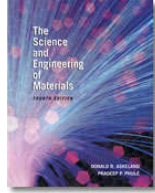


The Science and Engineering of Materials, 4th ed

Donald R. Askeland – Pradeep P. Phulé

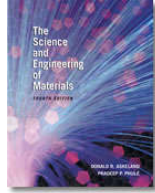
Chapter 1 – Introduction to Materials Science and Engineering





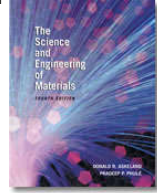
Objectives of Chapter 1

- ❑ Introduce the field of materials science and engineering (MSE)
- ❑ Provide introduction to the classification of materials



Chapter Outline

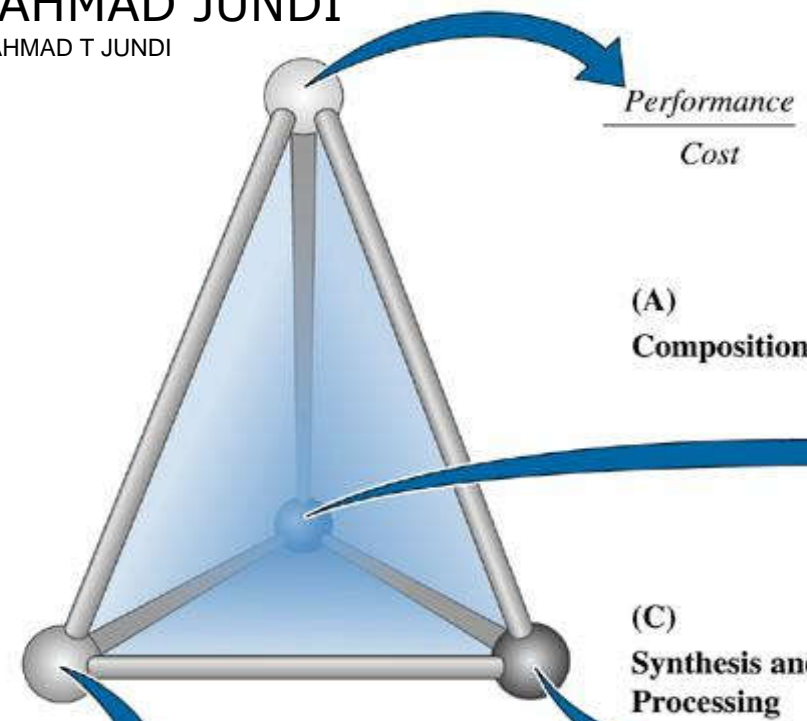
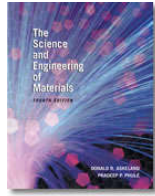
- 1.1 What is Materials Science and Engineering?
- 1.2 Classification of Materials
- 1.3 Functional Classification of Materials
- 1.4 Classification of Materials Based on Structure
- 1.5 Environmental and Other Effects
- 1.6 Materials Design and Selection



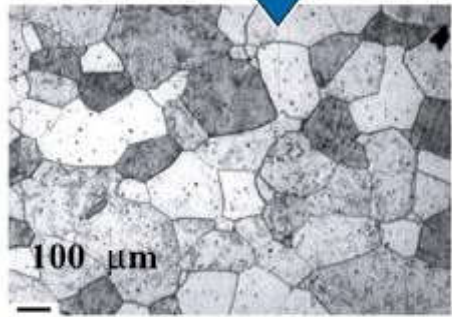
Section 1.1

What is Materials Science and Engineering?

- **Materials Science and Engineering**
- **Composition** means the chemical make-up of a material.
- **Structure** means a description of the arrangements of atoms or ions in a material.
- **Synthesis** is the process by which materials are made from naturally occurring or other chemicals.
- **Processing** means different ways for shaping materials into useful components or changing their properties.



(B) Microstructure



© 2003 Brooks/Cole Publishing / Thomson Learning™

Introduction to Chapter 1

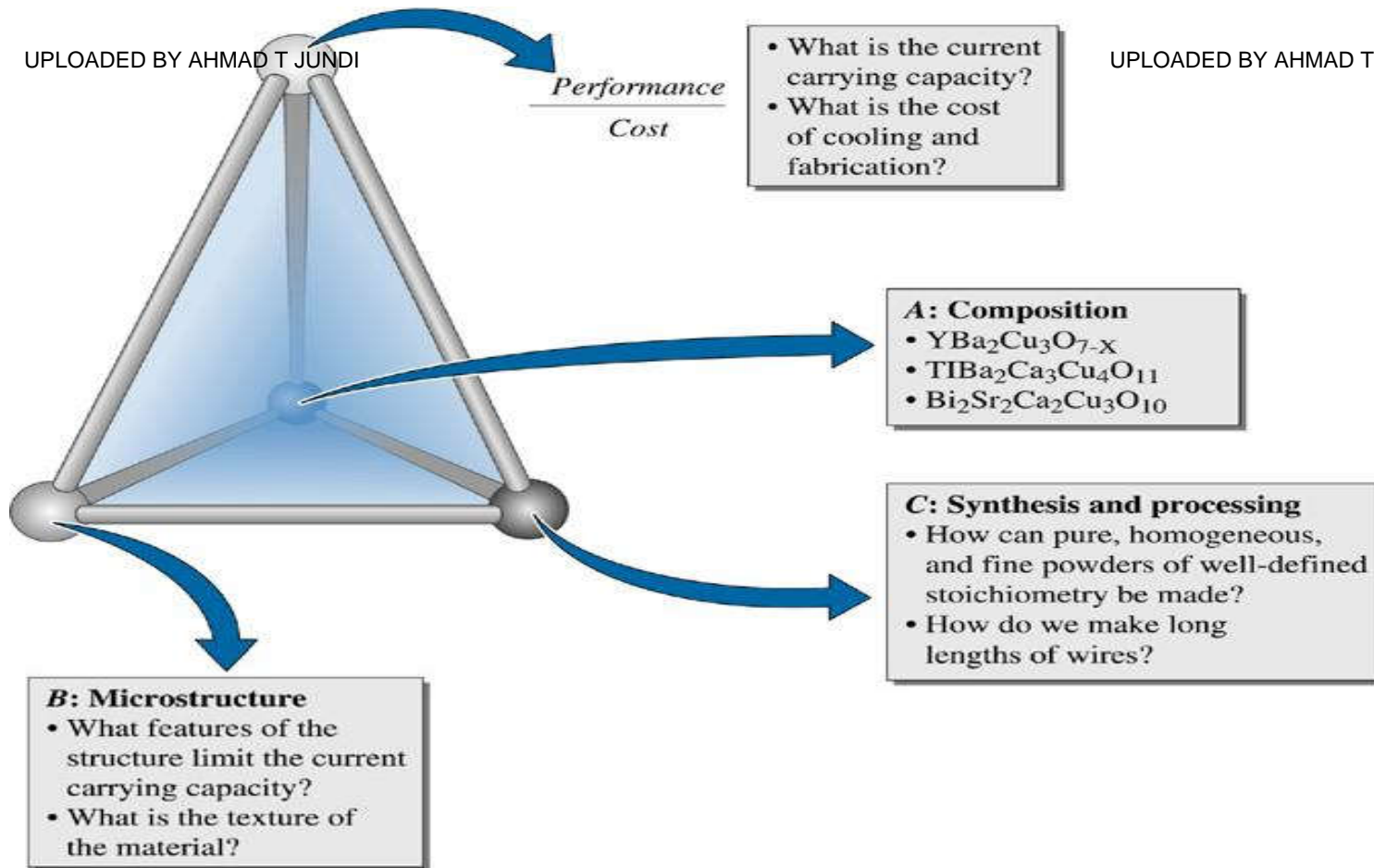
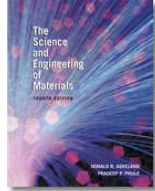


Figure 1.1 Application of the tetrahedron of materials science and engineering to ceramic superconductors. Note that the microstructure-synthesis and processing-composition are all interconnected and affect the performance-to-cost ratio

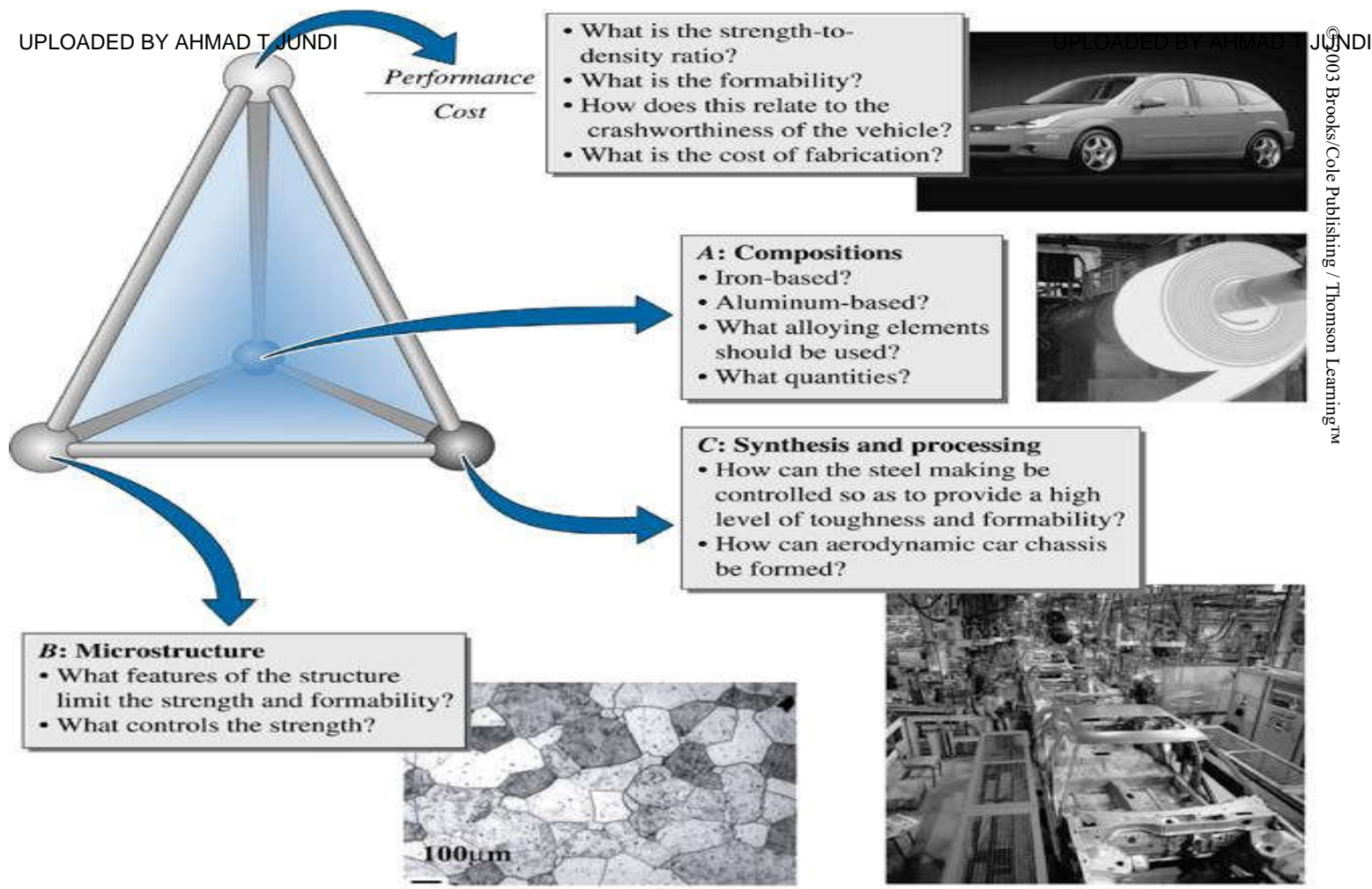


Figure 1.2 Application of the tetrahedron of materials science and engineering to sheet steels for automotive chassis. Note that the microstructure-synthesis and processing-composition are all interconnected and affect the performance-to-cost ratio

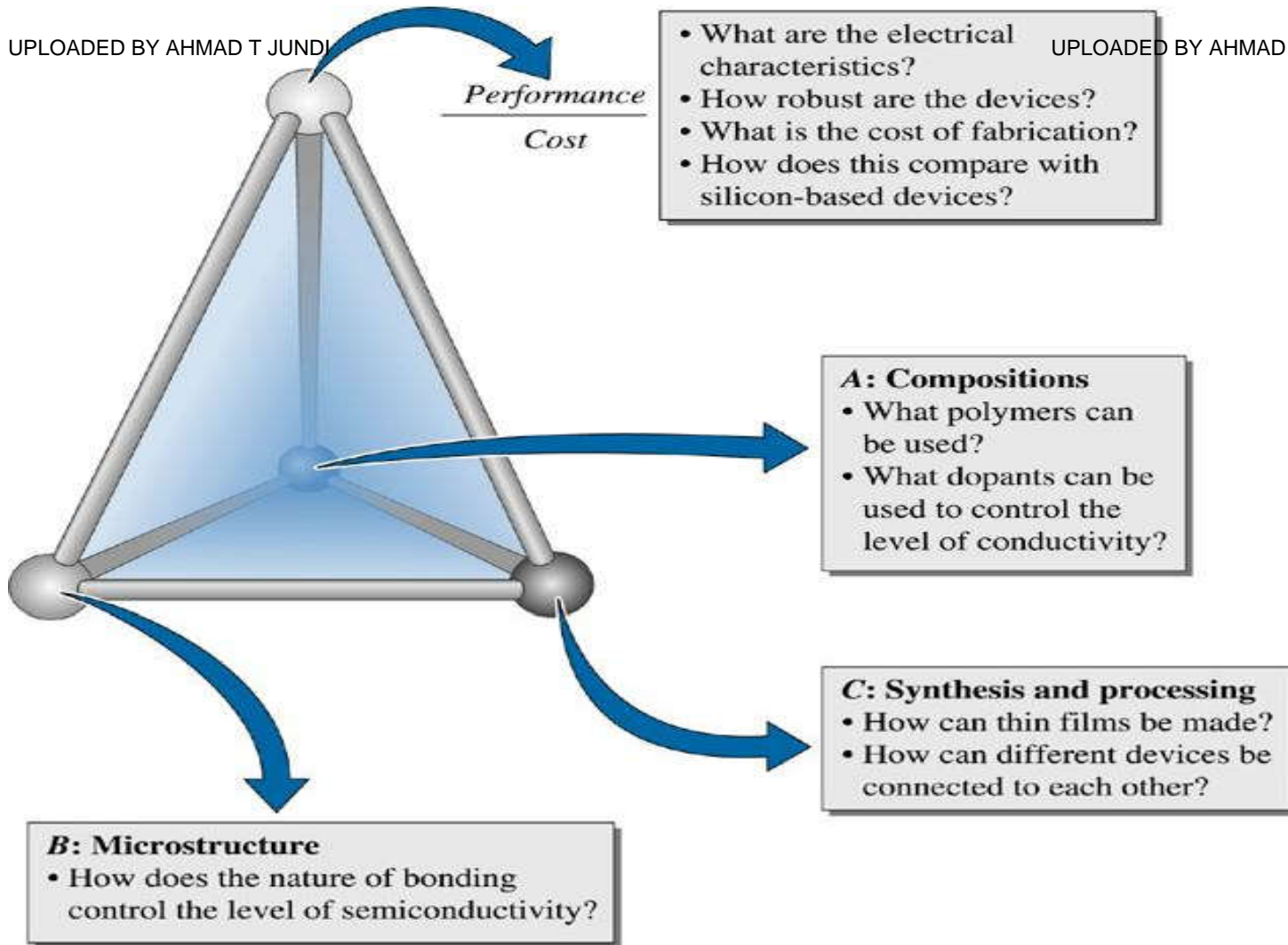
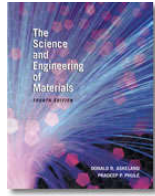
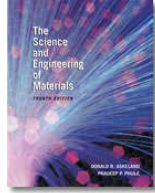


Figure 1.3 Application of the tetrahedron of materials science and engineering to semiconducting polymers for microelectronics



Section 1.2

Classification of Materials



- ❑ Metals and Alloys
- ❑ Ceramics, Glasses, and Glass-ceramics
- ❑ Polymers (plastics), Thermoplastics and Thermosets
- ❑ Semiconductors
- ❑ Composite Materials

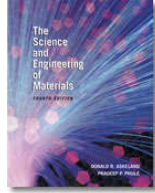


Table 1.1 Representative examples, applications, and properties for each category of materials

Example of Applications

Properties

Metals and Alloys

Gray cast iron

Automobile engine blocks

Castable, machinable, vibration damping

Ceramics and Glasses

$\text{SiO}_2\text{-Na}_2\text{O-CaO}$

Window glass

Optically transparent, thermally insulating

Polymers

Polyethylene

Food packaging

Easily formed into thin, flexible, airtight film



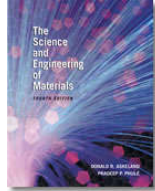


Table 1.1 Continued

Example of Applications

Properties

Semiconductors
Silicon

Transistors and integrated circuits

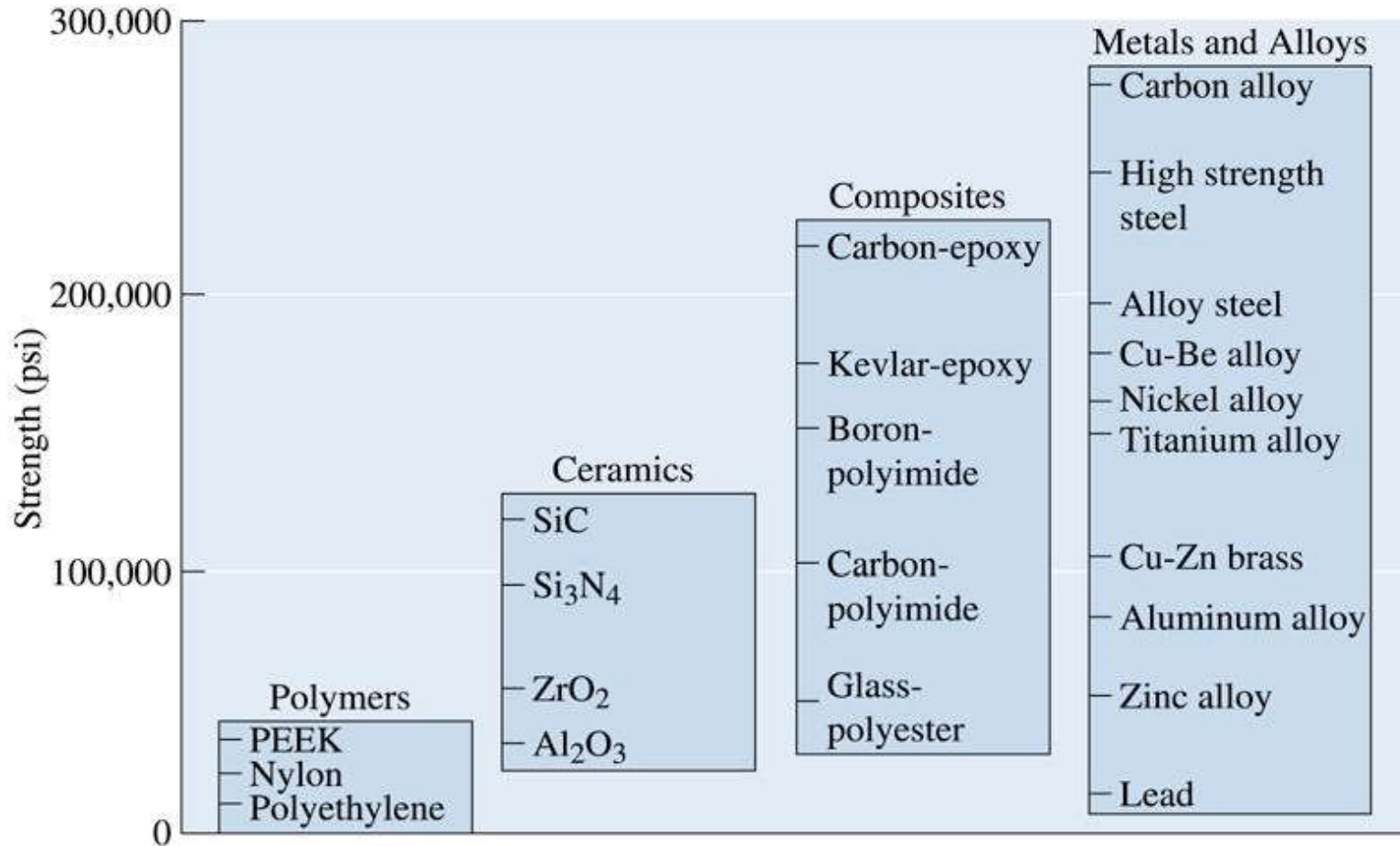
Unique electrical behavior

Composites
Tungsten carbide-cobalt (WC-Co)

Carbide cutting tools for machining

High hardness, yet good shock resistance





© 2003 Brooks/Cole Publishing / Thomson Learning™



Figure 1.4 Representative strengths of various categories of materials

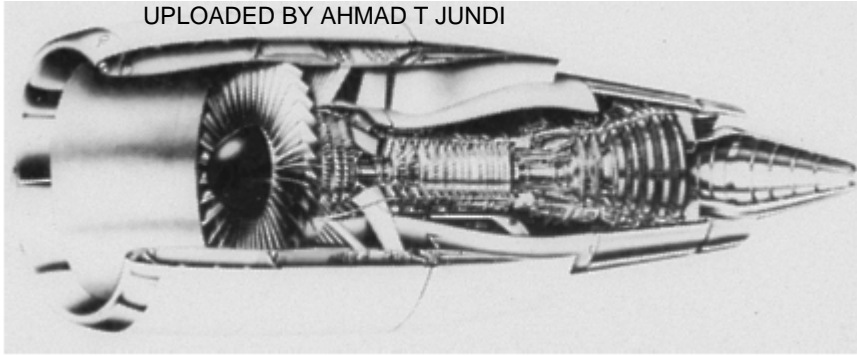
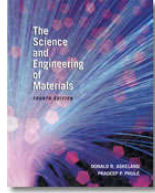
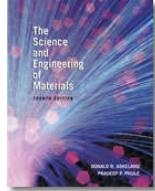


Figure 1.5 A section through a jet engine. The forward compression section operates at low to medium temperatures, and titanium parts are often used. The rear combustion section operates at high temperatures and nickel-based superalloys are required. The outside shell experiences low temperatures, and aluminum and composites are satisfactory. (Courtesy of GE Aircraft Engines.)



Figure 1.6 A variety of complex ceramic components, including impellers and blades, which allow turbine engines to operate more efficiently at higher temperatures. (Courtesy of Certech, Inc.)





© 2003 Brooks/Cole Publishing / Thomson Learning™

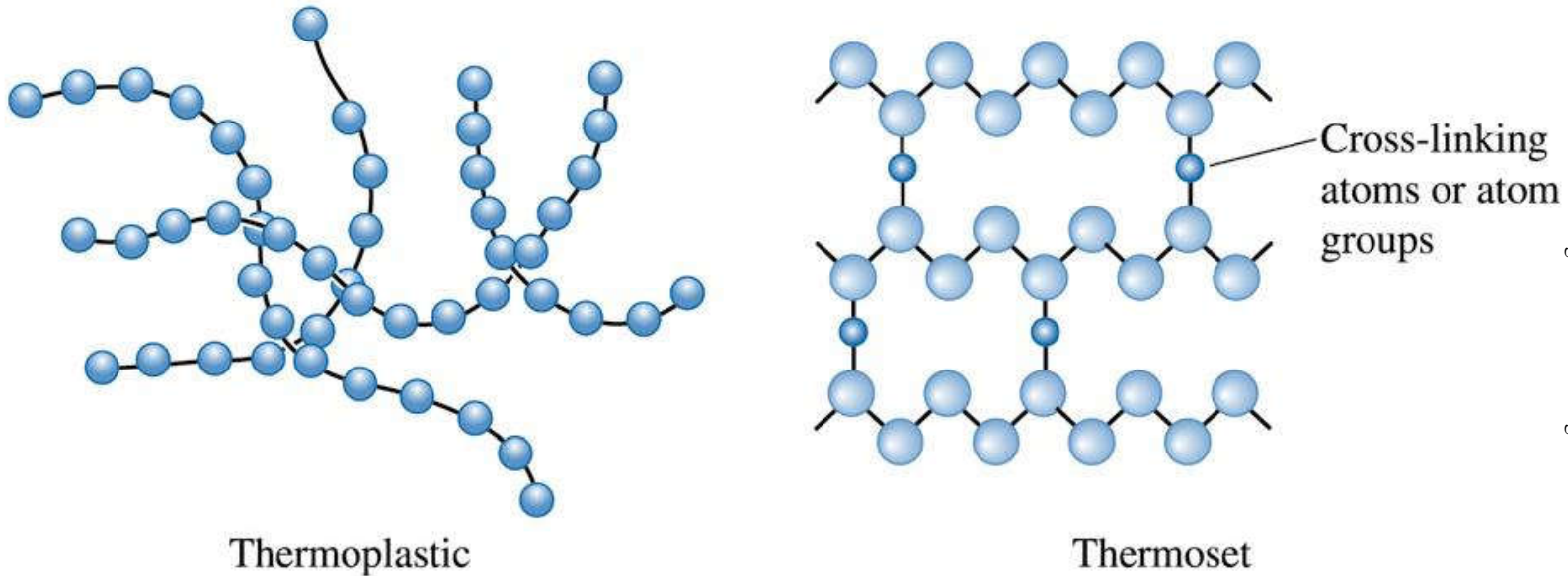


Figure 1.7 Polymerization occurs when small molecules, represented by the circles, combine to produce larger molecules, or polymers. The polymer molecules can have a structure that consists of many chains that are entangled but not connected (thermoplastics) or can form three-dimensional networks in which chains are cross-linked (thermosets)

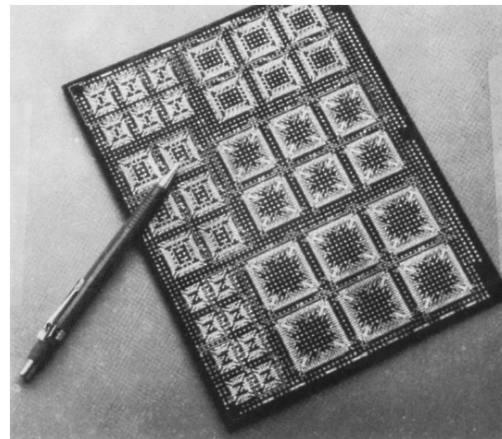
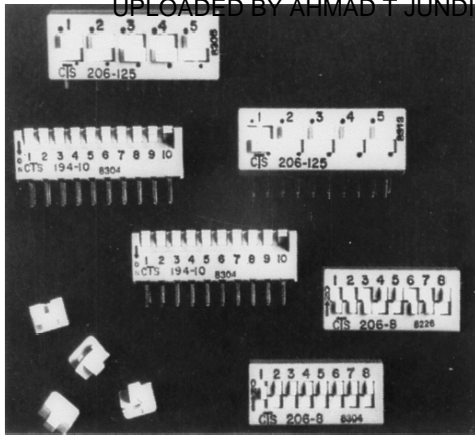
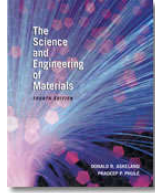


Figure 1.8 Polymers are used in a variety of electronic devices, including these computer dip switches, where moisture resistance and low conductivity are required. (Courtesy of CTS Corporation.)

Figure 1.9 Integrated circuits for computers and other electronic devices rely on the unique electrical behavior of semiconducting materials. (Courtesy of Rogers Corporation.)

Figure 1.10 The X-wing for advanced helicopters relies on a material composed of a carbon-fiber-reinforced polymer. (Courtesy of Sikorsky Aircraft Division—United Technologies Corporation.)



Section 1.3

Functional Classification of Materials

- Aerospace
- Biomedical
- Electronic Materials
- Energy Technology and Environmental Technology
- Magnetic Materials
- Photonic or Optical Materials
- Smart Materials
- Structural Materials

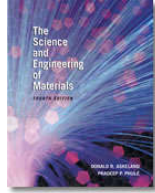
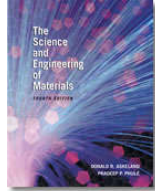


Figure 1.11 Functional classification of materials. Notice that metals, plastics, and ceramics occur in different categories. A limited number of examples in each category is provided



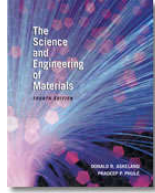
Section 1.4

Classification of Materials-Based on Structure

- ❑ **Crystalline** material is a material comprised of one or many crystals. In each crystal, atoms or ions show a long-range periodic arrangement.
- ❑ **Single crystal** is a crystalline material that is made of only one crystal (there are no grain boundaries).
- ❑ **Grains** are the crystals in a polycrystalline material.
- ❑ **Polycrystalline material** is a material comprised of many crystals (as opposed to a single-crystal material that has only one crystal).
- ❑ **Grain boundaries** are regions between grains of a polycrystalline material.

Section 1.5

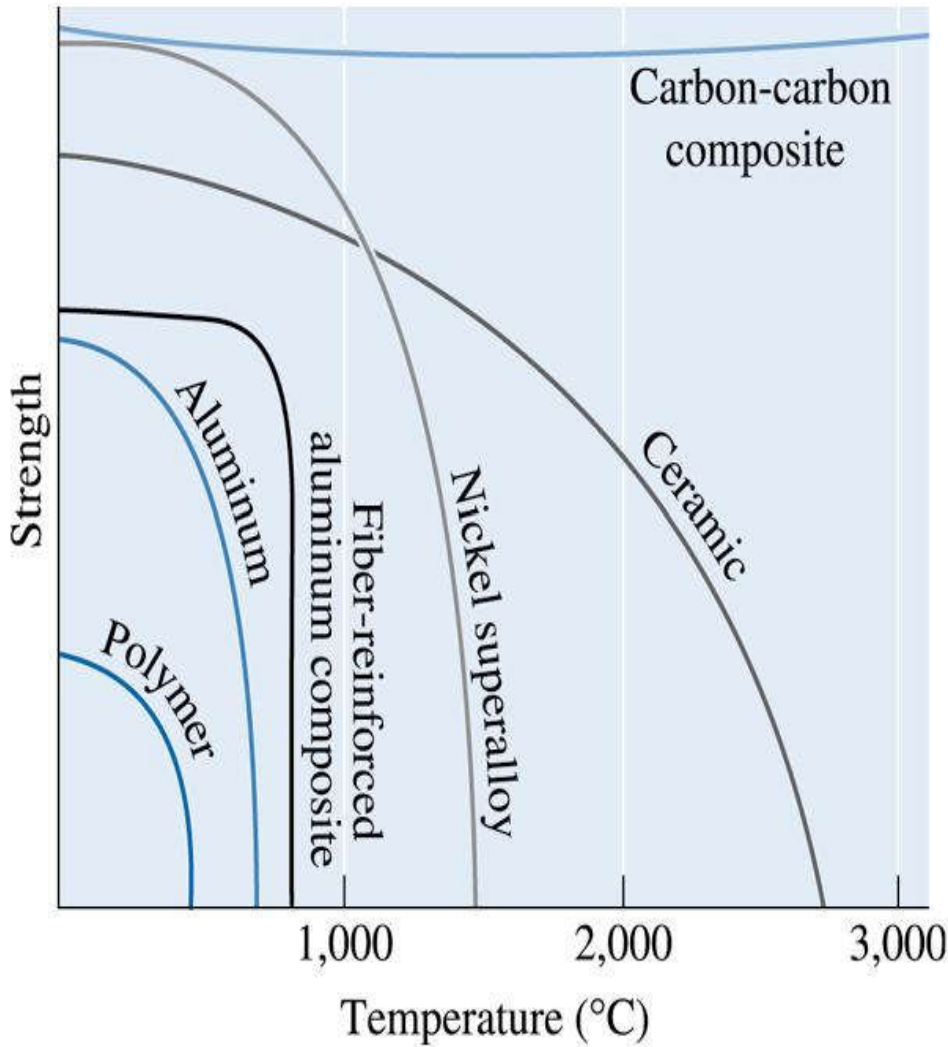
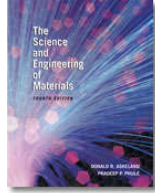
Environmental and Other Effects



Effects of following factors must be accounted for in design to ensure that components do not fail unexpectedly:

- Temperature
- Corrosion
- Fatigue
- Strain Rate





© 2003 Brooks/Cole Publishing / Thomson Learning™

Figure 1.12
Increasing temperature normally reduces the strength of a material. Polymers are suitable only at low temperatures. Some composites, special alloys, and ceramics, have excellent properties at high temperatures





Figure 1.13 Skin operating temperatures for aircraft have increased with the development of improved materials. (After M. Steinberg, Scientific American, October, 1986.)

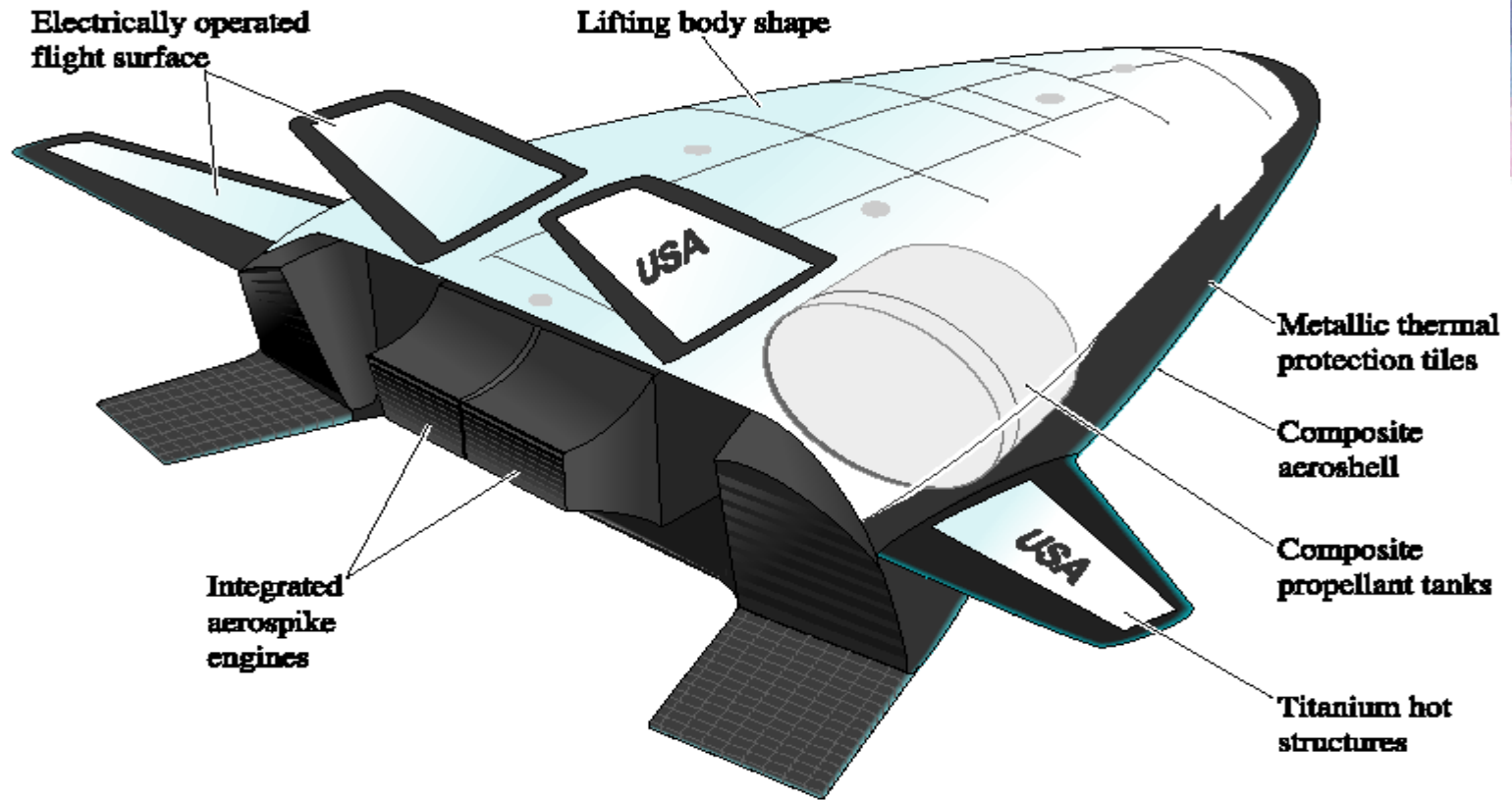
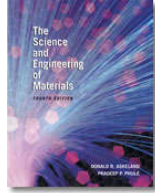
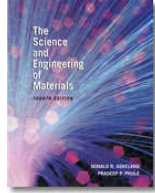


Figure 1-14 Schematic of a X-33 plane prototype. Notice the use of different materials for different parts. This type of vehicle will test several components for the Venturestar (From "A Simpler Ride into Space," by T.K. Mattingly, October, 1997, Scientific American, p. 125. Copyright © 1997 Slim Films.)

Section 1.6

Materials Design and Selection



- ❑ **Density** is mass per unit volume of a material, usually expressed in units of g/cm^3 or lb/in.^3
- ❑ **Strength-to-weight ratio** is the strength of a material divided by its density; materials with a high strength-to-weight ratio are strong but lightweight.

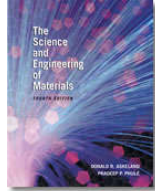


TABLE 1-2 ■ Strength-to-weight ratios of various materials

Material	Strength (lb/in.²)	Density (lb/in.³)	Strength-to-weight ratio (in.)
Polyethylene	1,000	0.030	0.03×10^6
Pure aluminum	6,500	0.098	0.07×10^6
Al ₂ O ₃	30,000	0.114	0.26×10^6
Epoxy	15,000	0.050	0.30×10^6
Heat-treated alloy steel	240,000	0.280	0.86×10^6
Heat-treated aluminum alloy	86,000	0.098	0.88×10^6
Carbon-carbon composite	60,000	0.065	0.92×10^6
Heat-treated titanium alloy	170,000	0.160	1.06×10^6
Kevlar-epoxy composite	65,000	0.050	1.30×10^6
Carbon-epoxy composite	80,000	0.050	1.60×10^6



The Science and Engineering of Materials, 4th ed

Donald R. Askeland – Pradeep P. Phulé

Chapter 2 – Atomic Structure





Objectives of Chapter 2

- ❑ The goal of this chapter is to describe the underlying physical concepts related to the structure of matter.
- ❑ To examine the relationships between structure of atoms-bonds-properties of engineering materials.
- ❑ Learn about different levels of structure i.e. atomic structure, nanostructure, microstructure, and macrostructure.





Chapter Outline

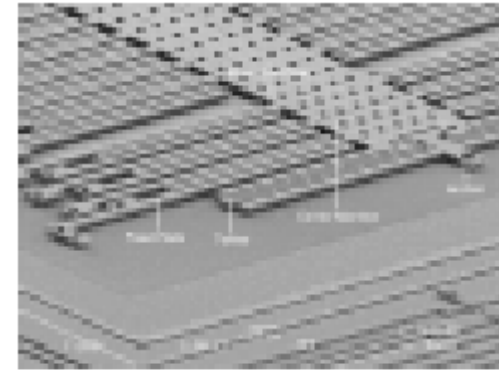
- 2.1 The Structure of Materials: Technological Relevance
- 2.2 The Structure of the Atom
- 2.3 The Electronic Structure of the Atom
- 2.4 The Periodic Table
- 2.5 Atomic Bonding
- 2.6 Binding Energy and Interatomic Spacing



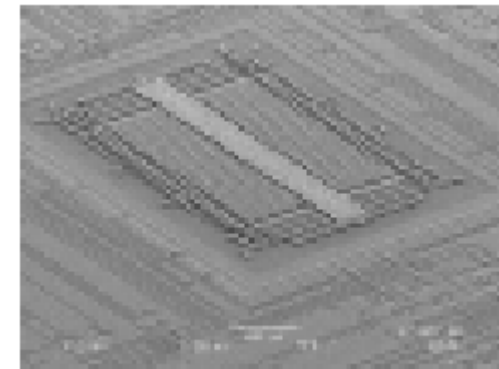


The Structure of Materials: Technological Relevance

- Nanotechnology
- Micro-electro-mechanical (MEMS) systems-Airbag sensors
- Nanostructures



(a)



(b)

Figure 2.1



Table 2.1 Levels of Structure

Level of Structure Example of Technologies

Atomic Structure Diamond – edge of cutting tools



Atomic Arrangements: Long-Range Order (LRO) Lead-zirconium-titanate [$Pb(Zr_x Ti_{1-x})$] or PZT – gas igniters



Atomic Arrangements: Short-Range Order (SRO) Amorphous silica - fiber optical communications industry



Figures 2.2 – 2.4





Table 2.1 (Continued)

Level of Structure **Example of Technologies**

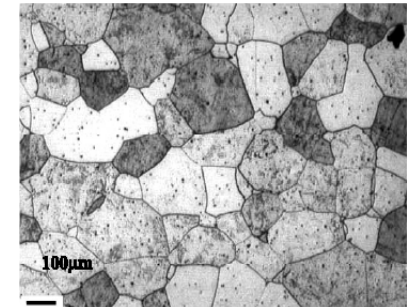
Nanostructure

Nano-sized particles of iron oxide – ferrofluids



Microstructure

Mechanical strength of metals and alloys



Macrostructure

Paints for automobiles for corrosion resistance



Figures 2.5 – 2.7





Section 2.2

The Structure of the Atom

- The **atomic number** of an element is equal to the number of electrons or protons in each atom.
- The **atomic mass** of an element is equal to the average number of protons and neutrons in the atom.
- The **Avogadro number** of an element is the number of atoms or molecules in a mole.
- The **atomic mass unit** of an element is the mass of an atom expressed as 1/12 the mass of a carbon atom.





Example 2.1

Calculate the Number of Atoms in Silver

Calculate the number of atoms in 100 g of silver.

Example 2.1 SOLUTION

$$\begin{aligned} \text{The number of silver atoms is} &= \frac{(100 \text{ g})(6.023 \times 10^{23} \text{ atoms/mol})}{(107.868 \text{ g/mol})} \\ &= 5.58 \times 10^{23} \end{aligned}$$





Example 2.2

Nano-Sized Iron-Platinum Particles For Information Storage

Scientists are considering using nano-particles of such magnetic materials as iron-platinum (Fe-Pt) as a medium for ultrahigh density data storage. Arrays of such particles potentially can lead to storage of trillions of bits of data per square inch—a capacity that will be 10 to 100 times higher than any other devices such as computer hard disks. If these scientists considered iron (Fe) particles that are 3 nm in diameter, what will be the number of atoms in one such particle?





Example 2.2 SOLUTION

The radius of a particle is 1.5 nm.

Volume of each iron magnetic nano-particle

$$= (4/3)\pi(1.5 \times 10^{-7} \text{ cm})^3$$

$$= 1.4137 \times 10^{-20} \text{ cm}^3$$

Density of iron = 7.8 g/cm³. Atomic mass of iron is 56 g/mol.

Mass of each iron nano-particle

$$= 7.8 \text{ g/cm}^3 \times 1.4137 \times 10^{-20} \text{ cm}^3$$

$$= 1.102 \times 10^{-19} \text{ g.}$$

One mole or 56 g of Fe contains 6.023×10^{23} atoms, therefore, the number of atoms in one Fe nano-particle will be 1186.





Dopant Concentration In Silicon Crystals

Silicon single crystals are used extensively to make computer chips. Calculate the concentration of silicon atoms in silicon, or the number of silicon atoms per unit volume of silicon. During the growth of silicon single crystals it is often desirable to deliberately introduce atoms of other elements (known as dopants) to control and change the electrical conductivity and other electrical properties of silicon. Phosphorus (P) is one such dopant that is added to make silicon crystals n -type semiconductors. Assume that the concentration of P atoms required in a silicon crystal is 10^{17} atoms/cm³. Compare the concentrations of atoms in silicon and the concentration of P atoms. What is the significance of these numbers from a technological viewpoint? Assume that density of silicon is 2.33 g/cm³.





Example 2.3 SOLUTION

Atomic mass of silicon = 28.09 g/mol.

So, 28.09 g of silicon contain 6.023×10^{23} atoms.

Therefore, 2.33 g of silicon will contain

$(2.33 \times 6.023 \times 10^{23} / 28.09)$ atoms = 4.99×10^{22} atoms. Mass of one cm^3 of Si is 2.33 g.

Therefore, the concentration of silicon atoms in pure silicon is $\sim 5 \times 10^{22}$ atoms/ cm^3 .





Example 2.3 SOLUTION (Continued)

Significance of comparing dopant and Si atom concentrations: If we were to add phosphorus (P) into this crystal, such that the concentration of P is 10^{17} atoms/cm³, the ratio of concentration of atoms in silicon to that of P will be

$(5 \times 10^{22}) / (10^{17}) = 5 \times 10^5$. This says that only 1 out of 500,000 atoms of the doped crystal will be that of phosphorus (P)! This is equivalent to one apple in 500,000 oranges! This explains why the single crystals of silicon must have exceptional purity and at the same time very small and uniform levels of dopants.





Section 2.3 The Electronic Structure of the Atom

- **Quantum numbers** are the numbers that assign electrons in an atom to discrete energy levels.
- A **quantum shell** is a set of fixed energy levels to which electrons belong.
- **Pauli exclusion principle** specifies that no more than two electrons in a material can have the same energy. The two electrons have opposite magnetic spins.
- The **valence** of an atom is the number of electrons in an atom that participate in bonding or chemical reactions.
- **Electronegativity** describes the tendency of an atom to gain an electron.





© 2003 Brooks/Cole Publishing / Thomson Learning™

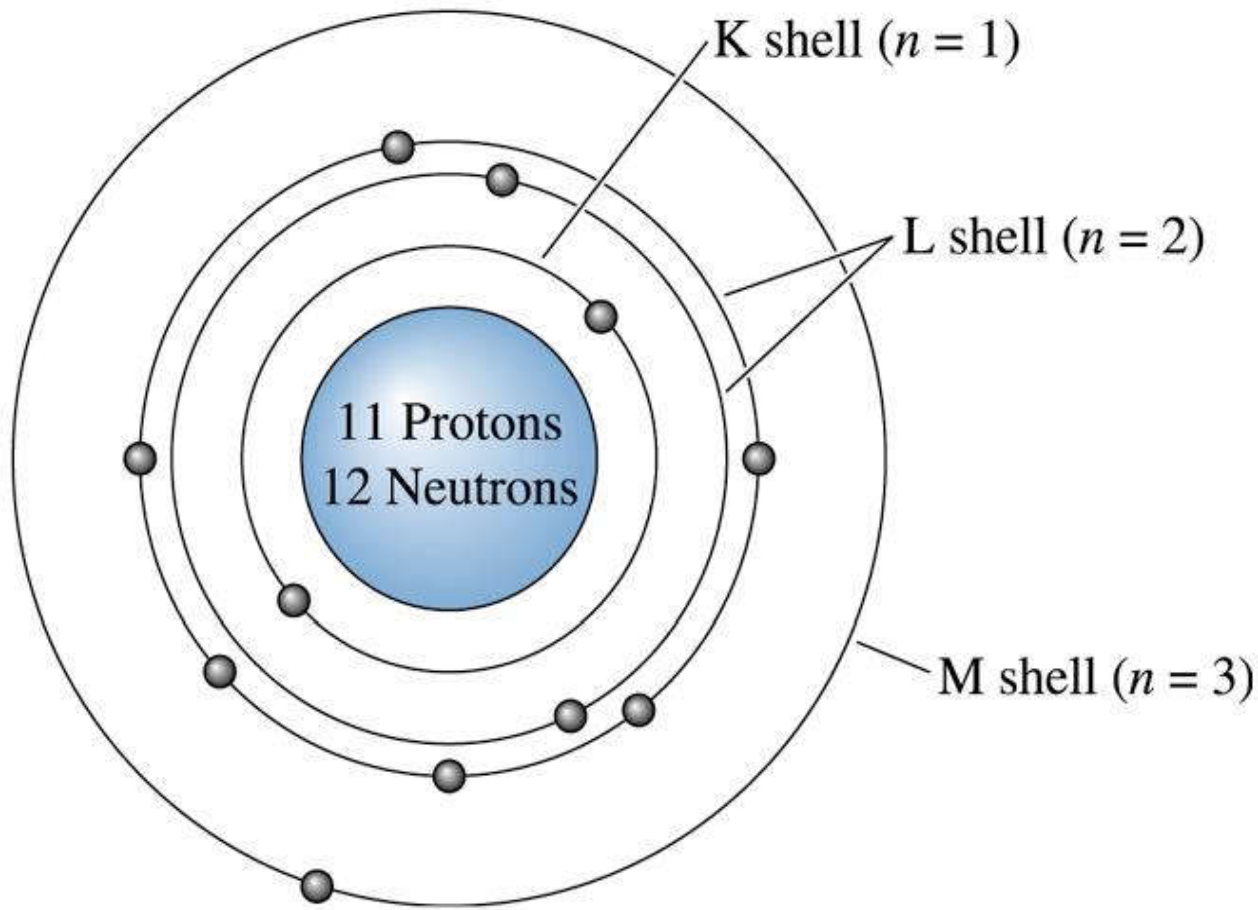


Figure 2.8 The atomic structure of sodium, atomic number 11, showing the electrons in the *K*, *L*, and *M* quantum shells





© 2003 Brooks/Cole Publishing / Thomson Learning™

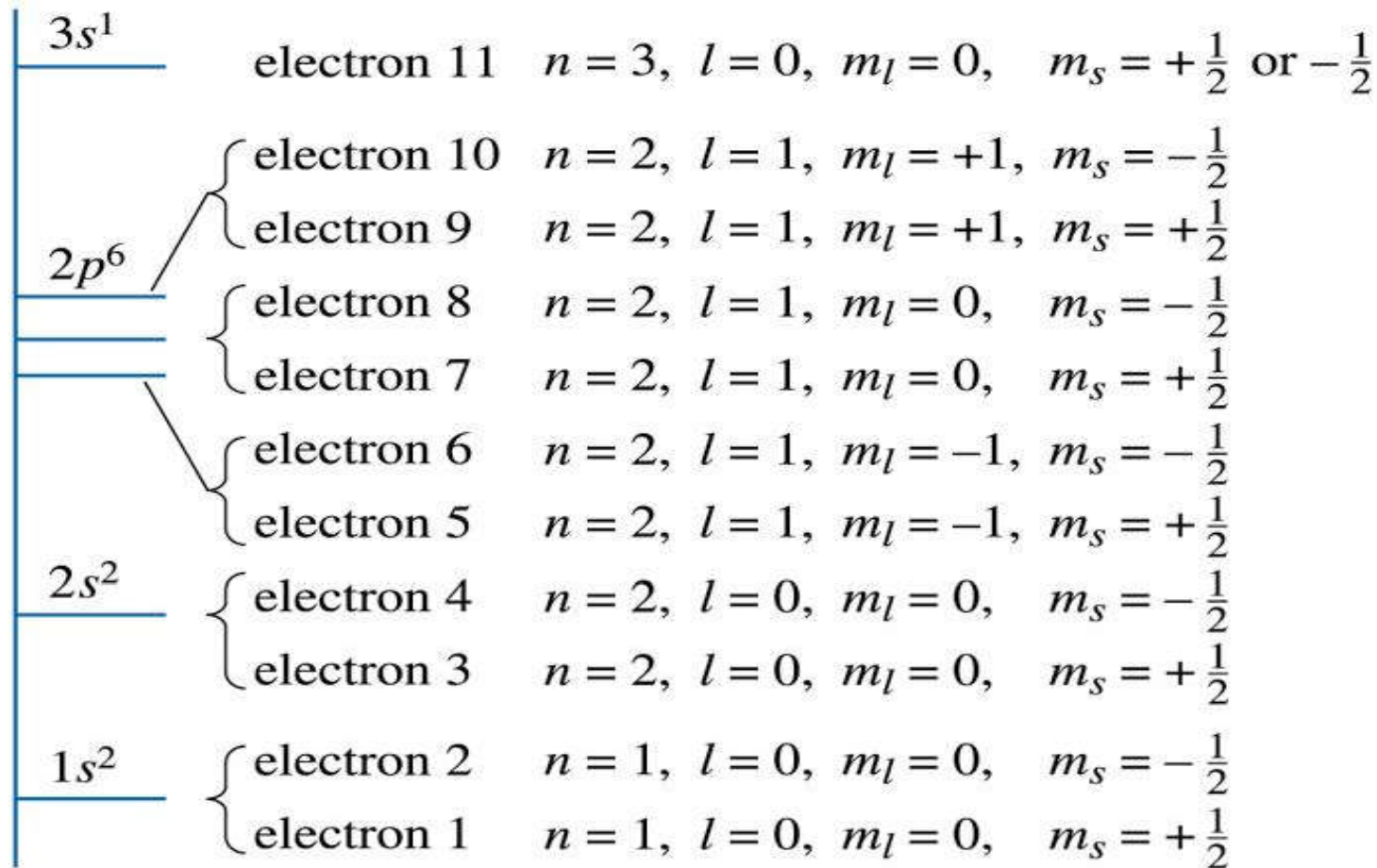


Figure 2.9 The complete set of quantum numbers for each of the 11 electrons in sodium



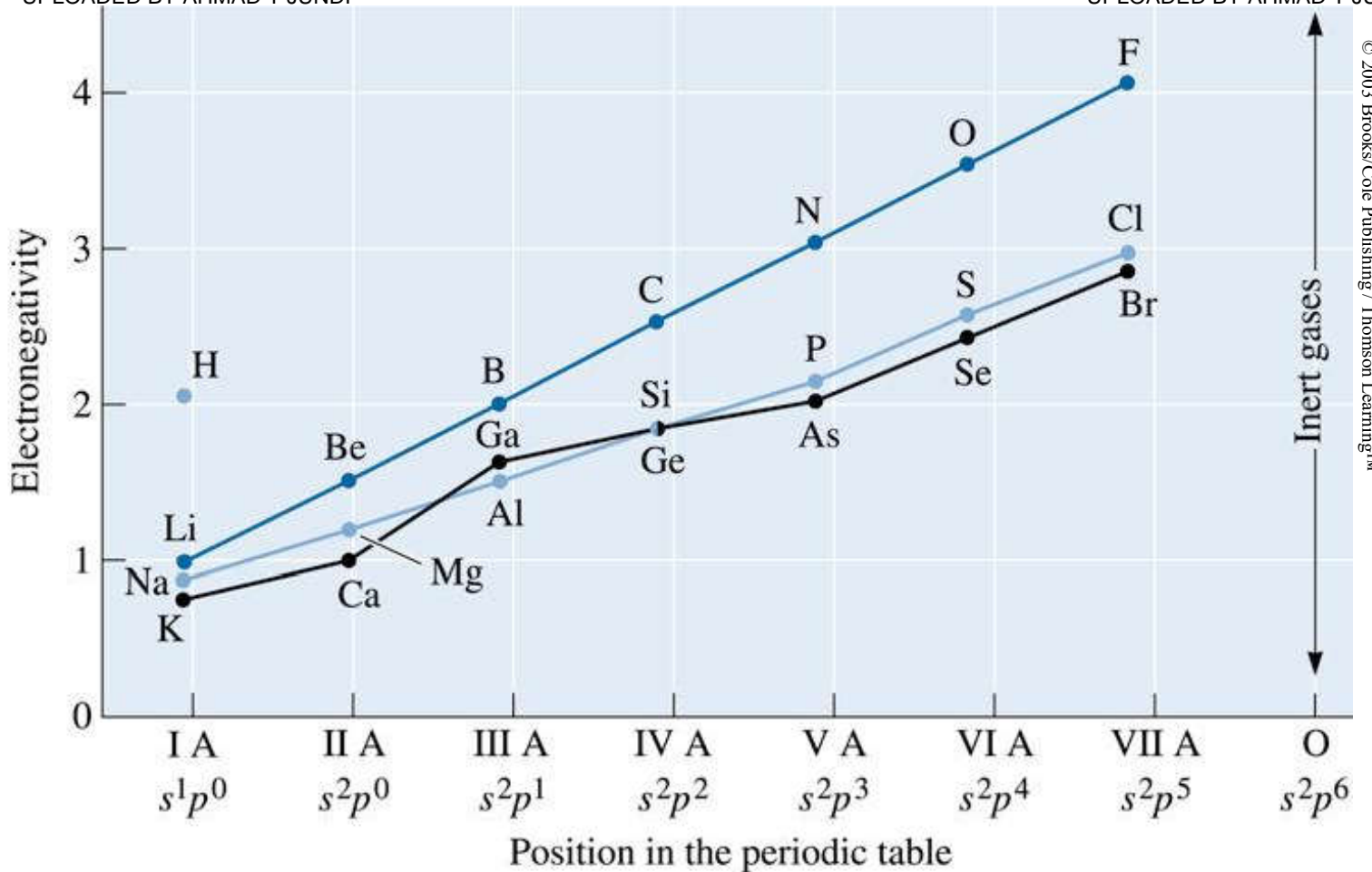


TABLE 2-2 ■ *The pattern used to assign electrons to energy levels*

	$l = 0$ (s)	$l = 1$ (p)	$l = 2$ (d)	$l = 3$ (f)	$l = 4$ (g)	$l = 5$ (h)
$n = 1$ (K)	2					
$n = 2$ (L)	2	6				
$n = 3$ (M)	2	6	10			
$n = 4$ (N)	2	6	10	14		
$n = 5$ (O)	2	6	10	14	18	
$n = 6$ (P)	2	6	10	14	18	22

Note: 2, 6, 10, 14, ... refer to the number of electrons in the energy level.





© 2003 Brooks/Cole Publishing / Thomson Learning™



Figure 2.10 The electronegativities of selected elements relative to the position of the elements in the periodic table



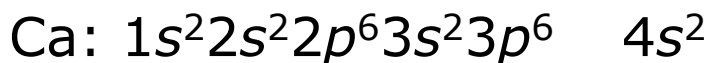
Example 16.9

Comparing Electronegativities

Using the electronic structures, compare the electronegativities of calcium and bromine.

Example 2.4 SOLUTION

The electronic structures, obtained from Appendix C, are:



Calcium has two electrons in its outer 4s orbital and bromine has seven electrons in its outer 4s4p orbital. Calcium, with an electronegativity of 1.0, tends to give up electrons and has low electronegativity, but bromine, with an electronegativity of 2.8, tends to accept electrons and is strongly electronegative. This difference in electronegativity values suggests that these elements may react readily to form a compound.





Section 2.4 The Periodic Table

- **III-V semiconductor** is a semiconductor that is based on group 3A and 5B elements (e.g. GaAs).
- **II-VI semiconductor** is a semiconductor that is based on group 2B and 6B elements (e.g. CdSe).
- **Transition elements** are the elements whose electronic configurations are such that their inner "d" and "f" levels begin to fill up.
- **Electropositive** element is an element whose atoms want to participate in chemical interactions by donating electrons and are therefore highly reactive.



© 2003 Brooks/Cole Publishing / Thomson Learning™

© 2003 Brooks/Cole Publishing / Thomson Learning™

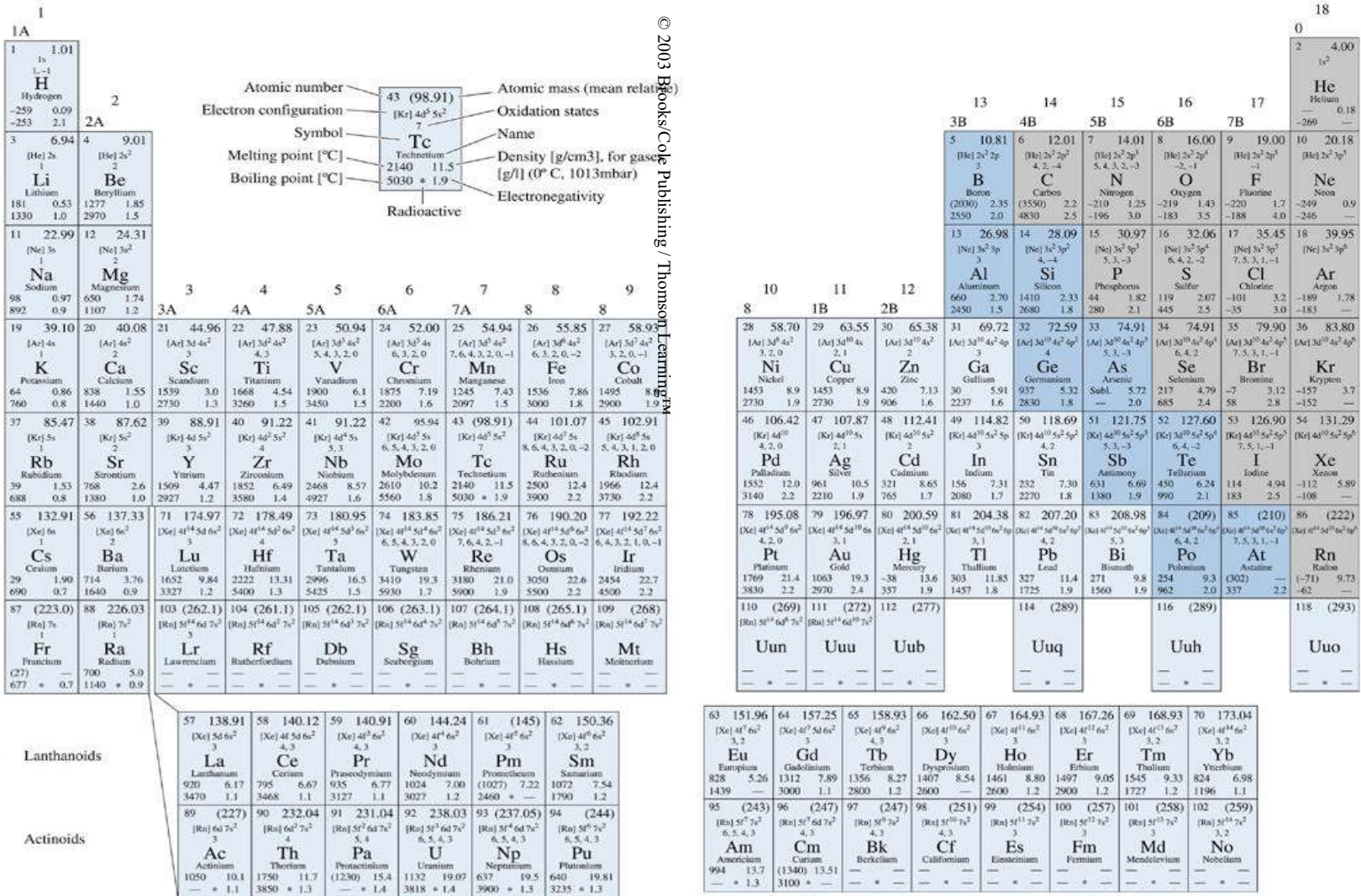


Figure 2.11 (a) and (b) Periodic Table of Elements





Section 2.5 Atomic Bonding

- **Metallic bond, Covalent bond, Ionic bond, van der Waals bond** are the different types of bonds.
- **Ductility** refers to the ability of materials to be stretched or bent without breaking
- Van der Waals interactions: **London forces, Debye interaction, Keesom interaction**
- **Glass temperature** is a temperature above which many polymers and inorganic glasses no longer behave as brittle materials
- **Intermetallic compound** is a compound such as Al_3V formed by two or more metallic atoms



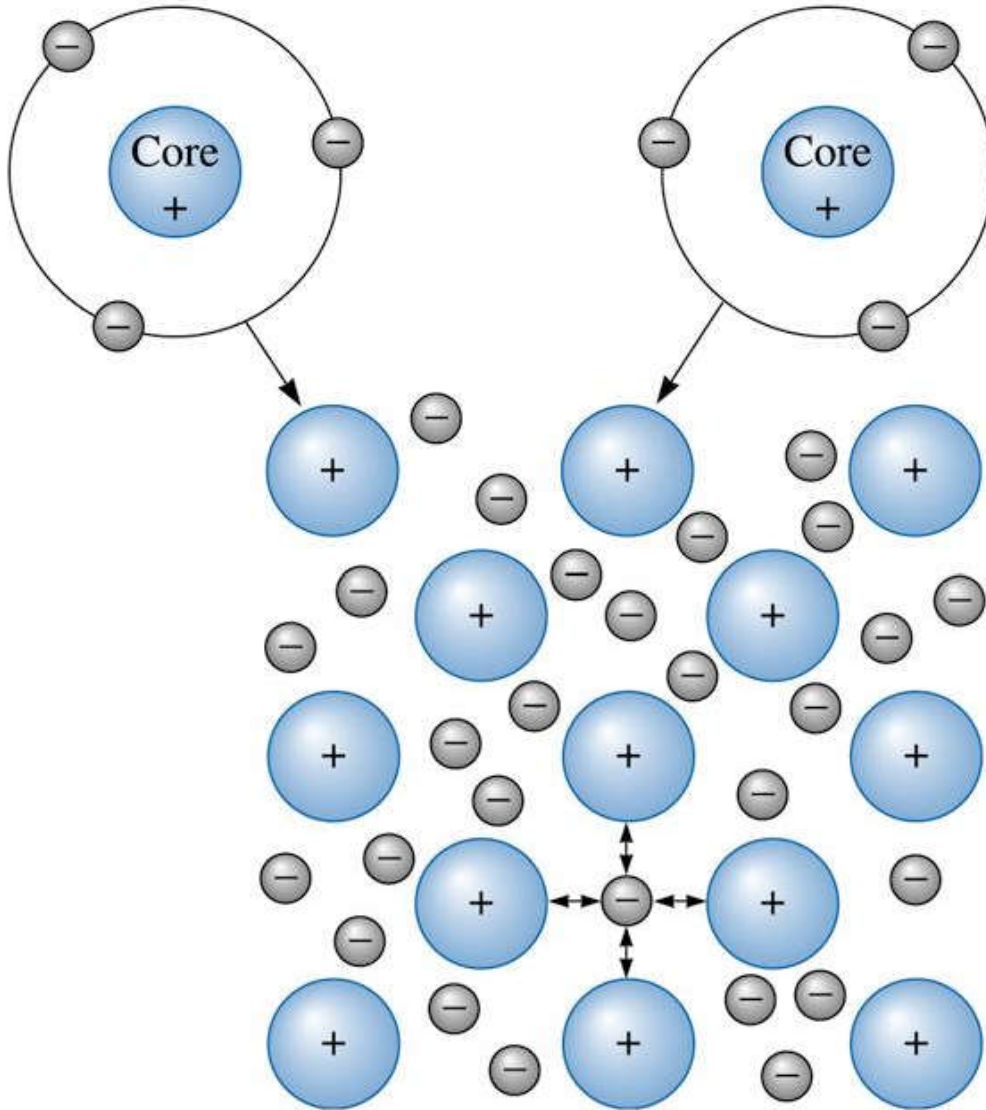


Figure 2.12 The metallic bond forms when atoms give up their valence electrons, which then form an electron sea. The positively charged atom cores are bonded by mutual attraction to the negatively charged electrons

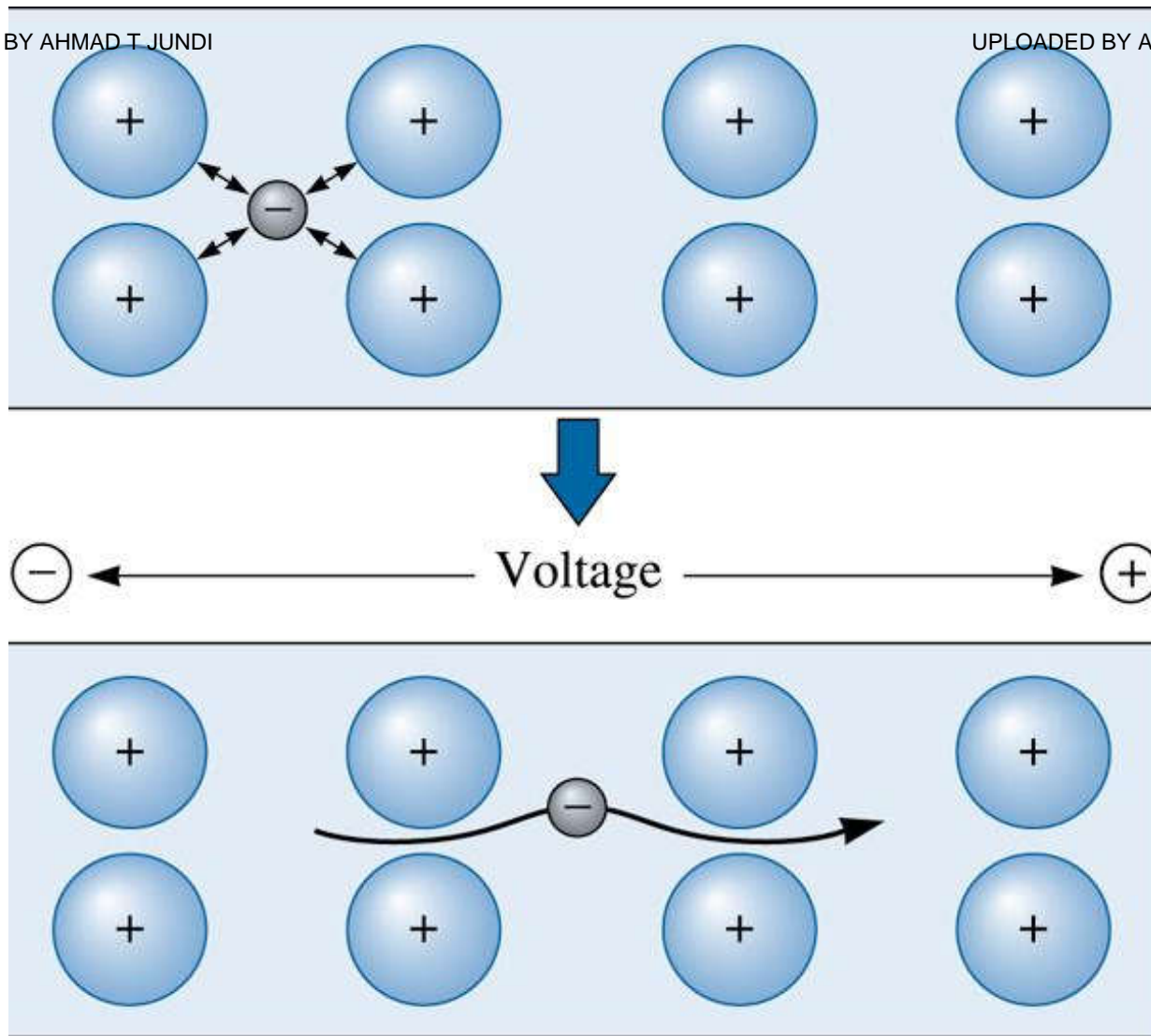


Figure 2.13 When voltage is applied to a metal, the electrons in the electron sea can easily move and carry a current



Example 2.5

Calculating the Conductivity of Silver

Calculate the number of electrons capable of conducting an electrical charge in ten cubic centimeters of silver.

Example 2.5 SOLUTION

The valence of silver is one, and only the valence electrons are expected to conduct the electrical charge. From Appendix A, we find that the density of silver is 10.49 g/cm³. The atomic mass of silver is 107.868 g/mol.

$$\text{Mass of } 10 \text{ cm}^3 = (10 \text{ cm}^3)(10.49 \text{ g/cm}^3) = 104.9 \text{ g}$$

$$\text{Atoms} = \frac{(104.9 \text{ g})(6.023 \times 10^{23} \text{ atoms / mol})}{107.868 \text{ g / mol}} = 5.85 \times 10^{23}$$

$$\begin{aligned} \text{Electrons} &= (5.85 \times 10^{23} \text{ atoms})(1 \text{ valence electron/atom}) \\ &= 5.85 \times 10^{23} \text{ valence electron/atom per } 10 \text{ cm}^3 \end{aligned}$$



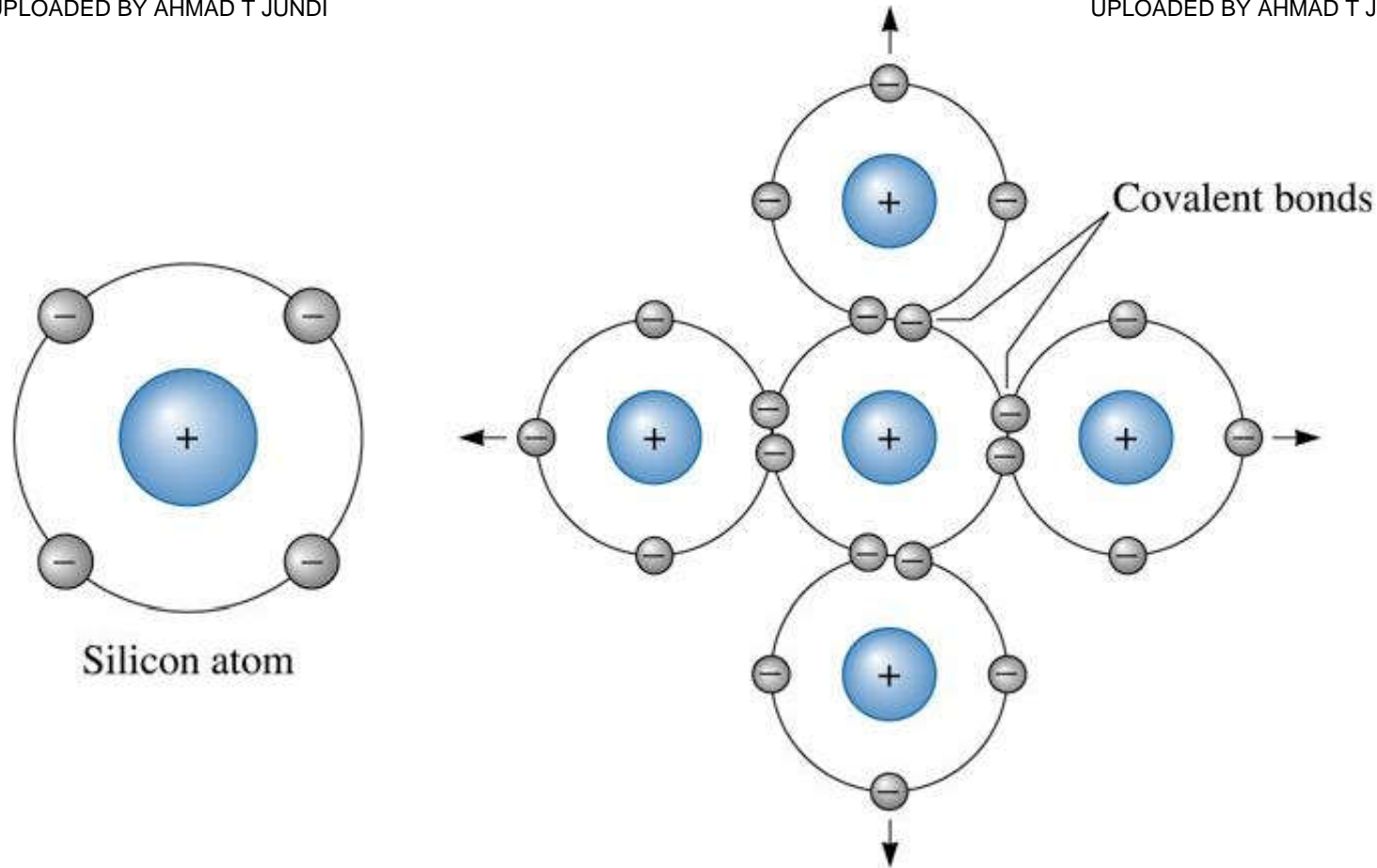


Figure 2.14 Covalent bonding requires that electrons be shared between atoms in such a way that each atom has its outer *sp* orbital filled. In silicon, with a valence of four, four covalent bonds must be formed

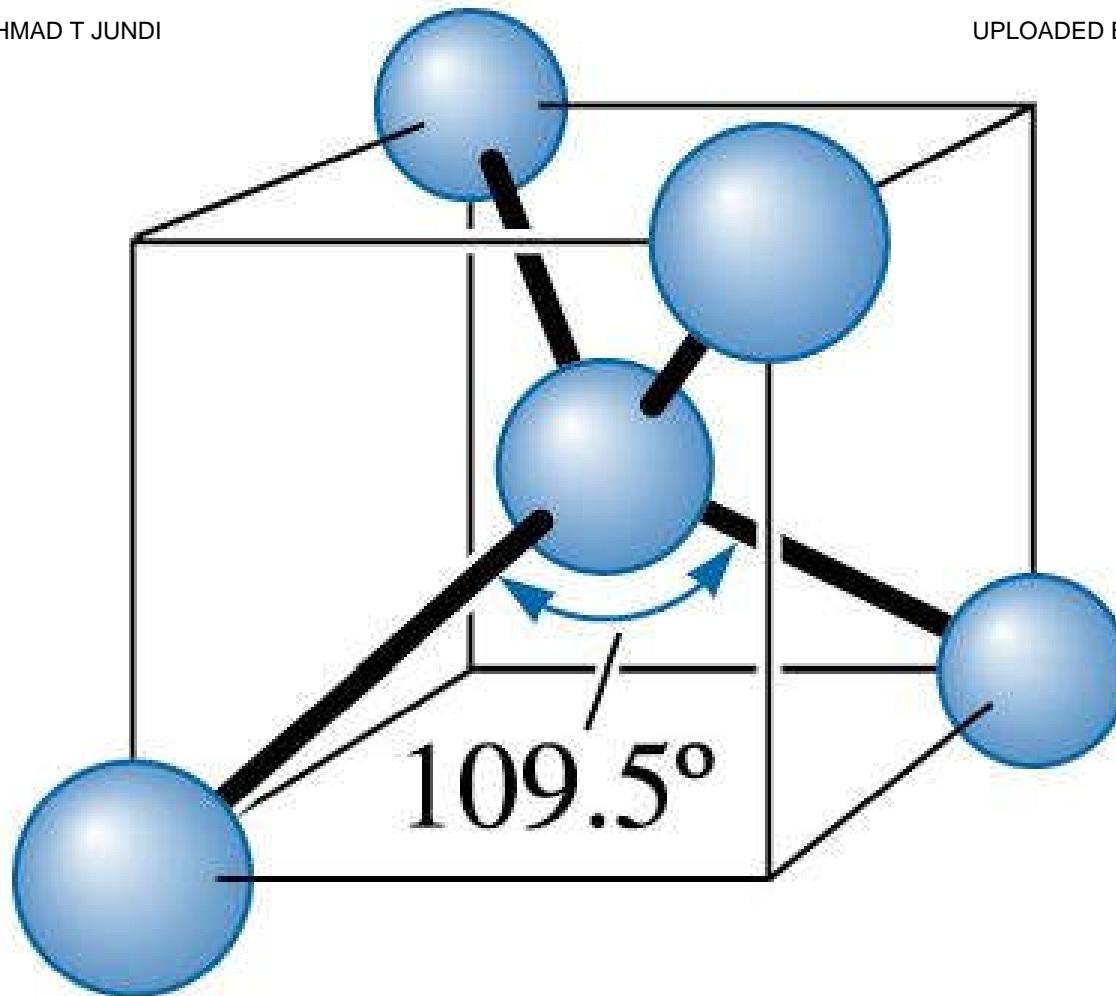


Figure 2.15 Covalent bonds are directional. In silicon, a tetrahedral structure is formed, with angles of 109.5° required between each covalent bond

Example 2.6



How Do Oxygen and Silicon Atoms Join to Form Silica?

Assuming that silica (SiO_2) has 100% covalent bonding, describe how oxygen and silicon atoms in silica (SiO_2) are joined.

Example 2.6 SOLUTION

Silicon has a valence of four and shares electrons with four oxygen atoms, thus giving a total of eight electrons for each silicon atom. However, oxygen has a valence of six and shares electrons with two silicon atoms, giving oxygen a total of eight electrons. Figure 2-16 illustrates one of the possible structures. Similar to silicon (Si), a tetrahedral structure also is produced. We will discuss later in this chapter how to account for the ionic and covalent nature of bonding in silica.



© 2003 Brooks/Cole Publishing / Thomson Learning™

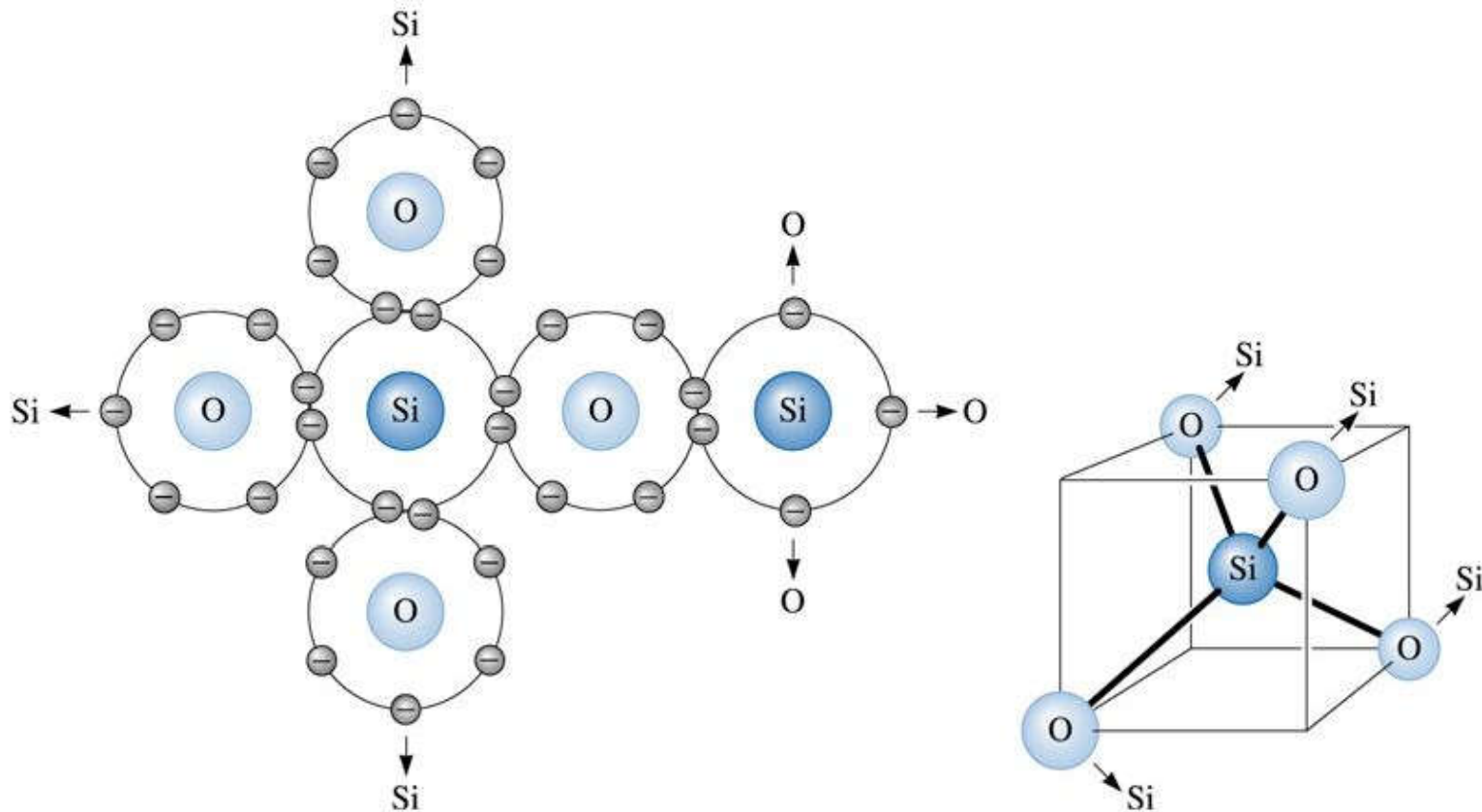


Figure 2.16 The tetrahedral structure of silica (SiO_2), which contains covalent bonds between silicon and oxygen atoms (for Example 2-6)





Example 2.7

Design of a Thermistor

A thermistor is a device used to measure temperature by taking advantage of the change in electrical conductivity when the temperature changes. Select a material that might serve as a thermistor in the 500 to 1000°C temperature range (see Figure 2-17).



Figure 2.17 Photograph of a commercially available thermistor (for Example 2-7). (Courtesy of Vishay Intertechnology, Inc.)





Example 2.7 SOLUTION

The resistance of a thermistor can be made to increase or decrease with increasing temperature. These are known as positive temperature coefficient of resistance (*PTCR*) or negative temperature coefficient of resistance (*NTCR*) thermistors, respectively. The fact that a thermistor changes its resistance in response to a temperature change is used to control temperature or switch (turn "on" and "off") the operation of an electrical circuit when a particular device (i.e., a refrigerator, hairdryer, furnace, oven, or reactor) reaches a certain temperature.



Example 2.7 SOLUTION (Continued)

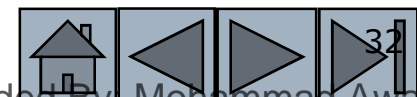
UPLOADED BY AHMAD T JUNDI

UPLOADED BY AHMAD T JUNDI



Two design requirements must be satisfied. First, a material with a high melting point must be selected. Second, the electrical conductivity of the material must show a systematic and reproducible change as a function of temperature. Covalently bonded materials might be suitable. They often have high melting temperatures, and, as more covalent bonds are broken when the temperature increases, increasing numbers of electrons become available to transfer electrical charge.

The semiconductor silicon is one choice: Silicon melts at 1410°C and is covalently bonded. A number of ceramic materials also have high melting points and behave as semiconducting materials. Silicon will have to be protected against oxidation. We will have to make sure the changes in conductivity in the temperature range are actually acceptable. Some thermistors that show a predictable decrease in the resistance with increasing temperature are made from semiconducting materials.

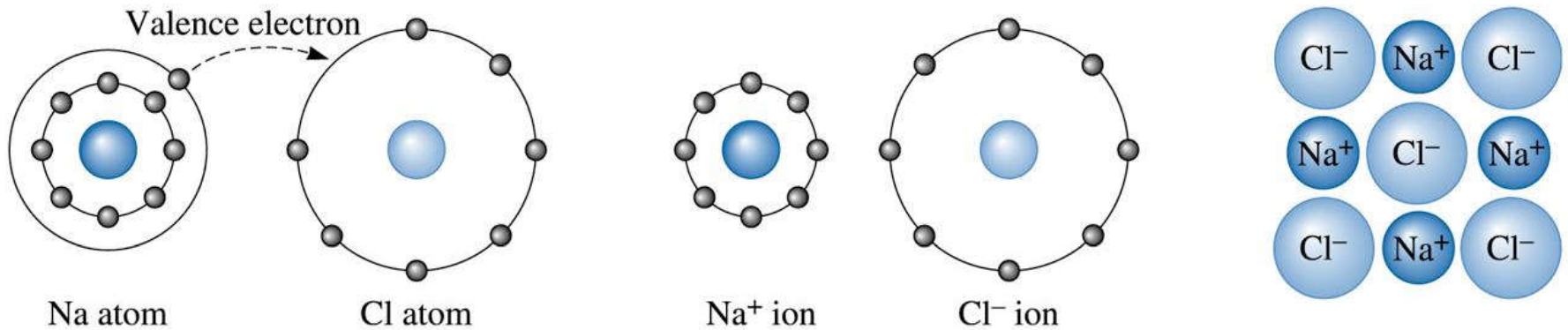




Example 2.7 SOLUTION (Continued)

Polymers would *not* be suitable, even though the major bonding is covalent, because of their relatively low melting, or decomposition, temperatures. Many thermistors that can be used for switching applications make use of barium titanate (BaTiO_3) based formulations. Many useful *NTCR* materials are based on Fe_3O_4 - ZnCr_2O_4 , Fe_3O_4 - MgCr_2O_4 , or Mn_3O_4 , doped with Ni, Co, or Cu.[4]

In almost any design situation, once the technical performance criteria are met we should always pay attention to and take into account the cost of raw materials, manufacturing costs, and other important factors such as the durability. In some applications, we also need to pay closer attention to the environmental impact including the ability to recycle materials.



© 2003 Brooks/Cole Publishing / Thomson Learning™

Figure 2.18 An ionic bond is created between two unlike atoms with different electronegativities. When sodium donates its valence electron to chlorine, each becomes an ion; attraction occurs, and the ionic bond is formed

Example 2.8

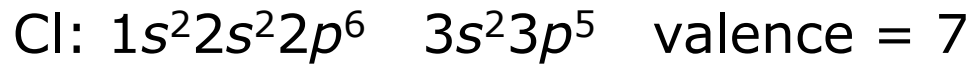


Describing the Ionic Bond Between Magnesium and Chlorine

Describe the ionic bonding between magnesium and chlorine.

Example 2.8 SOLUTION

The electronic structures and valences are:



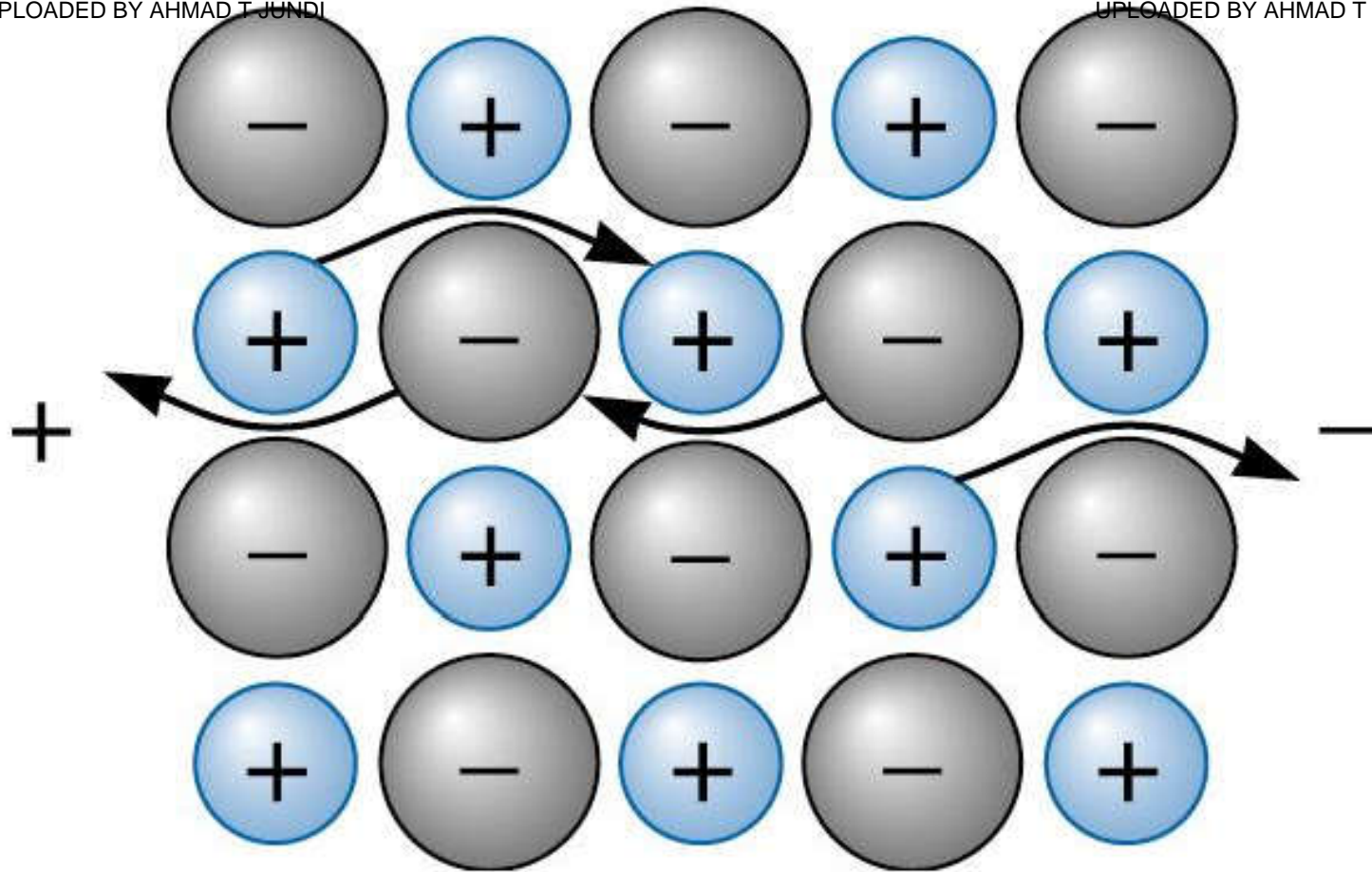
Each magnesium atom gives up its two valence electrons, becoming a Mg^{2+} ion. Each chlorine atom accepts one electron, becoming a Cl^- ion. To satisfy the ionic bonding, there must be twice as many chloride ions as magnesium ions present, and a compound, $MgCl_2$, is formed.





Example 2.8 SOLUTION (Continued)

Solids that exhibit considerable ionic bonding are also often mechanically strong because of the strength of the bonds. Electrical conductivity of ionically bonded solids is very limited. A large fraction of the electrical current is transferred via the movement of ions (Figure 2-19). Owing to their size, ions typically do not move as easily as electrons. However, in many technological applications we make use of the electrical conduction that can occur via movement of ions as a result of increased temperature, chemical potential gradient, or an electrochemical driving force. Examples of these include, lithium ion batteries that make use of lithium cobalt oxide, conductive indium tin oxide coatings on glass for touch sensitive screens for displays, and solid oxide fuel cells based on compositions based on zirconia (ZrO_2).



© 2003 Brooks/Cole Publishing / Thomson Learning™

Figure 2.19 When voltage is applied to an ionic material, entire ions must move to cause a current to flow. Ion movement is slow and the electrical conductivity is poor (for Example 2-8)

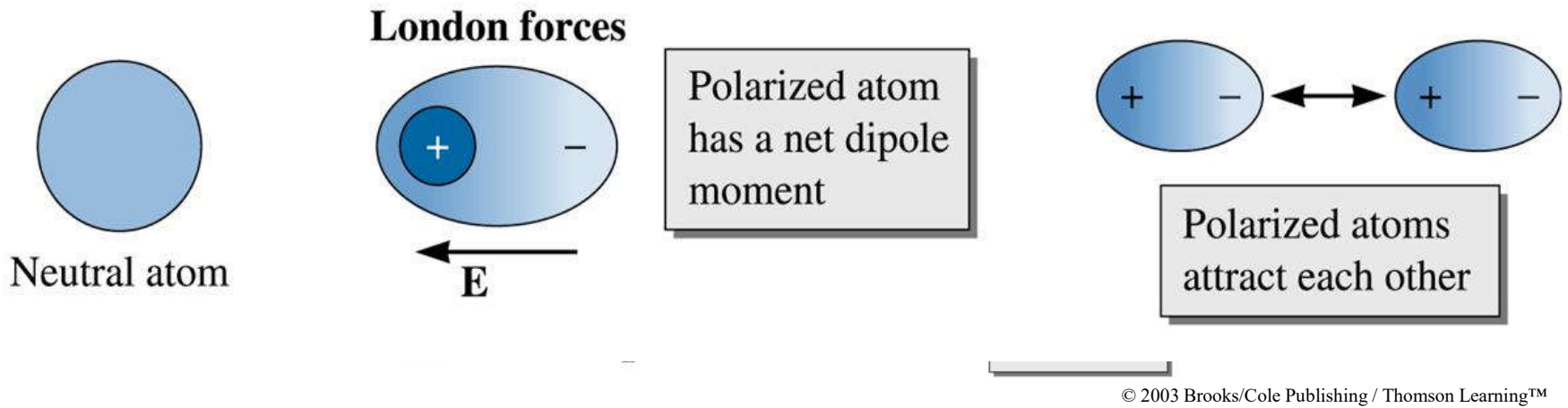
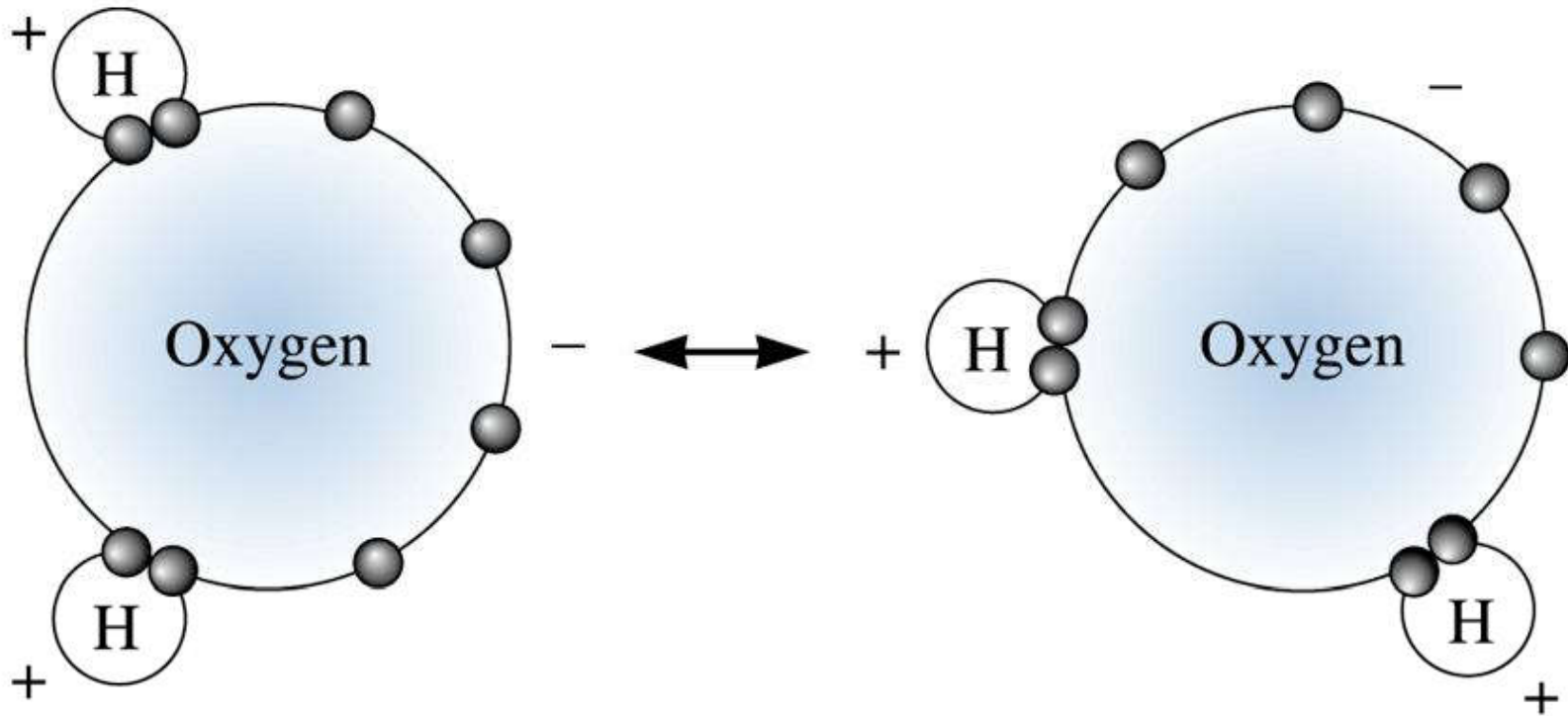


Figure 2.20 Illustration of London forces, a type of a van der Waals force, between atoms



© 2003 Brooks/Cole Publishing / Thomson Learning™

Figure 2.21 The Keesom interactions are formed as a result of polarization of molecules or groups of atoms. In water, electrons in the oxygen tend to concentrate away from the hydrogen. The resulting charge difference permits the molecule to be weakly bonded to other water molecules

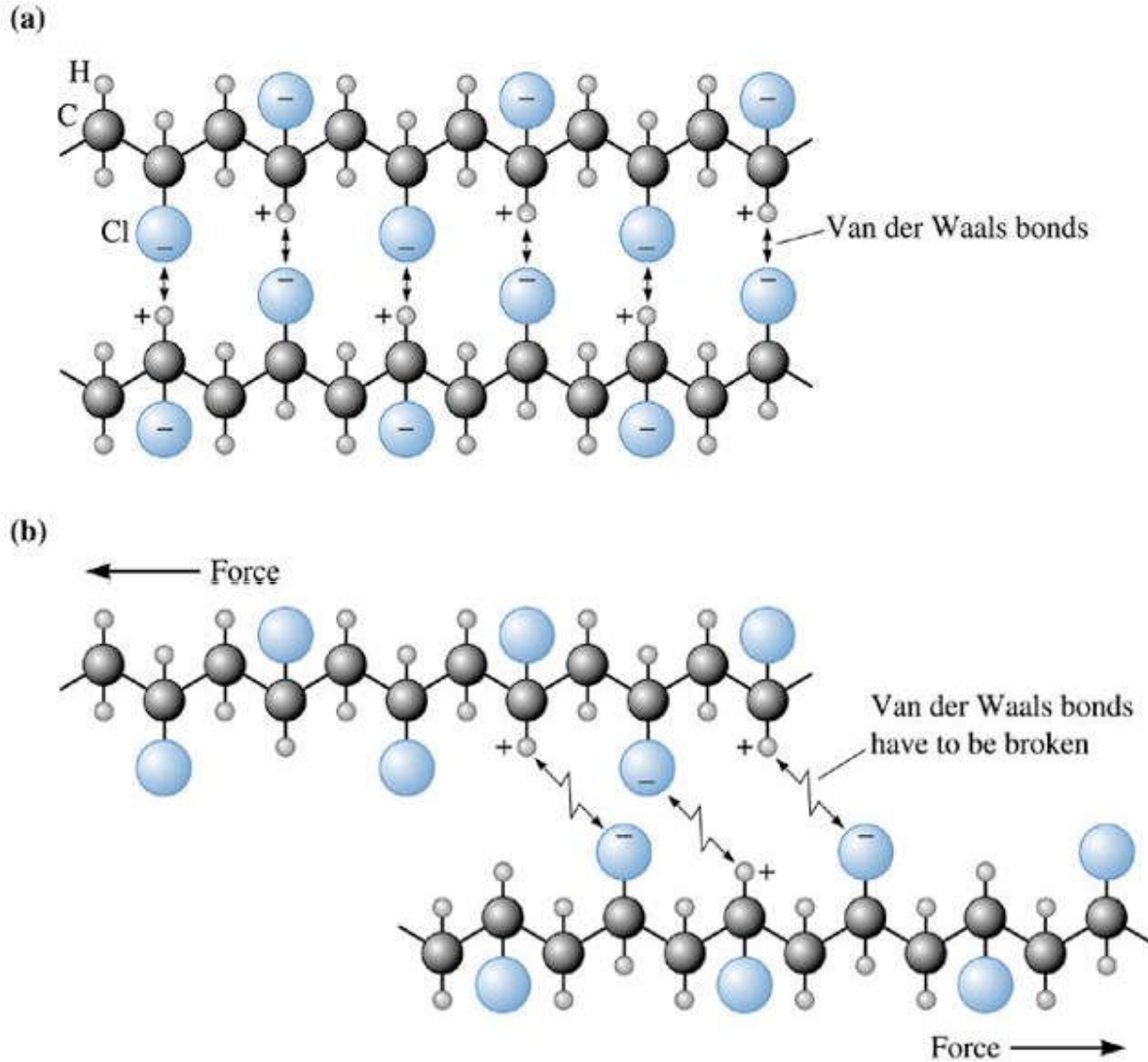


Figure 2.22 (a) In polyvinyl chloride (PVC), the chlorine atoms attached to the polymer chain have a negative charge and the hydrogen atoms are positively charged. The chains are weakly bonded by van der Waals bonds. This additional bonding makes PVC stiffer, (b) When a force is applied to the polymer, the van der Waals bonds are broken and the chains slide past one another

Example 2.9



Determine if Silica is Ionically or Covalently Bonded

In a previous example, we used silica (SiO_2) as an example of a covalently bonded material. In reality, silica exhibits ionic and covalent bonding. What fraction of the bonding is covalent? Give examples of applications in which silica is used.

Example 2.9 SOLUTION

From Figure 2-10, we estimate the electronegativity of silicon to be 1.8 and that of oxygen to be 3.5. The fraction of the bonding that is covalent is:

$$\text{Fraction covalent} = \exp[-0.25(3.5 - 1.8)^2] = \exp(-0.72) = 0.486$$

Although the covalent bonding represents only about half of the bonding, the directional nature of these bonds still plays an important role in the eventual structure of SiO_2 .





Example 2.9 SOLUTION (Continued)

Silica has many applications. Silica is used for making glasses and optical fibers. We add nano-sized particles of silica to tires to enhance the stiffness of the rubber. High-purity silicon (Si) crystals are made by reducing silica to silicon.





Example 2.10

Design Strategies for Silica Optical Fibers

Silica is used for making long lengths of optical fibers (Figure 2-4). Being a covalently and ionically bonded material, the strength of Si-O bonds is expected to be high. Other factors such as susceptibility of silica surfaces to react with water vapor in atmosphere have a deleterious effect on the strength of silica fibers. Given this, what design strategies can you think of such that silica fibers could still be bent to a considerable degree without breaking?



Example 2.10 SOLUTION

Based on the mixed ionic and covalent bonding in silica we know that the Si-O bonds are very strong. We also know that covalent bonds will be directional and hence we can anticipate silica to exhibit limited ductility. Therefore, our choices to enhance ductility of optical fibers are rather limited since the composition is essentially fixed. Most other glasses are also brittle. We can make an argument that silica fibers will exhibit better ductility at higher temperatures. However, we have to use them for making long lengths of optical fibers (most of which are to be buried underground or under the sea) and hence keeping them at an elevated temperature is not a practical option.





Example 2.10 SOLUTION (Continued)

Therefore, we need to understand, beyond what the nature of bonding consideration can offer us, why glass fibers exhibit limited ductility. Is this a property that is intrinsic to the glass or are there external variables that are causing a change in the chemistry and structure of the glass? Materials scientists and engineers have recognized that the lack of ductility in optical glass fibers is linked to the ability of the silica surface to react with water vapor in the atmosphere. They have found that water vapor in the atmosphere reacts with the surface of silica leading to micro-cracks on the surface. When subjected to stress these cracks grow rapidly and the fibers break quite easily! They have also tested silica fibers in a vacuum and found that the levels to which one can bend fibers are much higher.





Section 2.6 Binding Energy and Interatomic Spacing

- **Interatomic spacing** is the equilibrium spacing between the centers of two atoms.
- **Binding energy** is the energy required to separate two atoms from their equilibrium spacing to an infinite distance apart.
- **Modulus of elasticity** is the slope of the stress-strain curve in the elastic region (E).
- **Yield strength** is the level of stress above which a material begins to show permanent deformation.
- **Coefficient of thermal expansion (CTE)** is the amount by which a material changes its dimensions when the temperature changes.

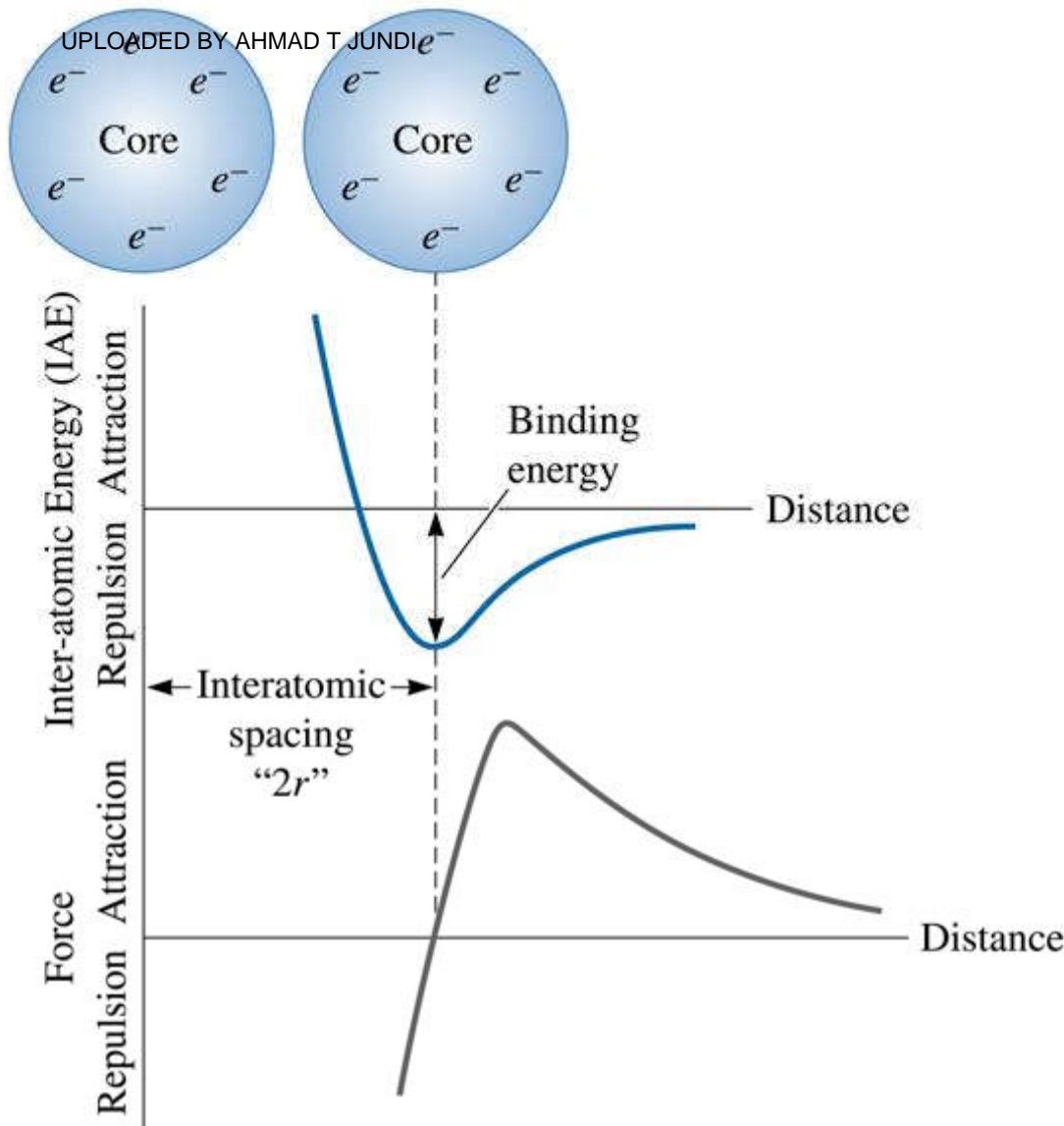


Figure 2.23 Atoms or ions are separated by and equilibrium spacing that corresponds to the minimum inter-atomic energy for a pair of atoms or ions (or when zero force is acting to repel or attract the atoms or ions)

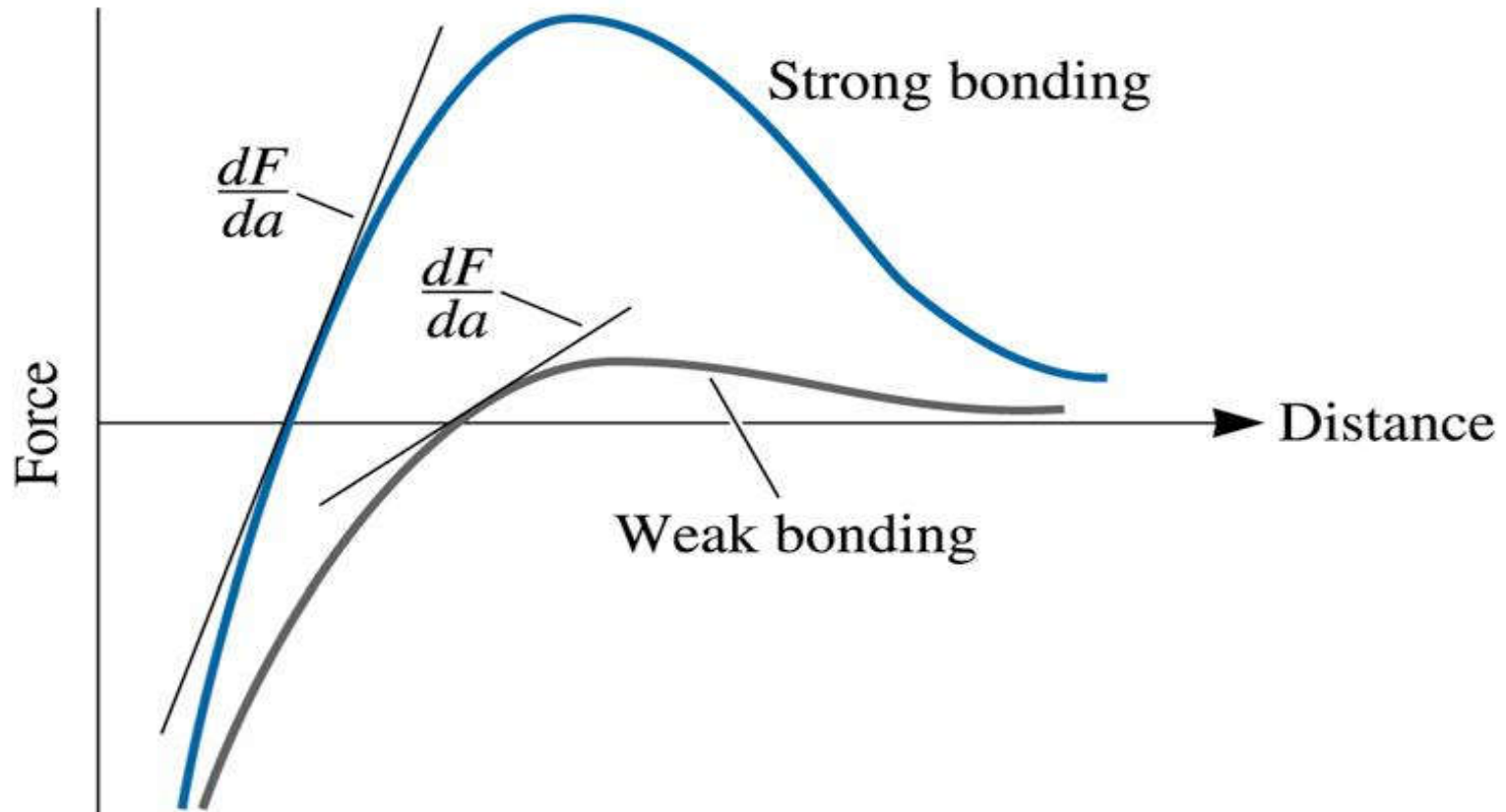




TABLE 2-3 ■ *Binding energies for the four bonding mechanisms*

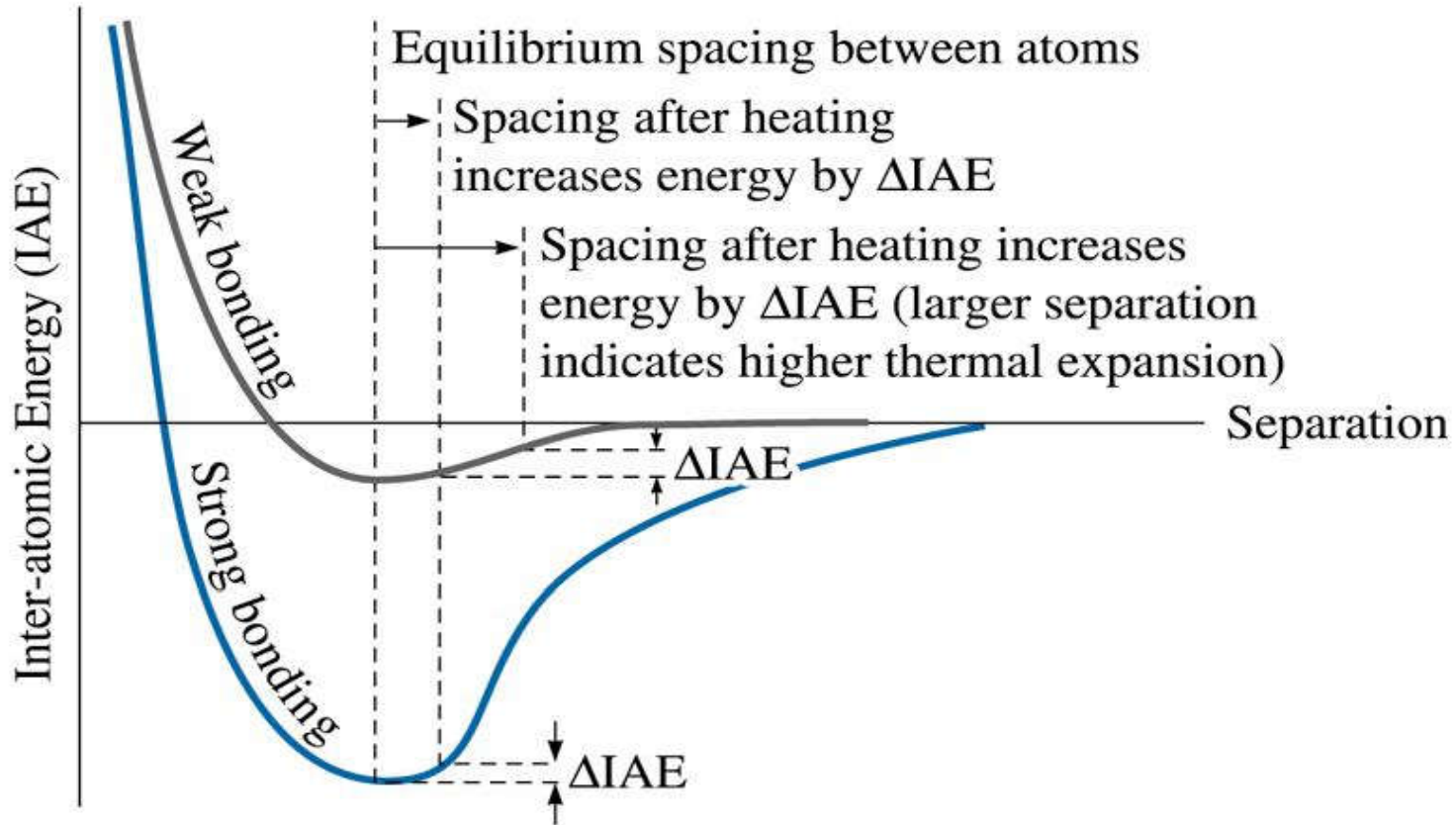
Bond	Binding Energy (kcal/mol)
Ionic	150–370
Covalent	125–300
Metallic	25–200
Van der Waals	<10





© 2003 Brooks/Cole Publishing / Thomson Learning™

Figure 2.24 The force-distance curve for two materials, showing the relationship between atomic bonding and the modulus of elasticity, a steep dF/da slope gives a high modulus



© 2003 Brooks/Cole Publishing / Thomson Learning™

Figure 2.25 The inter-atomic energy (IAE)-separation curve for two atoms. Materials that display a steep curve with a deep trough have low linear coefficients of thermal expansion



Example 2.11

Design of a Space Shuttle Arm

NASA's space shuttles have a long manipulator robot arm, also known as the Shuttle Remote Manipulator System or SRMS (Figure 2-26), that permits astronauts to launch and retrieve satellites. It is also used to view and monitor the outside of the space shuttle using a mounted video camera. Select a suitable material for this device.

Figure 2.26 NASA's Shuttle Remote Manipulator System: SRMS (for Example 2.11). Courtesy of Getty Images)





Example 2.11 SOLUTION

Let's look at two of the many material choices. First, the material should be stiff so that little bending occurs when a load is applied; this feature helps the operator maneuver the manipulator arm precisely. Generally, materials with strong bonding and high melting points also have a high modulus of elasticity, or stiffness. Second, the material should be light in weight to permit maximum payloads to be carried into orbit; a low density is thus desired. It is estimated that it costs about US \$100,000 to take the weight of a beverage can into space! Thus, the density must be as low as possible.



Example 2.11 SOLUTION (Continued)

Good stiffness is obtained from high-melting-point metals (such as beryllium and tungsten), from ceramics, and from certain fibers (such as carbon). Tungsten, however, has a very high density, while ceramics are very brittle. Beryllium, which has a modulus of elasticity that is greater than that of steel and a density that is less than that of aluminum, might be an excellent candidate. However, toxicity of Be and its compounds must be considered. The preferred material is a composite consisting of carbon fibers embedded in an epoxy matrix. The carbon fibers have an exceptionally high modulus of elasticity, while the combination of carbon and epoxy provides a very low-density material. Other factors such as exposure to low and high temperatures in space and on earth must also be considered. The current shuttle robot arm is about 45 feet long, 15 inches in diameter and weighs about 900 pounds. When in space it can manipulate weights up to 260 tons.



UPLOADED BY AHMAD JUNDI

The Science and Engineering of Materials, 4th ed

Donald R. Askeland – Pradeep P. Phulé

Chapter 3 – Atomic and Ionic Arrangements





Objectives of Chapter 3

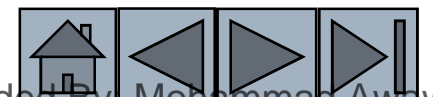
- ❑ To learn classification of materials based on atomic/ionic arrangements
- ❑ To describe the arrangements in crystalline solids based on lattice, basis, and crystal structure



Chapter Outline



- 3.1 Short-Range Order versus Long-Range Order
- 3.2 Amorphous Materials: Principles and Technological Applications
- 3.3 Lattice, Unit Cells, Basis, and Crystal Structures
- 3.4 Allotropic or Polymorphic Transformations
- 3.5 Points, Directions, and Planes in the Unit Cell
- 3.6 Interstitial Sites
- 3.7 Crystal Structures of Ionic Materials
- 3.8 Covalent Structures



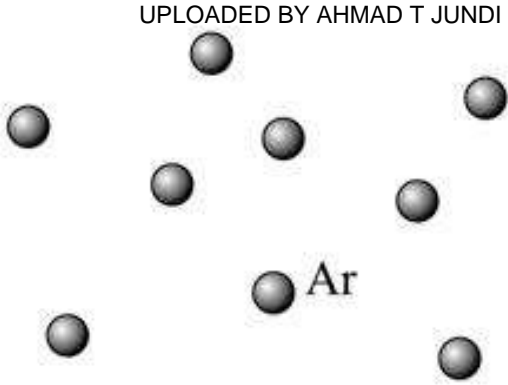


Section 3.1

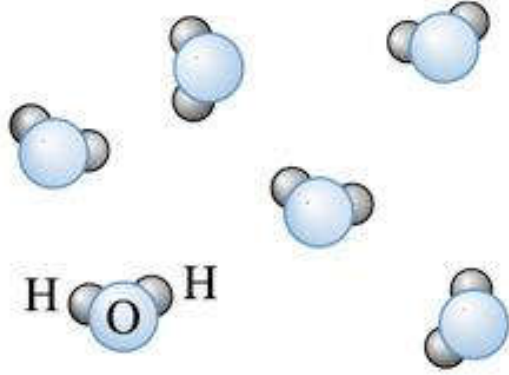
Short-Range Order versus Long-Range Order

- **Short-range order** - The regular and predictable arrangement of the atoms over a short distance - usually one or two atom spacings.
- **Long-range order (LRO)** - A regular repetitive arrangement of atoms in a solid which extends over a very large distance.
- **Bose-Einstein condensate (BEC)** - A newly experimentally verified state of a matter in which a group of atoms occupy the same quantum ground state.

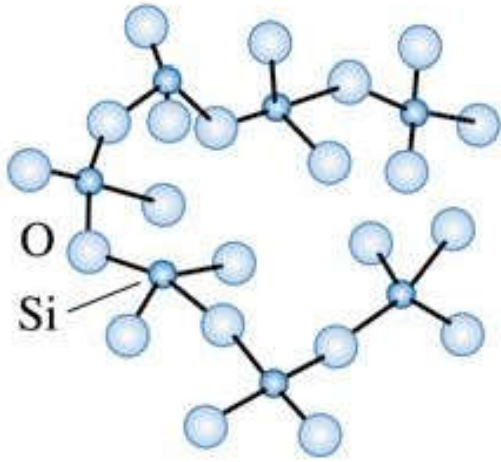




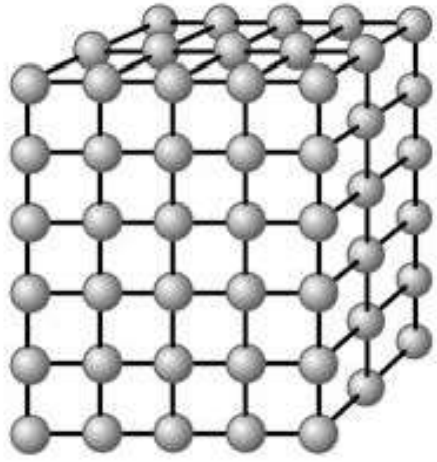
(a)



(b)



(c)



(d)

Figure 3.1 Levels of atomic arrangements in materials: (a) Inert monoatomic gases have no regular ordering of atoms: (b,c) Some materials, including water vapor, nitrogen gas, amorphous silicon and silicate glass have short-range order. (d) Metals, alloys, many ceramics and some polymers have regular ordering of atoms/ions that extends through the material.

(c) 2003 Brooks/Cole Publishing / Thomson Learning™

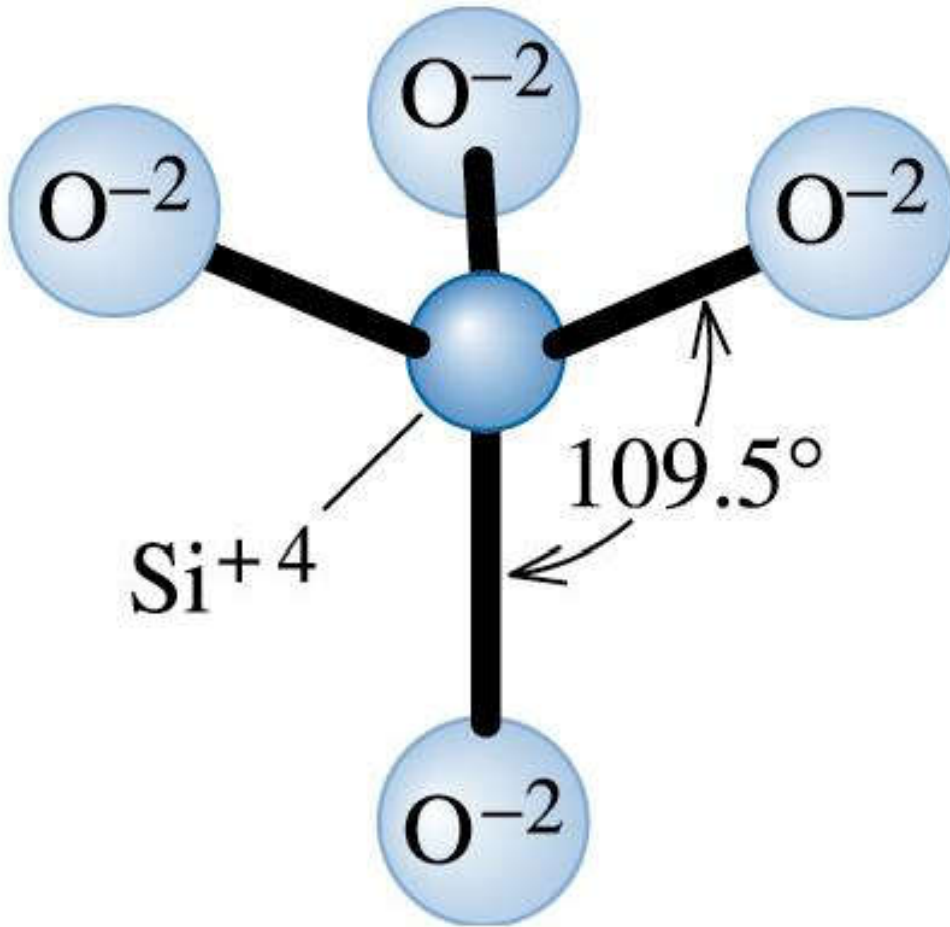


Figure 3.2 Basic *Si-O* tetrahedron in silicate glass.

(c) 2003 Brooks/Cole Publishing / Thomson Learning™



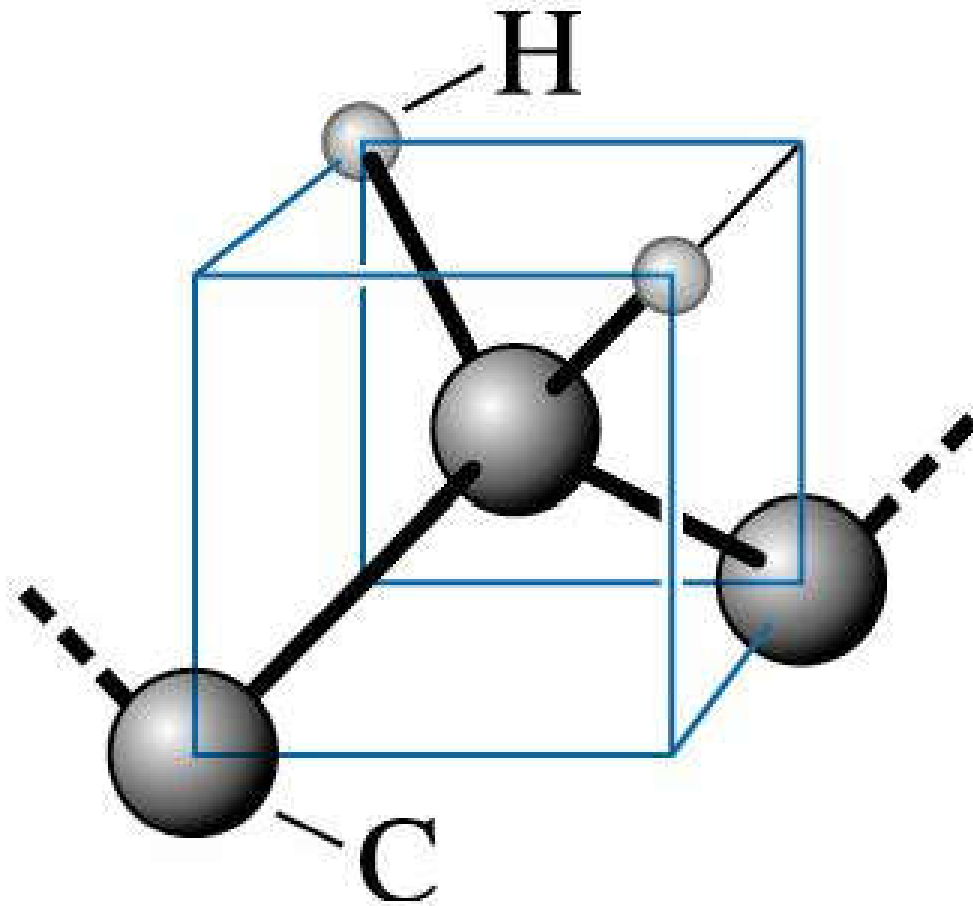
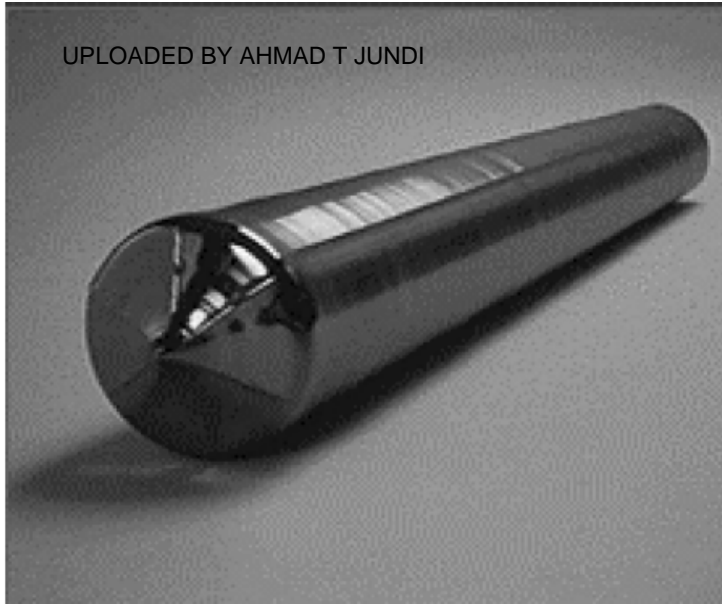


Figure 3.3 Tetrahedral arrangement of *C-H* bonds in polyethylene.

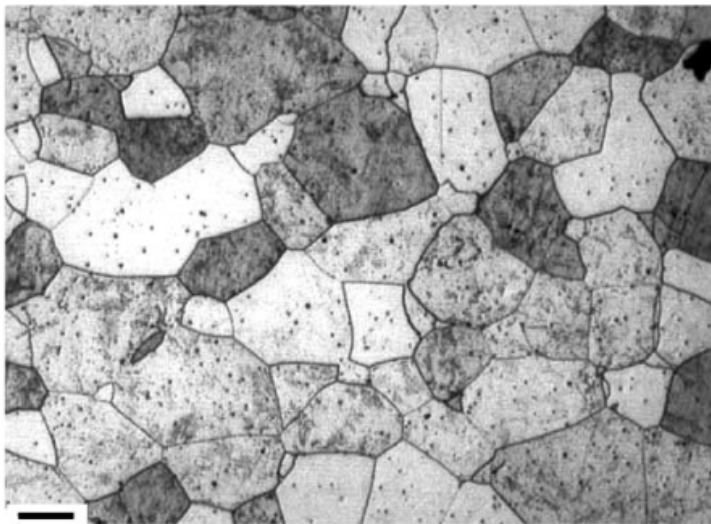
(c) 2003 Brooks/Cole Publishing / Thomson Learning™





(a)

Figure 3.4 (a) Photograph of a silicon single crystal. (b) Micrograph of a polycrystalline stainless steel showing grains and grain boundaries (Courtesy Dr. M. Hua, Dr. I. Garcia, and Dr. A.J. Deardo.)



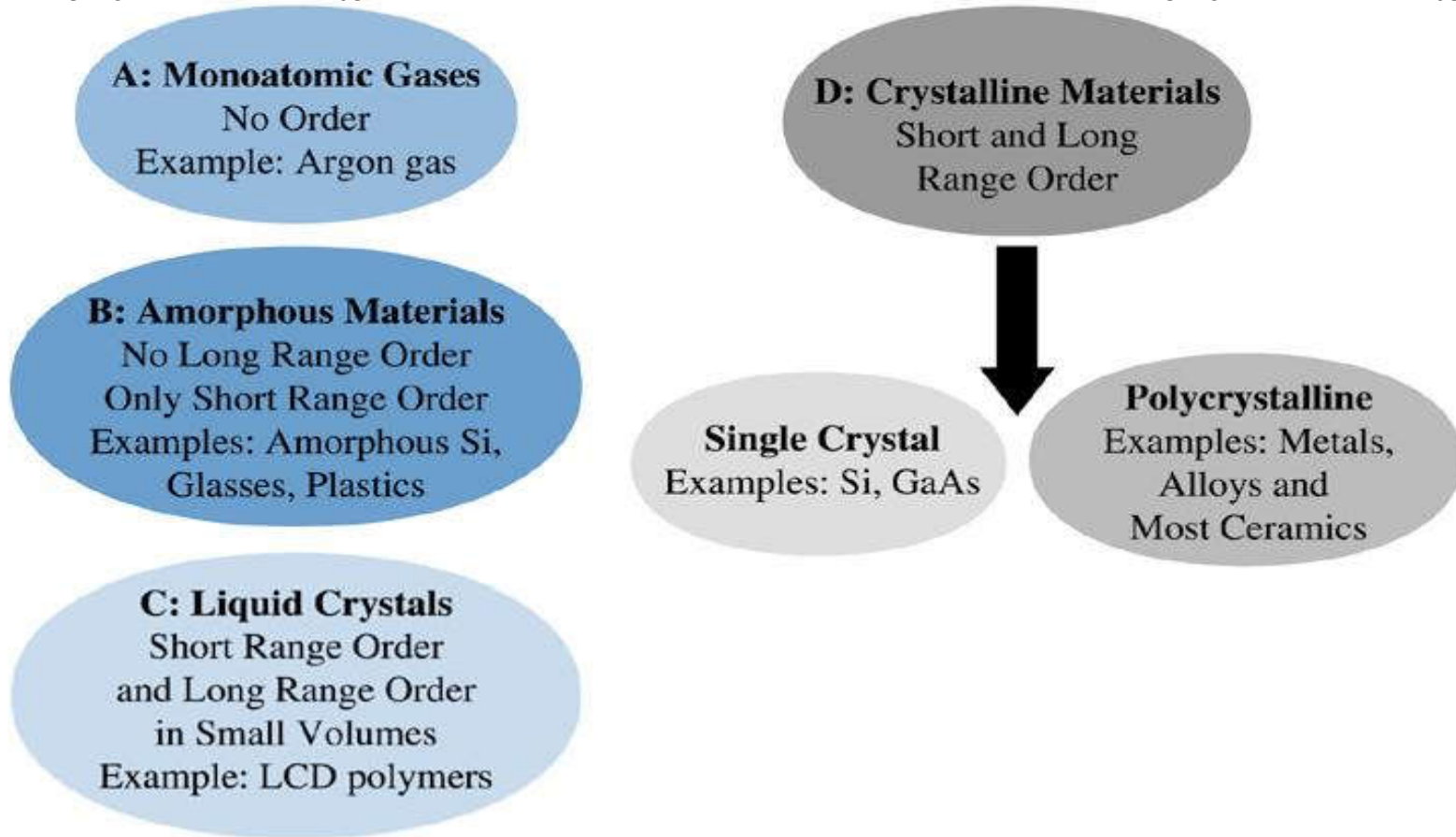
(b)





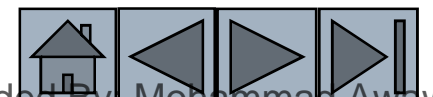
Figure 3.5 Liquid crystal display. These materials are amorphous in one state and undergo localized crystallization in response to an external electric field and are widely used in liquid crystal displays. (Courtesy of Nick Koudis/PhotoDisc/Getty Images.)





(c) 2003 Brooks/Cole Publishing / Thomson Learning™

Figure 3.7 Classification of materials based on the type of atomic order.



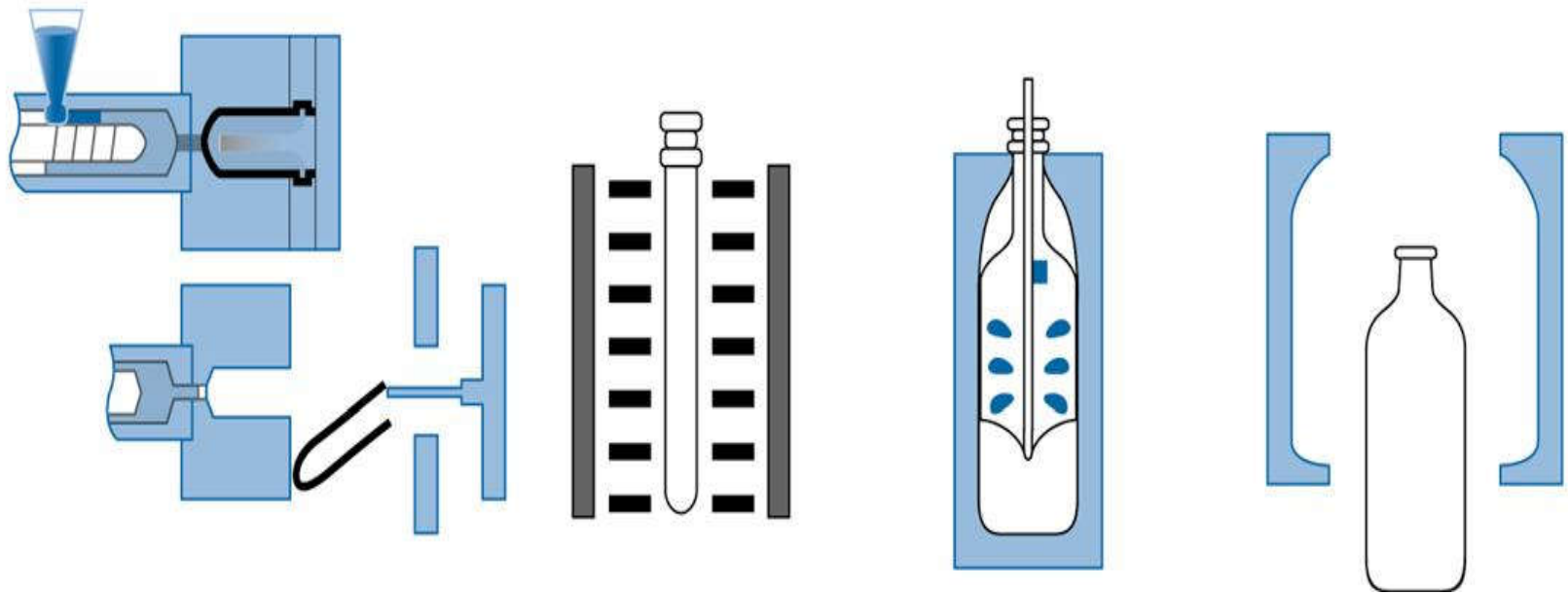


Section 3.2

Amorphous Materials: Principles and Technological Applications

- **Amorphous materials** - Materials, including glasses, that have no long-range order, or crystal structure.
- **Glasses** - Solid, non-crystalline materials (typically derived from the molten state) that have only short-range atomic order.
- **Glass-ceramics** - A family of materials typically derived from molten inorganic glasses and processed into crystalline materials with very fine grain size and improved mechanical properties.

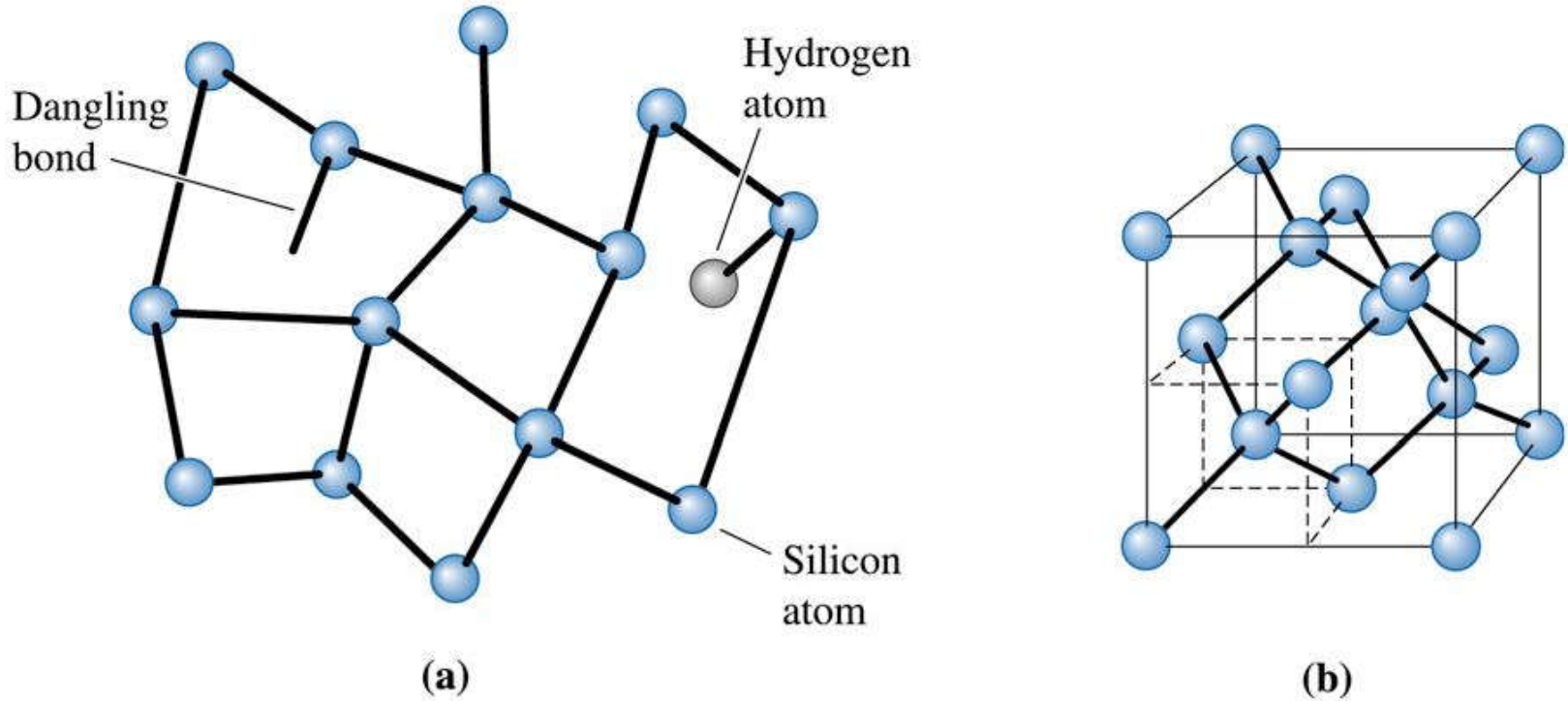




(c) 2003 Brooks/Cole Publishing / Thomson Learning™

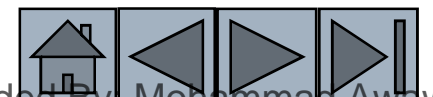
Figure 3.9 (b) This figure shows a schematic of the blow-stretch process used for fabrication of a standard two-liter PET (polyethylene terephthalate) bottle from a preform. The stress induced crystallization leads to formation of small crystals that help reinforce the remaining amorphous matrix.





(c) 2003 Brooks/Cole Publishing / Thomson Learning™

Figure 3.10 Atomic arrangements in crystalline silicon and amorphous silicon. (a) Amorphous silicon. (b) Crystalline silicon. Note the variation in the inter-atomic distance for amorphous silicon.



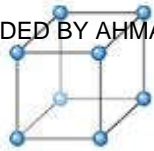


Section 3.3

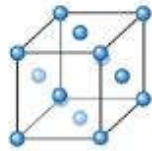
Lattice, Unit Cells, Basis, and Crystal Structures

- **Lattice** - A collection of points that divide space into smaller equally sized segments.
- **Basis** - A group of atoms associated with a lattice point.
- **Unit cell** - A subdivision of the lattice that still retains the overall characteristics of the entire lattice.
- **Atomic radius** - The apparent radius of an atom, typically calculated from the dimensions of the unit cell, using close-packed directions (depends upon coordination number).
- **Packing factor** - The fraction of space in a unit cell occupied by atoms.

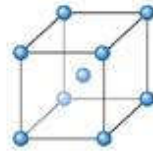




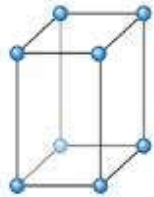
Simple cubic



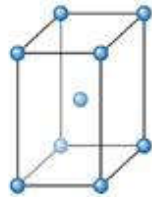
Face-centered cubic



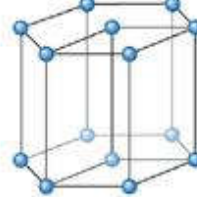
Body-centered cubic



Simple tetragonal

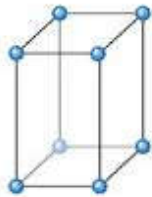


Body-centered tetragonal

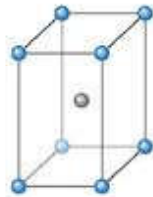


Hexagonal

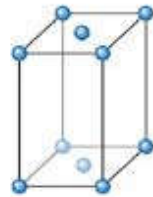
Figure 3.11 The fourteen types of Bravais lattices grouped in seven crystal systems. The actual unit cell for a hexagonal system is shown in Figures 3.12 and 3.16.



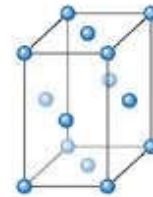
Simple orthorhombic



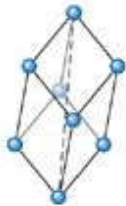
Body-centered orthorhombic



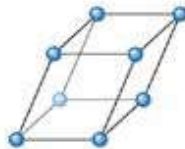
Base-centered orthorhombic



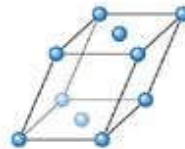
Face-centered orthorhombic



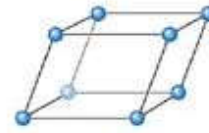
Rhombohedral



Simple monoclinic



Base-centered monoclinic



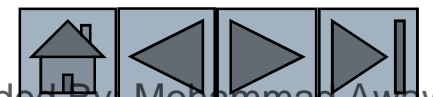
Triclinic





TABLE 3-1 ■ Characteristics of the seven crystal systems

Structure	Axes	Angles between Axes	Volume of the Unit Cell
Cubic	$a = b = c$	All angles equal 90°	a^3
Tetragonal	$a = b \neq c$	All angles equal 90°	a^2c
Orthorhombic	$a \neq b \neq c$	All angles equal 90°	abc
Hexagonal	$a = b \neq c$	Two angles equal 90° . One angle equals 120° .	$0.866a^2c$
Rhombohedral or trigonal	$a = b = c$	All angles are equal and none equals 90°	$a^3\sqrt{1 - 3 \cos^2 \alpha + 2 \cos^3 \alpha}$
Monoclinic	$a \neq b \neq c$	Two angles equal 90° . One angle (β) is not equal to 90°	$abc \sin \beta$
Triclinic	$a \neq b \neq c$	All angles are different and none equals 90°	$abc\sqrt{1 - \cos^2 \alpha - \cos^2 \beta - \cos^2 \gamma + 2 \cos \alpha \cos \beta \cos \gamma}$



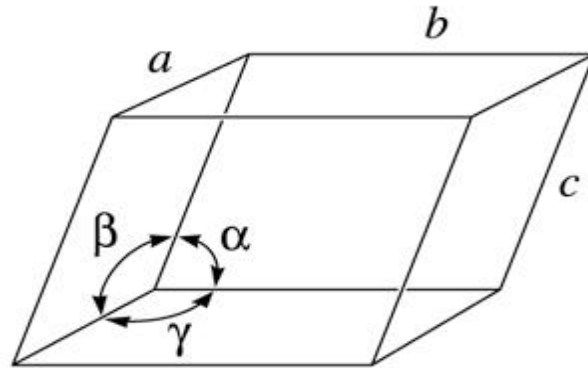
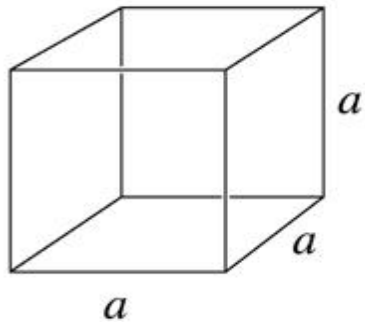
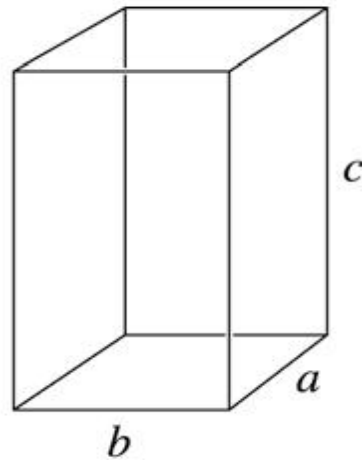


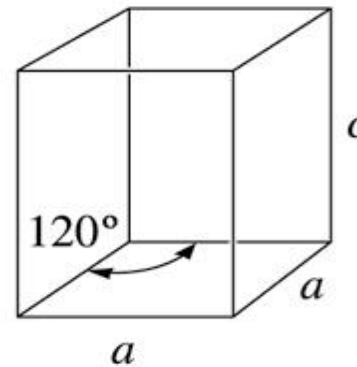
Figure 3.12
Definition of
the lattice
parameters and
their use in
cubic,
orthorhombic,
and hexagonal
crystal systems.



Cubic



Orthorhombic

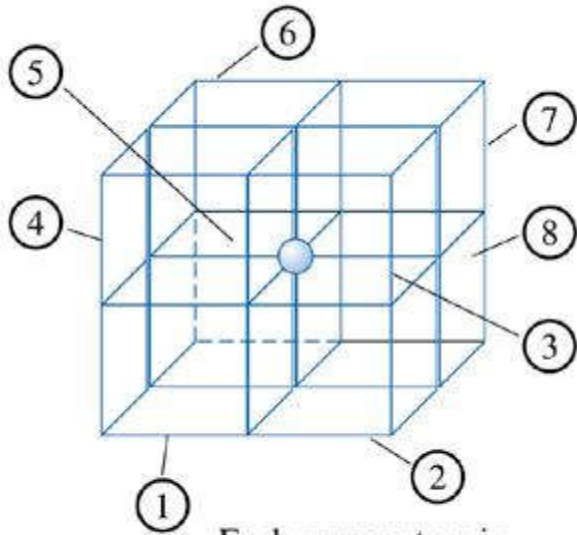
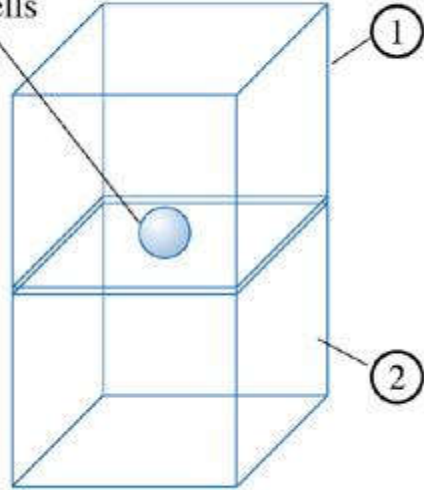


Hexagonal

(c) 2003 Brooks/Cole Publishing / Thomson Learning™

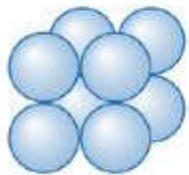


UPLOADED BY AHMAD T JUNDI
 Face centered atom shared between two unit cells

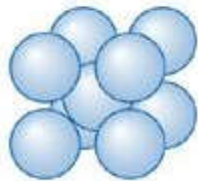


Each corner atom is shared by 8 unit cells (1-4 in front, 5-8 in back)

(a)

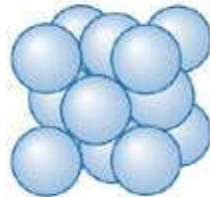


Simple cubic



Body-centered cubic

(b)



Face-centered cubic



UPLOADED BY AHMAD T JUNDI

Figure 3.13 (a) Illustration showing sharing of face and corner atoms. (b) The models for simple cubic (SC), body centered cubic (BCC), and face-centered cubic (FCC) unit cells, assuming only one atom per lattice point.





Determining the Number of Lattice Points in Cubic Crystal Systems

Determine the number of lattice points per cell in the cubic crystal systems. If there is only one atom located at each lattice point, calculate the number of atoms per unit cell.

Example 3.1 SOLUTION

In the SC unit cell: lattice point / unit cell = (8 corners) $1/8$ = 1

In BCC unit cells: lattice point / unit cell
= (8 corners) $1/8$ + (1 center)(1) = 2

In FCC unit cells: lattice point / unit cell
= (8 corners) $1/8$ + (6 faces)($1/2$) = 4

The number of atoms per unit cell would be 1, 2, and 4, for the simple cubic, body-centered cubic, and face-centered cubic, unit cells, respectively.

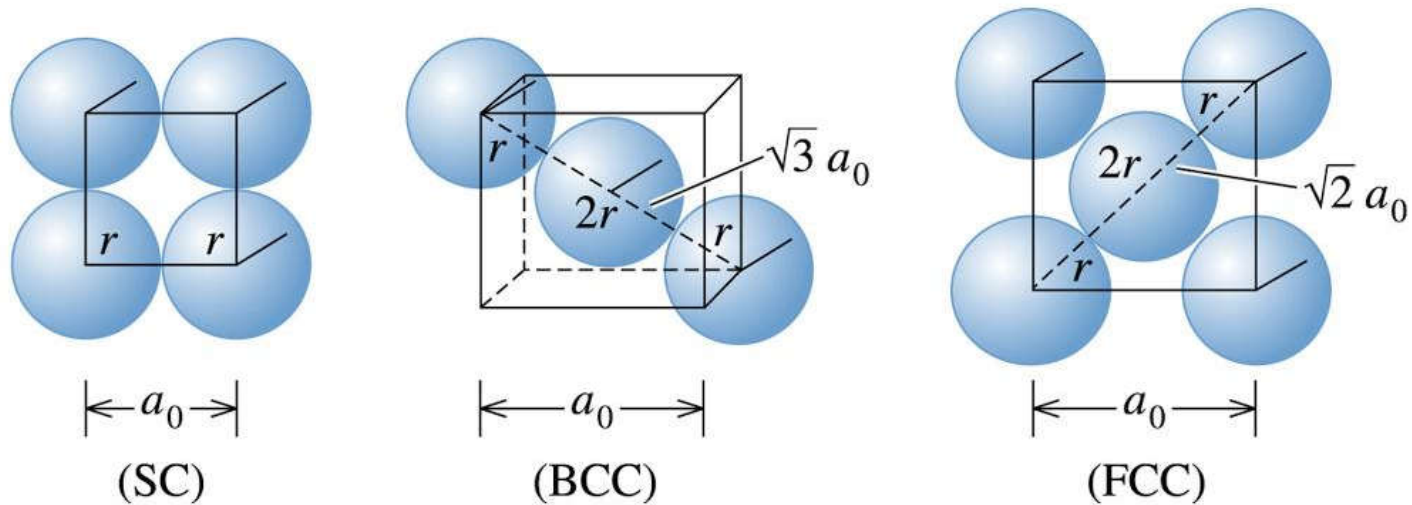




Example 3.2

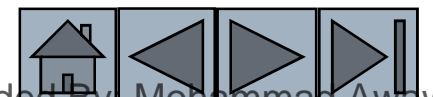
Determining the Relationship between Atomic Radius and Lattice Parameters

Determine the relationship between the atomic radius and the lattice parameter in SC, BCC, and FCC structures when one atom is located at each lattice point.



(c) 2003 Brooks/Cole Publishing / Thomson Learning™

Figure 3.14 The relationships between the atomic radius and the Lattice parameter in cubic systems (for Example 3.2).





Referring to Figure 3.14, we find that atoms touch along the edge of the cube in **SC structures**.

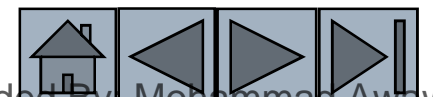
$$a_0 = 2r$$

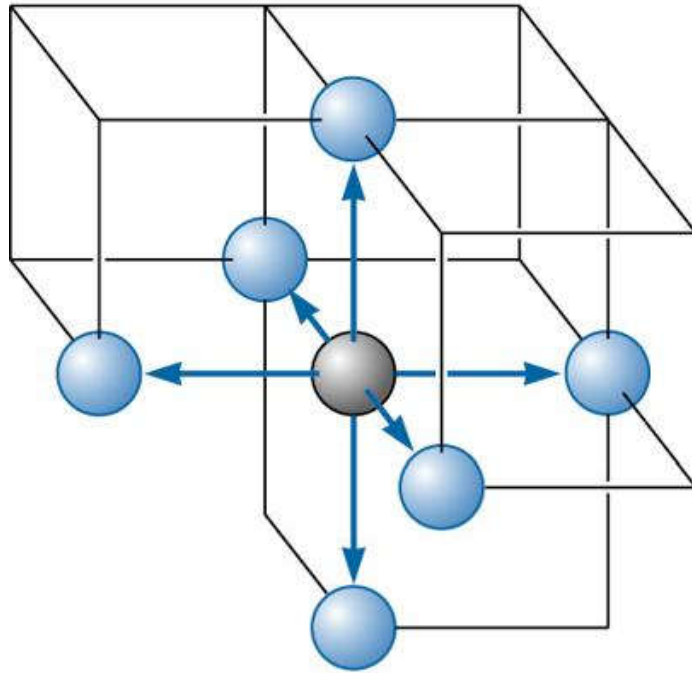
In **BCC structures**, atoms touch along the body diagonal. There are two atomic radii from the center atom and one atomic radius from each of the corner atoms on the body diagonal, so

$$a_0 = \frac{4r}{\sqrt{3}}$$

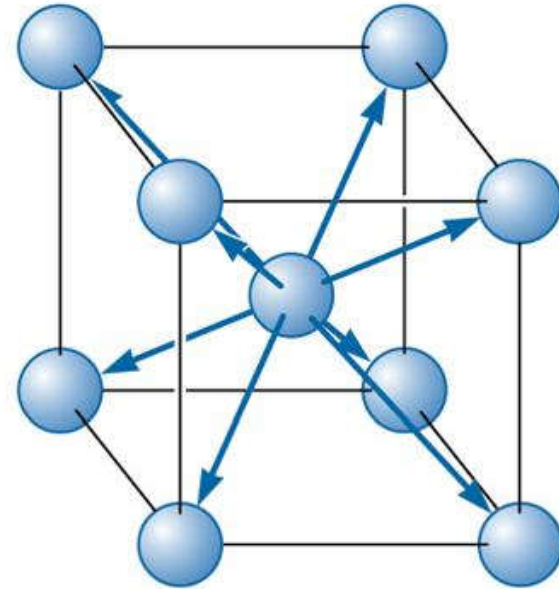
In **FCC structures**, atoms touch along the face diagonal of the cube. There are four atomic radii along this length—two radii from the face-centered atom and one radius from each corner, so:

$$a_0 = \frac{4r}{\sqrt{2}}$$





(a)



(b)

(c) 2003 Brooks/Cole Publishing / Thomson Learning™

Figure 3.15 Illustration of coordinations in (a) SC and (b) BCC unit cells. Six atoms touch each atom in SC, while the eight atoms touch each atom in the BCC unit cell.





Example 3.3

Calculating the Packing Factor

Calculate the packing factor for the FCC cell.

Example 3.3 SOLUTION

In a FCC cell, there are four lattice points per cell; if there is one atom per lattice point, there are also four atoms per cell. The volume of one atom is $\frac{4\pi r^3}{3}$ and the volume of the unit cell is a_0^3 .

$$\text{Packing Factor} = \frac{(4 \text{ atoms/cell})\left(\frac{4}{3} \pi r^3\right)}{a_0^3}$$

Since, for FCC unit cells, $a_0 = 4r/\sqrt{2}$

$$\text{Packing Factor} = \frac{(4)\left(\frac{4}{3} \pi r^3\right)}{\left(4r / \sqrt{2}\right)^3} = \frac{\pi}{\sqrt{18}} \cong 0.74$$





Determining the Density of BCC Iron

Determine the density of BCC iron, which has a lattice parameter of 0.2866 nm.

Example 3.4 SOLUTION

$$\text{Atoms/cell} = 2, a_0 = 0.2866 \text{ nm} = 2.866 \times 10^{-8} \text{ cm}$$

$$\text{Atomic mass} = 55.847 \text{ g/mol}$$

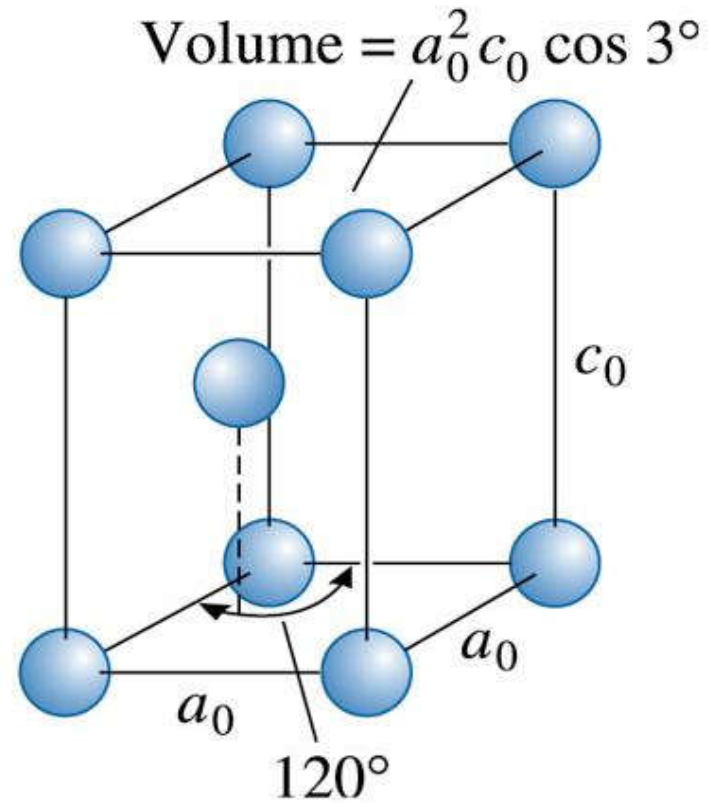
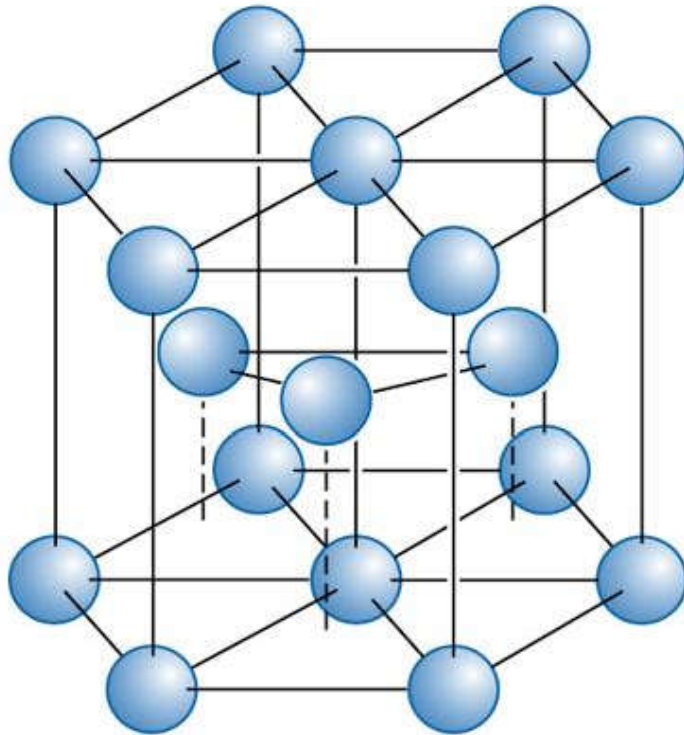
$$\text{Volume of unit cell} = a_0^3 = (2.866 \times 10^{-8} \text{ cm})^3 = 23.54 \times 10^{-24} \text{ cm}^3/\text{cell}$$

$$\text{Avogadro's number } N_A = 6.02 \times 10^{23} \text{ atoms/mol}$$

$$\text{Density } \rho = \frac{(\text{number of atoms/cell})(\text{atomic mass of iron})}{(\text{volume of unit cell})(\text{Avogadro's number})}$$

$$\rho = \frac{(2)(55.847)}{(23.54 \times 10^{-24})(6.02 \times 10^{23})} = 7.882 \text{ g / cm}^3$$





(c) 2003 Brooks/Cole Publishing / Thomson Learning™

Figure 3.16 The hexagonal close-packed (HCP) structure (left) and its unit cell.

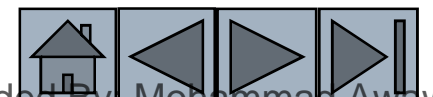




TABLE 3-2 ■ *Crystal structure characteristics of some metals*

Structure	a_0 versus r	Atoms per Cell	Coordination Number	Packing Factor	Examples
Simple cubic (SC)	$a_0 = 2r$	1	6	0.52	Polonium (Po), α -Mn
Body-centered cubic	$a_0 = 4r/\sqrt{3}$	2	8	0.68	Fe, Ti, W, Mo, Nb, Ta, K, Na, V, Zr, Cr
Face-centered cubic	$a_0 = 4r/\sqrt{2}$	4	12	0.74	Fe, Cu, Au, Pt, Ag, Pb, Ni
Hexagonal close-packed	$a_0 = 2r$ $c_0 \approx 1.633a_0$	2	12	0.74	Ti, Mg, Zn, Be, Co, Zr, Cd





Section 3.4

Allotropic or Polymorphic Transformations

- **Allotropy** - The characteristic of an element being able to exist in more than one crystal structure, depending on temperature and pressure.
- **Polymorphism** - Compounds exhibiting more than one type of crystal structure.





Figure 3.17 Oxygen gas sensors used in cars and other applications are based on stabilized zirconia compositions. (*Image courtesy of Bosch © Robert Bosch GmbH.*)





Example 3.5

Calculating Volume Changes in Polymorphs of Zirconia

Calculate the percent volume change as zirconia transforms from a tetragonal to monoclinic structure.[9] The lattice constants for the monoclinic unit cells are: $a = 5.156$, $b = 5.191$, and $c = 5.304 \text{ \AA}$, respectively. The angle β for the monoclinic unit cell is 98.9 . The lattice constants for the tetragonal unit cell are $a = 5.094$ and $c = 5.304 \text{ \AA}$, respectively.[10] Does the zirconia expand or contract during this transformation? What is the implication of this transformation on the mechanical properties of zirconia ceramics?



Example 3.5 SOLUTION

UPLOADED BY AHMAD T JUNDI

UPLOADED BY AHMAD T JUNDI



The volume of a tetragonal unit cell is given by
 $V = a^2c = (5.094)^2 (5.304) = 134.33 \text{ \AA}^3$.

The volume of a monoclinic unit cell is given by
 $V = abc \sin \beta = (5.156) (5.191) (5.304) \sin(98.9) = 140.25 \text{ \AA}^3$.

Thus, there is an expansion of the unit cell as ZrO_2 transforms from a tetragonal to monoclinic form.

The percent change in volume
 $= (\text{final volume} - \text{initial volume}) / (\text{initial volume}) \times 100$
 $= (140.25 - 134.33 \text{ \AA}^3) / 134.33 \text{ \AA}^3 \times 100 = 4.21\%$.

Most ceramics are very brittle and cannot withstand more than a 0.1% change in volume. The conclusion here is that ZrO_2 ceramics cannot be used in their monoclinic form since, when zirconia does transform to the tetragonal form, it will most likely fracture. Therefore, ZrO_2 is often stabilized in a cubic form using different additives such as CaO , MgO , and Y_2O_3 .





Example 3.6

Designing a Sensor to Measure Volume Change

To study how iron behaves at elevated temperatures, we would like to design an instrument that can detect (with a 1% accuracy) the change in volume of a 1-cm³ iron cube when the iron is heated through its polymorphic transformation temperature. At 911°C, iron is BCC, with a lattice parameter of 0.2863 nm. At 913°C, iron is FCC, with a lattice parameter of 0.3591 nm. Determine the accuracy required of the measuring instrument.

Example 3.6 SOLUTION

The volume of a unit cell of BCC iron before transforming is:

$$V_{BCC} = a_0^3 = (0.2863 \text{ nm})^3 = 0.023467 \text{ nm}^3$$





Example 3.6 SOLUTION (Continued)

The volume of the unit cell in FCC iron is:

$$V_{FCC} = a_0^3 = (0.3591 \text{ nm})^3 = 0.046307 \text{ nm}^3$$

But this is the volume occupied by *four* iron atoms, as there are four atoms per FCC unit cell. Therefore, we must compare two BCC cells (with a volume of $2(0.023467) = 0.046934 \text{ nm}^3$) with each FCC cell. The percent volume change during transformation is:

$$\text{Volume change} = \frac{(0.046307 - 0.046934)}{0.046934} \times 100 = -1.34\%$$

The 1-cm³ cube of iron contracts to $1 - 0.0134 = 0.9866 \text{ cm}^3$ after transforming; therefore, to assure 1% accuracy, the instrument must detect a change of:

$$\Delta V = (0.01)(0.0134) = 0.000134 \text{ cm}^3$$





Points, Directions, and Planes in the Unit Cell

- **Miller indices** - A shorthand notation to describe certain crystallographic directions and planes in a material. Denoted by [] brackets. A negative number is represented by a bar over the number.
- **Directions of a form** - Crystallographic directions that all have the same characteristics, although their “sense” is different. Denoted by $h\ i$ brackets.
- **Repeat distance** - The distance from one lattice point to the adjacent lattice point along a direction.
- **Linear density** - The number of lattice points per unit length along a direction.
- **Packing fraction** - The fraction of a direction (linear-packing fraction) or a plane (planar-packing factor) that is actually covered by atoms or ions.



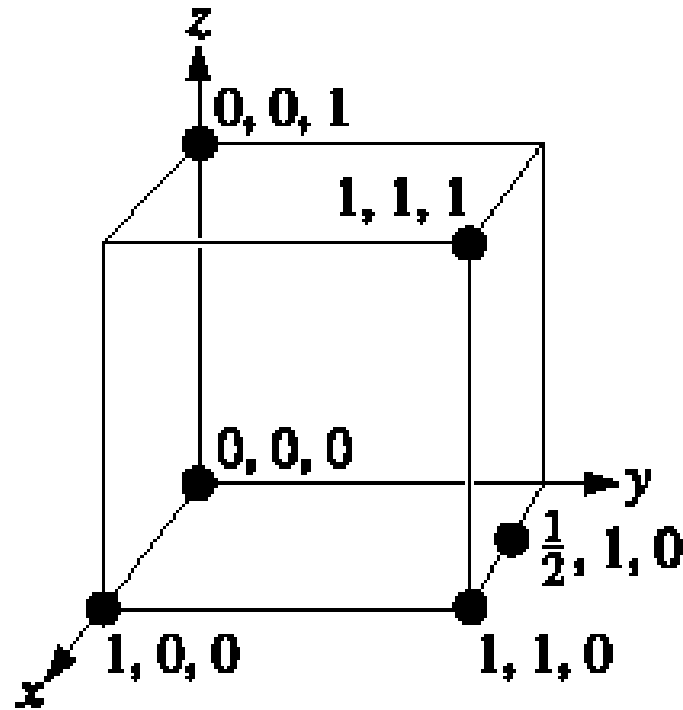


Figure 3.18 Coordinates of selected points in the unit cell. The number refers to the distance from the origin in terms of lattice parameters.





Example 3.7

Determining Miller Indices of Directions

Determine the Miller indices of directions *A*, *B*, and *C* in Figure 3.19.

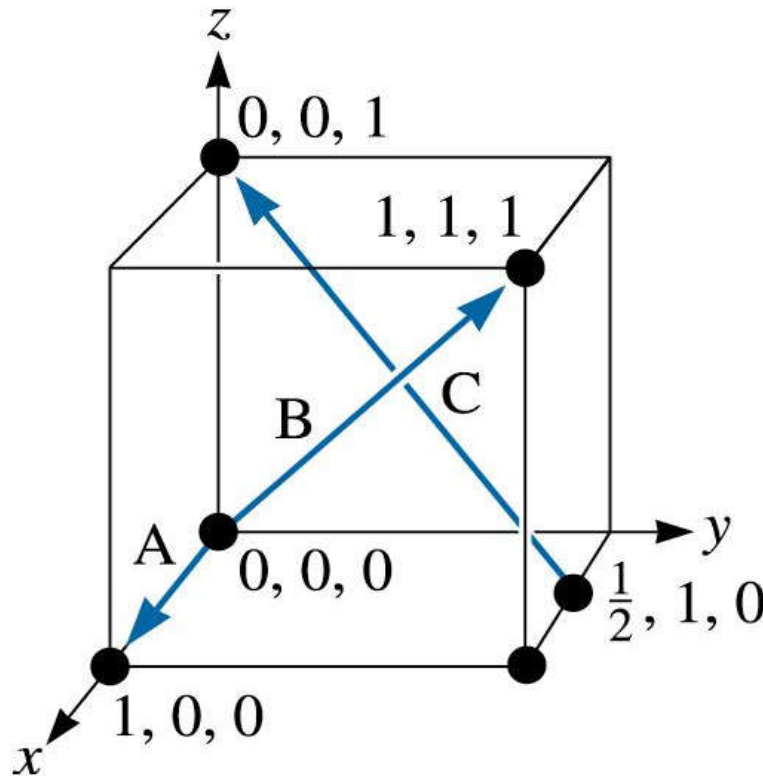
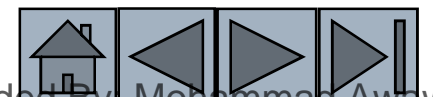


Figure 3.19 Crystallographic directions and coordinates (for Example 3.7).

(c) 2003 Brooks/Cole Publishing / Thomson Learning™





Example 3.7 SOLUTION

Direction A

1. Two points are 1, 0, 0, and 0, 0, 0
2. $1, 0, 0, -0, 0, 0 = 1, 0, 0$
3. No fractions to clear or integers to reduce
4. [100]

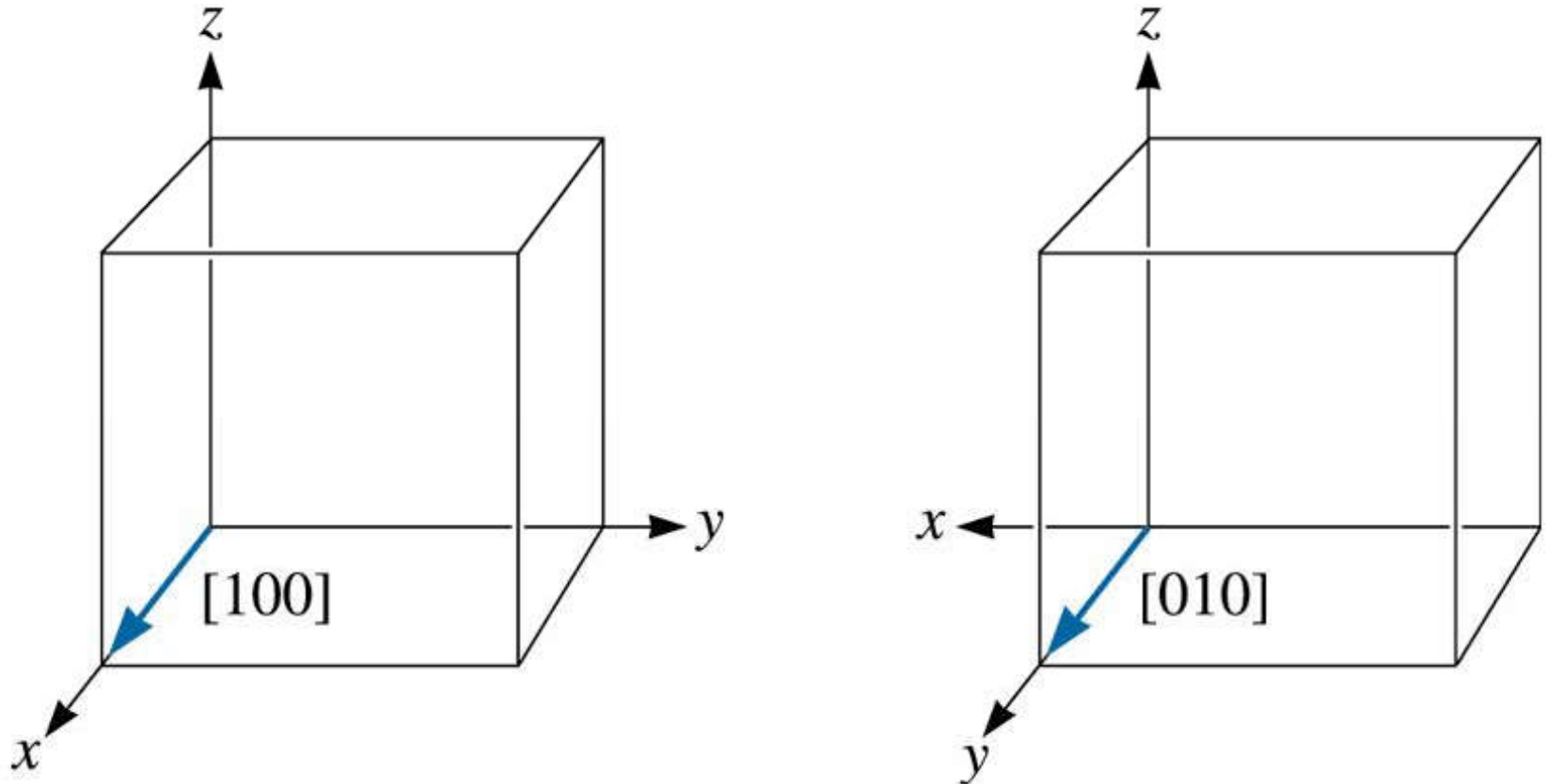
Direction B

1. Two points are 1, 1, 1 and 0, 0, 0
2. $1, 1, 1, -0, 0, 0 = 1, 1, 1$
3. No fractions to clear or integers to reduce
4. [111]

Direction C

1. Two points are 0, 0, 1 and $1/2, 1, 0$
2. $0, 0, 1 - 1/2, 1, 0 = -1/2, -1, 1$
3. $2(-1/2, -1, 1) = -1, -2, 2$
4. $[\bar{1}\bar{2}2]$





(c) 2003 Brooks/Cole Publishing / Thomson Learning™

Figure 3.20 Equivalency of crystallographic directions of a form in cubic systems.





TABLE 3-3 ■ *Directions of the form $\langle 110 \rangle$ in cubic systems*

$$\langle 110 \rangle = \left\{ \begin{array}{ll} [110] & [\bar{1}\bar{1}0] \\ [101] & [\bar{1}0\bar{1}] \\ [011] & [0\bar{1}\bar{1}] \\ [1\bar{1}0] & [\bar{1}10] \\ [10\bar{1}] & [\bar{1}01] \\ [01\bar{1}] & [0\bar{1}1] \end{array} \right.$$



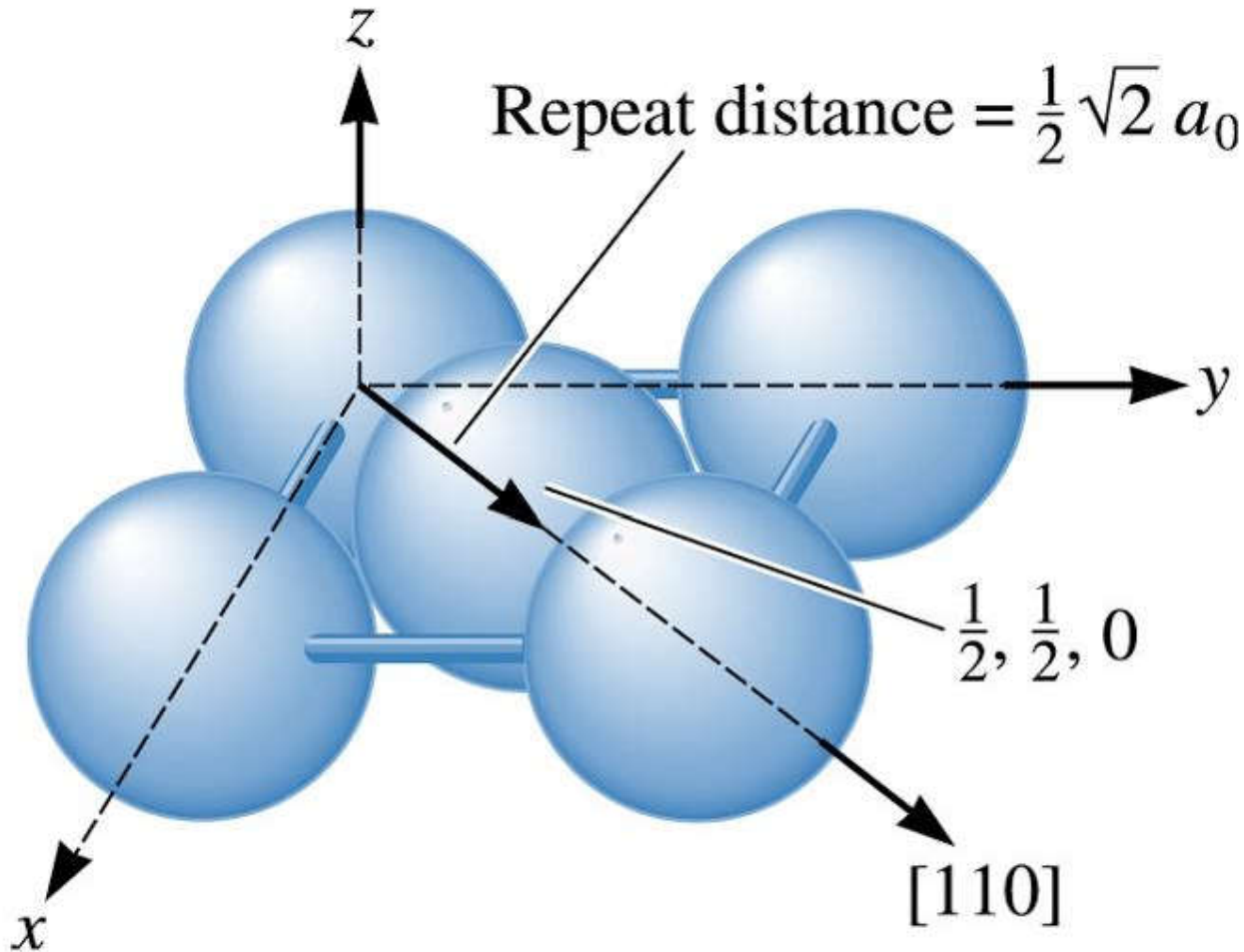
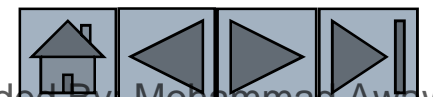


Figure 3.21
Determining the
repeat distance,
linear density,
and packing
fraction for
[110] direction
in FCC copper.

(c) 2003 Brooks/Cole Publishing / Thomson Learning™





Example 3.8

Determining Miller Indices of Planes

Determine the Miller indices of planes *A*, *B*, and *C* in Figure 3.22.

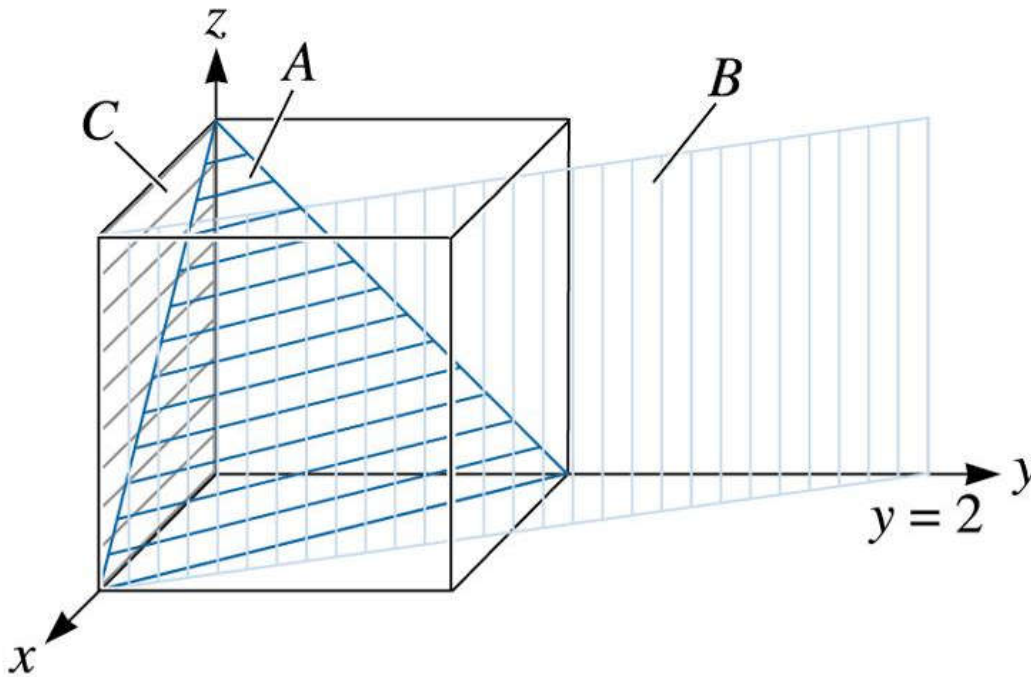
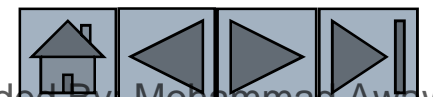


Figure 3.22
Crystallographic planes
and intercepts (for
Example 3.8)

(c) 2003 Brooks/Cole Publishing / Thomson Learning™



Example 3.8 SOLUTION

UPLOADED BY AHMAD T JUNDI

Plane A

1. $x = 1, y = 1, z = 1$
2. $1/x = 1, 1/y = 1, 1/z = 1$
3. No fractions to clear
4. (111)

Plane B

1. The plane never intercepts the z axis, so $x = 1, y = 2,$ and $z = \infty$
2. $1/x = 1, 1/y = 1/2, 1/z = 0$
3. Clear fractions:
 $1/x = 2, 1/y = 1, 1/z = 0$
4. (210)

Plane C

1. We must move the origin, since the plane passes through $0, 0, 0$. Let's move the origin one lattice parameter in the y-direction. Then, $x = \infty, y = -1,$ and $z = \infty$
2. $1/x = 0, 1/y = 1, 1/z = 0$
3. No fractions to clear.
4. $(0\bar{1}0)$

UPLOADED BY AHMAD T JUNDI





TABLE 3-4 ■ Planes of the form {1 10} in cubic systems

$$\{110\} \left\{ \begin{array}{l} (110) \\ (101) \\ (011) \\ (1\bar{1}0) \\ (10\bar{1}) \\ (01\bar{1}) \end{array} \right.$$

Note: The negatives of the planes are not unique planes.





Example 3.9

Calculating the Planar Density and Packing Fraction

Calculate the planar density and planar packing fraction for the (010) and (020) planes in simple cubic polonium, which has a lattice parameter of 0.334 nm.

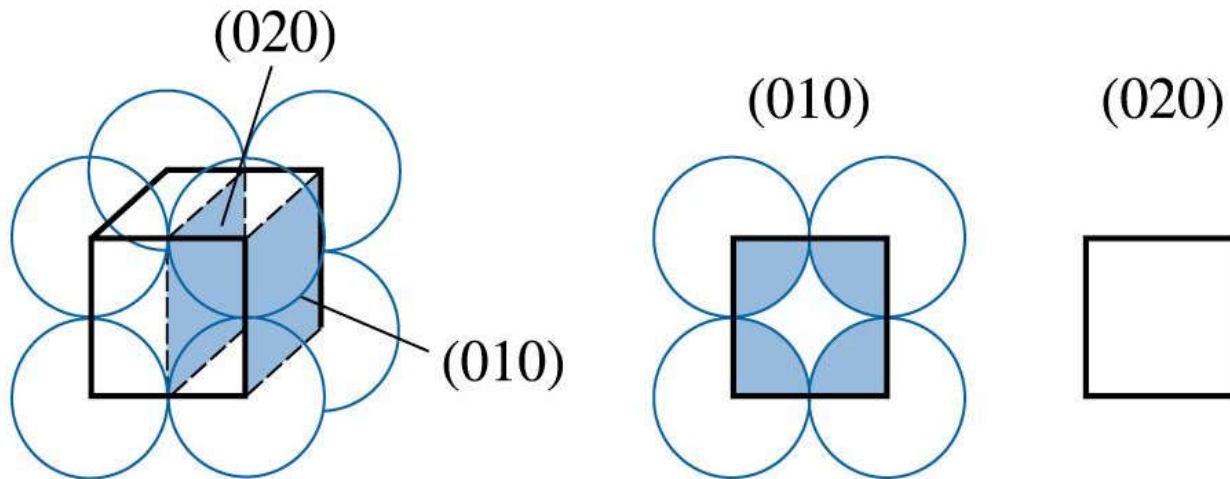
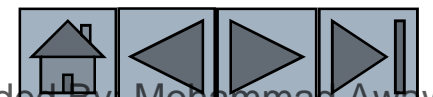


Figure 3.23 The planer densities of the (010) and (020) planes in SC unit cells are not identical (for Example 3.9).

(c) 2003 Brooks/Cole Publishing / Thomson Learning™





The total atoms on each face is one. The planar density is:

$$\begin{aligned} \text{Planar density (010)} &= \frac{\text{atom per face}}{\text{area of face}} = \frac{1 \text{ atom per face}}{(0.334)^2} \\ &= 8.96 \text{ atoms/nm}^2 = 8.96 \times 10^{14} \text{ atoms/cm}^2 \end{aligned}$$

The planar packing fraction is given by:

$$\begin{aligned} \text{Packing fraction (010)} &= \frac{\text{area of atoms per face}}{\text{area of face}} = \frac{(1 \text{ atom}) (\pi r^2)}{(a_0)^2} \\ &= \frac{\pi r^2}{(2r)^2} = 0.79 \end{aligned}$$

However, no atoms are centered on the (020) planes. Therefore, the planar density and the planar packing fraction are both zero. The (010) and (020) planes are not equivalent!





Example 3.10

Drawing Direction and Plane

Draw (a) the $[1\bar{2}1]$ direction and (b) the $(\bar{2}10)$ plane in a cubic unit cell.

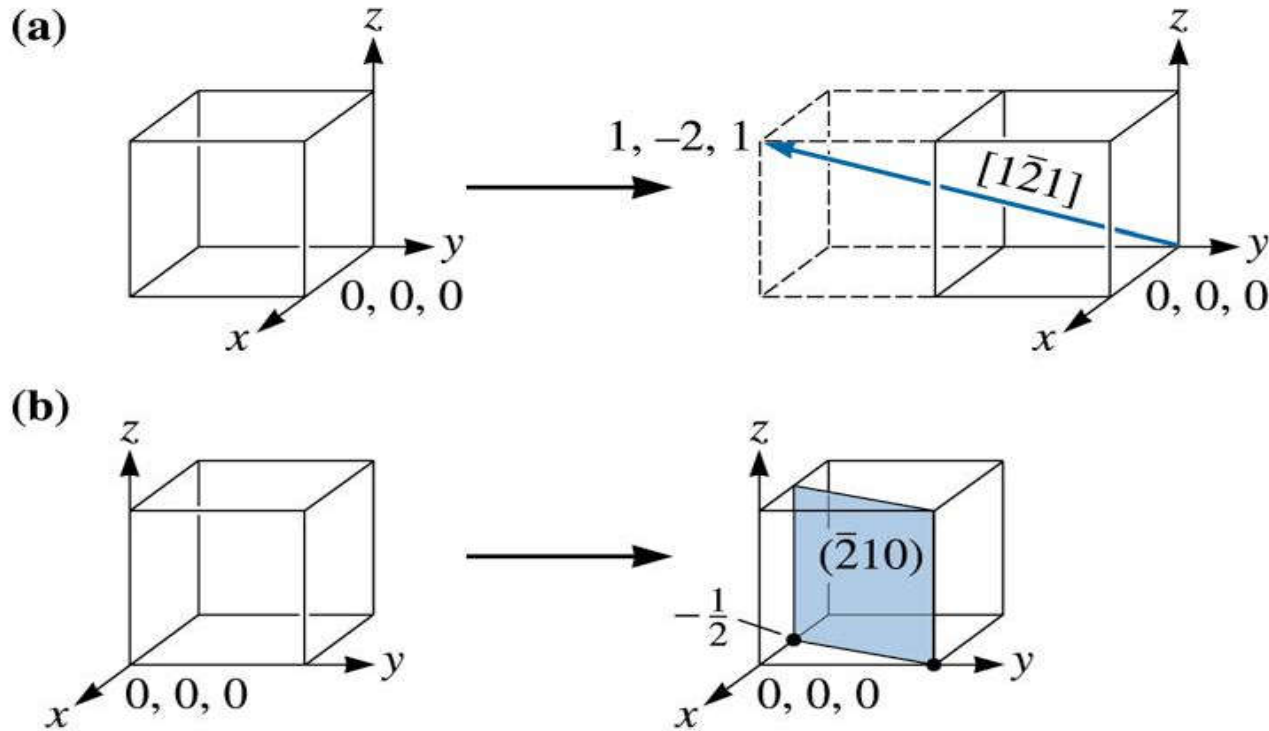
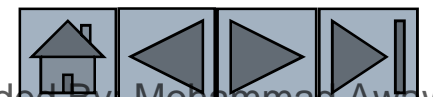


Figure 3.24
Construction
of a (a)
direction and
(b) plane
within a unit
cell (for
Example 3.10)

(c) 2003 Brooks/Cole Publishing / Thomson Learning™





Example 3.10 SOLUTION

a. Because we know that we will need to move in the negative y -direction, let's locate the origin at $0, +1, 0$. The "tail" of the direction will be located at this new origin. A second point on the direction can be determined by moving $+1$ in the x -direction, 2 in the y -direction, and $+1$ in the z direction [Figure 3.24(a)].

b. To draw in the $[\bar{2}10]$ plane, first take reciprocals of the indices to obtain the intercepts, that is:

$$x = 1/-2 = -1/2 \quad y = 1/1 = 1 \quad z = 1/0 = \infty$$

Since the x -intercept is in a negative direction, and we wish to draw the plane within the unit cell, let's move the origin $+1$ in the x -direction to $1, 0, 0$. Then we can locate the x -intercept at $1/2$ and the y -intercept at $+1$. The plane will be parallel to the z -axis [Figure 3.24(b)].



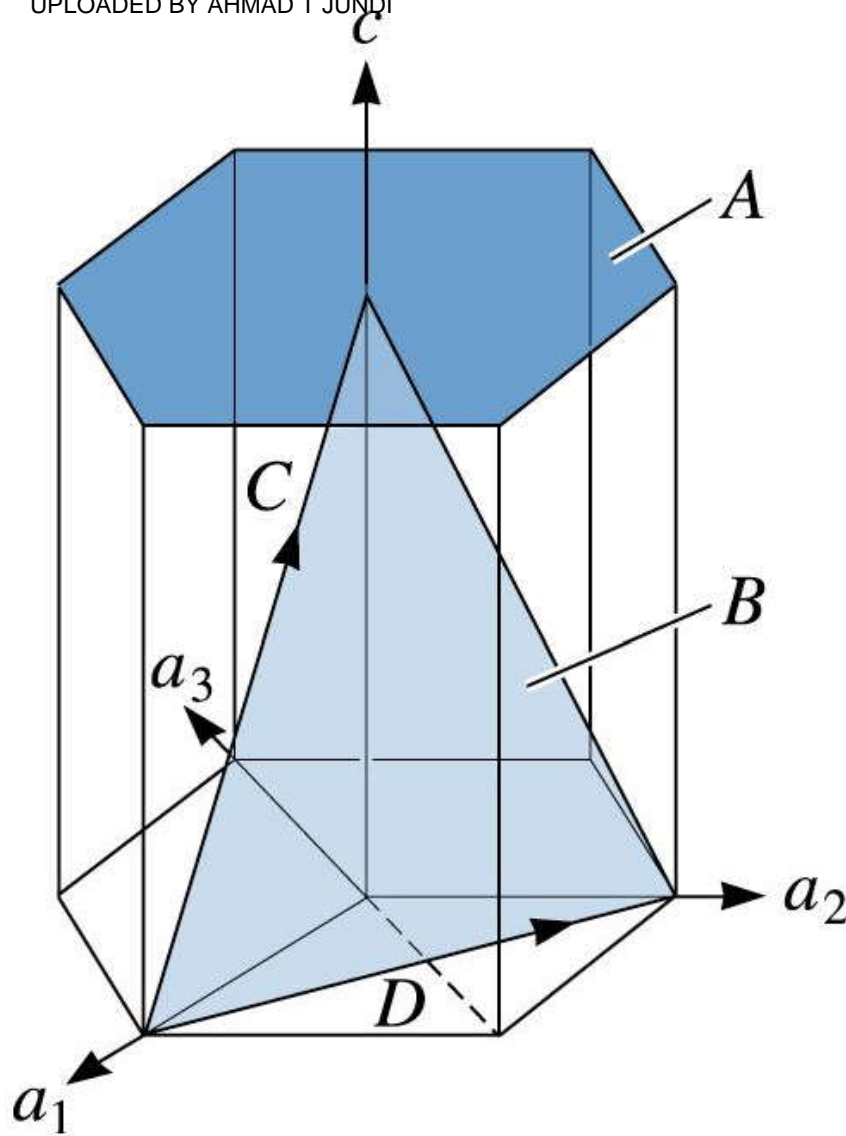
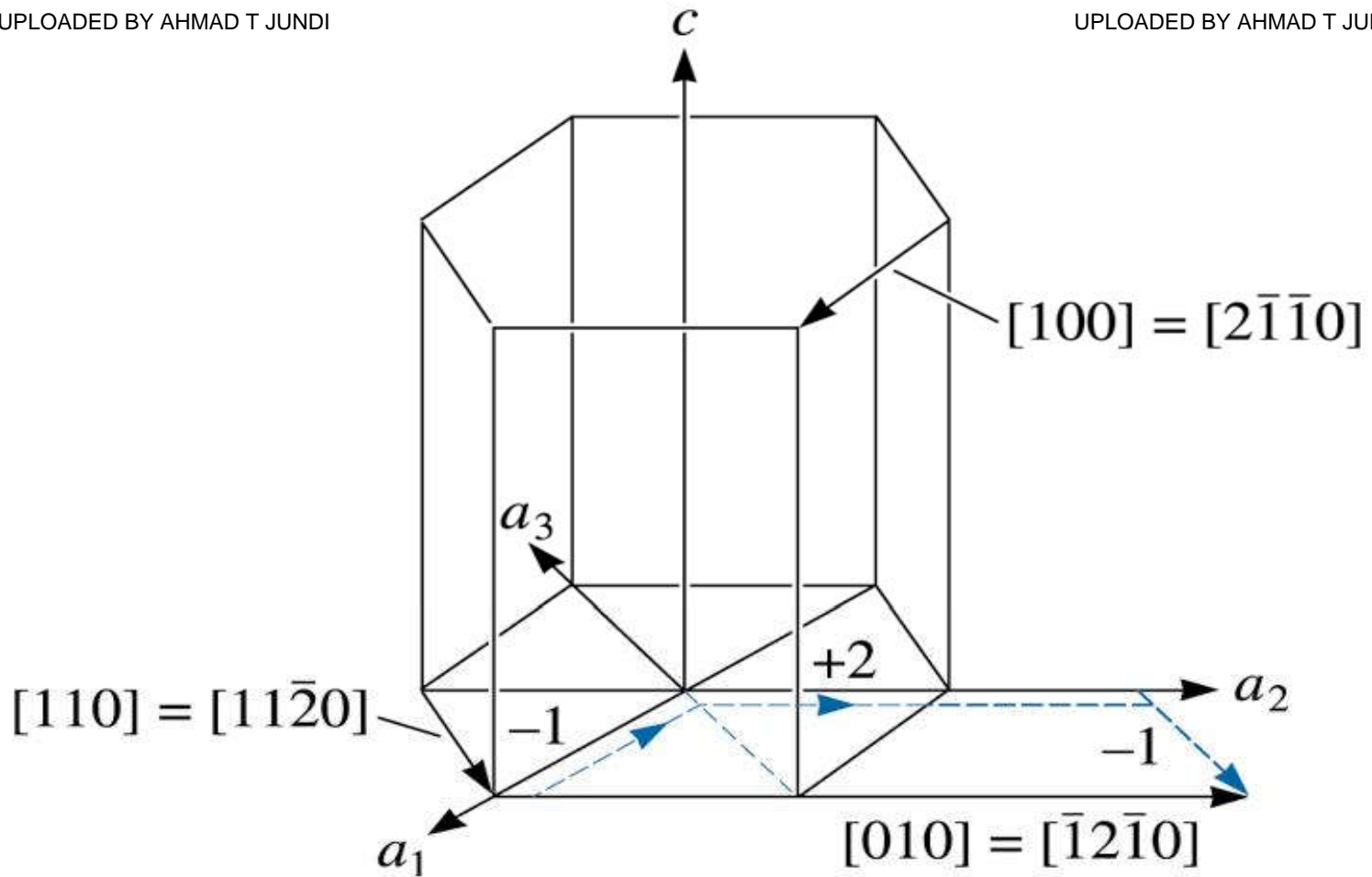


Figure 3.25 Miller-Bravais indices are obtained for crystallographic planes in HCP unit cells by using a four-axis coordinate system. The planes labeled A and B and the direction labeled C and D are those discussed in Example 3.11.





(c) 2003 Brooks/Cole Publishing / Thomson Learning™

Figure 3.26 Typical directions in the HCP unit cell, using both three-and-four-axis systems. The dashed lines show that the $[\bar{1}2\bar{1}0]$ direction is equivalent to a $[010]$ direction.





Example 3.11

Determining the Miller-Bravais Indices for Planes and Directions

Determine the Miller-Bravais indices for planes A and B and directions C and D in Figure 3.25.

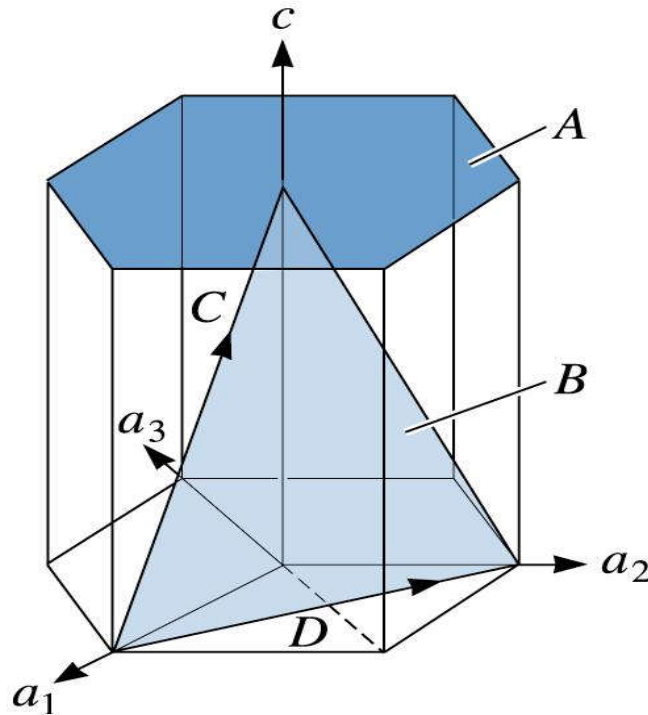
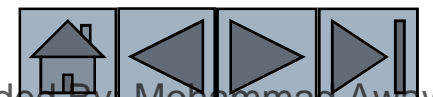


Figure 3.25 Miller-Bravais indices are obtained for crystallographic planes in HCP unit cells by using a four-axis coordinate system. The planes labeled A and B and the direction labeled C and D are those discussed in Example 3.11.

(c) 2003 Brooks/Cole Publishing / Thomson Learning™





Plane A

1. $a_1 = a_2 = a_3 = \infty$, $c = 1$
2. $1/a_1 = 1/a_2 = 1/a_3 = 0$, $1/c = 1$
3. No fractions to clear
4. (0001)

Plane B

1. $a_1 = 1$, $a_2 = 1$, $a_3 = -1/2$, $c = 1$
2. $1/a_1 = 1$, $1/a_2 = 1$, $1/a_3 = -2$, $1/c = 1$
3. No fractions to clear
4. $(11\bar{2}1)$

Direction C

1. Two points are 0, 0, 1 and 1, 0, 0.
2. $0, 0, 1, -1, 0, 0 = 1, 0, 1$
3. No fractions to clear or integers to reduce.
4. $[\bar{1}01]$ or $[\bar{2}113]$





Example 3.11 SOLUTION (Continued)

Direction D

1. Two points are $0, 1, 0$ and $1, 0, 0$.
2. $0, 1, 0, -1, 0, 0 = -1, 1, 0$
3. No fractions to clear or integers to reduce.
4. $[\bar{1} 10]$ or $[\bar{1} 100]$





TABLE 3-5 ■ *Close-packed planes and directions*

Structure	Directions	Planes
SC	$\langle 100 \rangle$	None
BCC	$\langle 111 \rangle$	None
FCC	$\langle 110 \rangle$	$\{111\}$
HCP	$\langle 100 \rangle$, $\langle 110 \rangle$ or $\langle 11\bar{2}0 \rangle$	(0001), (0002)



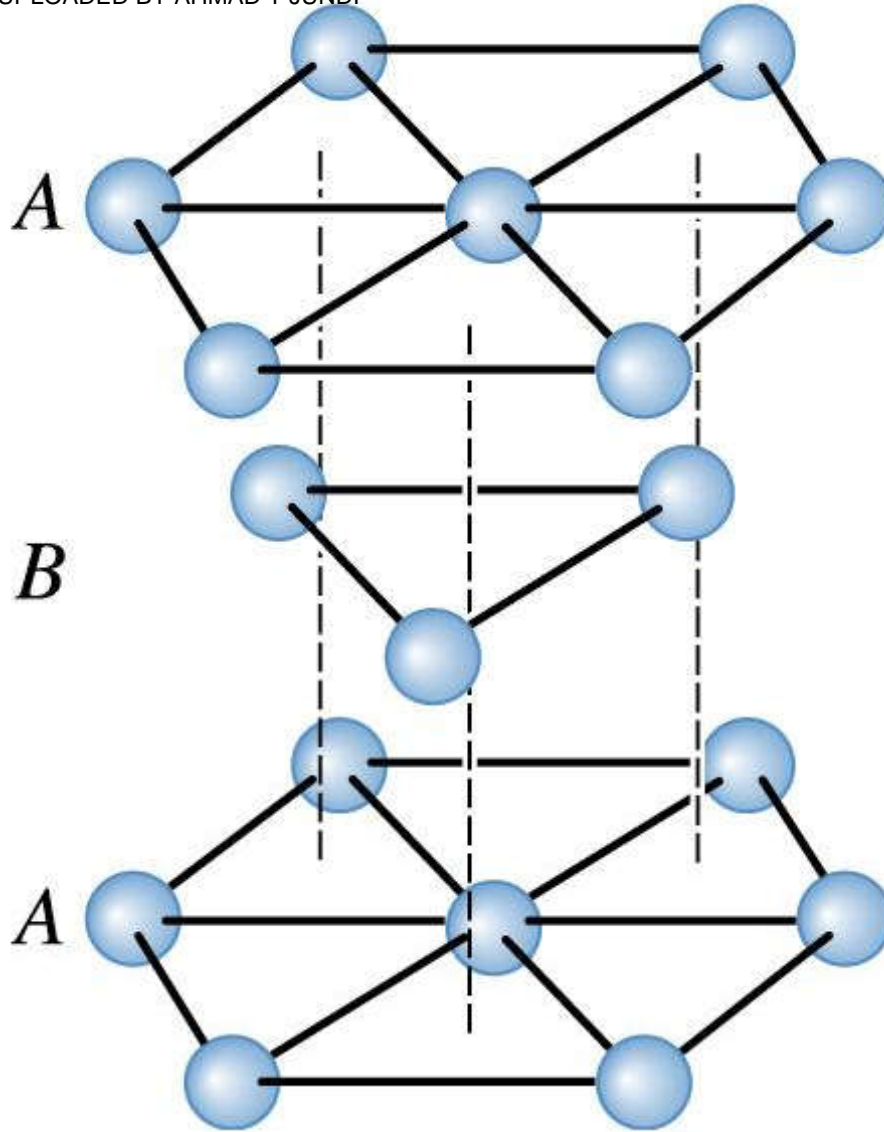
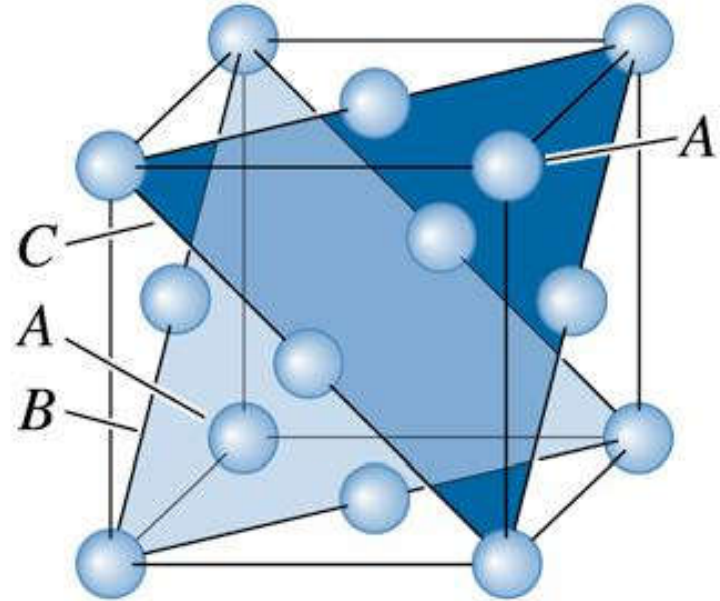
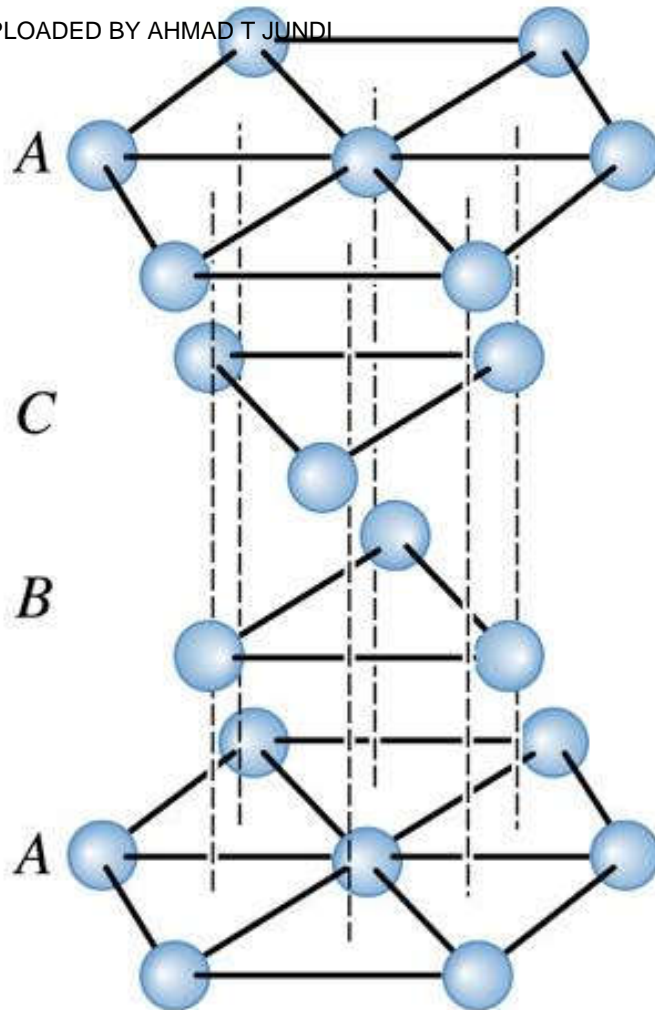


Figure 3.27 The **ABABAB** stacking sequence of close-packed planes produces the HCP structure.

(c) 2003 Brooks/Cole Publishing / Thomson Learning™





(c) 2003 Brooks/Cole Publishing / Thomson Learning™

Figure 3.28 The *ABCABCABC* stacking sequence of close-packed planes produces the FCC structure.

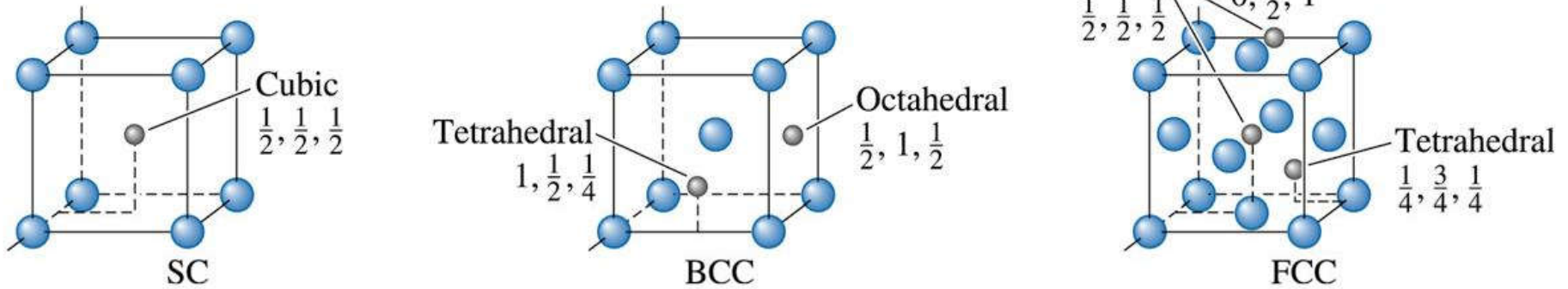


Section 3.6

Interstitial Sites

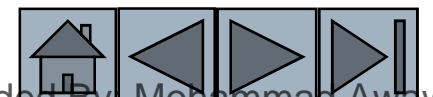
- ❑ **Interstitial sites** - Locations between the “normal” atoms or ions in a crystal into which another - usually different - atom or ion is placed. Typically, the size of this interstitial location is smaller than the atom or ion that is to be introduced.
- ❑ **Cubic site** - An interstitial position that has a coordination number of eight. An atom or ion in the cubic site touches eight other atoms or ions.
- ❑ **Octahedral site** - An interstitial position that has a coordination number of six. An atom or ion in the octahedral site touches six other atoms or ions.
- ❑ **Tetrahedral site** - An interstitial position that has a coordination number of four. An atom or ion in the tetrahedral site touches four other atoms or ions.





(c) 2003 Brooks/Cole Publishing / Thomson Learning™

Figure 3.29 The location of the interstitial sites in cubic unit cells. Only representative sites are shown.





Example 3.12

Calculating Octahedral Sites

Calculate the number of octahedral sites that *uniquely* belong to one FCC unit cell.

Example 3.12 SOLUTION

The octahedral sites include the 12 edges of the unit cell, with the coordinates

$$\begin{array}{cccc}
 \frac{1}{2}, 0, 0 & \frac{1}{2}, 1, 0 & \frac{1}{2}, 0, 1 & \frac{1}{2}, 1, 1 \\
 0, \frac{1}{2}, 0 & 1, \frac{1}{2}, 0 & 1, \frac{1}{2}, 1 & 0, \frac{1}{2}, 1 \\
 0, 0, \frac{1}{2} & 1, 0, \frac{1}{2} & 1, 1, \frac{1}{2} & 0, 1, \frac{1}{2}
 \end{array}$$

plus the center position, $\frac{1}{2}, \frac{1}{2}, \frac{1}{2}$.





Example 3.12 SOLUTION (Continued)

Each of the sites on the edge of the unit cell is shared between four unit cells, so only $1/4$ of each site belongs uniquely to each unit cell.

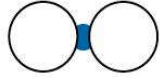
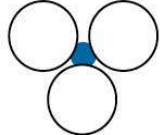
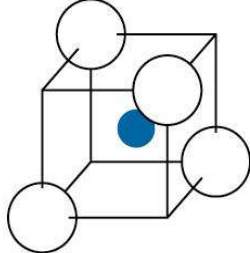
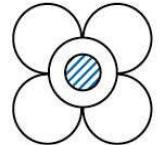
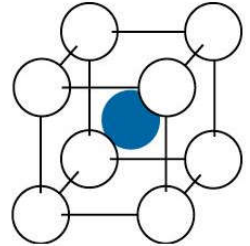
Therefore, the number of sites belonging uniquely to each cell is:

$$(12 \text{ edges}) (1/4 \text{ per cell}) + 1 \text{ center location} \\ = 4 \text{ octahedral sites}$$



TABLE 3-6 The coordination number and the radius ratio



Coordination Number	Interstitial Location of Number	Interstitial	Radius Ratio	Representation
2		Linear	0–0.155	
3		Center of triangle	0.155–0.225	
4		Center of tetrahedron	0.225–0.414	
6		Center of octahedron	0.414–0.732	
8		Center of cube	0.732–1.000	



Example 3.13



Design of a Radiation-Absorbing Wall

We wish to produce a radiation-absorbing wall composed of 10,000 lead balls, each 3 cm in diameter, in a face-centered cubic arrangement. We decide that improved absorption will occur if we fill interstitial sites between the 3-cm balls with smaller balls. Design the size of the smaller lead balls and determine how many are needed.

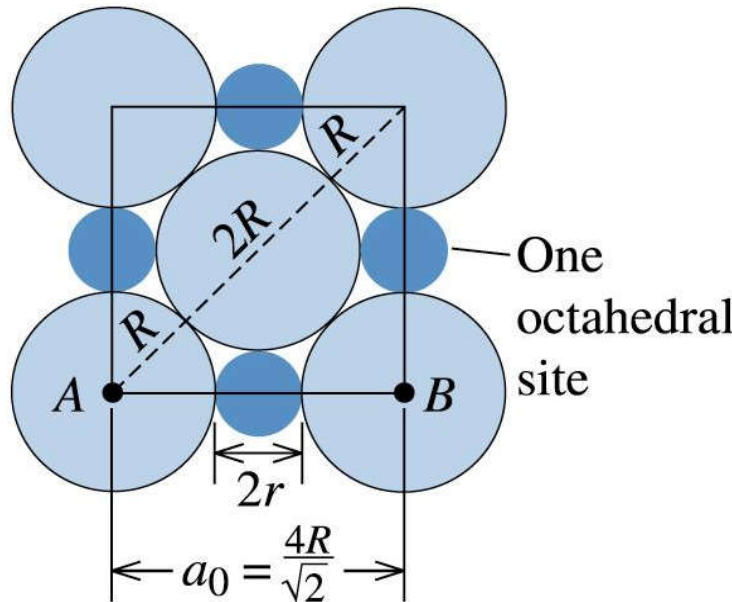


Figure 3.30 Calculation of an octahedral interstitial site (for Example 3.13).

(c) 2003 Brooks/Cole Publishing / Thomson Learning™



Example 3.13 SOLUTION

UPLOADED BY AHMAD T JUNDI

UPLOADED BY AHMAD T JUNDI



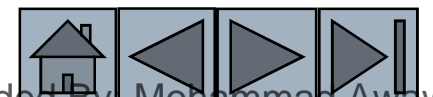
First, we can calculate the diameter of the octahedral sites located between the 3-cm diameter balls. Figure 3.30 shows the arrangement of the balls on a plane containing an octahedral site.

$$\begin{aligned}\text{Length } AB &= 2R + 2r = 2R\sqrt{2} \\ r &= \sqrt{2}R - R = (\sqrt{2} - 1)R \\ r/R &= 0.414\end{aligned}$$

This is consistent with Table 3-6. Since $r = R = 0.414$, the radius of the small lead balls is

$$r = 0.414 * R = (0.414)(3 \text{ cm}/2) = 0.621 \text{ cm.}$$

From Example 3-12, we find that there are four octahedral sites in the FCC arrangement, which also has four lattice points. **Therefore, we need the same number of small lead balls as large lead balls, or 10,000 small balls.**



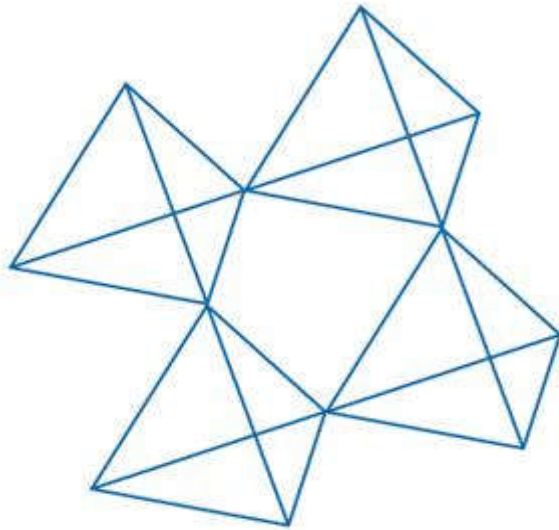


Section 3.7

Crystal Structures of Ionic Materials

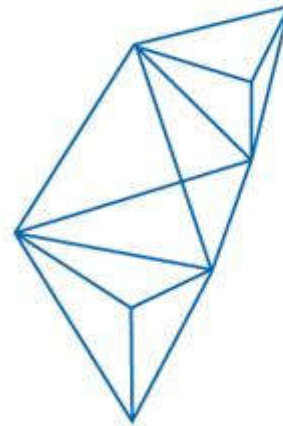
- Factors need to be considered in order to understand crystal structures of ionically bonded solids:
 - Ionic Radii
 - Electrical Neutrality
 - Connection between Anion Polyhedra
 - Visualization of Crystal Structures Using Computers





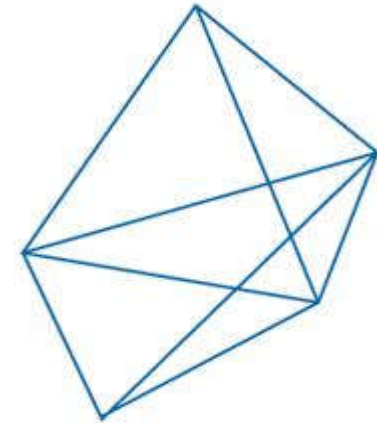
Corner-sharing tetrahedra

(a)



Edge-sharing tetrahedra

(b)



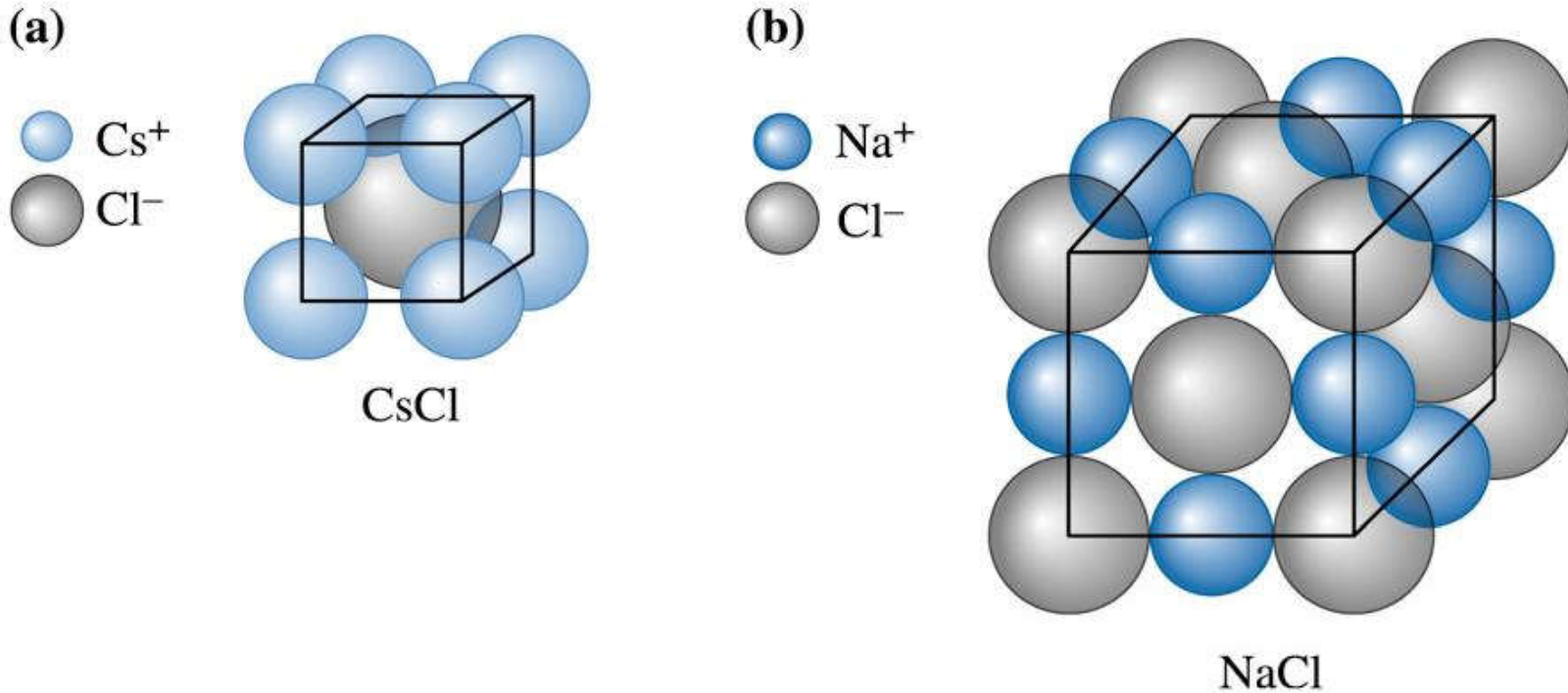
Face-sharing tetrahedra

(c)

(c) 2003 Brooks/Cole Publishing / Thomson Learning™

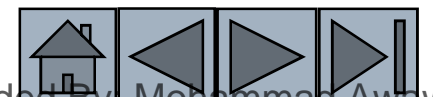
Figure 3.31 Connection between anion polyhedra. Different possible connections include sharing of corners, edges, or faces. In this figure, examples of connections between tetrahedra are shown.





(c) 2003 Brooks/Cole Publishing / Thomson Learning™

Figure 3.32 (a) The cesium chloride structure, a SC unit cell with two ions (Cs^+ and Cl^-) per lattice point. (b) The sodium chloride structure, a FCC unit cell with two ions (Na^+ + Cl^-) per lattice point. *Note: Ion sizes not to scale.*



Example 3.14

Radius Ratio for KCl



For potassium chloride (KCl), (a) verify that the compound has the cesium chloride structure and (b) calculate the packing factor for the compound.

Example 3.14 SOLUTION

a. From Appendix B, $r_{K^+} = 0.133$ nm and $r_{Cl^-} = 0.181$ nm, so:

$$r_{K^+}/r_{Cl^-} = 0.133/0.181 = 0.735$$

Since $0.732 < 0.735 < 1.000$, the coordination number for each type of ion is eight and the CsCl structure is likely.





Example 3.14 SOLUTION (Continued)

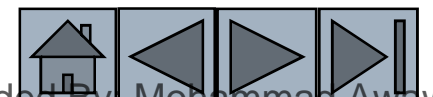
b. The ions touch along the body diagonal of the unit cell, so:

$$a_0 = 2r_{K^+} + 2r_{Cl^-} = 2(0.133) + 2(0.181) = 0.628 \text{ nm}$$

$$a_0 = 0.363 \text{ nm}$$

$$\text{Packing factor} = \frac{\frac{4}{3} \pi r_{K^+}^3 (1 \text{ K ion}) + \frac{4}{3} \pi r_{Cl^-}^3 (1 \text{ Cl ion})}{a_0^3}$$

$$= \frac{\frac{4}{3} \pi (0.133)^3 + \frac{4}{3} \pi (0.181)^3}{(0.363)^3} = 0.725$$





Example 3.15

Illustrating a Crystal Structure and Calculating Density

Show that MgO has the sodium chloride crystal structure and calculate the density of MgO.

Example 3.15 SOLUTION

From Appendix B, $r_{\text{Mg}^{+2}} = 0.066 \text{ nm}$ and $r_{\text{O}^{-2}} = 0.132 \text{ nm}$, so:

$$r_{\text{Mg}^{+2}}/r_{\text{O}^{-2}} = 0.066/0.132 = 0.50$$

Since $0.414 < 0.50 < 0.732$, the coordination number for each ion is six, and the sodium chloride structure is possible.





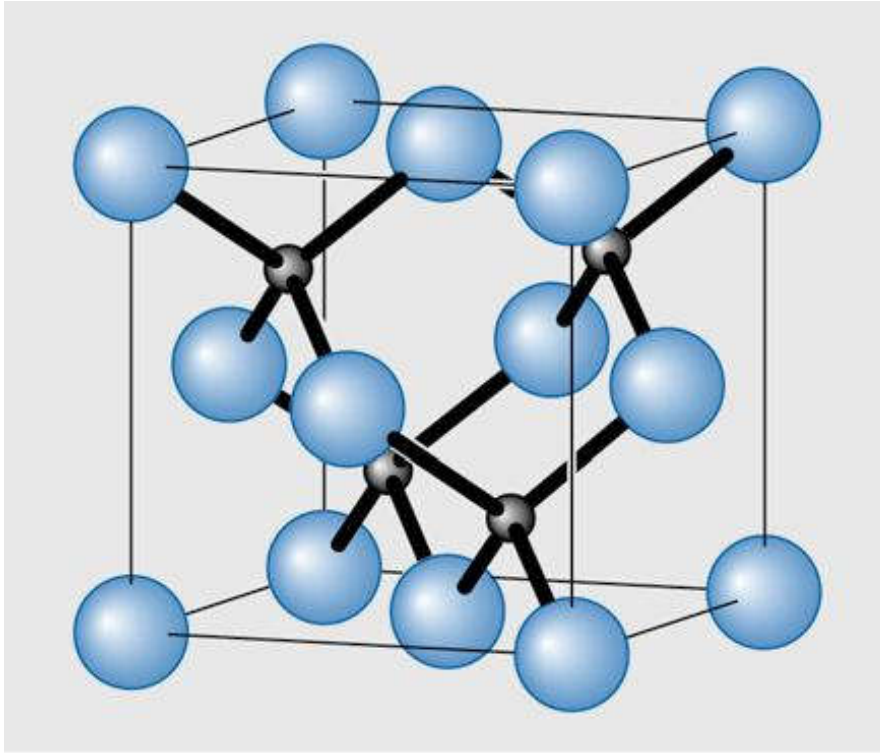
Example 3.15 SOLUTION

The atomic masses are 24.312 and 16 g/mol for magnesium and oxygen, respectively. The ions touch along the edge of the cube, so:

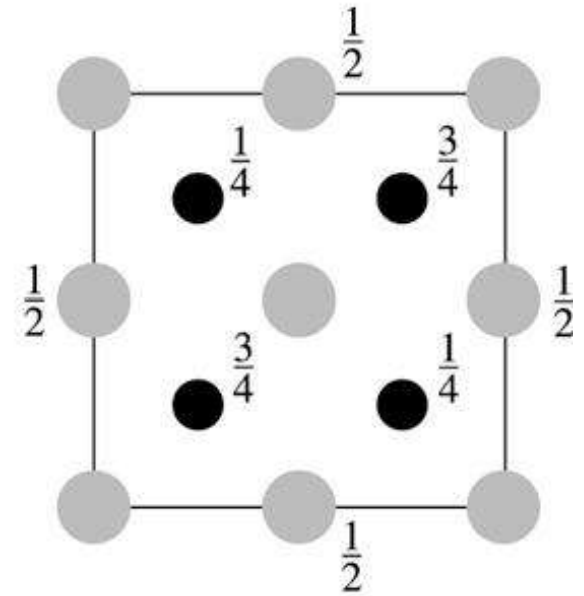
$$\begin{aligned} a_0 &= 2 r_{\text{Mg}^{+2}} + 2 r_{\text{O}^{-2}} = 2(0.066) + 2(0.132) \\ &= 0.396 \text{ nm} = 3.96 \times 10^{-8} \text{ cm} \end{aligned}$$

$$\rho = \frac{(4\text{Mg}^{+2})(24.312) + (4\text{O}^{-2})(16)}{(3.96 \times 10^{-8} \text{ cm})^3 (6.02 \times 10^{23})} = 4.31 \text{ g} / \text{cm}^3$$





(a)



(b)

(c) 2003 Brooks/Cole Publishing / Thomson Learning™

Figure 3.33 (a) The zinc blende unit cell, (b) plan view.





Example 3.16

Calculating the Theoretical Density of GaAs

The lattice constant of gallium arsenide (GaAs) is 5.65 Å. Show that the theoretical density of GaAs is 5.33 g/cm³.

Example 3.16 SOLUTION

For the “zinc blende” GaAs unit cell, there are four Ga and four As atoms per unit cell.

From the periodic table (Chapter 2):

Each mole (6.023×10^{23} atoms) of Ga has a mass of 69.7 g. Therefore, the mass of four Ga atoms will be $(4 * 69.7 / 6.023 \times 10^{23})$ g.





Example 3.16 SOLUTION (Continued)

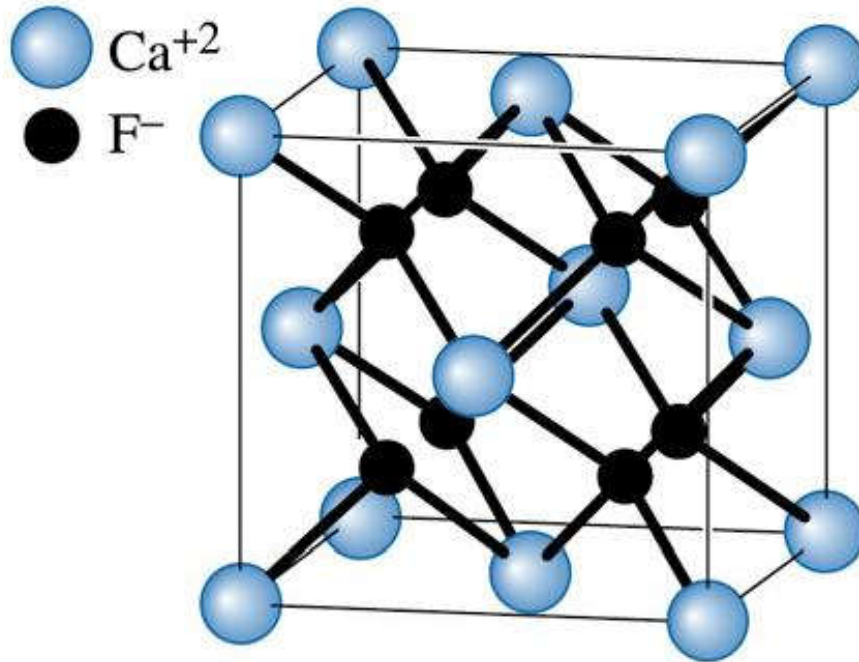
Each mole (6.023×10^{23} atoms) of As has a mass of 74.9 g.

Therefore, the mass of four As atoms will be ($4 * 74.9 / 6.023 \times 10^{23}$) g. These atoms occupy a volume of $(5.65 \times 10^{-8})^3 \text{ cm}^3$.

$$\text{density} = \frac{\text{mass}}{\text{volume}} = \frac{4(69.7 + 74.9) / 6.023 \times 10^{23}}{(5.65 \times 10^{-8} \text{ cm})^3}$$

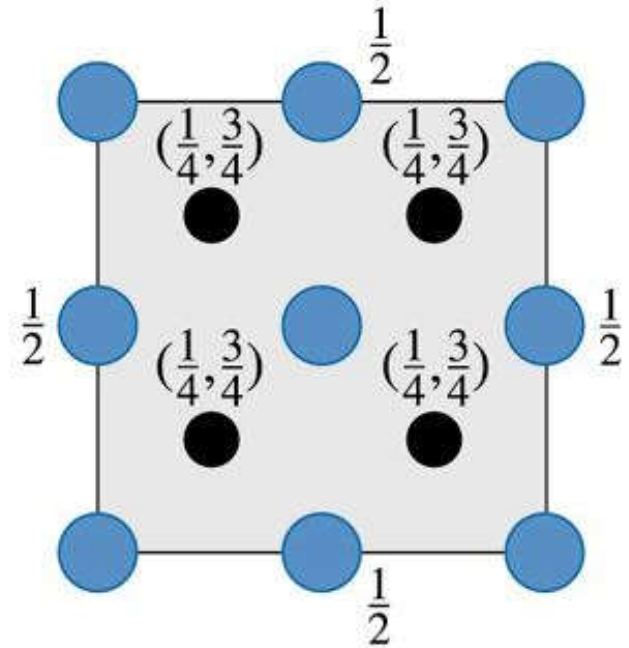
Therefore, the theoretical density of GaAs will be 5.33 g/cm³.





Fluorite cell

(a)

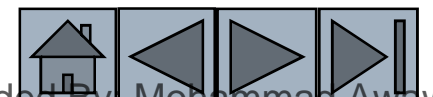


Plan view

(b)

(c) 2003 Brooks/Cole Publishing / Thomson Learning™

Figure 3.34 (a) Fluorite unit cell, (b) plan view.



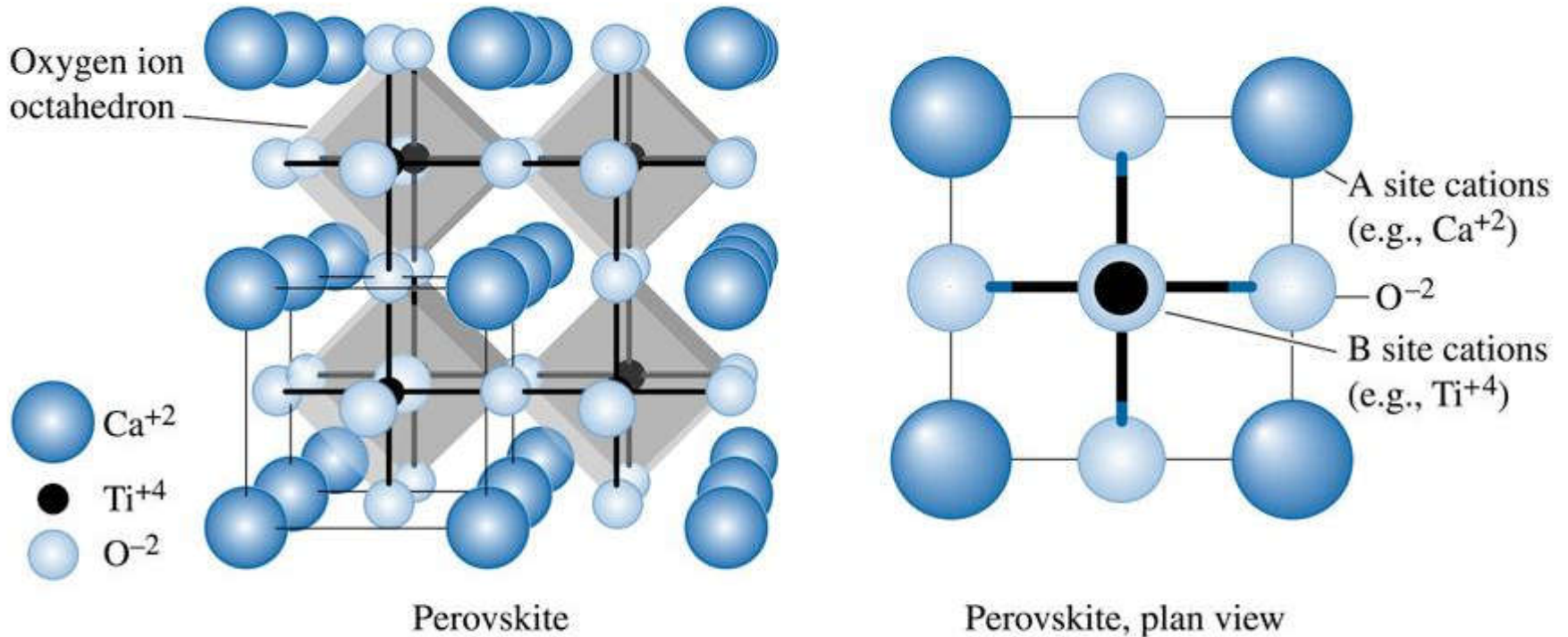
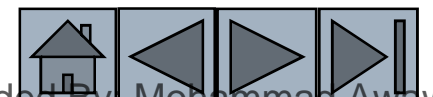


Figure 3.35 The perovskite unit cell showing the A and B site cations and oxygen ions occupying the face-center positions of the unit cell. *Note:* Ions are not show to scale.

(c) 2003 Brooks/Cole Publishing / Thomson Learning



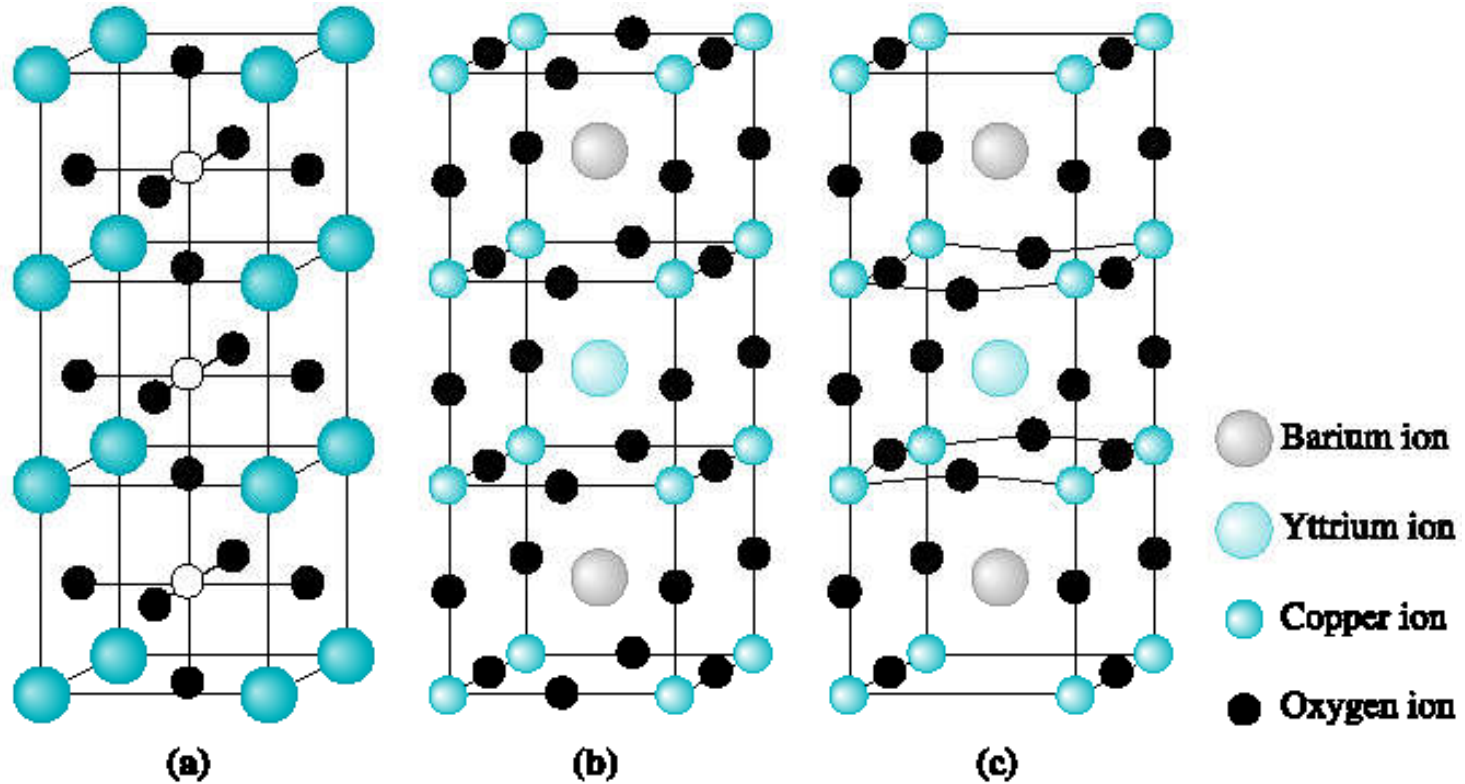
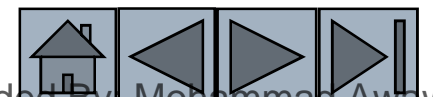


Figure 3.36 Crystal structure of a new high T_c ceramic superconductor based on a yttrium barium copper oxide. These materials are unusual in that they are ceramics, yet at low temperatures their electrical resistance vanishes. (Source: ill.fr/dif/3D-crystals/superconductor.html; © M. Hewat 1998.)





© 2003 Brooks/Cole Publishing / Thomson Learning

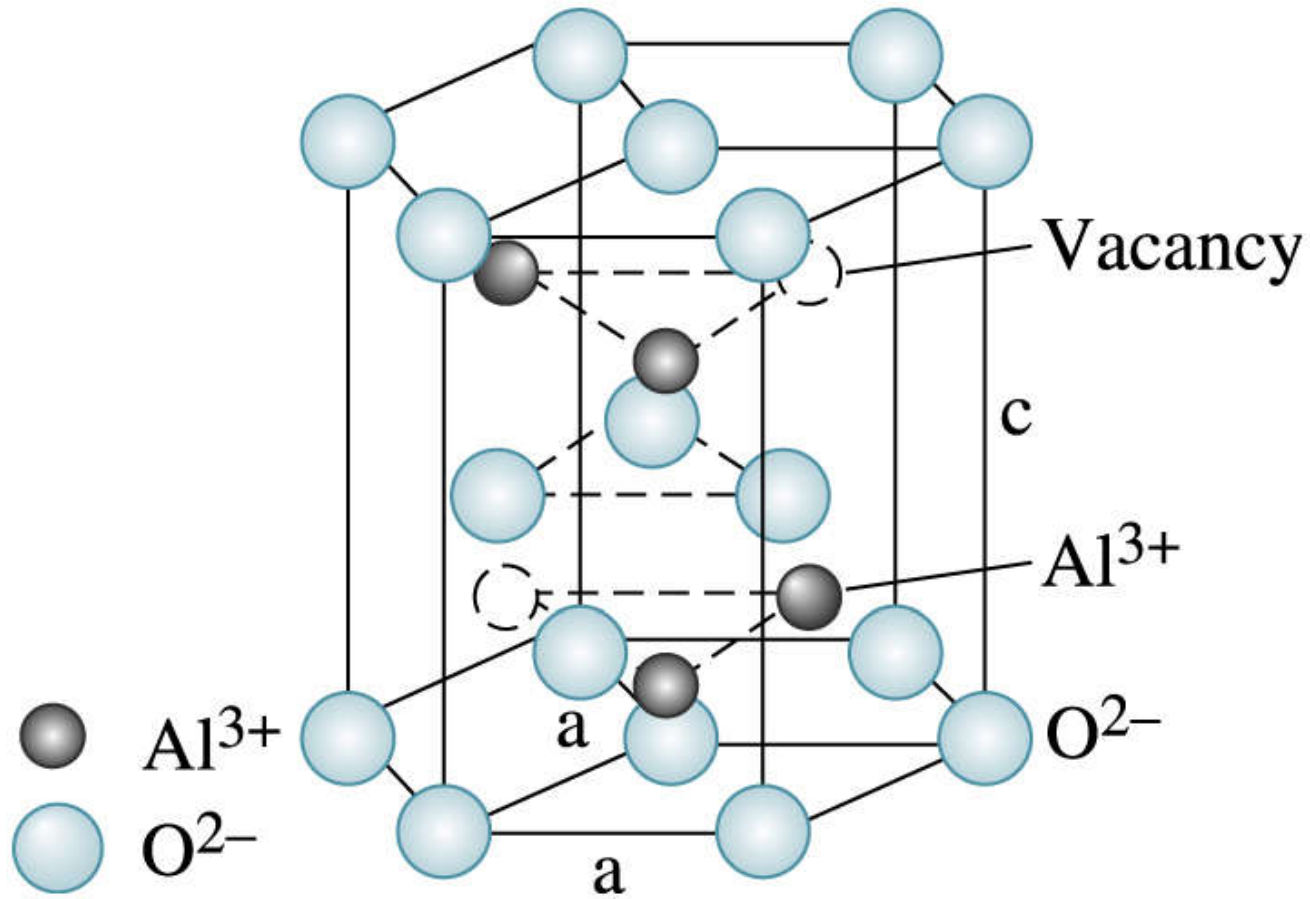


Figure 3.37 Corundum structure of alpha-alumina ($\alpha\text{-Al}_2\text{O}_3$).



Section 3.8

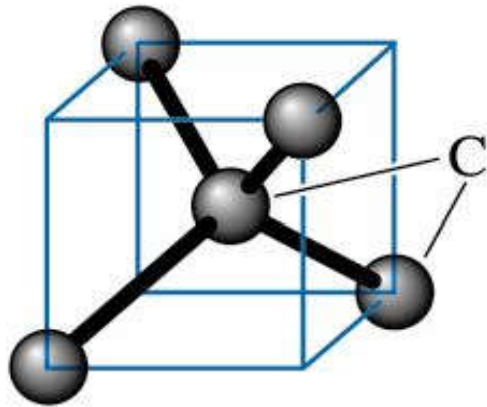
Covalent Structures

- **Covalently bonded materials** frequently have complex structures in order to satisfy the directional restraints imposed by the bonding.
- **Diamond cubic (DC)** - A special type of face-centered cubic crystal structure found in carbon, silicon, and other covalently bonded materials.

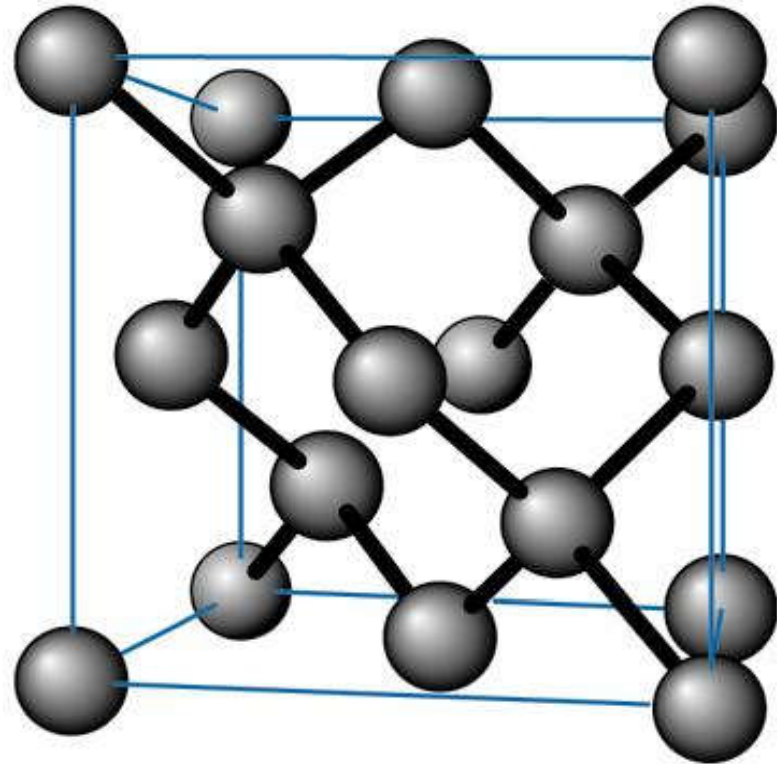
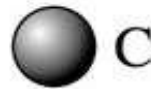




(c) 2003 Brooks/Cole Publishing / Thomson Learning



(a)



Diamond

(b)

Figure 3.38 (a) Tetrahedron and (b) the diamond cubic (DC) unit cell. This open structure is produced because of the requirements of covalent bonding.





Example 3.17

Determining the Packing Factor for Diamond Cubic Silicon

Determine the packing factor for diamond cubic silicon.

© 2003 Brooks/Cole Publishing / Thomson Learning

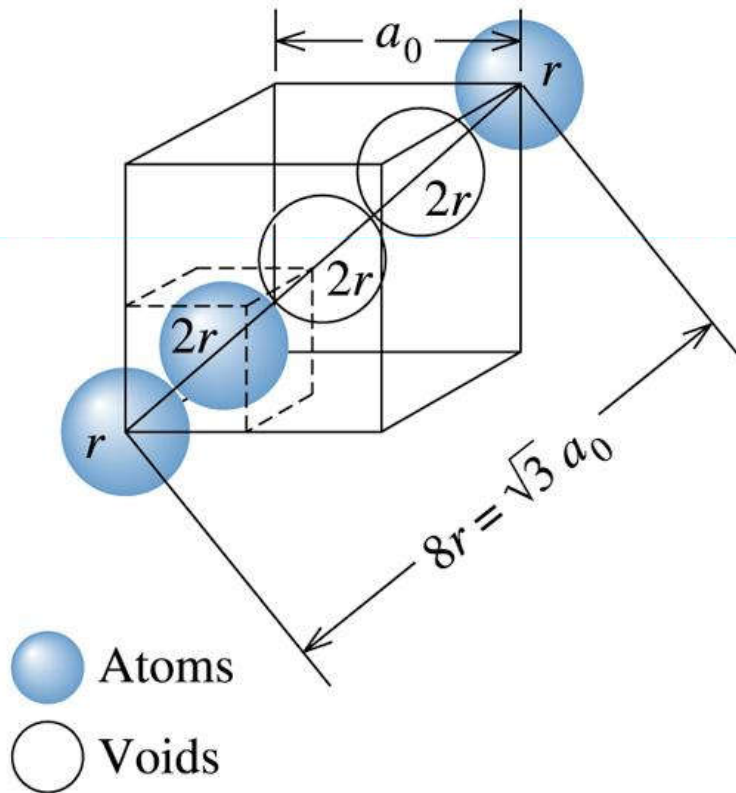
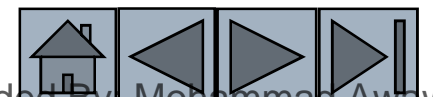


Figure 3.39
Determining the relationship between lattice parameter and atomic radius in a diamond cubic cell (for Example 3.17).



Example 3.17 SOLUTION

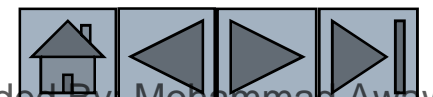


We find that atoms touch along the body diagonal of the cell (Figure 3.39). Although atoms are not present at all locations along the body diagonal, there are voids that have the same diameter as atoms. Consequently:

$$\sqrt{3}a_0 = 8r$$

$$\begin{aligned} \text{Packing factor} &= \frac{(8 \text{ atoms/cell})\left(\frac{4}{3} \pi r^3\right)}{a_0^3} \\ &= \frac{(8)\left(\frac{4}{3} \pi r^3\right)}{(8r / \sqrt{3})^3} \\ &= 0.34 \end{aligned}$$

Compared to close packed structures this is a relatively open structure.





Example 3.18

Calculating the Radius, Density, and Atomic Mass of Silicon

The lattice constant of Si is 5.43 \AA . What will be the radius of a silicon atom? Calculate the theoretical density of silicon. The atomic mass of Si is 28.1 gm/mol .

Example 3.18 SOLUTION

For the diamond cubic structure, $\sqrt{3} a_0 = 8r$
 Therefore, substituting $a = 5.43 \text{ \AA}$,
 the radius of silicon atom = 1.176 \AA .

There are eight Si atoms per unit cell.

$$\text{density} = \frac{\text{mass}}{\text{volume}} = \frac{8(28.1) / 6.023 \times 10^{23}}{(5.43 \times 10^{-8} \text{ cm})^3} = 2.33 \text{ g} / \text{cm}^3$$



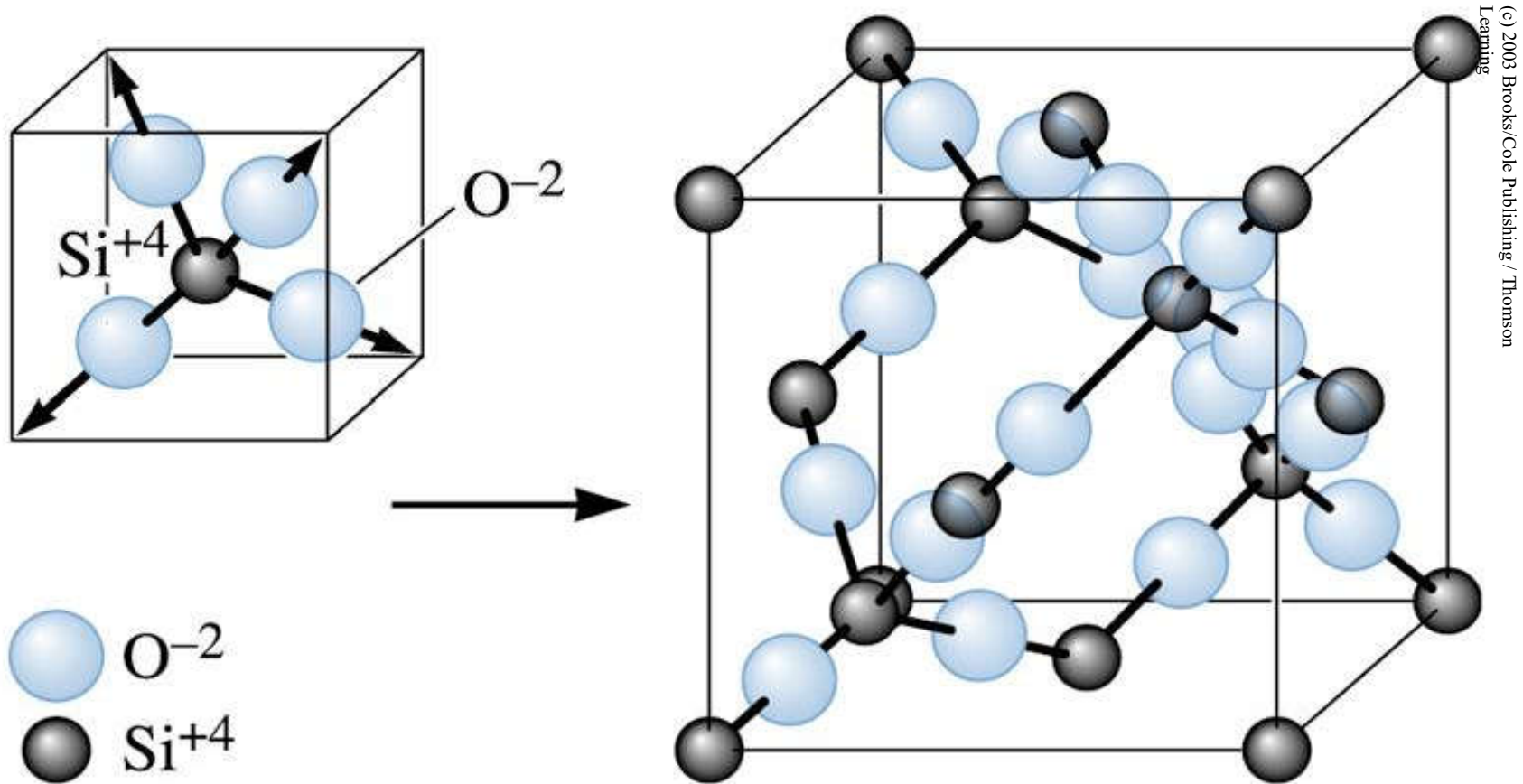


Figure 3.40 The silicon-oxygen tetrahedron and the resultant β -cristobalite form of silica.





(c) 2003 Brooks/Cole Publishing / Thomson Learning

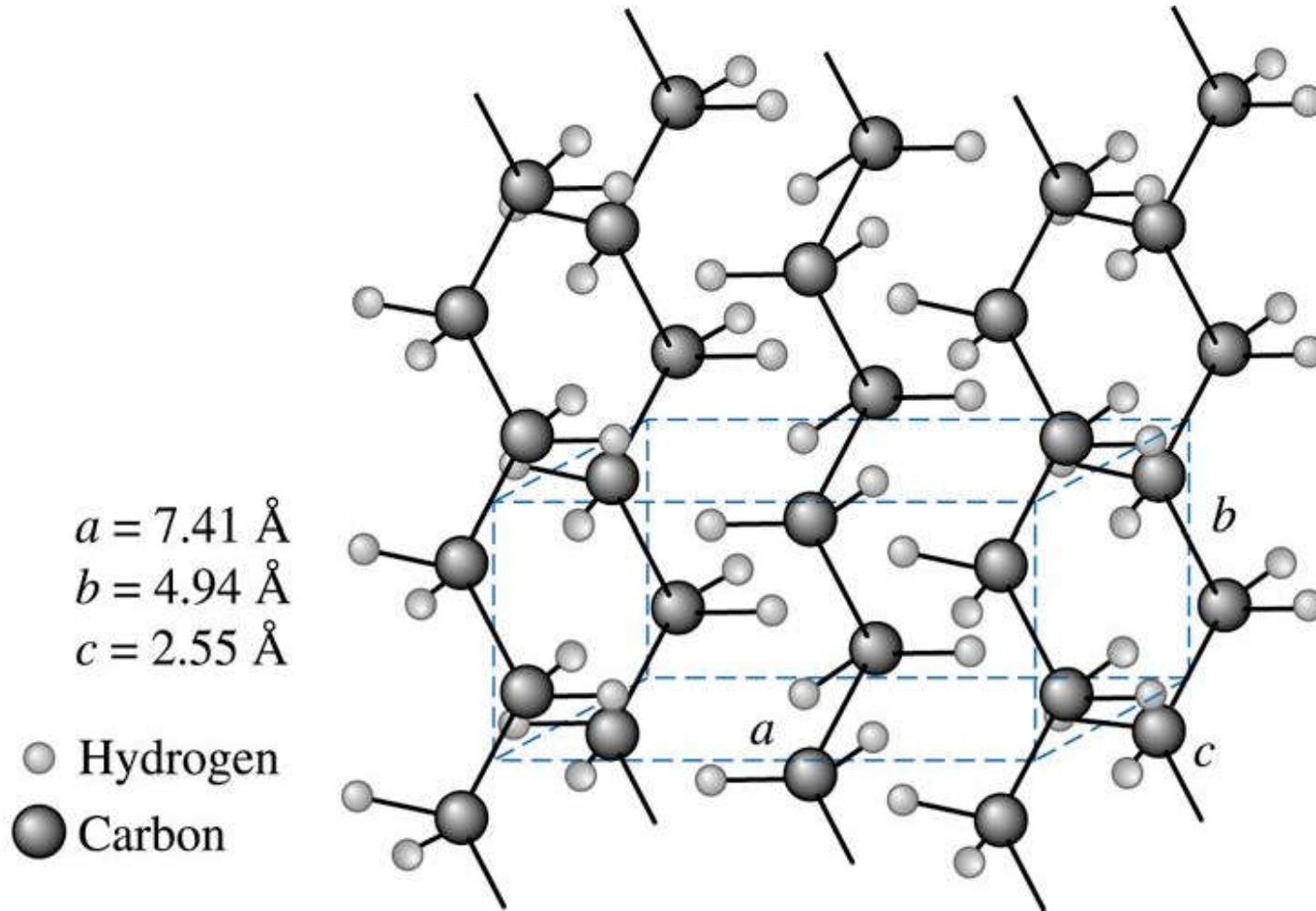


Figure 3.41 The unit cell of crystalline polyethylene.



Example 3.19



Calculating the Number of Carbon and Hydrogen Atoms in Crystalline Polyethylene

How many carbon and hydrogen atoms are in each unit cell of crystalline polyethylene? There are twice as many hydrogen atoms as carbon atoms in the chain. The density of polyethylene is about 0.9972 g/cm³.

Example 3.19 SOLUTION

If we let x be the number of carbon atoms, then $2x$ is the number of hydrogen atoms. From the lattice parameters shown in Figure 3.41:

$$\rho = \frac{(x)(12g / mol) + (2x)(1g / mol)}{(7.41 \times 10^{-8} cm)(4.94 \times 10^{-8} cm)(2.55 \times 10^{-8} cm)(6.02 \times 10^{23})}$$

$x = 4$ carbon atoms per cell

$2x = 8$ hydrogen atoms per cell



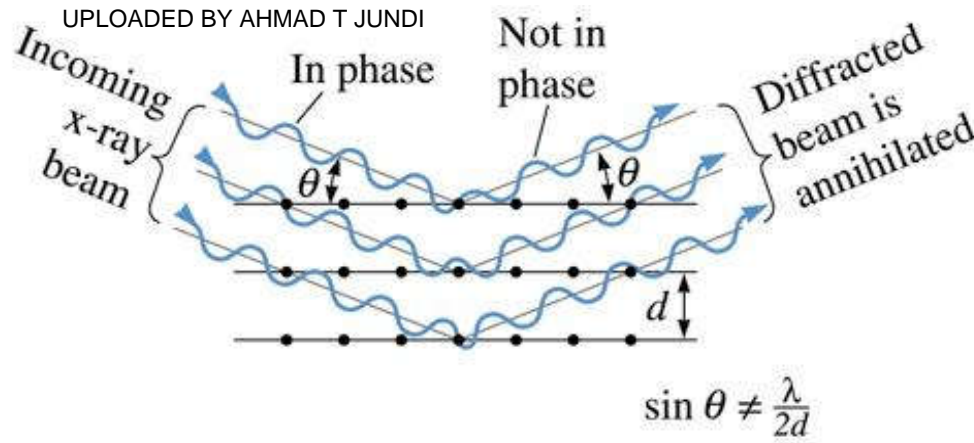


Section 3.9

Diffraction Techniques for Crystal Structure Analysis

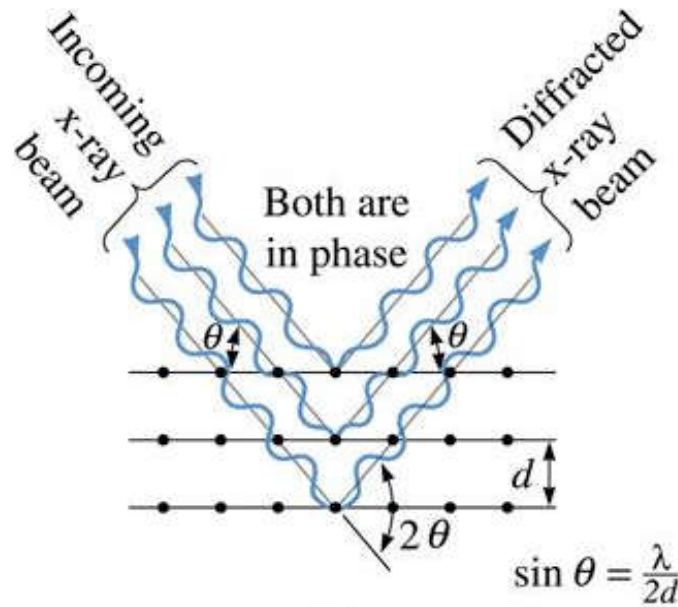
- **Diffraction** - The constructive interference, or reinforcement, of a beam of x-rays or electrons interacting with a material. The diffracted beam provides useful information concerning the structure of the material.
- **Bragg's law** - The relationship describing the angle at which a beam of x-rays of a particular wavelength diffracts from crystallographic planes of a given interplanar spacing.
- **In a diffractometer** a moving x-ray detector records the 2θ angles at which the beam is diffracted, giving a characteristic diffraction pattern





(a)

Figure 3.43 (a) Destructive and (b) reinforcing interactions between x-rays and the crystalline material. Reinforcement occurs at angles that satisfy Bragg's law.



(b)



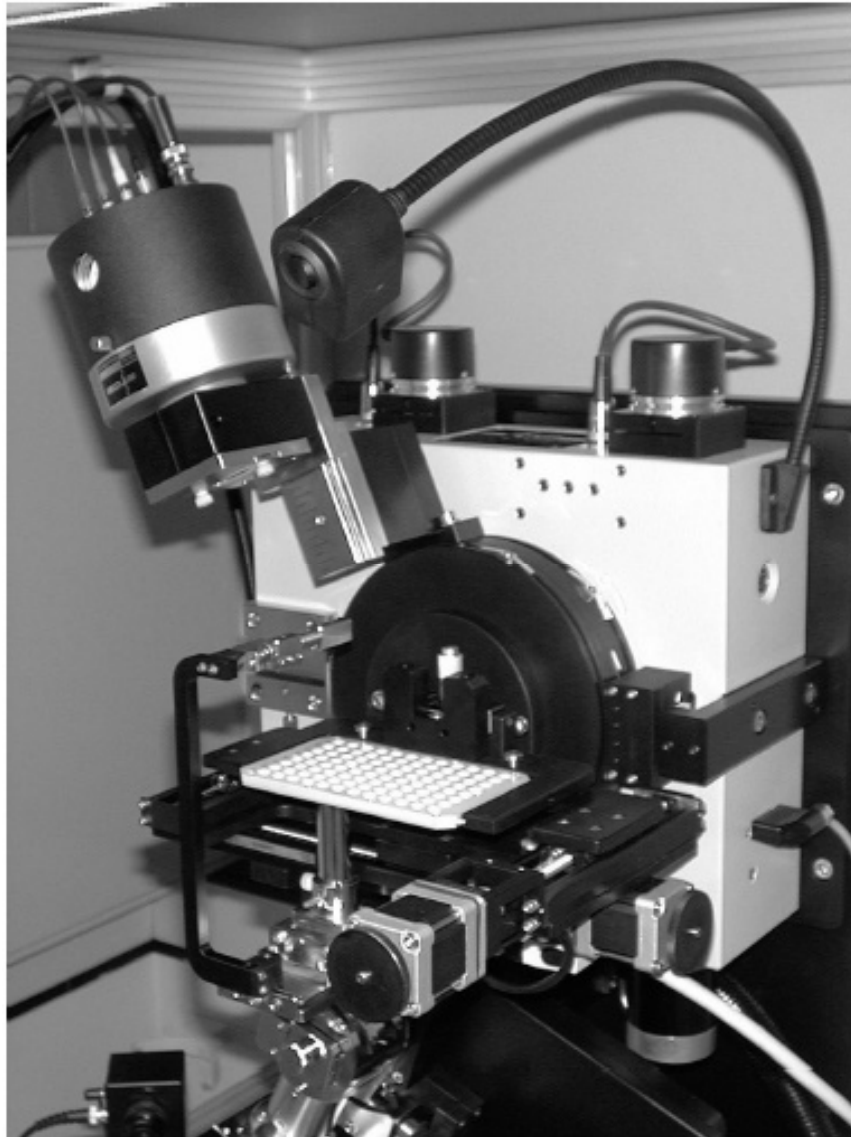


Figure 3.44 Photograph of a XRD diffractometer. (Courtesy of H&M Analytical Services.)



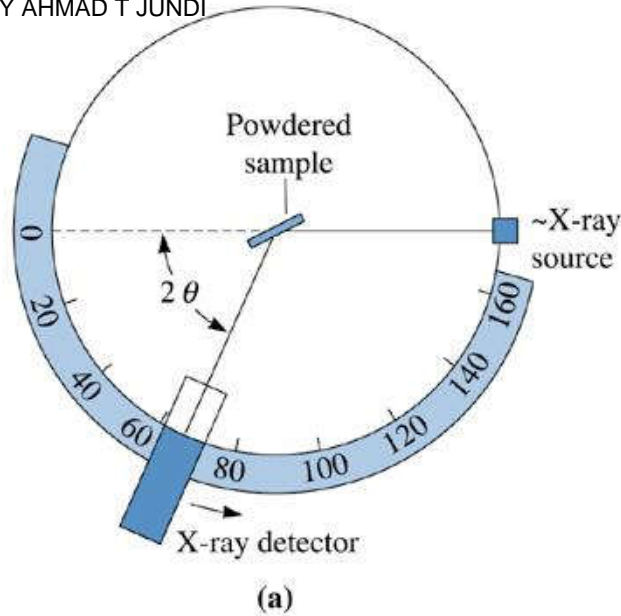
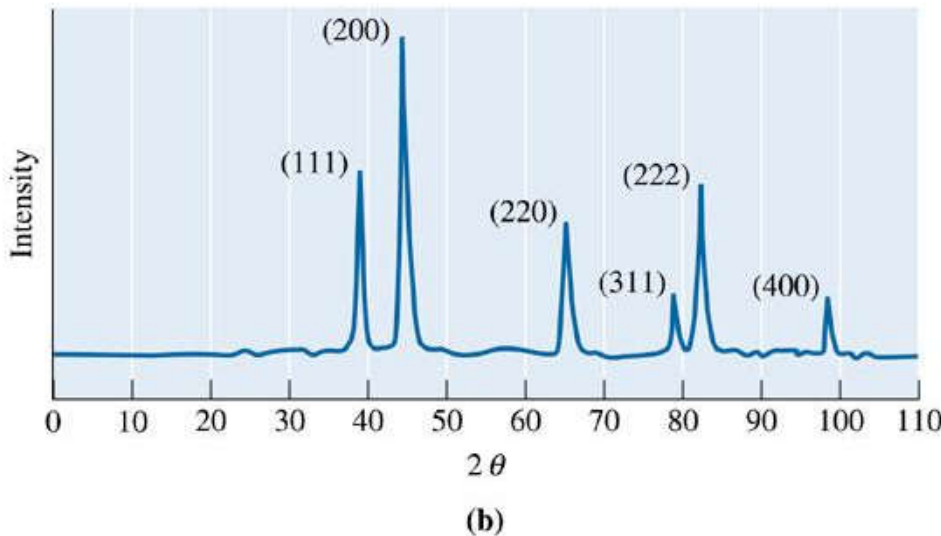


Figure 3.45 (a) Diagram of a diffractometer, showing powder sample, incident and diffracted beams. (b) The diffraction pattern obtained from a sample of gold powder.





Example 3.20

Examining X-ray Diffraction

The results of a x-ray diffraction experiment using x-rays with $\lambda = 0.7107 \text{ \AA}$ (a radiation obtained from molybdenum (Mo) target) show that diffracted peaks occur at the following 2θ angles:

Peak	2θ	Peak	2θ
1	20.20	5	46.19
2	28.72	6	50.90
3	35.36	7	55.28
4	41.07	8	59.42

Determine the crystal structure, the indices of the plane producing each peak, and the lattice parameter of the material.





Example 3.20 SOLUTION

We can first determine the $\sin^2 \theta$ value for each peak, then divide through by the lowest denominator, 0.0308.

Peak	2θ	$\sin^2 \theta$	$\sin^2 \theta / 0.0308$	$h^2 + k^2 + l^2$	(hkl)
1	20.20	0.0308	1	2	(110)
2	28.72	0.0615	2	4	(200)
3	35.36	0.0922	3	6	(211)
4	41.07	0.1230	4	8	(220)
5	46.19	0.1539	5	10	(310)
6	50.90	0.1847	6	12	(222)
7	55.28	0.2152	7	14	(321)
8	59.42	0.2456	8	16	(400)





Example 3.20 SOLUTION (Continued)

We could then use 2θ values for any of the peaks to calculate the interplanar spacing and thus the lattice parameter. Picking peak 8:

$$2\theta = 59.42 \text{ or } \theta = 29.71$$

$$d_{400} = \frac{\lambda}{2 \sin \theta} = \frac{0.7107}{2 \sin(29.71)} = 0.71699 \text{ \AA}$$

$$a_0 = d_{400} \sqrt{h^2 + k^2 + l^2} = (0.71699)(4) = 2.868 \text{ \AA}$$

This is the lattice parameter for body-centered cubic iron.



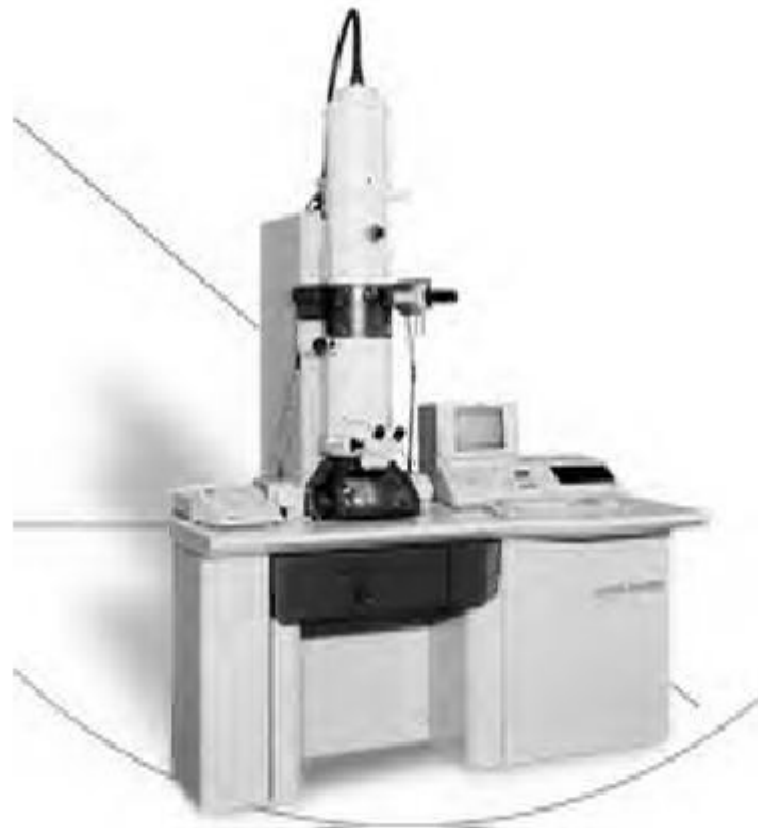


Figure 3.46 Photograph of a transmission electron microscope (TEM) used for analysis of the microstructure of materials. (Courtesy of JEOL USA, Inc.)



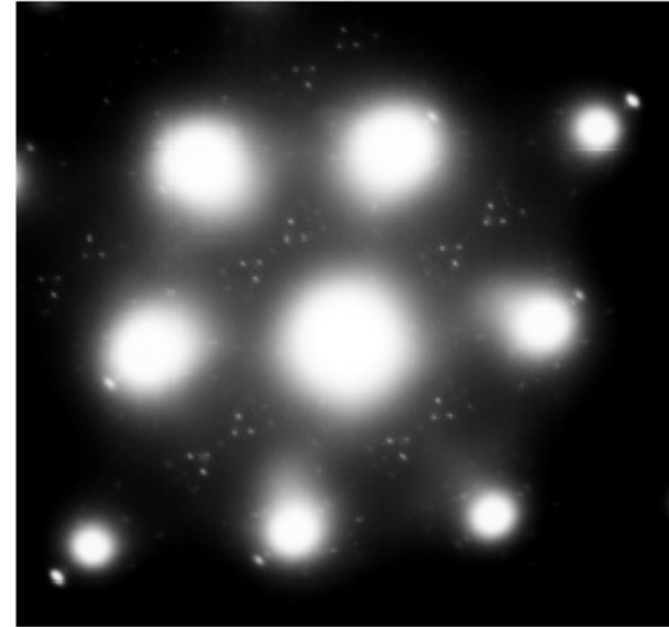
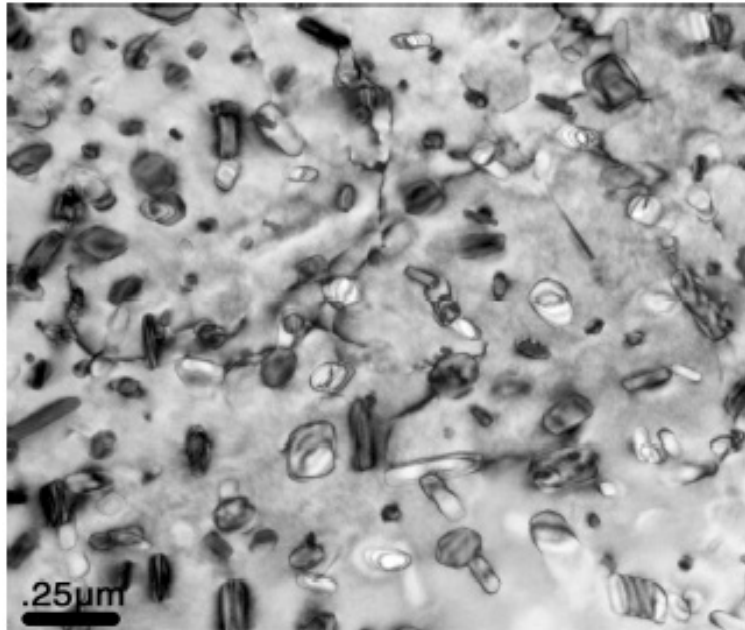


Figure 3.47 A TEM micrograph of an aluminum alloy (Al-7055) sample. The diffraction pattern at the right shows large bright spots that represent diffraction from the main aluminum matrix grains. The smaller spots originate from the nano-scale crystals of another compound that is present in the aluminum alloy. (Courtesy of Dr. Jörg M.K. Wiezorek, University of Pittsburgh.)





(c) 2003 Brooks/Cole Publishing / Thomson Learning

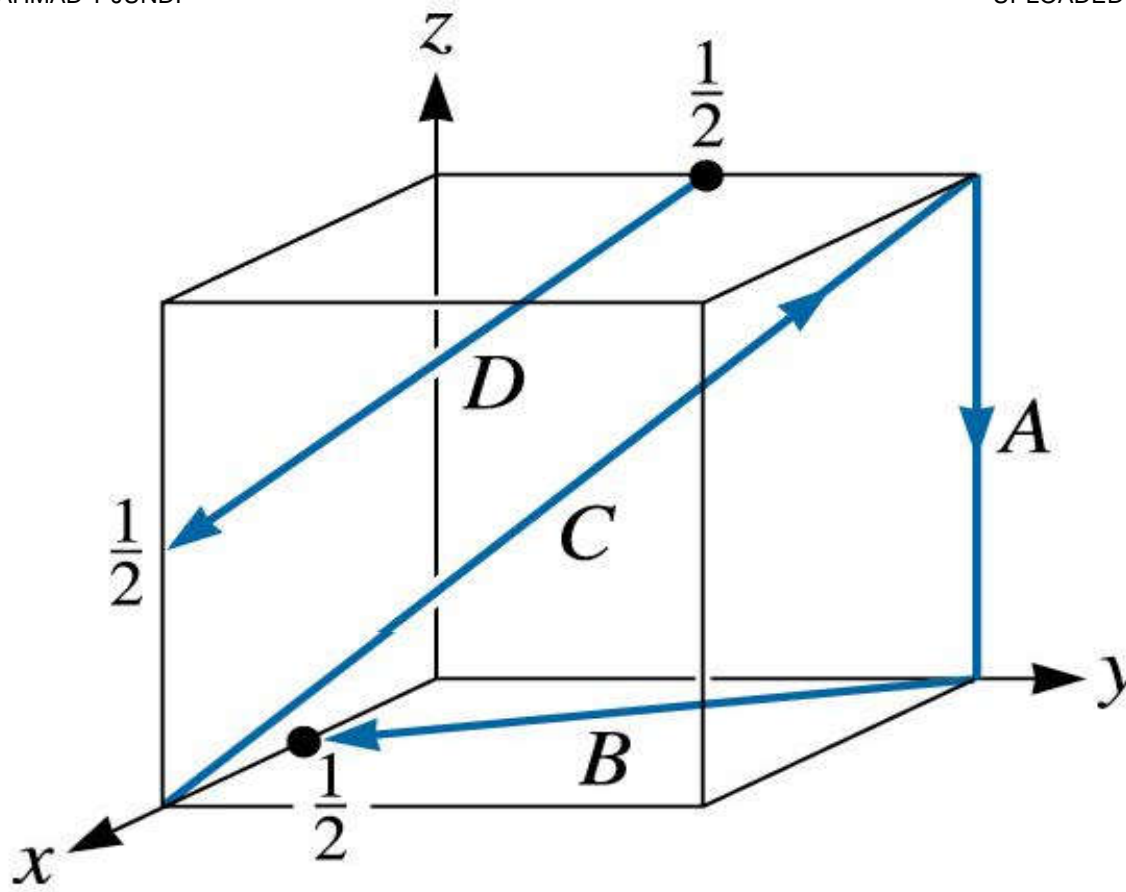


Figure 3.48 Directions in a cubic unit cell for Problem 3.51





(c) 2003 Brooks/Cole Publishing / Thomson Learning

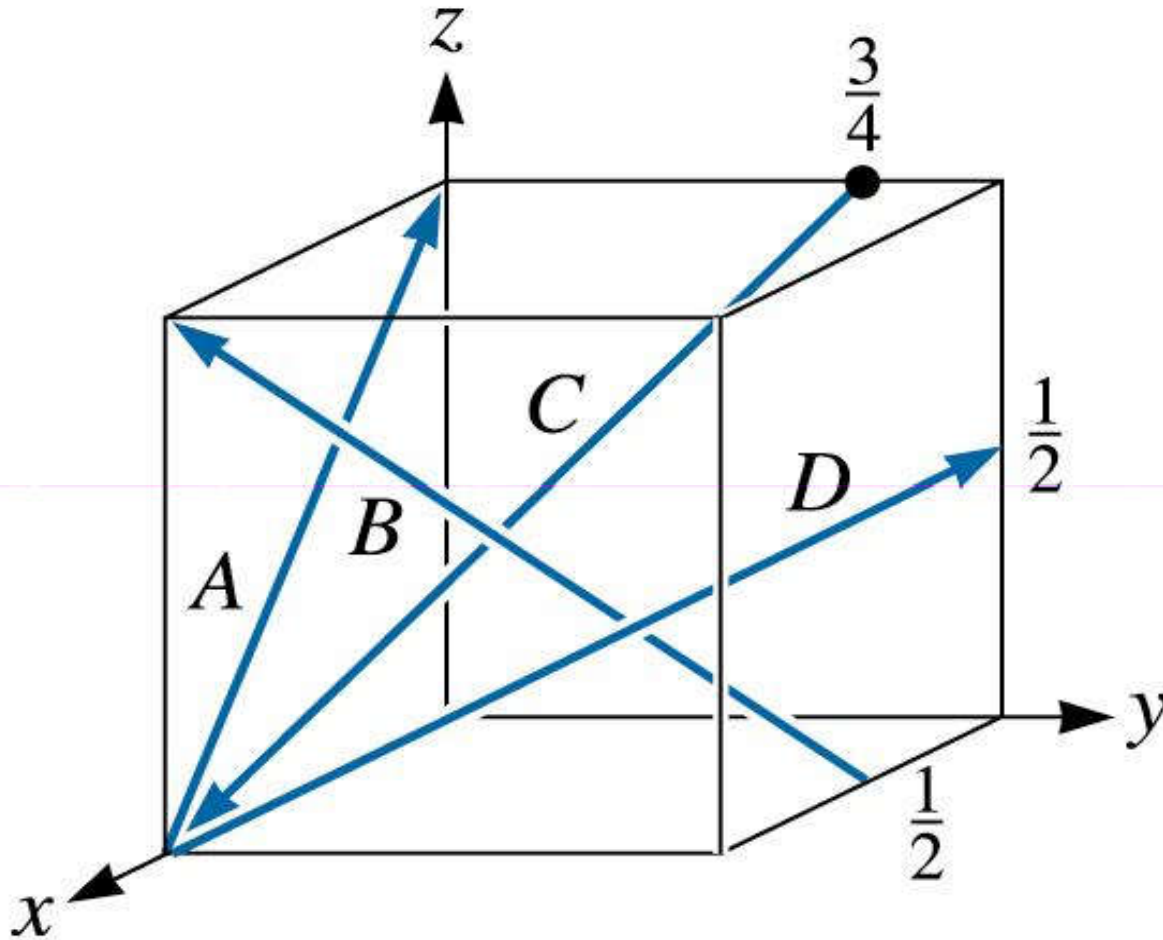


Figure 3.49
Directions in a cubic
unit cell for Problem
3.52.





(c) 2003 Brooks/Cole Publishing / Thomson Learning

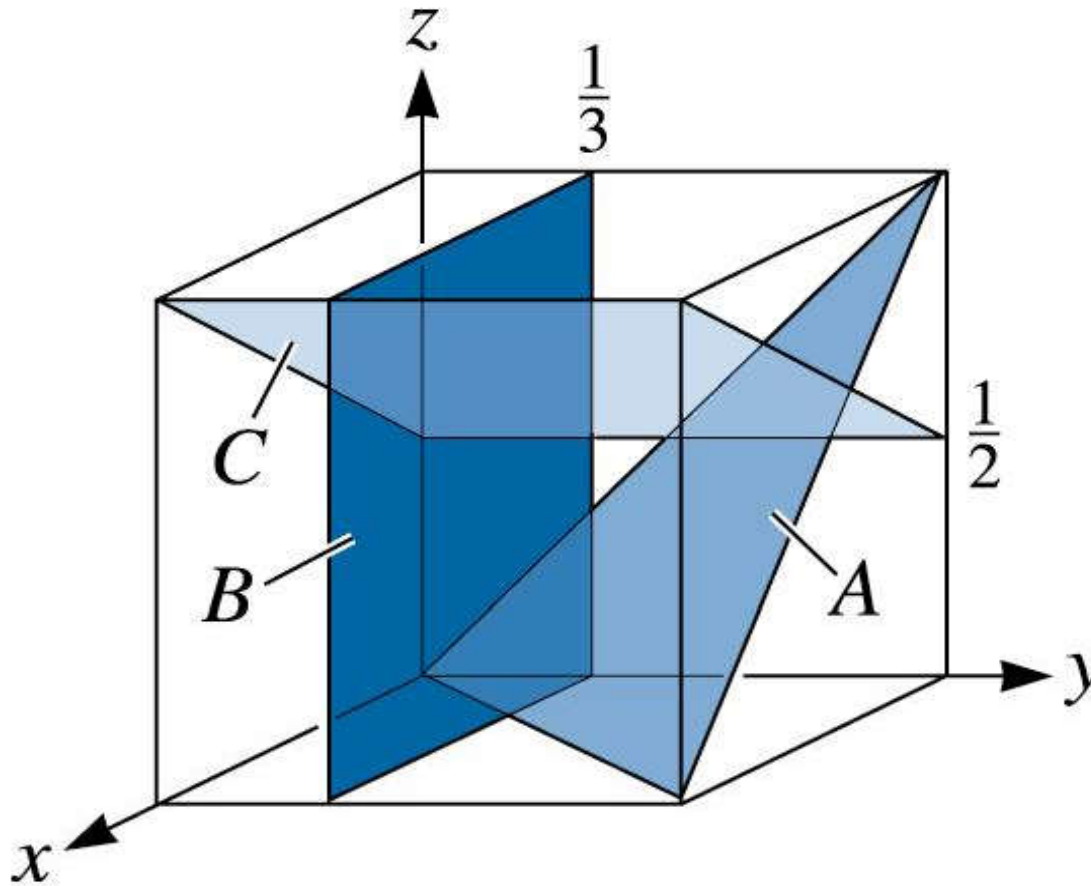


Figure 3.50 Planes in a cubic unit cell for Problem 3.53.

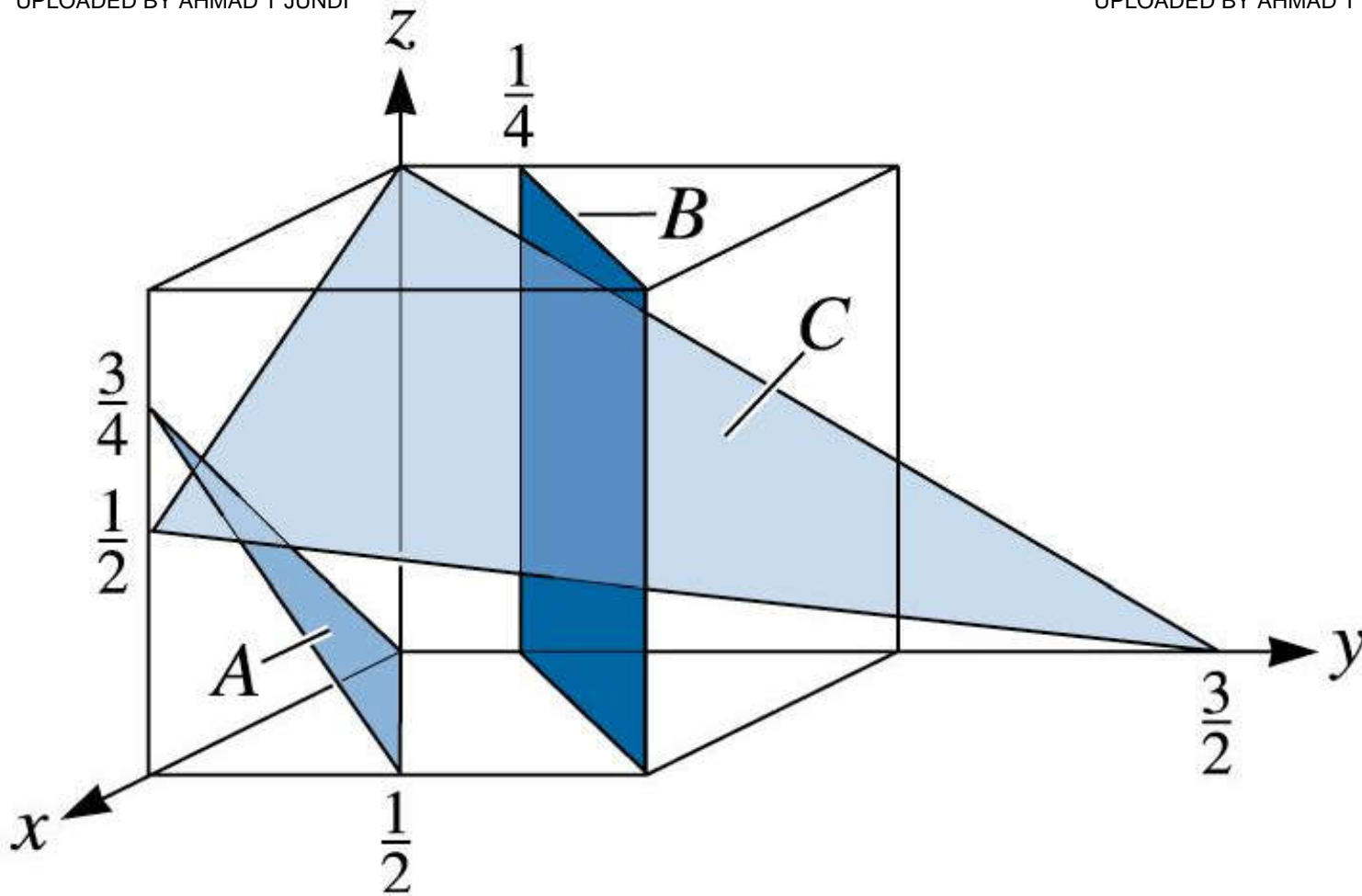


Figure 3.51 Planes in a cubic unit cell for Problem 3.54.



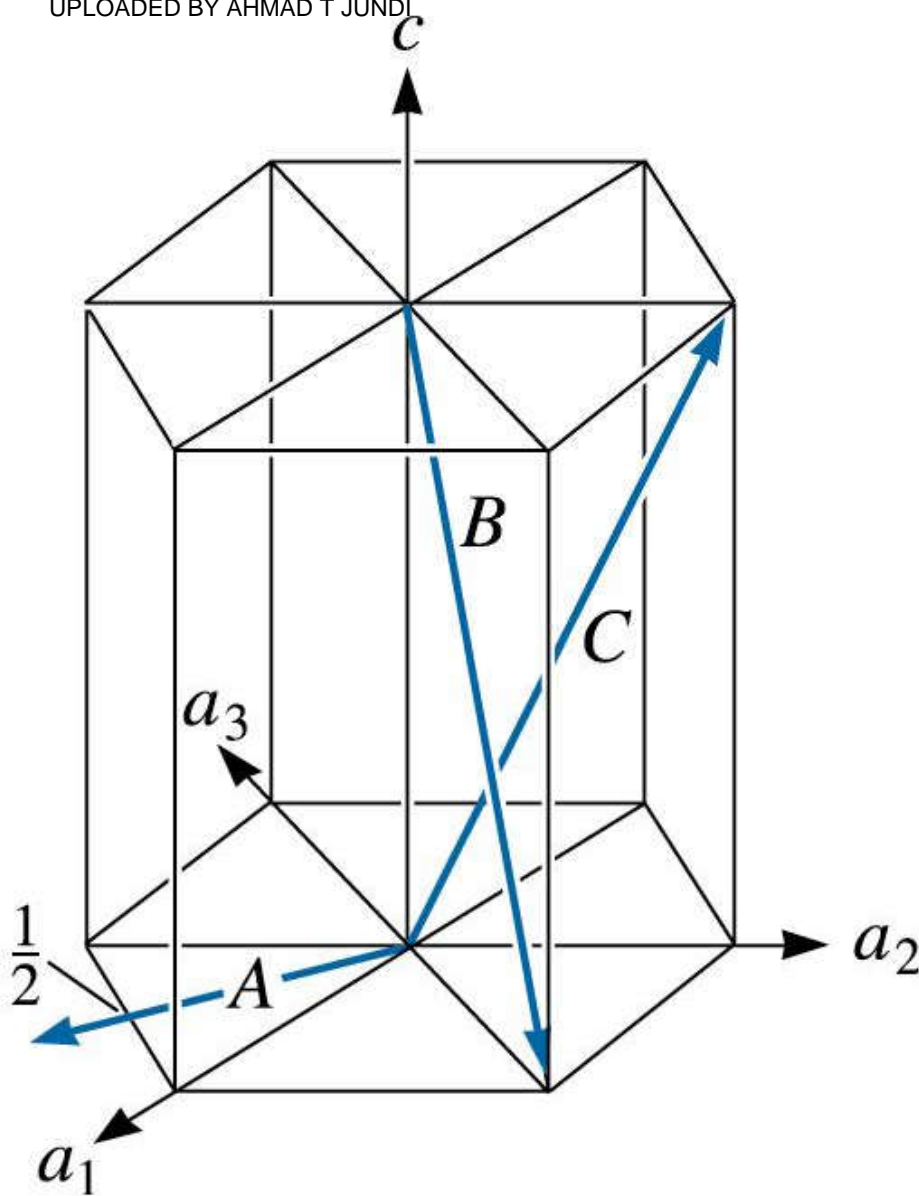


Figure 3.52
Directions in a
hexagonal lattice for
Problem 3.55.

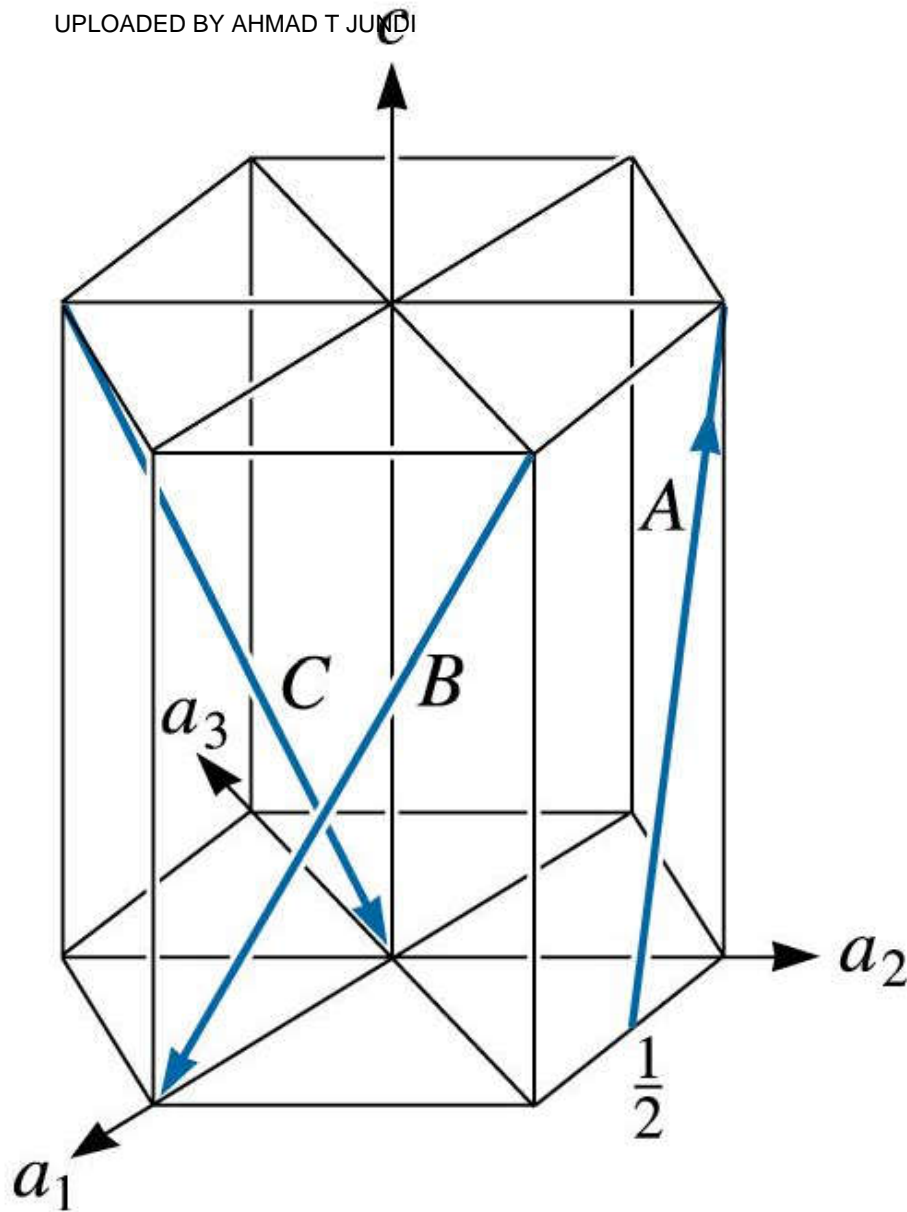


Figure 3.53 Directions in a hexagonal lattice for Problem 3.56.



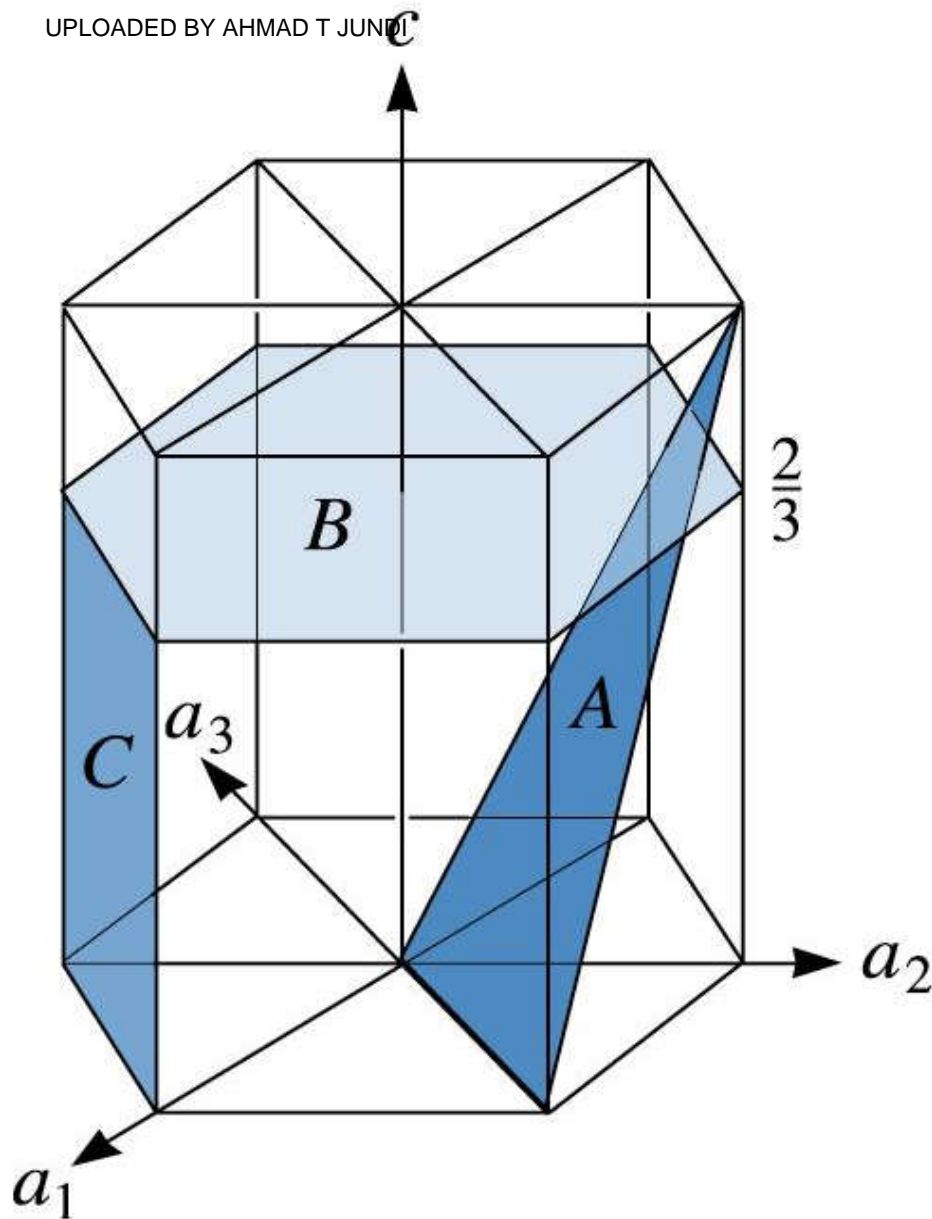


Figure 3.54 Planes in a hexagonal lattice for Problem 3.57.

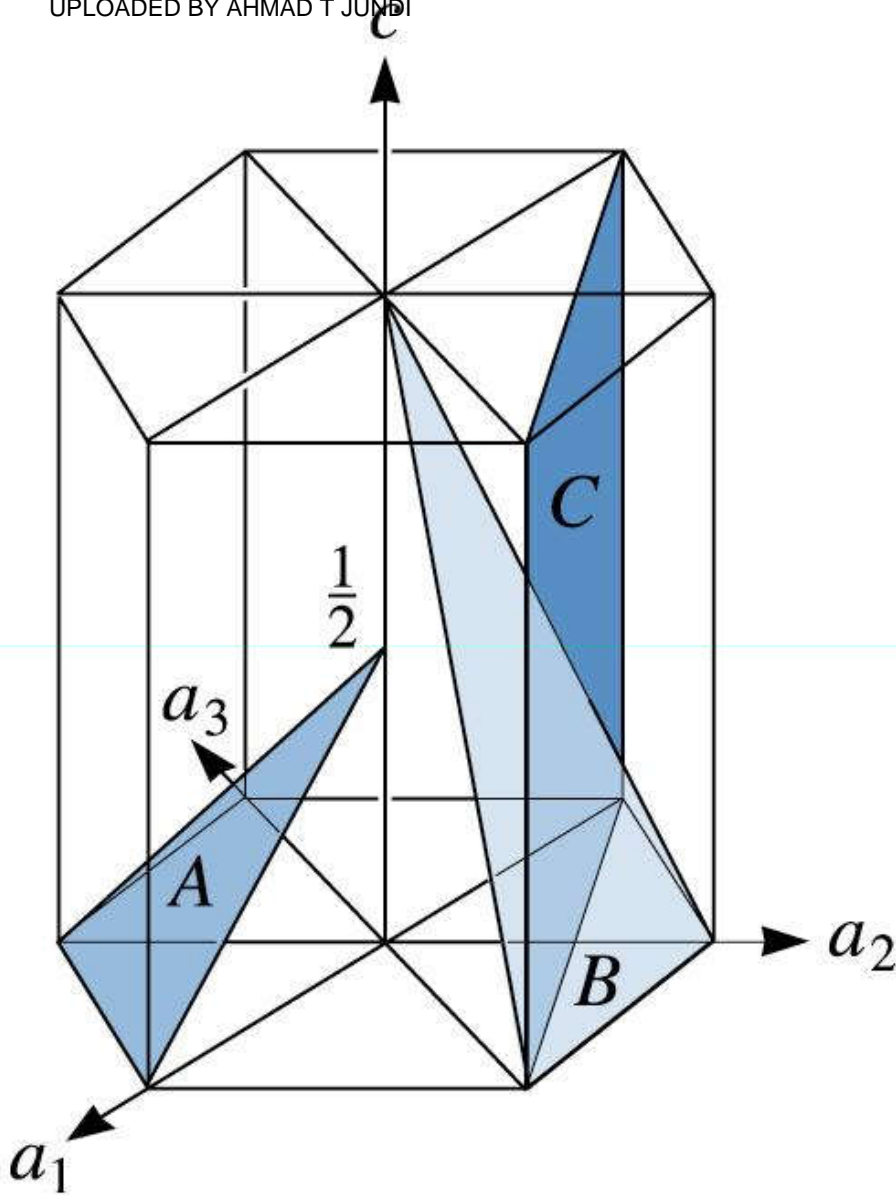


Figure 3.55 Planes in a hexagonal lattice for Problem 3.58.



(c) 2003 Brooks/Cole Publishing / Thomson Learning

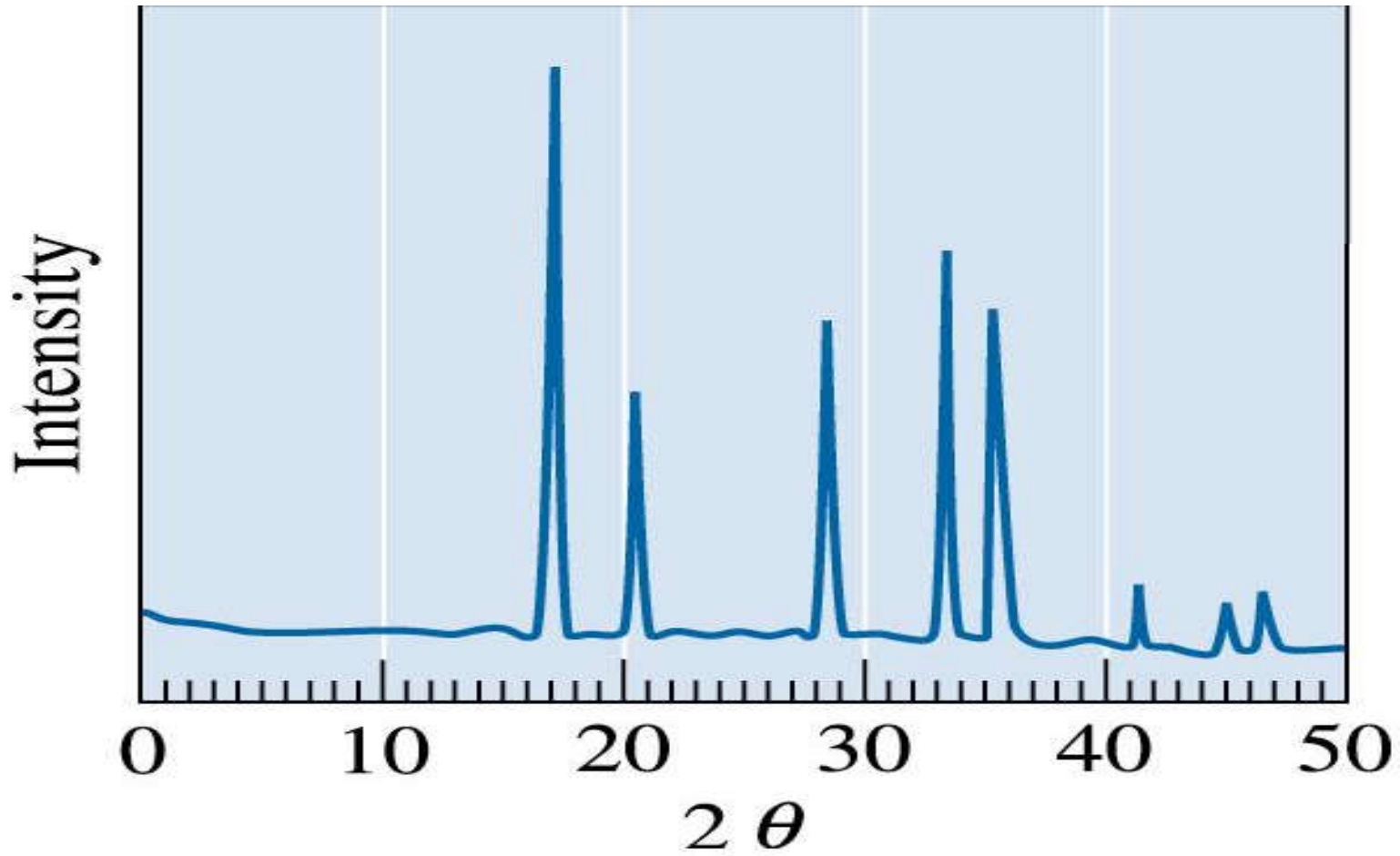


Figure 3.56 XRD pattern for Problem 3.107.





(c) 2003 Brooks/Cole Publishing / Thomson Learning

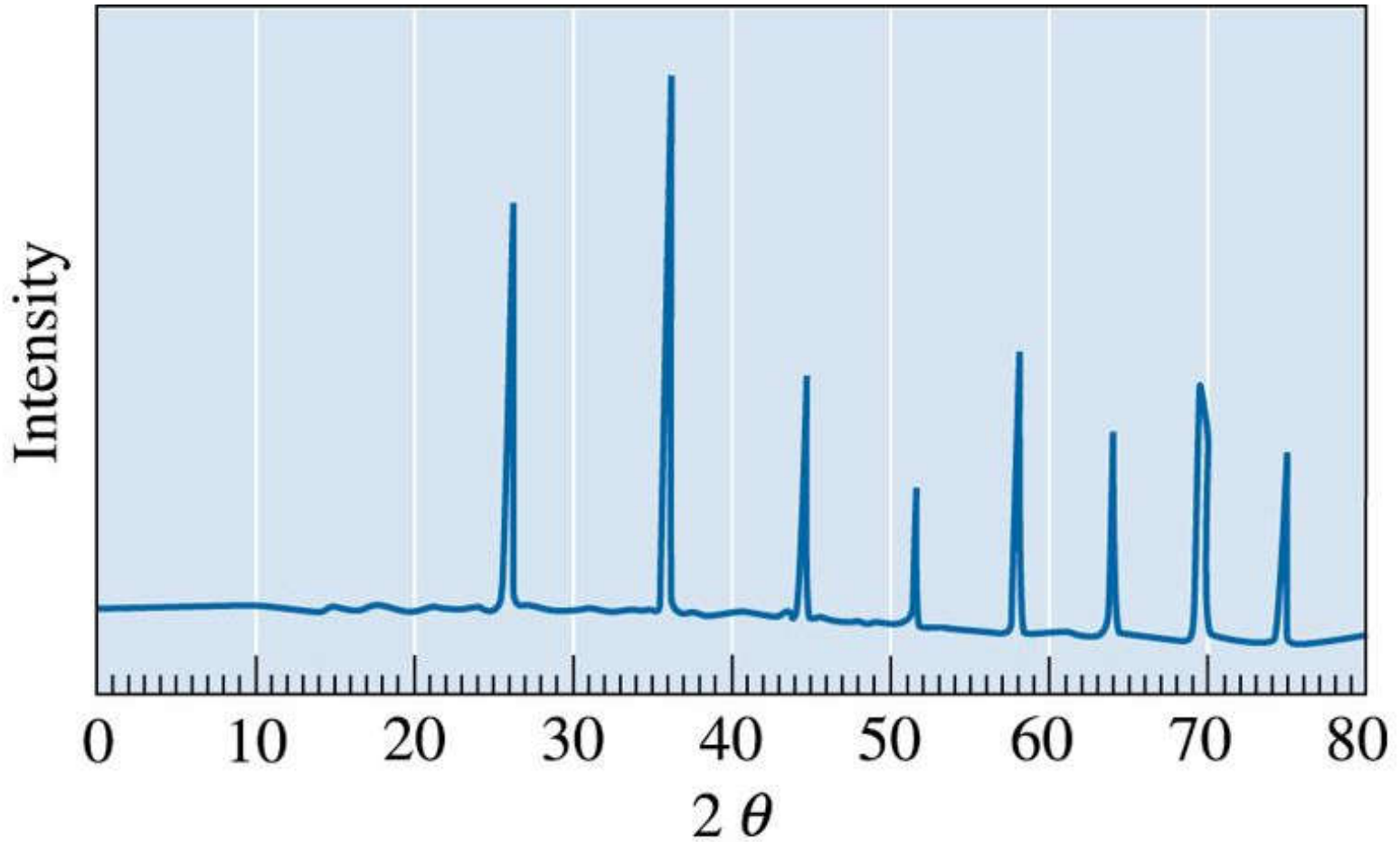


Figure 3.57 XRD pattern for Problem 3.108.



The Science and Engineering of Materials, 4th ed

Donald R. Askeland – Pradeep P. Phulé

Chapter 4 – Imperfections in the Atomic and Ionic Arrangements





Objectives of Chapter 4

- Introduce the three basic types of imperfections: point defects, line defects (or dislocations), and surface defects.
- Explore the nature and effects of different types of defects.





Chapter Outline

- 4.1 Point Defects
- 4.2 Other Point Defects
- 4.3 Dislocations
- 4.4 Observing Dislocations
- 4.5 Significance of Dislocations
- 4.6 Schmid's Law
- 4.7 Influence of Crystal Structure
- 4.8 Surface Defects
- 4.9 Importance of Defects



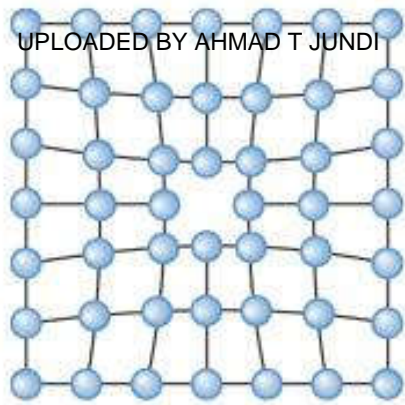


Section 4.1

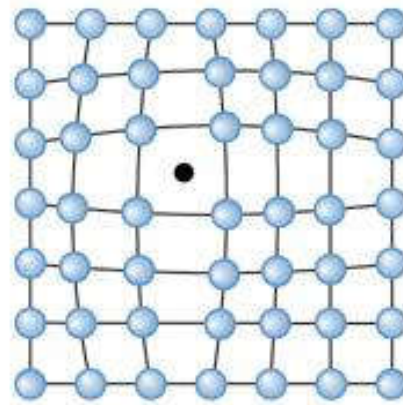
Point Defects

- **Point defects** - Imperfections, such as vacancies, that are located typically at one (in some cases a few) sites in the crystal.
- **Extended defects** - Defects that involve several atoms/ions and thus occur over a finite volume of the crystalline material (e.g., dislocations, stacking faults, etc.).
- **Vacancy** - An atom or an ion missing from its regular crystallographic site.
- **Interstitial defect** - A point defect produced when an atom is placed into the crystal at a site that is normally not a lattice point.
- **Substitutional defect** - A point defect produced when an atom is removed from a regular lattice point and replaced with a different atom, usually of a different size.

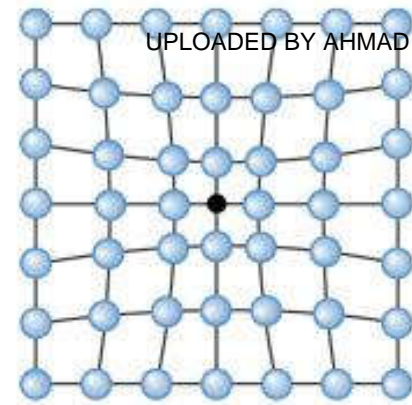




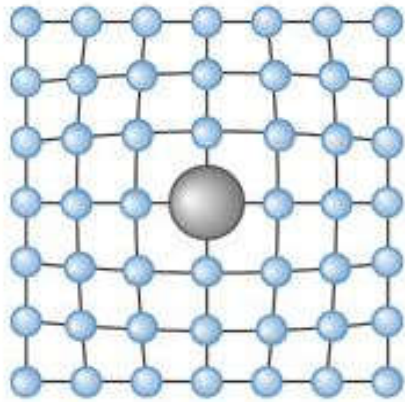
(a)



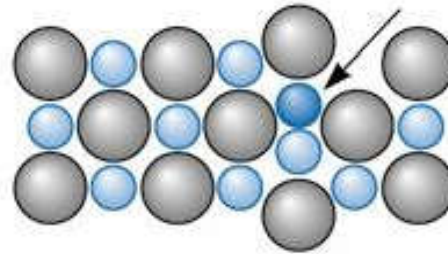
(b)



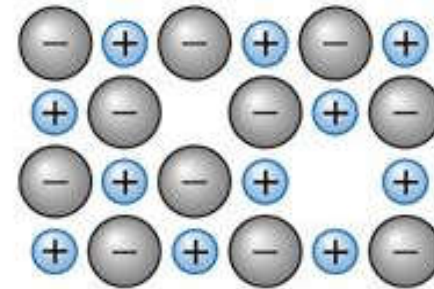
(c)



(d)



(e)



(f)

Figure 4.1 Point defects: (a) vacancy, (b) interstitial atom, (c) small substitutional atom, (d) large substitutional atom, (e) Frenkel defect, (f) Schottky defect. All of these defects disrupt the perfect arrangement of the surrounding atoms.



Example 4.1

The Effect of Temperature on Vacancy Concentrations

Calculate the concentration of vacancies in copper at room temperature (25°C). What temperature will be needed to heat treat copper such that the concentration of vacancies produced will be 1000 times more than the equilibrium concentration of vacancies at room temperature? Assume that 20,000 cal are required to produce a mole of vacancies in copper.

Example 4.1 SOLUTION

The lattice parameter of FCC copper is 0.36151 nm. The basis is 1, therefore, the number of copper atoms, or lattice points, per cm³ is:

$$n = \frac{4 \text{ atoms/cell}}{(3.6151 \times 10^{-8} \text{ cm})^3} = 8.47 \times 10^{22} \text{ copper atoms/cm}^3$$



Example 4.1 SOLUTION (Continued)

UPLOADED BY AHMAD T JUNDI

UPLOADED BY AHMAD T JUNDI



At room temperature, $T = 25 + 273 = 298 \text{ K}$:

$$\begin{aligned}n_v &= n \exp\left(\frac{Q_v}{RT}\right) \\&= \left(8.47 \times 10^{22} \frac{\text{atoms}}{\text{cm}^3}\right) \cdot \exp\left(\frac{-20,000 \frac{\text{cal}}{\text{mol}}}{1.987 \frac{\text{cal}}{\text{mol} \cdot \text{K}} \times 298\text{K}}\right) \\&= 1.815 \times 10^8 \text{ vacancies/cm}^3\end{aligned}$$

We could do this by heating the copper to a temperature at which this number of vacancies forms:

$$\begin{aligned}n_v &= 1.815 \times 10^{11} = n \exp\left(\frac{Q_v}{RT}\right) \\&= (8.47 \times 10^{22}) \exp(-20,000 / (1.987 \times T)), \quad T = 102^\circ \text{C}\end{aligned}$$





Example 4.2

Vacancy Concentrations in Iron

Determine the number of vacancies needed for a BCC iron crystal to have a density of 7.87 g/cm^3 . The lattice parameter of the iron is $2.866 \times 10^{-8} \text{ cm}$.

Example 4.2 SOLUTION

The expected theoretical density of iron can be calculated from the lattice parameter and the atomic mass.

$$\rho = \frac{(2 \text{ atoms/cell})(55.847 \text{ g/mol})}{(2.866 \times 10^{-8} \text{ cm})^3 (6.02 \times 10^{23} \text{ atoms/mol})} = 7.8814 \text{ g/cm}^3$$





Example 4.2 SOLUTION (Continued)

Let's calculate the number of iron atoms and vacancies that would be present in each unit cell for the required density of 7.87 g/cm³:

$$\rho = \frac{(X \text{ atoms/cell})(55.847 \text{ g/mol})}{(2.866 \times 10^{-8} \text{ cm})^3 (6.02 \times 10^{23} \text{ atoms/mol})} = 7.87 \text{ g/cm}^3$$

$$X \text{ atoms/cell} = \frac{(7.87)(2.866 \times 10^{-8})^3 (6.02 \times 10^{23})}{55.847} = 1.9971$$

Or, there should be 2.00 - 1.9971 = 0.0029 vacancies per unit cell. The number of vacancies per cm³ is:

$$\text{Vacancies/cm}^3 = \frac{0.0029 \text{ vacancies/cell}}{(2.866 \times 10^{-8} \text{ cm})^3} = 1.23 \times 10^{20}$$





Example 4.3

Sites for Carbon in Iron

In FCC iron, carbon atoms are located at *octahedral* sites at the center of each edge of the unit cell $(1/2, 0, 0)$ and at the center of the unit cell $(1/2, 1/2, 1/2)$. In BCC iron, carbon atoms enter tetrahedral sites, such as $1/4, 1/2, 0$. The lattice parameter is 0.3571 nm for FCC iron and 0.2866 nm for BCC iron. Assume that carbon atoms have a radius of 0.071 nm. (1) Would we expect a greater distortion of the crystal by an interstitial carbon atom in FCC or BCC iron? (2) What would be the atomic percentage of carbon in each type of iron if all the interstitial sites were filled?



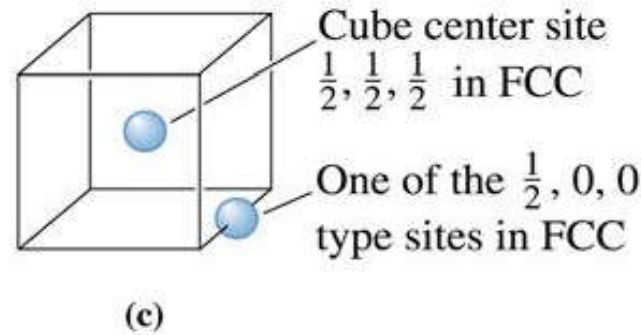
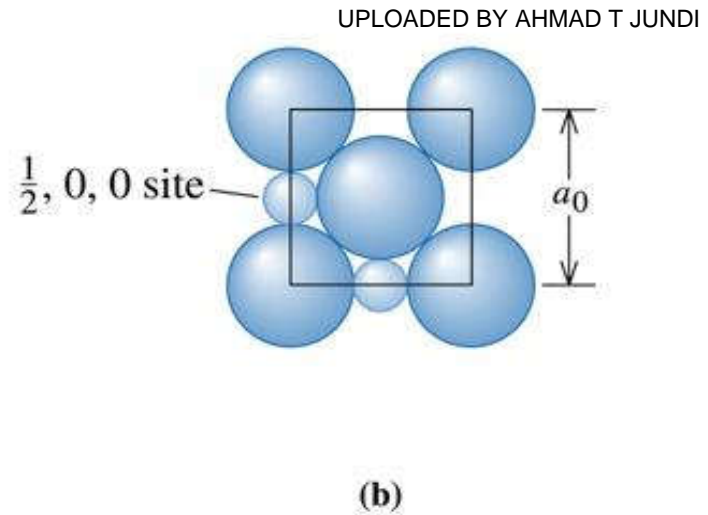
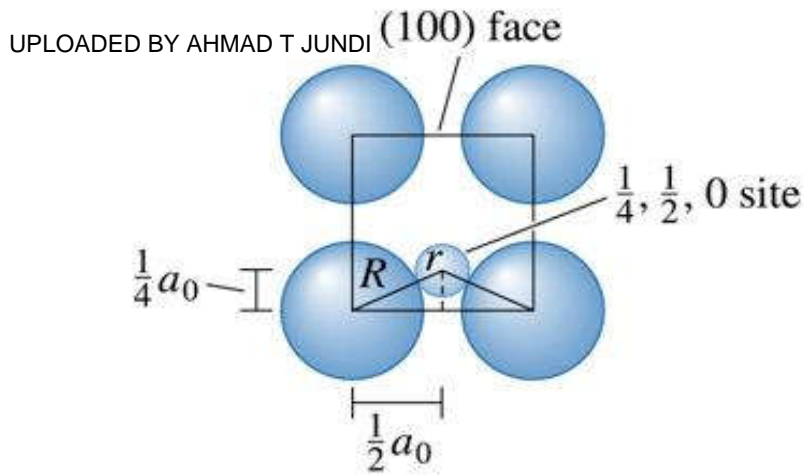


Figure 4.2 (a) The location of the $\frac{1}{4}, \frac{1}{2}, 0$ interstitial site in BCC metals, showing the arrangement of the normal atoms and the interstitial atom (b) $\frac{1}{2}, 0, 0$ site in FCC metals, (for Example 4.3). (c) Edge centers and cube centers are some of the interstitial sites in the FCC structure (Example 4.3).

(c) 2003 Brooks/Cole Publishing / Thomson Learning



Example 4.3 SOLUTION

1. We could calculate the size of the interstitial site at the 1/4, 1/2, 0 location with the help of Figure 4.2(a). The radius R_{BCC} of the iron atom is:

$$R_{\text{BCC}} = \frac{\sqrt{3}a_0}{4} = \frac{(\sqrt{3})(0.2866)}{4} = 0.1241 \text{ nm}$$

From Figure 4.2(a), we find that:

$$\left(\frac{1}{2}a_0\right)^2 + \left(\frac{1}{4}a_0\right)^2 = (r_{\text{interstitial}} + R_{\text{BCC}})^2$$

$$r_{\text{interstitial}} = \sqrt{0.02567} - 0.1241 = 0.0361 \text{ nm}$$

For FCC iron, the interstitial site such as the 1/2, 0, 0 lies along $\langle 100 \rangle$ directions. Thus, the radius of the iron atom and the radius of the interstitial site are [Figure 4.2(b)]:





Example 4.3 SOLUTION (Continued)

$$R_{\text{FCC}} = \frac{\sqrt{2}a_0}{4} = \frac{(\sqrt{2})(0.3571)}{4} = 0.1263 \text{ nm}$$

$$2r_{\text{interstitial}} + 2R_{\text{FCC}} = a_0$$

$$r_{\text{interstitial}} = \frac{0.3571 - (2)(0.1263)}{2} = 0.0522 \text{ nm}$$

The interstitial site in the BCC iron is smaller than the interstitial site in the FCC iron. Although both are smaller than the carbon atom, carbon distorts the BCC crystal structure more than the FCC crystal. As a result, fewer carbon atoms are expected to enter interstitial positions in BCC iron than in FCC iron.





Example 4.3 SOLUTION (Continued)

2. We can find a total of 24 interstitial sites of the type $1/4$, $1/2$, 0 ; however, since each site is located at a face of the unit cell, only half of each site belongs uniquely to a single cell. Thus:

$$(24 \text{ sites})(1/2) = 12 \text{ interstitial sites per unit cell}$$

Atomic percentage of carbon in BCC iron would be:

$$\text{at \% C} = \frac{12 \text{ C atoms}}{12 \text{ C atoms} + 2 \text{ Fe atoms}} \times 100 = 86\%$$

In FCC iron, the number of octahedral interstitial sites is:

$$(12 \text{ edges}) (1/4) + 1 \text{ center} = 4 \text{ interstitial sites per unit cell}$$

Atomic percentage of carbon in BCC iron would be:

$$\text{at \% C} = \frac{4 \text{ C atoms}}{4 \text{ C atoms} + 4 \text{ Fe atoms}} \times 100 = 50\%$$





Dopants in Germanium Semiconductor

Three separate samples of germanium (Ge) crystals contain small concentrations of either silicon (Si), arsenic (As), or boron (B) as dopants. Based on the valence of these elements, what type of semiconductivity is expected from these materials? Assume that these elements will occupy Ge sites.

Example 4.4 SOLUTION

When Si is added to Ge, silicon atoms can form four bonds with neighboring Ge atoms. As a result, there is no need to donate or accept an electron. The resultant material then does not show either “*n*-type” or “*p*-type” conductivity.

When we add As, we expect *n*-type conductivity since each As atom brings in five valence electrons.

When we add small concentrations of B to Ge we expect *p*-type conductivity for the resultant material, since B has a valence of 3.



Section 4.2

Other Point Defects

- **Interstitialcy** - A point defect caused when a “normal” atom occupies an interstitial site in the crystal.
- **Frenkel defect** - A pair of point defects produced when an ion moves to create an interstitial site, leaving behind a vacancy.
- **Schottky defect** - A point defect in ionically bonded materials. In order to maintain a neutral charge, a stoichiometric number of cation and anion vacancies must form.
- **Kröger-Vink notation** - A system used to indicate point defects in materials. The main body of the notation indicates the type of defect or the element involved.



(c) 2003 Brooks/Cole Publishing / Thomson Learning

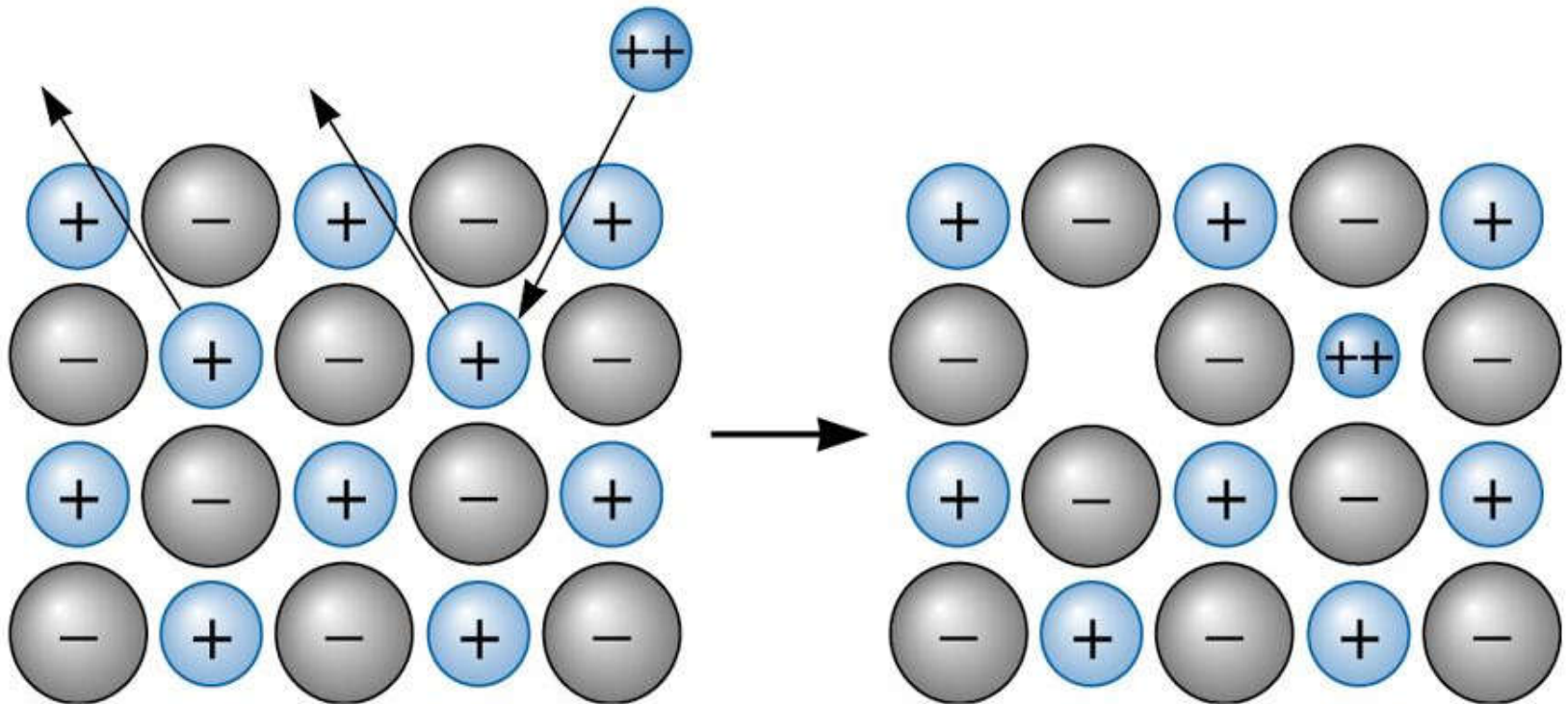


Figure 4.3 When a divalent cation replaces a monovalent cation, a second monovalent cation must also be removed, creating a vacancy.





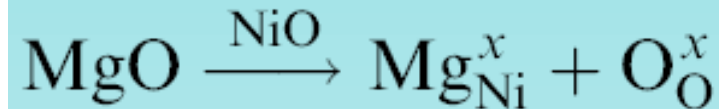
Example 4.5

Application of the Kröger-Vink Notation

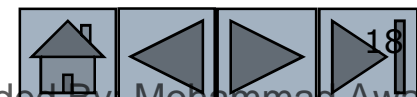
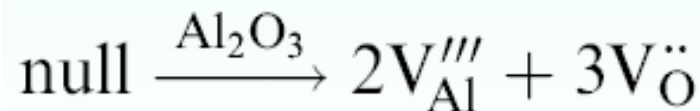
Write the appropriate defect reactions for (1) incorporation of magnesium oxide (MgO) in nickel oxide (NiO), and (2) formation of a Schottky defect in alumina (Al₂O₃).

Example 4.5 SOLUTION

1. MgO is the guest and NiO is the host material. We will assume that Mg⁺² ions will occupy Ni⁺² sites and oxygen anions from MgO will occupy O⁻² sites of NiO.



2. Thus V_{Al}''' describes one vacancy of an Al⁺³. Similarly, $V_{\text{O}}\ddot{}$ represents an oxygen ion vacancy.



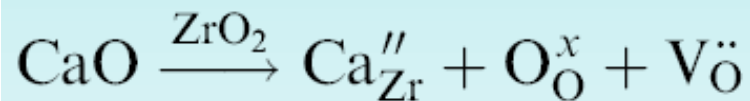


Point Defects in Stabilized Zirconia for Solid Electrolytes

Write the appropriate defect reactions for the incorporation of calcium oxide (CaO) in zirconia (ZrO₂) using the Kröger-Vink notation.

Example 4.6 SOLUTION

We will assume that Ca⁺² will occupy Zr⁺⁴ sites. If we send one Ca⁺² to Zr⁺⁴, the site will have an effective negative charge of -2 (instead of having a charge of +4 we have a charge of +2). We have used one Zr⁺⁴ site and site balance would require us to utilize *two oxygen sites*. We can send one O⁻² from CaO to one of the O⁻² sites in ZrO₂. The other oxygen site must be used and since mass balance must also be maintained we will have to keep this site vacant.





Section 4.3 Dislocations

- **Dislocation** - A line imperfection in a crystalline material.
- **Screw dislocation** - A dislocation produced by skewing a crystal so that one atomic plane produces a spiral ramp about the dislocation.
- **Edge dislocation** - A dislocation introduced into the crystal by adding an "extra half plane" of atoms.
- **Mixed dislocation** - A dislocation that contains partly edge components and partly screw components.
- **Slip** - Deformation of a metallic material by the movement of dislocations through the crystal.





© 2003 Brooks/Cole Publishing / Thomson Learning

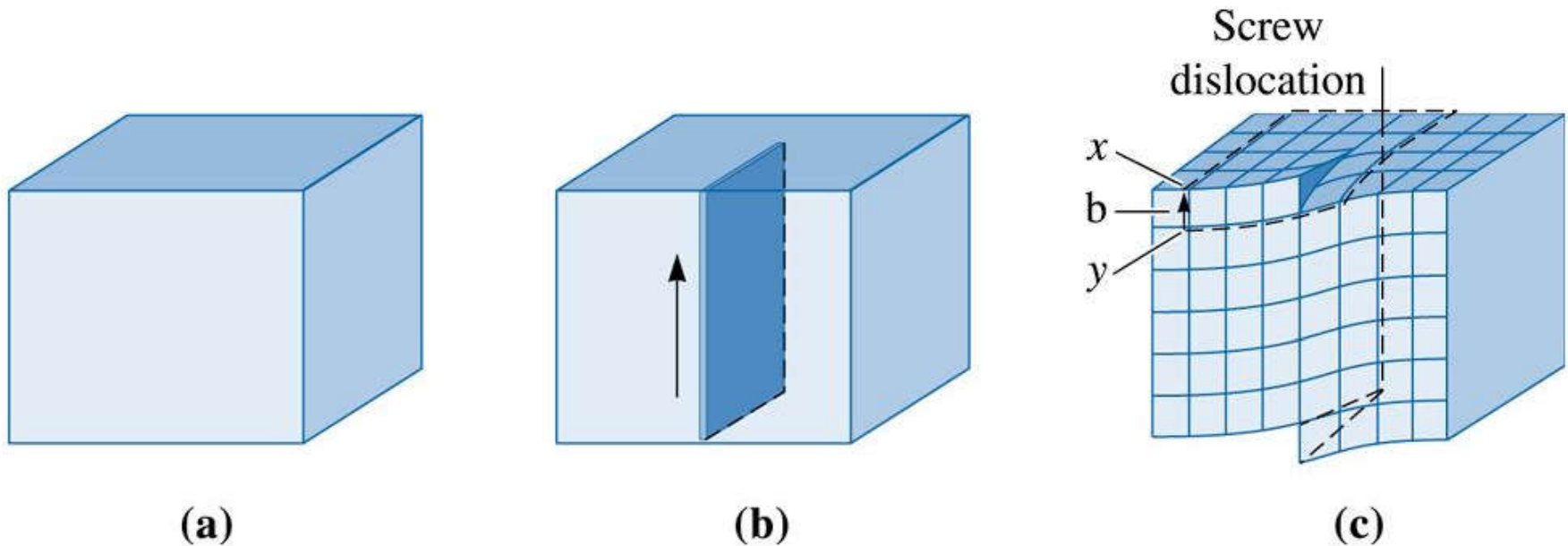


Figure 4.4 the perfect crystal (a) is cut and sheared one atom spacing, (b) and (c). The line along which shearing occurs is a screw dislocation. A Burgers vector b is required to close a loop of equal atom spacings around the screw dislocation.



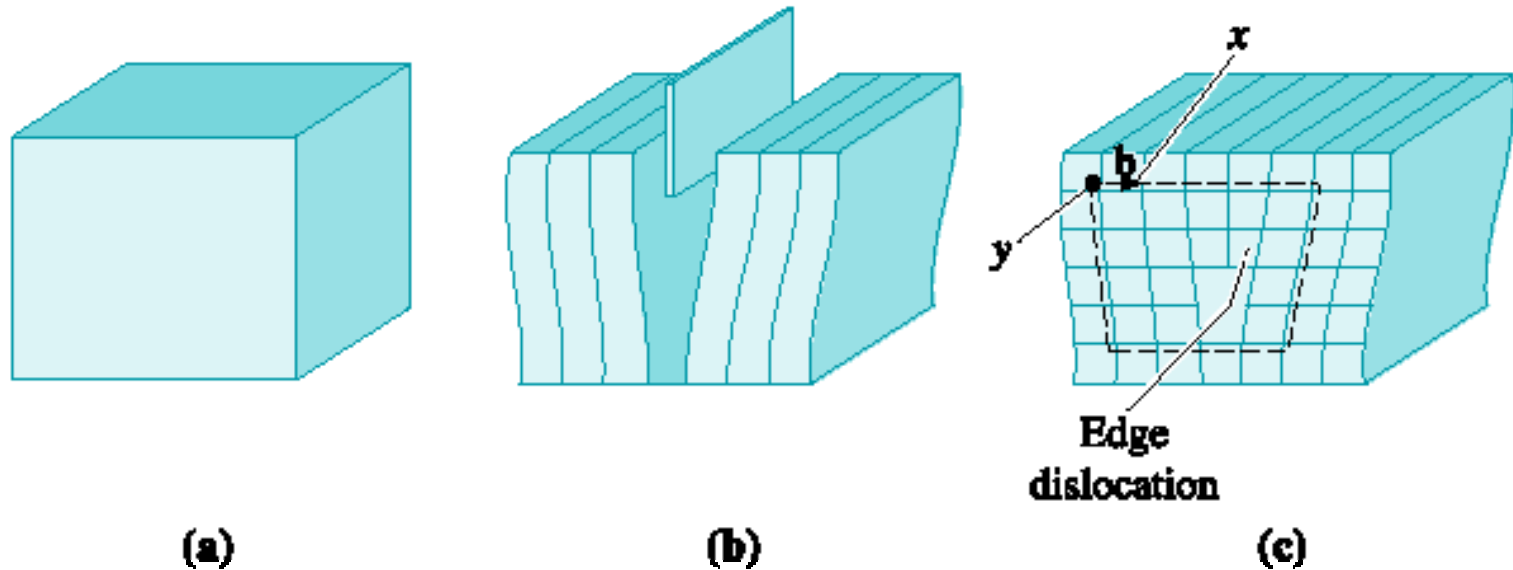


Figure 4.5 The perfect crystal in (a) is cut and an extra plane of atoms is inserted (b). The bottom edge of the extra plane is an edge dislocation (c). A Burgers vector b is required to close a loop of equal atom spacings around the edge dislocation. (*Adapted from J.D. Verhoeven, Fundamentals of Physical Metallurgy, Wiley, 1975.*)

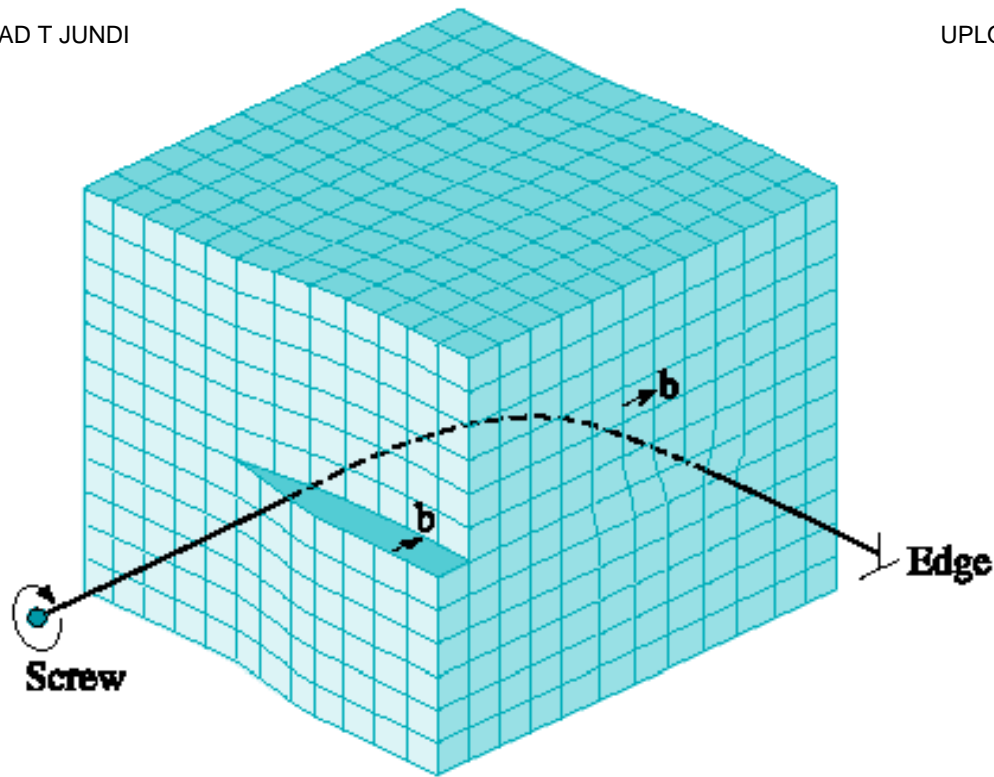


Figure 4.6 A mixed dislocation. The screw dislocation at the front face of the crystal gradually changes to an edge dislocation at the side of the crystal. (Adapted from W.T. Read, Dislocations in Crystals. McGraw-Hill, 1953.)

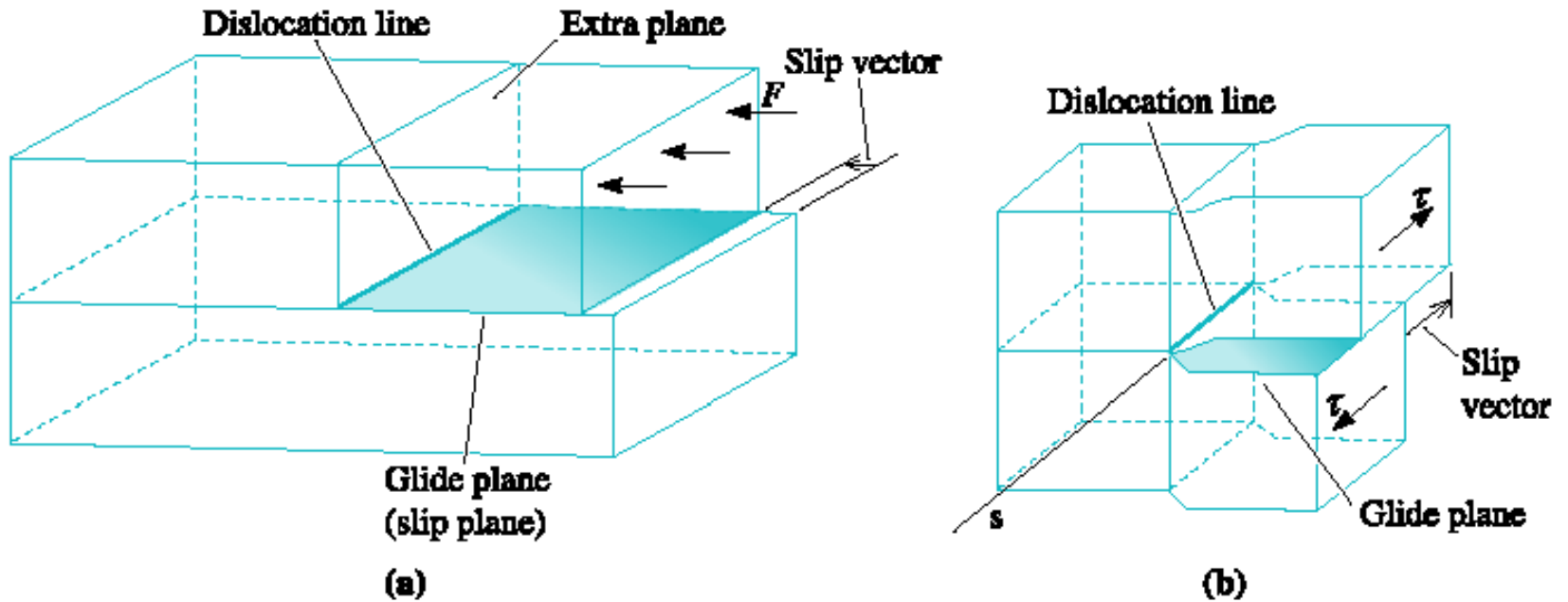


Figure 4.7 Schematic of slip line, slip plane, and slip (Burgers) vector for (a) an edge dislocation and (b) for a screw dislocation. (Adapted from J.D. Verhoeven, Fundamentals of Physical Metallurgy, Wiley, 1975.)

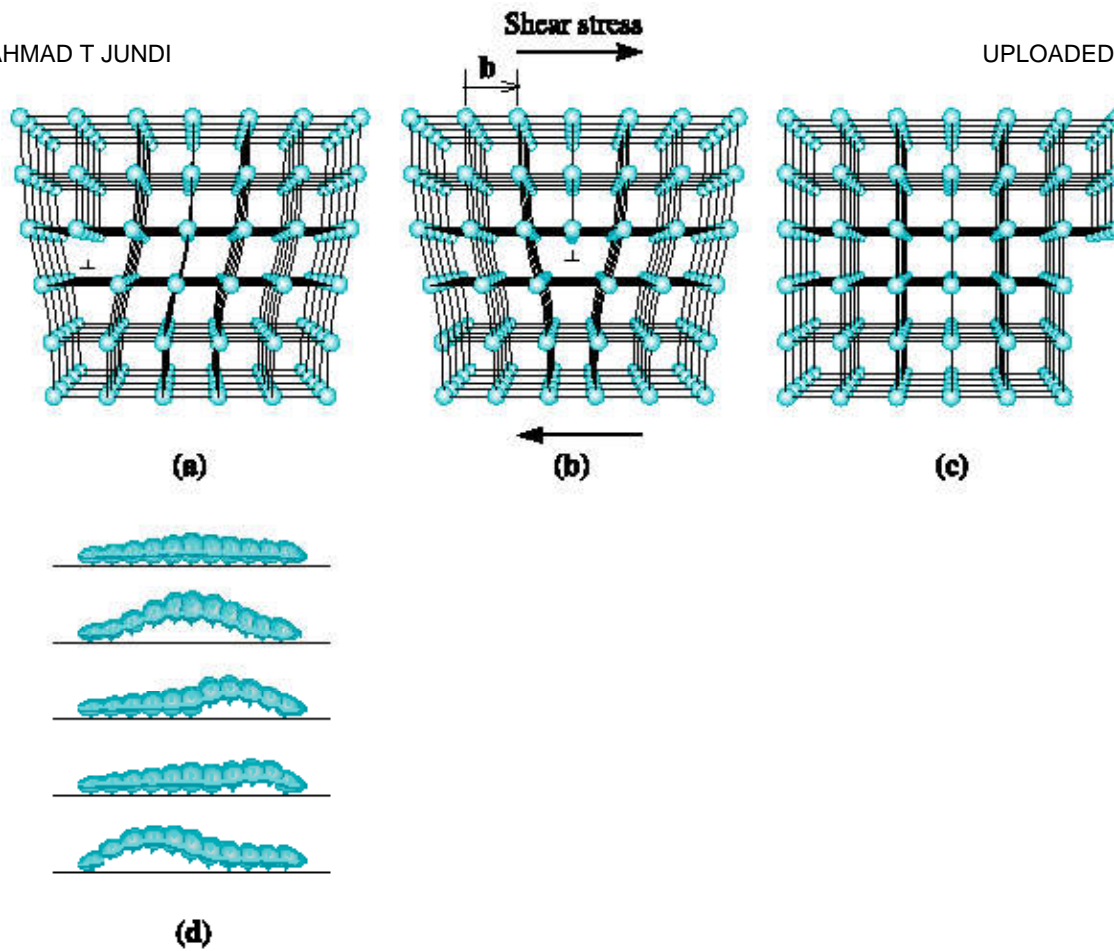


Figure 4.8 (a) When a shear stress is applied to the dislocation in (a), the atoms are displaced, causing the dislocation to move one Burgers vector in the slip direction (b). Continued movement of the dislocation eventually creates a step (c), and the crystal is deformed. *(Adapted from A.G. Guy, Essentials of Materials Science, McGraw-Hill, 1976.)*
(b) Motion of caterpillar is analogous to the motion of a dislocation.



TABLE 4-1 ■ Slip planes and directions in metallic structures

Crystal Structure	Slip Plane	Slip Direction
BCC metals	{110} {112} {123}	$\langle 111 \rangle$
FCC metals	{111}	$\langle 110 \rangle$
HCP metals	{0001}	$\langle 100 \rangle$
	{11 $\bar{2}$ 0}	$\langle 110 \rangle$
	{10 $\bar{1}$ 0}	or $\langle 11\bar{2}0 \rangle$
	{10 $\bar{1}$ 1}	
MgO, NaCl (ionic)	{110}	$\langle 110 \rangle$
Silicon (covalent)	{111}	$\langle 110 \rangle$

Note: These planes are active in some metals and alloys or at elevated temperatures.





Example 4.7

Dislocations in Ceramic Materials

A sketch of a dislocation in magnesium oxide (MgO), which has the sodium chloride crystal structure and a lattice parameter of 0.396 nm, is shown in Figure 4.9. Determine the length of the Burgers vector.

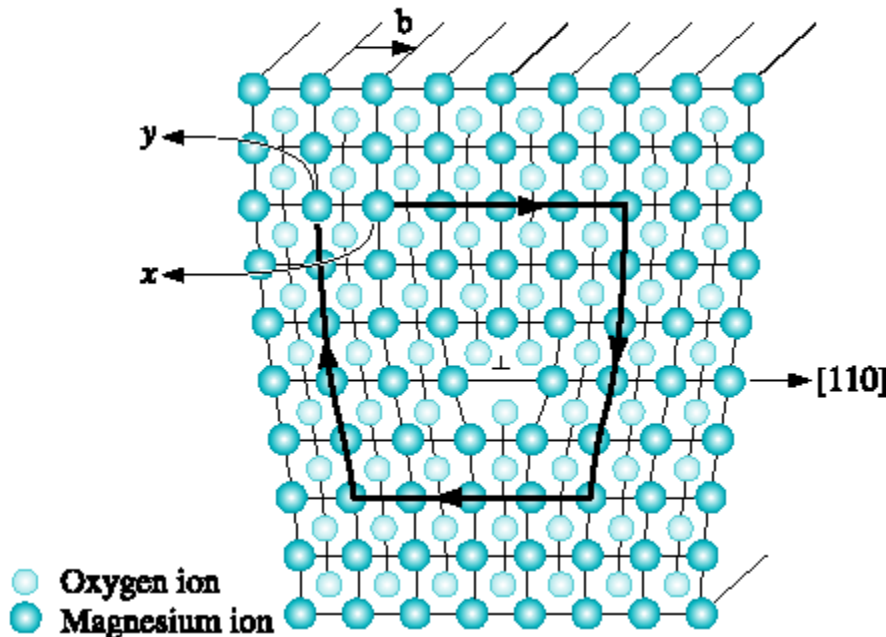


Figure 4.9 An edge dislocation in MgO showing the slip direction and Burgers vector (for Example 4.7). (Adapted from W.D. Kingery, H.K. Bowen, and D.R. Uhlmann, Introduction to Ceramics, John Wiley, 1976.) for Example 4.7)



Example 4.7 SOLUTION

In Figure 4.9, we begin a clockwise loop around the dislocation at point x , then move equal atom spacings to finish at point y . The vector \mathbf{b} is the Burgers vector. Because \mathbf{b} is a $[110]$ direction, it must be perpendicular to $\{110\}$ planes. The length of \mathbf{b} is the distance between two adjacent (110) planes. From Equation 3-7,

$$d_{110} = \frac{a_0}{\sqrt{h^2 + k^2 + l^2}} = \frac{0.396}{\sqrt{1^2 + 1^2 + 0^2}} = 0.280 \text{ nm}$$

Note that this formula for calculating the magnitude of the Burgers vector will not work for non-cubic systems. It is better to consider the magnitude of the Burgers vector as equal to the repeat distance in the slip direction.



Example 4.8

Burgers Vector Calculation

Calculate the length of the Burgers vector in copper.

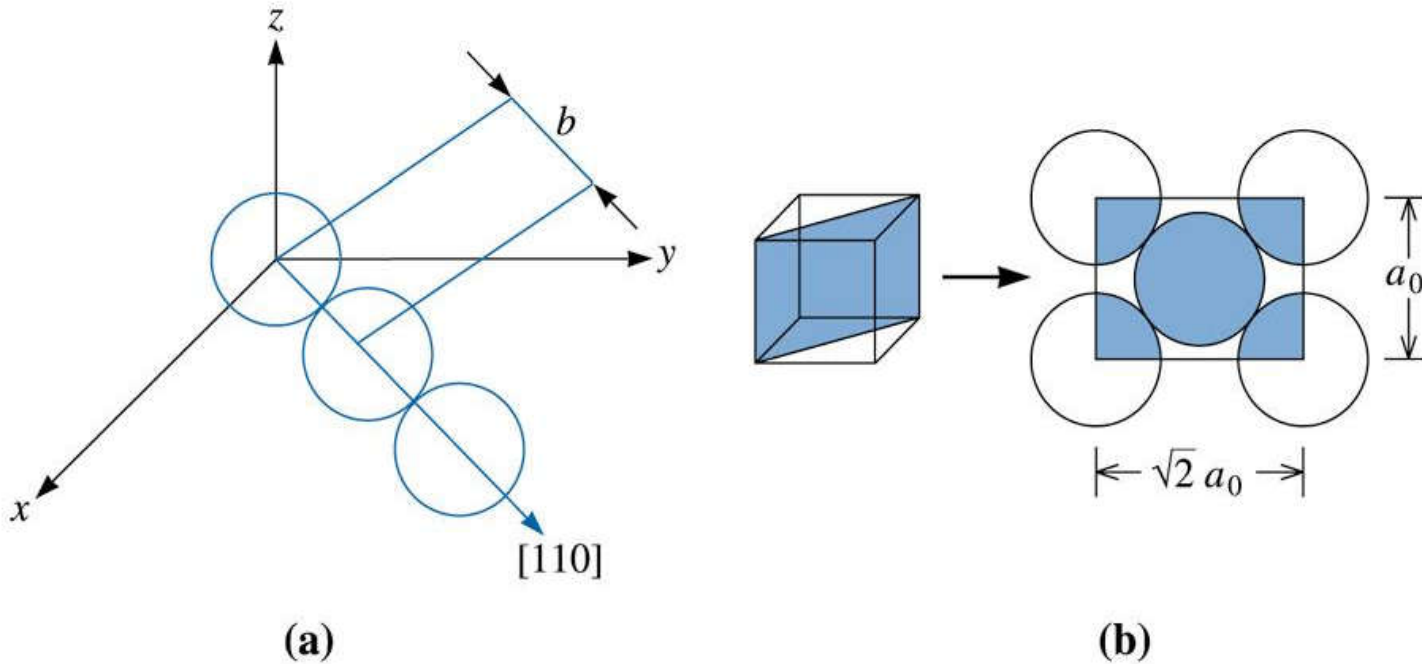


Figure 4.10
(a) Burgers vector for FCC copper. (b) The atom locations on a (110) plane in a BCC unit cell (for example 4.8 and 4.9, respectively)

© 2003 Brooks/Cole Publishing / Thomson Learning



Example 4.8 SOLUTION

Copper has an FCC crystal structure. The lattice parameter of copper (Cu) is 0.36151 nm. The close-packed directions, or the directions of the Burgers vector, are of the form $\langle 110 \rangle$. The repeat distance along the $\langle 110 \rangle$ directions is one-half the face diagonal, since lattice points are located at corners and centers of faces [Figure 4.10(a)].

$$\text{Face diagonal} = \sqrt{2}a_0 = (\sqrt{2})(0.36151) = 0.51125 \text{ nm}$$

The length of the Burgers vector, or the repeat distance, is:

$$b = 1/2(0.51125 \text{ nm}) = 0.25563 \text{ nm}$$





Example 4.9

Identification of Preferred Slip Planes

The planar density of the (112) plane in BCC iron is 9.94×10^{14} atoms/cm². Calculate (1) the planar density of the (110) plane and (2) the interplanar spacings for both the (112) and (110) planes. On which plane would slip normally occur?

© 2003 Brooks/Cole Publishing / Thomson Learning

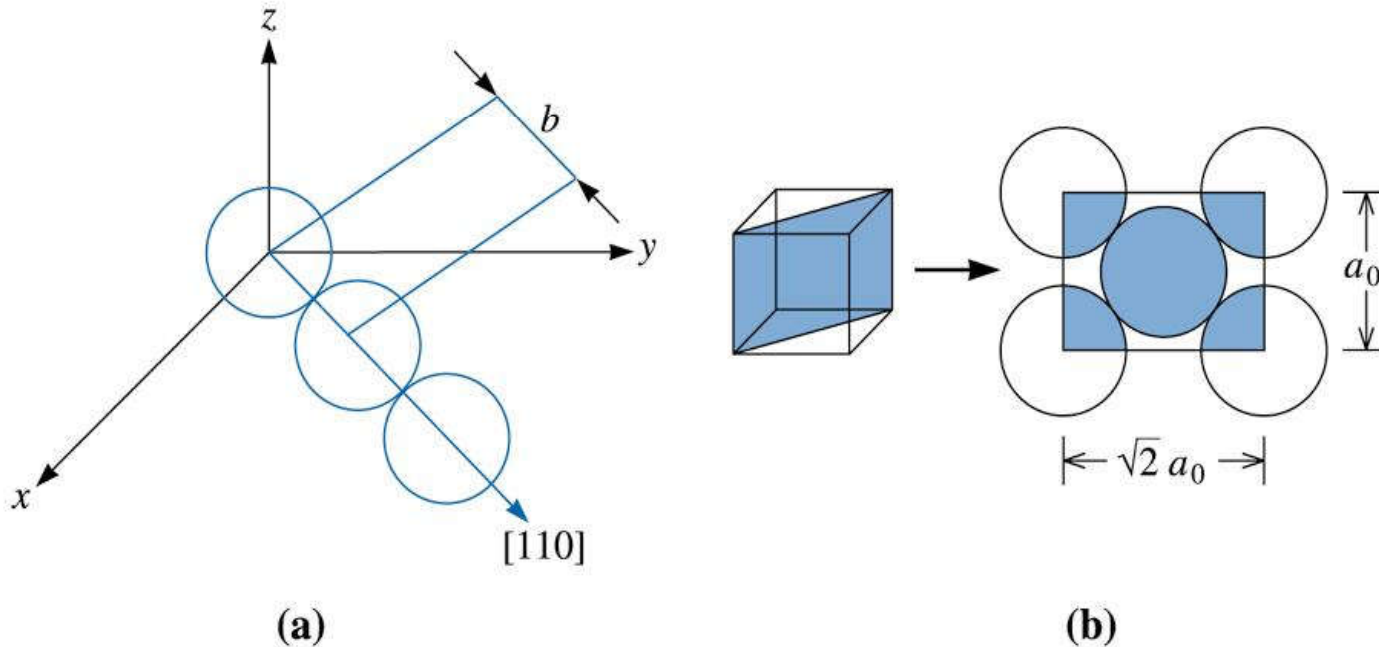
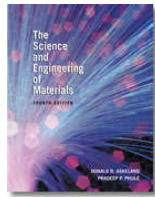


Figure 4.10
(a) Burgers vector for FCC copper.
(b) The atom locations on a (110) plane in a BCC unit cell (for example 4.8 and 4.9, respectively)





UPLOADED BY AHMAD T. JUNDI

Example 4.9 SOLUTION

1. The planar density is:

$$\begin{aligned}\text{Planar density (110)} &= \frac{\text{atoms}}{\text{area}} = \frac{2}{(\sqrt{2})(2.866 \times 10^{-8} \text{ cm})^2} \\ &= 1.72 \times 10^{15} \text{ atoms/cm}^2\end{aligned}$$

$$\text{Planar density (112)} = 0.994 \times 10^{15} \text{ atoms/cm}^2 \text{ (from problem statement)}$$

2. The interplanar spacings are:

$$d_{110} = \frac{2.866 \times 10^{-8}}{\sqrt{1^2 + 1^2 + 0}} = 2.0266 \times 10^{-8} \text{ cm}$$

$$d_{112} = \frac{2.866 \times 10^{-8}}{\sqrt{1^2 + 1^2 + 2^2}} = 1.17 \times 10^{-8} \text{ cm}$$

The planar density and interplanar spacing of the (110) plane are larger than those for the (112) plane; therefore, the (110) plane would be the preferred slip plane.





Section 4.4

Observing Dislocations

- **Etch pits** - Tiny holes created at areas where dislocations meet the surface. These are used to examine the presence and number density of dislocations.
- **Slip line** - A visible line produced at the surface of a metallic material by the presence of several thousand dislocations.
- **Slip band** - Collection of many slip lines, often easily visible.





© 2003 Brooks/Cole Publishing / Thomson Learning

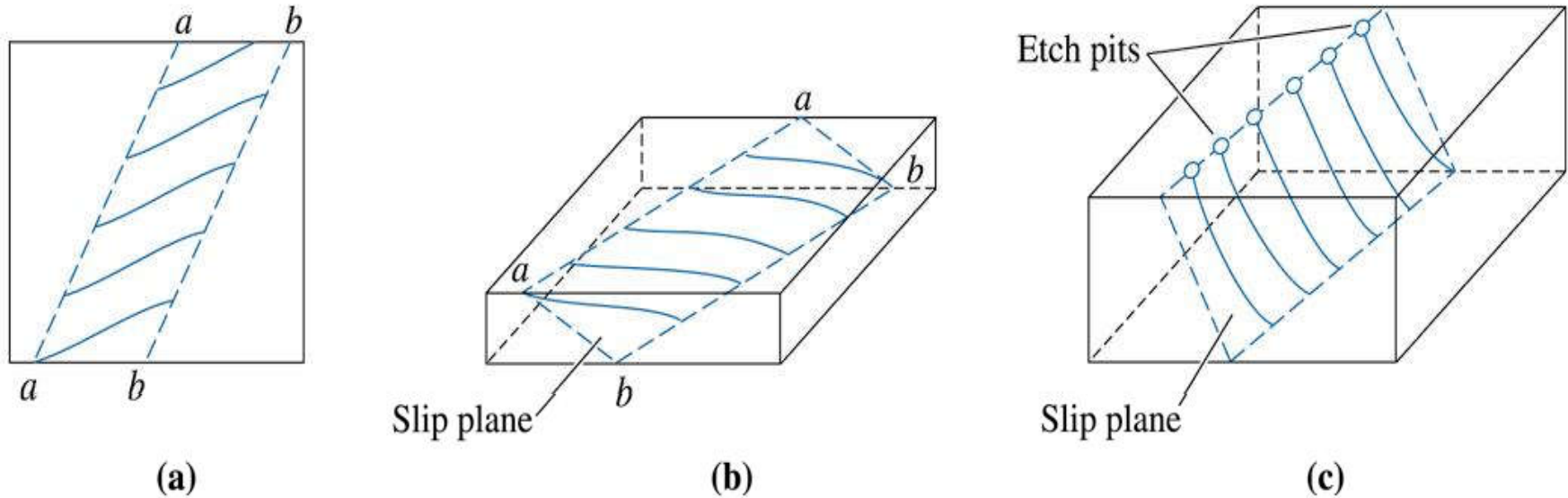


Figure 4.11 A sketch illustrating dislocations, slip planes, and etch pit locations. (Source: Adapted from Physical Metallurgy Principles, Third Edition, by R.E. Reed-Hill and R. Abbaschian, p. 92, Figs. 4-7 and 4-8. Copyright (c) 1992 Brooks/Cole Thomson Learning. Adapted by permission.)

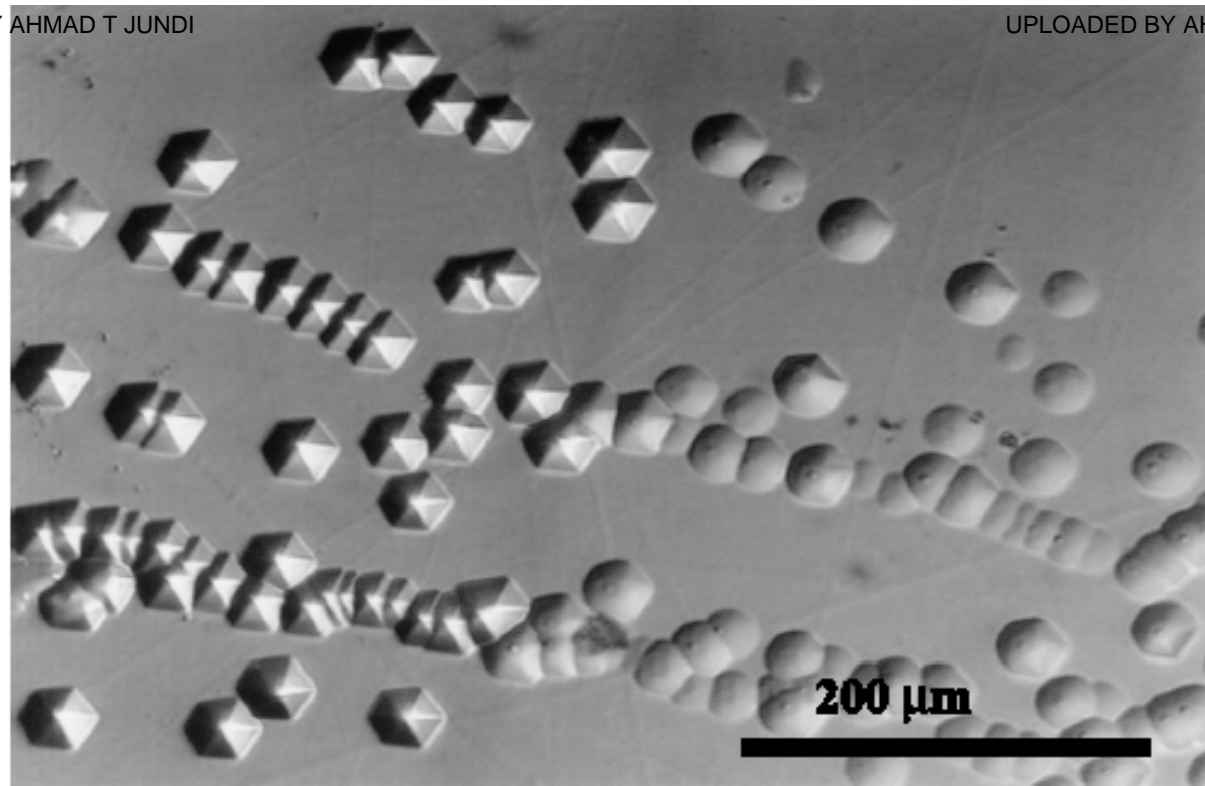
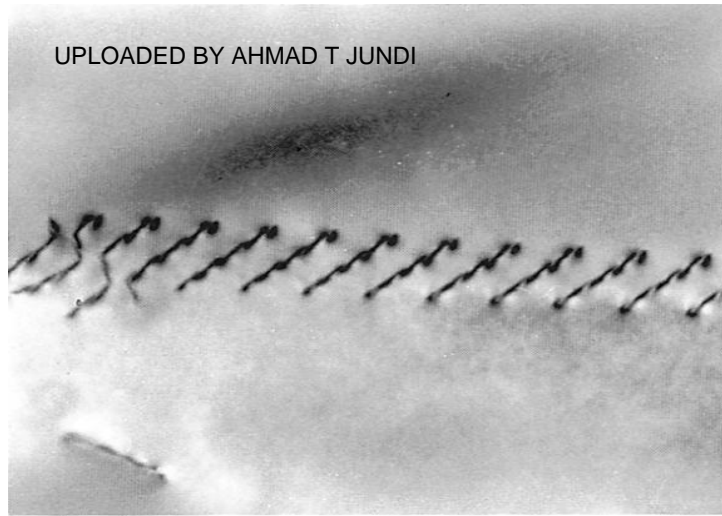
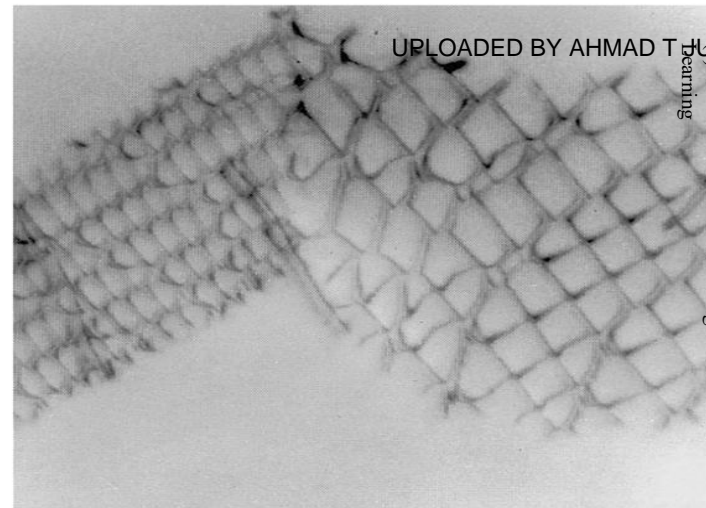


Figure 4.12 Optical image of etch pits in silicon carbide (SiC). The etch pits correspond to intersection points of pure edge dislocations with Burgers vector $a/3 \langle 1120 \rangle$ and the dislocation line direction along $[0001]$ (perpendicular to the etched surface). Lines of etch pits represent low angle grain boundaries (Courtesy of Dr. Marek Skowronski, Carnegie Mellon University.)



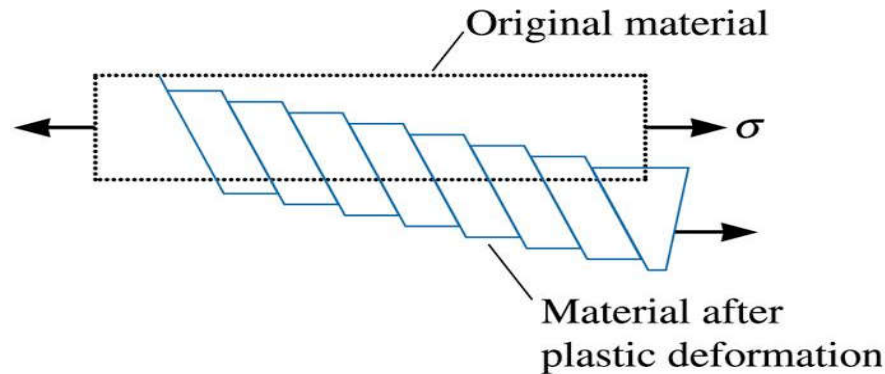
UPLOADED BY AHMAD T JUNDI

(a)



UPLOADED BY AHMAD T JUNDI

(b)



(c)

(c)2003 Brooks/Cole, a division of Thomson Learning, Inc. Thomson Learningsm is a trademark used herein under license.

Figure 4.13 Electron photomicrographs of dislocations in Ti_3Al : (a) Dislocation pileups (x26,500). (b) Micrograph at x 100 showing slip lines and grain boundaries in Al. (c) Schematic of slip bands development.



Section 4.5

Significance of Dislocations

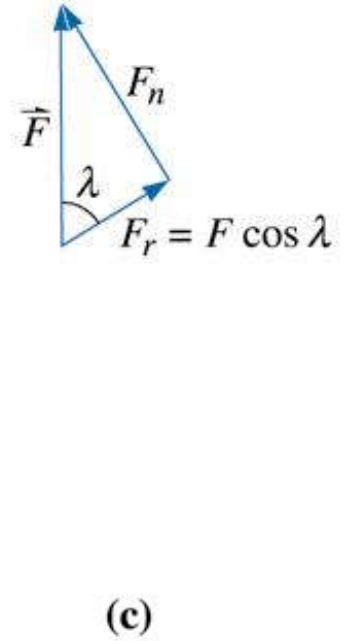
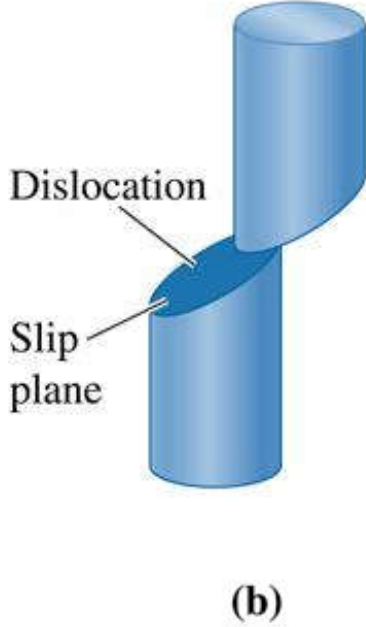
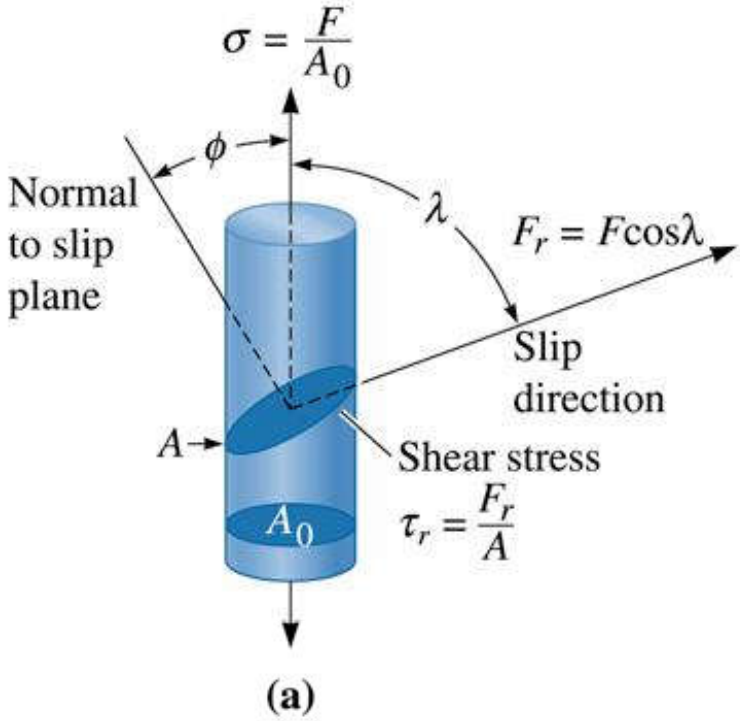
- ❑ **Plastic deformation** refers to irreversible deformation or change in shape that occurs when the force or stress that caused it is removed.
- ❑ **Elastic deformation** - Deformation that is fully recovered when the stress causing it is removed.
- ❑ **Dislocation density** - The total length of dislocation line per cubic centimeter in a material.



Section 4.6

Schmid's Law

- **Schmid's law** -The relationship between shear stress, the applied stress, and the orientation of the slip system— that is, $\tau = \sigma \cos \lambda \cos \phi$
- **Critical resolved shear stress** - The shear stress required to cause a dislocation to move and cause slip.



(c)2003 Brooks/Cole, a division of Thomson Learning, Inc. Thomson Learning[™] is a trademark used herein under license.

Figure 4.14 (a) A resolved shear stress τ is produced on a slip system. (Note: $(\phi + \lambda)$ does not have to be 90° .) (b) Movement of dislocations on the slip system deforms the material. (c) Resolving the force.



Example 4.10

Calculation of Resolved Shear Stress

Apply the Schmid's law for a situation in which the single crystal is at an orientation so that the slip plane is perpendicular to the applied tensile stress.

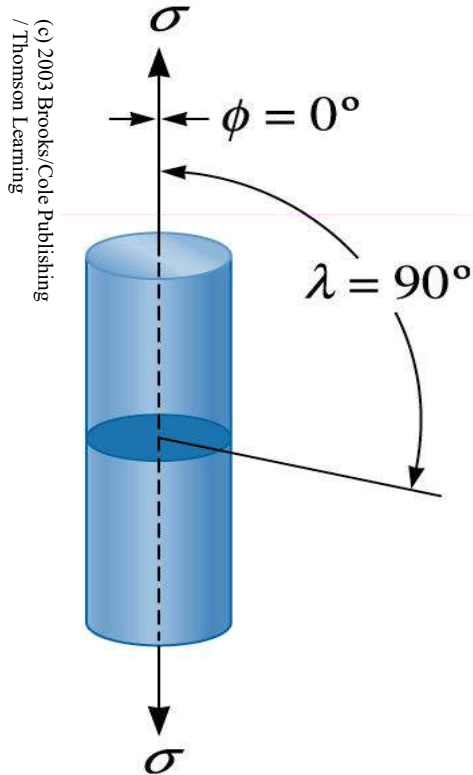


Figure 14.15 When the slip plane is perpendicular to the applied stress σ , the angle λ is 90° and no shear stress is resolved.



Example 4.10 SOLUTION

Suppose the slip plane is perpendicular to the applied stress σ , as in Figure 4.15. Then, $\phi = 0^\circ$, $\lambda = 90^\circ$, $\cos \lambda = 0$, and therefore $\tau_r = 0$. As noted before, the angles ϕ and λ can but do not always add up to 90° . Even if the applied stress s is enormous, no resolved shear stress develops along the slip direction and the dislocation cannot move. Slip cannot occur if the slip system is oriented so that either λ or ϕ is 90° .





Example 4.11

Design of a Single Crystal Casting Process

We wish to produce a rod composed of a single crystal of pure aluminum, which has a critical resolved shear stress of 148 psi. We would like to orient the rod in such a manner that, when an axial stress of 500 psi is applied, the rod deforms by slip in a 45° direction to the axis of the rod and actuates a sensor that detects the overload. Design the rod and a method by which it might be produced.

Example 4.11 SOLUTION

Dislocations begin to move when the resolved shear stress τ_r equals the critical resolved shear stress, 148 psi. From Schmid's law:

$$\tau_r = \sigma \cos \lambda \cos \phi; \text{ or}$$

$$148 \text{ psi} = (500 \text{ psi}) \cos \lambda \cos \phi$$



Example 4.11 SOLUTION (Continued)

UPLOADED BY AHMAD T JUNDI

UPLOADED BY AHMAD T JUNDI



Because we wish slip to occur at a 45° angle to the axis of the rod, $\lambda = 45^\circ$, and:

$$\cos \phi = \frac{148}{500 \cos 45} = \frac{148}{(500)(0.707)} = 0.419$$
$$\phi = 65.2^\circ$$

Therefore, we must produce a rod that is oriented such that $\lambda = 45^\circ$ and $\phi = 65.2^\circ$. Note that ϕ and λ do not add to 90° .

We might do this by a solidification process. We would orient a seed crystal of solid aluminum at the bottom of a mold. Liquid aluminum could be introduced into the mold. The liquid begins to solidify from the starting crystal and a single crystal rod of the proper orientation is produced.



Section 4.7

Influence of Crystal Structure

- Critical Resolved Shear Stress
- Number of Slip Systems
- Cross-slip - A change in the slip system of a dislocation.





TABLE 4-2 ■ *Summary of factors affecting slip in metallic structures*

Factor	FCC	BCC	HCP ($\frac{c}{a} > 1.633$)
Critical resolved shear stress (psi)	50–100	5,000–10,000	50–100 ^a
Number of slip systems	12	48	3 ^b
Cross-slip	Can occur	Can occur	Cannot occur ^b
Summary of properties	Ductile	Strong	Relatively brittle

^a For slip on basal planes.

^b By alloying or heating to elevated temperatures, additional slip systems are active in HCP metals, permitting cross-slip to occur and thereby improving ductility.





Example 4.12

Ductility of HCP Metal Single Crystals and Polycrystalline Materials

A single crystal of magnesium (Mg), which has a HCP crystal structure, can be stretched into a ribbon-like shape four to six times its original length. However, *polycrystalline* Mg and other metals with a HCP structure show limited ductilities. Use the values of critical resolved shear stress for metals with different crystal structures and the nature of deformation in polycrystalline materials to explain this observation.



TABLE 4-2 ■ *Summary of factors affecting slip in metallic structures*

Factor	FCC	BCC	HCP ($\frac{c}{a} > 1.633$)
Critical resolved shear stress (psi)	50–100	5,000–10,000	50–100 ^a
Number of slip systems	12	48	3 ^b
Cross-slip	Can occur	Can occur	Cannot occur ^b
Summary of properties	Ductile	Strong	Relatively brittle

^a For slip on basal planes.

^b By alloying or heating to elevated temperatures, additional slip systems are active in HCP metals, permitting cross-slip to occur and thereby improving ductility.



Example 4.12 SOLUTION



From Table 4-2, we note that for HCP metals such as Mg, the critical resolved shear stress is low (50–100 psi). We also note that slip in HCP metals will occur readily on the basal plane—the primary slip plane. When a single crystal is deformed, assuming the basal plane is suitably oriented with applied stress, a very large deformation can occur. This explains why single crystal Mg can be stretched into a ribbon four to six times the original size.

When we have a polycrystalline Mg, the deformation is not as simple. Each crystal must deform such that the strain developed in any one crystal is accommodated by its neighbors. In HCP metals, there are no intersecting slip systems, thus dislocations cannot glide over from one slip plane in one crystal (grain) onto another slip plane in a neighboring crystal. As a result, polycrystalline HCP metals such as Mg show limited ductility.



Section 4.8

Surface Defects

- **Surface defects** - Imperfections, such as grain boundaries, that form a two-dimensional plane within the crystal.
- **Hall-Petch equation** - The relationship between yield strength and grain size in a metallic material—that is,
$$\sigma_y = \sigma_0 + Kd^{-1/2}$$
- **ASTM grain size number (n)** - A measure of the size of the grains in a crystalline material obtained by counting the number of grains per square inch a magnification $\times 100$.
- **Small angle grain boundary** - An array of dislocations causing a small misorientation of the crystal across the surface of the imperfection.

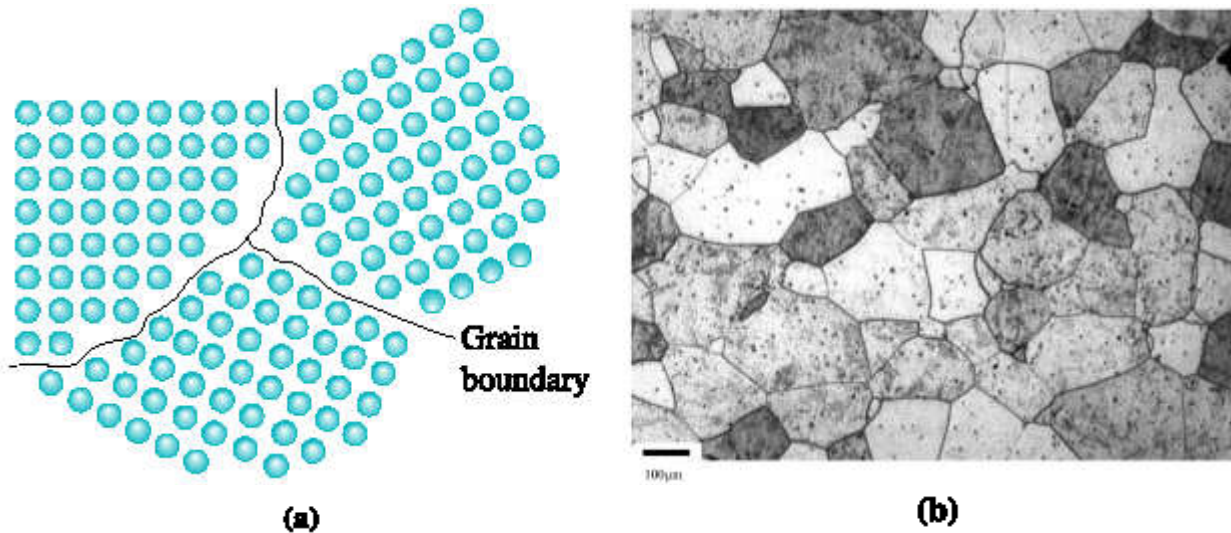


Figure 4.16 (a) The atoms near the boundaries of the three grains do not have an equilibrium spacing or arrangement. (b) Grains and grain boundaries in a stainless steel sample. (Courtesy Dr. A. Deardo.)



© 2003 Brooks/Cole Publishing / Thomson Learning

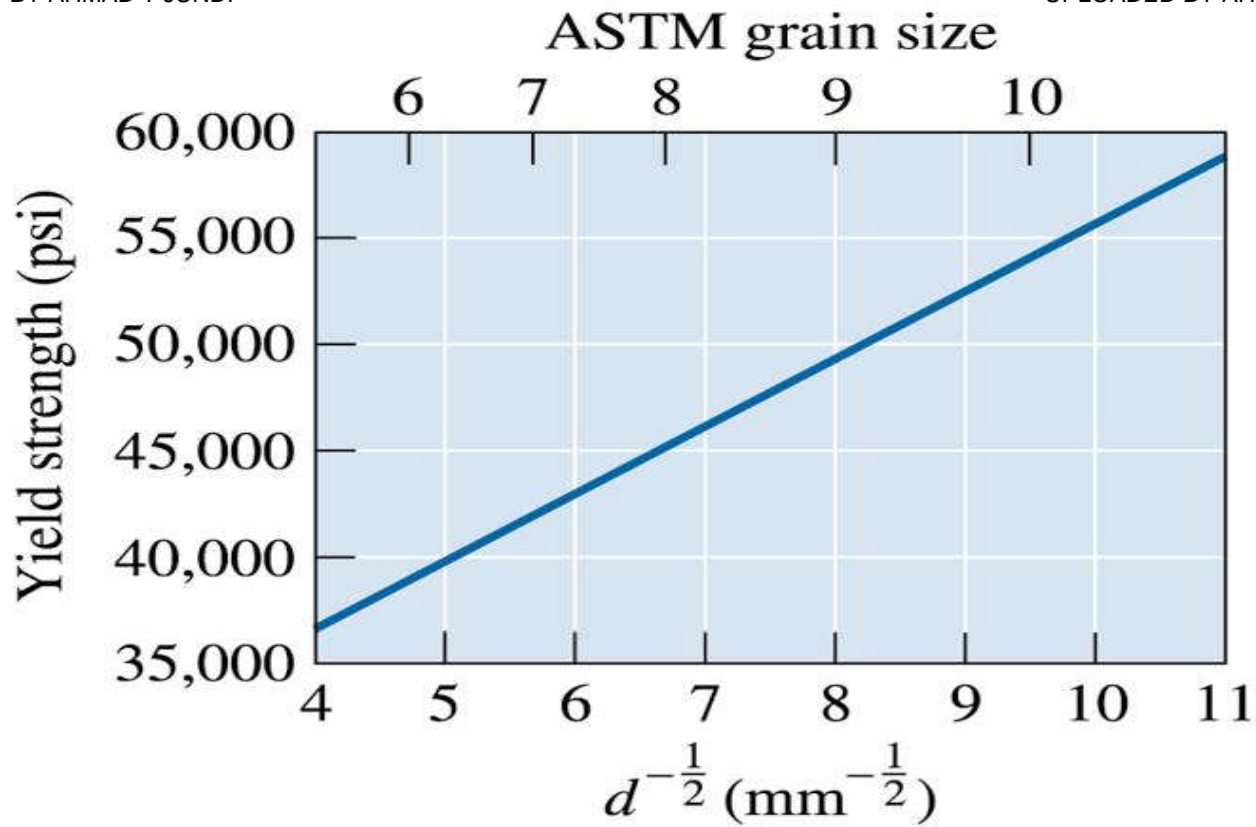


Figure 4.17 The effect of grain size on the yield strength of steel at room temperature.





Example 4.13

Design of a Mild Steel

The yield strength of mild steel with an average grain size of 0.05 mm is 20,000 psi. The yield stress of the same steel with a grain size of 0.007 mm is 40,000 psi. What will be the average grain size of the same steel with a yield stress of 30,000 psi? Assume the Hall-Petch equation is valid and that changes in the observed yield stress are due to changes in dislocation density.

Example 4.13 SOLUTION

$$\sigma_y = \sigma_0 + Kd^{-1/2}$$

Thus, for a grain size of 0.05 mm the yield stress is
 $20 \times 6.895 \text{ MPa} = 137.9 \text{ MPa}$.

(Note: 1,000 psi = 6.895 MPa). Using the Hall-Petch equation





Example 4.13 SOLUTION (Continued)

$$137.9 = \sigma_0 + \frac{K}{\sqrt{0.05}}$$

For the grain size of 0.007 mm, the yield stress is $40 \times 6.895 \text{ MPa} = 275.8 \text{ MPa}$. Therefore, again using the Hall-Petch equation:

$$275.8 = \sigma_0 + \frac{K}{\sqrt{0.007}}$$

Solving these two equations $K = 18.43 \text{ MPa}\cdot\text{mm}^{1/2}$, and $\sigma_0 = 55.5 \text{ MPa}$. Now we have the Hall-Petch equation as

$$\sigma_y = 55.5 + 18.43 d^{-1/2}$$

If we want a yield stress of 30,000 psi or $30 \times 6.895 = 206.9 \text{ MPa}$, the grain size will be 0.0148 mm.



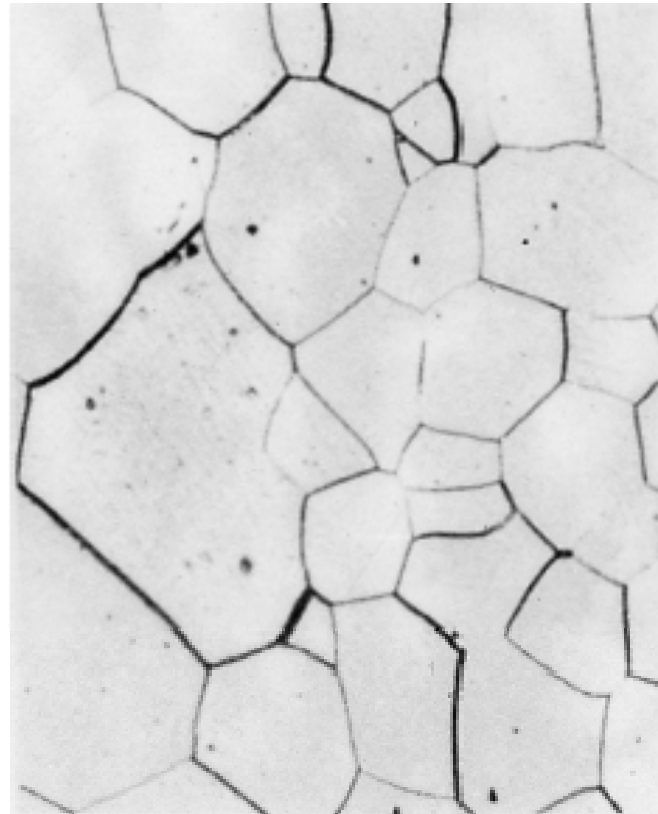


Figure 4.18 Microstructure of palladium (x 100). (From ASM Handbook, Vol. 9, Metallography and Microstructure (1985), ASM International, Materials Park, OH 44073.)



Example 4.14

Calculation of ASTM Grain Size Number

Suppose we count 16 grains per square inch in a photomicrograph taken at magnification $\times 250$. What is the ASTM grain size number?

Example 4.14 SOLUTION

If we count 16 grains per square inch at magnification $\times 250$, then at magnification $\times 100$ we must have:

$$N = (250/100)^2 (16) = 100 \text{ grains/in.}^2 = 2^{n-1}$$

$$\text{Log } 100 = (n - 1) \log 2$$

$$2 = (n - 1)(0.301)$$

$$n = 7.64$$

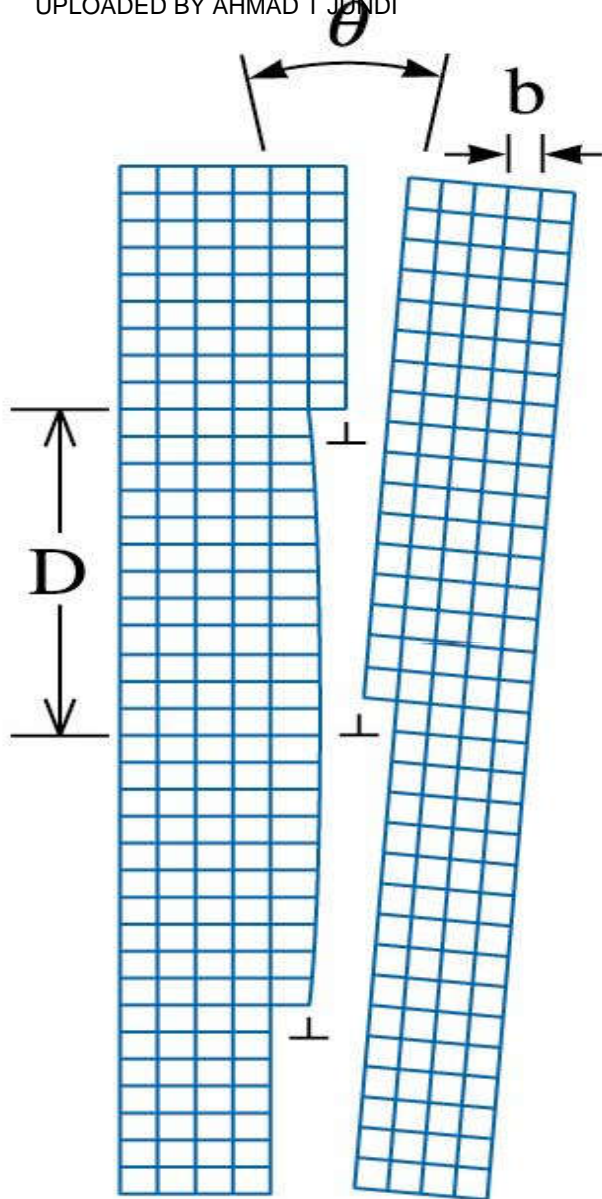
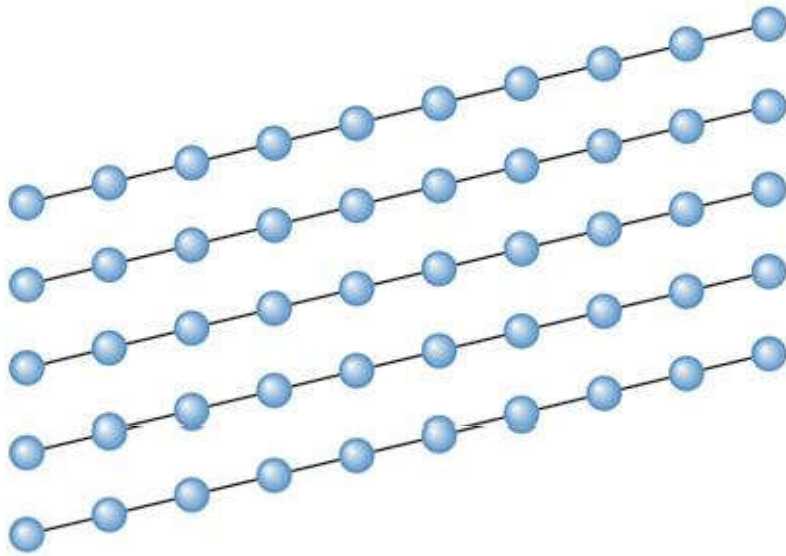


Figure 4.19 The small angle grain boundary is produced by an array of dislocations, causing an angular mismatch θ between lattices on either side of the boundary.

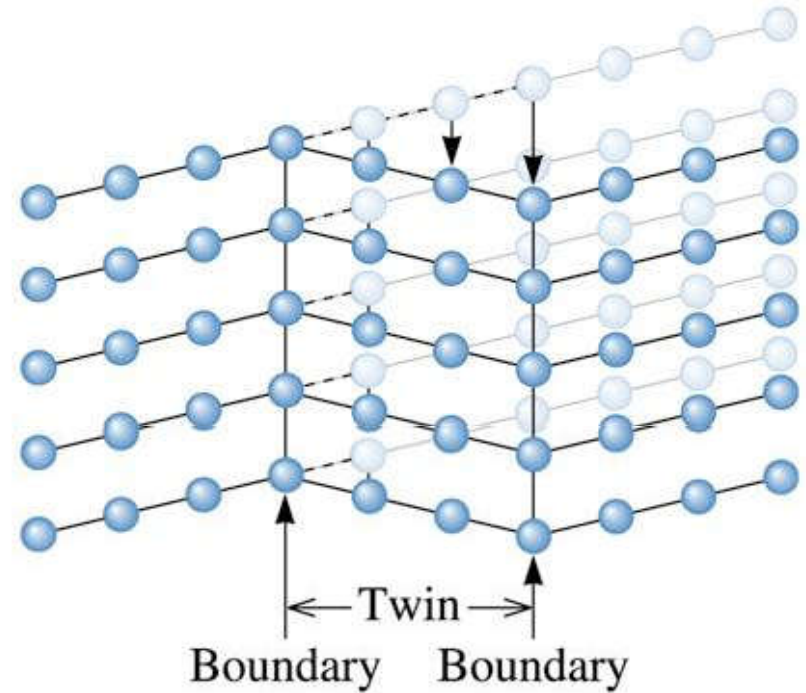
(c) 2003 Brooks/Cole Publishing / Thomson Learning



© 2003 Brooks/Cole Publishing / Thomson Learning

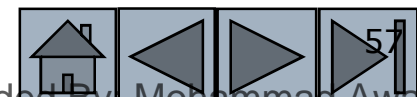


(a)



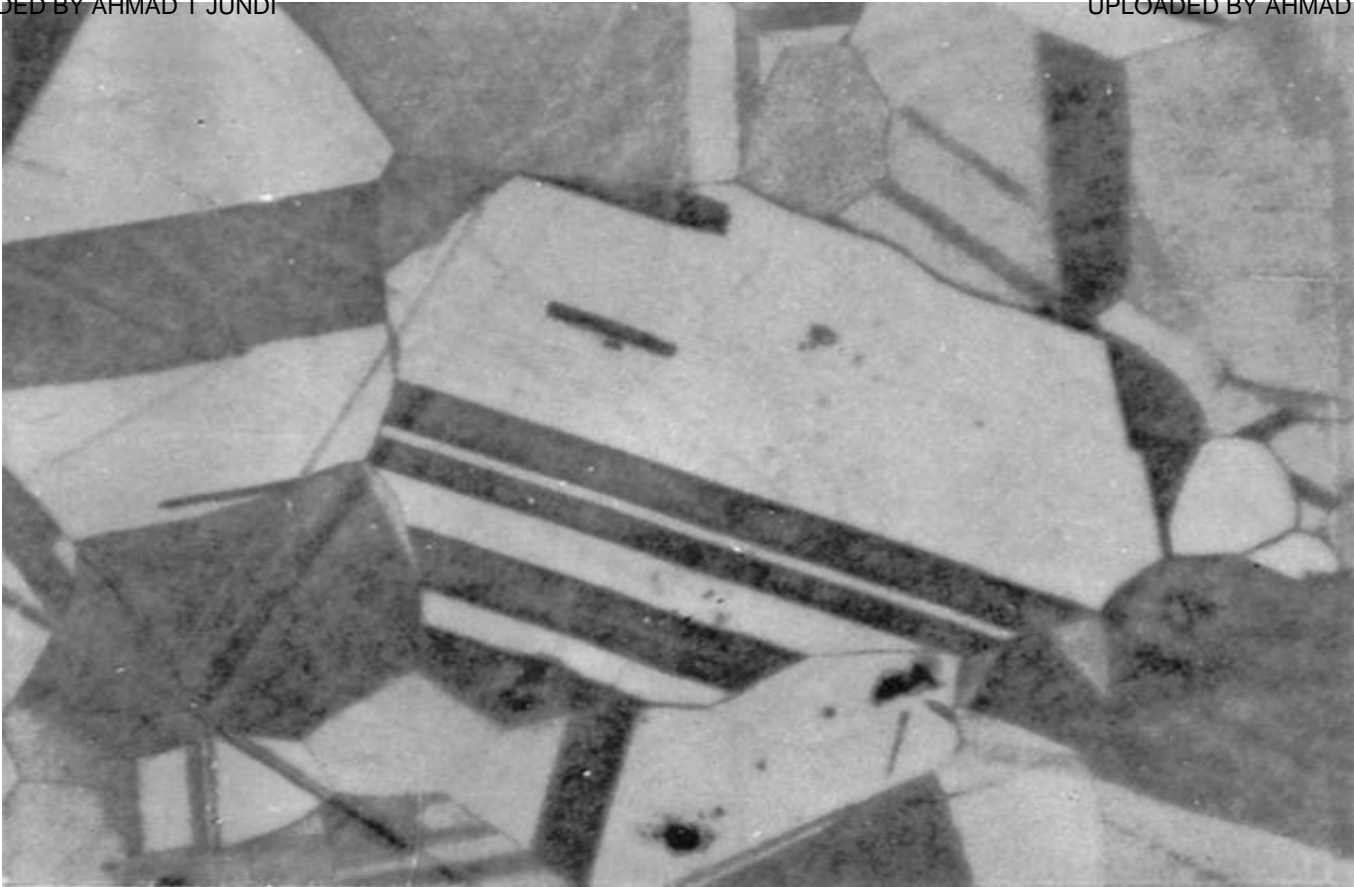
(b)

Figure 4.20 Application of a stress to the perfect crystal (a) may cause a displacement of the atoms, (b) causing the formation of a twin. Note that the crystal has deformed as a result of twinning.





© 2003 Brooks/Cole Publishing / Thomson Learning



(c)

Figure 4.20 (c) A micrograph of twins within a grain of brass (x250).



TABLE 4-3 ■ *Energies of surface imperfections in selected metals*

Surface Imperfection (energy/cm ²)	Al	Cu	Pt	Fe
Stacking fault	200	75	95	—
Twin boundary	120	45	195	190
Grain boundary	625	645	1000	780



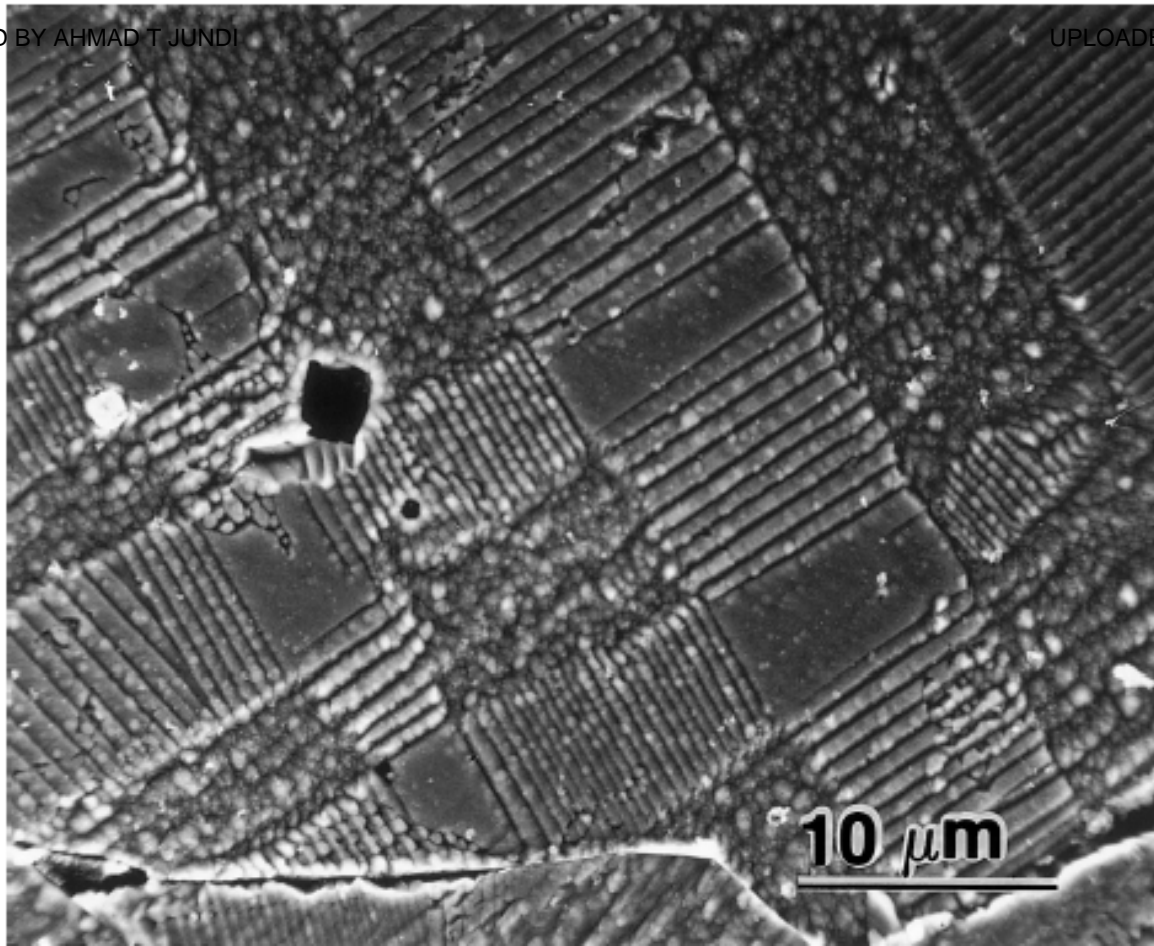


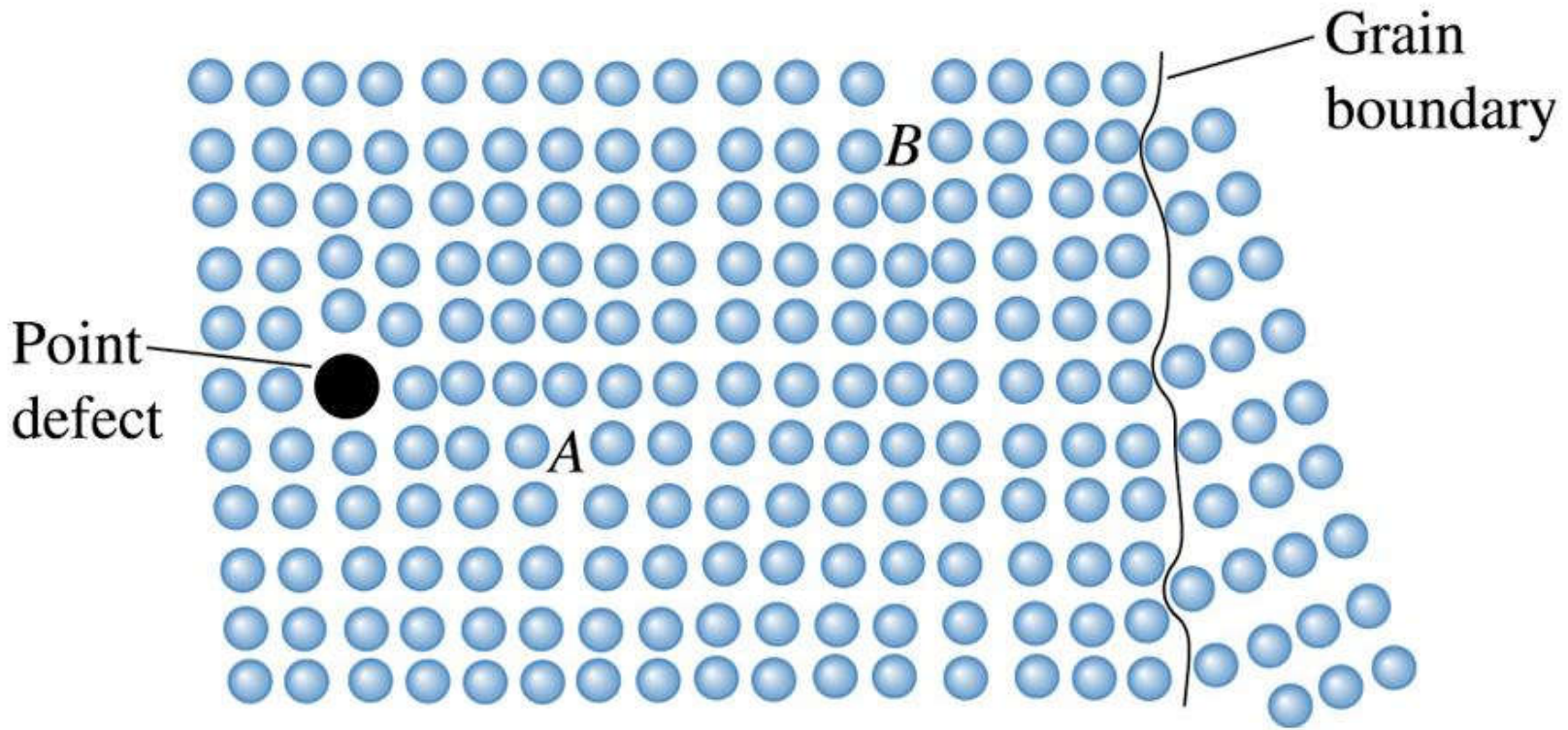
Figure 4.21 Domains in ferroelectric barium titanate. (Courtesy of Dr. Rodney Roseman, University of Cincinnati.) Similar domain structures occur in ferromagnetic and ferrimagnetic materials.



Section 4.9

Importance of Defects

- Effect on Mechanical Properties via Control of the Slip Process
- Strain Hardening
- Solid-Solution Strengthening
- Grain-Size Strengthening
- Effects on Electrical, Optical, and Magnetic Properties



(c)2003 Brooks/Cole, a division of Thomson Learning, Inc. Thomson Learningsm is a trademark used herein under license.

Figure 4.22 If the dislocation at point A moves to the left, it is blocked by the point defect. If the dislocation moves to the right, it interacts with the disturbed lattice near the second dislocation at point B. If the dislocation moves farther to the right, it is blocked by a grain boundary.



Example 4.15

Design/Materials Selection for a Stable Structure

We would like to produce a bracket to hold ceramic bricks in place in a heat-treating furnace. The bracket should be strong, should possess some ductility so that it bends rather than fractures if overloaded, and should maintain most of its strength up to 600°C. Design the material for this bracket, considering the various crystal imperfections as the strengthening mechanism.

Example 4.15 SOLUTION

In order to serve up to 600°C, the bracket should not be produced from a polymer material. Instead, a metal or ceramic would be considered.



Example 4.15 SOLUTION (Continued)

In order to have some ductility, dislocations must move and cause slip. Because slip in ceramics is difficult, the bracket should be produced from a metallic material.

We might add carbon to the iron as interstitial atoms or substitute vanadium atoms for iron atoms at normal lattice points. These point defects continue to interfere with dislocation movement and help to keep the strength stable.

Of course, other design requirements may be important as well. For example, the steel bracket may deteriorate by oxidation or may react with the ceramic brick.

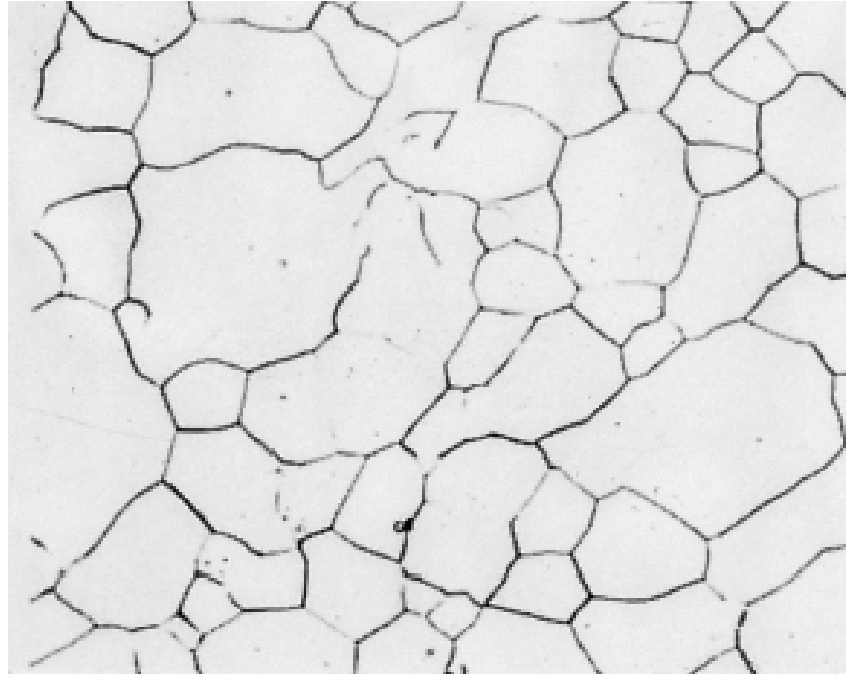


Figure 4.23 Microstructure of iron, for Problem 4-54 (x500). (From ASM Handbook, Vol. 9, Metallography and Microstructure (1985), ASM International, Materials Park, OH 44073.)

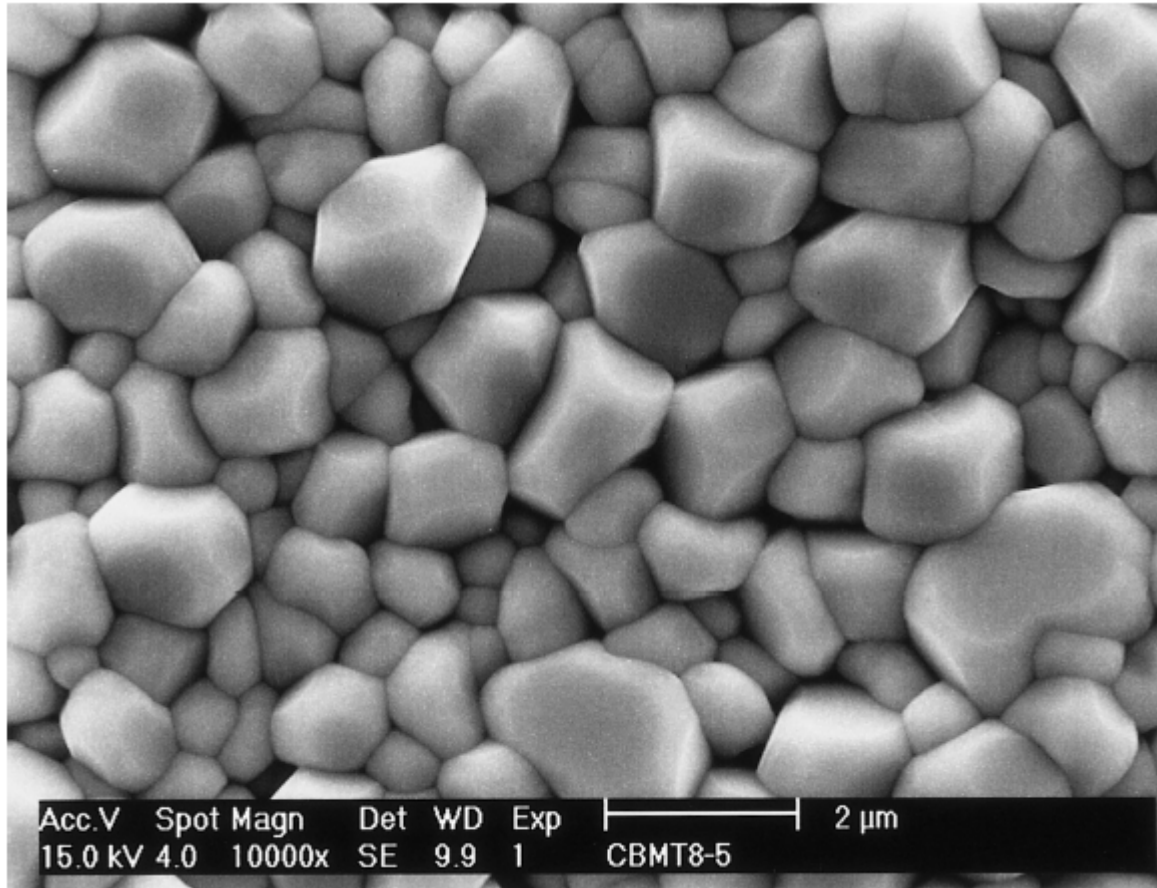


Figure 4.24 The microstructure of BMT ceramics obtained by compaction and sintering of BMT powders. (Courtesy of H. Shirey.)

The Science and Engineering of Materials, 4th ed

Donald R. Askeland – Pradeep P. Phulé

Chapter 5 – Atom and Ion Movements in Materials





Objectives of Chapter 5

- Examine the principles and applications of diffusion in materials.
- Discuss, how diffusion is used in the synthesis and processing of advanced materials as well as manufacturing of components using advanced materials.





Chapter Outline

- 5.1 Applications of Diffusion
- 5.2 Stability of Atoms and Ions
- 5.3 Mechanisms for Diffusion
- 5.4 Activation Energy for Diffusion
- 5.5 Rate of Diffusion (Fick's First Law)
- 5.6 Factors Affecting Diffusion
- 5.7 Permeability of Polymers
- 5.8 Composition Profile (Fick's Second Law)
- 5.9 Diffusion and Materials Processing





Section 5.1

Applications of Diffusion

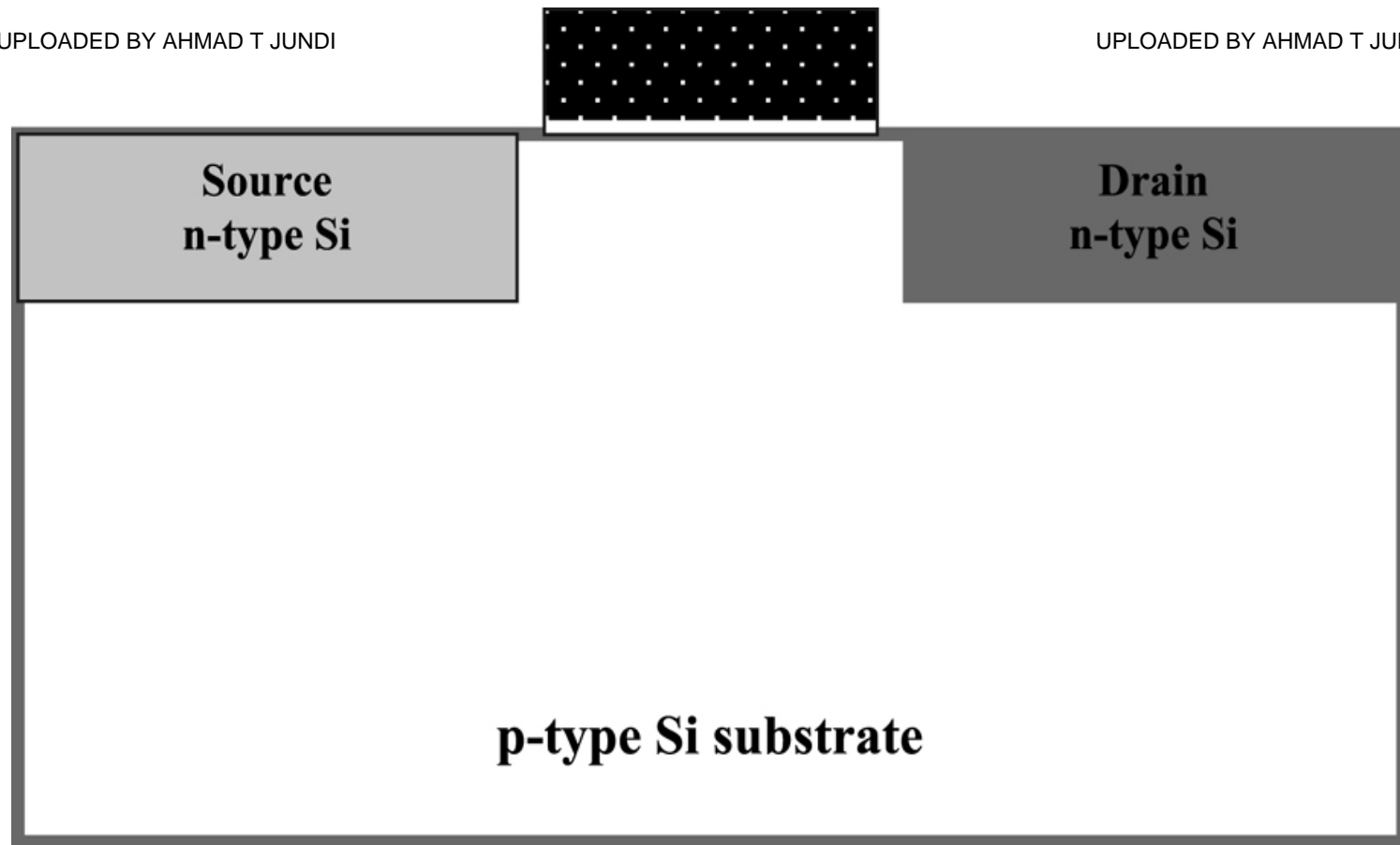
- ❑ **Nitriding** - Carburization for Surface Hardening of Steels
- ❑ **p-n junction** - Dopant Diffusion for Semiconductor Devices
- ❑ **Manufacturing of Plastic Beverage Bottles/Mylar™ Balloons**
- ❑ **Sputtering, Annealing** - Magnetic Materials for Hard Drives
- ❑ **Hot dip galvanizing** - Coatings and Thin Films
- ❑ **Thermal Barrier Coatings** for Turbine Blades





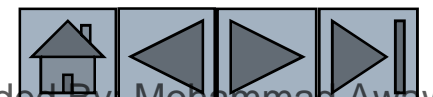
Figure 5.1 Furnace for heat treating steel using the carburization process. (Courtesy of Cincinnati Steel Treating).

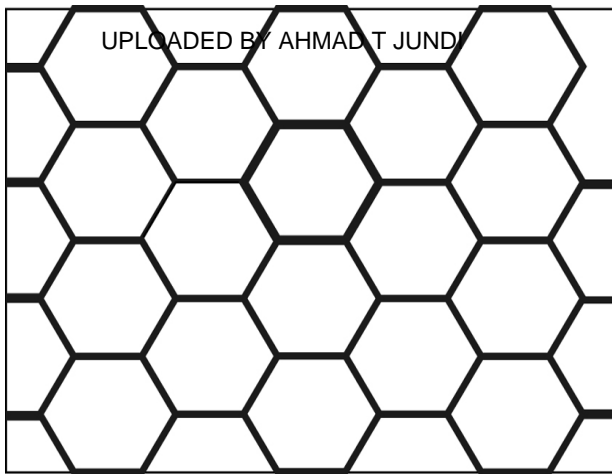




©2003 Brooks/Cole, a division of Thomson Learning, Inc. Thomson LearningSM is a trademark used herein under license.

Figure 5.2 Schematic of a n-p-n transistor. Diffusion plays a critical role in formation of the different regions created in the semiconductor substrates. The creation of millions of such transistors is at the heart of microelectronics technology





©2003 Brooks/Cole, a division of Thomson Learning, Inc. Thomson Learning, is a trademark used herein under license.

Figure 5.3 Schematic of the microstructure of the Co-Pt-Ta-Cr film after annealing. Most of the chromium diffuses from the grains to the grain boundaries after the annealing process. This helps improve the magnetic properties of the hard disk



Figure 5.4 Hot dip galvanized parts and structures prevent corrosion. (Courtesy of Casey Young and Barry Dugan of the Zinc Corporation of America)



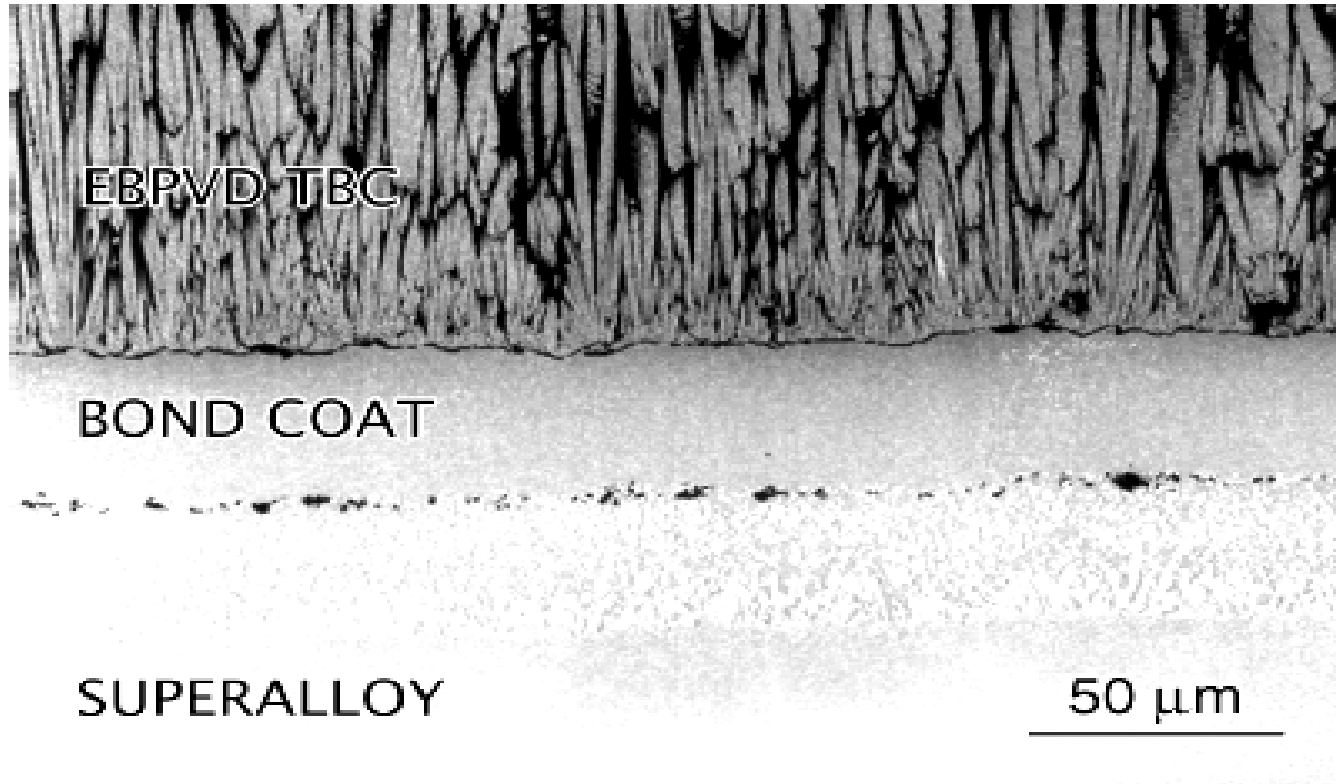
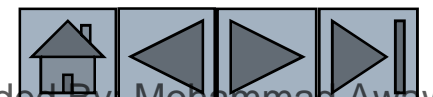


Figure 5.5 A thermal barrier coating on nickel-based superalloy. (Courtesy of Dr. F.S. Pettit and Dr. G.H. Meier, University of Pittsburgh.)





Example 5.1

Diffusion of Ar/He and Cu/Ni

Consider a box containing an impermeable partition that divides the box into equal volumes (Figure 5.6). On one side, we have pure argon (Ar) gas; on the other side, we have pure helium (He) gas. Explain what will happen when the partition is opened? What will happen if we replace the Ar side with a Cu single crystal and the He side with a Ni single crystal?

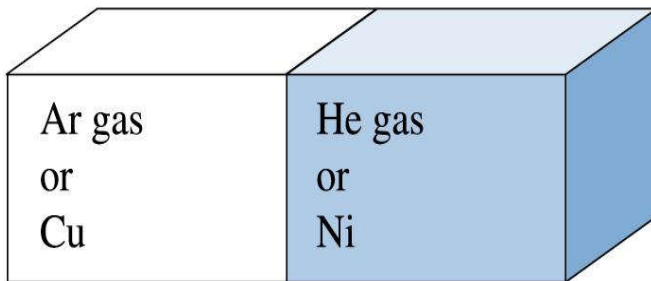
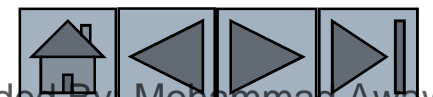


Figure 5.6 Illustration for Diffusion of Ar/He and Cu/Ni (for Example 5.1)

©2003 Brooks/Cole, a division of Thomson Learning, Inc. Thomson Learning, is a trademark used herein under license.





Example 5.1 SOLUTION

Before the partition is opened, one compartment has no argon and the other has no helium (i.e., there is a concentration gradient of Ar and He). When the partition is opened, Ar atoms will diffuse toward the He side, and vice versa.

If we open the hypothetical partition between the Ni and Cu single crystals at room temperature, we would find that, similar to the Ar/He situation, the concentration gradients exist but the temperature is too low to see any significant diffusion of Cu atoms into Ni single crystal and vice-versa.





Diffusion and Drift of Charge Carriers in a Semiconductor

The p-n junction is the basis for all transistors (Figure 5.2) and other devices.[1] A p-n junction is formed in single crystal silicon (Si) by doping the n-side with phosphorous (P) atoms and the p-side with boron (B) atoms (Figure 5.7). The doping can be achieved by diffusing atoms from a liquid, solid, or gaseous source of dopant atoms known as a precursor. Sometimes, the ion implantation process, in which dopant atoms are incorporated using high-energy ion beams, is also used instead of thermally diffusing dopant atoms. As discussed in Chapter 3, each phosphorus (P) atom makes available an extra electron, and each boron (B) atom added on the p-side has a deficit of one electron. We call this missing electron a hole and treat it as a particle having a positive charge. The magnitude of the charge is the same as that of an electron (1.6×10^{-19} C).



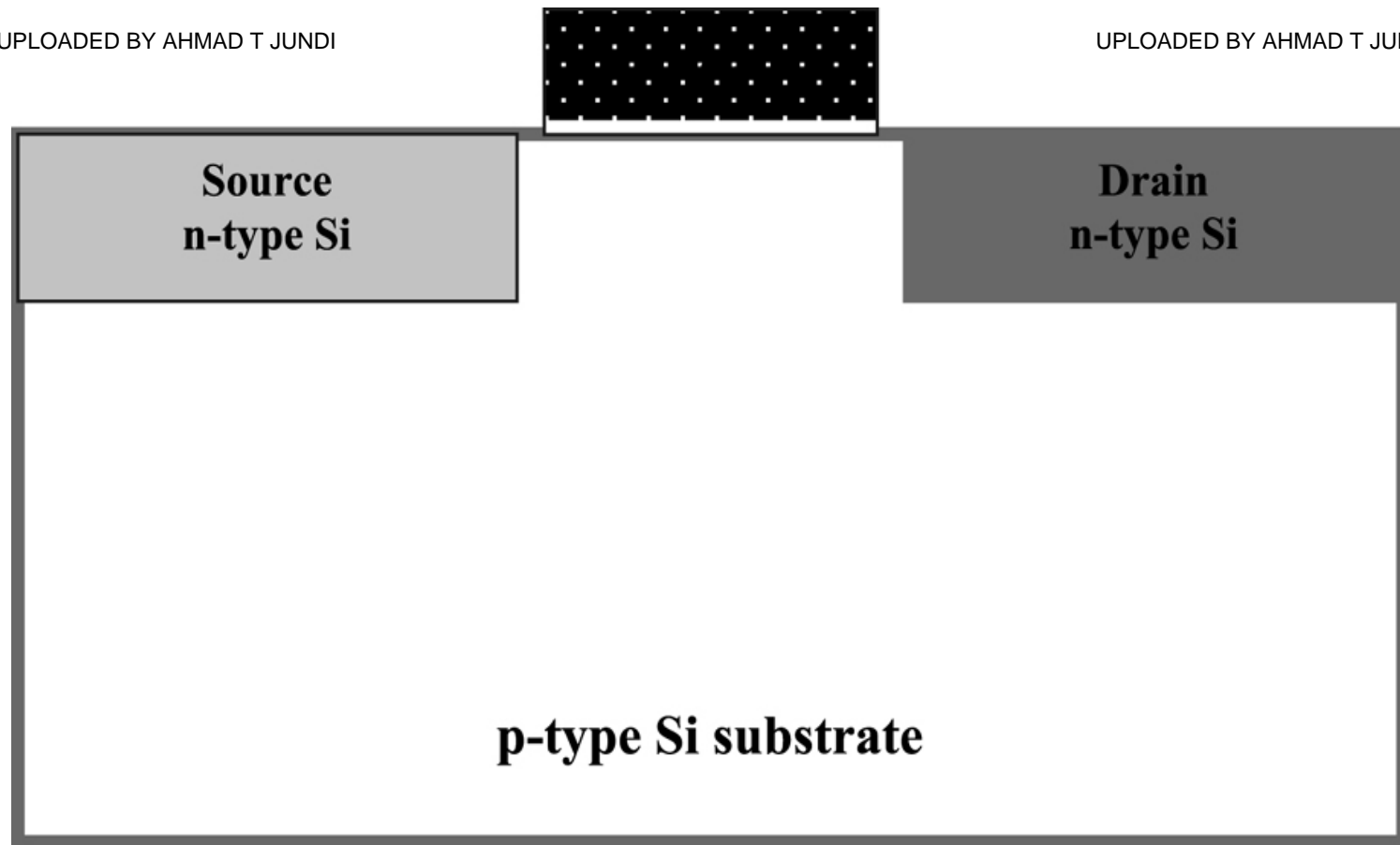


Example 5.2 (Continued)

Consider that diffusion of a species is initiated by temperature and concentration gradients and that external electric and magnetic fields can initiate the drift of carriers, then:

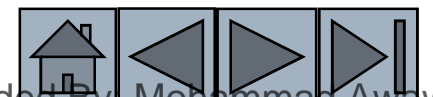
- (a) Show schematically which way the electrons and holes will diffuse when a p-n junction is formed.
- (b) Compare this situation with the diffusion of Cu and Ni atoms in the previous example.
- (c) Based on this comment on the electric field driven drift of electrons and holes in the p-n junction. Assume the temperature is 300 K.

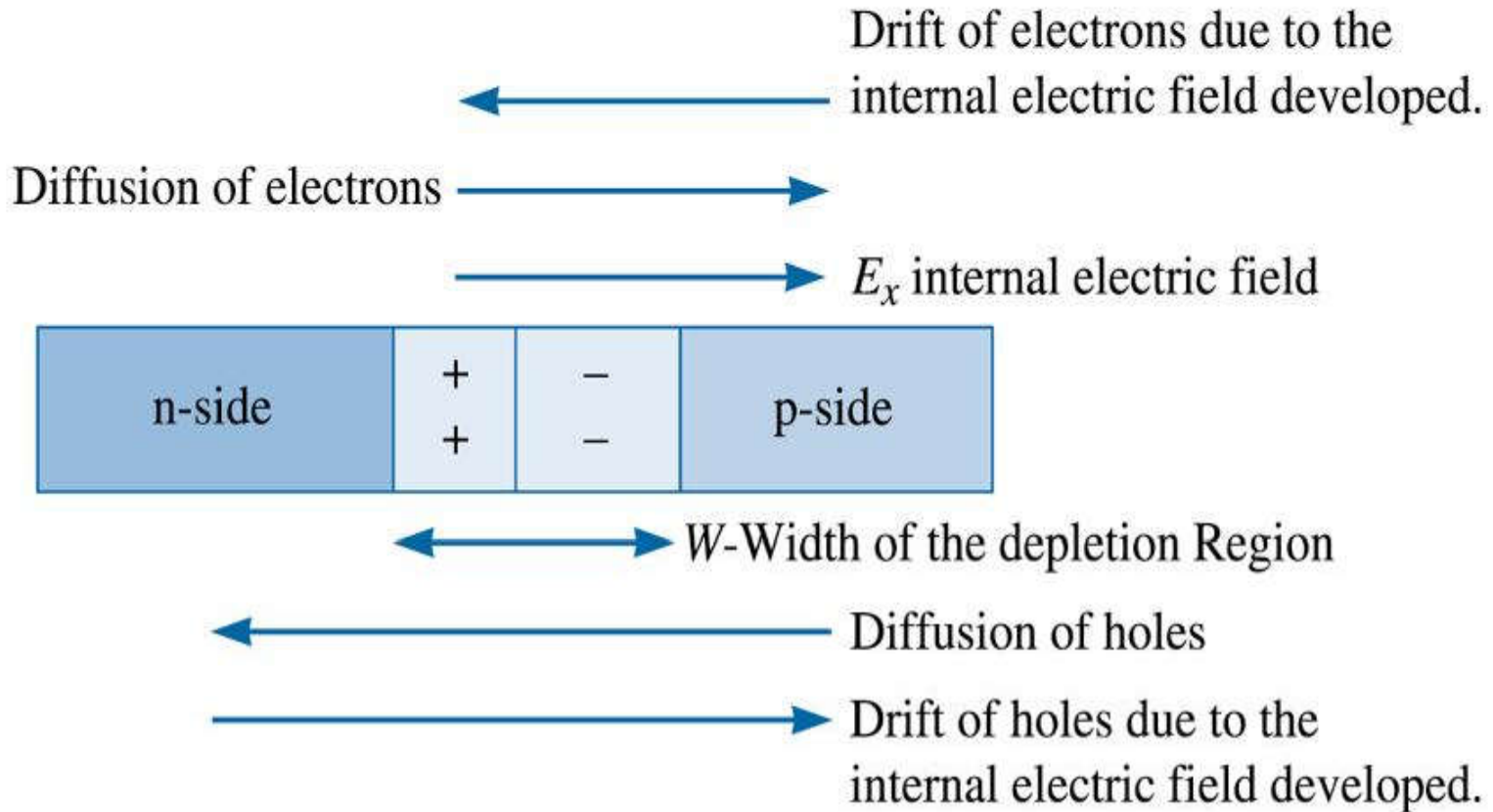




©2003 Brooks/Cole, a division of Thomson Learning, Inc. Thomson LearningSM is a trademark used herein under license.

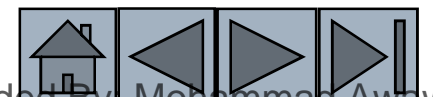
Figure 5.2 Schematic of a n-p-n transistor. Diffusion plays a critical role in formation of the different regions created in the semiconductor substrates. The creation of millions of such transistors is at the heart of microelectronics technology





©2003 Brooks/Cole, a division of Thomson Learning, Inc. Thomson Learning,™ is a trademark used herein under license.

Figure 5.7 Directions for diffusion and drift of charge carriers in a semiconductor (for Example 5.2)





Section 5.2

Stability of Atoms and Ions

- Arrhenius equation
- Activation energy -The energy required to cause a particular reaction to occur.



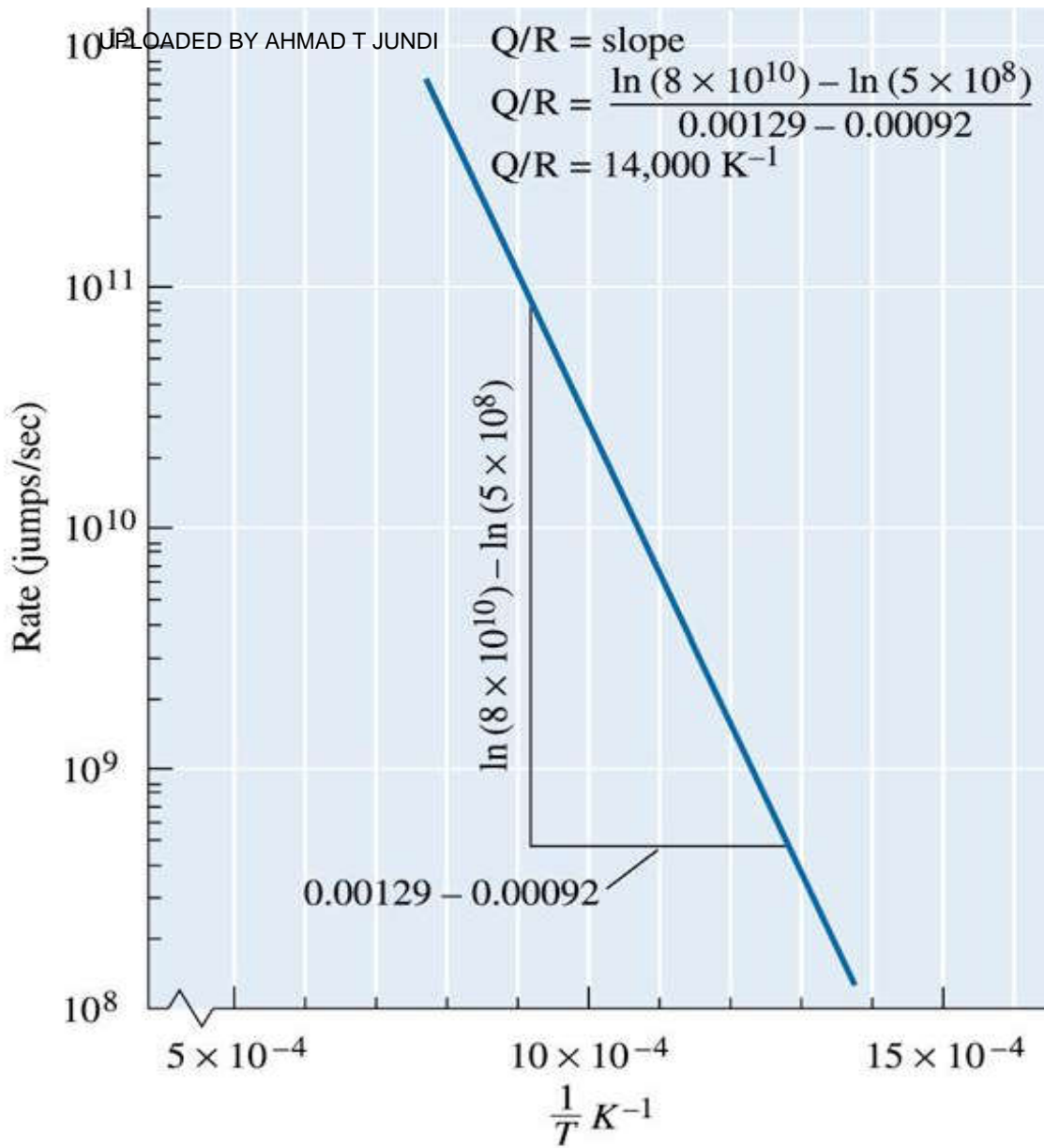
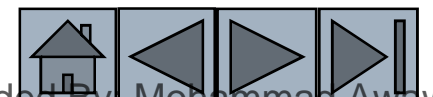


Figure 5.8 The Arrhenius plot of $\ln(\text{rate})$ versus $1/T$ can be used to determine the activation energy required for a reaction





Example 5.3

Activation Energy for Interstitial Atoms

Suppose that interstitial atoms are found to move from one site to another at the rates of 5×10^8 jumps/s at 500°C and 8×10^{10} jumps/s at 800°C . Calculate the activation energy Q for the process.





Example 5.3 SOLUTION

Figure 5.8 represents the data on a $\ln(\text{rate})$ versus $1/T$ plot; the slope of this line, as calculated in the figure, gives $Q/R = 14,000 \text{ K}^{-1}$, or $Q = 27,880 \text{ cal/mol}$. Alternately, we could write two simultaneous equations:

$$\text{Rate}\left(\frac{\text{jumps}}{s}\right) = C_0 \exp\left(\frac{-Q}{RT}\right)$$
$$Q = \frac{5.075}{0.000182} = 27,880 \text{ cal/mol}$$





Section 5.3

Mechanisms for Diffusion

- **Self-diffusion** - The random movement of atoms within an essentially pure material.
- **Vacancy diffusion** - Diffusion of atoms when an atom leaves a regular lattice position to fill a vacancy in the crystal.
- **Interstitial diffusion** - Diffusion of small atoms from one interstitial position to another in the crystal structure.



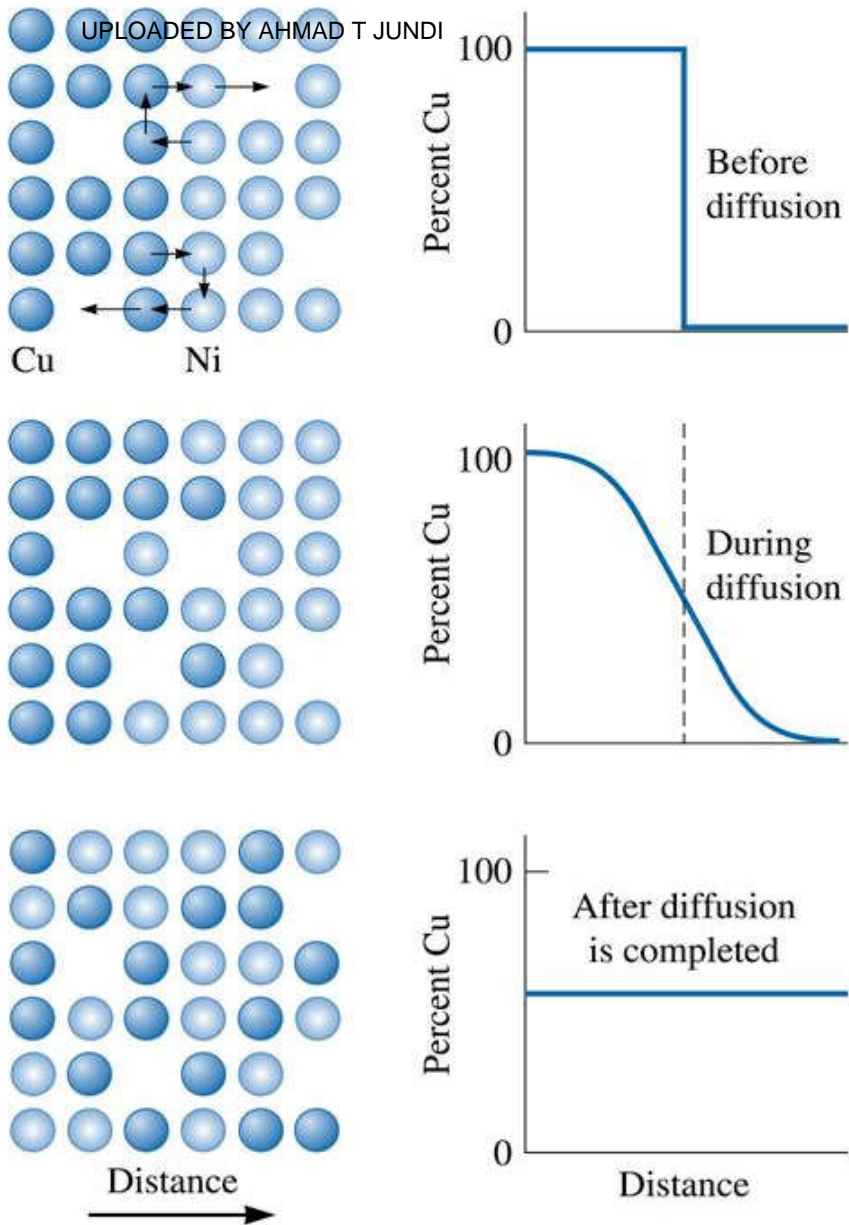
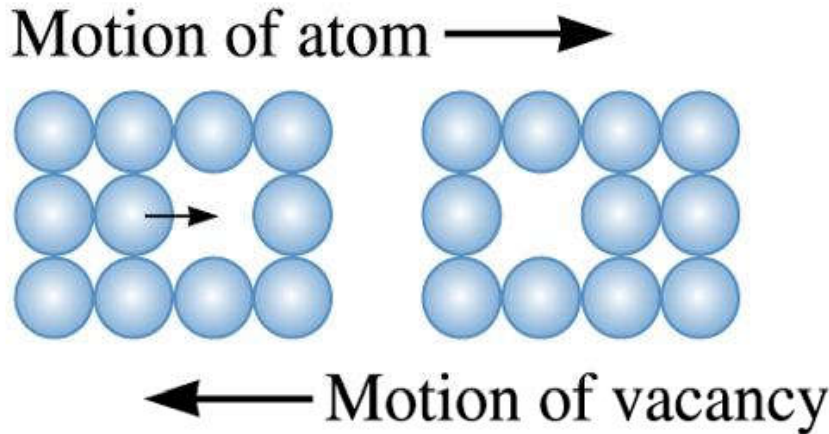
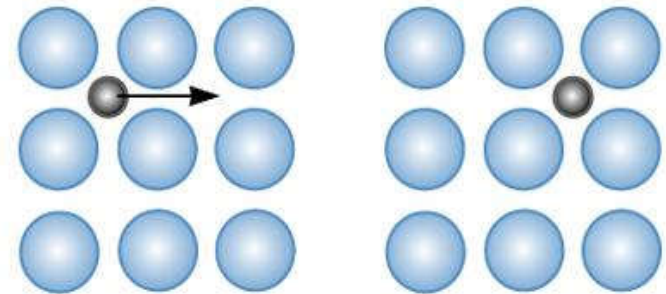


Figure 5.10 Diffusion of copper atoms into nickel. Eventually, the copper atoms are randomly distributed throughout the nickel



(a) Vacancy mechanism



(b) Interstitial mechanism

©2003 Brooks/Cole, a division of Thomson Learning, Inc. Thomson Learning,™ is a trademark used herein under license.

Figure 5.11 Diffusion mechanisms in material: (a) vacancy or substitutional atom diffusion and (b) interstitial diffusion





Activation Energy for Diffusion

- **Diffusion couple** - A combination of elements involved in diffusion studies

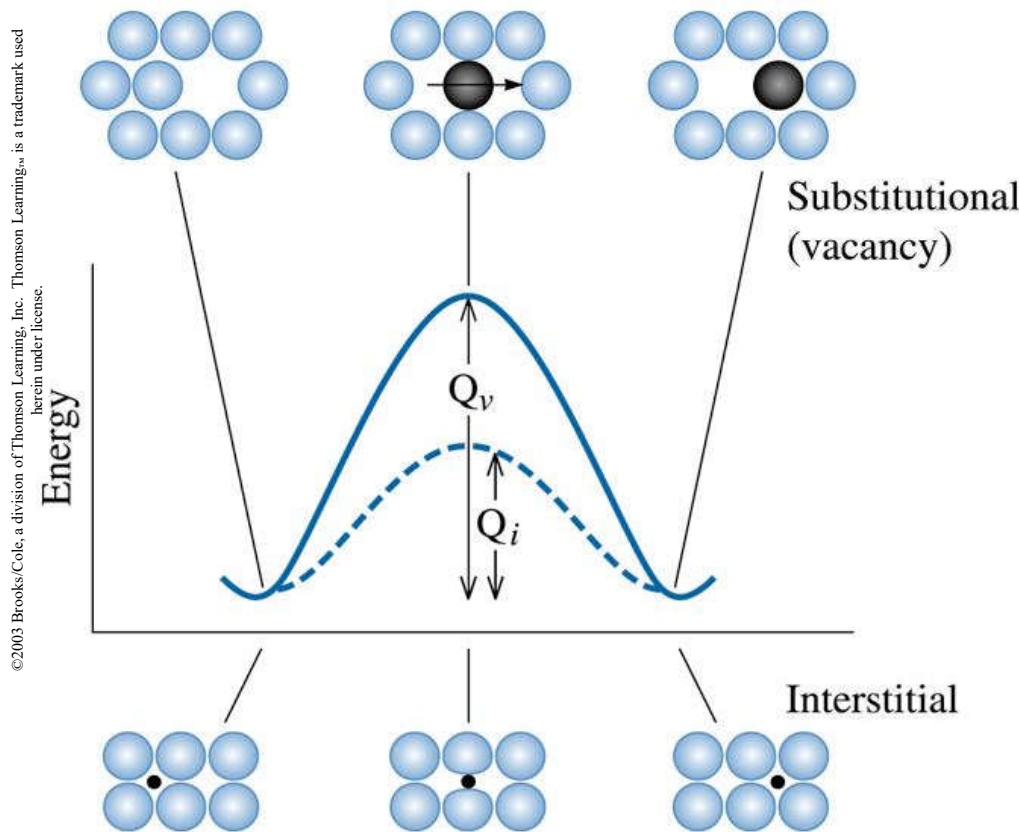


Figure 5.12 A high energy is required to squeeze atoms past one another during diffusion. This energy is the activation energy Q . Generally more energy is required for a substitutional atom than for an interstitial atom



TABLE 5-1 ■ Diffusion data for selected materials

UPLOADED BY AHMAD T JUNDI

UPLOADED BY AHMAD T JUNDI



Diffusion Couple	Q (cal/mol)	D_0 (cm²/s)
Interstitial diffusion:		
C in FCC iron	32,900	0.23
C in BCC iron	20,900	0.011
N in FCC iron	34,600	0.0034
N in BCC iron	18,300	0.0047
H in FCC iron	10,300	0.0063
H in BCC iron	3,600	0.0012
Self-diffusion (vacancy diffusion):		
Pb in FCC Pb	25,900	1.27
Al in FCC Al	32,200	0.10
Cu in FCC Cu	49,300	0.36
Fe in FCC Fe	66,700	0.65
Zn in HCP Zn	21,800	0.1
Mg in HCP Mg	32,200	1.0
Fe in BCC Fe	58,900	4.1
W in BCC W	143,300	1.88
Si in Si (covalent)	110,000	1800.0
C in C (covalent)	163,000	5.0
Heterogeneous diffusion (vacancy diffusion):		
Ni in Cu	57,900	2.3
Cu in Ni	61,500	0.65
Zn in Cu	43,900	0.78
Ni in FCC iron	64,000	4.1
Au in Ag	45,500	0.26
Ag in Au	40,200	0.072
Al in Cu	39,500	0.045
Al in Al ₂ O ₃	114,000	28.0
O in Al ₂ O ₃	152,000	1900.0
Mg in MgO	79,000	0.249
O in MgO	82,100	0.000043

From several sources, including Adda, Y. and Philibert, J., La Diffusion dans les Solides, Vol. 2, 1966.





Section 5.5

Rate of Diffusion (Fick's First Law)

- **Fick's first law** - The equation relating the flux of atoms by diffusion to the diffusion coefficient and the concentration gradient.
- **Diffusion coefficient (D)** - A temperature-dependent coefficient related to the rate at which atoms, ions, or other species diffuse.
- **Concentration gradient** - The rate of change of composition with distance in a nonuniform material, typically expressed as atoms/cm³·cm or at%/cm.





©2003 Brooks/Cole, a division of Thomson Learning, Inc. Thomson Learning, Inc. is a trademark used herein under license.

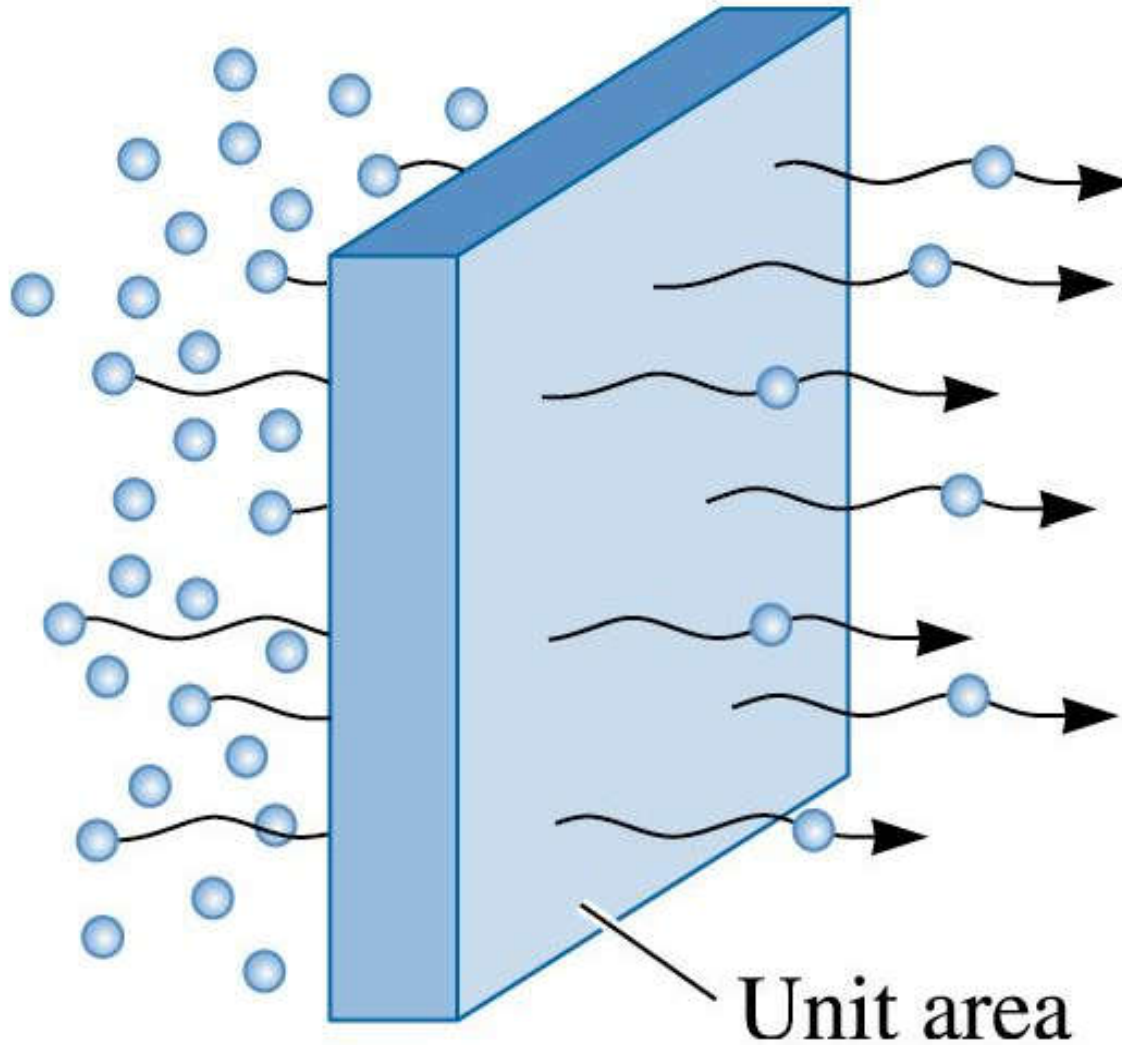


Figure 5.14 The flux during diffusion is defined as the number of atoms passing through a plane of unit area per unit time

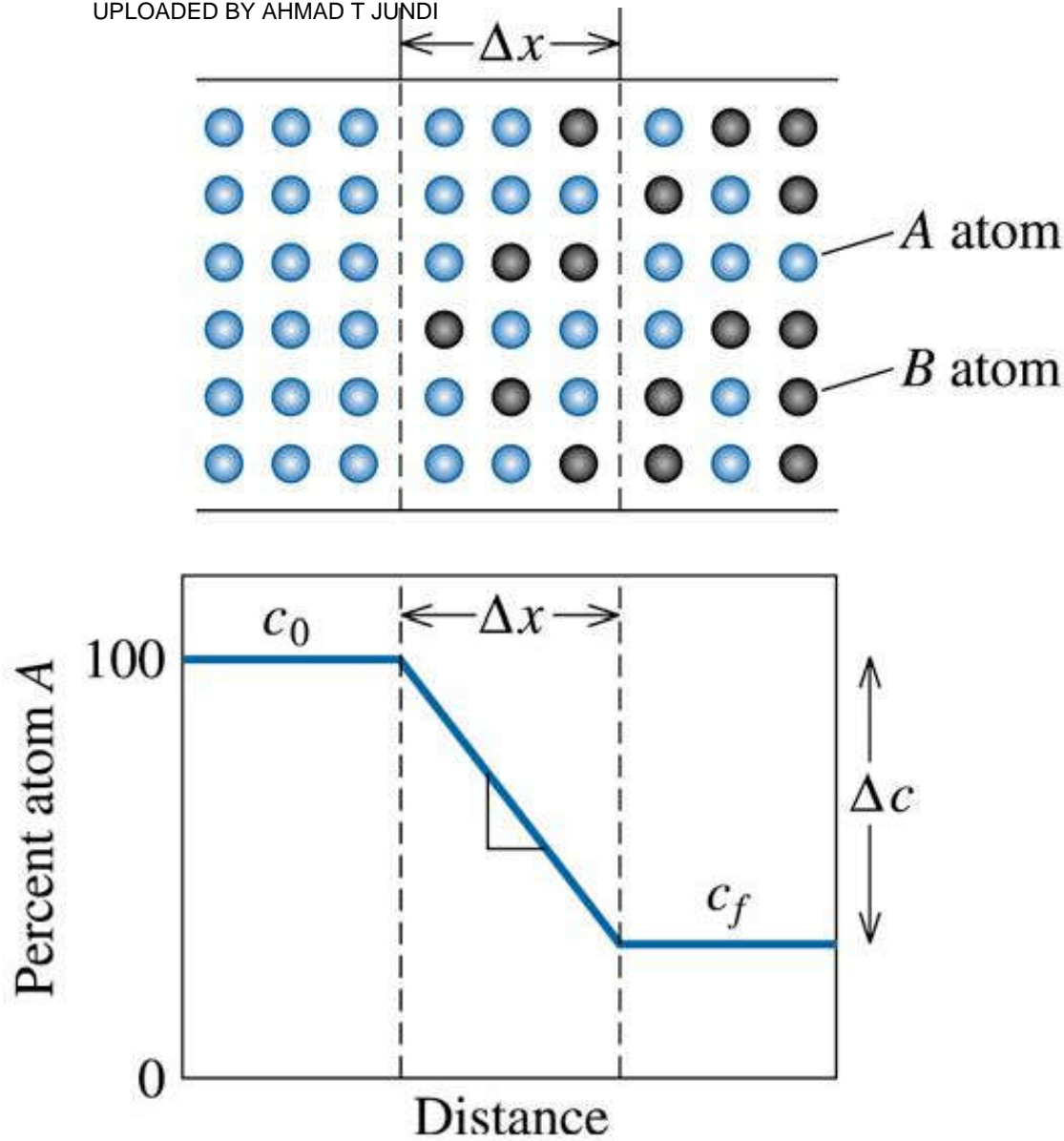


Figure 5.15
Illustration of the
concentration
gradient

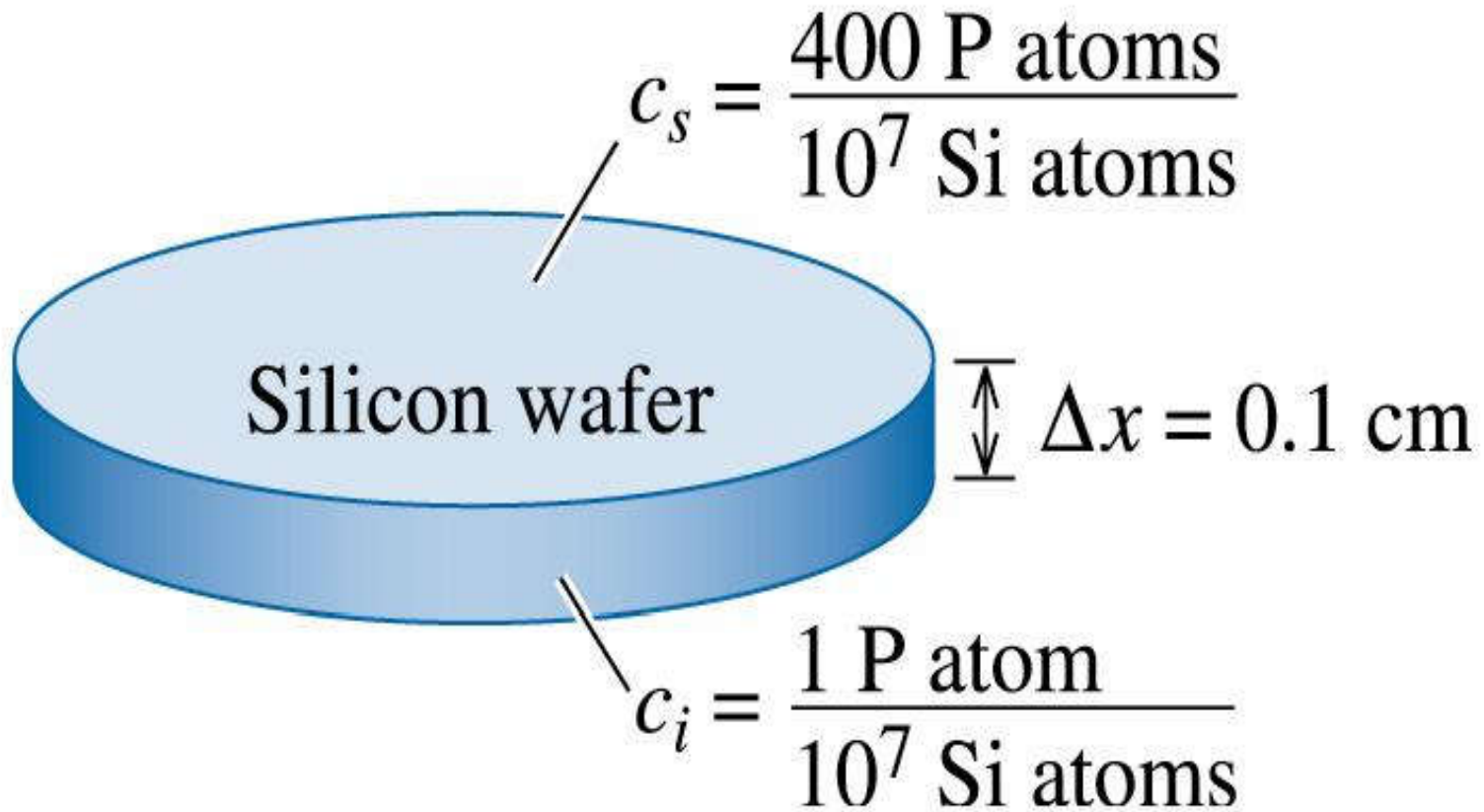


Example 5.4

Semiconductor Doping

One way to manufacture transistors, which amplify electrical signals, is to diffuse impurity atoms into a semiconductor material such as silicon (Si). Suppose a silicon wafer 0.1 cm thick, which originally contains one phosphorus atom for every 10 million Si atoms, is treated so that there are 400 phosphorous (P) atoms for every 10 million Si atoms at the surface (Figure 5.16). Calculate the concentration gradient (a) in atomic percent/cm and (b) in atoms /cm³.cm. The lattice parameter of silicon is 5.4307 Å.





©2003 Brooks/Cole, a division of Thomson Learning, Inc. Thomson Learning™ is a trademark used herein under license.

Figure 5.16 Silicon wafer showing variation in concentration of P atoms (for Example 5.4)





Example 5.4 SOLUTION

a) Calculate the initial and surface compositions in atomic percent.

$$C_i = \frac{1P_{atom}}{10^7 atoms} \times 100 = 0.00001at\%P$$

$$C_s = \frac{400P_{atom}}{10^7 atoms} \times 100 = 0.004at\%P$$

$$\frac{\Delta c}{\Delta x} = \frac{0.00001 - 0.004at\%P}{0.1cm} = -0.0399 \frac{at\%P}{cm}$$



Example 5.4 SOLUTION (Continued)



UPLOADED BY AHMAD T JUNDI

b) The volume of the unit cell:

$$V_{\text{cell}} = (5.4307 \times 10^{-8} \text{ cm})^3 = 1.6 \times 10^{-22} \text{ cm}^3/\text{cell}$$

The volume occupied by 10^7 Si atoms, which are arranged in a diamond cubic (DC) structure with 8 atoms/cell, is:

$$V = 2 \times 10^{-16} \text{ cm}^3$$

The compositions in atoms/cm³ are:

$$c_i = \frac{1 \text{ P atom}}{2 \times 10^{-16} \text{ cm}^3} = 0.005 \times 10^{18} \text{ P} \left(\frac{\text{atoms}}{\text{cm}^3} \right)$$

$$c_s = \frac{400 \text{ P atoms}}{2 \times 10^{-16} \text{ cm}^3} = 2 \times 10^{18} \text{ P} \left(\frac{\text{atoms}}{\text{cm}^3} \right)$$

$$\frac{\Delta c}{\Delta x} = \frac{0.005 \times 10^{18} - 2 \times 10^{18} \text{ P} \left(\frac{\text{atoms}}{\text{cm}^3} \right)}{0.1 \text{ cm}}$$

$$= -1.995 \times 10^{19} \text{ P} \frac{\text{atoms}}{\text{cm}^3 \cdot \text{cm}}$$



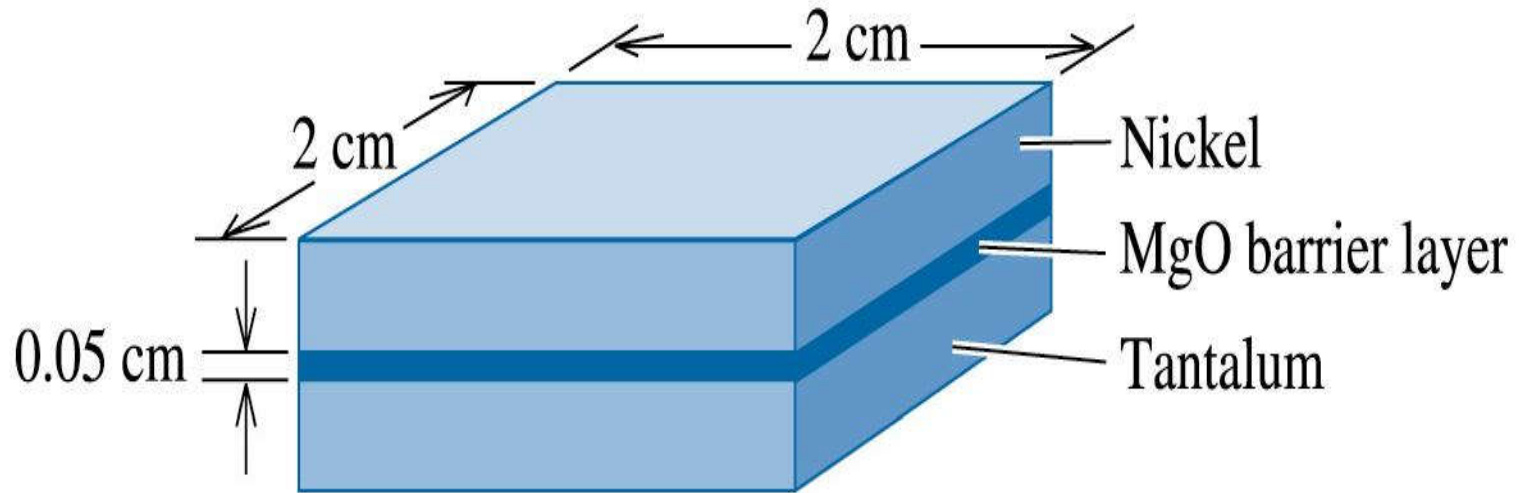


Example 5.5

Diffusion of Nickel in Magnesium Oxide (MgO)

A 0.05 cm layer of magnesium oxide (MgO) is deposited between layers of nickel (Ni) and tantalum (Ta) to provide a diffusion barrier that prevents reactions between the two metals (Figure 5.17). At 1400°C, nickel ions are created and diffuse through the MgO ceramic to the tantalum. Determine the number of nickel ions that pass through the MgO per second. The diffusion coefficient of nickel ions in MgO is 9×10^{-12} cm²/s, and the lattice parameter of nickel at 1400°C is 3.6×10^{-8} cm.





©2003 Brooks/Cole, a division of Thomson Learning, Inc. Thomson Learning™ is a trademark used herein under license.

Figure 5.17 Diffusion couple (for Example 5.5)





Example 5.5 SOLUTION

The composition of nickel at the Ni/MgO interface is 100% Ni, or

$$C_{Ni / MgO} = \frac{4Ni \frac{atoms}{unitcell}}{(3.6 \times 10^{-8} cm)^3} = 8.57 \times 10^{22} \frac{atoms}{cm^3}$$

The composition of nickel at the Ta/MgO interface is 0% Ni. Thus, the concentration gradient is:

$$\frac{\Delta c}{\Delta x} = \frac{0 - 8.57 \times 10^{22} \frac{atoms}{cm^3}}{0.05cm} = -1.71 \times 10^{24} \frac{atoms}{cm^3.cm}$$





Example 5.5 SOLUTION (Continued)

The flux of nickel atoms through the MgO layer is:

$$J = -D \frac{\Delta c}{\Delta x} = (9 \times 10^{-12} \text{ cm}^2 / \text{s})(-1.71 \times 10^{24} \frac{\text{atoms}}{\text{cm}^3 \cdot \text{cm}})$$

$$J = 1.54 \times 10^{13} \frac{\text{Ni atoms}}{\text{cm}^2 \cdot \text{s}}$$

The total number of nickel atoms crossing the 2 cm × 2 cm interface per second is:

$$\begin{aligned} \text{Total Ni atoms per second} &= J(\text{Area}) \\ &= (1.54 \times 10^{13} \text{ atoms/cm}^2 \cdot \text{s}) (2 \text{ cm})(2 \text{ cm}) \\ &= 6.16 \times 10^{13} \text{ Ni atoms/s} \end{aligned}$$





Section 5.6

Factors Affecting Diffusion

- Temperature and the Diffusion Coefficient (D)
- Types of Diffusion - volume diffusion, grain boundary diffusion, Surface diffusion
- Time
- Dependence on Bonding and Crystal Structure
- Dependence on Concentration of Diffusing Species and Composition of Matrix



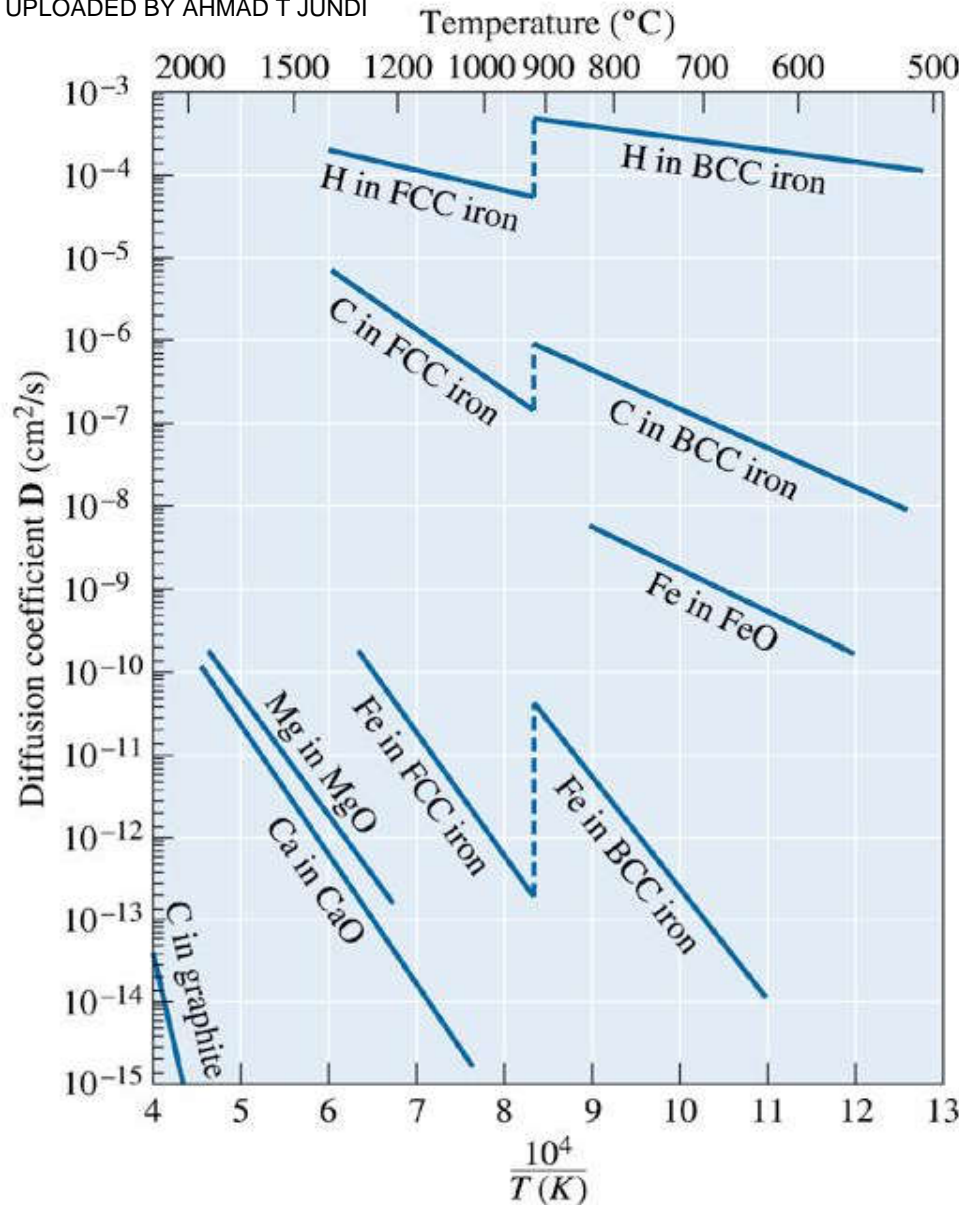


Figure 5.18 The diffusion coefficient D as a function of reciprocal temperature for some metals and ceramics. In the Arrhenius plot, D represents the rate of the diffusion process. A steep slope denotes a high activation energy

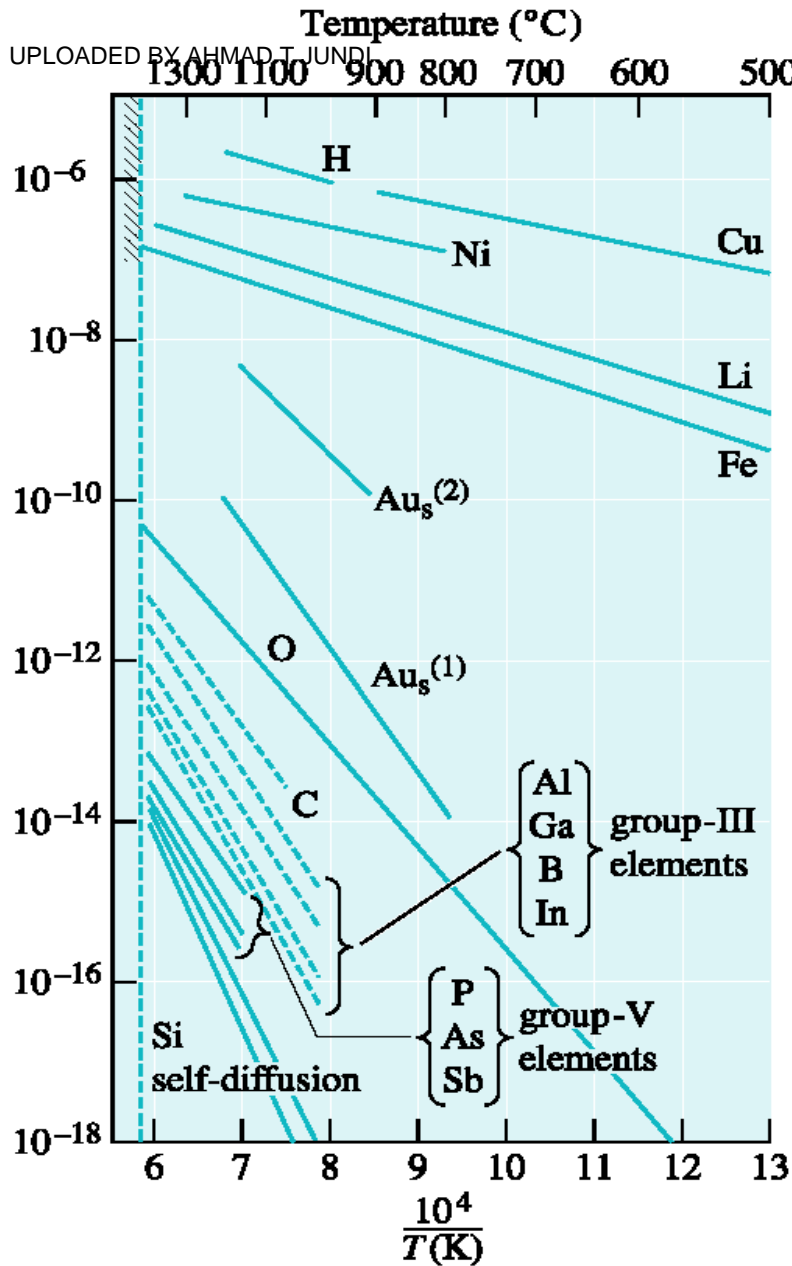
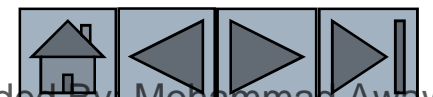
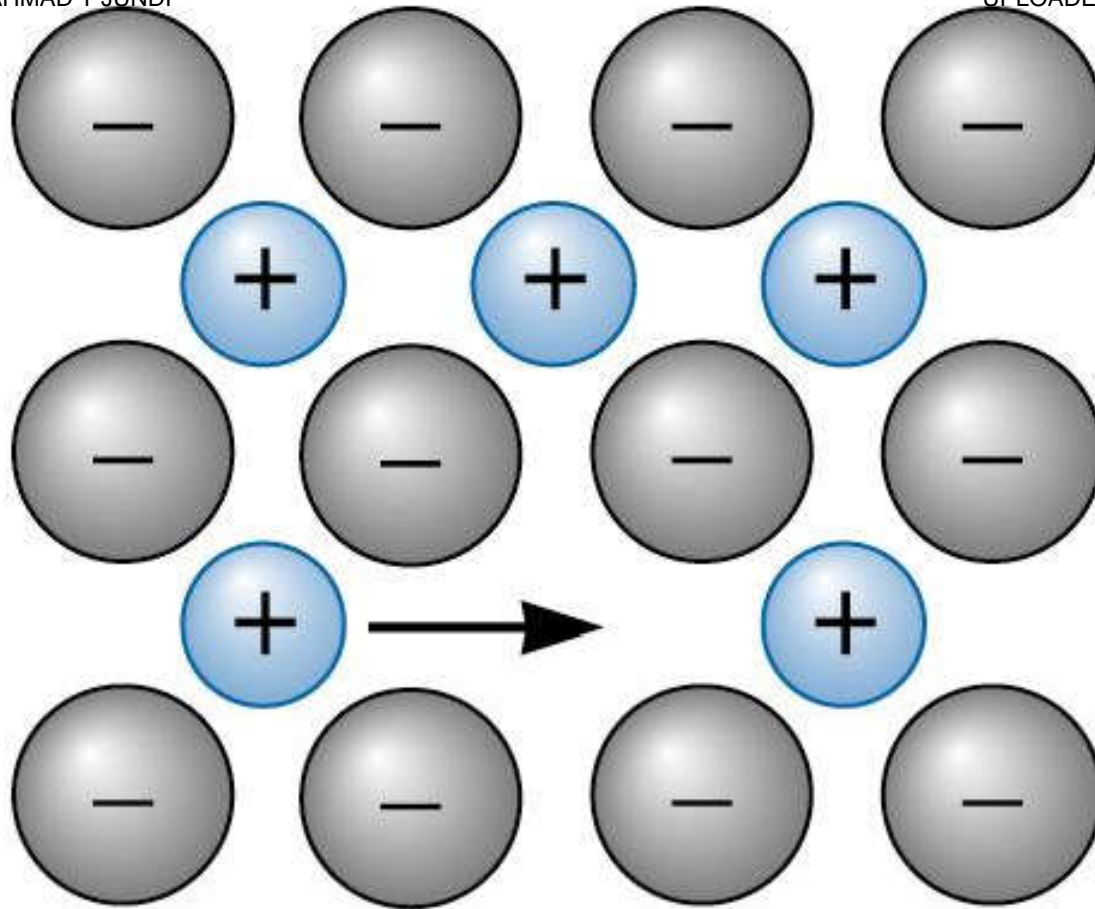


Figure 5.19 Diffusion coefficients for different dopants in silicon.
(Source: From "Diffusion and Diffusion Induced Defects in Silicon," by U. Gösele. In R. Bloor, M. Flemings, and S. Mahajan (Eds.), Encyclopedia of Advanced Materials, Vol. 1, 1994, p. 631, Fig. 2. Copyright © 1994 Pergamon Press. Reprinted with permission of the authors.)





©2003 Brooks/Cole, a division of Thomson Learning, Inc. Thomson Learningsm is a trademark used herein under license.

Figure 5.20 Diffusion in ionic compounds. Anions can only enter other anion sites. Smaller cations tend to diffuse faster

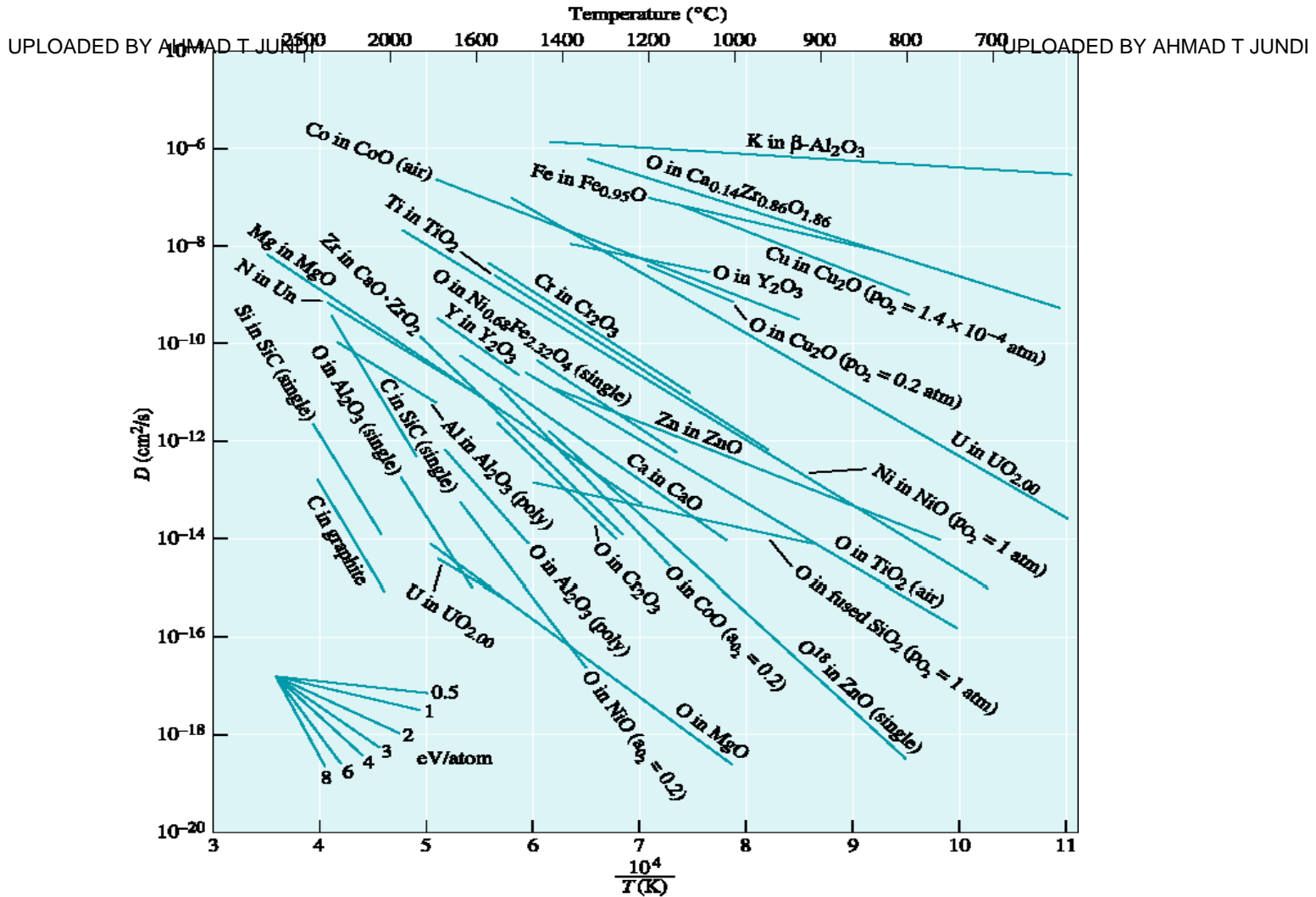


Figure 5.21 Diffusion coefficients of ions in different oxides. (Source: Adapted from Physical Ceramics: Principles for Ceramic Science and Engineering, by Y.M. Chiang, D. Birnie, and W.D. Kingery, Fig. 3-1. Copyright © 1997 John Wiley & Sons. Adapted with permission.)



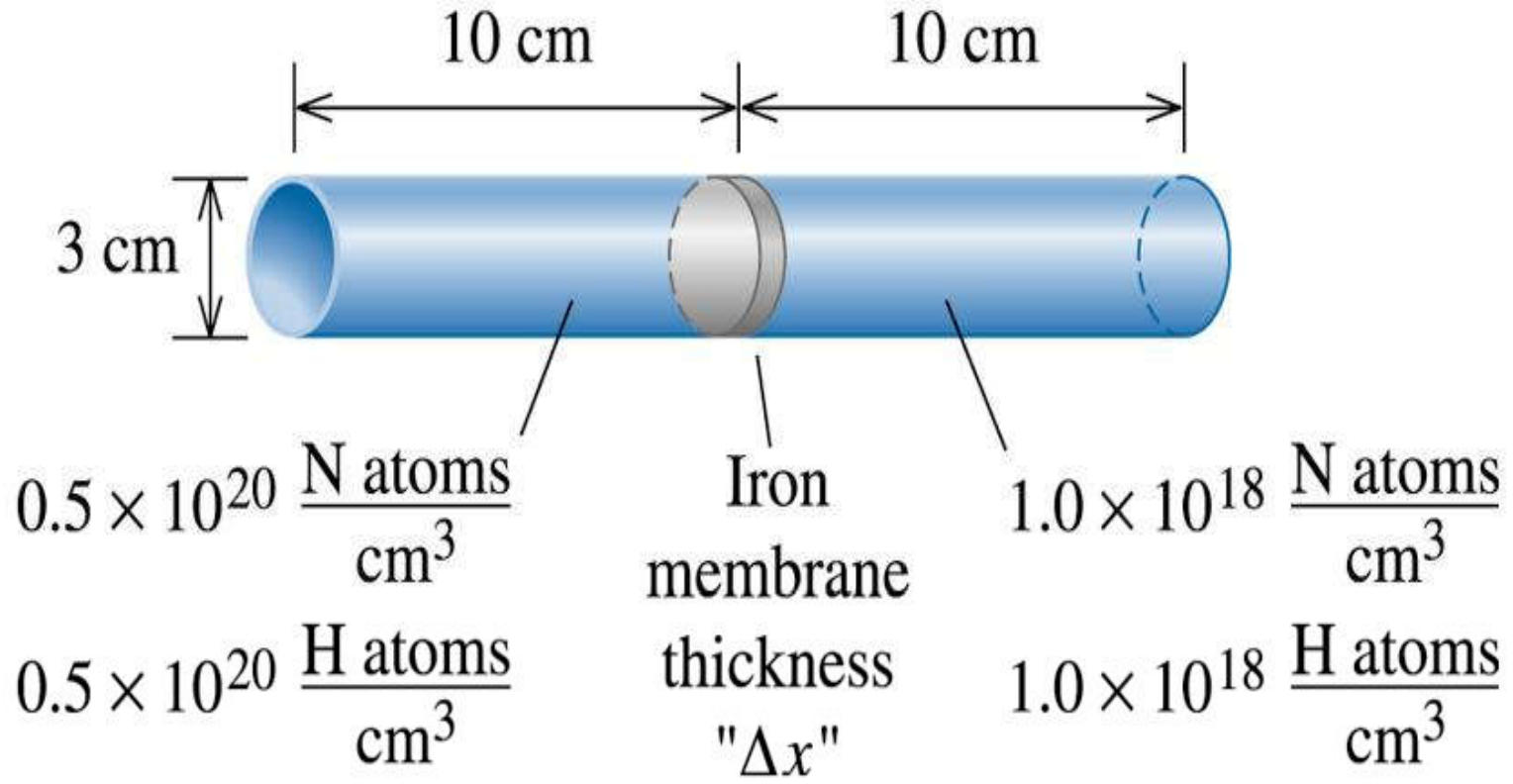


Example 5.6

Design of an Iron Membrane

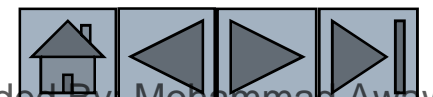
An impermeable cylinder 3 cm in diameter and 10 cm long contains a gas that includes 0.5×10^{20} N atoms per cm^3 and 0.5×10^{20} H atoms per cm^3 on one side of an iron membrane (Figure 5.22). Gas is continuously introduced to the pipe to assure a constant concentration of nitrogen and hydrogen. The gas on the other side of the membrane includes a constant 1×10^{18} N atoms per cm^3 and 1×10^{18} H atoms per cm^3 . The entire system is to operate at 700°C , where the iron has the BCC structure. Design an iron membrane that will allow no more than 1% of the nitrogen to be lost through the membrane each hour, while allowing 90% of the hydrogen to pass through the membrane per hour.





©2003 Brooks/Cole, a division of Thomson Learning, Inc. Thomson Learning,™ is a trademark used herein under license.

Figure 5.22 Design of an ion membrane (for Example 5.6)





Example 5.6 SOLUTION

The total number of nitrogen atoms in the container is:

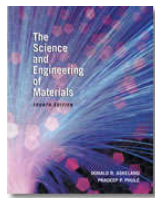
$$(0.5 \times 10^{20} \text{ N/cm}^3)(\pi/4)(3 \text{ cm})^2(10 \text{ cm}) = 35.343 \times 10^{20} \text{ N atoms}$$

The flux is then:

$$J = \frac{(0.0098 \times 10^{18} \text{ (N atoms/s)})}{\left(\frac{\pi}{4}\right)(3 \text{ cm})^2}$$

$$= 0.00139 \times 10^{18} \text{ N } \frac{\text{atoms}}{\text{cm}^2 \cdot \text{s}}$$



UPLOADED BY AHMAD T JUNDI
Example 5.6 SOLUTION(Continued)

$$D = D_0 \exp\left(\frac{-Q}{RT}\right)$$

In a similar manner, the maximum thickness of the membrane that will permit 90% of the hydrogen to pass can be calculated:

$$\text{H atom loss per h} = (0.90)(35.343 \times 10^{20}) = 31.80 \times 10^{20}$$

$$\text{H atom loss per s} = 0.0088 \times 10^{20}$$

$$J = 0.125 \times 10^{18} \frac{\text{H atoms}}{\text{cm}^2 \cdot \text{s}}$$

$\Delta x = 0.0128 \text{ cm} = \text{minimum thickness of the membrane}$

$$\Delta x = \frac{\left(1.86 \times 10^{-4} \frac{\text{cm}^2}{\text{s}}\right) \left(49 \times 10^{18} \frac{\text{H atoms}}{\text{cm}^3}\right)}{0.125 \times 10^{18} \frac{\text{H atoms}}{\text{cm}^2 \cdot \text{s}}}$$

$$= 0.0729 \text{ cm} = \text{maximum thickness}$$

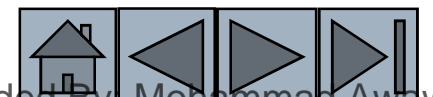




TABLE 5-2 ■ *The effect of the type of diffusion for thorium in tungsten and for self-diffusion in silver**

Diffusion Type	Diffusion Coefficient (<i>D</i>)			
	Thorium in Tungsten		Silver in Silver	
	D_0 cm ² /s	<i>Q</i> cal/mole	D_0 cm ² /s	<i>Q</i> cal/mole
Surface	0.47	66,400	0.068	8,900
Grain boundary	0.74	90,000	0.24	22,750
Volume	1.00	120,000	0.99	45,700

* Given by parameters for Equation 5-4.





Example 5.7

Tungsten Thorium Diffusion Couple

Consider a diffusion couple setup between pure tungsten and a tungsten alloy containing 1 at.% thorium. After several minutes of exposure at 2000°C , a transition zone of 0.01 cm thickness is established. What is the flux of thorium atoms at this time if diffusion is due to (a) volume diffusion, (b) grain boundary diffusion, and (c) surface diffusion? (See Table 5.2.)

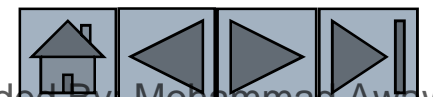




TABLE 5-2 ■ *The effect of the type of diffusion for thorium in tungsten and for self-diffusion in silver**

Diffusion Type	Diffusion Coefficient (<i>D</i>)			
	Thorium in Tungsten		Silver in Silver	
	<u>D_0 cm²/s</u>	<u>Q cal/mole</u>	<u>D_0 cm²/s</u>	<u>Q cal/mole</u>
Surface	0.47	66,400	0.068	8,900
Grain boundary	0.74	90,000	0.24	22,750
Volume	1.00	120,000	0.99	45,700

* Given by parameters for Equation 5-4.





Example 5.7 SOLUTION

The lattice parameter of BCC tungsten is about 3.165 Å. Thus, the number of tungsten atoms/cm³ is:

$$\frac{W \text{ atoms}}{\text{cm}^3} = \frac{2 \text{ atoms/cell}}{(3.165 \times 10^{-8})^3 \text{ cm}^3/\text{cell}} = 6.3 \times 10^{22}$$

In the tungsten-1 at.% thorium alloy, the number of thorium atoms is:

$$c_{\text{Th}} = (0.01)(6.3 \times 10^{22}) = 6.3 \times 10^{20} \text{ Th atoms/cm}^3$$

In the pure tungsten, the number of thorium atoms is zero. Thus, the concentration gradient is:

$$\frac{\Delta c}{\Delta x} = \frac{0 - 6.3 \times 10^{20} \frac{\text{atoms}}{\text{cm}^3}}{0.01 \text{ cm}} = -6.3 \times 10^{22} \text{ Th} \frac{\text{atoms}}{\text{cm}^3 \cdot \text{cm}}$$





Example 5.7 SOLUTION(Continued)

1. Volume diffusion

$$= 18.2 \times 10^{10} \frac{\text{Th atoms}}{\text{cm}^2 \cdot \text{s}}$$

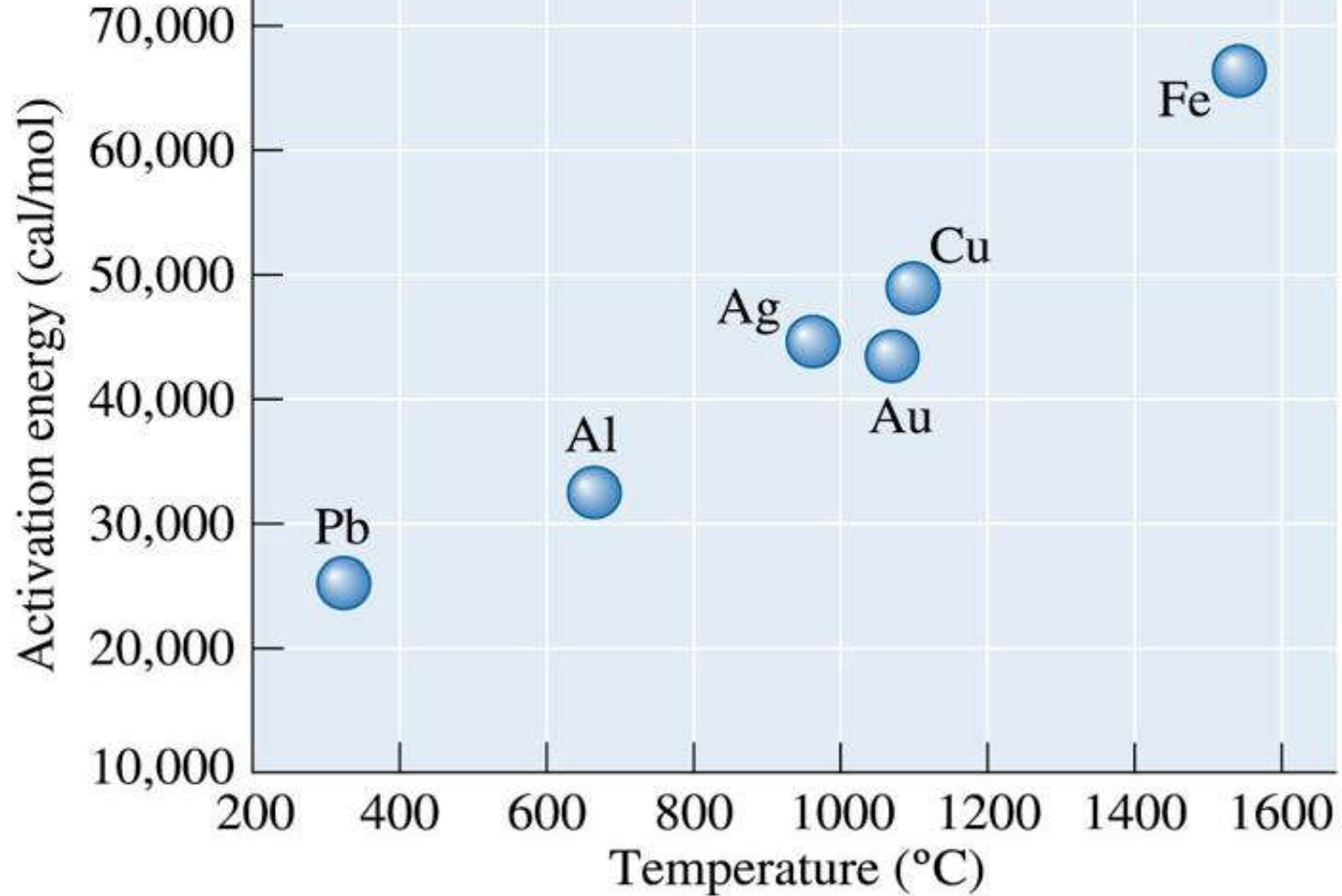
2. Grain boundary diffusion

$$= 10.3 \times 10^{13} \frac{\text{Th atoms}}{\text{cm}^2 \cdot \text{s}}$$

3. Surface diffusion

$$= 12.2 \times 10^{15} \frac{\text{Th atoms}}{\text{cm}^2 \cdot \text{s}}$$





©2003 Brooks/Cole, a division of Thomson Learning, Inc. Thomson Learning, is a trademark used herein under license.

Figure 5.23 The activation energy for self-diffusion increases as the melting point of the metal increases



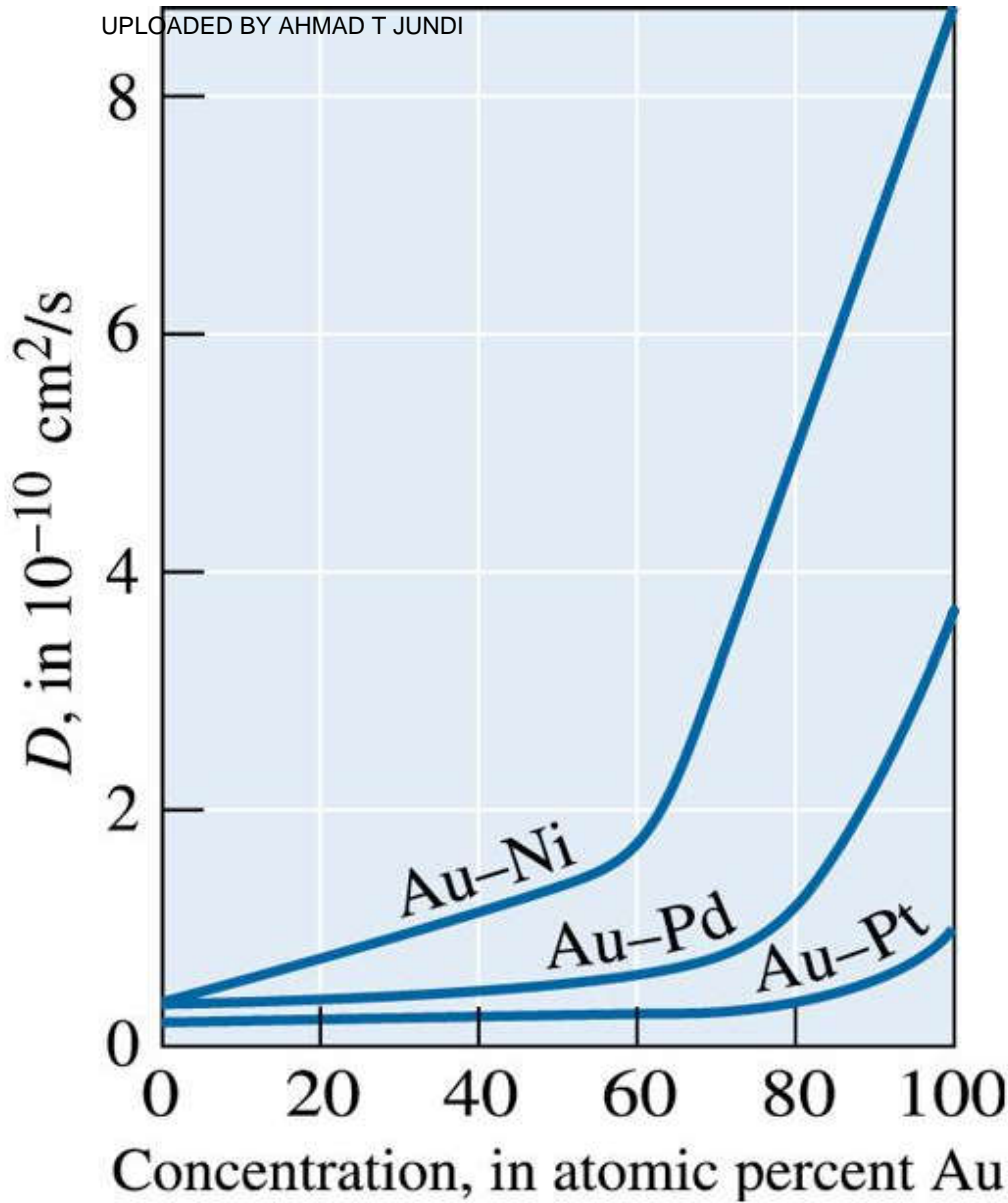


Figure 5.24 The dependence of diffusion coefficient of Au on concentration. (*Source: Adapted from Physical Metallurgy Principles, Third Edition, by R.E. Reed-Hill and R. Abbaschian, p. 363, Fig. 12-3. Copyright © 1991 Brooks/Cole Thomson Learning. Adapted with permission.*)





Example 5.8

Diffusion in Ionic Conductors

Consider two compositions of yttria (yttrium oxide, Y_2O_3)-stabilized zirconia (ZrO_2). The first sample contains 6 mole percent yttria (Y_2O_3). [9] Since each mole of yttria contains two moles of yttrium, the mole fraction of element yttrium (Y) in the first sample would be 0.12. The second sample of yttria-stabilized zirconia contains 15 mole percent yttria (Y_2O_3). Therefore, in the second sample, the mole fraction of element yttrium (Y) is 0.30. The introduction of yttria (Y_2O_3) creates oxygen vacancies and defects into which the yttrium ions go on the Zr^{+4} sites. Write down the defect chemistry equation using the Kröger-Vink notation. Show that the concentration of oxygen ion vacancies would be approximately one-half the concentration of yttrium oxide (Y_2O_3). Given this, predict which composition of yttria (Y_2O_3) will likely exhibit higher diffusivity of oxygen ions. Compare your prediction with the data shown in Figure 5.25. [6,10]



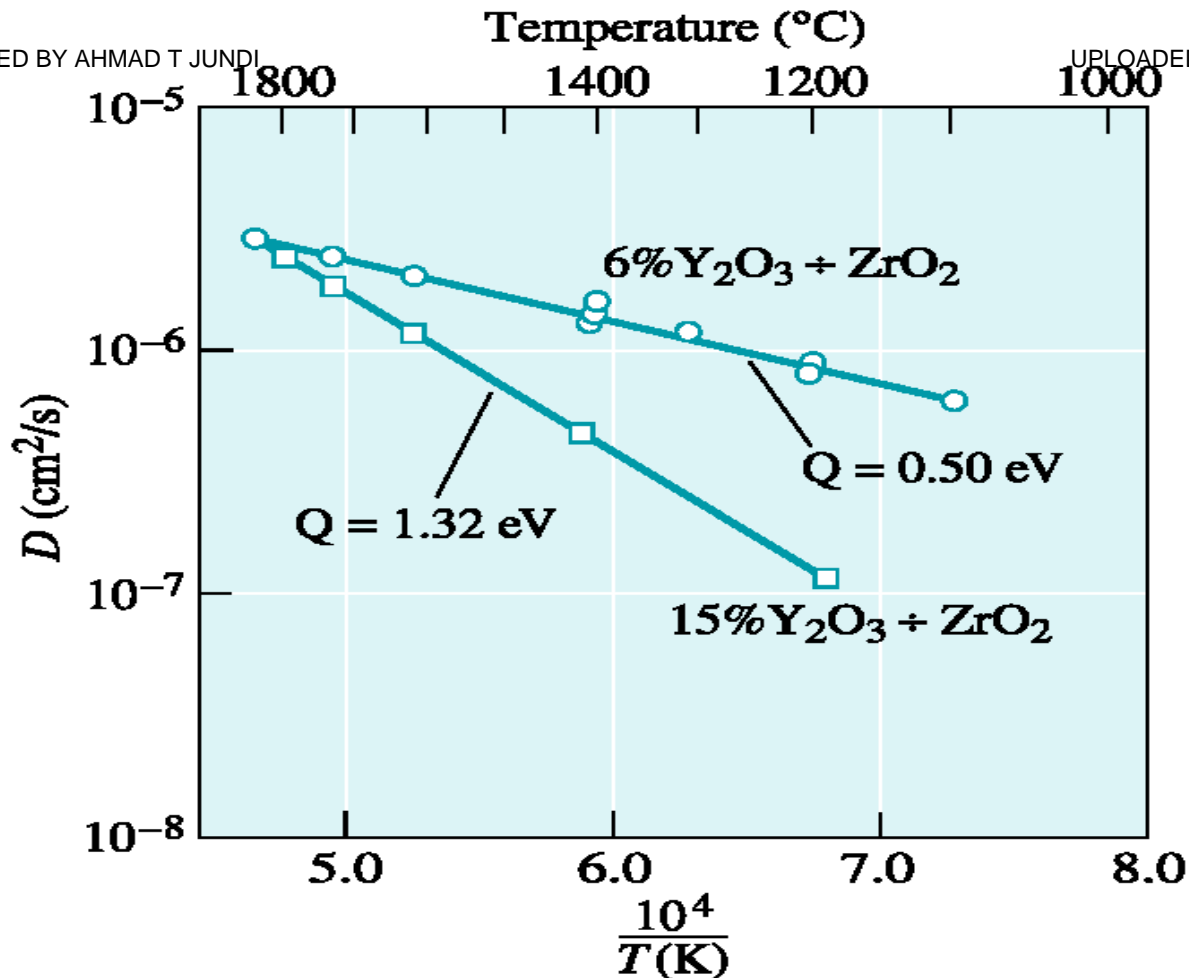


Figure 5.25 Diffusivity of oxygen ions in yttria stabilized zirconia ceramics (for Example 5-8). (Source: Adapted from *Physical Ceramics: Principles for Ceramic Science and Engineering*, by Y.M. Chiang, D. Birnie, and W.D. Kingery, Fig. 3-14. Copyright © 1997 John Wiley & Sons, Inc. Based on *Transport in Nonstoichiometric Compounds*, by G. Simkovich and U.S. Stubican (Eds.), p. 188–202, Plenum Press. Adapted with permission.)





Example 5.8 SOLUTION

Equation to express the addition of yttrium oxide



For every $2Y'_{Zr}$ defect, there is one oxygen ion vacancy $V_o^{..}$

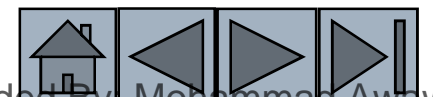
Therefore,

$$[Y'_{Zr}] = 2[V_o^{..}]$$

The concentration of oxygen ion vacancies would be given by the following equations:

$$[Y'_{Zr}] = 12\% = 2[V_o^{..}]$$

$$\therefore [V_o^{..}] = 6\%$$





Section 5.7

Permeability of Polymers

Permeability is expressed in terms of the volume of gas or vapor that can permeate per unit area, per unit time, or per unit thickness at a specified temperature and relative humidity.





Example 5.9

Design of Carbonated Beverage Bottles

You want to select a polymer for making plastic bottles that can be used for storing carbonated beverages. What factors would you consider in choosing a polymer for this application?





Example 5.9 SOLUTION

- First, since the bottles are to be used for storing carbonated beverages, a plastic material with a **small diffusivity for carbon dioxide gas** should be chosen.
- The bottles should **have enough strength** so that they can survive a fall of about six feet. This is often tested using a “drop test.”
- The **surface of the polymer** should also be amenable to printing of labels or other product information.
- The effect of processing on the **resultant microstructure** of polymers must also be considered.



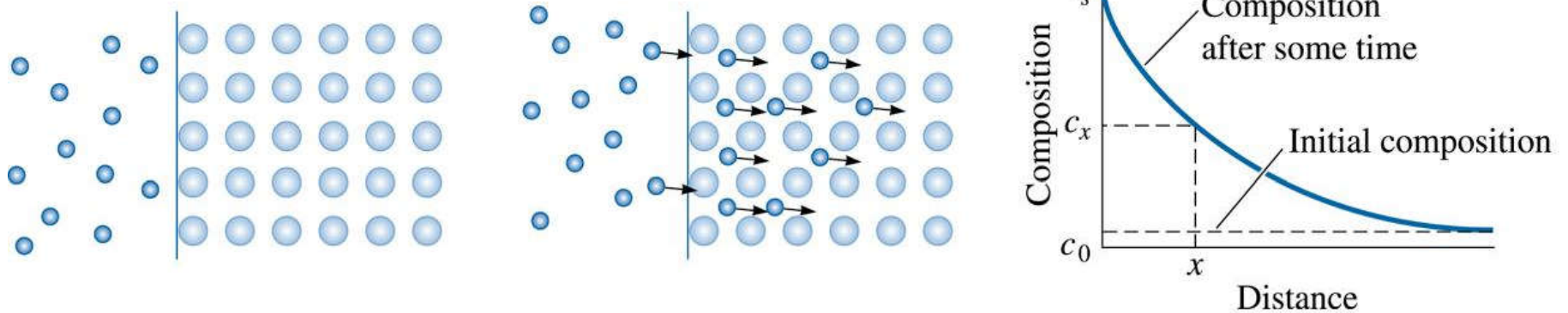


Section 5.8

Composition Profile (Fick's Second Law)

- **Fick's second law** - The partial differential equation that describes the rate at which atoms are redistributed in a material by diffusion.
- **Interdiffusion** - Diffusion of different atoms in opposite directions.
- **Kirkendall effect** - Physical movement of an interface due to unequal rates of diffusion of the atoms within the material.
- **Purple plague** - Formation of voids in gold-aluminum welds due to unequal rates of diffusion of the two atoms; eventually failure of the weld can occur.





©2003 Brooks/Cole, a division of Thomson Learning, Inc. Thomson Learning[®] is a trademark used herein under license.

Figure 5.26 Diffusion of atoms into the surface of a material illustrating the use of Fick's second law



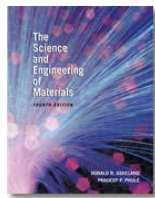


TABLE 5-3 ■ Error function values for Fick's second law

Argument of the error function $\frac{x}{2\sqrt{Dt}}$	Value of the error function $\text{erf} \frac{x}{2\sqrt{Dt}}$
0	0
0.10	0.1125
0.20	0.2227
0.30	0.3286
0.40	0.4284
0.50	0.5205
0.60	0.6039
0.70	0.6778
0.80	0.7421
0.90	0.7970
1.00	0.8427
1.50	0.9661
2.00	0.9953

Note that error function values are available on many software packages found on personal computers.





©2003 Brooks/Cole, a division of Thomson Learning, Inc. Thomson Learning, Inc. is a trademark used herein under license.

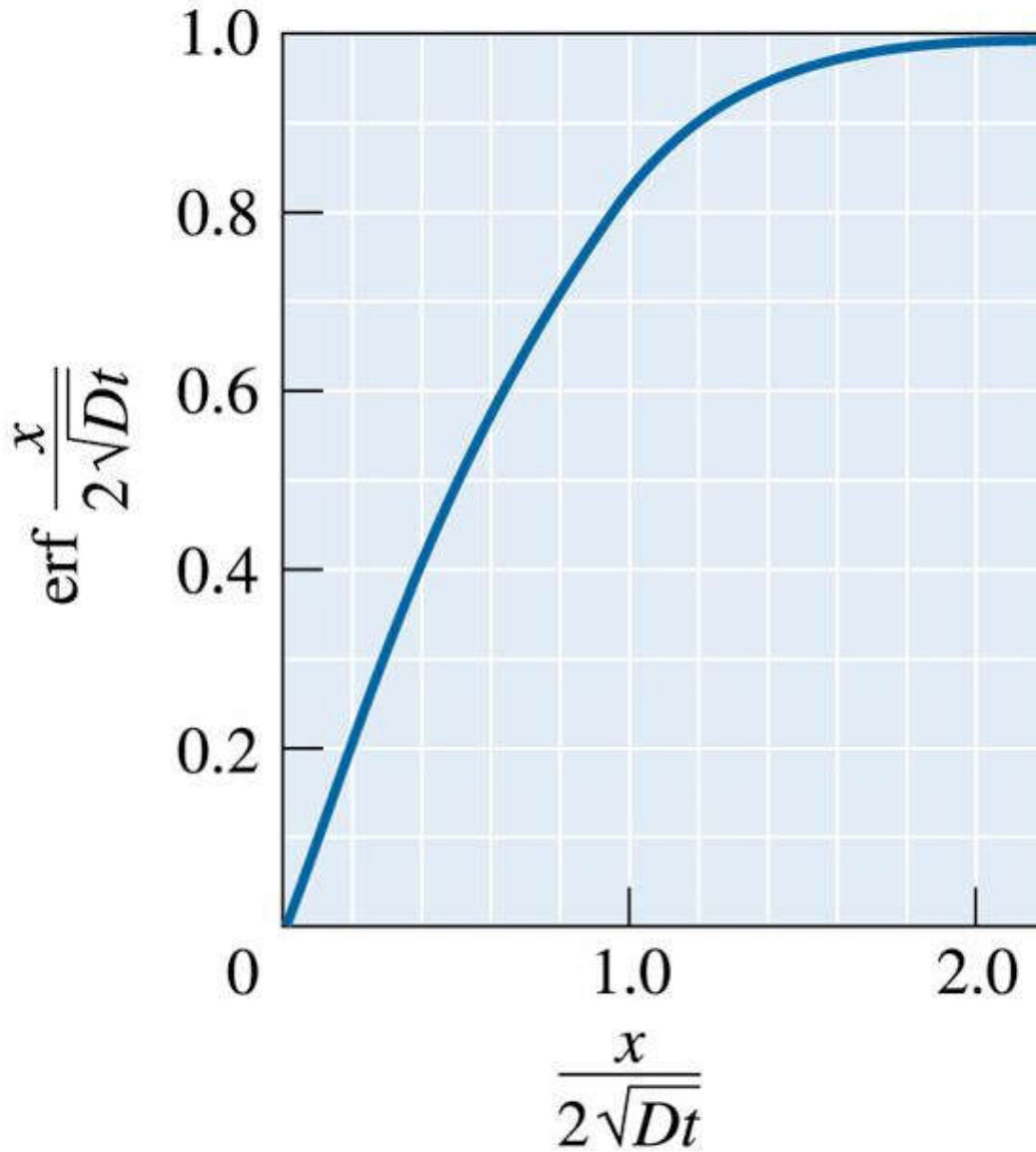


Figure 5.27 Graph showing the argument and value of error function encountered in Fick's second law





Example 5.10

Design of a Carburizing Treatment

The surface of a 0.1% C steel gears is to be hardened by carburizing. In gas carburizing, the steel gears are placed in an atmosphere that provides 1.2% C at the surface of the steel at a high temperature (Figure 5.1). Carbon then diffuses from the surface into the steel. For optimum properties, the steel must contain 0.45% C at a depth of 0.2 cm below the surface. Design a carburizing heat treatment that will produce these optimum properties. Assume that the temperature is high enough (at least 900°C) so that the iron has the FCC structure.





Figure 5.1 Furnace for heat treating steel using the carburization process. (Courtesy of Cincinnati Steel Treating).



Example 5.10 SOLUTION



Since the boundary conditions for which Equation 5-7 was derived are assumed to be valid we can use this equation.

$$\frac{c_s - c_x}{c_s - c_0} = \text{erf}\left(\frac{x}{2\sqrt{Dt}}\right)$$

From Table 5-3, we find that:

$$\frac{0.1 \text{ cm}}{\sqrt{Dt}} = 0.71 \quad \text{or} \quad Dt = \left(\frac{0.1}{0.71}\right)^2 = 0.0198 \text{ cm}^2$$

Any combination of D and t whose product is 0.0198 cm^2 will work. For carbon diffusing in FCC iron, the diffusion coefficient is related to temperature by Equation 5-4:

$$D = D_0 \exp\left(\frac{-Q}{RT}\right)$$

From Table 5-1:

$$D = 0.23 \exp\left(\frac{-32,900 \text{ cal/mol}}{1.987 \frac{\text{cal}}{\text{mol-K}} T(\text{K})}\right) = 0.23 \exp\left(\frac{-16,558}{T}\right)$$





Example 5.10 SOLUTION(Continued)

Therefore, the temperature and time of the heat treatment are related by:

$$t = \frac{0.0198 \text{ cm}^2}{D \frac{\text{cm}^2}{\text{s}}} = \frac{0.0198 \text{ cm}^2}{0.23 \exp(-16,558/T) \frac{\text{cm}^2}{\text{s}}} = \frac{0.0861}{\exp(-16,558/T)}$$

Some typical combinations of temperatures and times are:

If $T = 900^\circ\text{C} = 1173 \text{ K}$, then $t = 116,174 \text{ s} = 32.3 \text{ h}$

If $T = 1000^\circ\text{C} = 1273 \text{ K}$, then $t = 36,360 \text{ s} = 10.7 \text{ h}$

If $T = 1100^\circ\text{C} = 1373 \text{ K}$, then $t = 14,880 \text{ s} = 4.13 \text{ h}$

If $T = 1200^\circ\text{C} = 1473 \text{ K}$, then $t = 6,560 \text{ s} = 1.82 \text{ h}$





Example 5.11

Design of a More Economical Heat Treatment

We find that 10 h are required to successfully carburize a batch of 500 steel gears at 900°C , where the iron has the FCC structure. We find that it costs \$1000 per hour to operate the carburizing furnace at 900°C and \$1500 per hour to operate the furnace at 1000°C . Is it economical to increase the carburizing temperature to 1000°C ? What other factors must be considered?





Example 5.11 SOLUTION

Again assuming, we can use the solution to Ficks's second law given by Equation 5-7

$$\frac{c_s - c_x}{c_s - c_0} = \text{erf}\left(\frac{x}{2\sqrt{Dt}}\right)$$

Note that, since we are dealing with only changes in heat treatment time and temperature, the term Dt must be constant.

To achieve the same carburizing treatment at 1000°C as at 900°C :

$$D_{1273}t_{1273} = D_{1173}t_{1173}$$

At 900°C , the cost per part is $(\$1000/\text{h}) (10 \text{ h})/500 \text{ parts} = \$20/\text{part}$

At 1000°C , the cost per part is $(\$1500/\text{h}) (3.299 \text{ h})/500 \text{ parts} = \$9.90/\text{part}$





Example 5.12

Silicon Device Fabrication

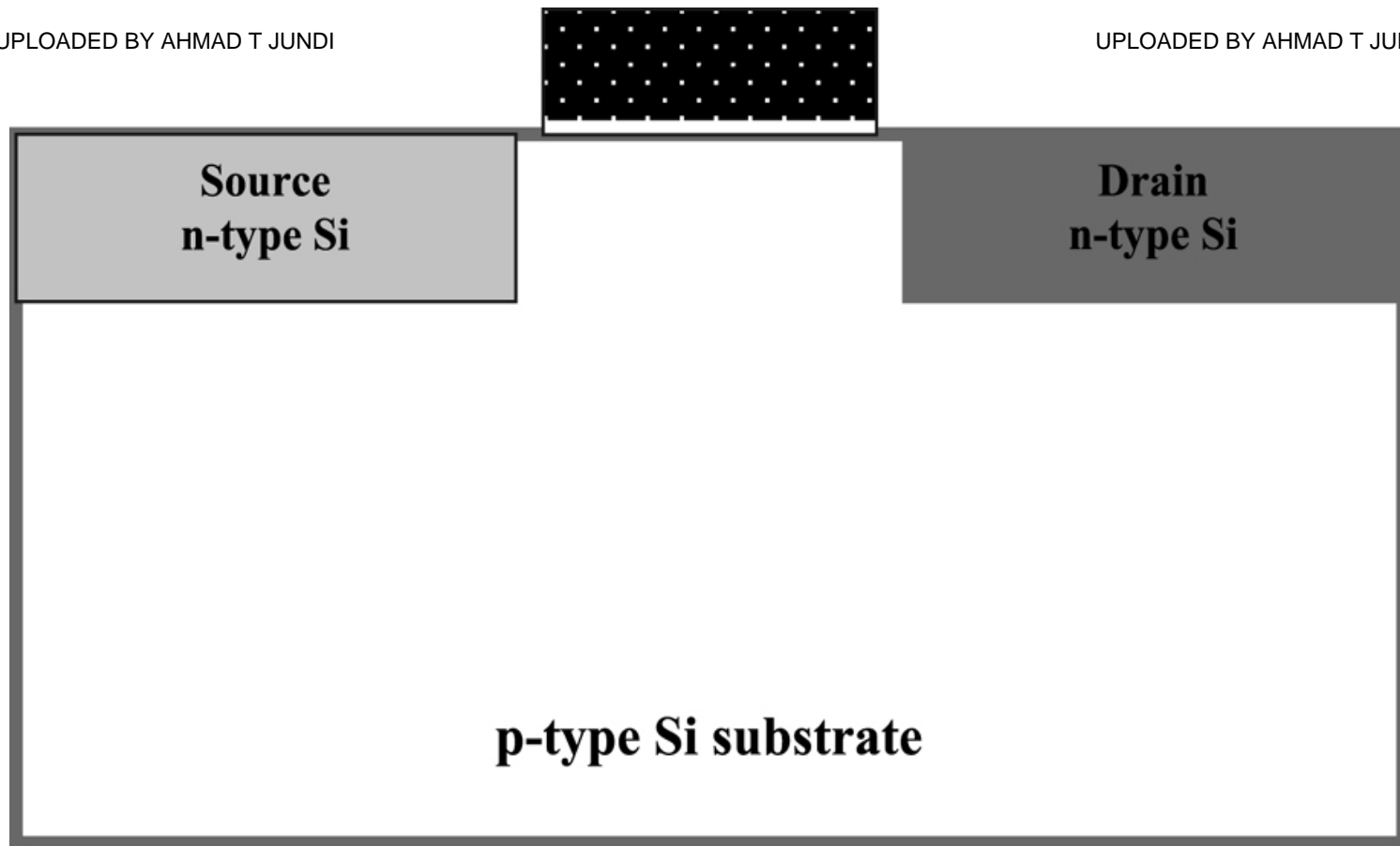
Devices such as transistors (Figure 5.2) are made by doping semiconductors with different dopants to generate regions that have p- or n-type semiconductivity.[1] The diffusion coefficient of phosphorus (P) in Si is $D = 65 \times 10^{-13} \text{ cm}^2/\text{s}$ at a temperature of 1100°C . [13] Assume the source provides a surface concentration of $10^{20} \text{ atoms/cm}^3$ and the diffusion time is one hour. Assume that the silicon wafer contains no P to begin with.

(a) Calculate the depth at which the concentration of P will be $10^{18} \text{ atoms/cm}^3$. State any assumptions you have made while solving this problem.

(b) What will happen to the concentration profile as we cool the Si wafer containing P?

(c) What will happen if now the wafer has to be heated again for boron (B) diffusion for creating a p-type region?





©2003 Brooks/Cole, a division of Thomson Learning, Inc. Thomson LearningSM is a trademark used herein under license.

Figure 5.2 Schematic of a n-p-n transistor. Diffusion plays a critical role in formation of the different regions created in the semiconductor substrates. The creation of millions of such transistors is at the heart of microelectronics technology





Example 5.12 SOLUTION

(a) We assume that we can use one of the solutions to Fick's second law (i.e., Equation 5-7):

$$\frac{c_s - c_x}{c_s - c_0} = \text{erf}\left(\frac{x}{2\sqrt{Dt}}\right)$$

If $\text{erf}(z) = 0.99$, $z = 1.82$, therefore,

$$1.82 = \frac{x}{9.67 \times 10^{-5}}$$

or

$$x = 1.76 \times 10^{-4} \text{ cm}$$



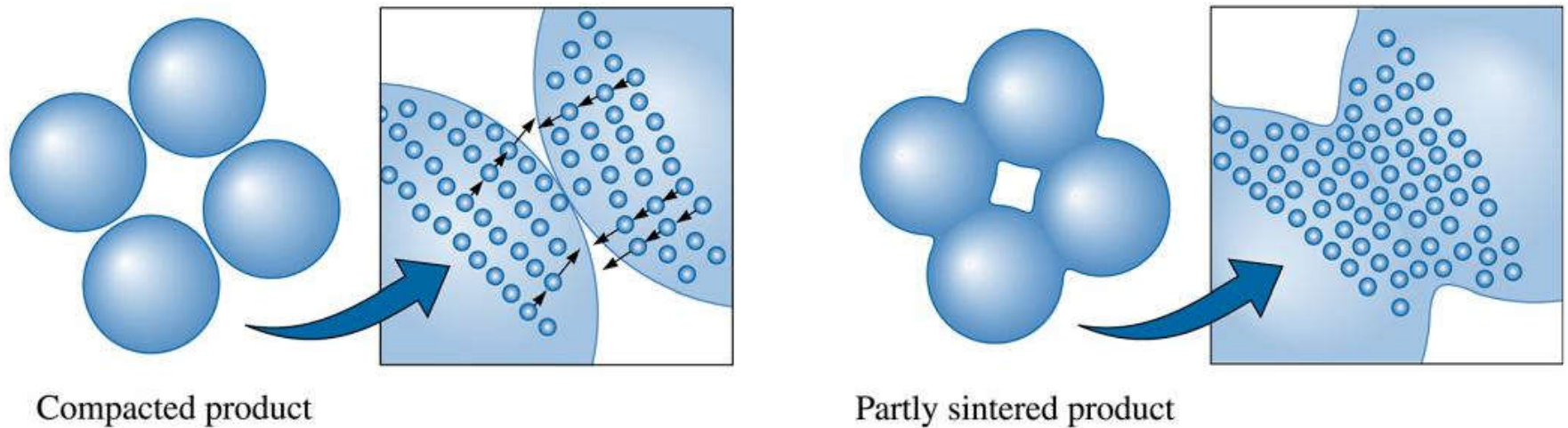


Section 5.9

Diffusion and Materials Processing

- **Sintering** - A high-temperature treatment used to join small particles.
- **Powder metallurgy** - A method for producing monolithic metallic parts.
- **Dielectric resonators** - Hockey puck-like pieces of ceramics such as barium magnesium tantalate (BMT) or barium zinc tantalate (BZN).
- **Grain growth** - Movement of grain boundaries by diffusion in order to reduce the amount of grain boundary area.
- **Diffusion bonding** - A joining technique in which two surfaces are pressed together at high pressures and temperatures.





©2003 Brooks/Cole, a division of Thomson Learning, Inc. Thomson Learning[®] is a trademark used herein under license.

Figure 5.28 Diffusion processes during sintering and powder metallurgy. Atoms diffuse to points of contact, creating bridges and reducing the pore size



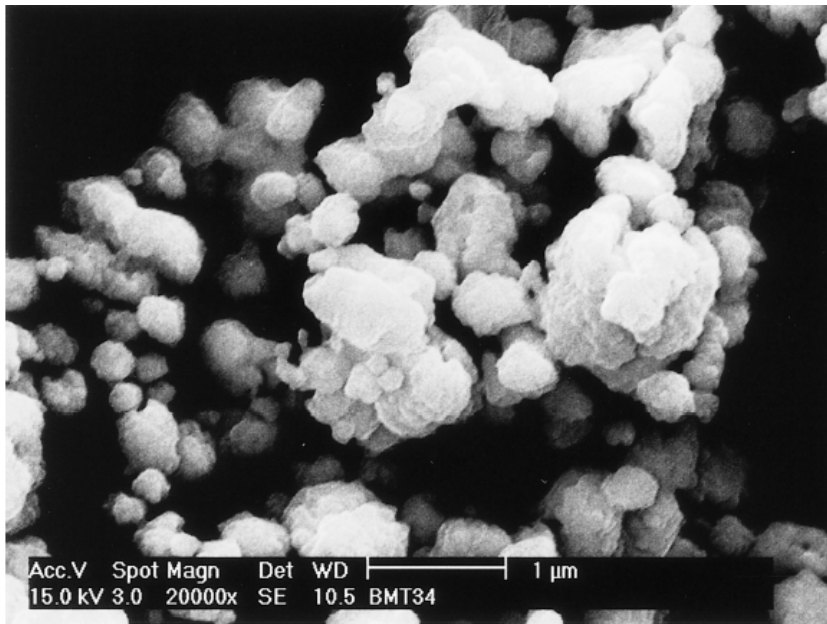


Figure 5.29 Particles of barium magnesium tantalate (BMT) ($\text{Ba}(\text{Mg}_{1/3}\text{Ta}_{2/3})\text{O}_3$) powder are shown. This ceramic material is useful in making electronic components known as dielectric resonators that are used for wireless communications. (Courtesy of H. Shirey.)

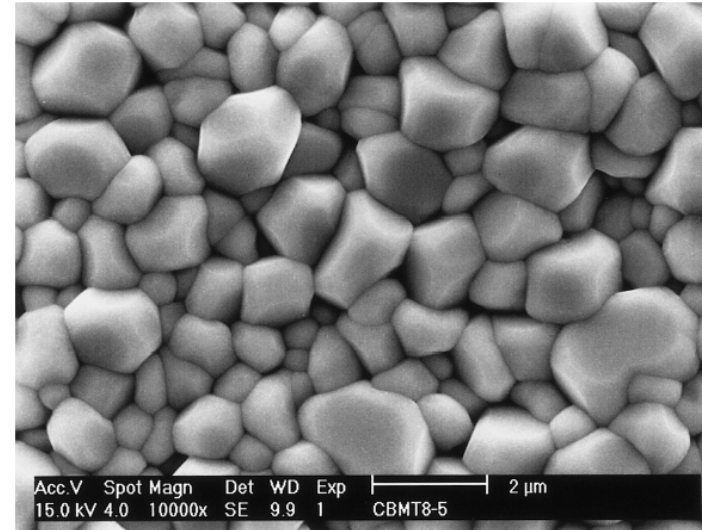
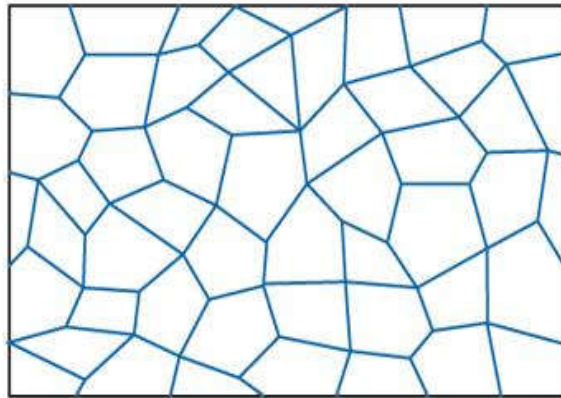
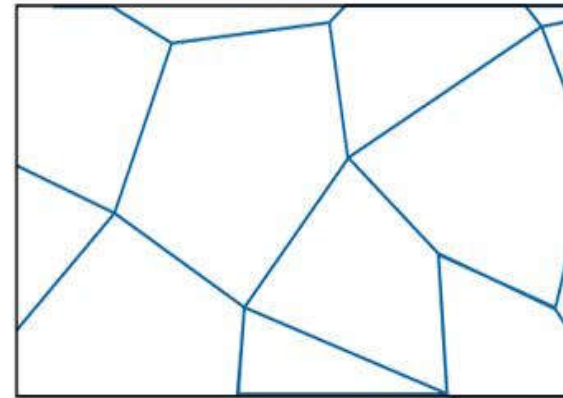


Figure 5.30 The microstructure of BMT ceramics obtained by compaction and sintering of BMT powders. (Courtesy of H. Shirey.)





(a) Initial microstructure

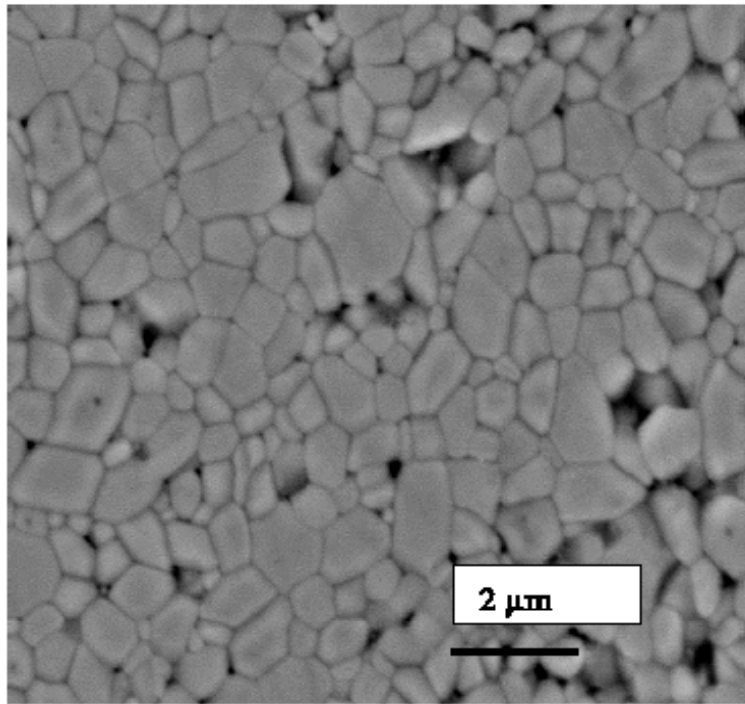


(b) Microstructure after grain growth

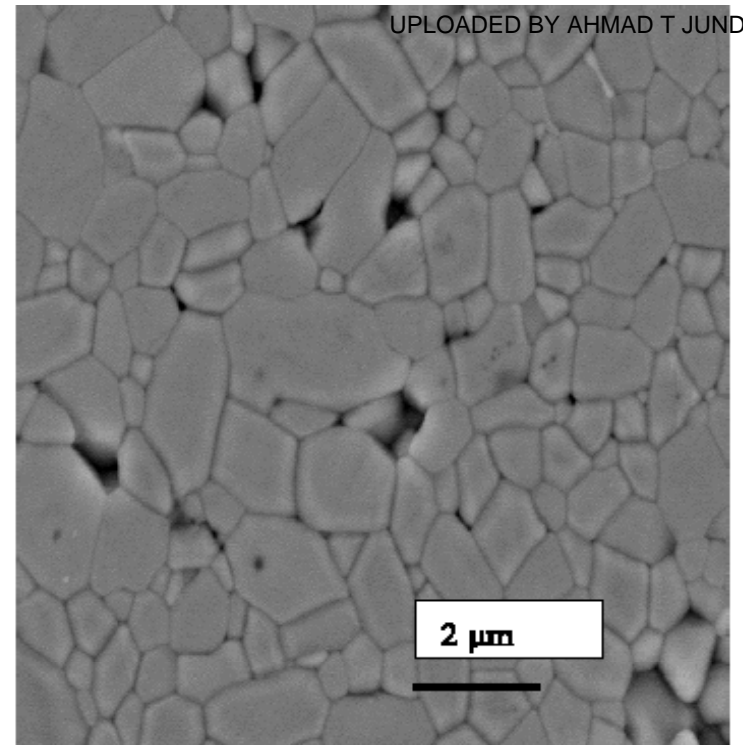
©2003 Brooks/Cole, a division of Thomson Learning, Inc. Thomson Learning[®] is a trademark used herein under license.

Figure 5.31 Grain growth occurs as atoms diffuse across the grain boundary from one grain to another





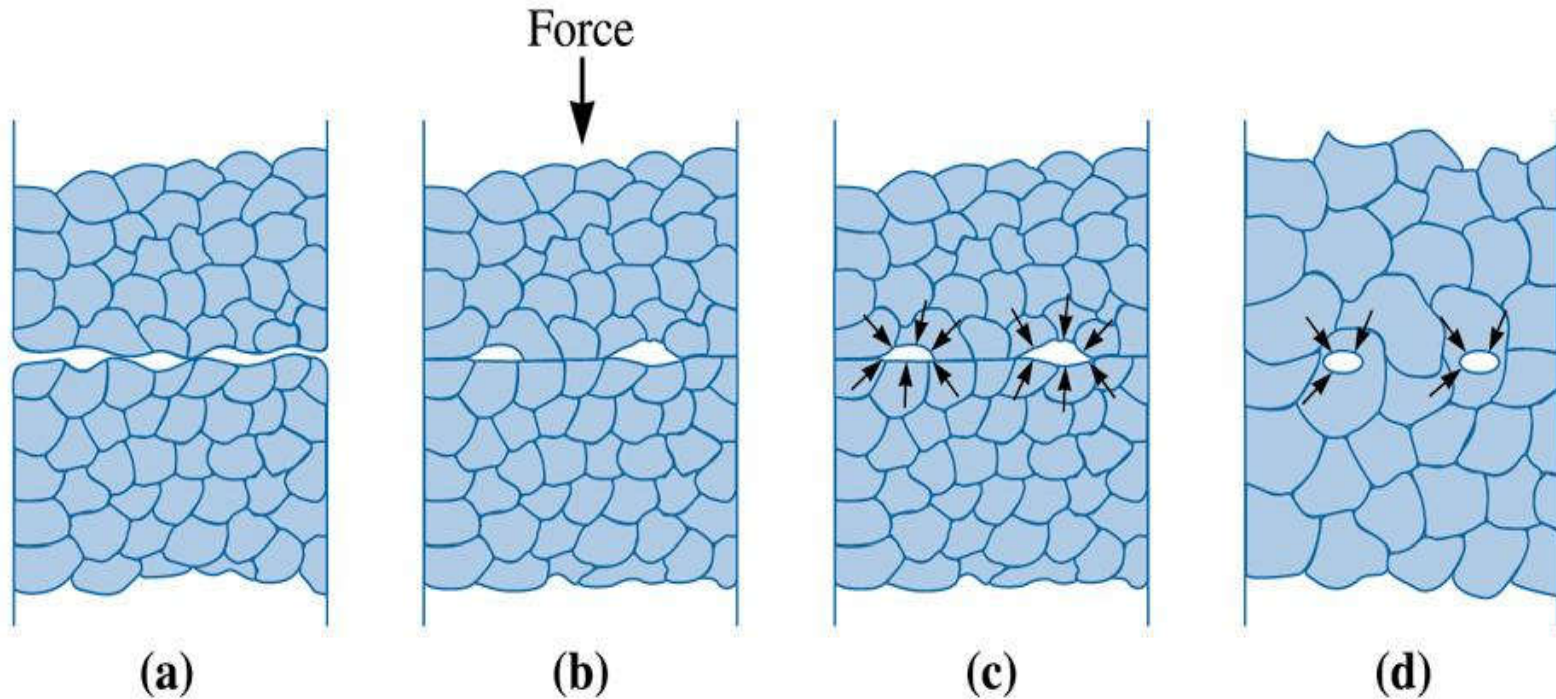
(a)



(b)

Figure 5.32 Grain growth in alumina ceramics can be seen from the SEM micrographs of alumina ceramics. (a) The left micrograph shows the microstructure of an alumina ceramic sintered at 1350°C for 150 hours. (b) The right micrograph shows a sample sintered at 1350°C for 30 hours. (Courtesy of I. Nettleship and R. McAfee.)





©2003 Brooks/Cole, a division of Thomson Learning, Inc. Thomson Learning™ is a trademark used herein under license.

Figure 5.33 The steps in diffusion bonding: (a) Initially the contact area is small; (b) application of pressure deforms the surface, increasing the bonded area; (c) grain boundary diffusion permits voids to shrink; and (d) final elimination of the voids requires volume diffusion





The Science and Engineering of Materials, 4th ed

Donald R. Askeland – Pradeep P. Phulé

Chapter 6 – Mechanical Properties and Behavior





Objectives of Chapter 6

- ❑ Introduce the basic concepts associated with mechanical properties of materials.
- ❑ Evaluate factors that affect the mechanical properties of materials.
- ❑ Review some of the basic testing procedures that engineers use to evaluate many of these properties.





Chapter Outline

- 6.1 Technological Significance
- 6.2 Terminology for Mechanical Properties
- 6.3 The Tensile Test: Use of the Stress-Strain Diagram
- 6.4 Properties Obtained from the Tensile Test
- 6.5 True Stress and True Strain
- 6.6 The Bend Test for Brittle Materials
- 6.7 Hardness of Materials
- 6.8 Strain Rate Effects and Impact Behavior
- 6.9 Properties Obtained from the Impact Test
- 6.10 Fracture Mechanics
- 6.11 The Importance of Fracture Mechanics





Chapter Outline(Continued)

- 6.12 Microstructural Features of Fracture in Metallic Materials
- 6.13 Microstructural Features of Fracture in Ceramics, Glasses, and Composites
- 6.14 Weibull Statistics for Failure Strength Analysis
- 6.15 Fatigue
- 6.16 Results of the Fatigue Test
- 6.17 Application of Fatigue Testing
- 6.18 Creep, Stress Rupture, and Stress Corrosion
- 6.19 Evaluation of Creep Behavior
- 6.20 Use of Creep Data
- 6.21 Superplasticity





Technological Significance



Figure 6.1 Aircraft, such as the one shown here, makes use of aluminum alloys and carbon-fiber-reinforced composites. (Courtesy of Getty Images.)



Figure 6.2 The materials used in sports equipment must be lightweight, stiff, tough, and impact resistant. (Courtesy of Getty Images.)



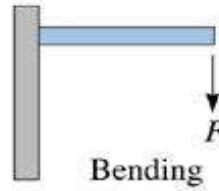


Terminology for Mechanical Properties

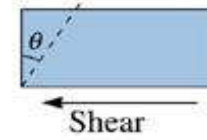
- ❑ **Stress** - Force or load per unit area of cross-section over which the force or load is acting.
- ❑ **Strain** - Elongation change in dimension per unit length.
- ❑ **Young's modulus** - The slope of the linear part of the stress-strain curve in the elastic region, same as modulus of elasticity.
- ❑ **Shear modulus (G)** - The slope of the linear part of the shear stress-shear strain curve.
- ❑ **Viscosity (η)** - Measure of resistance to flow, defined as the ratio of shear stress to shear strain rate (units Poise or Pa-s).
- ❑ **Thixotropic behavior** - Materials that show shear thinning and also an apparent viscosity that at a constant rate of shear decreases with time.



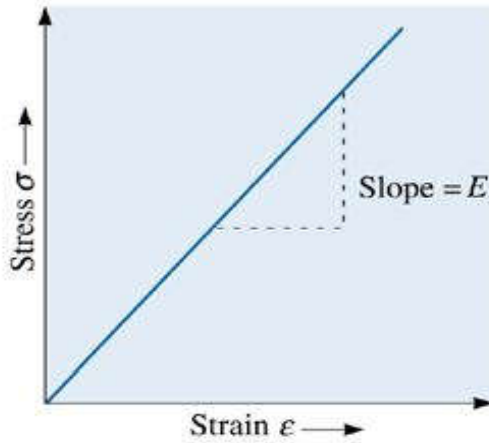
UPLOADED BY AHMAD T JUNDI



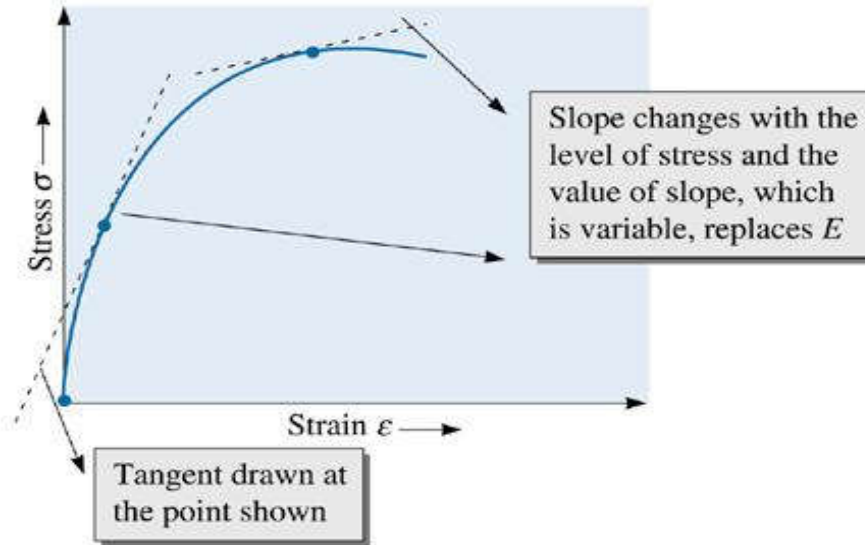
UPLOADED BY AHMAD T JUNDI



(a)

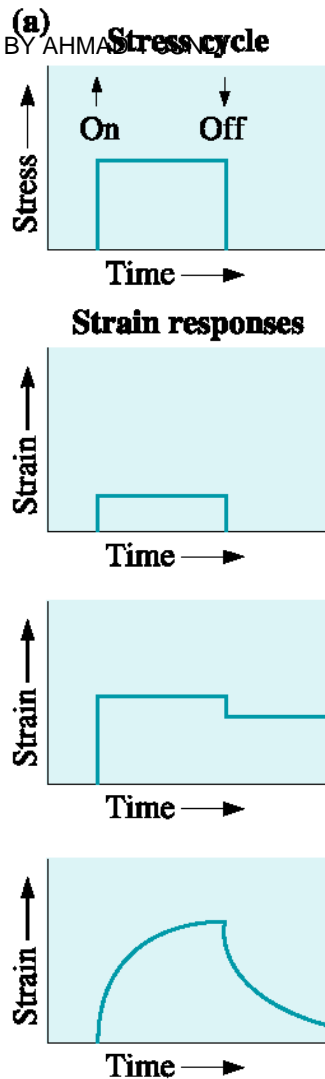


(b) Elastic material



(c) Nonlinear material

Figure 6.3 (a) Tensile, compressive, shear and bending stresses. (b) Illustration showing how Young's modulus is defined for elastic material. (c) For nonlinear materials, we use the slope of a tangent as a variable quantity that replaces the Young's modulus constant



Specimen is loaded to a given stress and subsequently unloaded

Ideal elastic solid: elastic strain only, constant with time

Elastic plus plastic deformation: elastic strain is recovered on removal of stress, plastic strain is permanent

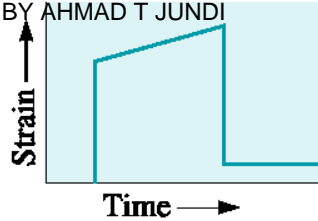
Viscoelastic: some instantaneous elastic strain followed by elastic strain which increases with time under stress and recovers slowly; some viscous (plastic) flow may also occur

Metals (below yield stress), thermoplastics [well below (T_g)], thermosets, ceramics and glasses

Ductile materials above yield stress

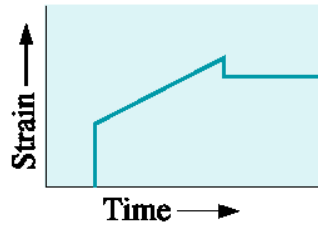
Thermoplastics at temperatures around T_g

Figure 6.4 (a) Various types of strain response to an imposed stress. (Source: Reprinted from Materials Principles and Practice, by C. Newey and G. Weaver (Eds.), 1991 p. 300, Fig. 6-9. Copyright © 1991 Butterworth-Heinemann. Reprinted with permission from Elsevier Science.)



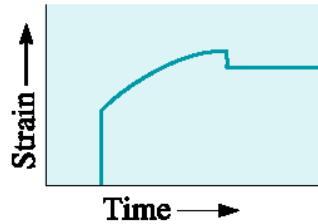
Rubbery: extensive elastic strain plus some nonrecoverable (plastic) strain

Elastomers (rubbers) and some thermoplastics at temperatures above the viscoelastic range



Viscous flow: behaves like a viscous liquid, plastic flow increases with time, small elastic recovery when stress is removed

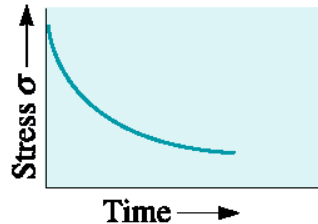
Thermoplastics and glasses well above T_g , some metals above $0.5 T_m$ under special conditions



Creep: plastic strain increasing with time, some elastic recovery when stress is removed

Metals and ceramics above about $0.4 T_m$

(b) Stress response



Strain is constant, stress decreases with time.

Thermoplastics

Figure 6.4 (Continued) (a) Various types of strain response to an imposed stress. (Source: Reprinted from Materials Principles and Practice, by C. Newey and G. Weaver (Eds.), 1991 p. 300, Fig. 6-9. Copyright © 1991 Butterworth-Heinemann. Reprinted with permission from Elsevier Science.) (b) Stress relaxation in a viscoelastic material. Note the y-axis is stress. Strain is constant.

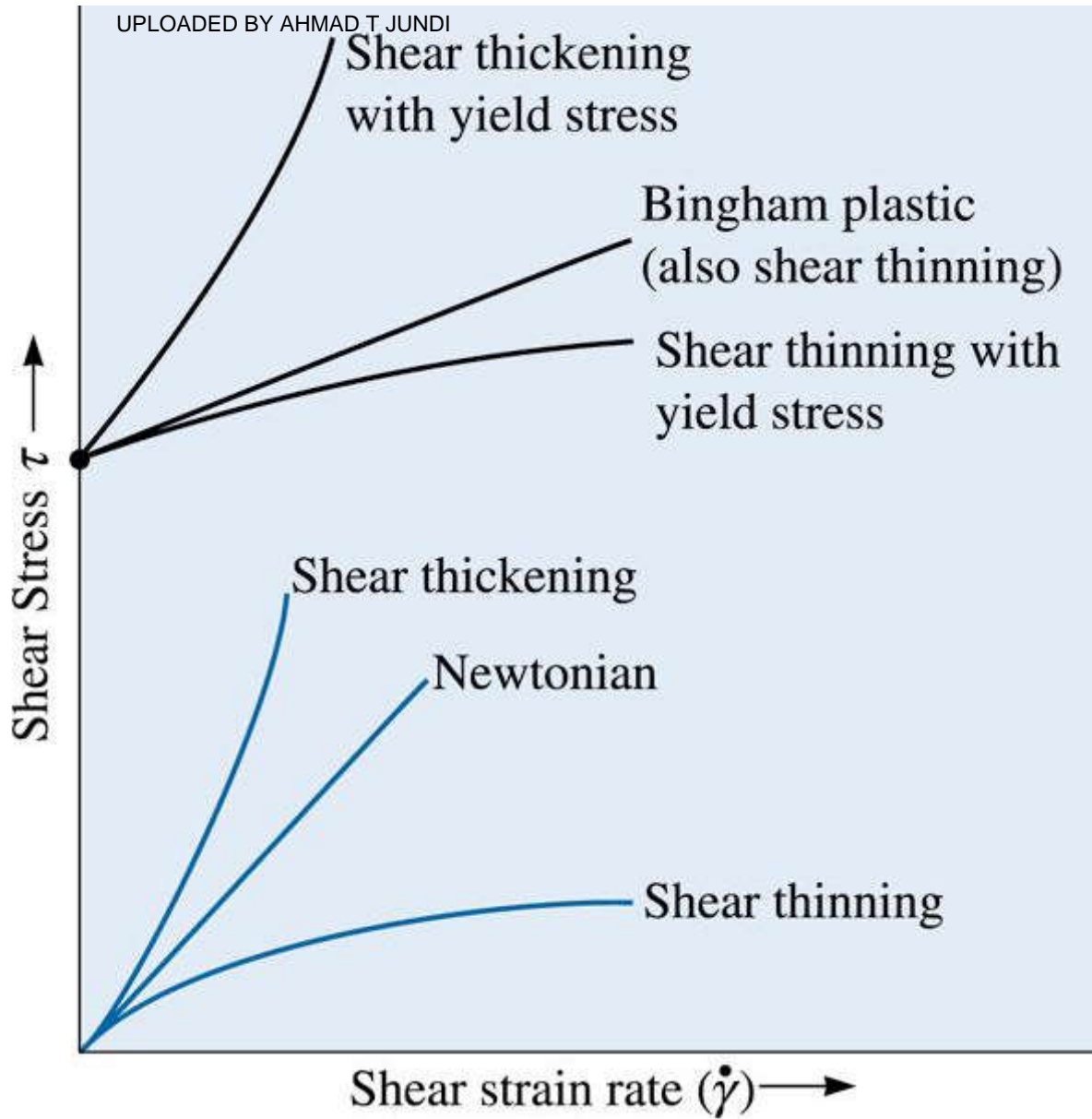


Figure 6.5 Shear stress strain rate relationships for Newtonian and non-Newtonian materials

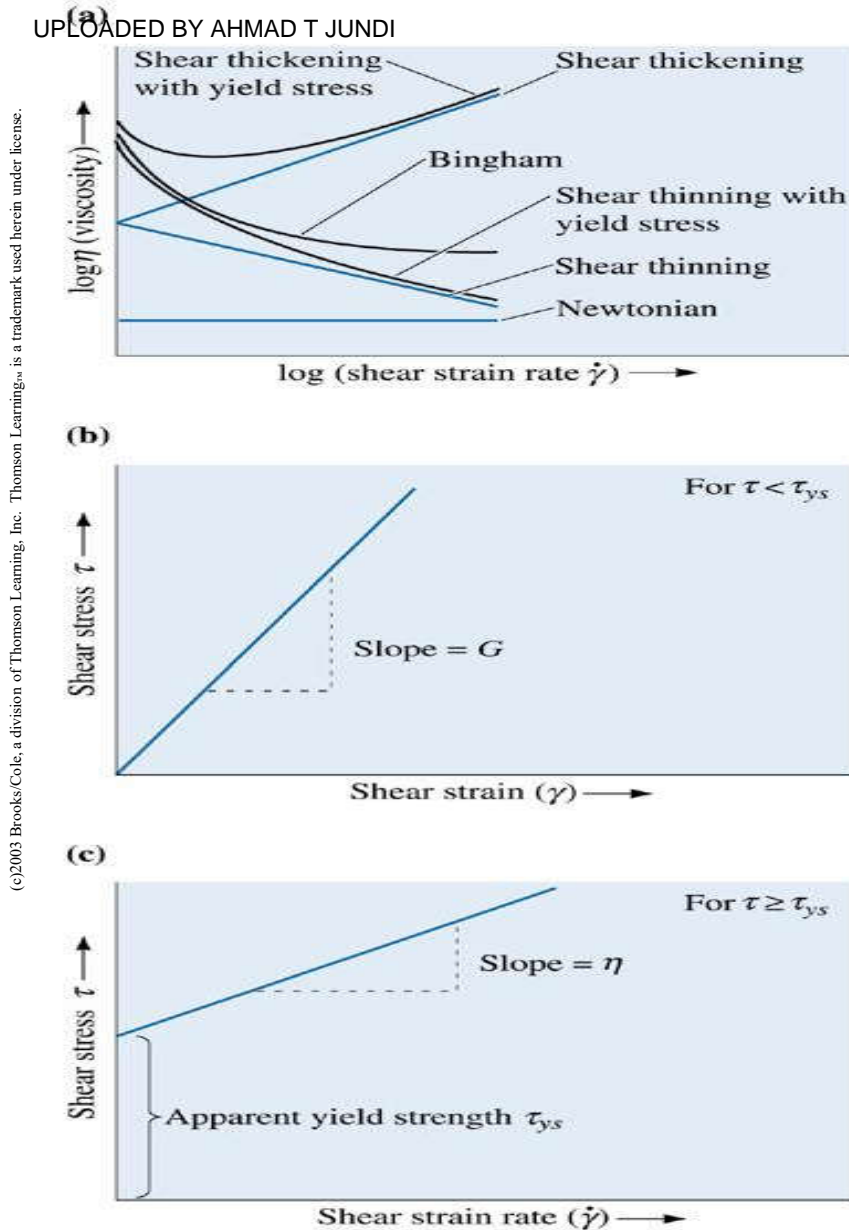


Figure 6.6 (a) Apparent viscosity as a function of shear log (shear rate $\dot{\gamma}$) strain rate. (b) and (c) illustration of a Bingham plastic (Equations 6-3a & b). Note the x-axis on (b) is shear strain

(c)2003 Brooks/Cole, a division of Thomson Learning, Inc. Thomson Learningsm is a trademark used herein under license.





Section 6.3

The Tensile Test: Use of the Stress-Strain Diagram

- **Load** - The force applied to a material during testing.
- **Strain gage or Extensometer** - A device used for measuring change in length and hence strain.
- **Glass temperature (T_g)** - A temperature below which an otherwise ductile material behaves as if it is brittle.
- **Engineering stress** - The applied load, or force, divided by the original cross-sectional area of the material.
- **Engineering strain** - The amount that a material deforms per unit length in a tensile test.





©2003 Brooks/Cole, a division of Thomson Learning, Inc. Thomson Learning is a trademark used herein under license.

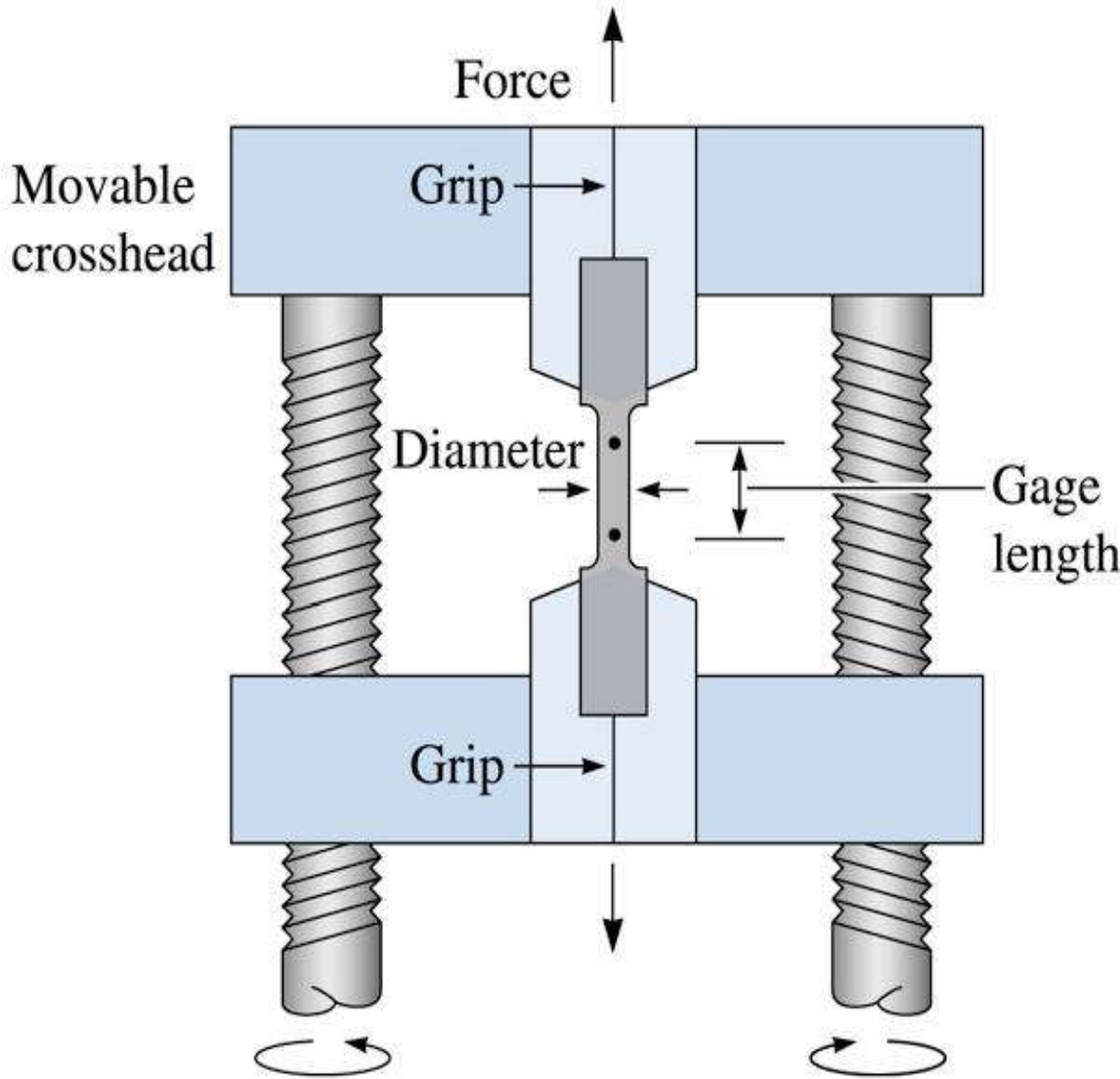
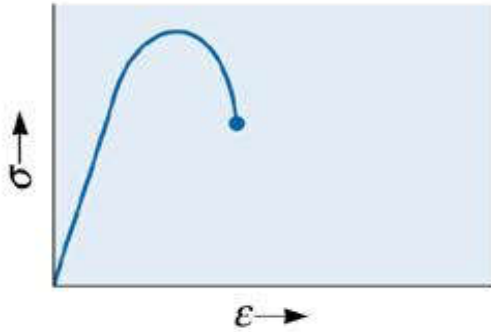


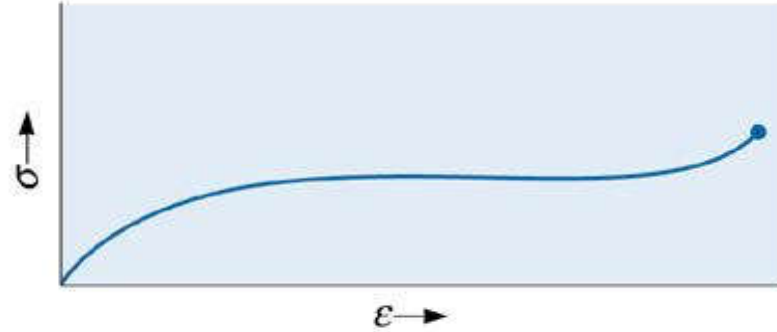
Figure 6.7 A unidirectional force is applied to a specimen in the tensile test by means of the moveable crosshead. The cross-head movement can be performed using screws or a hydraulic mechanism



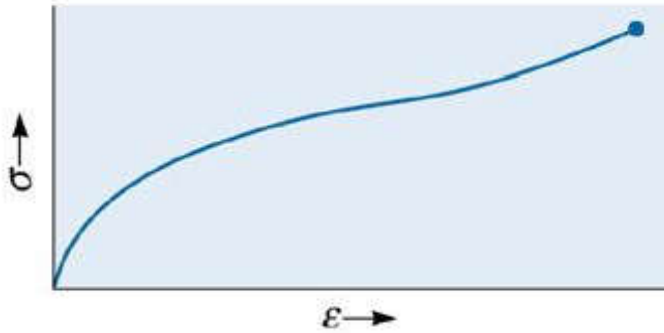
(a) Metal



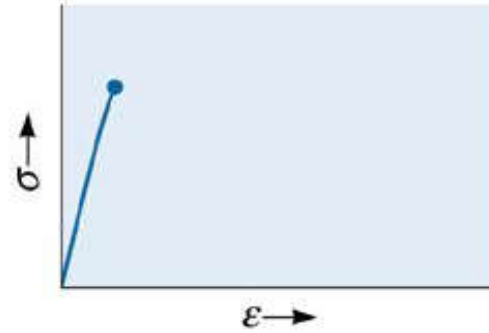
(b) Thermoplastic material above T_g



(c) Elastomer



(d) Ceramics, glasses, and concrete



©2003 Brooks/Cole, a division of Thomson Learning, Inc. Thomson Learning, is a trademark used herein under license.

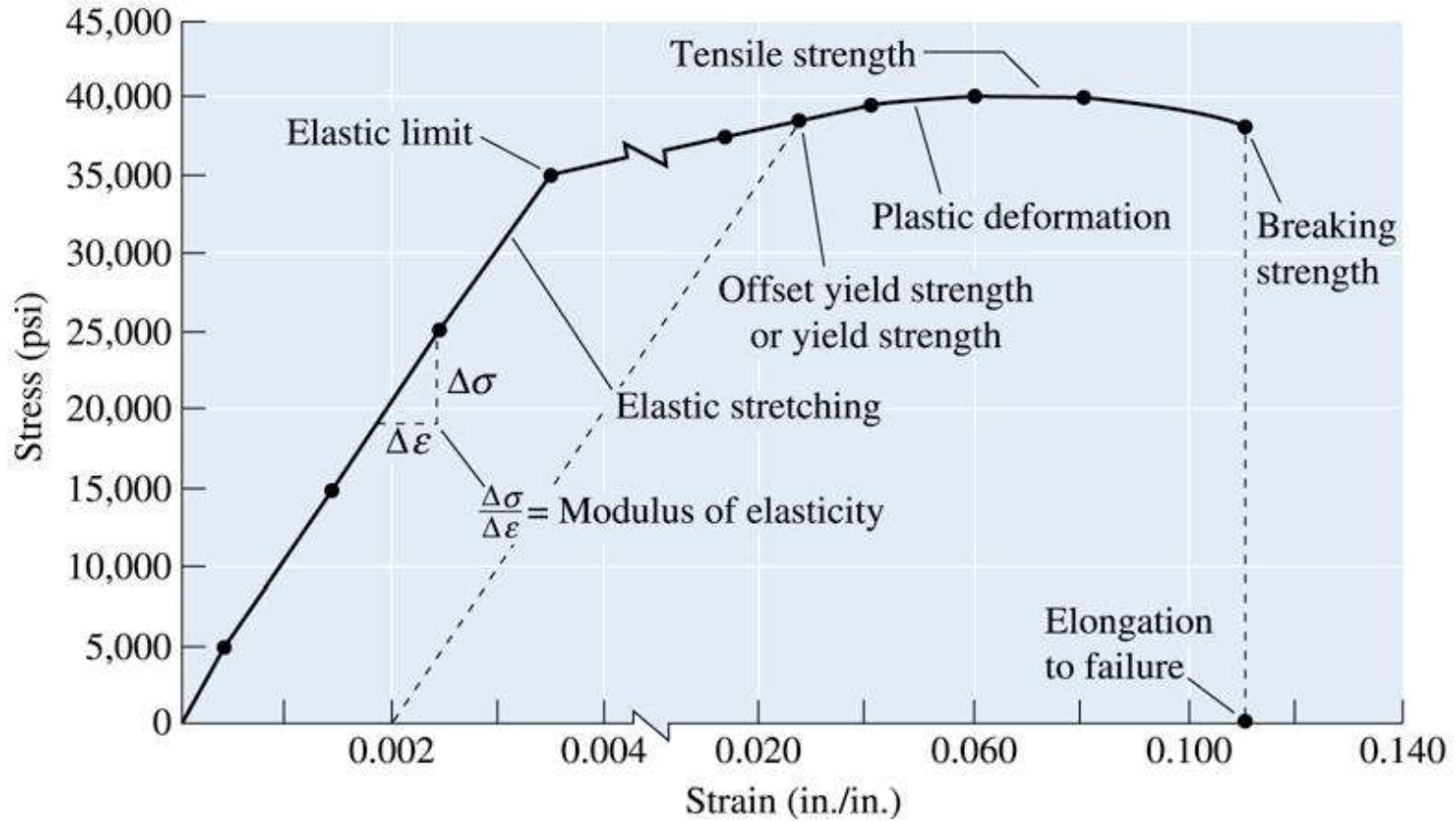
Figure 6.9 Tensile stress-strain curves for different materials. Note that these are qualitative



TABLE 6-1 ■ *The results of a tensile test of a 0.505-in. diameter aluminum alloy test bar, initial length (l_0) = 2 in.*

Measured Change in Length (Δl)		Calculated	
		Stress (psi)	Strain (in./in.)
Load (lb)	(in.)		
0	0.000	0	0
1000	0.001	5,000	0.0005
3000	0.003	15,000	0.0015
5000	0.005	25,000	0.0025
7000	0.007	35,000	0.0035
7500	0.030	37,500	0.0150
7900	0.080	39,500	0.0400
8000 (maximum load)	0.120	40,000	0.0600
7950	0.160	39,700	0.0800
7600 (fracture)	0.205	38,000	0.1025





(c)2003 Brooks/Cole, a division of Thomson Learning, Inc. Thomson Learning™ is a trademark used herein under license.

Figure 6.10 The stress-strain curve for an aluminum alloy from Table 6-1





Tensile Testing of Aluminum Alloy

Convert the change in length data in Table 6-1 to engineering stress and strain and plot a stress-strain curve.

TABLE 6-1 ■ *The results of a tensile test of a 0.505-in. diameter aluminum alloy test bar, initial length (l_0) = 2 in.*

Measured Change in Length (Δl)		Calculated	
Load (lb)	(in.)	Stress (psi)	Strain (in./in.)
0	0.000	0	0
1000	0.001	5,000	0.0005
3000	0.003	15,000	0.0015
5000	0.005	25,000	0.0025
7000	0.007	35,000	0.0035
7500	0.030	37,500	0.0150
7900	0.080	39,500	0.0400
8000 (maximum load)	0.120	40,000	0.0600
7950	0.160	39,700	0.0800
7600 (fracture)	0.205	38,000	0.1025





Example 6.1 SOLUTION

For the 1000-lb load:

$$\sigma = \frac{F}{A_0} = \frac{1000 \text{ lb}}{(\pi/4)(0.505 \text{ in.})^2} = \frac{1000 \text{ lb}}{0.2 \text{ in.}^2} = 5000 \text{ psi}$$

$$\varepsilon = \frac{\Delta l}{l_0} = \frac{0.001 \text{ in.}}{2.000 \text{ in.}} = 0.0005 \text{ in./in.}$$

The results of similar calculations for each of the remaining loads are given in Table 6-1 and are plotted in Figure 6-10.





TABLE 6-2 ■ *Units and conversion factors*

1 pound (lb) = 4.448 Newtons (N)

1 psi = pounds per square inch

1 MPa = MegaPascal = MegaNewtons per square meter (MN/m^2)
= Newtons per square millimeter (N/mm^2) = 1,000,000 Pa

1 GPa = 1000 MPa = GigaPascal

1 ksi = 1000 psi = 6.895 MPa

1 psi = 0.006895 MPa

1 MPa = 0.145 ksi = 145 psi





Design of a Suspension Rod

An aluminum rod is to withstand an applied force of 45,000 pounds. To assure a sufficient safety, the maximum allowable stress on the rod is limited to 25,000 psi. The rod must be at least 150 in. long but must deform elastically no more than 0.25 in. when the force is applied. Design an appropriate rod.

Example 6.2 SOLUTION

We can use the definition of engineering stress to calculate the required cross-sectional area of the rod:

$$A_0 = \frac{F}{\sigma} = \frac{45,000}{25,000} = 1.8 \text{ in.}^2$$

$$A_0 = \frac{\pi d^2}{4} = 1.8 \text{ in.}^2 \quad \text{or} \quad d = 1.51 \text{ in.}$$



Example 6.2 SOLUTION(Continued)

However, the minimum length of the rod is specified as 150 in. To produce a longer rod, we might make the cross-sectional area of the rod larger. The minimum strain allowed for the 150-in. rod is:

$$\varepsilon = \frac{\Delta l}{l_0} = \frac{0.25 \text{ in.}}{150 \text{ in.}} = 0.001667 \text{ in./in.}$$

$$A_0 = \frac{F}{\sigma} = \frac{45,000 \text{ psi}}{16,670 \text{ lb}} = 2.70 \text{ in.}^2$$

In order to satisfy both the maximum stress and the minimum elongation requirements, cross-sectional area of the rod must be at least 2.7 in.^2 , or a minimum diameter of 1.85 in.

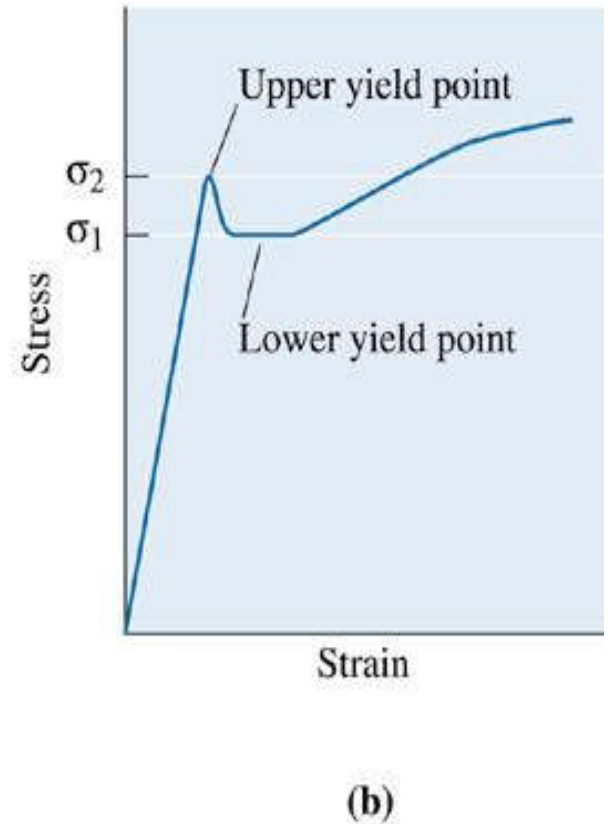
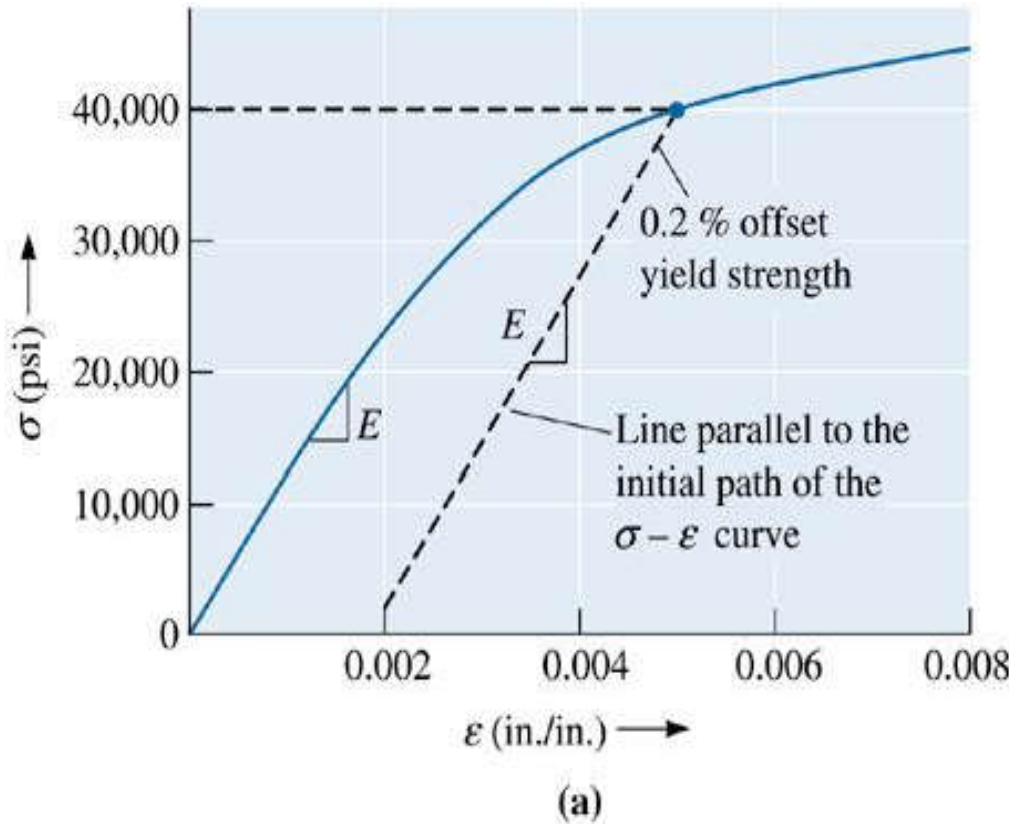




Section 6.4

Properties Obtained from the Tensile Test

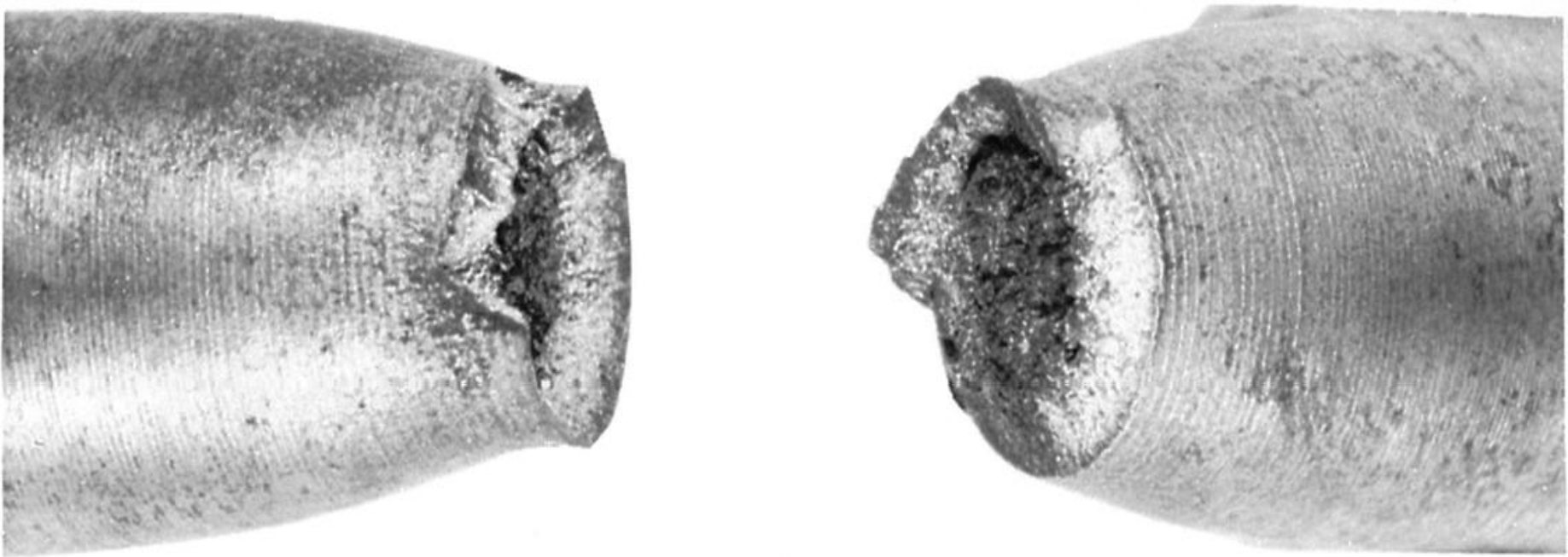
- Elastic limit
- Tensile strength, Necking
- Hooke's law
- Poisson's ratio
- Modulus of resilience (E_r)
- Tensile toughness
- Ductility



(c)2003 Brooks/Cole, a division of Thomson Learning, Inc. Thomson Learning, is a trademark used herein under license.

Figure 6.11 (a) Determining the 0.2% offset yield strength in gray cast iron, and (b) upper and lower yield point behavior in a low-carbon steel





(c)2003 Brooks/Cole, a division of Thomson Learning, Inc. Thomson Learning, Inc. is a trademark used herein under license.

Figure 6.12 Localized deformation of a ductile material during a tensile test produces a necked region. The micrograph shows necked region in a fractured sample

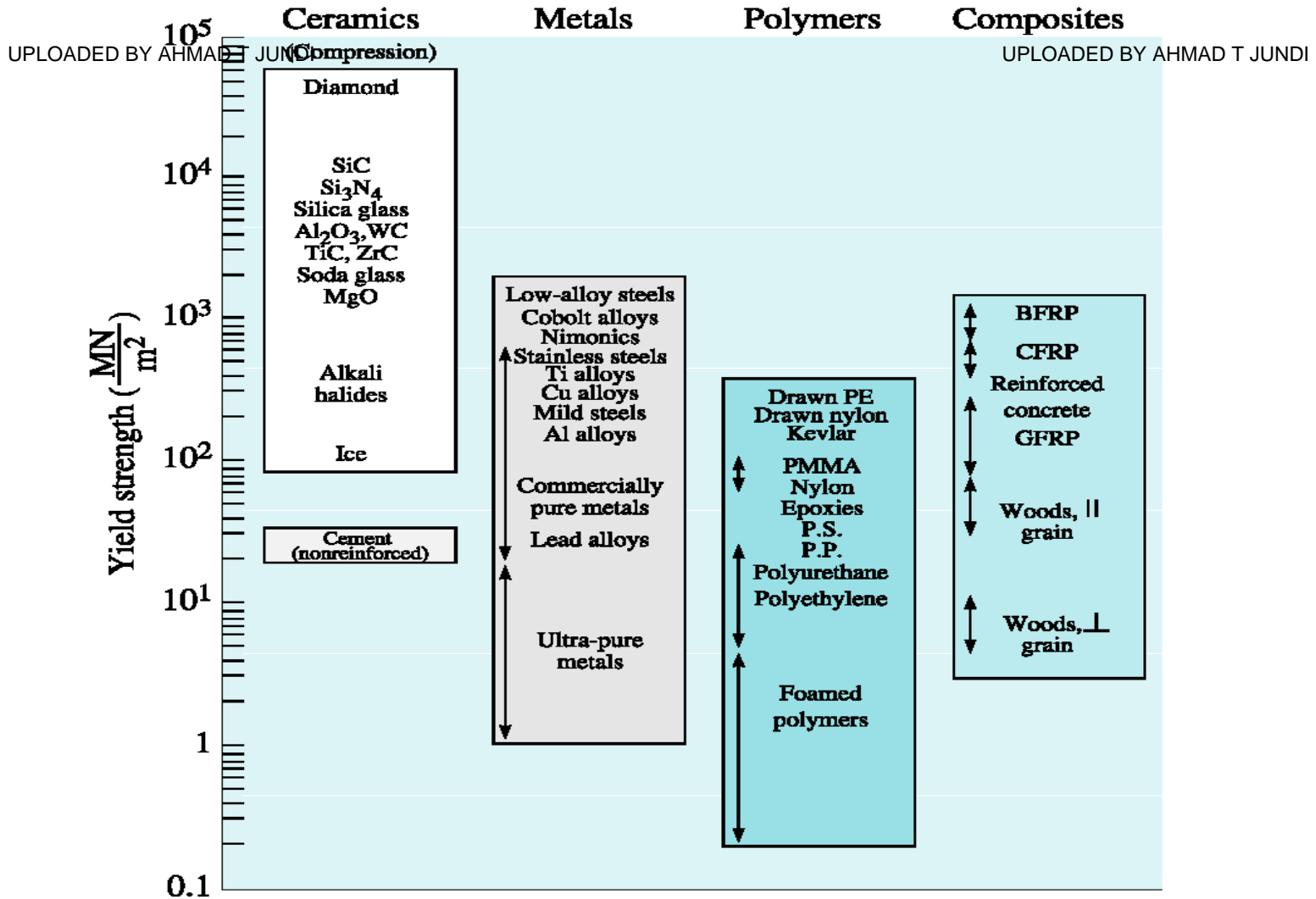


Figure 6.13 Typical yield strength values for different engineered materials. (Source: Reprinted from Engineering Materials I, Second Edition, M.F. Ashby and D.R.H. Jones, 1996, Fig. 8-12, p. 85. Copyright © Butterworth-Heinemann. Reprinted with permission from Elsevier Science.)





TABLE 6-3 ■ *Elastic properties and melting temperature (T_m) of selected materials*

Material	T_m (°C)	E (psi)	Poisson's ratio (μ)
Pb	327	2.0×10^6	0.45
Mg	650	6.5×10^6	0.29
Al	660	10.0×10^6	0.33
Cu	1085	18.1×10^6	0.36
Fe	1538	30.0×10^6	0.27
W	3410	59.2×10^6	0.28
Al_2O_3	2020	55.0×10^6	0.26
Si_3N_4		44.0×10^6	0.24



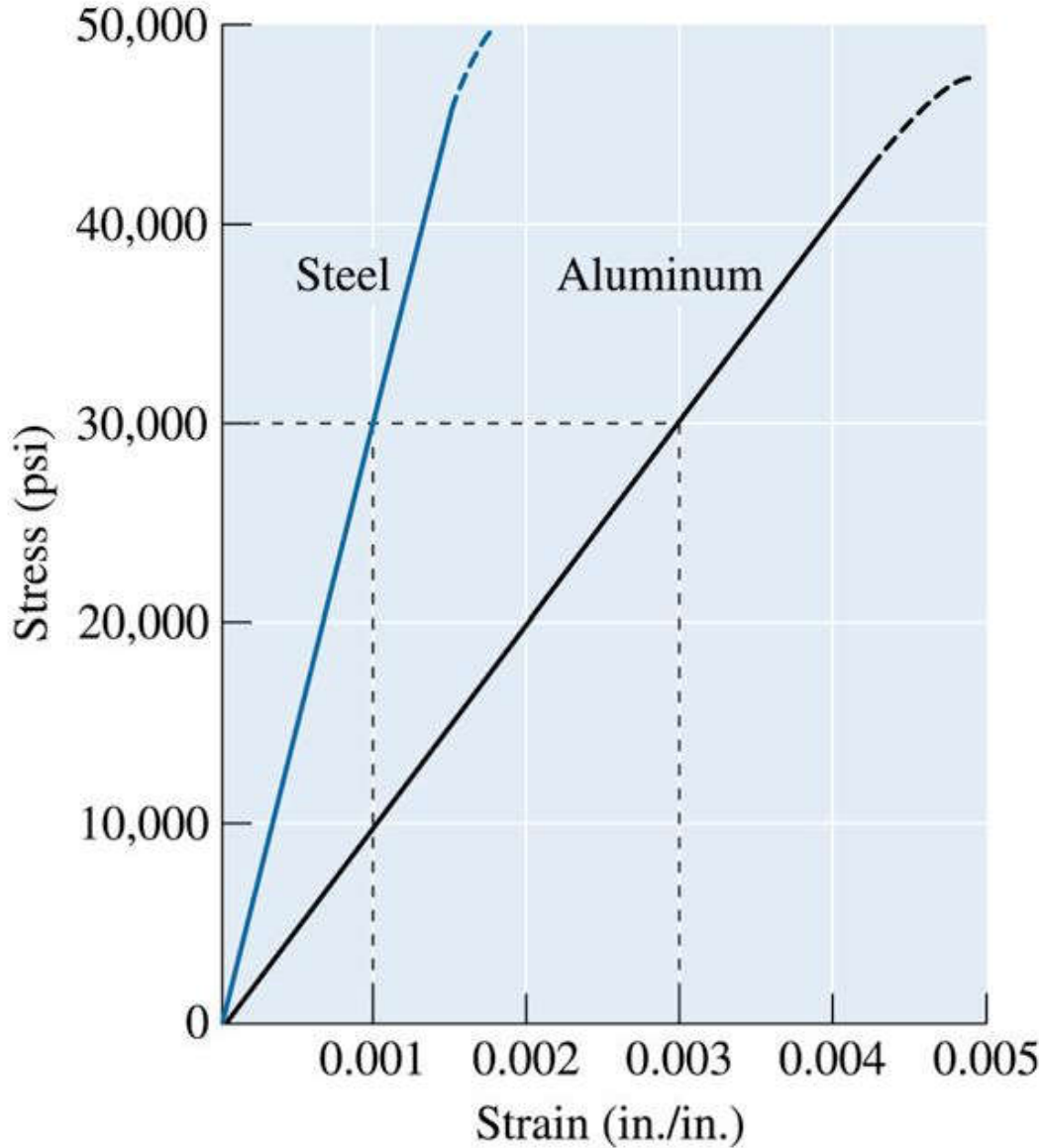


Figure 6.14
Comparison of the elastic behavior of steel and aluminum. For a given stress, aluminum deforms elastically three times as much as does steel

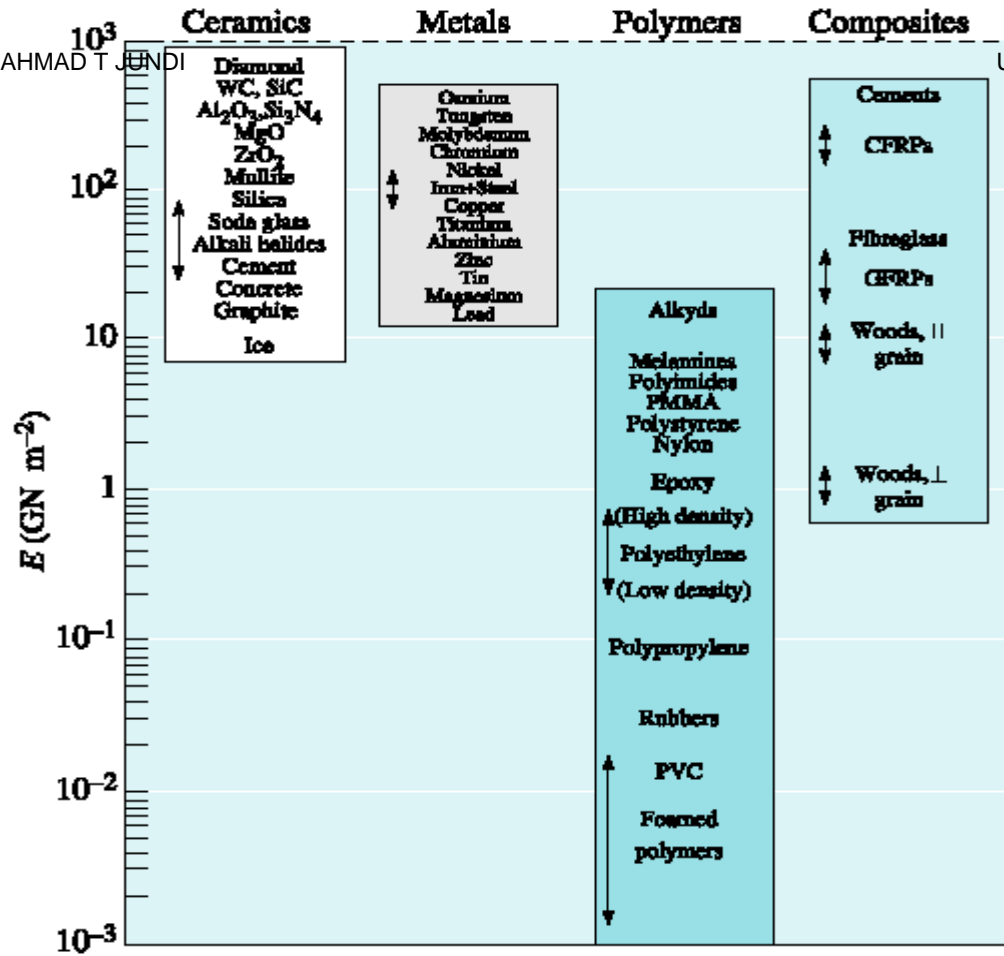


Figure 6.15 Range of elastic moduli for different engineered materials. (Source: Reprinted from Engineering Materials I, Second Edition, M.F. Ashby and D.R.H. Jones, 1996, Fig. 3-5, p. 35, Copyright © 1996 Butterworth-Heinemann. Reprinted with permission from Elsevier Science.)



Young's Modulus of Aluminum Alloy

From the data in Example 6.1, calculate the modulus of elasticity of the aluminum alloy. Use the modulus to determine the length after deformation of a bar of initial length of 50 in. Assume that a level of stress of 30,000 psi is applied.

Example 6.3 SOLUTION

When a stress of 35,000 psi is applied, a strain of 0.0035 in./in. is produced. Thus:

$$\text{Modulus of elasticity} = E = \frac{\sigma}{\varepsilon} = \frac{35,000 \text{ psi}}{0.0035} = 10 \times 10^6 \text{ psi}$$

From Hooke's law:

$$\varepsilon = \frac{\sigma}{E} = \frac{30,000 \text{ psi}}{10 \times 10^6} = 0.0003 = \text{in./in.} = \frac{l - l_0}{l_0}$$

$$l = l_0 + \varepsilon l_0 = 50 + (0.003)(50) = 50.15 \text{ in.}$$

Example 6.4

Ductility of an Aluminum Alloy



The aluminum alloy in Example 6.1 has a final length after failure of 2.195 in. and a final diameter of 0.398 in. at the fractured surface. Calculate the ductility of this alloy.

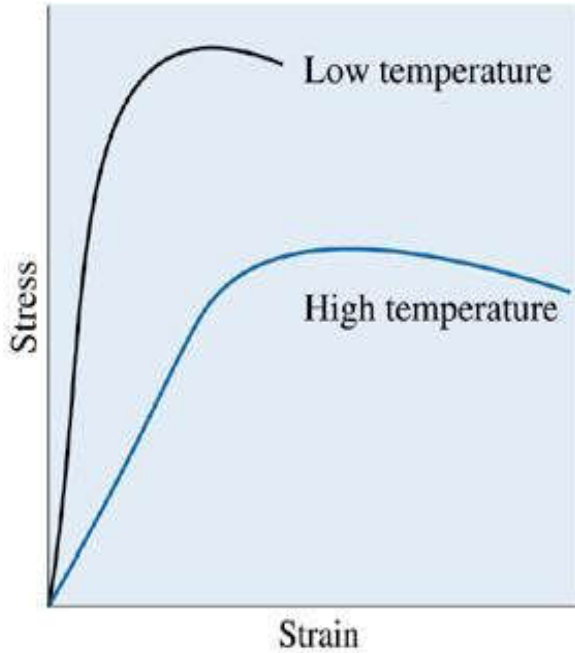
Example 6.4 SOLUTION

$$\% \text{ Elongation} = \frac{l_f - l_0}{l_0} \times 100 = \frac{2.195 - 2.000}{2.000} \times 100 = 9.75\%$$

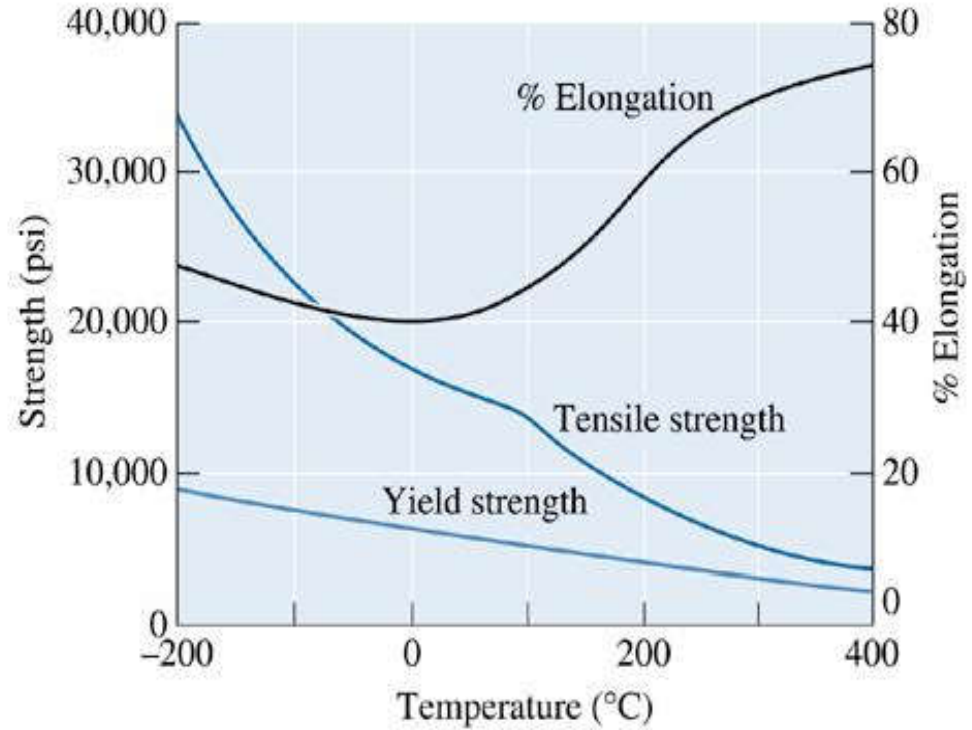
$$\begin{aligned} \% \text{ Reduction in area} &= \frac{A_0 - A_f}{A_0} \times 100 \\ &= \frac{(\pi/4)(0.505)^2 - (\pi/4)(0.398)^2}{(\pi/4)(0.505)^2} \times 100 \\ &= 37.9\% \end{aligned}$$

The final length is less than 2.205 in. (see Table 6-1) because, after fracture, the elastic strain is recovered.





(a)



(b)

(c)2003 Brooks/Cole, a division of Thomson Learning, Inc. Thomson Learning,™ is a trademark used herein under license.

Figure 6.16 The effect of temperance (a) on the stress-strain curve and (b) on the tensile properties of an aluminum alloy





True Stress and True Strain

- ❑ **True stress** The load divided by the actual cross-sectional area of the specimen at that load.
- ❑ **True strain** The strain calculated using actual and not original dimensions, given by $\epsilon_t \ln(l/l_0)$.

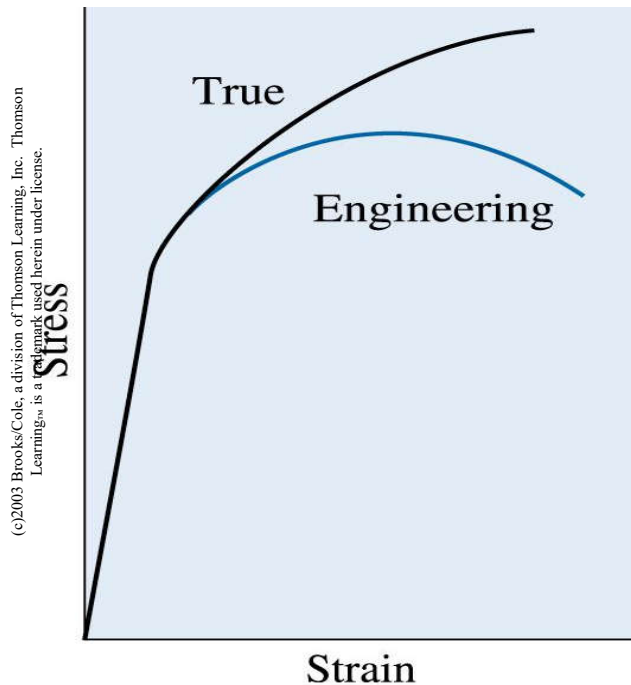


Figure 6.17 The relation between the true stress-true strain diagram and engineering stress-engineering strain diagram. The curves are identical to the yield point





True Stress and True Strain Calculation

Compare engineering stress and strain with true stress and strain for the aluminum alloy in Example 6.1 at (a) the maximum load and (b) fracture. The diameter at maximum load is 0.497 in. and at fracture is 0.398 in.

Example 6.5 SOLUTION

(a) At the tensile or maximum load:

$$\text{Engineering stress} = \frac{F}{A_0} = \frac{8000 \text{ lb}}{(\pi/4)(0.505 \text{ in.})^2} = 40,000 \text{ psi}$$

$$\text{True stress} = \frac{F}{A} = \frac{8000}{(\pi/4)(0.497)^2} = 41,237 \text{ psi}$$

$$\text{Engineering strain} = \frac{l - l_0}{l_0} = \frac{2.120 - 2.000}{2.000} = 0.060 \text{ in./in.}$$

$$\text{True strain} = \ln\left(\frac{l}{l_0}\right) = \ln\left(\frac{2.120}{2.000}\right) = 0.058 \text{ in./in.}$$



Example 6.5 SOLUTION (Continued)

(b) At fracture:

$$\text{Engineering stress} = \frac{F}{A_0} = \frac{7600 \text{ lb}}{(\pi/4)(0.505 \text{ in.})^2} = 38,000 \text{ psi}$$

$$\text{True stress} = \frac{F}{A} = \frac{7600}{(\pi/4)(0.398 \text{ in.})^2} = 61,090 \text{ psi}$$

$$\text{Engineering strain} = \frac{\Delta l}{l_0} = \frac{0.205}{2.000} = 0.1025 \text{ in./in.}$$

$$\begin{aligned} \text{True strain} &= \ln\left(\frac{A_0}{A_f}\right) = \ln\left[\frac{(\pi/4)(0.505)^2}{(\pi/4)(0.398)^2}\right] \\ &= \ln(1.610) = 0.476 \text{ in./in.} \end{aligned}$$

The true stress becomes much greater than the engineering stress only after necking begins.

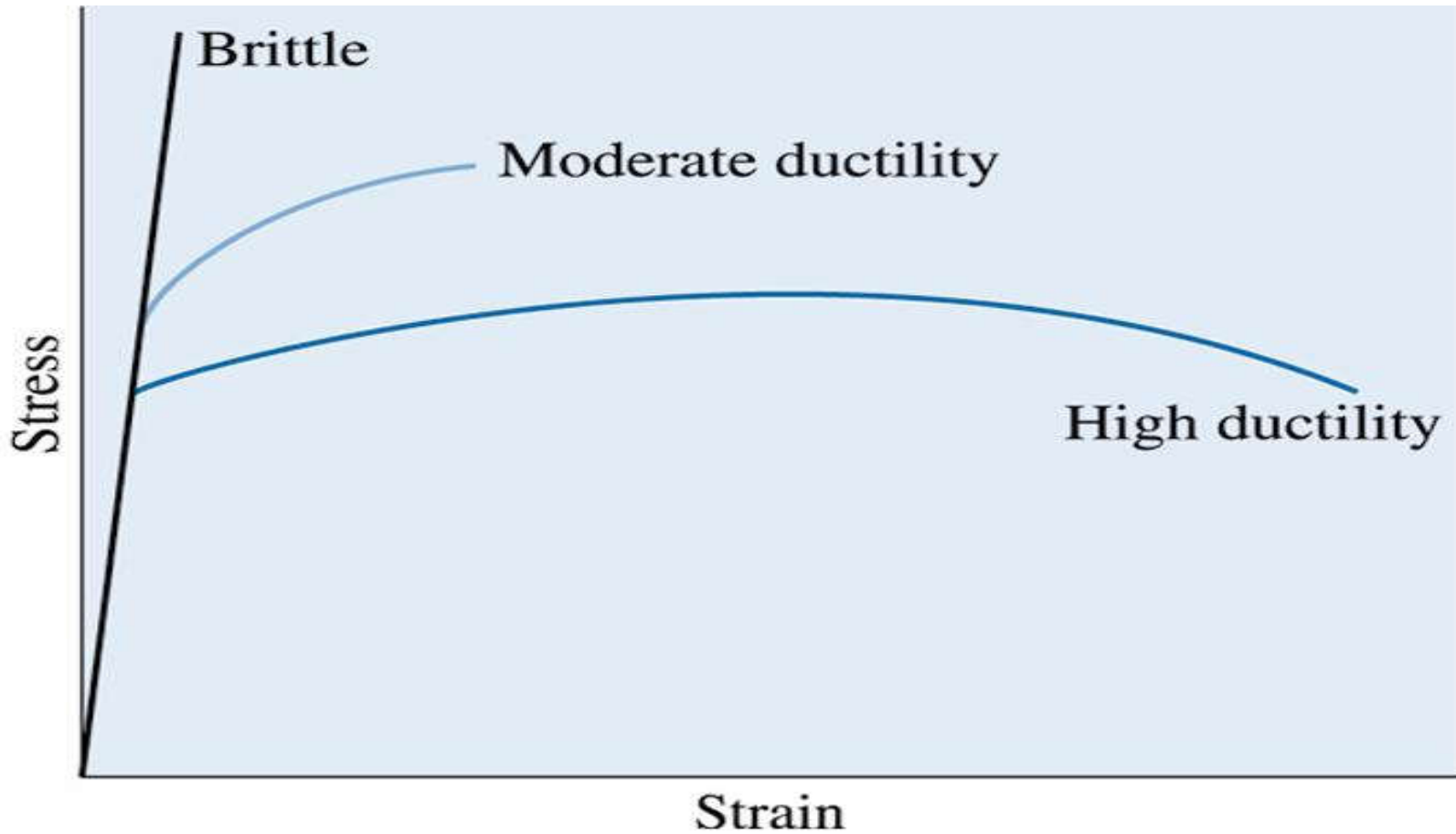




Section 6.6

The Bend Test for Brittle Materials

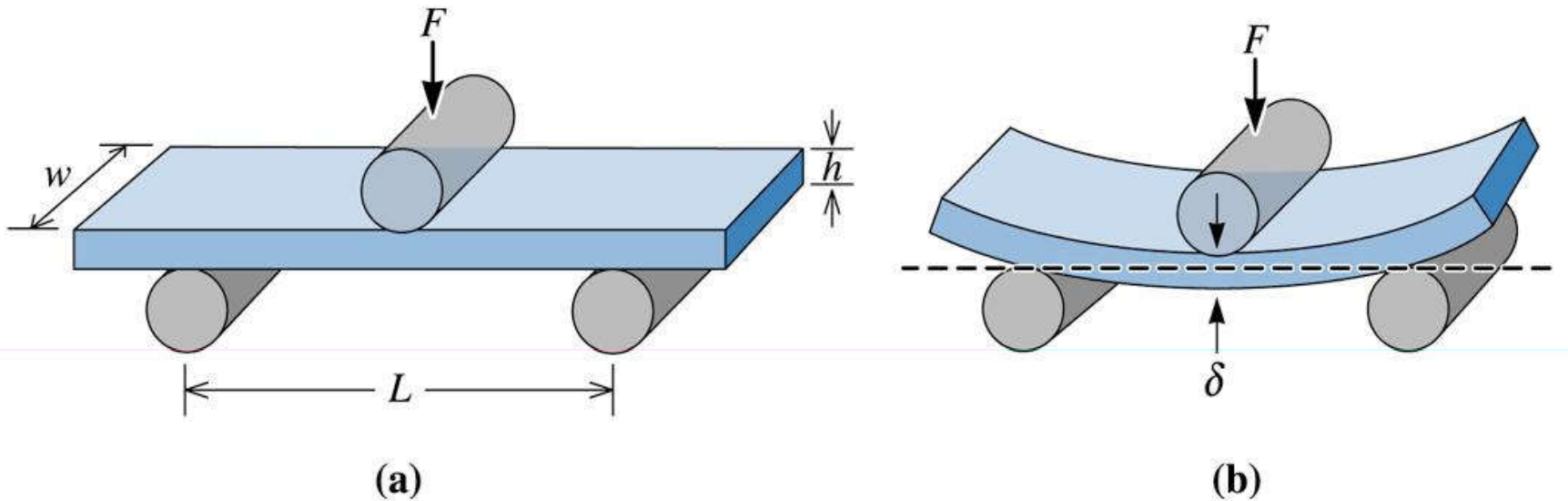
- **Bend test** - Application of a force to the center of a bar that is supported on each end to determine the resistance of the material to a static or slowly applied load.
- **Flexural strength or modulus of rupture** -The stress required to fracture a specimen in a bend test.
- **Flexural modulus** - The modulus of elasticity calculated from the results of a bend test, giving the slope of the stress-deflection curve.



(c)2003 Brooks/Cole, a division of Thomson Learning, Inc. Thomson Learningsm is a trademark used herein under license.

Figure 6.18 The stress-strain behavior of brittle materials compared with that of more ductile materials





(c)2003 Brooks/Cole, a division of Thomson Learning, Inc. Thomson Learningsm is a trademark used herein under license.

Figure 6.19 (a) The bend test often used for measuring the strength of brittle materials, and (b) the deflection δ obtained by bending



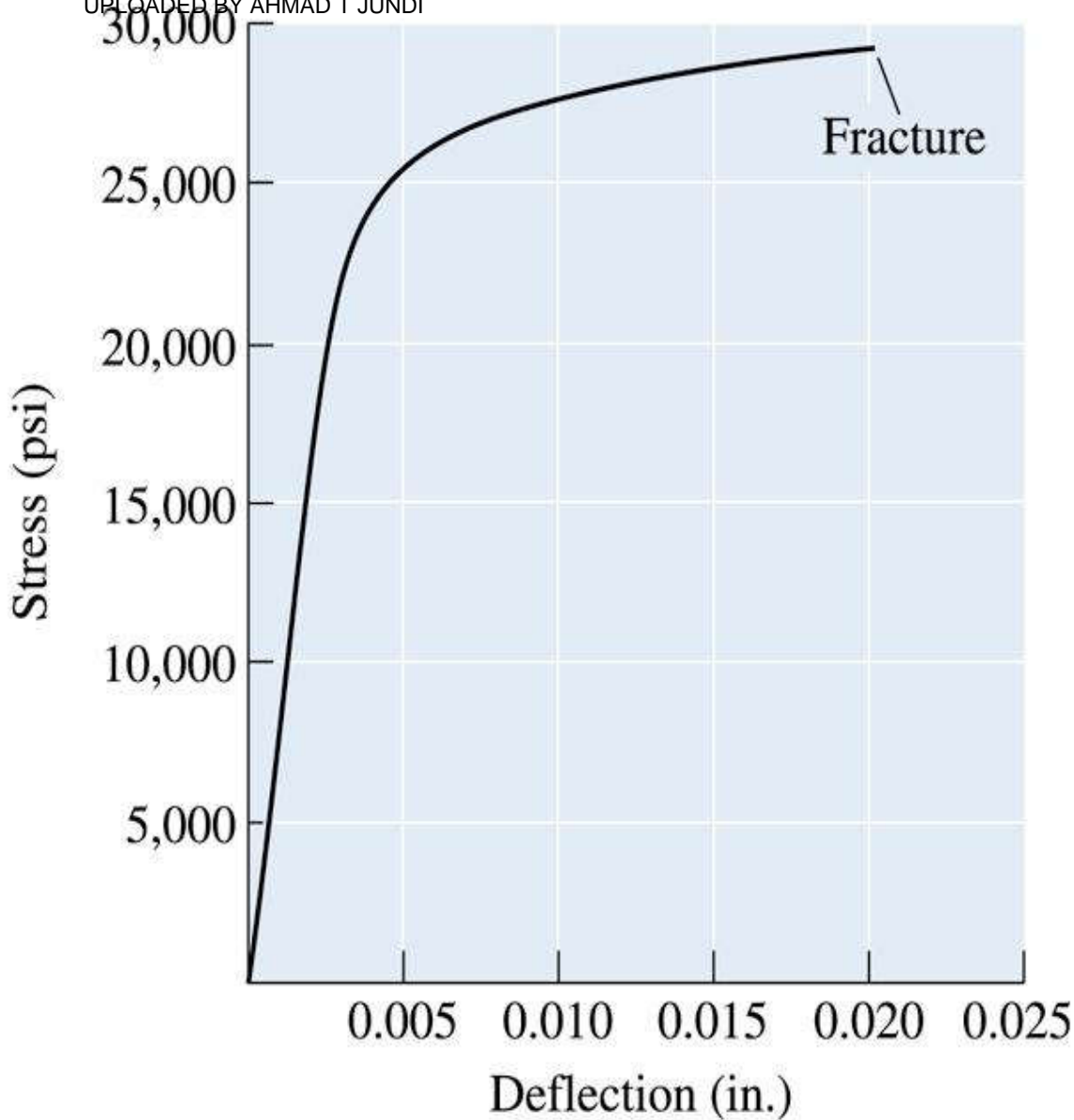
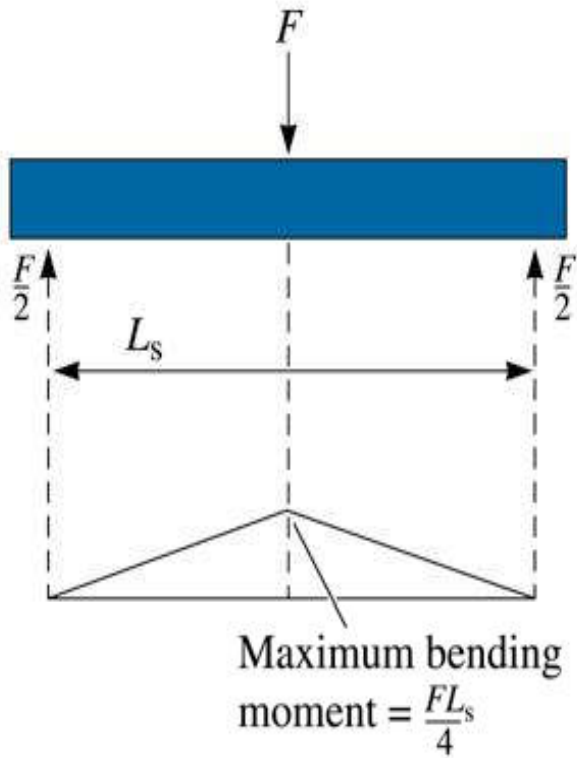
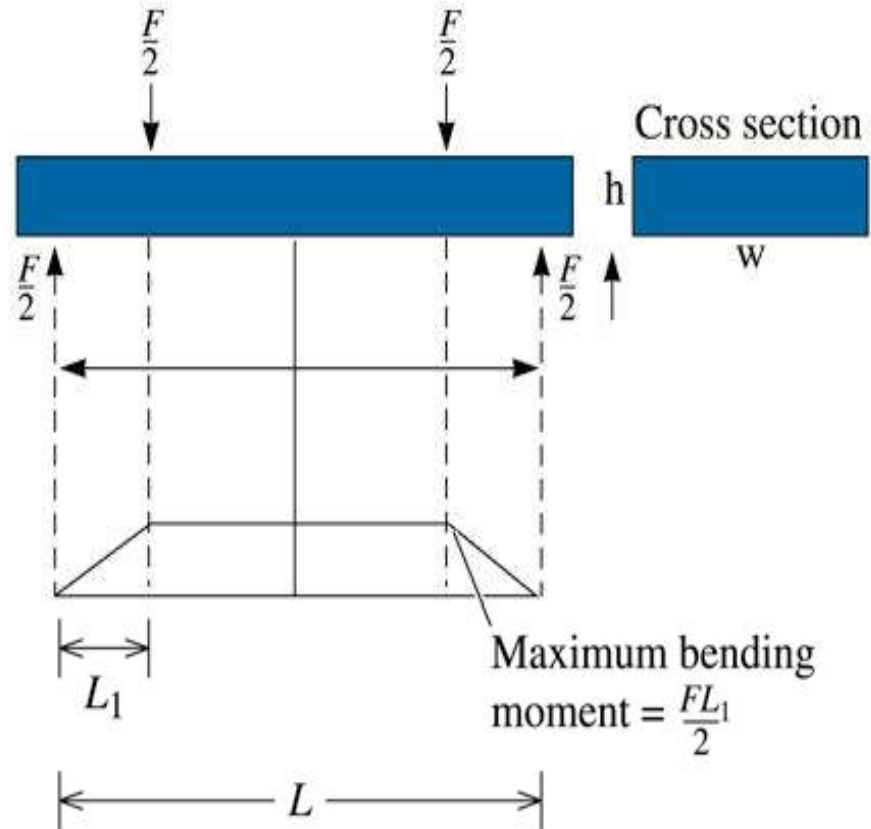


Figure 6.20
Stress-
deflection
curve for MgO
obtained from
a bend test



(a)



(b)

(c)2003 Brooks/Cole, a division of Thomson Learning, Inc. Thomson Learning,™ is a trademark used herein under license.

Figure 6.21 (a) Three point and (b) four-point bend test setup



TABLE 6-4 ■ *Comparison of the tensile, compressive, and flexural strengths of selected ceramic and composite materials*

Material	Tensile Strength (psi)	Compressive Strength (psi)	Flexural Strength (psi)
Polyester—50% glass fibers	23,000	32,000	45,000
Polyester—50% glass fiber fabric	37,000	27,000 ^a	46,000
Al ₂ O ₃ (99% pure)	30,000	375,000	50,000
SiC (pressureless-sintered)	25,000	560,000	80,000

^a A number of composite materials are quite poor in compression.



Flexural Strength of Composite Materials



The flexural strength of a composite material reinforced with glass fibers is 45,000 psi and the flexural modulus is 18×10^6 psi. A sample, which is 0.5 in. wide, 0.375 in. high, and 8 in. long, is supported between two rods 5 in. apart. Determine the force required to fracture the material and the deflection of the sample at fracture, assuming that no plastic deformation occurs.

Example 6.6 SOLUTION

Based on the description of the sample, $w = 0.5$ in., $h = 0.375$ in., and $L = 5$ in. From Equation 6-15:

$$45,000 \text{ psi} = \frac{3FL}{2wh^2} = \frac{(3)(F \text{ lb})(5 \text{ in.})}{(2)(0.5 \text{ in.})(0.375 \text{ in.})^2} = 106.7F$$

$$F = \frac{45,000}{106.7} = 422 \text{ lb}$$





Example 6.6 SOLUTION (Continued)

Therefore, the deflection, from Equation 6-14, is:

$$18 \times 10^6 \text{ psi} = \frac{L^3 F}{4wh^3\delta} = \frac{(5 \text{ in.})^3(422 \text{ lb})}{(4)(0.5 \text{ in.})(0.375 \text{ in.})^3\delta}$$
$$\delta = 0.0278 \text{ in.}$$

In this calculation, we did assume that there is no viscoelastic behavior and a linear behavior of stress versus strain.[8]

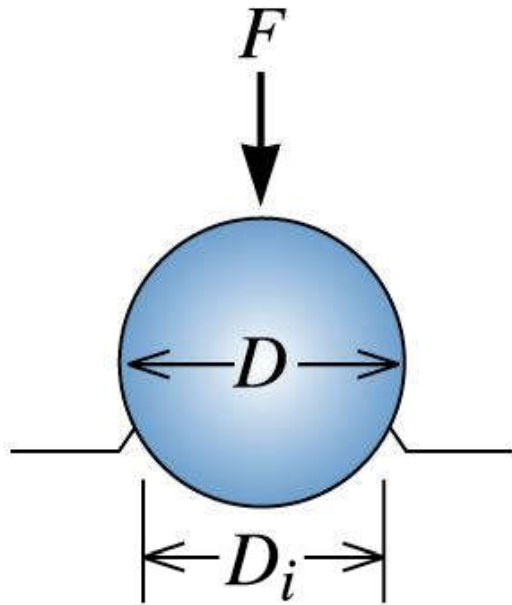




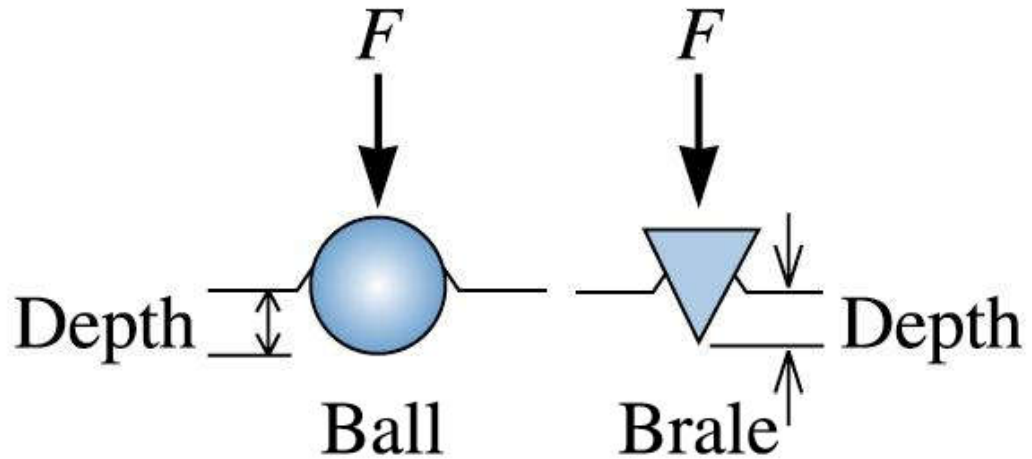
Section 6.7

Hardness of Materials

- **Hardness test** - Measures the resistance of a material to penetration by a sharp object.
- **Macrohardness** - Overall bulk hardness of materials measured using loads >2 N.
- **Microhardness** Hardness of materials typically measured using loads less than 2 N using such test as Knoop (HK).
- **Nano-hardness** - Hardness of materials measured at 1–10 nm length scale using extremely small (~ 100 μN) forces.



Brinell test



Rockwell test

(c)2003 Brooks/Cole, a division of Thomson Learning, Inc. Thomson Learning[®] is a trademark used herein under license.

Figure 6.23 Indentors for the Brinell and Rockwell hardness tests





TABLE 6-5 ■ *Comparison of typical hardness tests*

Test	Indentor	Load	Application
Brinell	10-mm ball	3000 kg	Cast iron and steel
Brinell	10-mm ball	500 kg	Nonferrous alloys
Rockwell <i>A</i>	Brale	60 kg	Very hard materials
Rockwell <i>B</i>	1/16-in. ball	100 kg	Brass, low-strength steel
Rockwell <i>C</i>	Brale	150 kg	High-strength steel
Rockwell <i>D</i>	Brale	100 kg	High-strength steel
Rockwell <i>E</i>	1/8-in. ball	100 kg	Very soft materials
Rockwell <i>F</i>	1/16-in. ball	60 kg	Aluminum, soft materials
Vickers	Diamond pyramid	10 kg	All materials
Knoop	Diamond pyramid	500 g	All materials

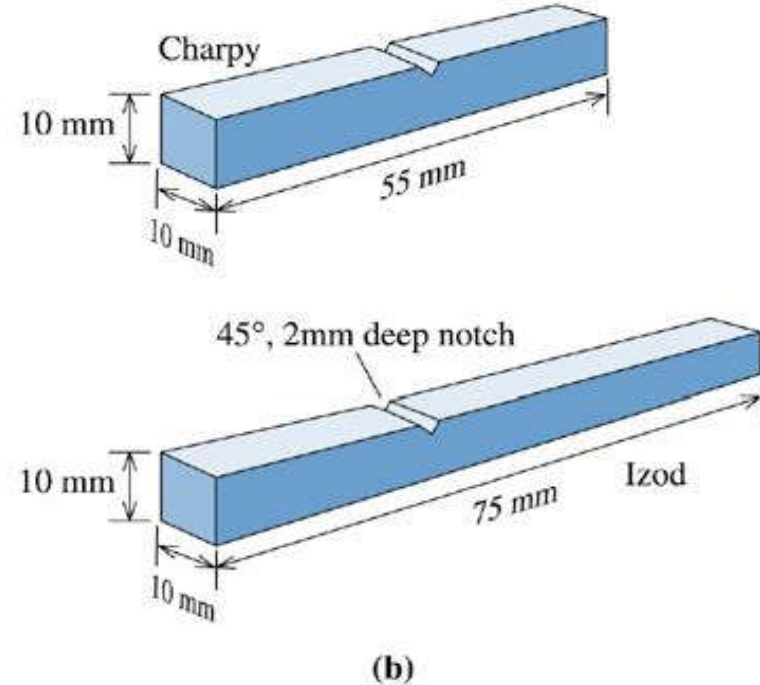
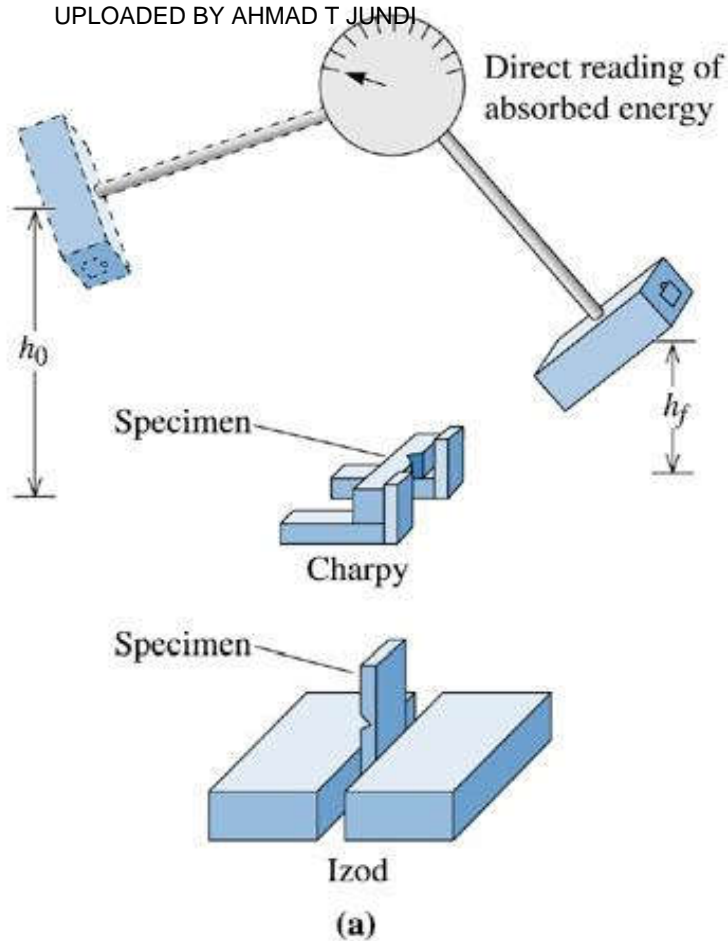




Section 6.8

Strain Rate Effects and Impact Behavior

- ❑ **Impact test** - Measures the ability of a material to absorb the sudden application of a load without breaking.
- ❑ **Impact energy** - The energy required to fracture a standard specimen when the load is applied suddenly.
- ❑ **Impact toughness** - Energy absorbed by a material, usually notched, during fracture, under the conditions of impact test.
- ❑ **Fracture toughness** - The resistance of a material to failure in the presence of a flaw.



(c)2003 Brooks/Cole, a division of Thomson Learning, Inc. Thomson Learning,™ is a trademark used herein under license.

Figure 6.26 The impact test: (a) The Charpy and Izod tests, and (b) dimensions of typical specimens



Section 6.9

Properties Obtained from the Impact Test

- **Ductile to brittle transition temperature (DBTT)** - The temperature below which a material behaves in a brittle manner in an impact test.
- **Notch sensitivity** - Measures the effect of a notch, scratch, or other imperfection on a material's properties, such as toughness or fatigue life.

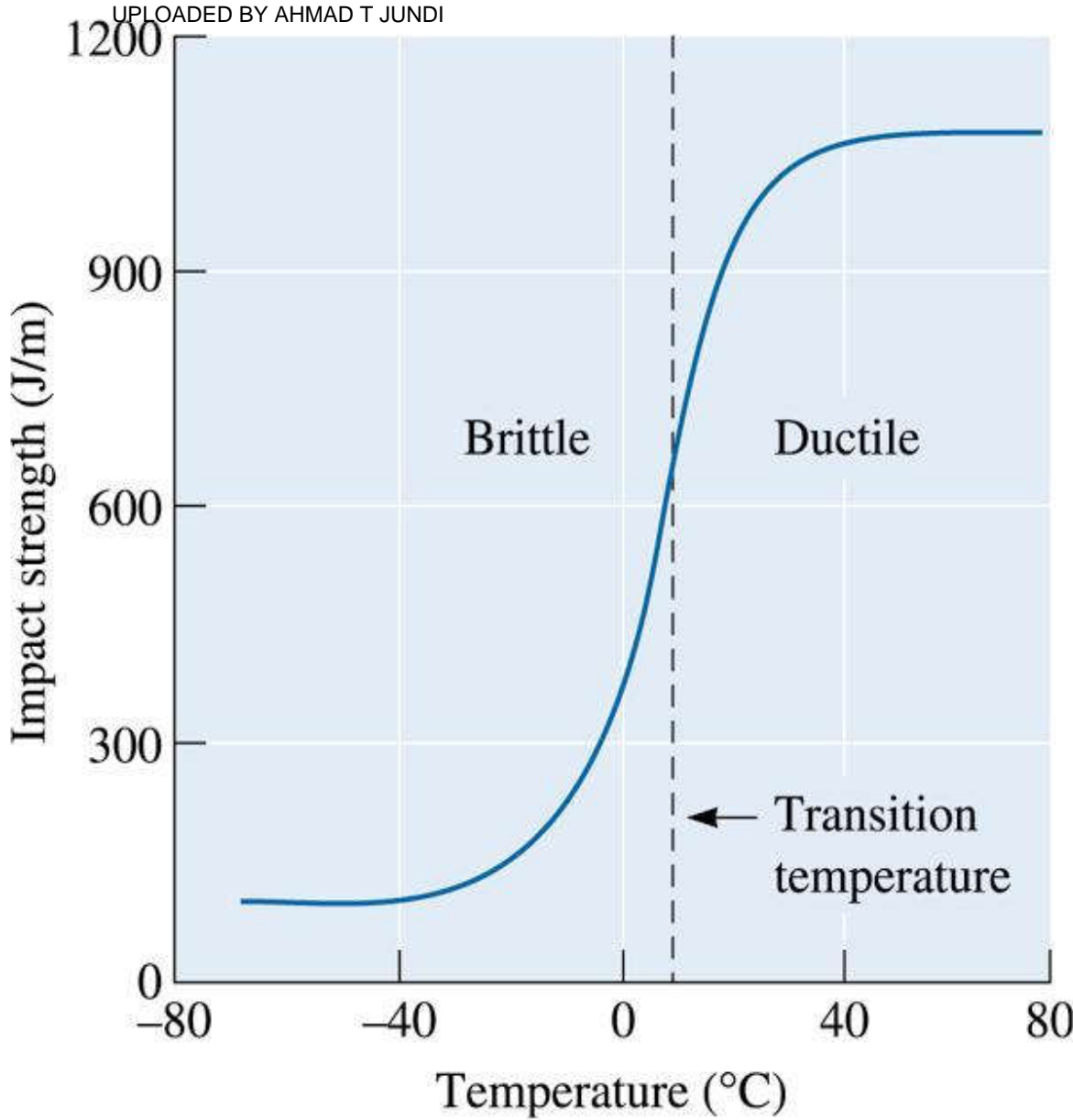


Figure 6.27 Results from a series of Izod impact tests for a super-tough nylon thermoplastic polymer



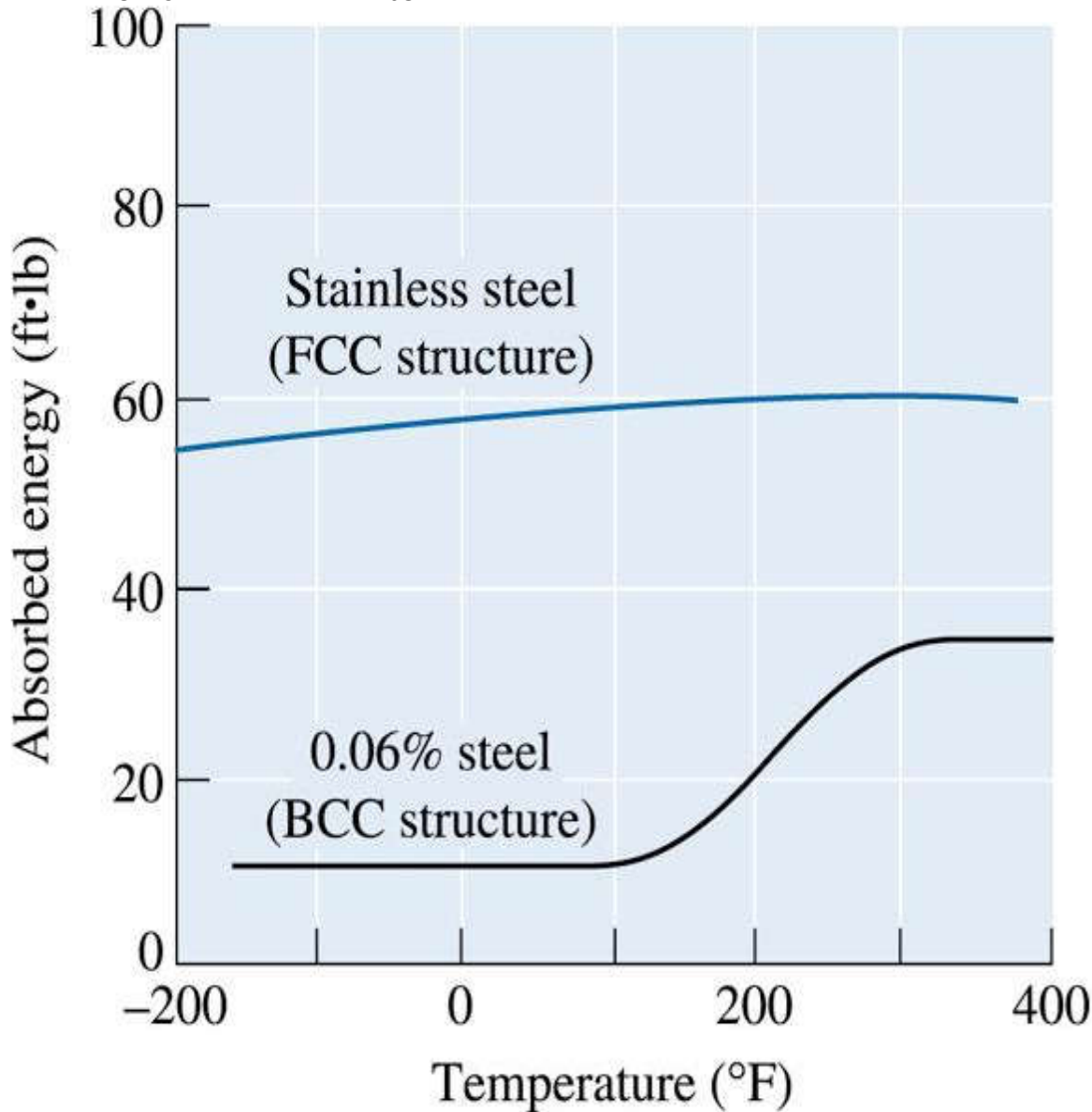


Figure 6.28 The Charpy V-notch properties for a BCC carbon steel and a FCC stainless steel. The FCC crystal structure typically leads to higher absorbed energies and no transition temperature

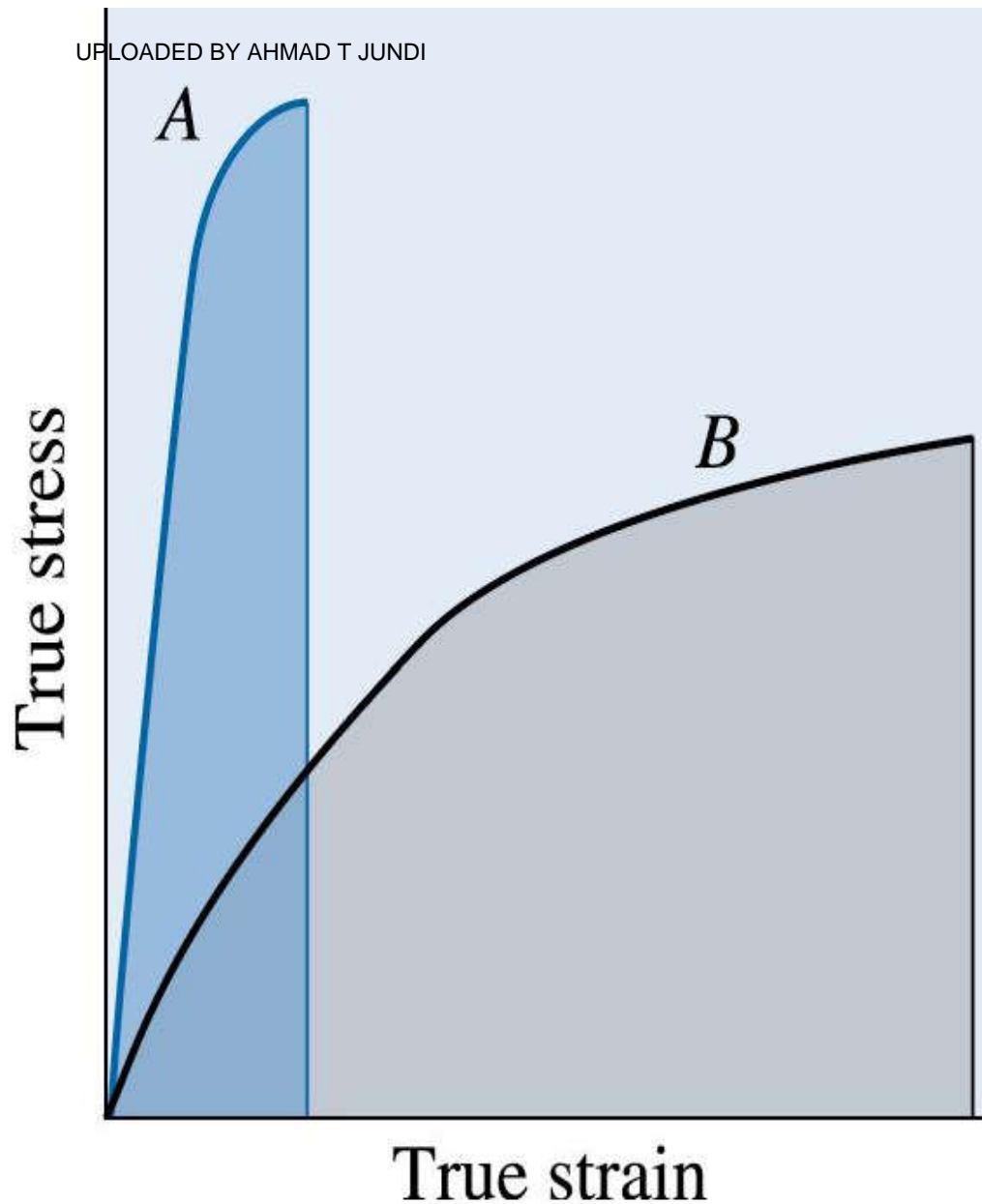


Figure 6.29 The area contained within the true stress-true strain curve is related to the tensile toughness. Although material *B* has a lower yield strength, it absorbs a greater energy than material *A*. The energies from these curves may not be the same as those obtained from impact test data



Example 6.7

Design of a Sledgehammer



The flexural strength of a composite material reinforced with glass fibers is 45,000 psi and the flexural modulus is 18×10^6 psi. A sample, which is 0.5 in. wide, 0.375 in. high, and 8 in. long, is supported between two rods 5 in. apart. Determine the force required to fracture the material and the deflection of the sample at fracture, assuming that no plastic deformation occurs.

Example 6.7 SOLUTION

Design requirements to be met by the sledgehammer. A partial list:

1. The handle should be light in weight, yet tough enough that it will not catastrophically break.
2. The head must not break or chip during use, even in subzero temperatures.
3. The head must not deform during continued use.
4. The head must be large enough to assure that the user doesn't miss the fence post, and it should not include sharp notches that might cause chipping.
5. The sledgehammer should be inexpensive.



Section 6.10

Fracture Mechanics

- **Fracture mechanics** - The study of a material's ability to withstand stress in the presence of a flaw.
- **Fracture toughness** - The resistance of a material to failure in the presence of a flaw.

©2003 Brooks/Cole, a division of Thomson Learning, Inc. Thomson Learning is a trademark used herein under license.

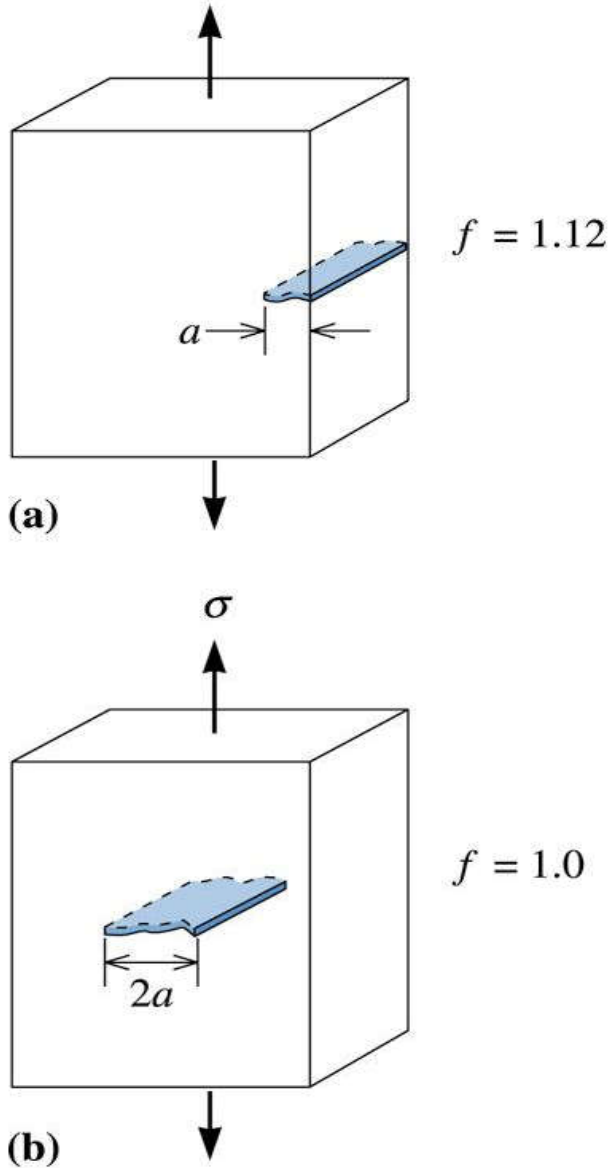


Figure 6.30 Schematic drawing of fracture toughness specimens with (a) edge and (b) internal flaws

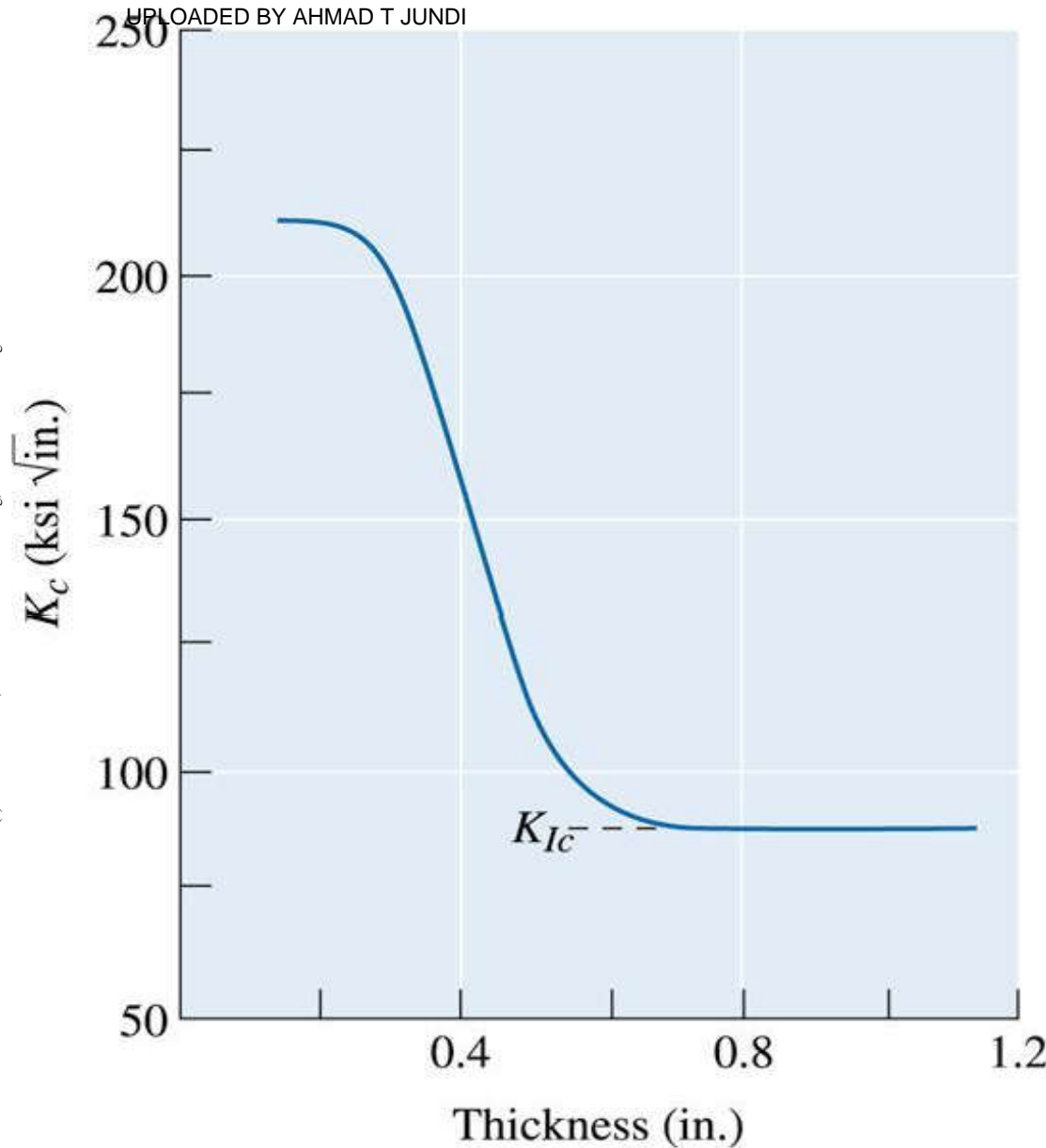


Figure 6.31 The fracture toughness K_c of a 3000,000psi yield strength steel decreases with increasing thickness, eventually leveling off at the plane strain fracture toughness K_{Ic}



TABLE 6-6 ■ *The plane strain fracture toughness K_{Ic} of selected materials*

Material	Fracture Toughness K_{Ic} (psi $\sqrt{\text{in.}}$)	Yield Strength or Ultimate Strength (for Brittle Solids) (psi)
Al-Cu alloy	22,000	66,000
	33,000	47,000
Ti-6% Al-4% V	50,000	130,000
	90,000	125,000
Ni-Cr steel	45,800	238,000
	80,000	206,000
Al ₂ O ₃	1,600	30,000
Si ₃ N ₄	4,500	80,000
Transformation toughened ZrO ₂	10,000	60,000
Si ₃ N ₄ -SiC composite	51,000	120,000
Polymethyl methacrylate polymer	900	4,000
Polycarbonate polymer	3,000	8,400



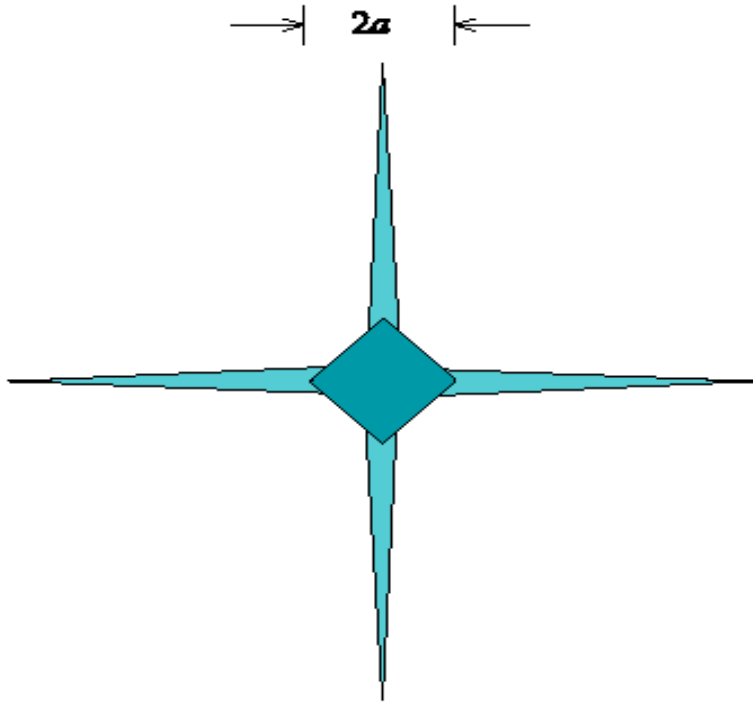


Figure 6-32 Secondary cracks developed during hardness testing can be used to assess the fracture toughness of brittle materials

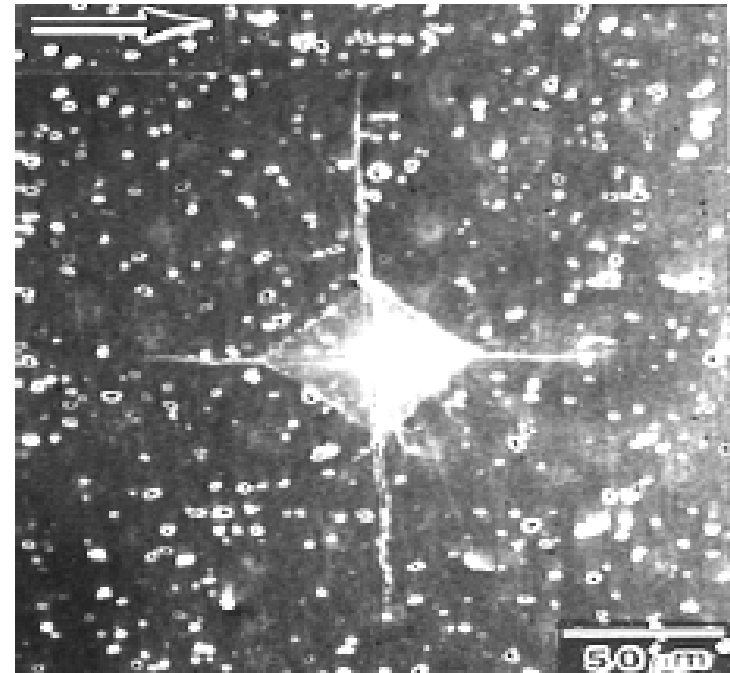


Figure 6-33 A scanning electron micrograph showing crack propagation in a PZT ceramic. (Courtesy of Wang and Raj N. Singh, *Ferroelectrics*, 207, 555–575 (1998).)

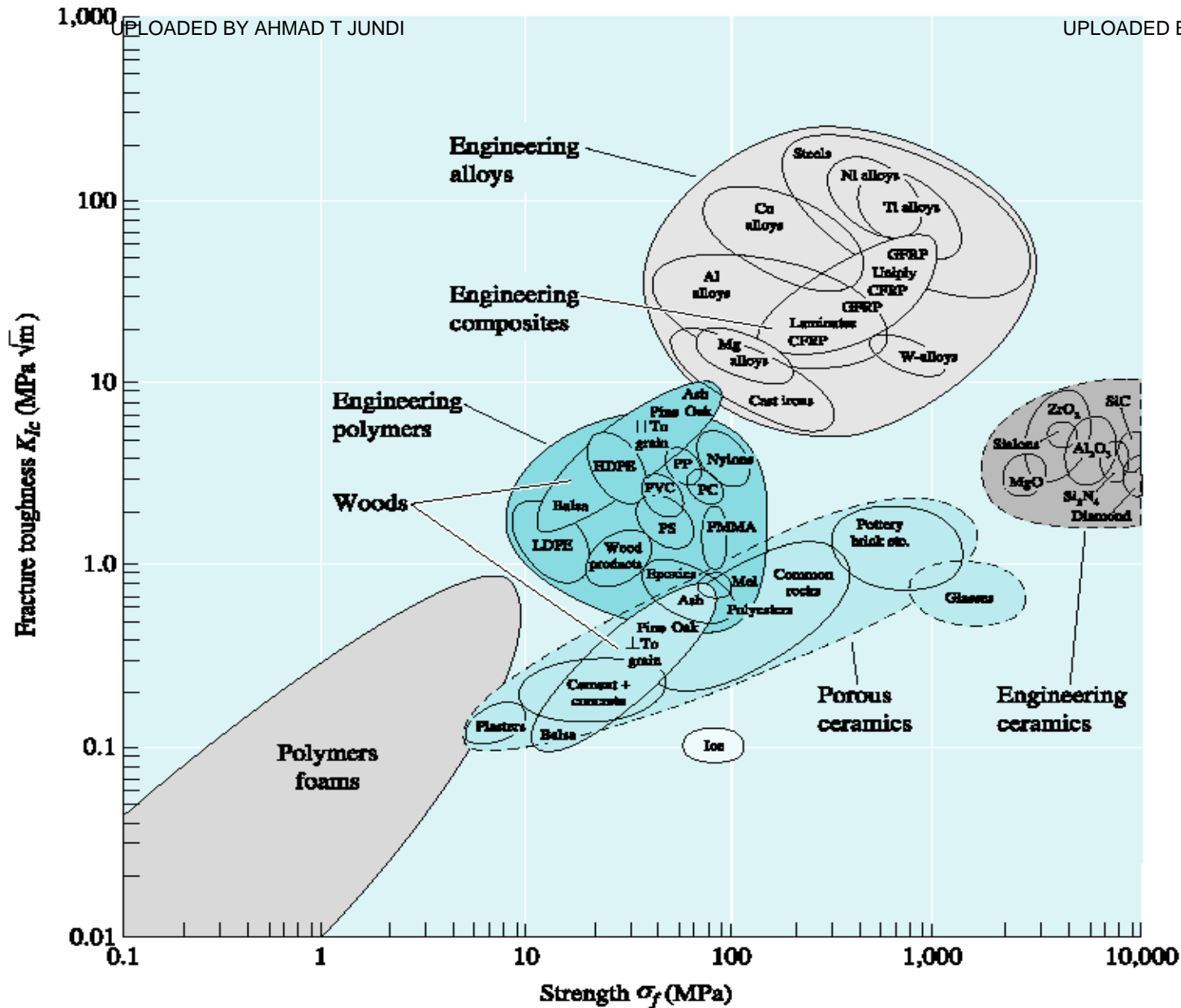
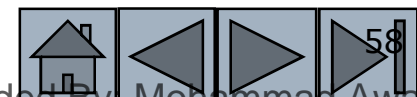


Figure 6-34 Fracture toughness versus strength of different engineered materials. (Source: Adapted from Mechanical Behavior of Materials, by T.H. Courtney, 2000, p. 434, Fig. 9-18. Copyright © 2000 The McGraw-Hill Companies. Adapted with permission.)





Section 6.11

The Importance of Fracture Mechanics

- Selection of a Material
- Design of a Component
- Design of a Manufacturing or Testing Method
- Griffith flaw - A crack or flaw in a material that concentrates and magnifies the applied stress.



Design of a Nondestructive Test

A large steel plate used in a nuclear reactor has a plane strain fracture toughness of $80,000 \text{ psi}\sqrt{\text{in.}}$ and is exposed to a stress of $45,000 \text{ psi}$ during service. Design a testing or inspection procedure capable of detecting a crack at the edge of the plate before the crack is likely to grow at a catastrophic rate.

Example 6.8 SOLUTION

We need to determine the minimum size of a crack that will propagate in the steel under these conditions. From Equation 6-18, assuming that $f = 1.12$:

$$K_{Ic} = f\sigma\sqrt{a\pi}$$

$$80,000 = (1.12)(45,000)\sqrt{a\pi}$$

$$a = 0.8 \text{ in.}$$

(c)2003 Brooks/Cole, a division of Thomson Learning, Inc. Thomson Learning is a trademark used herein under license.

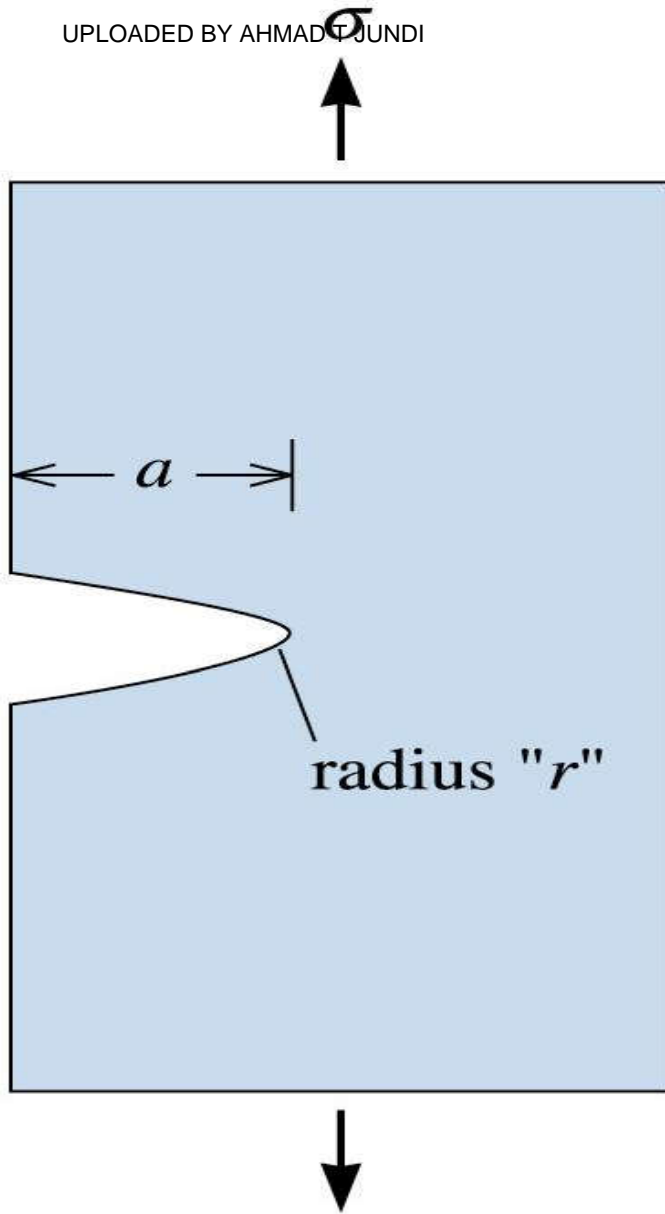


Figure 6.35 Schematic diagram of the Griffith flaw in a ceramic



Properties of SiAlON Ceramics

Assume that an advanced ceramic, sialon (acronym for SiAlON or silicon aluminum oxynitride), has a tensile strength of 60,000 psi. Let us assume that this value is for a flaw-free ceramic. (In practice, it is almost impossible to produce flaw-free ceramics.) A thin crack 0.01 in. deep is observed before a sialon part is tested. The part unexpectedly fails at a stress of 500 psi by propagation of the crack. Estimate the radius of the crack tip.

Example 6.9 SOLUTION

The failure occurred because the 500-psi applied stress, magnified by the stress concentration at the tip of the crack, produced an actual stress equal to the tensile strength. From Equation 6-21:

$$\sigma_{\text{actual}} = 2\sigma\sqrt{a/r}$$

$$60,000 \text{ psi} = (2)(500 \text{ psi})\sqrt{0.01 \text{ in.}/r}$$

$$\sqrt{0.01/r} = 60 \quad \text{or} \quad 0.01/r = 3600$$

$$r = 2.8 \times 10^{-6} \text{ in.} = 7.1 \times 10^{-6} \text{ cm} = 710 \text{ \AA}$$





Design of a Ceramic Support

Design a supporting 3-in.-wide plate made of sialon, which has a fracture toughness of $9,000 \text{ psi}\sqrt{\text{in.}}$, that will withstand a tensile load of 40,000 lb. The part is to be nondestructively tested to assure that no flaws are present that might cause failure.

Example 6.10 SOLUTION

From our fracture toughness equation, assuming that $f = 1$:

$$\sigma_{\max} = \frac{K_{Ic}}{\sqrt{\pi a}} = \frac{F}{A}$$

$$A = \frac{F\sqrt{\pi a}}{K_{Ic}} = \frac{(40,000)(\sqrt{\pi})(\sqrt{a})}{9,000}$$

$$A = 7.88\sqrt{a} \text{ in.}^2 \quad \text{and} \quad \text{thickness} = (7.88 \text{ in.}^2 / 3 \text{ in.})\sqrt{a} = 2.63\sqrt{a}$$





Section 6.12

Microstructural Features of Fracture in Metallic Materials

- ❑ **Transgranular** - Meaning across the grains (e.g., a transgranular fracture would be fracture in which cracks would go through the grains).
- ❑ **Microvoids** - Development of small holes in a material.
- ❑ **Intergranular** - In between grains or along the grain boundaries.
- ❑ **Chevron pattern** - A common fracture feature produced by separate crack fronts propagating at different levels in the material.

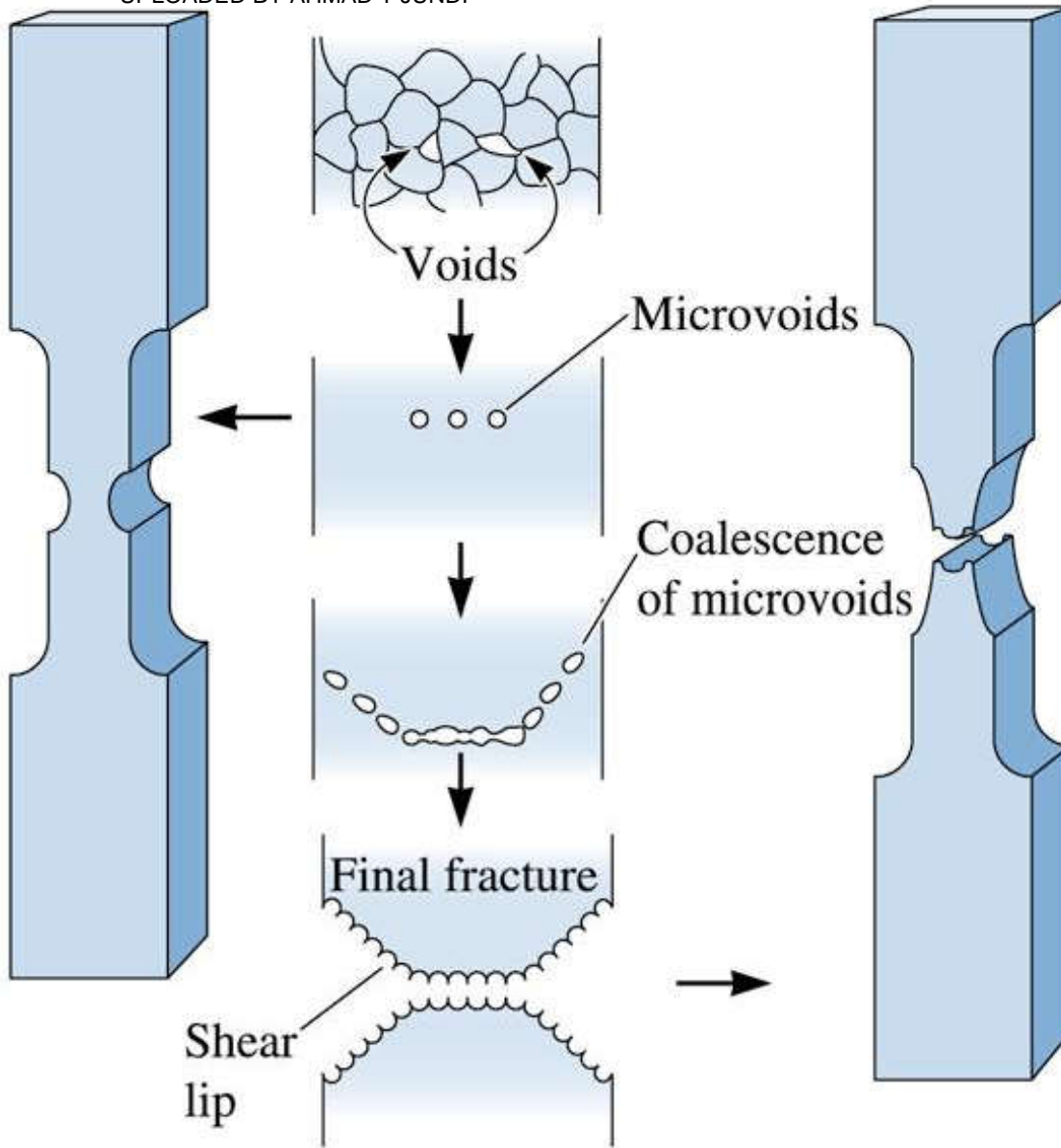
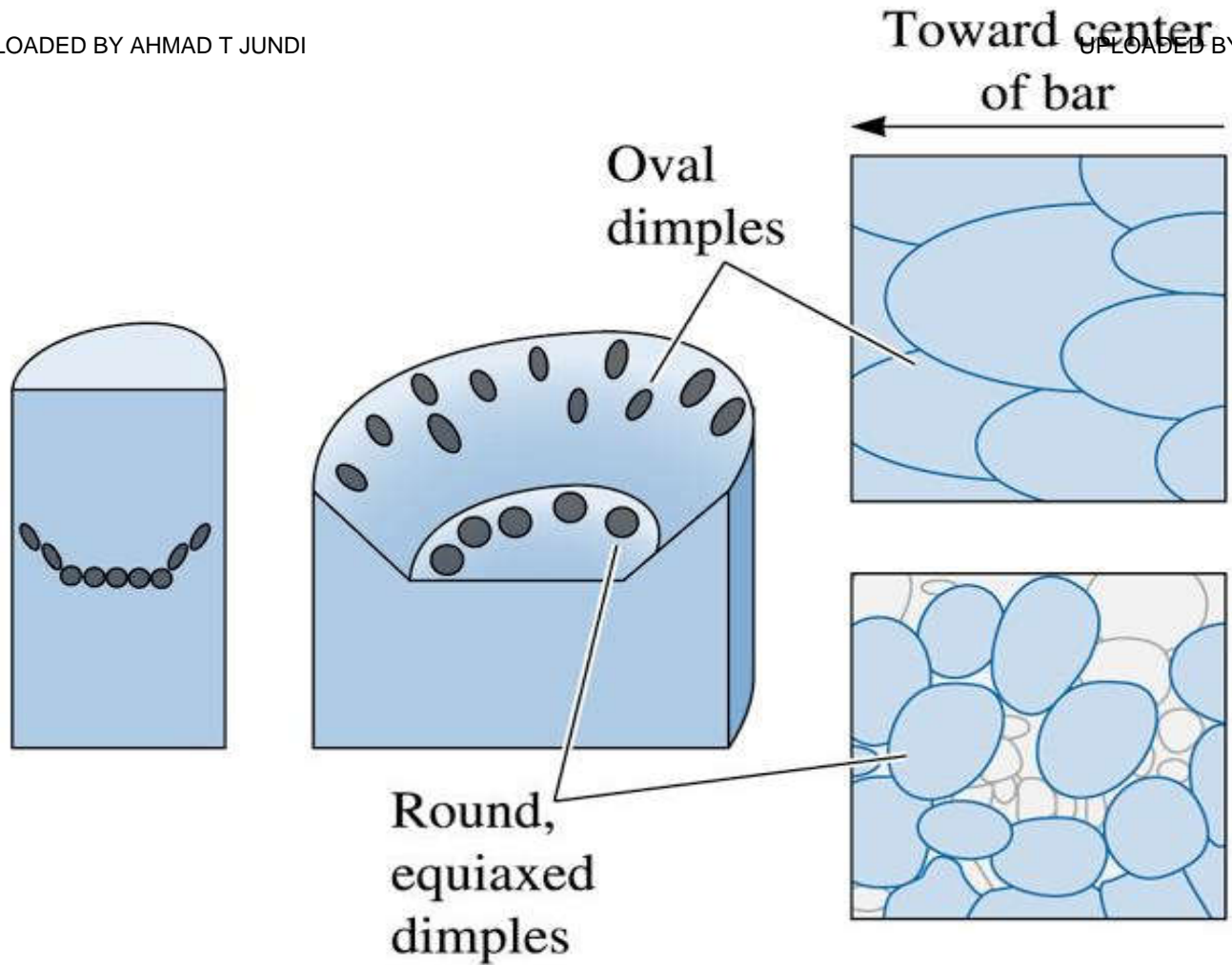
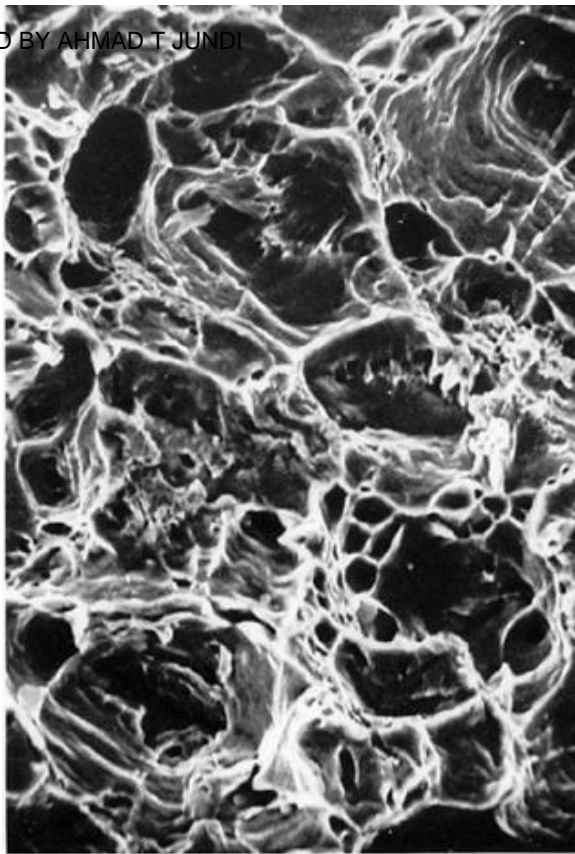


Figure 6.36 When a ductile material is pulled in a tensile test, necking begins and voids form – starting near the center of the bar – by nucleation at grain boundaries or inclusions. As deformation continues a 45° shear lip may form, producing a final cup and cone fracture



(c)2003 Brooks/Cole, a division of Thomson Learning, Inc. Thomson Learning,™ is a trademark used herein under license.

Figure 6.37 Dimples form during ductile fracture. Equiaxed dimples form in the center, where microvoids grow. Elongated dimples, pointing toward the origin of failure, form on the shear lip



(a)



(b)

(c)2003 Brooks/Cole, a division of Thomson Learning, Inc. Thomson Learning, is a trademark used herein under license.

Figure 6.38 Scanning electron micrographs of an annealed 1018 steel exhibiting ductile fracture in a tensile test. (a) Equiaxed dimples at the flat center of the cup and cone, and (b) elongated dimples at the shear lip (x 1250)

Example 6.11

Hoist Chain Failure Analysis



A chain used to hoist heavy loads fails. Examination of the failed link indicates considerable deformation and necking prior to failure. List some of the possible reasons for failure.

Example 6.11 SOLUTION

1. The load exceeded the hoisting capacity of the chain. Thus, the stress due to the load exceeded the yield strength of the chain, permitting failure. Comparison of the load to the manufacturer's specifications will indicate that the chain was not intended for such a heavy load. This is the fault of the user!
2. The chain was of the wrong composition or was improperly heattreated. Consequently, the yield strength was lower than intended by the manufacturer and could not support the load. This may be the fault of the manufacturer!

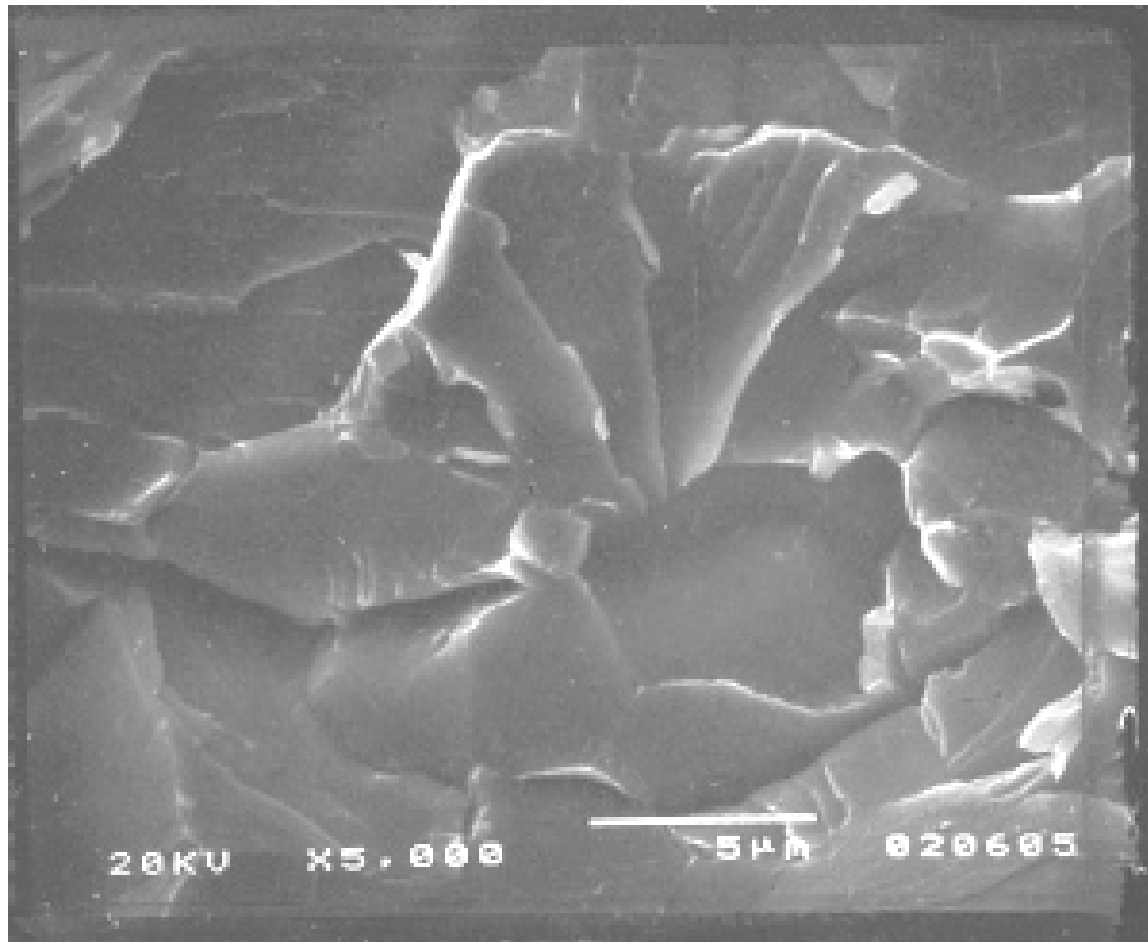
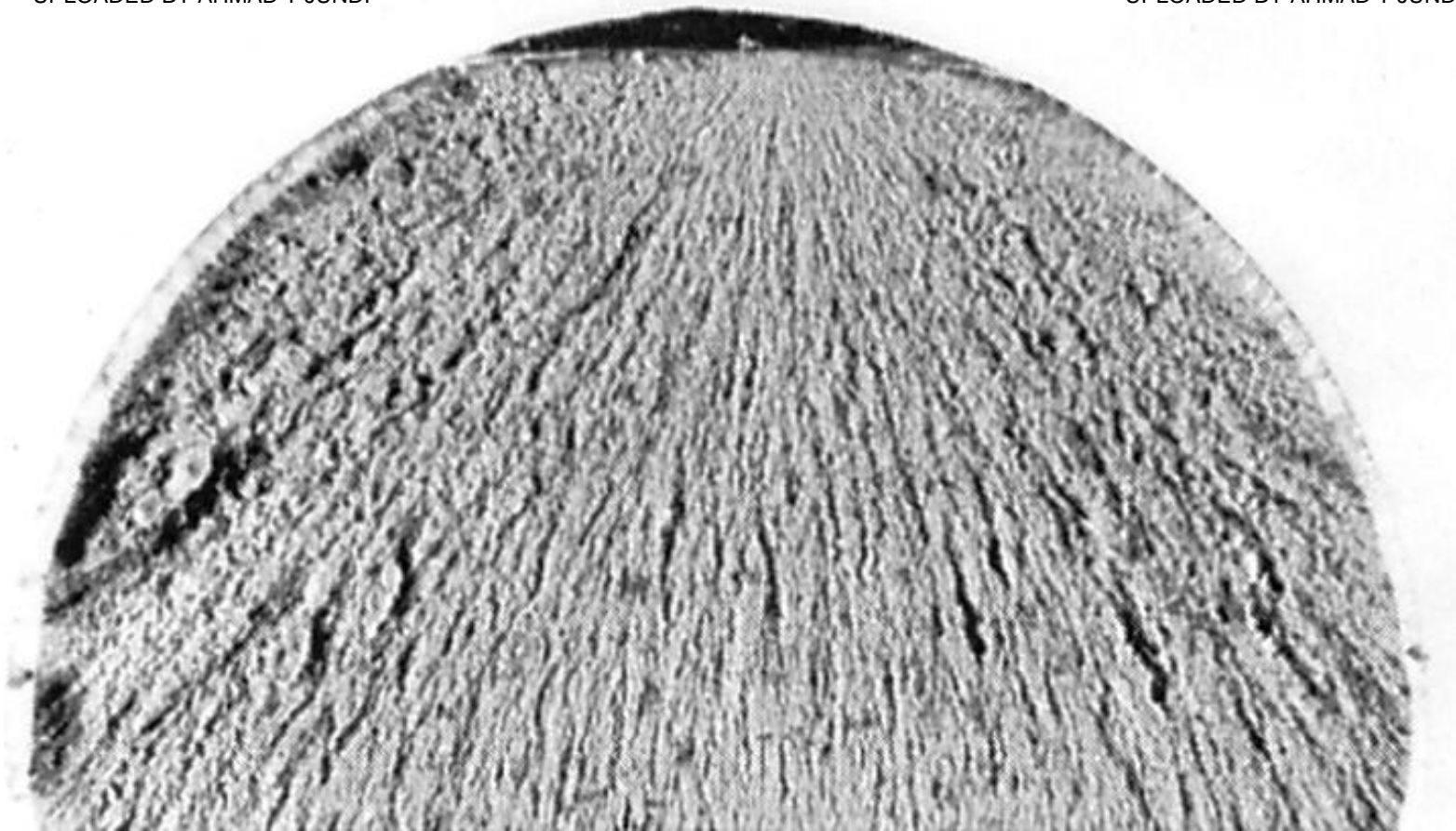


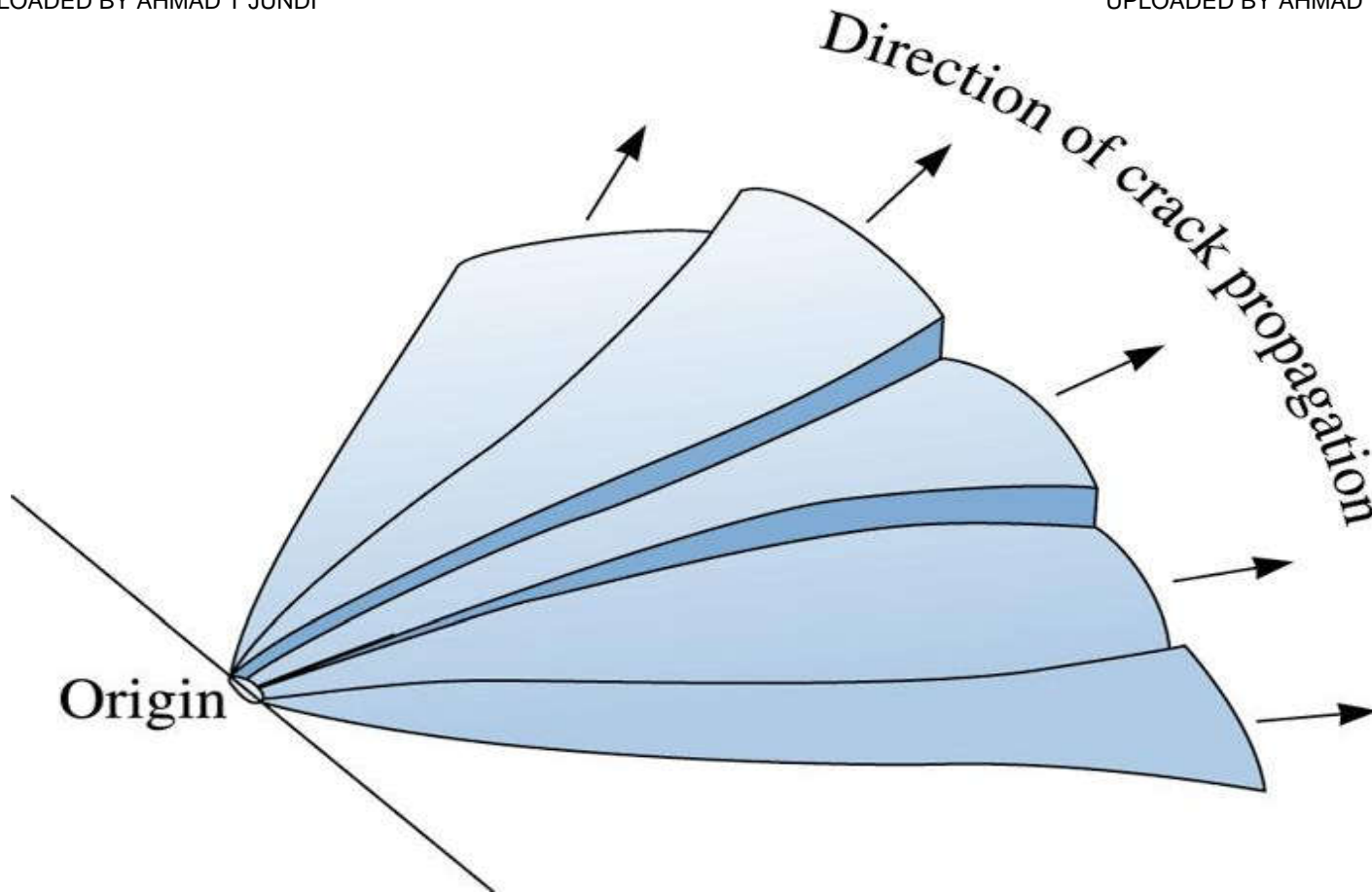
Figure 6.39 Scanning electron micrograph of a brittle fracture surface of a quenched 1010 steel (x 5000). (Courtesy of C.W. Ramsay.)



(c)2003 Brooks/Cole, a division of Thomson Learning, Inc. Thomson Learning,™ is a trademark used herein under license.

Figure 6.40 The Chevron pattern in a 0.5-in.-diameter quenched 4340 steel. The steel failed in a brittle manner by an impact blow





(c)2003 Brooks/Cole, a division of Thomson Learning, Inc. Thomson Learning, is a trademark used herein under license.

Figure 6.41 The Chevron pattern forms as the crack propagates from the origin at different levels. The pattern points back to the origin





Example 6.12

Automobile Axle Failure Analysis

An engineer investigating the cause of an automobile accident finds that the right rear wheel has broken off at the axle. The axle is bent. The fracture surface reveals a Chevron pattern pointing toward the surface of the axle. Suggest a possible cause for the fracture.

Example 6.12 SOLUTION

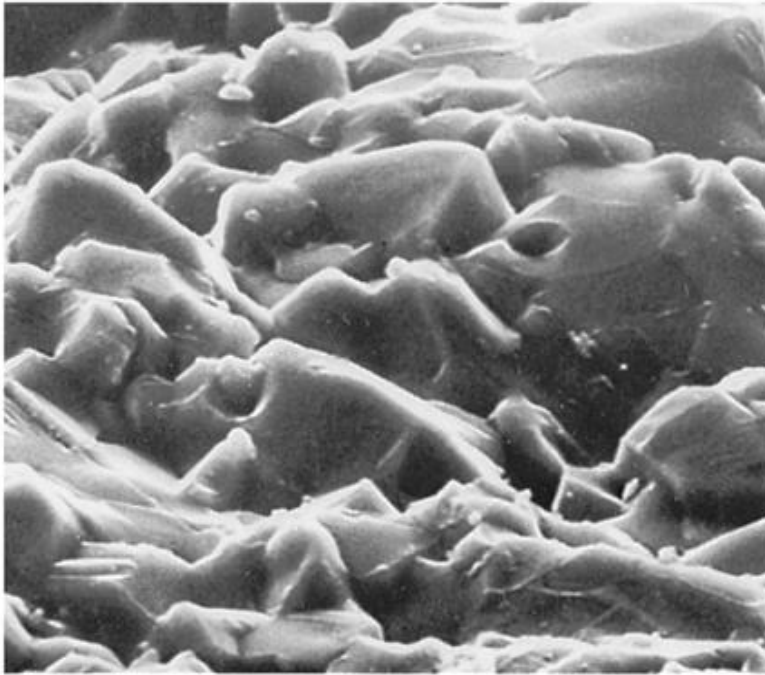
- The Chevron pattern indicates that the wheel was subjected to an intense impact blow, which was transmitted to the axle, causing failure.
- Further examination of the fracture surface, microstructure, composition, and properties may verify that the axle was manufactured properly.



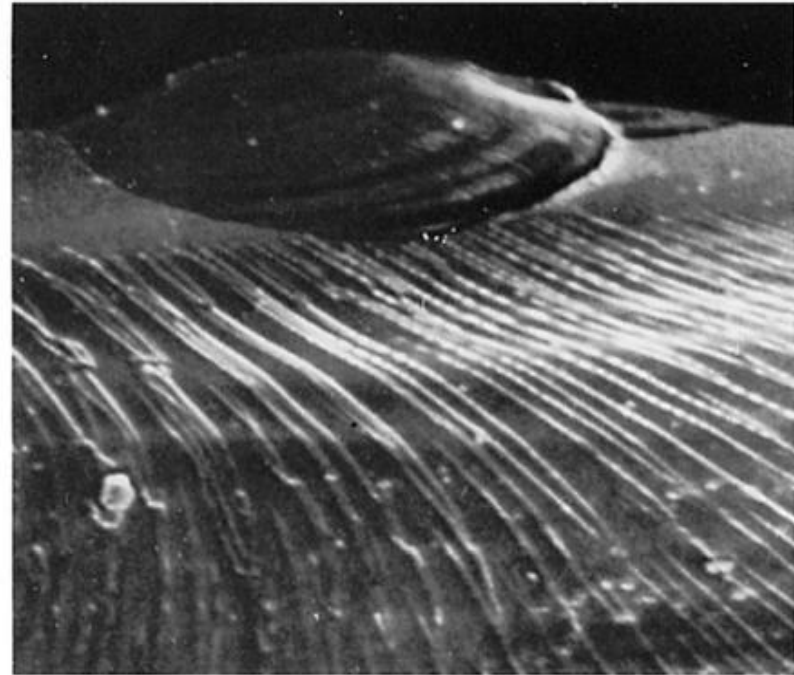
Section 6.13

Microstructural Features of Fracture in Ceramics, Glasses, and Composites

- ❑ **Conchoidal fracture** - Fracture surface containing a very smooth mirror zone near the origin of the fracture, with tear lines comprising the remainder of the surface.
- ❑ **Delamination** - The process by which different layers in a composite will begin to debond.



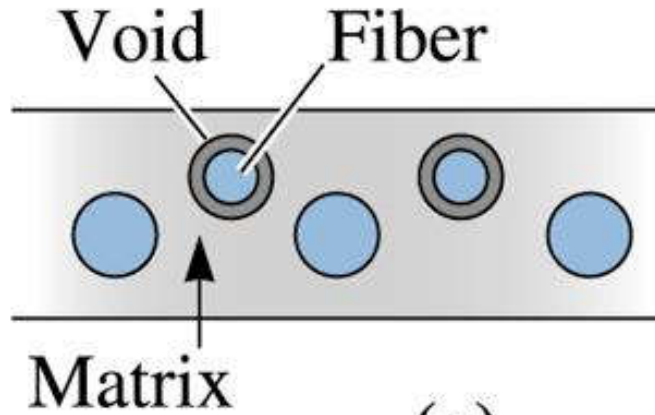
(a)



(b)

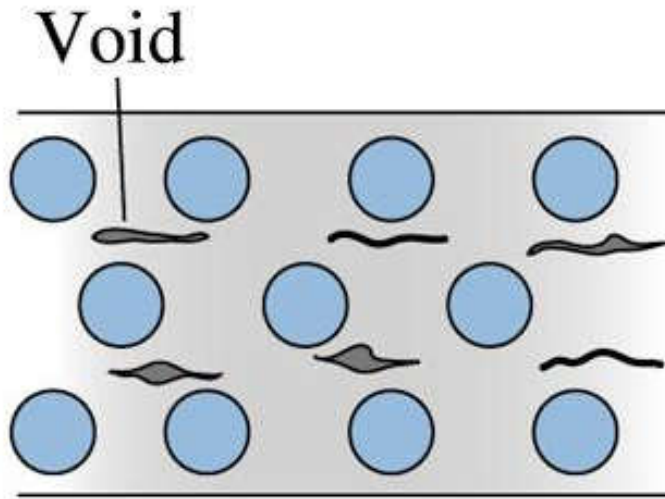
(c)2003 Brooks/Cole, a division of Thomson Learning, Inc. Thomson Learning, Inc. is a trademark used herein under license.

Figure 6.42 Scanning electron micrographs of fracture surfaces in ceramics. (a) The fracture surface Al_2O_3 , showing the cleavage faces (x 1250), and (b) the fracture surface of glass, showing the mirror zone (top) and tear lines characteristic of conchoidal fracture (x 300)

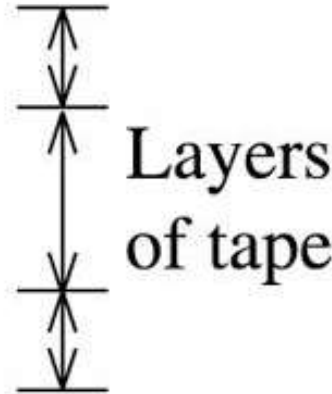


(a)

Figure 6.43 Fiber-reinforced composites can fail by several mechanisms. (a) Due to weak bonding between the matrix and fibers, fibers can pull out of the matrix, creating voids. (b) if the individual layers of the matrix are poorly bonded, the matrix may delaminate, creating voids



(b)





Example 6.13

Fracture in Composites

Describe the difference in fracture mechanism between a boron-reinforced aluminum composite and a glass fiber-reinforced epoxy composite.

Example 6.13 SOLUTION

In the boron-aluminum composite, the aluminum matrix is soft and ductile; thus we expect the matrix to fail in a ductile manner. Boron fibers, in contrast, fail in a brittle manner. Both glass fibers and epoxy are brittle; thus the composite as a whole should display little evidence of ductile fracture.

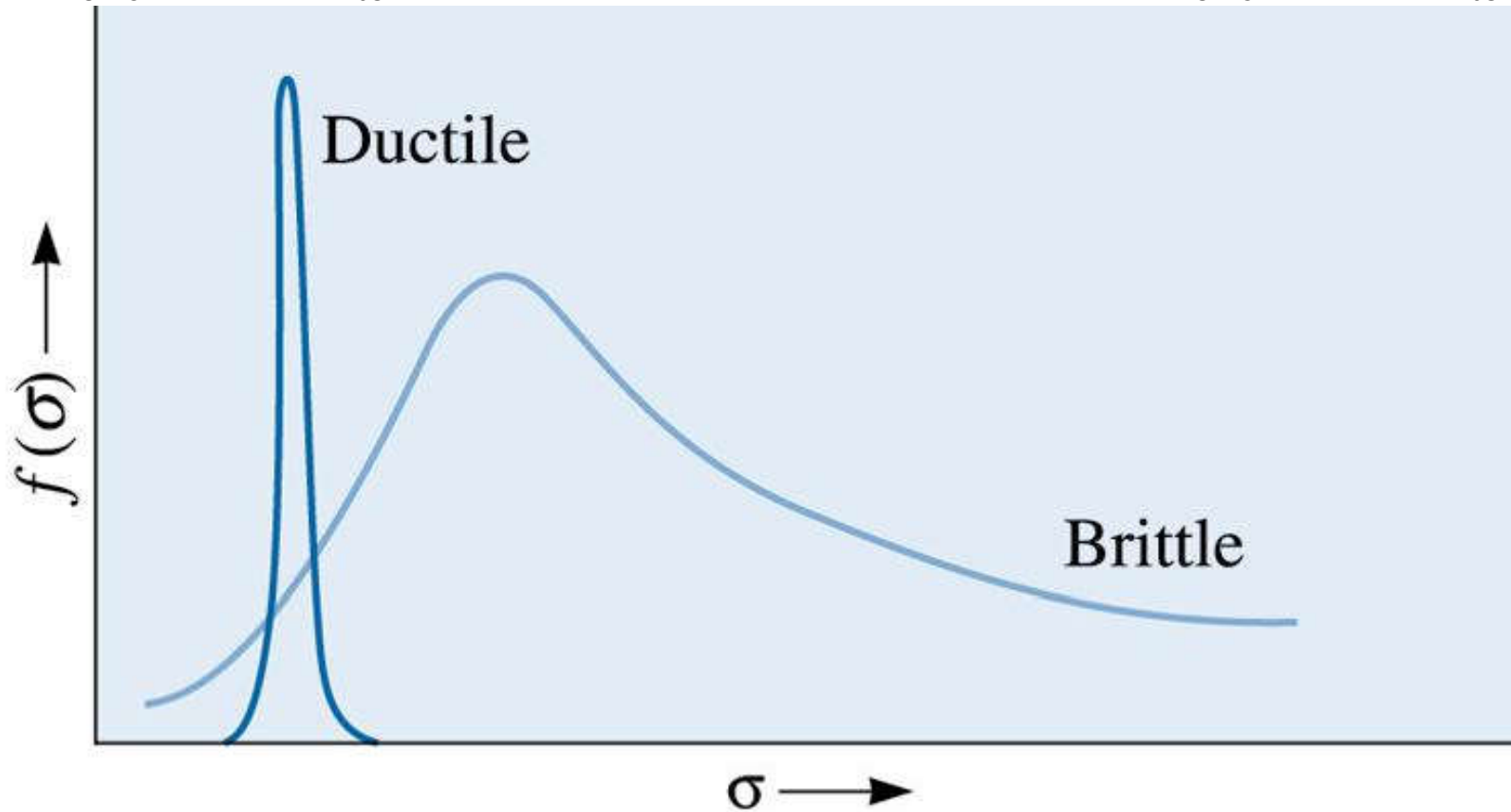


Section 6.14

Weibull Statistics for Failure Strength Analysis

- **Weibull distribution** - A mathematical distribution showing the probability of failure or survival of a material as a function of the stress.





(c)2003 Brooks/Cole, a division of Thomson Learning, Inc. Thomson Learning™ is a trademark used herein under license.

Figure 6.44 The Weibull distribution describes the fraction of the samples that fail at any given applied stress



Example 6.14

Weibull Modulus for Steel and Alumina Ceramics

Figure 6.45 shows the log-log plots of the probability of failure and strength of a 0.2% plain carbon steel, an alumina ceramics prepared using conventional powder processing in which alumina powders are compacted in a press and sintered into a dense mass at high temperature. Also, included is a plot for alumina ceramics prepared using special techniques that leads to much more uniform and controlled particle size. This in turn minimizes the flaws. These samples are labeled as controlled particle size (CPS). Comment on the nature of these graphs.

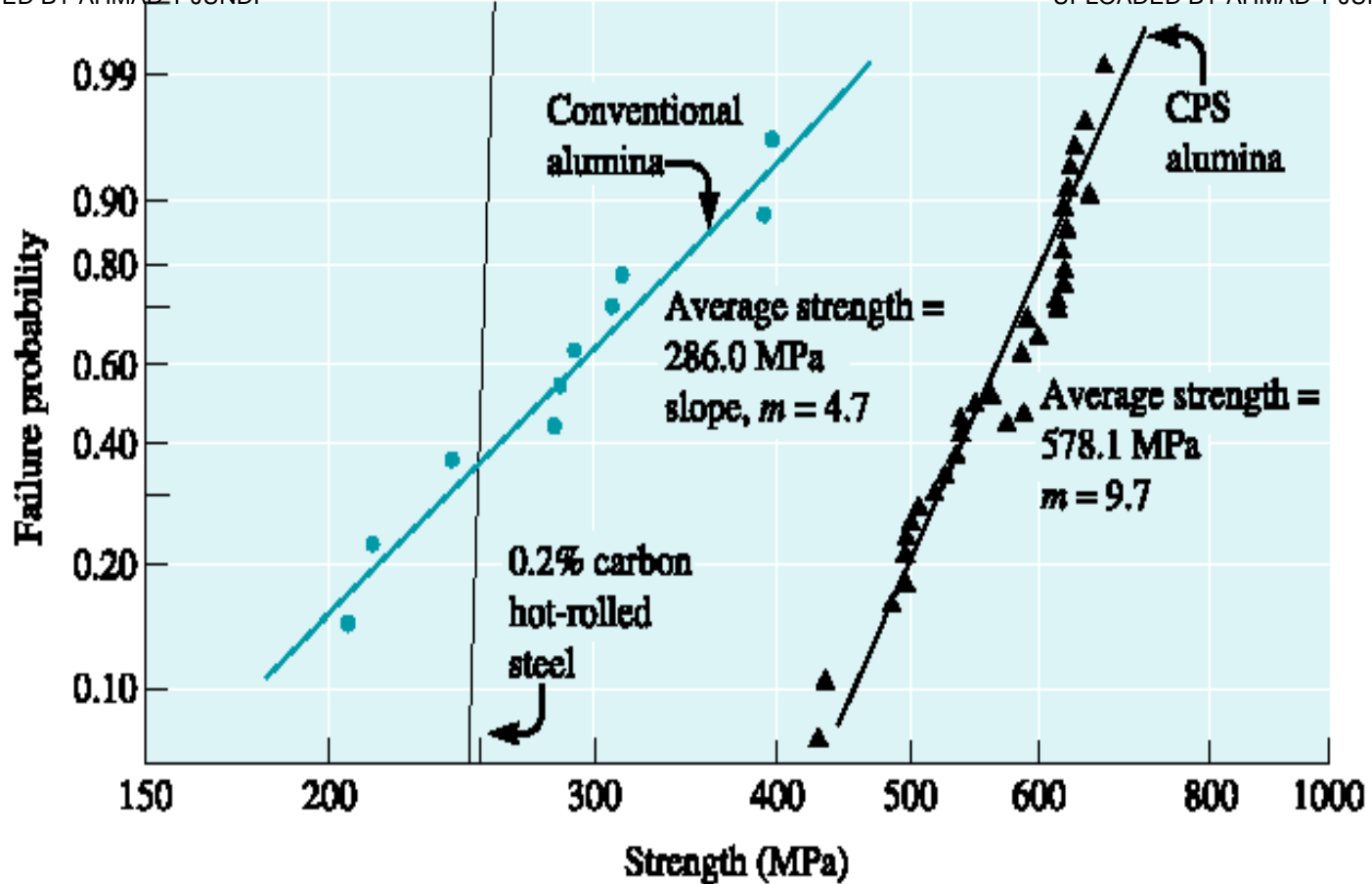
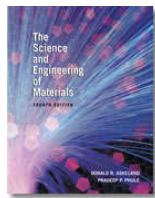


Figure 6-45 A cumulative plot (using special graph paper) of the probability that a sample will fail at any given stress yields the Weibull modulus or slope. Alumina produced by two different methods is compared with low carbon steel. Good reliability in design is obtained for a high Weibull modulus. (Source: From Mechanical Behavior of Materials, by M.A. Meyers and K.K. Chawla, 1999. Copyright © 1999 Prentice-Hall. Used with permission of Pearson Education, Inc., Upper Saddle River, NJ.)





Example 6.14 SOLUTION

For plain carbon steel the line is almost vertical (i.e., slope or m value is essentially approaching large values). This means that there is very little variation (5 to 10%) in the strength of different samples of the 0.2% C steel.

For alumina ceramics prepared using traditional processing, the variability is high (i.e., m is low ~ 4.7).

For ceramics prepared using improved and controlled processing techniques the m is higher ~ 9.7 indicating a more uniform distribution of flaws. The average strength is also higher (~ 578 MPa) suggesting lesser number of flaws that will lead to fracture.





Example 6.15

Strength of Ceramics and Probability of Failure

An advanced engineered ceramic has a Weibull modulus $m = 9$. The flexural strength is 250 MPa at a probability of failure $F = 0.4$. What is the level of flexural strength if the probability of failure has to be 0.1?

Example 6.15 SOLUTION



UPLOADED BY AHMAD T JUNDI

Equation 6.27

$$1 - F(V) = \exp \left[- \left(\frac{\sigma}{\sigma_0} \right)^m \right]$$

Now, we want to determine the value of σ for $F = 0.1$. We know that $m = 9$ and $\sigma_0 = 269.4$ MPa, so we need to get the value of σ . We substitute these values into Equation 6-29:

$$\ln \left[\ln \left(\frac{1}{1 - 0.1} \right) \right] = 9(\ln \sigma - \ln 269.4)$$

$$\ln \left[\ln \left(\frac{1}{0.9} \right) \right] = 9(\ln \sigma - \ln 269.4)$$

$$\ln(\ln 1.11111) = \ln(0.105361) = -2.25037 = 9(\ln \sigma - 5.596097),$$

$$\therefore -0.25004 = \ln \sigma - 5.596097, \quad \text{or}$$

$$\ln \sigma = 5.346056$$

or $\sigma = 209.8$ MPa. As expected, as we lowered the probability of failure to 0.1, we also decreased the level of stress that can be supported.





Example 6.16

Weibull Modulus Parameter Determination

Seven silicon carbide specimens were tested and the following fracture strengths were obtained: 23, 49, 34, 30, 55, 43, and 40 MPa. Estimate the Weibull modulus for the data by fitting the data to Equation 6.29. Discuss the reliability of the ceramic.

Equation 6.29

$$\ln \left[\ln \left(\frac{1}{1 - F(V)} \right) \right] = m(\ln \sigma - \ln \sigma_0)$$



(c) 2003 Brooks/Cole, a division of Thomson Learning, Inc. Thomson Learning is a trademark used herein under license.

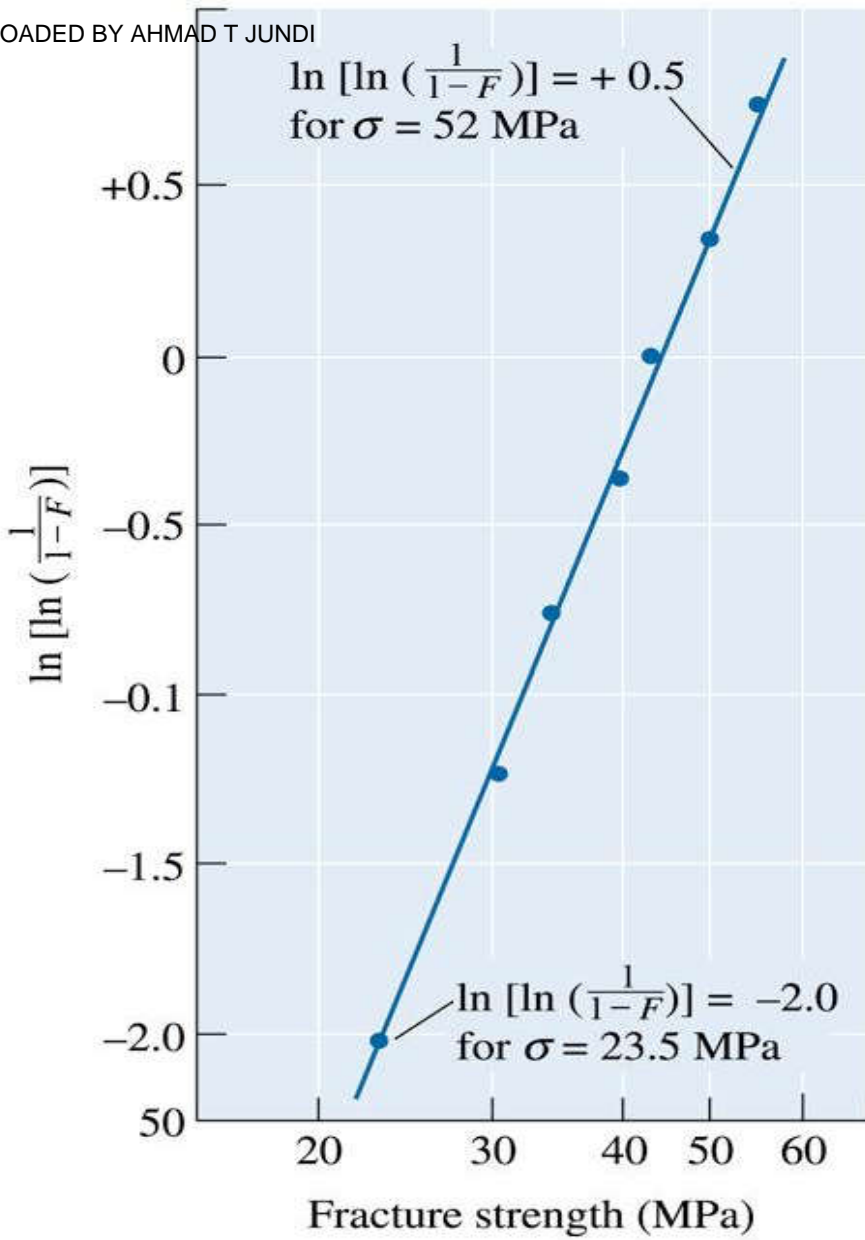


Figure 6.46 Plot of cumulative probability of failure versus fracture stress. Note the fracture strength is plotted on a log scale





Example 6.16 SOLUTION

j^{th} Specimen	σ (MPa)	$F(V_0)$	$\ln\{\ln 1/[1 - F(V_0)]\}$
1	23	$1/8 = 0.125$	-2.013
2	30	$2/8 = 0.250$	-1.246
3	34	$3/8 = 0.375$	-0.755
4	40	$4/8 = 0.500$	-0.367
5	43	$5/8 = 0.625$	-0.019
6	49	$6/8 = 0.750$	+0.327
7	55	$7/8 = 0.875$	+0.732

The slope of the fitted line, or the Weibull modulus m , is (using the two points indicated on the curve):

$$m = \frac{0.5 - (-2.0)}{\ln(52) - \ln(23.5)} = \frac{2.5}{3.951 - 3.157} = 3.15$$

This low Weibull modulus of 3.15 suggests that the ceramic has a highly variable fracture strength, making it difficult to use reliably in high load-bearing applications.





Section 6.15

Fatigue

- ❑ **Fatigue** is the lowering of strength or failure of a material due to repetitive stress which may be above or below the yield strength.
- ❑ **Creep** - A time dependent, permanent deformation at high temperatures, occurring at constant load or constant stress.
- ❑ **Beach or clamshell marks** - Patterns often seen on a component subjected to fatigue.
- ❑ **Rotating cantilever beam test** - An older test for fatigue testing.
- ❑ **S-N curve (also known as the Wöhler curve)** - A graph showing stress as a function of number of cycles in fatigue.

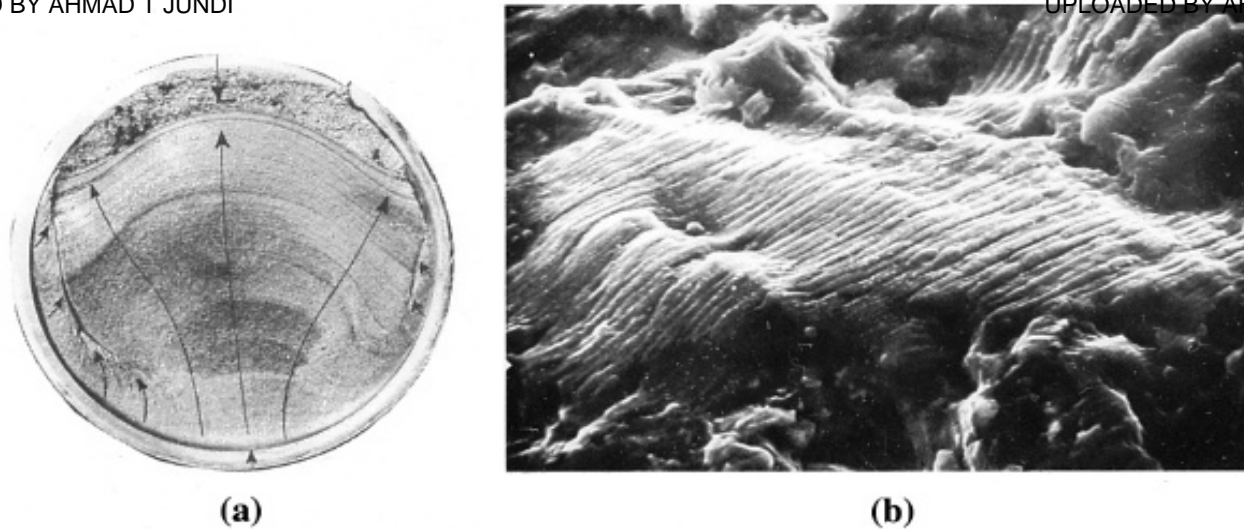


Figure 6.47 Fatigue fracture surface. (a) At low magnifications, the beach mark pattern indicates fatigue as the fracture mechanism. The arrows show the direction of growth of the crack front, whose origin is at the bottom of the photograph. (*Image (a) is from C.C. Cottell, "Fatigue Failures with Special Reference to Fracture Characteristics," Failure Analysis: The British Engine Technical Reports, American Society for Metals, 1981, p. 318.*) (b) At very high magnifications, closely spaced striations formed during fatigue are observed (x 1000)

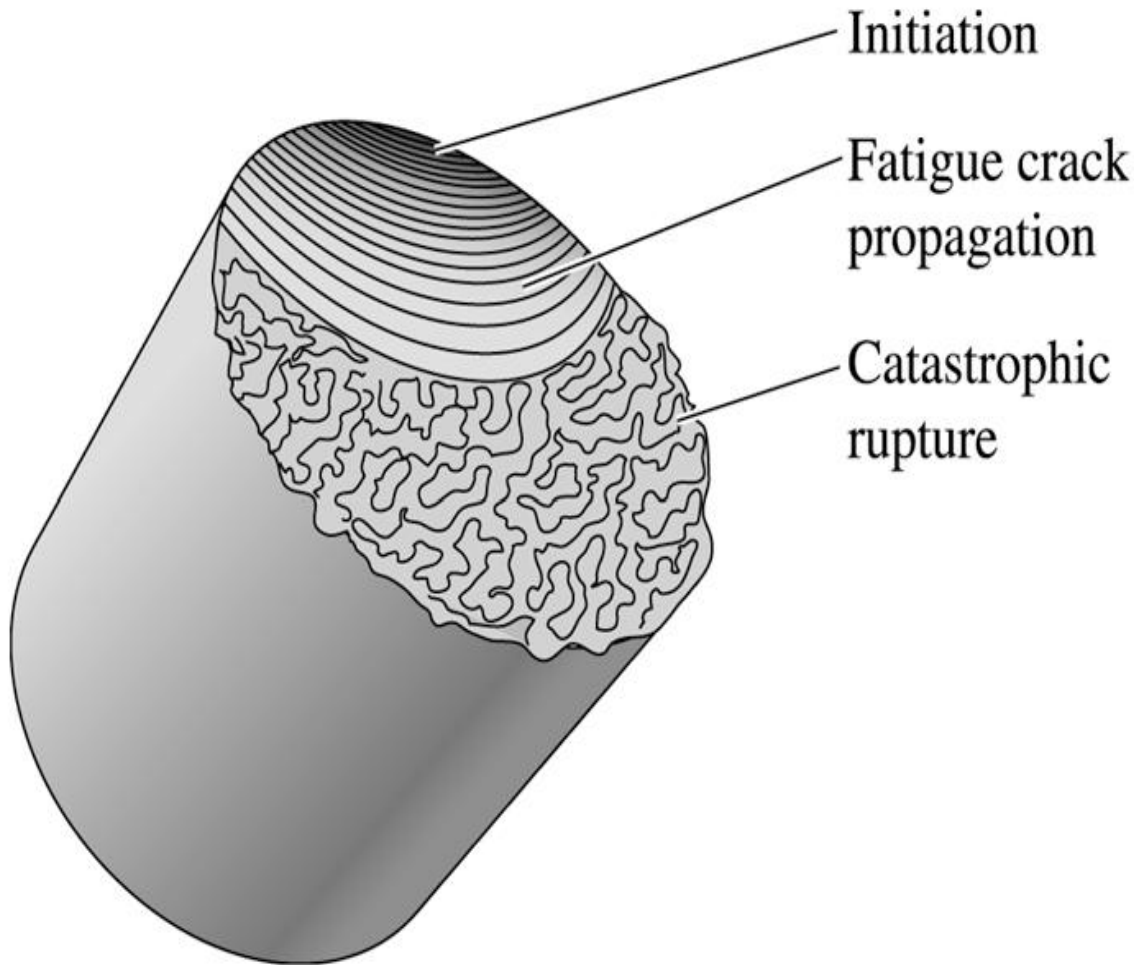


Figure 6.48
Schematic representation of a fatigue fracture surface in a steel shaft, showing the initiation region, the propagation of fatigue crack (with beam markings), and catastrophic rupture when the crack length exceeds a critical value at the applied stress

(c)2003 Brooks/Cole, a division of Thomson Learning, Inc. Thomson Learning[™] is a trademark used herein under license.



Example 6.17

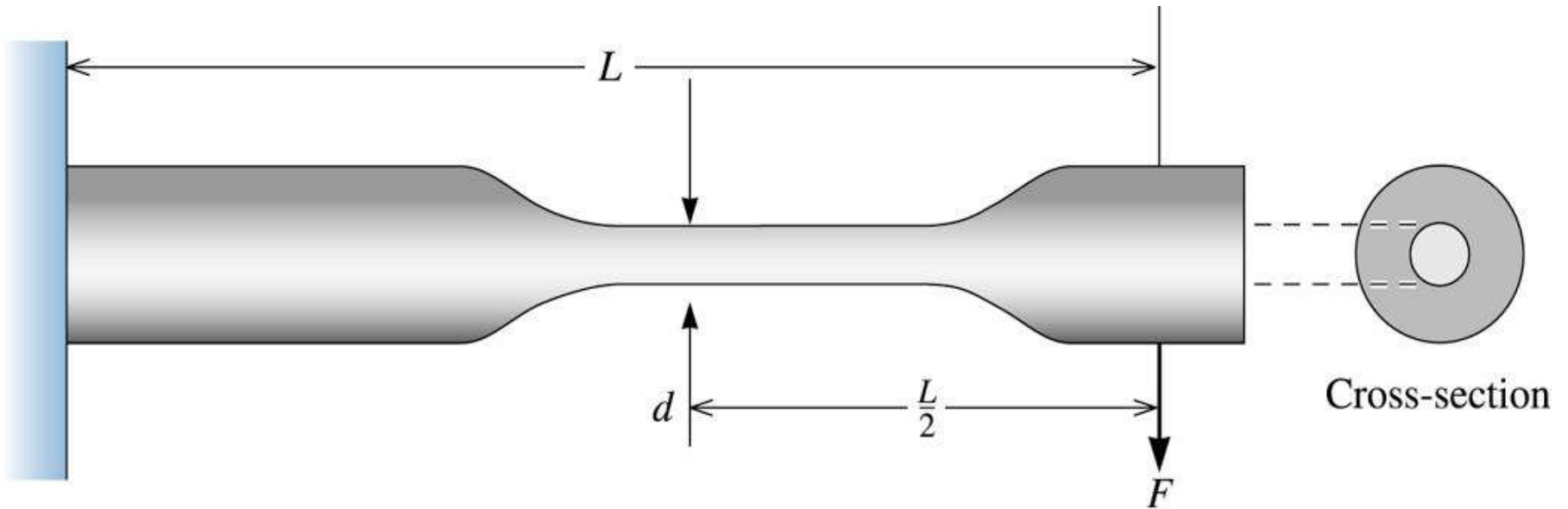
Fatigue Failure Analysis of a Crankshaft

A crankshaft in a diesel engine fails. Examination of the crankshaft reveals no plastic deformation. The fracture surface is smooth. In addition, several other cracks appear at other locations in the crankshaft. What type of failure mechanism would you expect?

Example 6.17 SOLUTION

Since the crankshaft is a rotating part, the surface experiences cyclical loading. We should immediately suspect fatigue. The absence of plastic deformation supports our suspicion. Furthermore, the presence of other cracks is consistent with fatigue; the other cracks didn't have time to grow to the size that produced catastrophic failure. Examination of the fracture surface will probably reveal beach marks or fatigue striations.

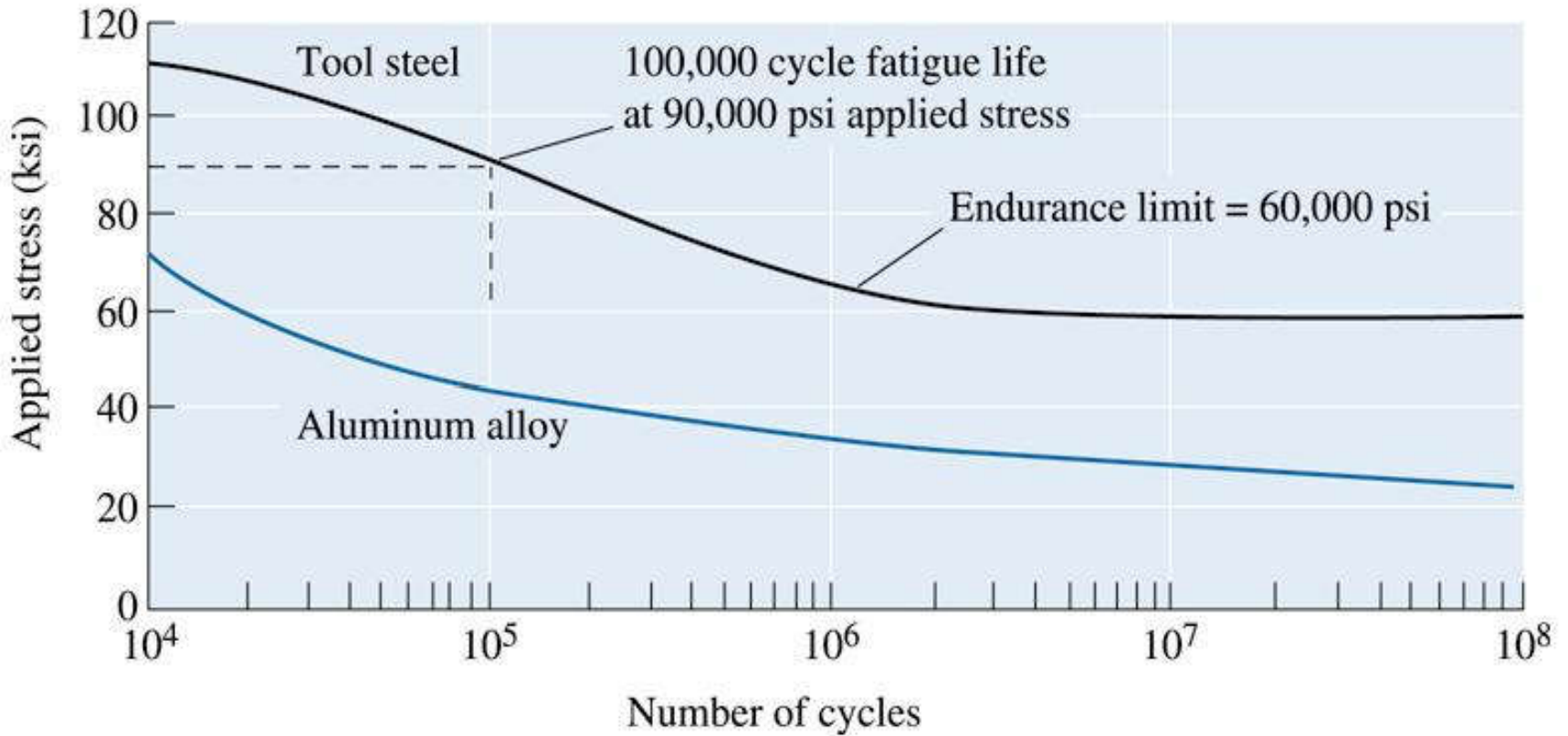




(c)2003 Brooks/Cole, a division of Thomson Learning, Inc. Thomson Learning, is a trademark used herein under license.

Figure 6.49 Geometry for the rotating cantilever beam specimen setup





(c)2003 Brooks/Cole, a division of Thomson Learning, Inc. Thomson Learning,™ is a trademark used herein under license.

Figure 6.50 The stress-number of cycles to failure (S-N) curves for a tool steel and an aluminum alloy





Section 6.16

Results of the Fatigue Test

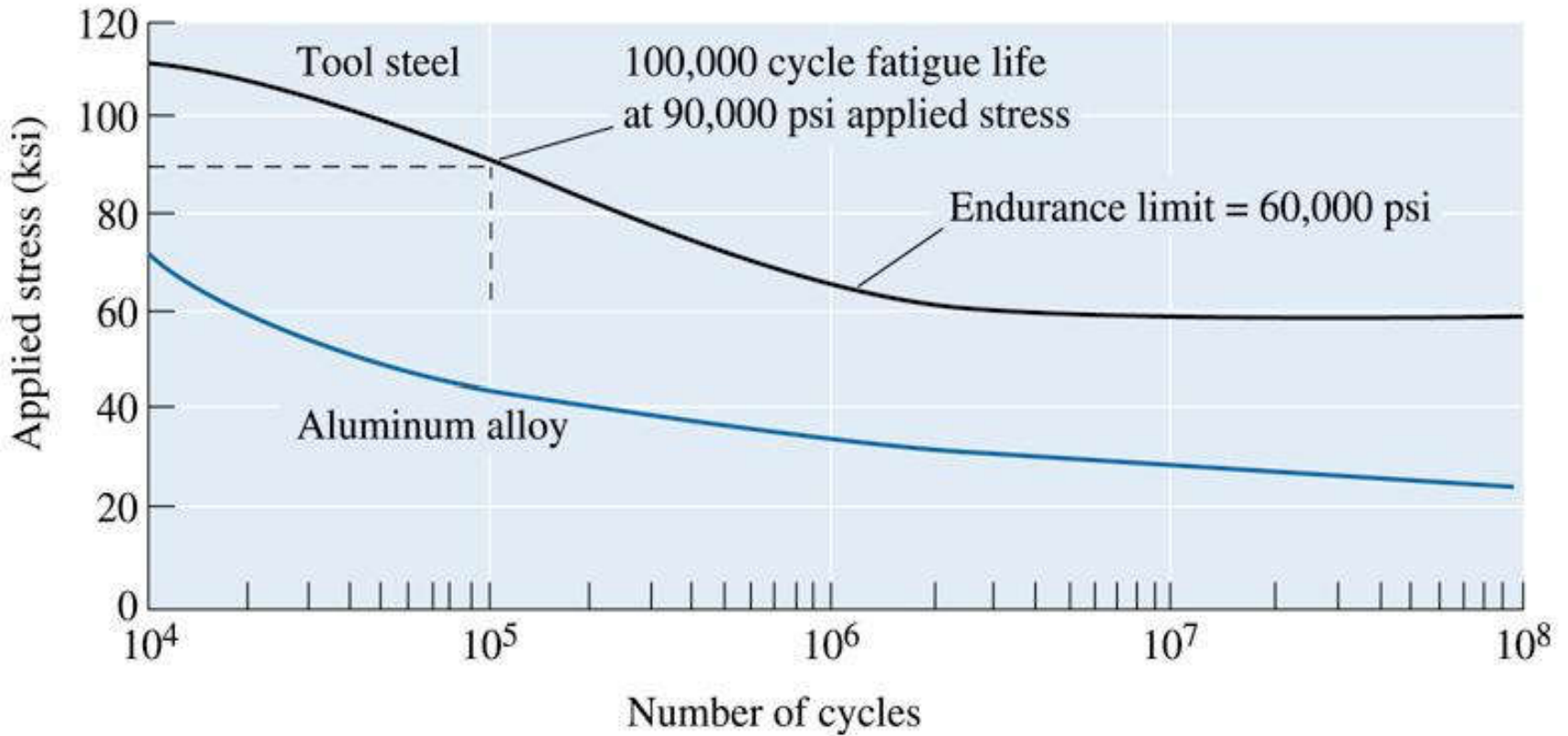
- **Endurance limit** - An older concept that defined a stress below which a material will not fail in a fatigue test.
- **Fatigue life** - The number of cycles permitted at a particular stress before a material fails by fatigue.
- **Fatigue strength** - The stress required to cause failure by fatigue in a given number of cycles, such as 500 million cycles.
- **Notch sensitivity** - Measures the effect of a notch, scratch, or other imperfection on a material's properties, such as toughness or fatigue life.
- **Shot peening** - A process in which metal spheres are shot at a component.



Example 6.18

Design of a Rotating Shaft

A solid shaft for a cement kiln produced from the tool steel in Figure 6.50 must be 96 in. long and must survive continuous operation for one year with an applied load of 12,500 lb. The shaft makes one revolution per minute during operation. Design a shaft that will satisfy these requirements.



(c)2003 Brooks/Cole, a division of Thomson Learning, Inc. Thomson Learning,™ is a trademark used herein under license.

Figure 6.50 The stress-number of cycles to failure (S-N) curves for a tool steel and an aluminum alloy



Example 6-18 SOLUTION



From Figure 6-50, the applied stress therefore must be less than about 72,000 psi. If Equation 6-31 is appropriate, then the diameter of the shaft must be:

$$\pm\sigma = \frac{16FL}{\pi d^3} = 5.09 \frac{FL}{d^3}$$

$$72,000 \text{ psi} = \frac{(5.09)(96 \text{ in.})(12,500 \text{ lb})}{d^3}$$

$$d = 4.39 \text{ in.}$$

Let us assume the factor of safety to be 2 (i.e., we will assume that the maximum allowed stress level will be $72,000/2 = 36,000$ psi). The minimum diameter required to prevent failure would now be:

$$36,000 \text{ psi} = \frac{(5.09)(96 \text{ in.})(12,500 \text{ lb})}{d^3}$$

$$d = 5.53 \text{ in.}$$





Application of Fatigue Testing

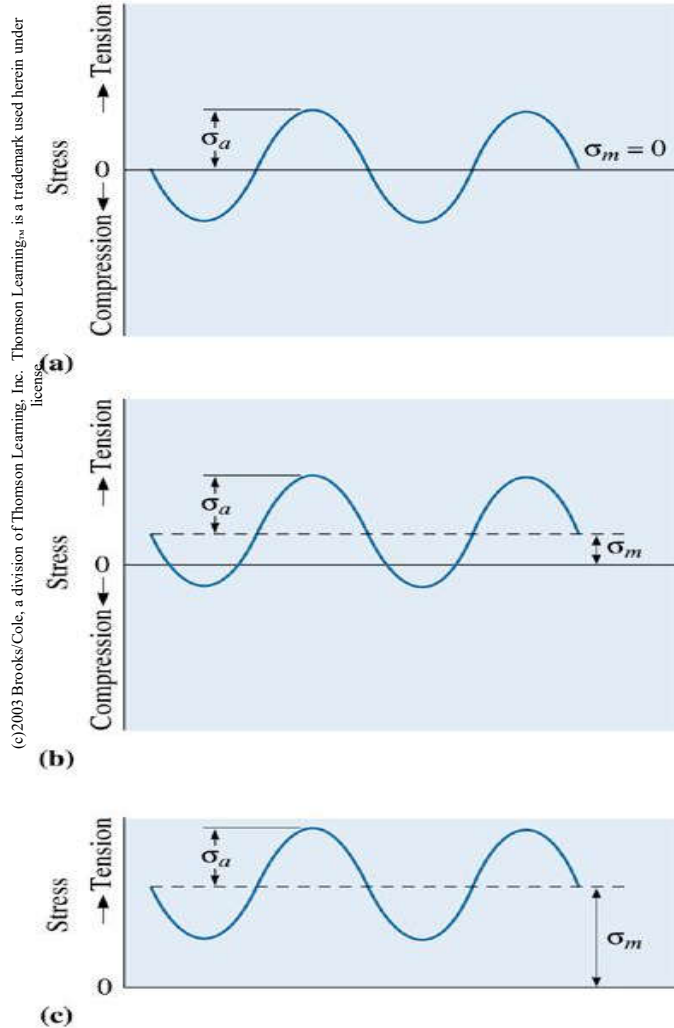


Figure 6.51 Examples of stress cycles. (a) Equal stress in tension and compression, (b) greater tensile stress than compressive stress, and (c) all of the stress is tensile

(c) 2003 Brooks/Cole, a division of Thomson Learning, Inc. Thomson Learning, Inc. is a trademark used herein under license.

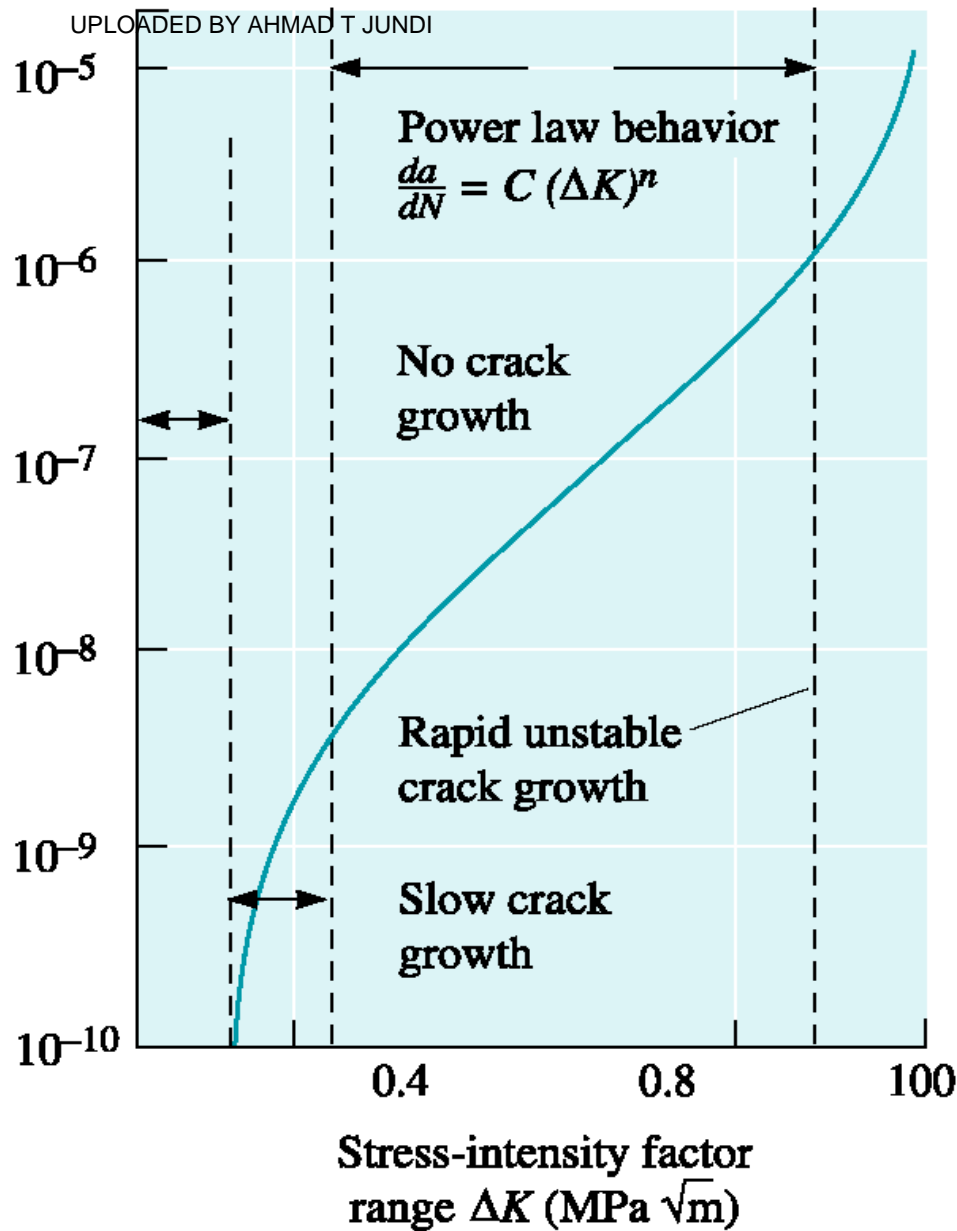


Figure 6.52 Crack growth rate versus stress-intensity factor range for a high-strength steel. For this steel, $C = 1.62 \times 10^{12}$ and $n = 3.2$ for the units shown





Example 6.19

Design of a Fatigue-Resistant Plate

A high-strength steel plate (Figure 6.52), which has a plane strain fracture toughness of $80 \text{ MPa} \sqrt{m}$, is alternately loaded in tension to 500 MPa and in compression to 60 MPa. The plate is to survive for 10 years, with the stress being applied at a frequency of once every 5 minutes. Design a manufacturing and testing procedure that assures that the component will serve as intended.

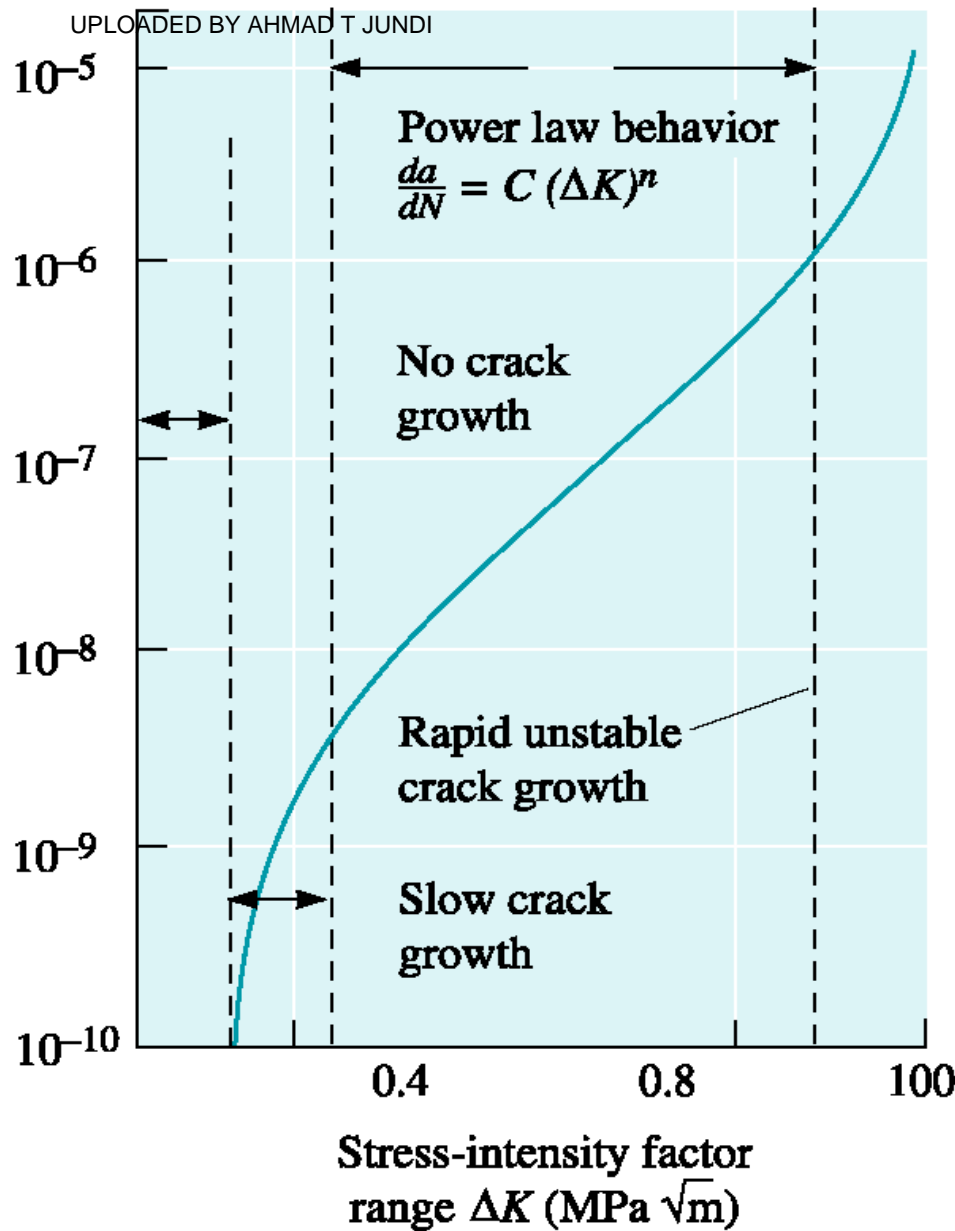


Figure 6.52 Crack growth rate versus stress-intensity factor range for a high-strength steel. For this steel, $C = 1.62 \times 10^{12}$ and $n = 3.2$ for the units shown





The critical crack size (a_c), using the fracture toughness and the maximum stress, is:

$$K_{Ic} = f\sigma\sqrt{\pi a_c}$$

$$80 \text{ MPa}\sqrt{\text{m}} = (1)(500 \text{ MPa})\sqrt{\pi a_c}$$

$$a_c = 0.0081 \text{ m} = 8.1 \text{ mm}$$

We need to determine the minimum number of cycles that the plate must withstand:

$$a_i = 1.82 \times 10^{-6} \text{ m} = 0.00182 \text{ mm for surface flaws}$$

$$2a_i = 0.00364 \text{ mm for internal flaws}$$

The manufacturing process must produce surface flaws smaller than 0.00182 mm in length. We can conduct a similar calculation for specifying a limit on edge cracks. In addition, nondestructive tests must be available to assure that cracks exceeding this length are not present.

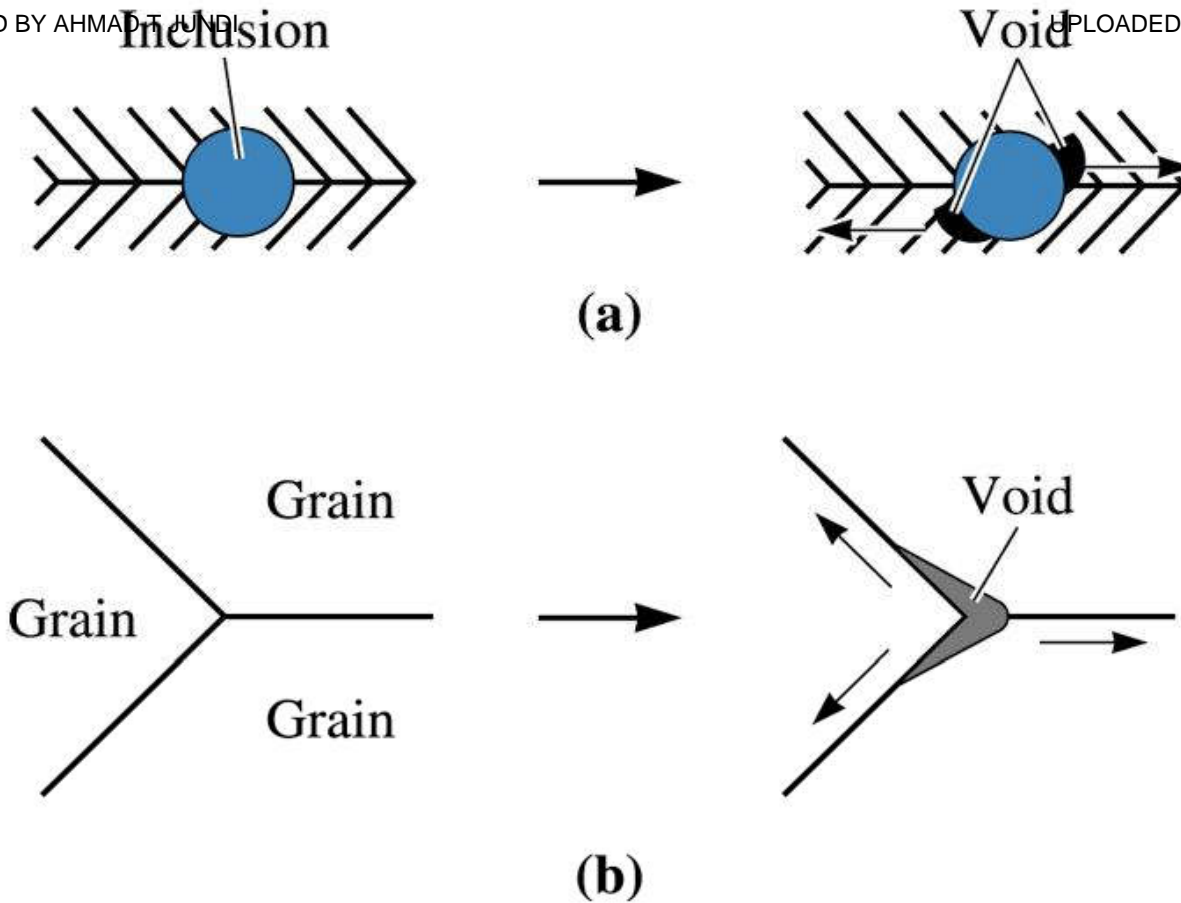




Section 6.18

Creep, Stress Rupture, and Stress Corrosion

- **Stress-rupture curve** - A method of reporting the results of a series of creep tests by plotting the applied stress versus the rupture time.
- **Stress-corrosion** - A phenomenon in which materials react with corrosive chemicals in the environment leading to the formation of cracks and lowering of strength.



(c)2003 Brooks/Cole, a division of Thomson Learning, Inc. Thomson Learning,™ is a trademark used herein under license.

Figure 6.53 Grain boundary sliding during creep causes (a) the creation of voids at an inclusion trapped at the grain boundary, and (b) the creation of a void at a triple point where three grains are in contact

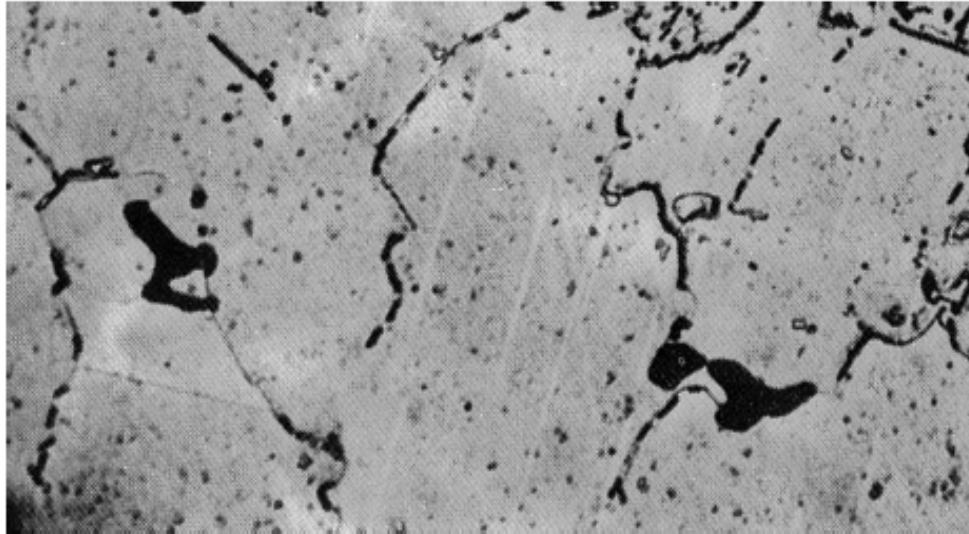


Figure 6.54 Creep cavities formed at grain boundaries in an austenitic stainless steel (x 500). (From ASM Handbook, Vol. 7, (1972) ASM International, Materials Park, OH 44073.)

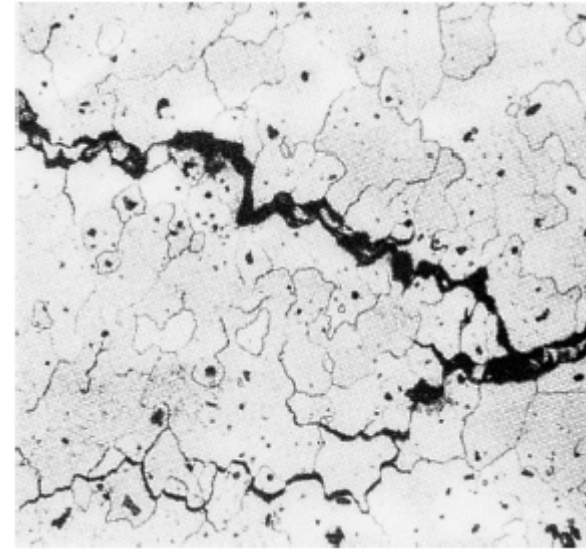


Figure 6.55 Photomicrograph of a metal near a stress-corrosion fracture, showing the many intergranular cracks formed as a result of the corrosion process (x 200). (From ASM Handbook, Vol. 7, (1972) ASM International, Materials Park, OH 44073.)



Example 6.20

Failure Analysis of a Pipe

A titanium pipe used to transport a corrosive material at 400°C is found to fail after several months. How would you determine the cause for the failure?

Example 6.20 SOLUTION

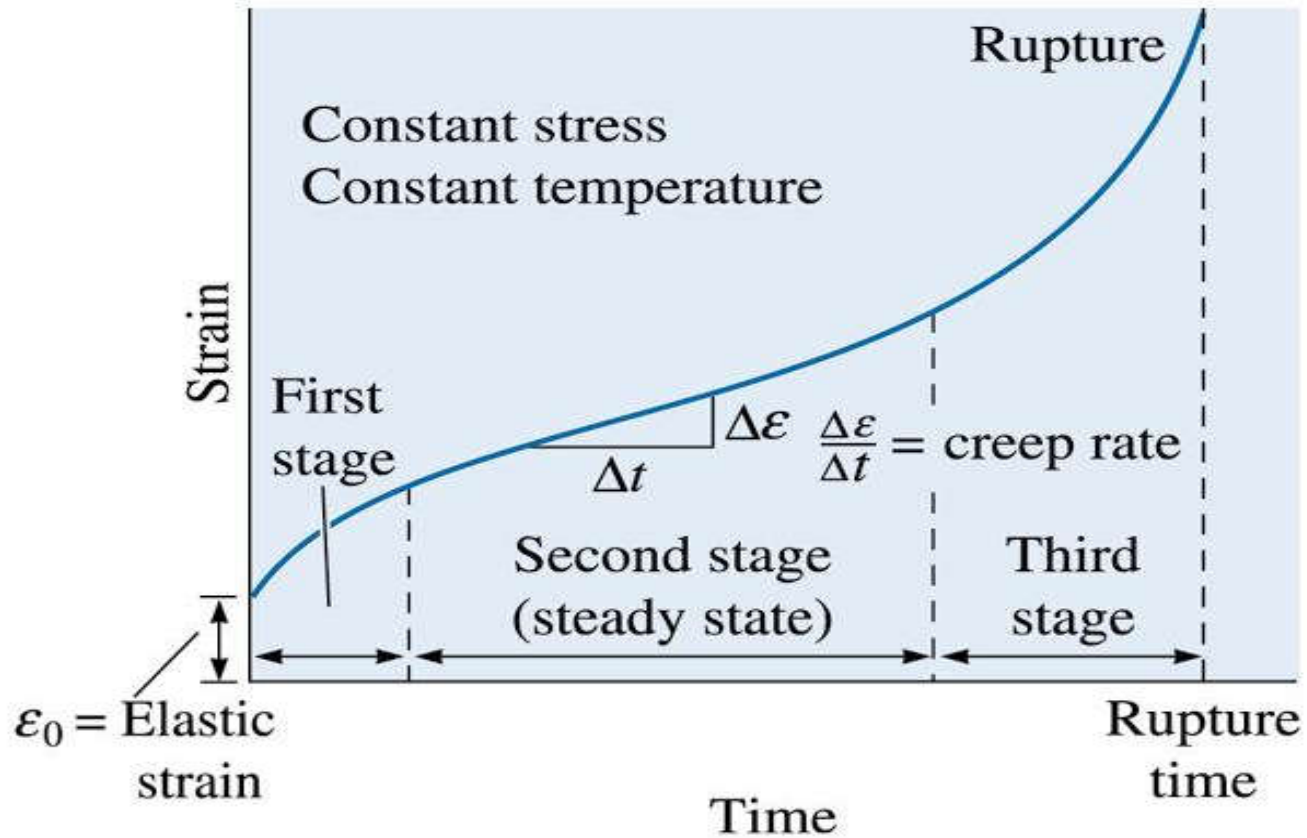
Since a period of time at a high temperature was required before failure occurred, we might first suspect a creep or stress-corrosion mechanism for failure. Microscopic examination of the material near the fracture surface would be advisable. If many tiny, branched cracks leading away from the surface are noted, stress-corrosion is a strong possibility. However, if the grains near the fracture surface are elongated, with many voids between the grains, creep is a more likely culprit.



Section 6.19

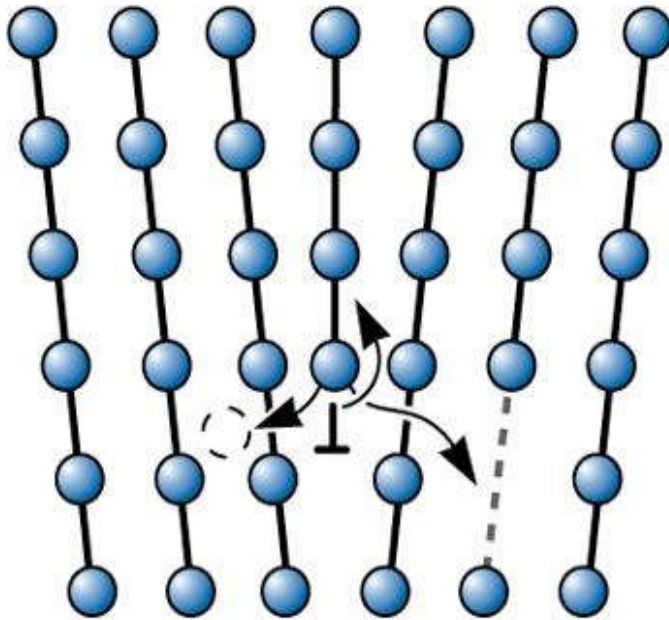
Evaluation of Creep Behavior

- **Creep test** - Measures the resistance of a material to deformation and failure when subjected to a static load below the yield strength at an elevated temperature.
- **Climb** - Movement of a dislocation perpendicular to its slip plane by the diffusion of atoms to or from the dislocation line.
- **Creep rate** - The rate at which a material deforms when a stress is applied at a high temperature.
- **Rupture time** - The time required for a specimen to fail by creep at a particular temperature and stress.

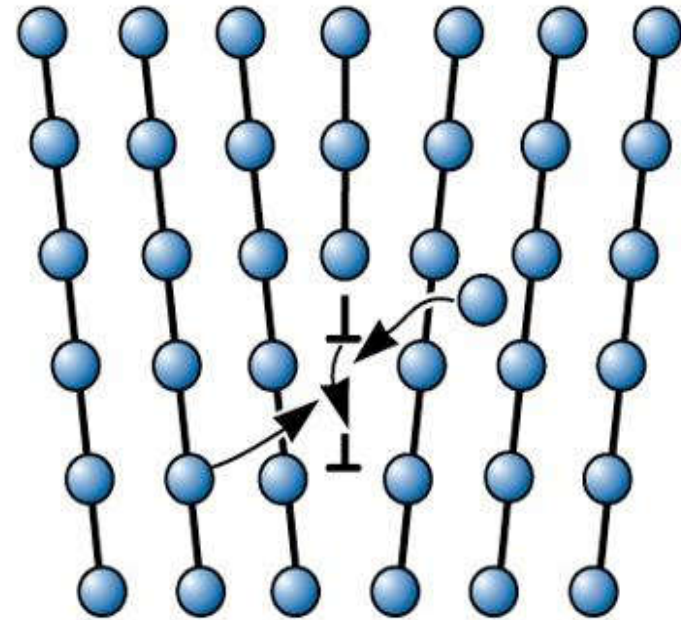


(c)2003 Brooks/Cole, a division of Thomson Learning, Inc. Thomson Learning,™ is a trademark used herein under license.

Figure 6.56 A typical creep curve showing the strain produced as a function of time for a constant stress and temperature



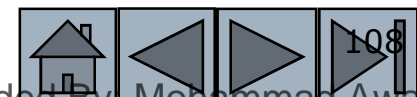
(a)

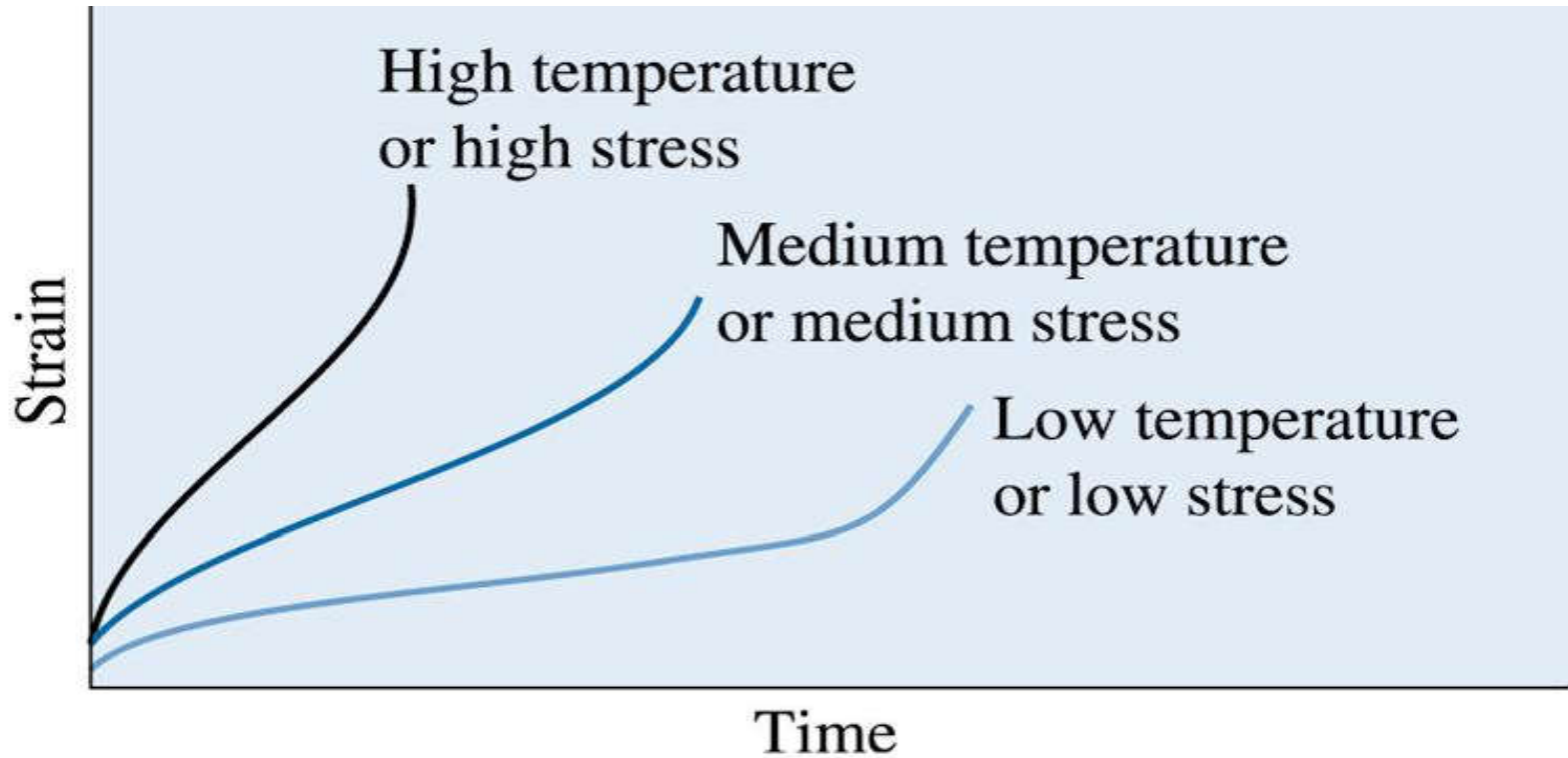


(b)

(c)2003 Brooks/Cole, a division of Thomson Learning, Inc. Thomson Learning[™] is a trademark used herein under license.

Figure 6.57 Dislocations can climb (a) when atoms leave the dislocation line to create interstitials or to fill vacancies or (b) when atoms are attached to the dislocation line by creating vacancies or eliminating interstitials





(c)2003 Brooks/Cole, a division of Thomson Learning, Inc. Thomson LearningTM is a trademark used herein under license.

Figure 6.58 The effect of temperature or applied stress on the creep curve



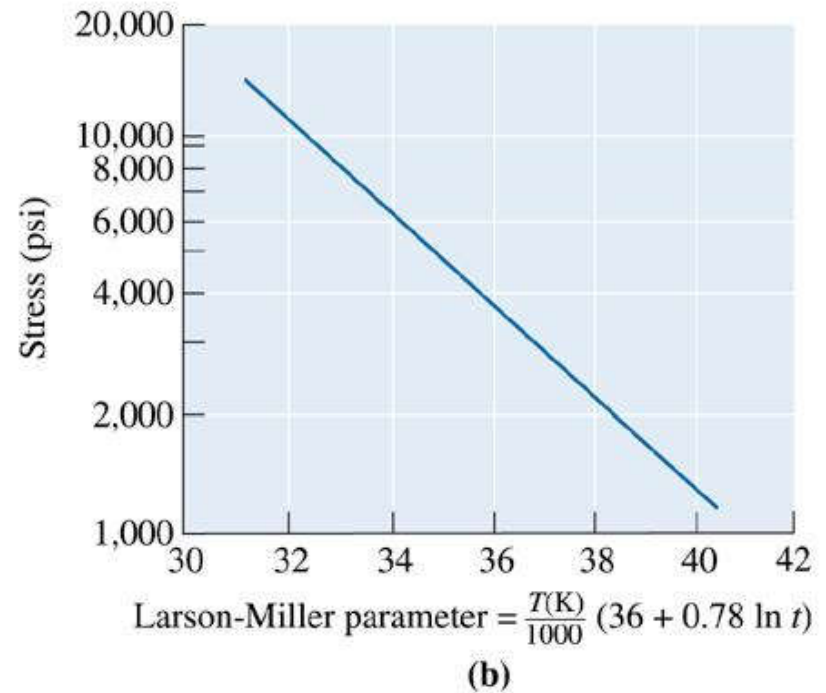
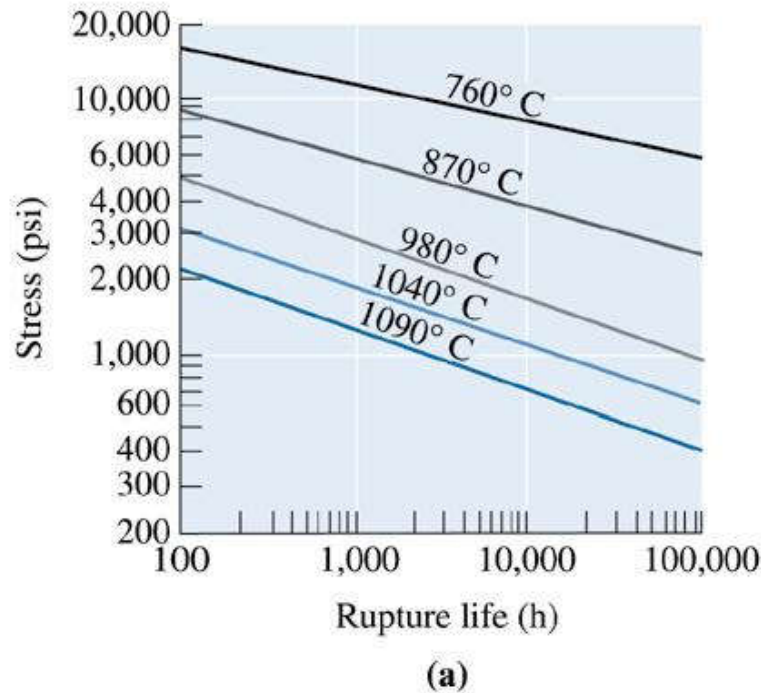


Section 6.20

Use of Creep Data

- **Stress-rupture curve** - A method of reporting the results of a series of creep tests by plotting the applied stress versus the rupture time.
- **Larson-Miller parameter** - A parameter used to relate the stress, temperature, and rupture time in creep.





(c)2003 Brooks/Cole, a division of Thomson Learning, Inc. Thomson Learning[®] is a trademark used herein under license.

Figure 6.59 Results from a series of creep tests. (a) Stress-rupture curves for an iron-chromium-nickel alloy and (b) the Larson-Miller parameter for ductile cast iron





Example 6.21

Design of Links for a Chain

Design a ductile cast iron chain (Figure 6.60) to operate in a furnace used to fire ceramic bricks. The furnace is to operate without rupturing for five years at 600°C, with an applied load of 5000 lbs.

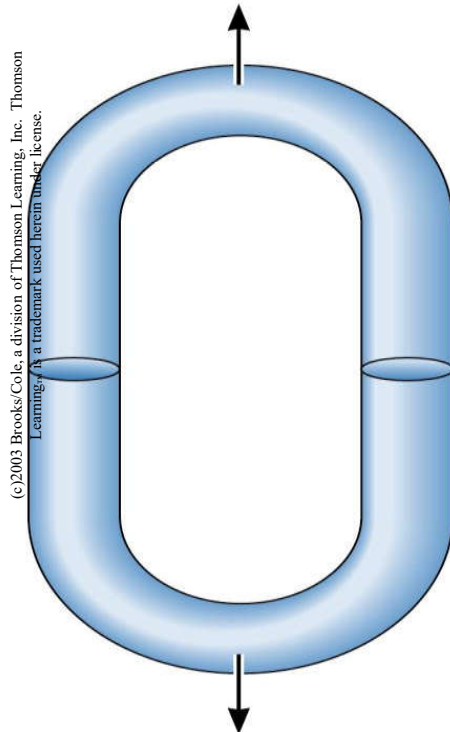


Figure 6.60 Sketch of chain link (for Example 6.21)





The Larson-Miller parameter for ductile cast iron is:

$$L.M. = \frac{T(36 + 0.78 \ln t)}{1000}$$

Let us assume a **factor of safety** of 2, this will mean the applied stress should not be more than $2000/2 = 1000$ psi.

The total cross-sectional area of the chain required to support the 5000 lb load is:

$$A = F/\sigma = \frac{5000 \text{ lb}}{1000 \text{ psi}} = 5 \text{ in.}^2$$

The cross-sectional area of each “half” of the iron link is then 2.5 in.^2 and, assuming a round cross-section:

$$d^2 = (4/\pi)A = (4/\pi)(2.5) = 3.18$$

$$d = 1.78 \text{ in.}$$



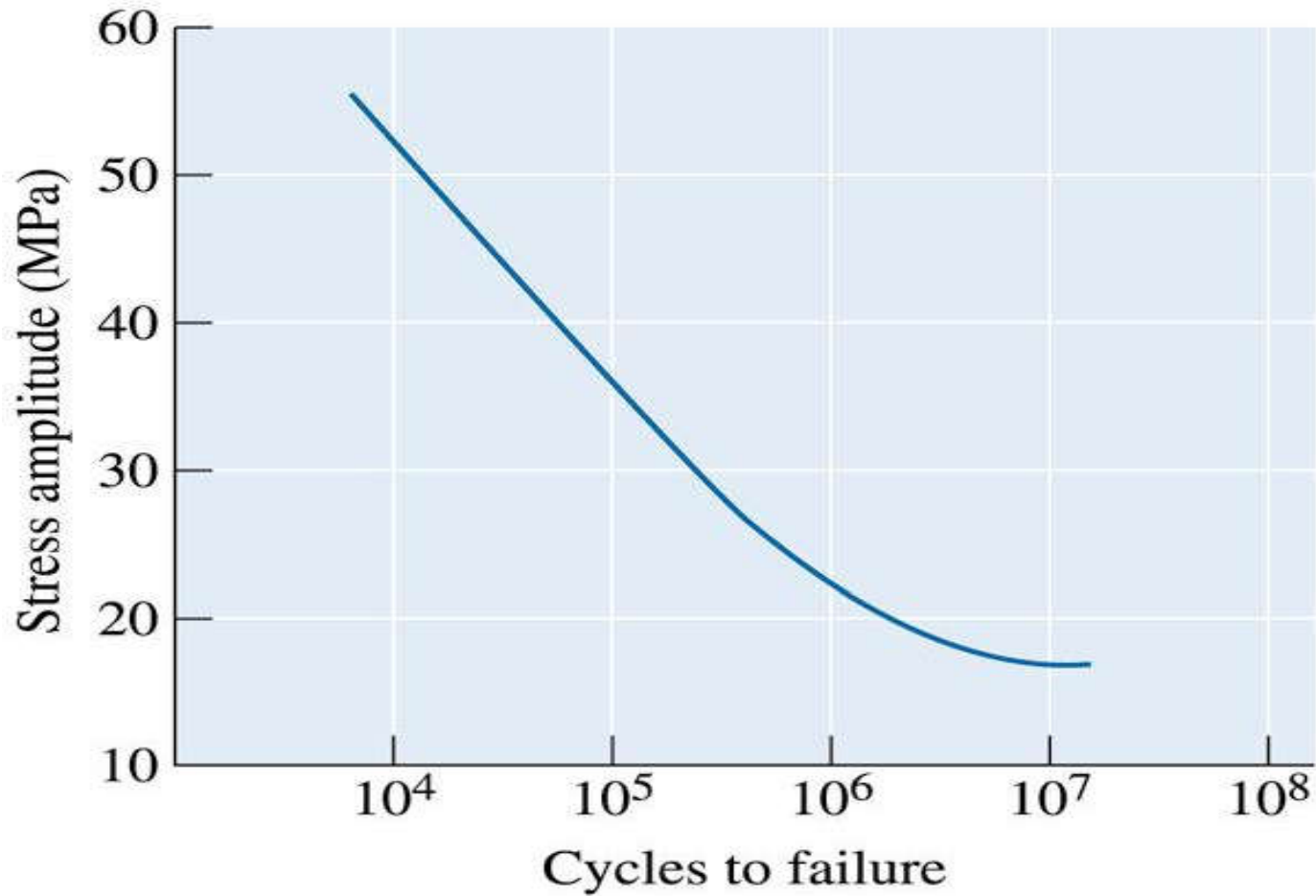


Section 6.21

Superplasticity

- **Superplasticity** - Large deformations in materials, resulting from high temperatures and low strain rates.





(c)2003 Brooks/Cole, a division of Thomson Learning, Inc. Thomson Learning[®] is a trademark used herein under license.

Figure 6.61 The S-N fatigue curve for an acetal polymer (for Problems 6.87, 6.89, and 6.90)





(c)2003 Brooks/Cole, a division of Thomson Learning, Inc. Thomson Learning, Inc. is a trademark used herein under license.

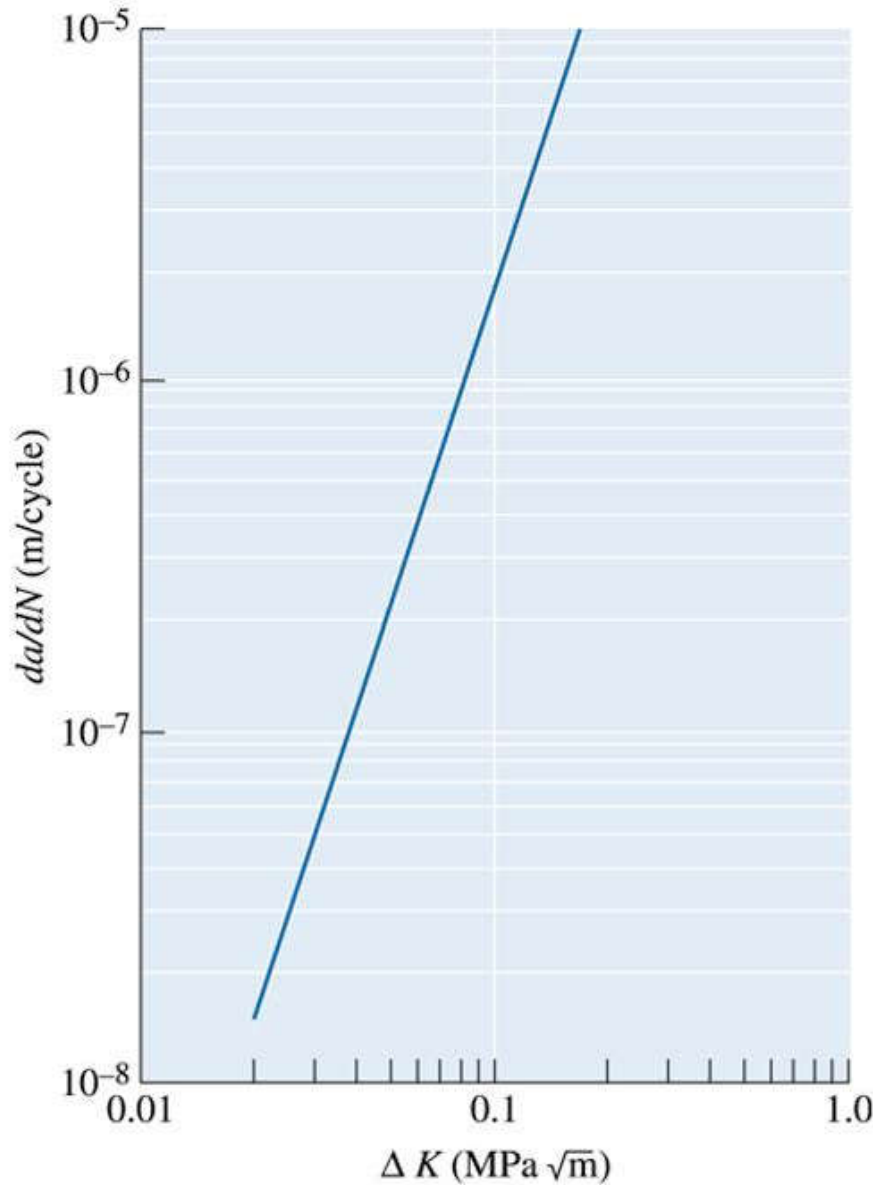


Figure 6.62 The crack growth rate for an acrylic polymer (for Problems 6.93, 6.94, 6.95)





(c) 2003 Brooks/Cole, a division of Thomson Learning, Inc. Thomson Learning, Inc. is a trademark used herein under license.

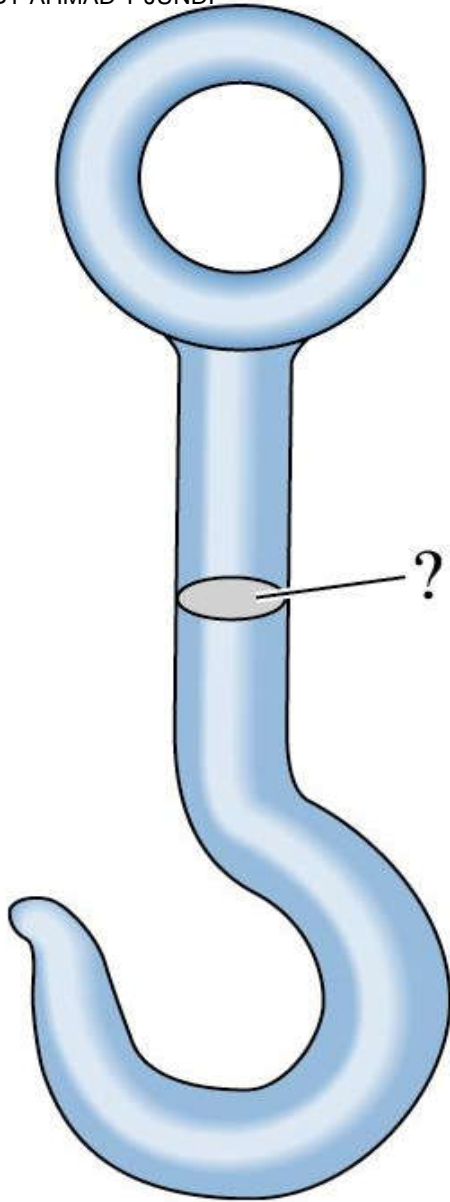
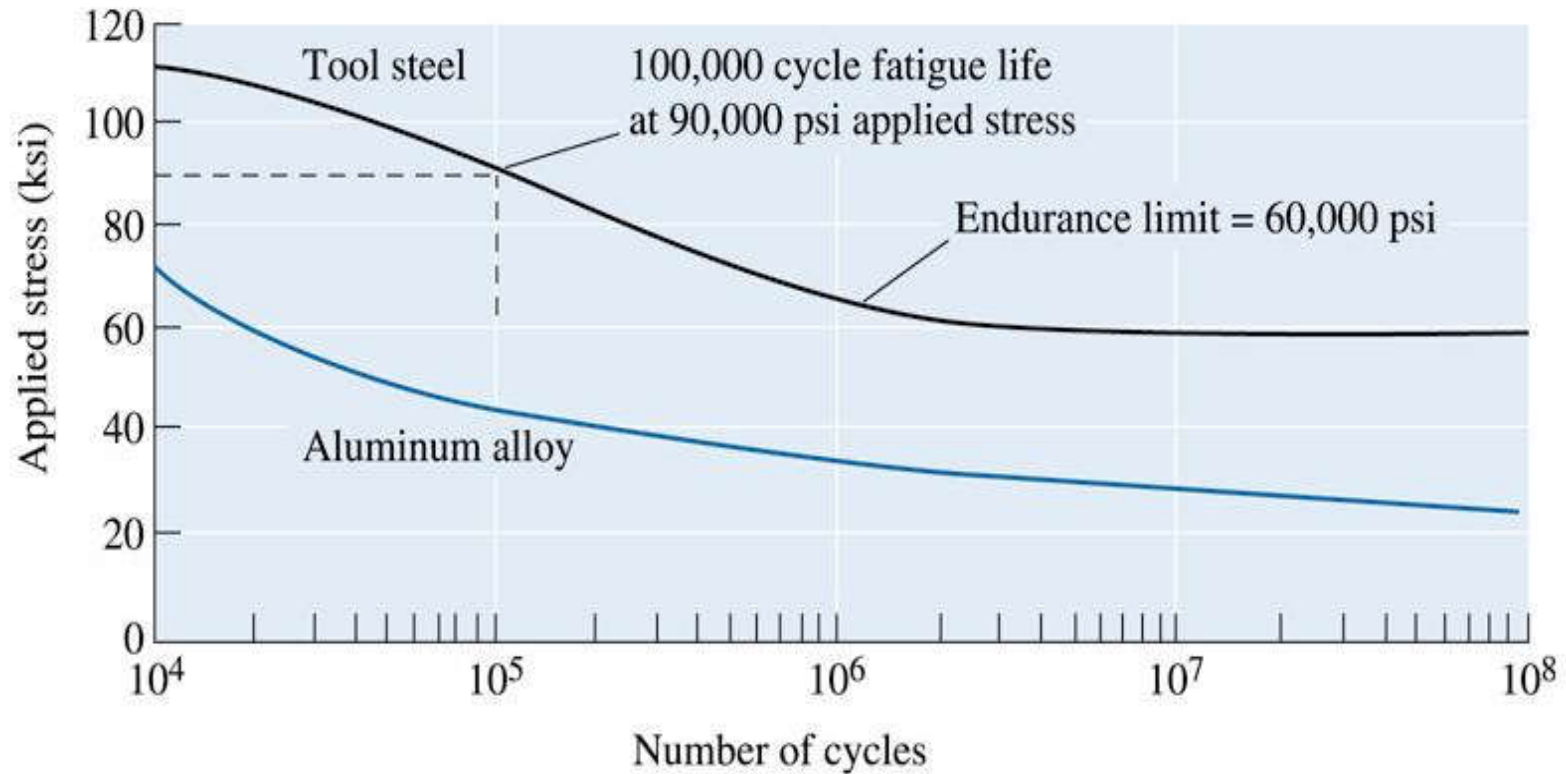


Figure 6.63 Hook (For Problem 6.113)





(c)2003 Brooks/Cole, a division of Thomson Learning, Inc. Thomson LearningSM is a trademark used herein under license.

Figure 6.50 (Repeated for Problems 6.86, and 6.88) The stress-number of cycles to failure (S-N) curves for a tool steel and an aluminum alloy



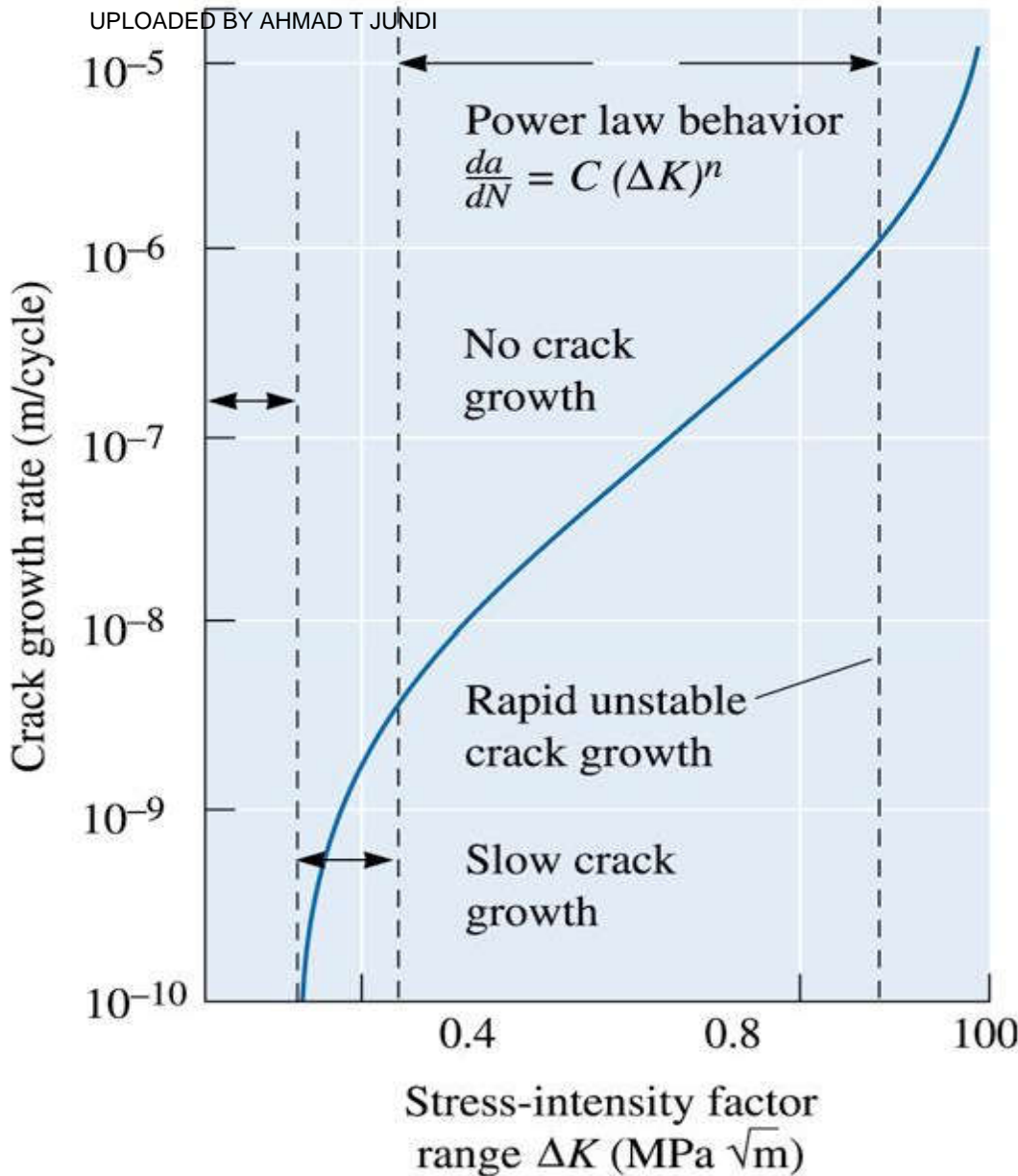
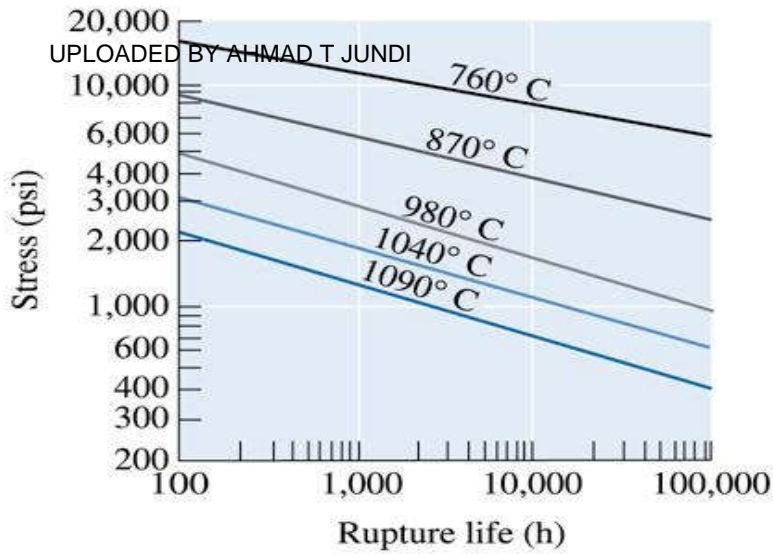
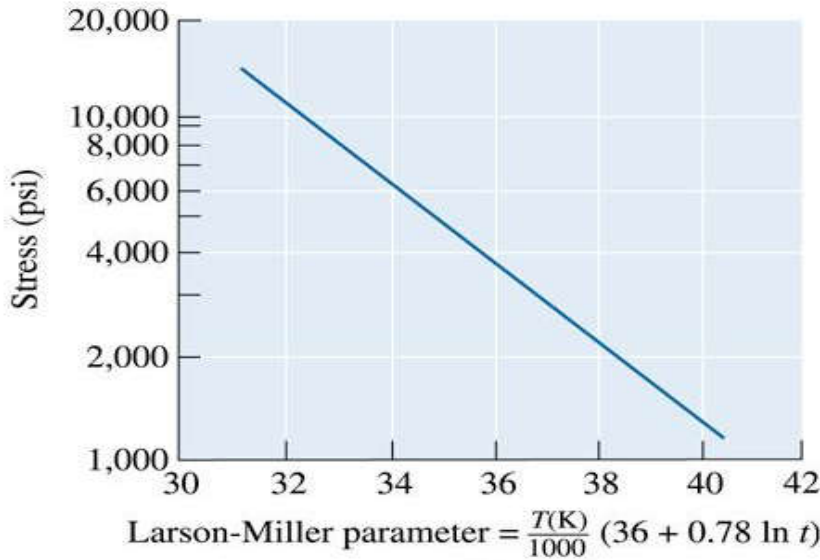


Figure 6.52
(Repeated for Problems 6.91 and 6.92) Crack growth rate versus stress-intensity factor range for a high-strength steel. For this steel, $C = 1.62 \times 10^{-12}$ and $n = 3.2$ for the units shown



(a)



(b)

Figure 6.59 (Repeated for Problems 6.106 through 6.112) Results from a series of creep tests. (a) Stress-rupture curves for an iron-chromium-nickel alloy and (b) the Larson-Miller parameter for ductile cast iron



The Science and Engineering of Materials, 4th ed

Donald R. Askeland – Pradeep P. Phulé

Chapter 7 – Strain Hardening and Annealing





Objectives of Chapter 7

- ❑ To learn how the strength of metals and alloys is influenced by mechanical processing and heat treatments.
- ❑ To learn how to enhance the strength of metals and alloys using cold working.
- ❑ To learn how to enhance ductility using annealing heat treatment.





Chapter Outline

- 7.1 Relationship of Cold Working to the Stress-Strain Curve
- 7.2 Strain-Hardening Mechanisms
- 7.3 Properties versus Percent Cold Work
- 7.4 Microstructure, Texture Strengthening, and Residual Stresses
- 7.5 Characteristics of Cold Working
- 7.6 The Three Stages of Annealing
- 7.7 Control of Annealing
- 7.8 Annealing and Materials Processing
- 7.9 Hot Working
- 7.10 Superplastic Forming (SPF)



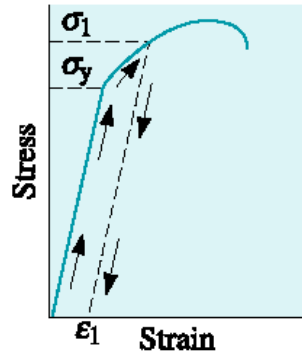


Section 7.1

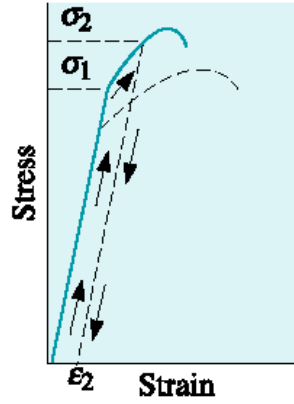
Relationship of Cold Working to the Stress-Strain Curve

- Flow stress
- Strain hardening
- Strain hardening exponent (n)
- Strain-rate sensitivity (m)
- Bauschinger effect

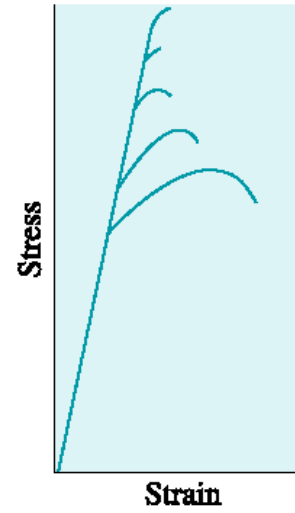




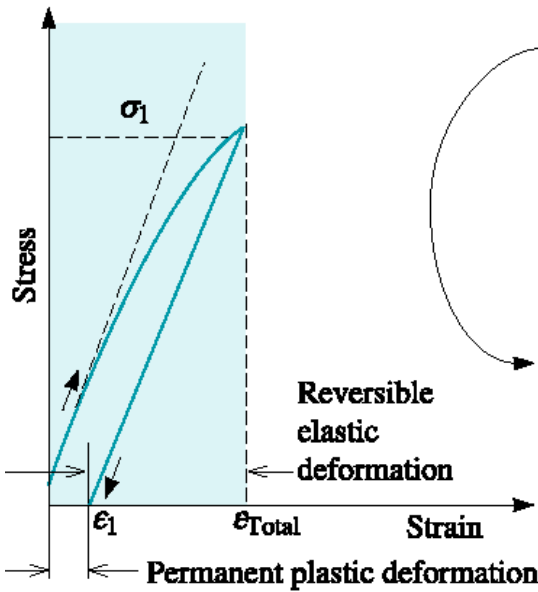
(a)



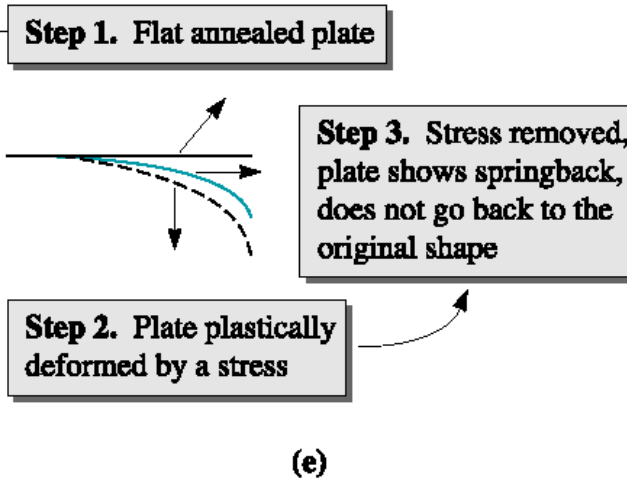
(b)



(c)

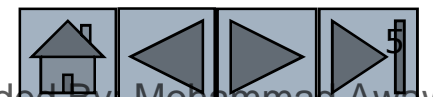


(d)



(e)

Figure 7.1
Development of
strain hardening
from the stress-
strain diagram



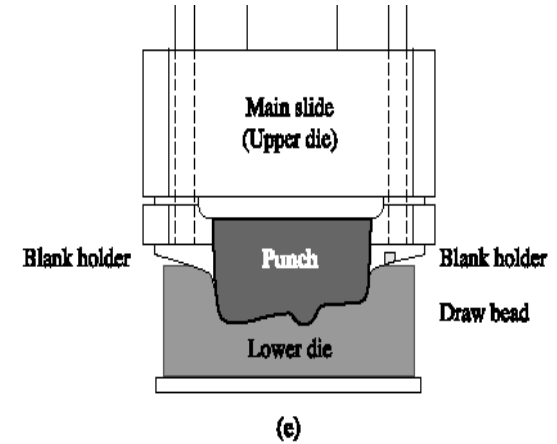
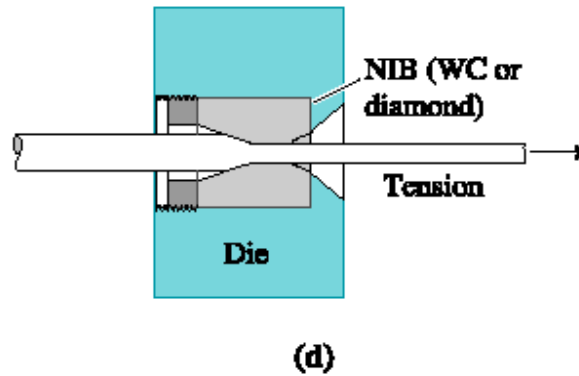
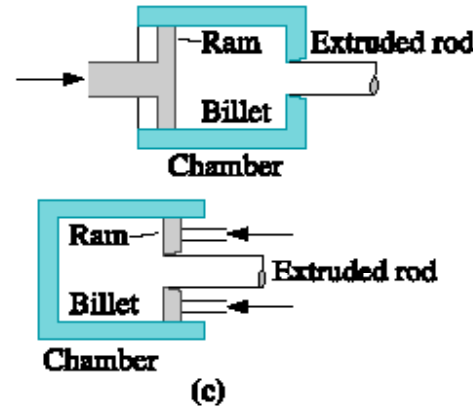
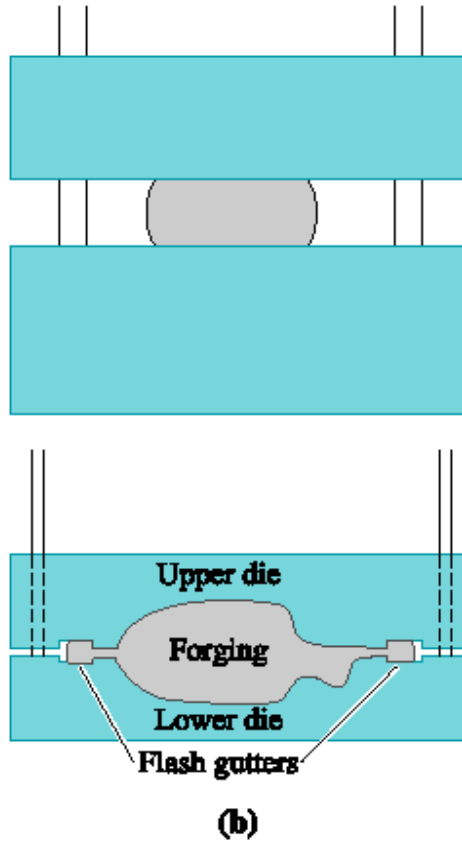
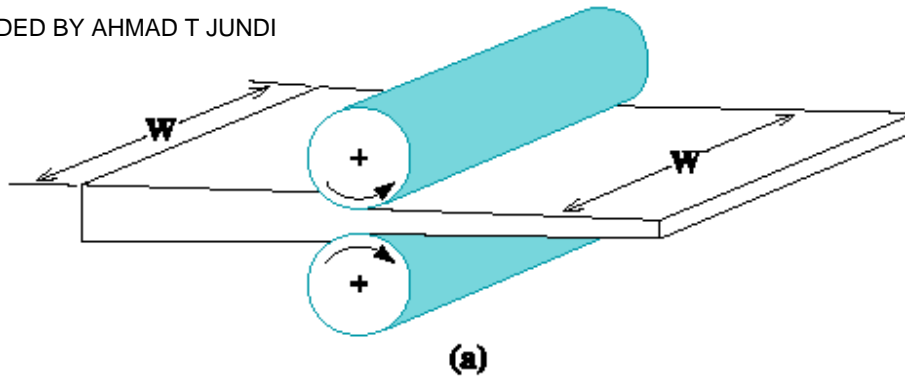


Figure 7.2
Manufacturing processes that make use of cold working as well as hot working. Common metalworking methods



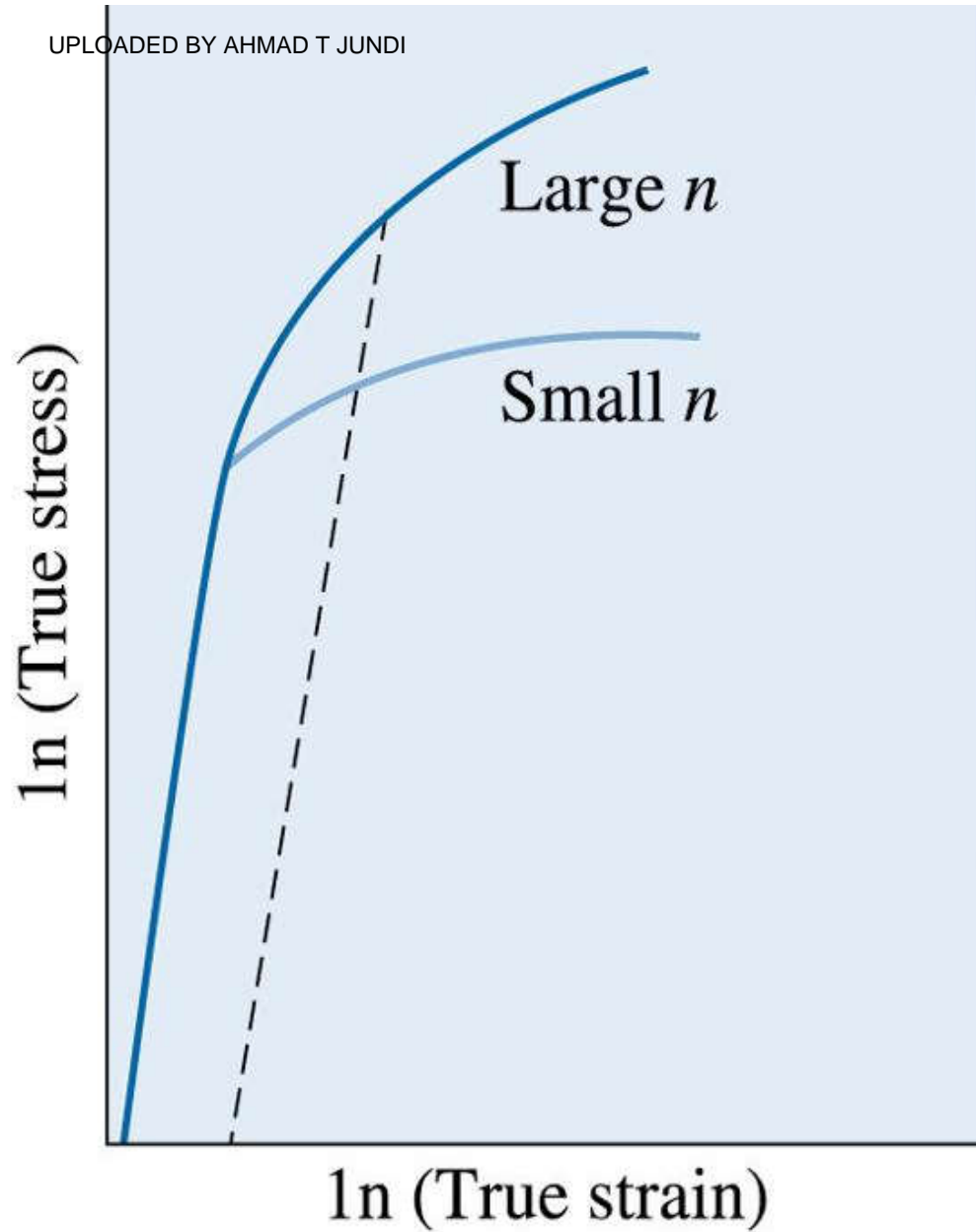


Figure 7.3 The true stress-true strain curves for metals with large and small strain-hardening exponents. Larger degrees of strengthening are obtained for a given strain for the metal with the larger n

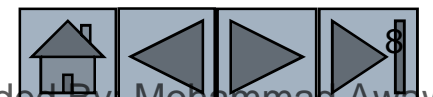




TABLE 7-1 ■ Strain-hardening exponents and strength coefficients of typical metals and alloys

Metal	Crystal Structure	<i>n</i>	K (psi)
Titanium	HCP	0.05	175,000
Annealed alloy steel	BCC	0.15	93,000
Quenched and tempered medium-carbon steel	BCC	0.10	228,000
Molybdenum	BCC	0.13	105,000
Copper	FCC	0.54	46,000
Cu-30% Zn	FCC	0.50	130,000
Austenitic stainless steel	FCC	0.52	220,000

Adapted from G. Dieter, Mechanical Metallurgy, McGraw-Hill, 1961, and other sources.



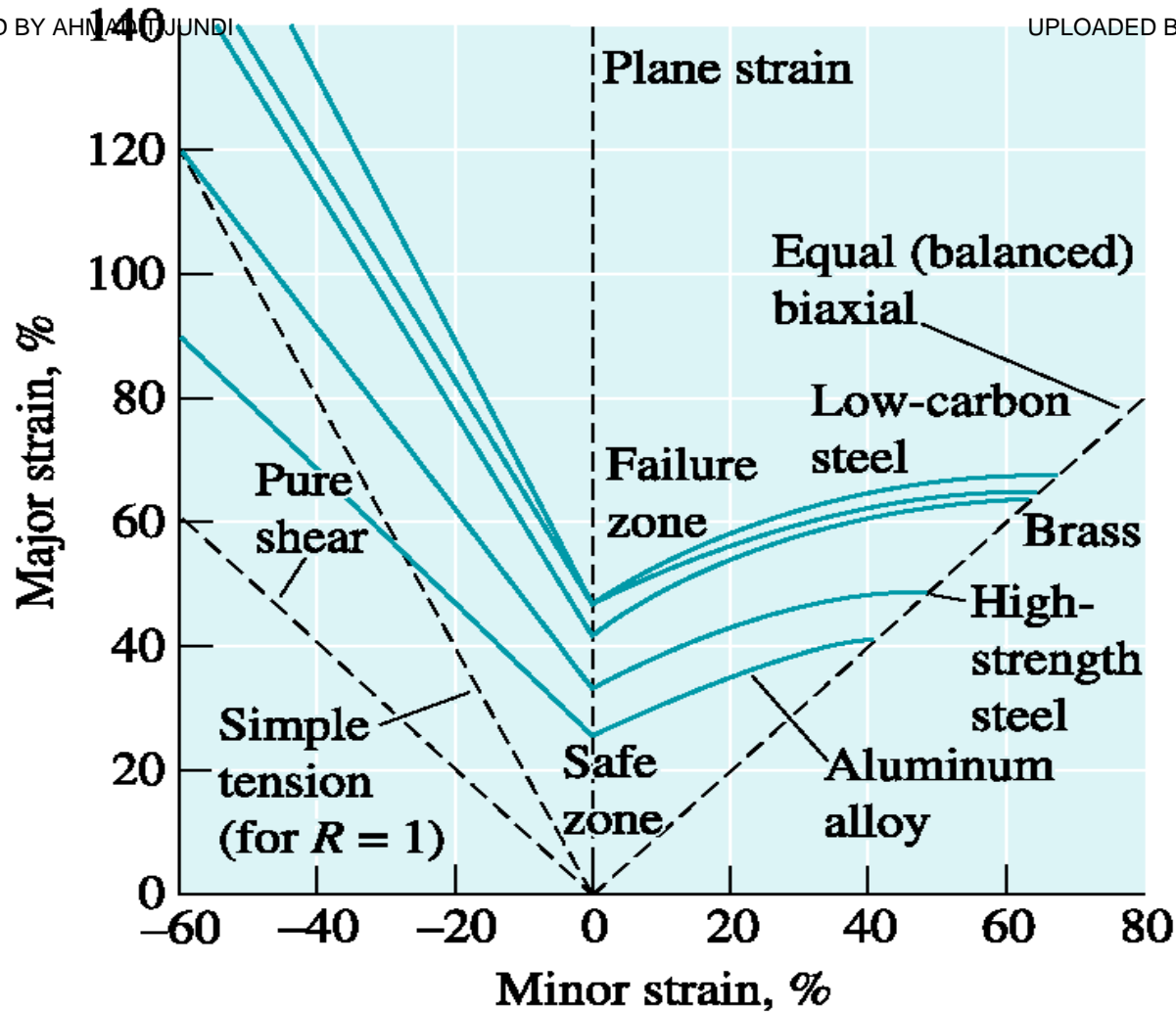


Figure 7.4 Forming limit diagram for different materials. (Source: Reprinted from Metals Handbook—Desk Edition, Second Edition, ASM International, Materials Park, OH 44073, p. 146, Fig. 5 © 1998 ASM International. Reprinted by permission.)





Section 7.2

Strain-Hardening Mechanisms

- **Frank-Read source** - A pinned dislocation that, under an applied stress, produces additional dislocations. This mechanism is at least partly responsible for strain hardening.
- **Thermoplastics** - A class of polymers that consist of large, long spaghetti-like molecules that are intertwined (e.g., polyethylene, nylon, PET, etc.).



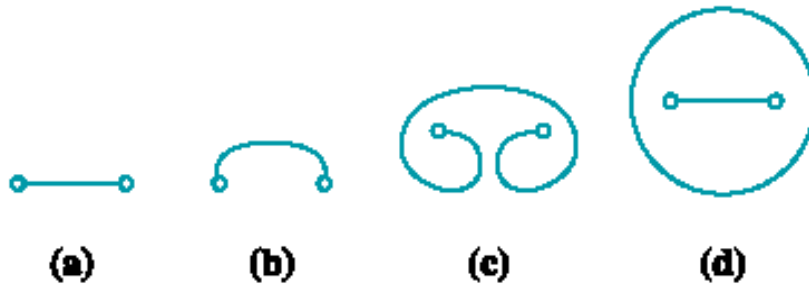
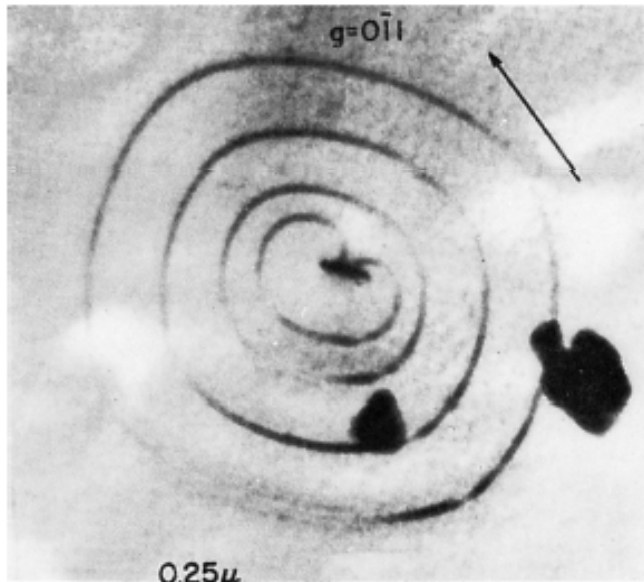


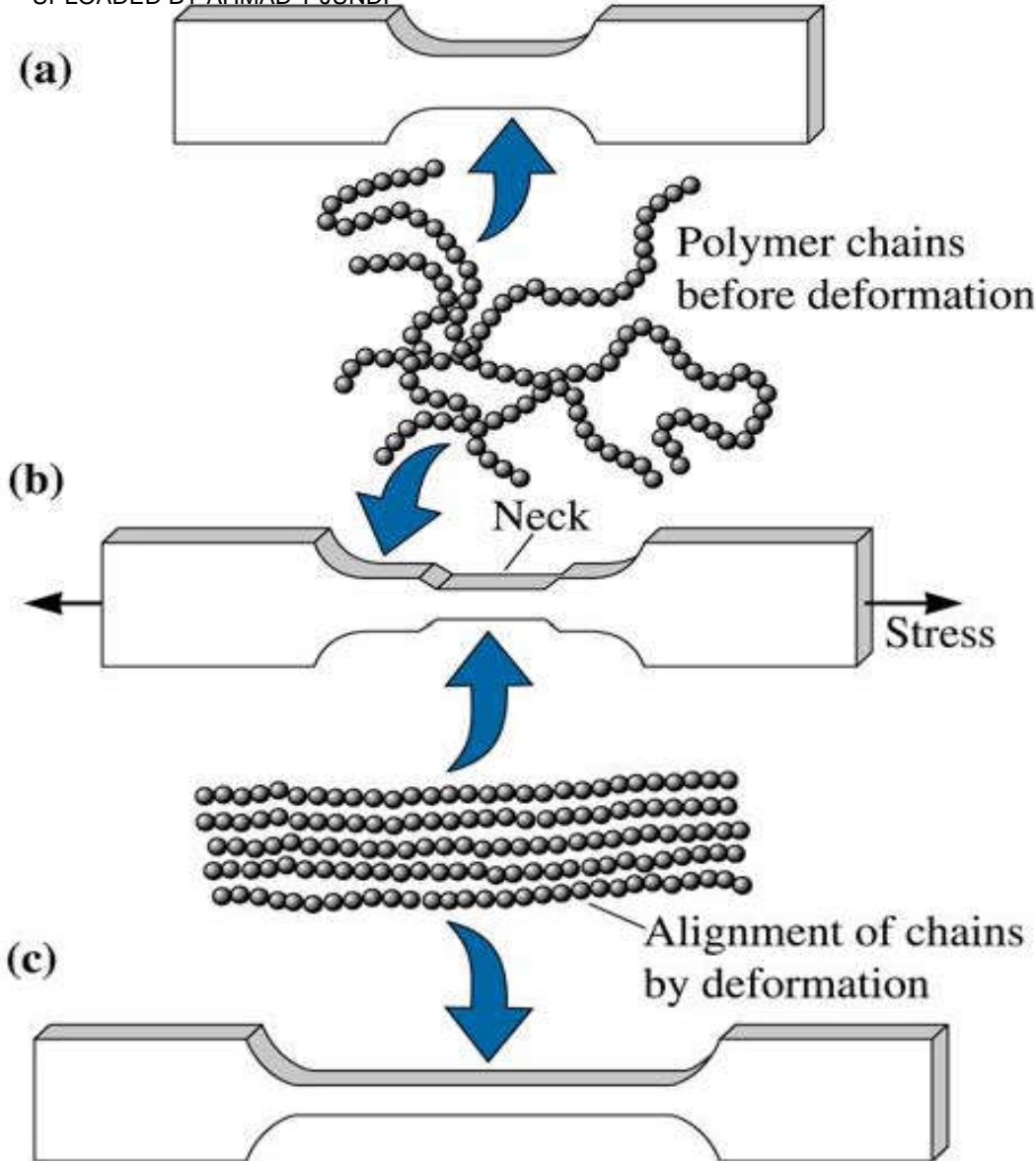
Figure 7.5 The Frank-Read source can generate dislocations. (a) A dislocation is pinned at its ends by lattice defects. (b) As the dislocation continues to move, the dislocation bows, eventually bending back on itself. (c) finally the dislocation loop forms, and (d) a new dislocation is created. (e) Electron micrograph of a Frank-Read source (330,000). (Adapted from Brittain, J., "Climb Sources in Beta Prime-NiAl," Metallurgical Transactions, Vol. 6A, April 1975.)



(e)



Figure 7.6 In an undeformed thermoplastic polymer tensile bar, (a) the polymer chains are randomly oriented. (b) When a stress is applied, a neck develops as chains become aligned locally. The neck continues to grow until the chains in the entire gage length have aligned. (c) The strength of the polymer is increased

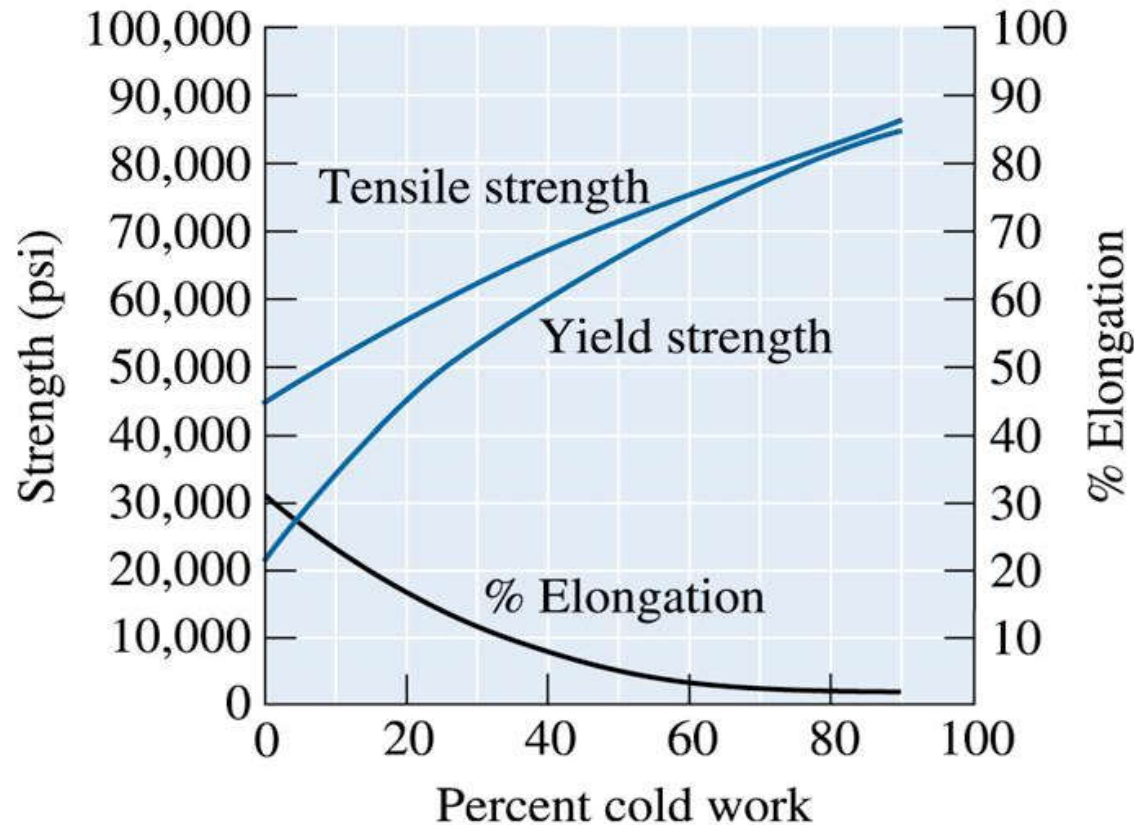


©2003 Brooks/Cole, a division of Thomson Learning, Inc. Thomson Learning, Inc. is a trademark used herein under license.

Section 7.3



Properties versus Percent Cold Work



©2003 Brooks/Cole, a division of Thomson Learning, Inc. Thomson Learning,™ is a trademark used herein under license.

Figure 7.7 The effect of cold work on the mechanical properties of copper



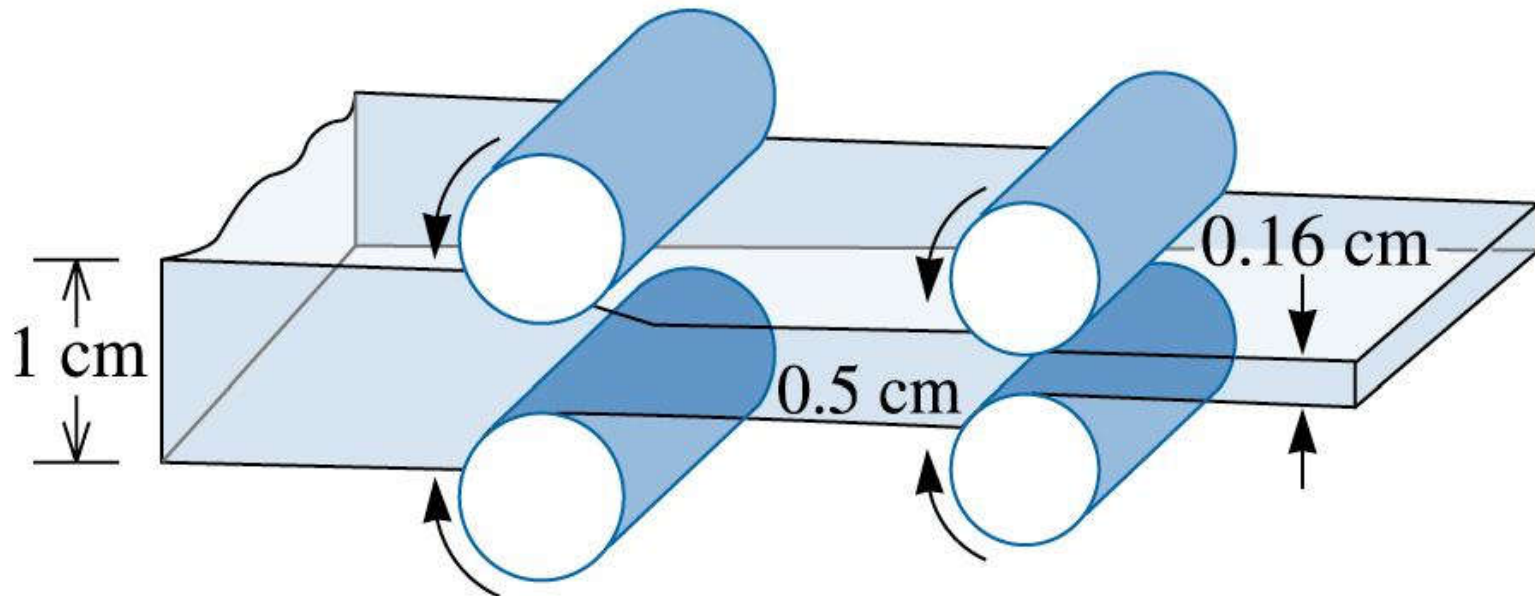


Example 7.1

Cold Working a Copper Plate

A 1-cm-thick copper plate is cold-reduced to 0.50 cm, and later further reduced to 0.16 cm. Determine the total percent cold work and the tensile strength of the 0.16-cm plate. (See Figure 7.8.)





©2003 Brooks/Cole, a division of Thomson Learning, Inc. Thomson Learning[™] is a trademark used herein under license.

Figure 7.8 Diagram showing the rolling of a 1-cm plate (for Example 7.1)



Example 7.1 SOLUTION

Our definition of cold work is the percentage change between the original and final cross-sectional areas; it makes no difference how many intermediate steps are involved. Thus, the total cold work is actually

$$\% \text{ CW} = \left[\frac{t_0 - t_f}{t_0} \right] \times 100 = \left[\frac{1 \text{ cm} - 0.16 \text{ cm}}{1 \text{ cm}} \right] \times 100 = 84\%$$

and, from Figure 7-7, the tensile strength is about 82,000 psi.





Design of a Cold Working Process

Design a manufacturing process to produce a 0.1-cm-thick copper plate having at least 65,000 psi tensile strength, 60,000 psi yield strength, and 5% elongation.

Example 7.2 SOLUTION

To produce the plate, a cold-rolling process would be appropriate. The original thickness of the copper plate prior to rolling can be calculated from Equation 7-4, assuming that the width of the plate does not change. Because there is a range of allowable cold work—between 40% and 45%—there is a range of initial plate thicknesses:



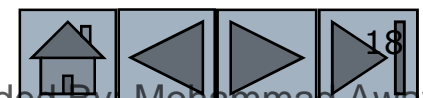


Example 7.2 SOLUTION (Continued)

$$\% CW_{\min} = 40 = \left[\frac{t_{\min} \text{ cm} - 0.1 \text{ cm}}{t_{\min} \text{ cm}} \right] \times 100, \quad \therefore t_{\min} = 0.167 \text{ cm}$$

$$\% CW_{\max} = 45 = \left[\frac{t_{\max} \text{ cm} - 0.1 \text{ cm}}{t_{\max} \text{ cm}} \right] \times 100, \quad \therefore t_{\max} = 0.182 \text{ cm}$$

To produce the 0.1-cm copper plate, we begin with a 0.167- to 0.182-cm copper plate in the softest possible condition, then cold roll the plate 40% to 45% to achieve the 0.1 cm thickness.

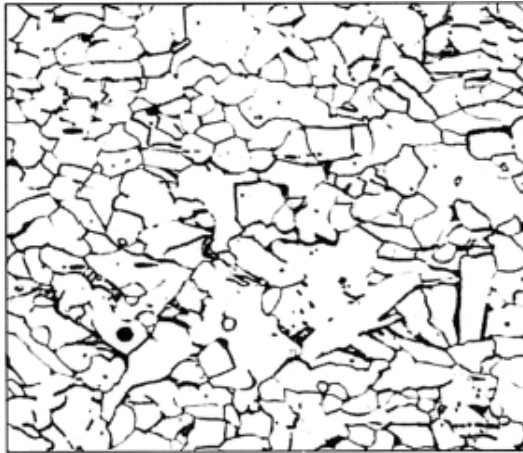




Section 7.4

Microstructure, Texture Strengthening, and Residual Stresses

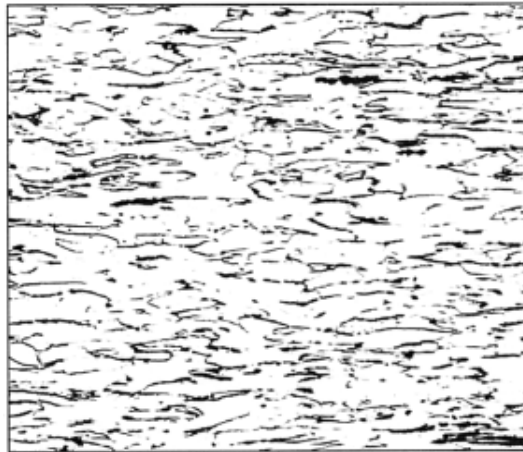
- Fiber texture, Sheet texture
- Pole figure analysis, Orientation microscopy
- Residual stresses, Stress-relief anneal
- Annealing glass, Tempered glass



(a)



(b)



(c)



(d)

Figure 7.9 The fibrous grain structure of a low carbon steel produced by cold working: (a) 10% cold work, (b) 30% cold work, (c) 60% cold work, and (d) 90% cold work (250). (Source: From ASM Handbook Vol. 9, Metallography and Microstructure, (1985) ASM International, Materials Park, OH 44073. Used with permission.)



©2003 Brooks/Cole, a division of Thomson Learning, Inc. Thomson Learning, Inc. is a trademark used herein under license.

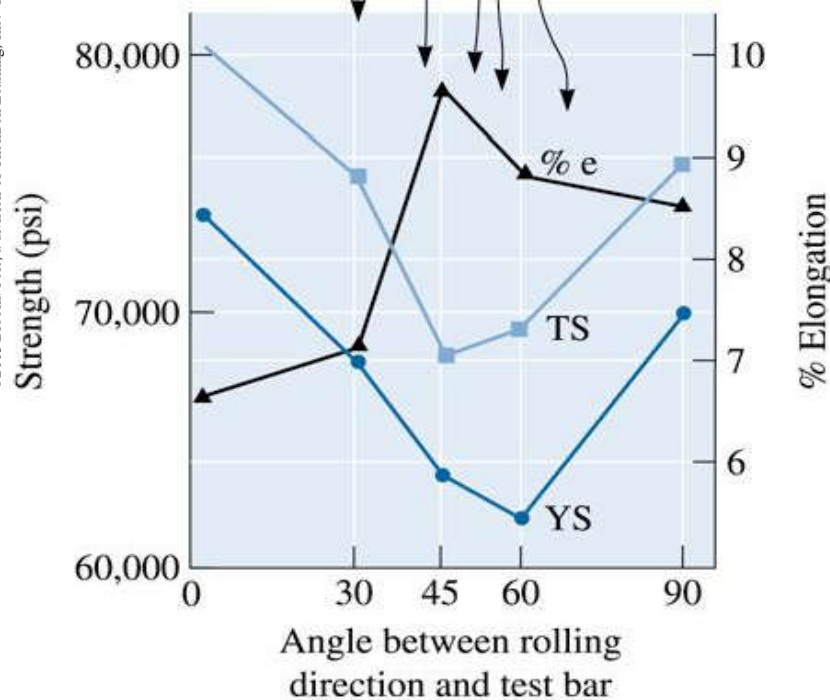
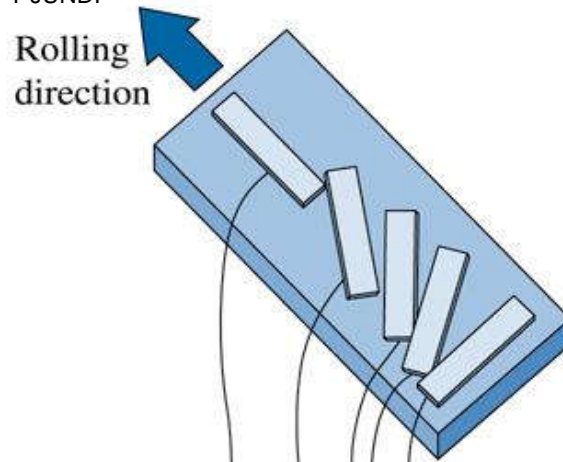


Figure 7.10 Anisotropic behavior in a rolled aluminum-lithium sheet material used in aerospace applications. The sketch relates the position of tensile bars to the mechanical properties that are obtained





Table 7-2 ■ Common wire drawing and extrusion, and sheet textures in materials[8]

Crystal Structure	Wire Drawing and Extrusion (Fiber Texture) (Direction Parallel to Wire Axis)	Sheet or Rolling Texture
FCC	$\langle 111 \rangle$ and $\langle 100 \rangle$	{110} planes parallel to rolling plane $\langle 112 \rangle$ directions parallel to rolling direction
BCC	$\langle 110 \rangle$	{001} planes parallel to rolling plane $\langle 110 \rangle$ directions parallel to rolling direction
HCP	$\langle 1\bar{0}10 \rangle$	{0001} planes parallel to rolling plane $\langle 11\bar{2}0 \rangle$ directions parallel to rolling direction



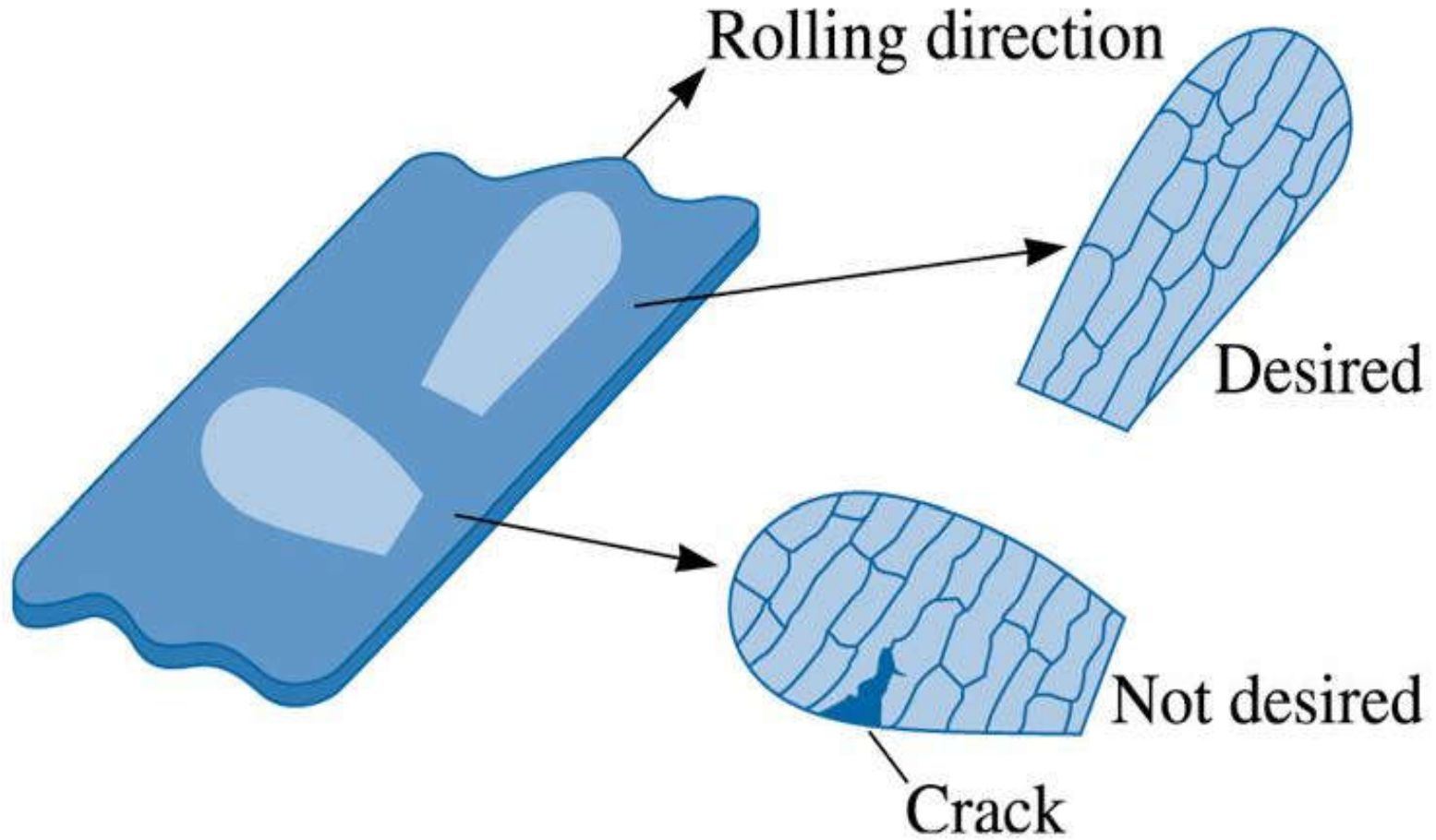


Example 7.3

Design of a Stamping Process

One method for producing fans for cooling automotive and truck engines is to stamp the blades from cold-rolled steel sheet, then attach the blades to a “spider” that holds the blades in the proper position. A number of fan blades, all produced at the same time, have failed by the initiation and propagation of a fatigue crack transverse to the axis of the blade (Figure 7.11). All other fan blades perform satisfactorily. Provide an explanation for the failure of the blades and redesign the manufacturing process to prevent these failures.

Example 7.3 (continued)



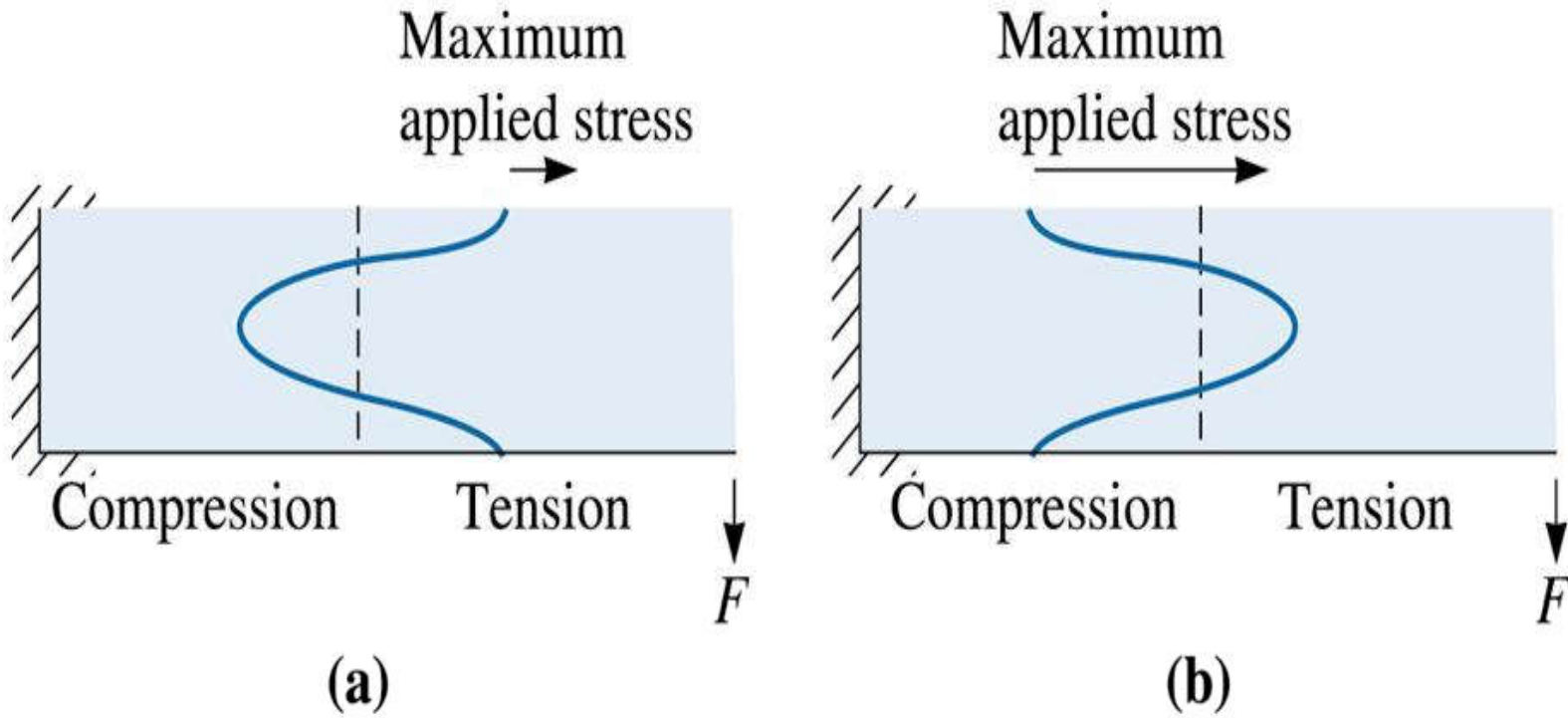
©2003 Brooks/Cole, a division of Thomson Learning, Inc. Thomson Learning, is a trademark used herein under license.

Figure 7.11 Orientations of samples (for Example 7.3)



Example 7.3 SOLUTION

- The wrong type of steel may have been selected.
- The dies used to stamp the blades from the sheet may be worn.
- The clearance between the parts of the dies may be incorrect, producing defects that initiate fatigue failure.
- The failures could also be related to the anisotropic behavior of the steel sheet caused by rolling.



©2003 Brooks/Cole, a division of Thomson Learning, Inc. Thomson Learning,™ is a trademark used herein under license.

Figure 7.12 The compressive residual stresses can be harmful or beneficial. (a) A bending force applies a tensile stress on the top of the beam. Since there are already tensile residual stresses at the top, the load-carrying characteristics are poor. (b) The top contains compressive residual stresses. Now the load-carrying characteristics are very good



Example 7.4

Design of a Fatigue-Resistant Shaft

Your company has produced several thousand shafts that have a fatigue strength of 20,000 psi. The shafts are subjected to high-bending loads during rotation. Your sales engineers report that the first few shafts placed into service failed in a short period of time by fatigue. Design a process by which the remaining shafts can be salvaged by improving their fatigue properties.





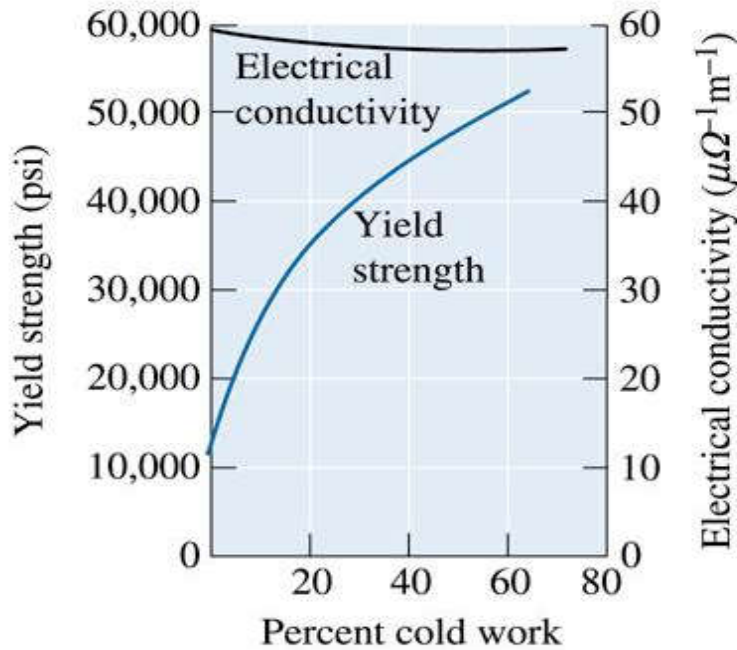
Example 7.4 SOLUTION

- Increasing the strength at the surface improves the fatigue life of the shaft – carburizing
- Cold working the shaft
- Shot peen the shaft

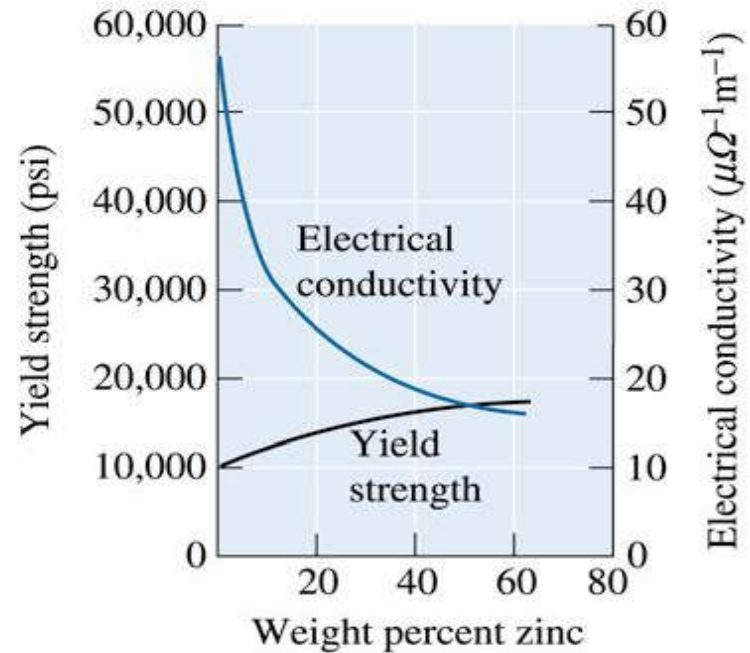




Characteristics of Cold Working



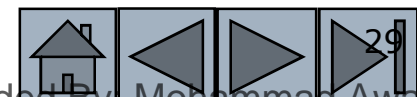
(a)



(b)

©2003 Brooks/Cole, a division of Thomson Learning, Inc. Thomson Learning[®] is a trademark used herein under license.

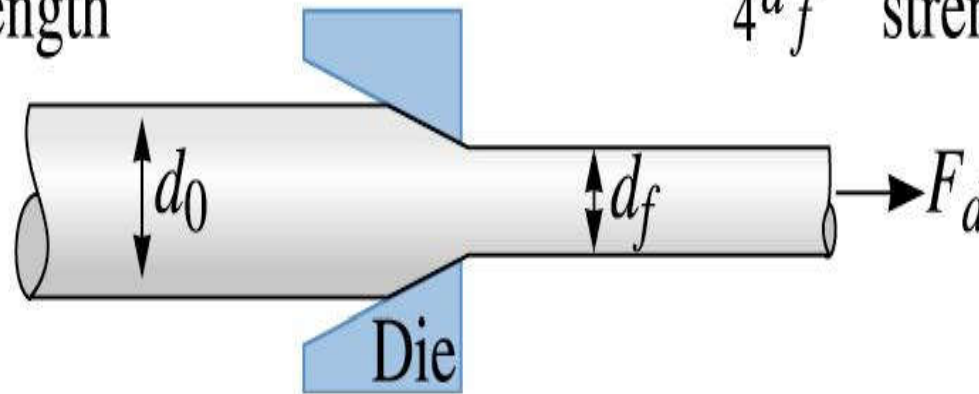
Figure 7.13 A comparison of strengthening copper by (a) cold working and (b) alloying with zinc. Note that cold working produces greater strengthening, yet has little effect on electrical conductivity





$$\text{Stress} = \frac{F_d}{\frac{\pi}{4}d_0^2} > \text{Original yield strength}$$

$$\text{Stress} = \frac{F_d}{\frac{\pi}{4}d_f^2} < \text{Final yield strength}$$



©2003 Brooks/Cole, a division of Thomson Learning, Inc. Thomson Learning[™] is a trademark used herein under license.

Figure 7.14 The wire-drawing process. The force F_d acts on both the original and final diameters. Thus, the stress produced in the final wire is greater than that in the original. If the wire did not strain harden during drawing, the final wire would break before the original wire was drawn through the die



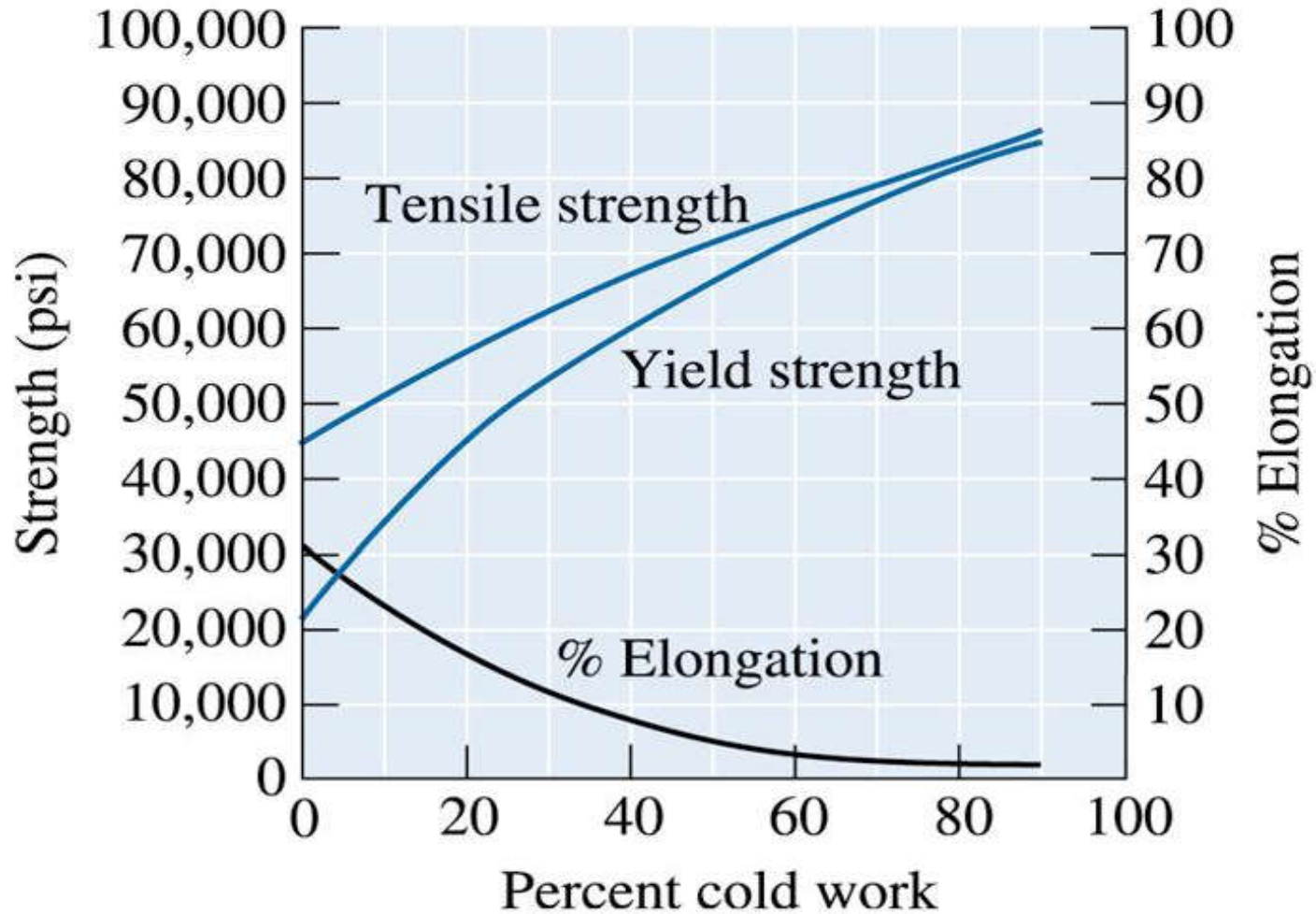


Example 7.5

Design of a Wire Drawing Process

Design a process to produce 0.20-in. diameter copper wire. The mechanical properties of copper are to be assumed as those shown in Figure 7.7.





©2003 Brooks/Cole, a division of Thomson Learning, Inc. Thomson Learning[®] is a trademark used herein under license.

Figure 7.7 The effect of cold work on the mechanical properties of copper





TABLE 7-3 ■ *Mechanical properties of copper wire (see Example 7-5)*

d_0 (in.)	% CW	Yield Strength of Drawn Wire (psi)	Force (lb)	Draw Stress on Drawn Wire (psi)
0.25	36	58,000	1080	34,380
0.30	56	68,000	1555	49,500
0.35	67	74,000	2117	67,390
0.40	75	77,500	2765	88,010

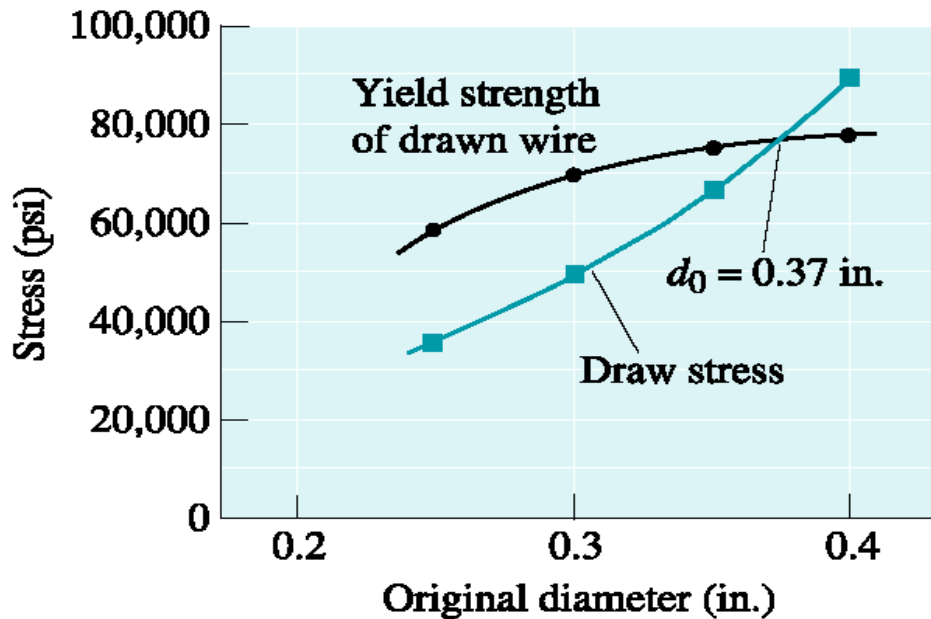


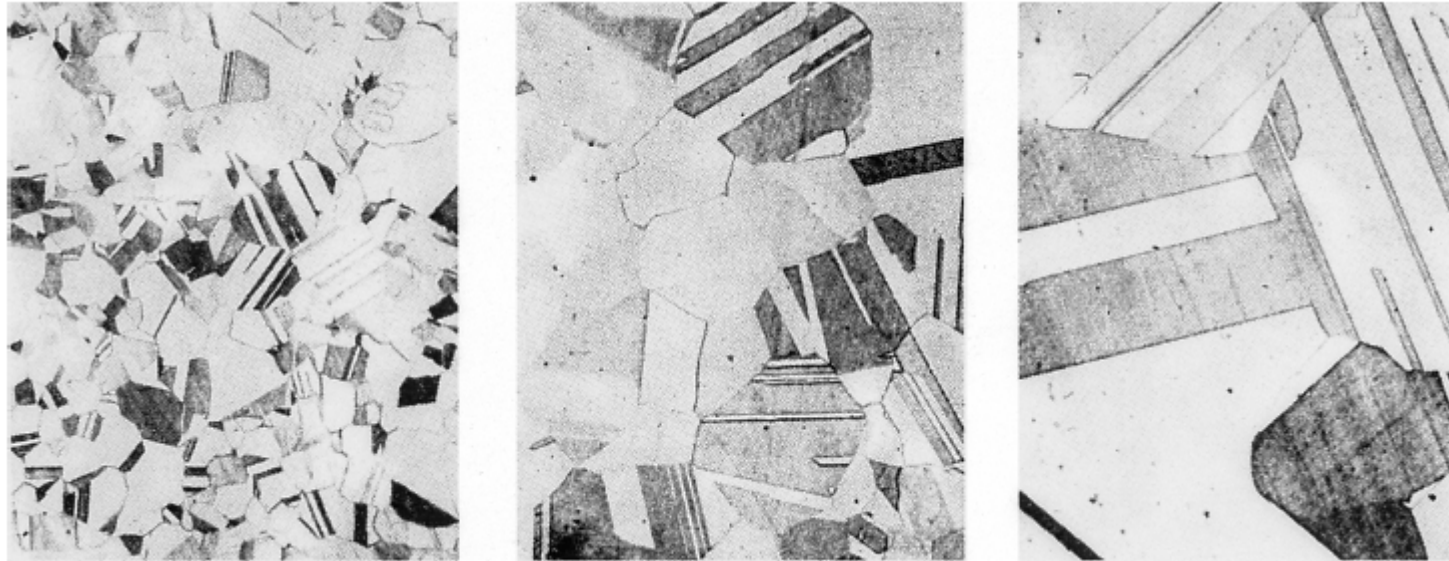
Figure 7-15
Yield strength and draw stress of wire (for Example 7-5).





The Three Stages of Annealing

- **Recovery** - A low-temperature annealing heat treatment designed to eliminate residual stresses introduced during deformation without reducing the strength of the cold-worked material.
- **Recrystallization** - A medium-temperature annealing heat treatment designed to eliminate all of the effects of the strain hardening produced during cold working.
- **Grain growth** - Movement of grain boundaries by diffusion in order to reduce the amount of grain boundary area.

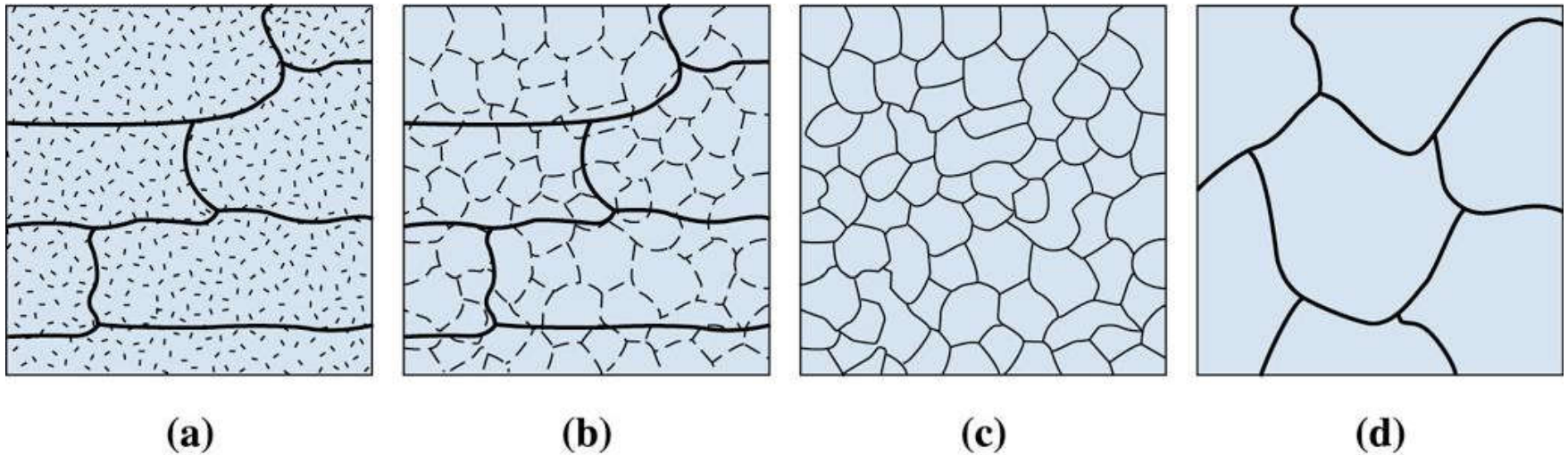


(a)

(b)

(c)

Figure 7.16 Photomicrographs showing the effect of annealing temperature on grain size in brass. Twin boundaries can also be observed in the structures. (a) Annealed at 400°C, (b) annealed at 650°C, and (c) annealed at 800°C (75). (Adapted from Brick, R. and Phillips, A., *The Structure and Properties of Alloys*, 1949: McGraw-Hill.)



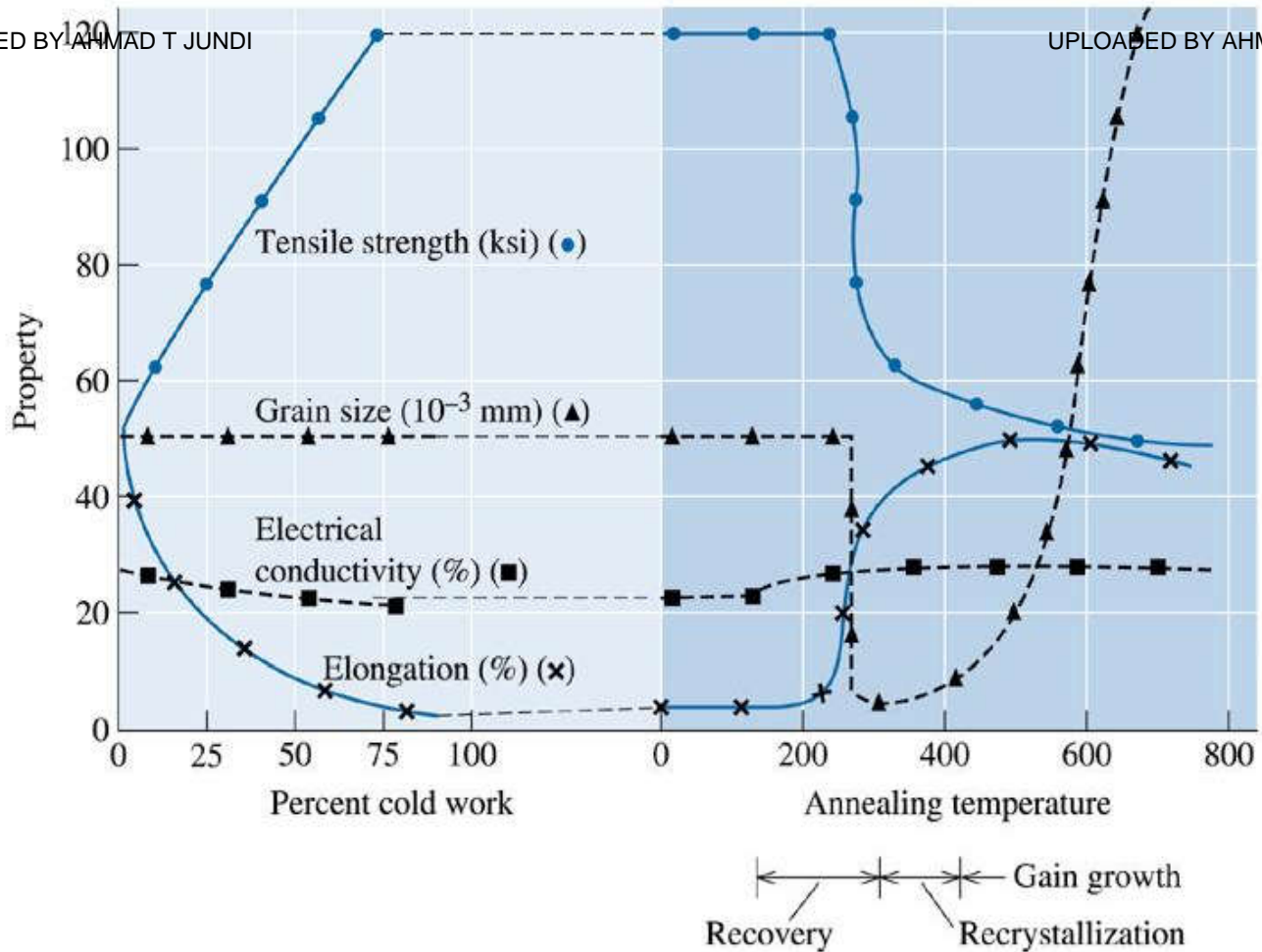
©2003 Brooks/Cole, a division of Thomson Learning, Inc. Thomson Learning™ is a trademark used herein under license.

Figure 7.17 The effect of annealing temperature on the microstructure of cold-worked metals. (a) cold-worked, (b) after recovery, (c) after recrystallization, and (d) after grain growth



UPLOADED BY AHMAD T JUNDI

UPLOADED BY AHMAD T JUNDI



©2003 Brooks/Cole, a division of Thomson Learning, Inc. Thomson Learning™ is a trademark used herein under license.

Figure 7.18 The effect of cold work on the properties of a Cu-35% Zn alloy and the effect of annealing temperature on the properties of a Cu-35% Zn alloy that is cold-worked 75%

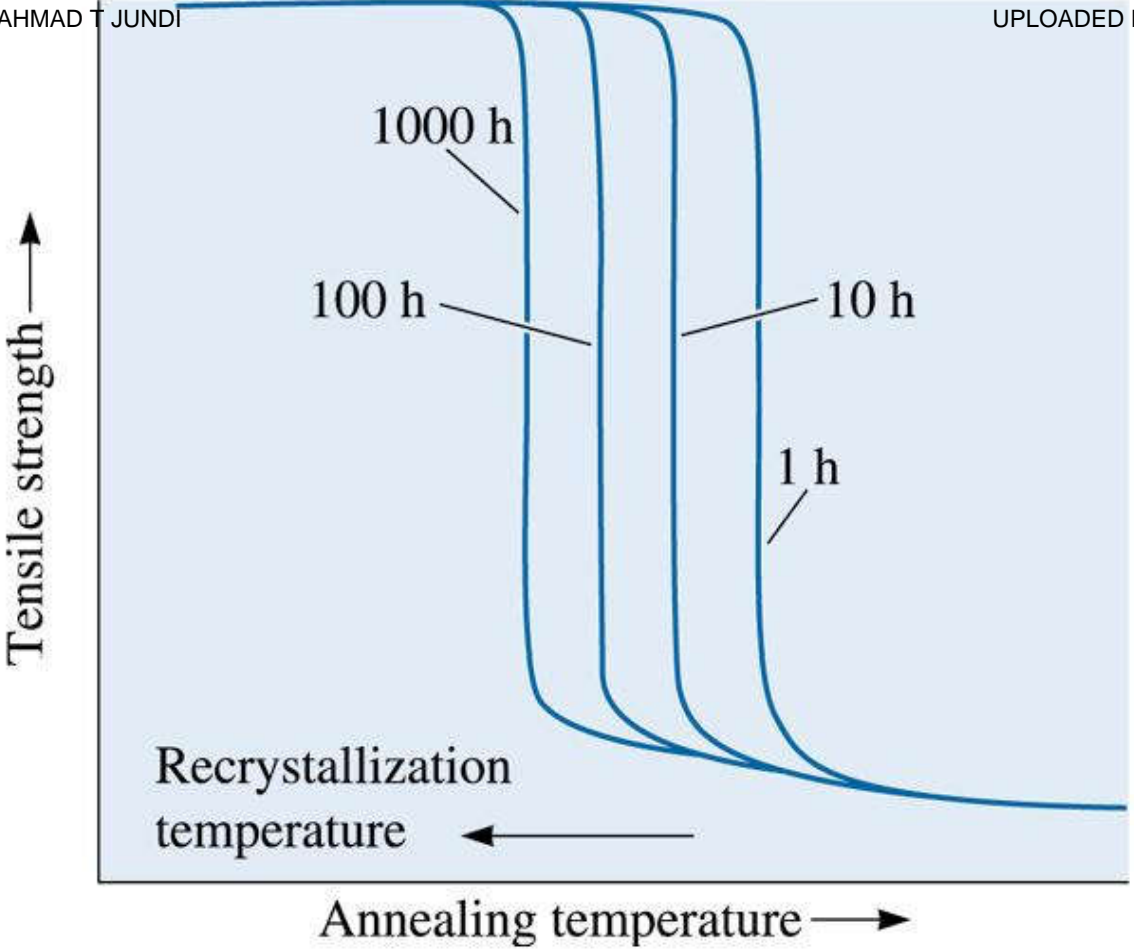


Section 7.7

Control of Annealing



- **Warm working** - A term used to indicate the processing of metallic materials in a temperature range that is between those that define cold and hot working (usually a temperature between 0.3 to 0.6 of melting temperature in K).



©2003 Brooks/Cole, a division of Thomson Learning, Inc. Thomson Learning[®] is a trademark used herein under license.

Figure 7.19 Longer annealing times reduce the recrystallization temperature. Note that the recrystallization temperature is not a fixed temperature

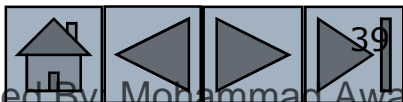




TABLE 7-4 ■ Typical recrystallization temperatures for selected metals

Metal	Melting Temperature (°C)	Recrystallization Temperature (°C)
Sn	232	-4
Pb	327	-4
Zn	420	10
Al	660	150
Mg	650	200
Ag	962	200
Cu	1085	200
Fe	1538	450
Ni	1453	600
Mo	2610	900
W	3410	1200

(Source: Adapted from Structure and Properties of Engineering Materials, by R. Brick, A. Pense, and R. Gordon, 1977. Copyright © 1977 The McGraw-Hill Companies. Adapted by permission.)





Section 7.8

Annealing and Materials Processing

- **Heat-affected zone (HAZ)** - The volume of material adjacent to a weld that is heated during the welding process above some critical temperature at which a change in the structure, such as grain growth or recrystallization, occurs.



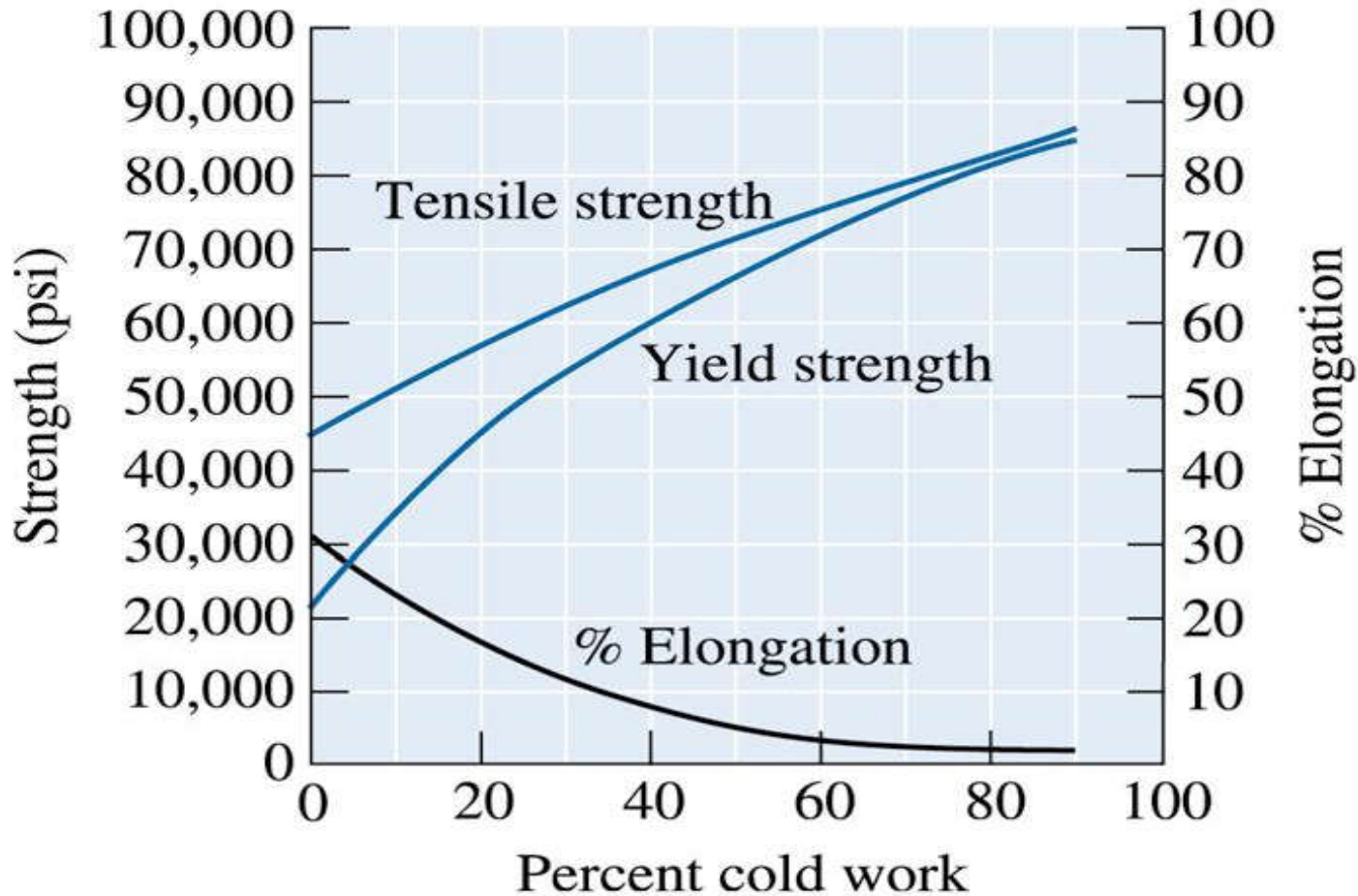


Example 7.6

Design of a Process to Produce Copper Strip

We wish to produce a 0.1-cm-thick, 6-cm-wide copper strip having at least 60,000 psi yield strength and at least 5% elongation. We are able to purchase 6-cm-wide strip only in thicknesses of 5 cm. Design a process to produce the product we need.





©2003 Brooks/Cole, a division of Thomson Learning, Inc. Thomson Learning™ is a trademark used herein under license.

Figure 7.7 The effect of cold work on the mechanical properties of copper





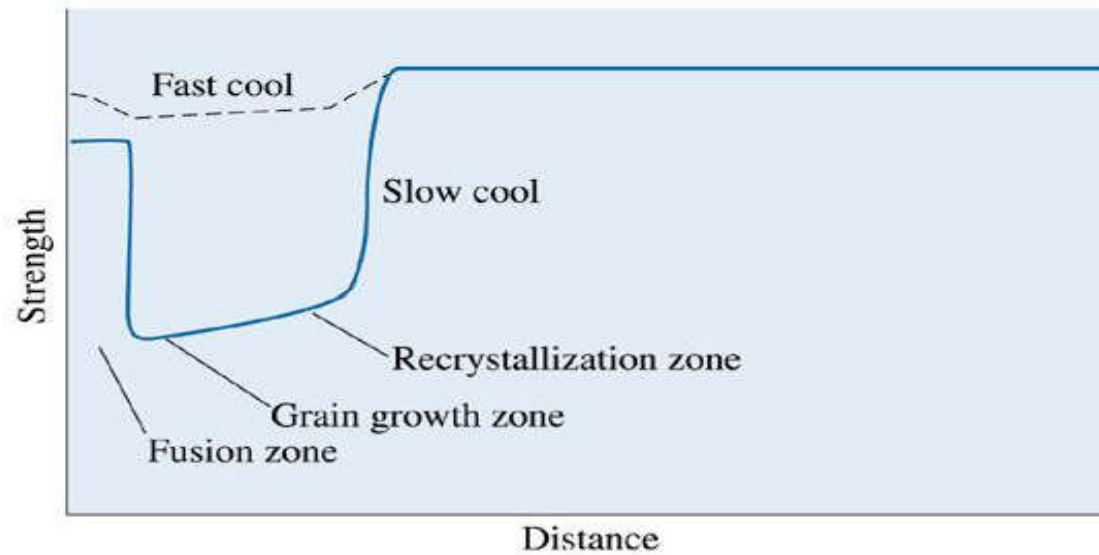
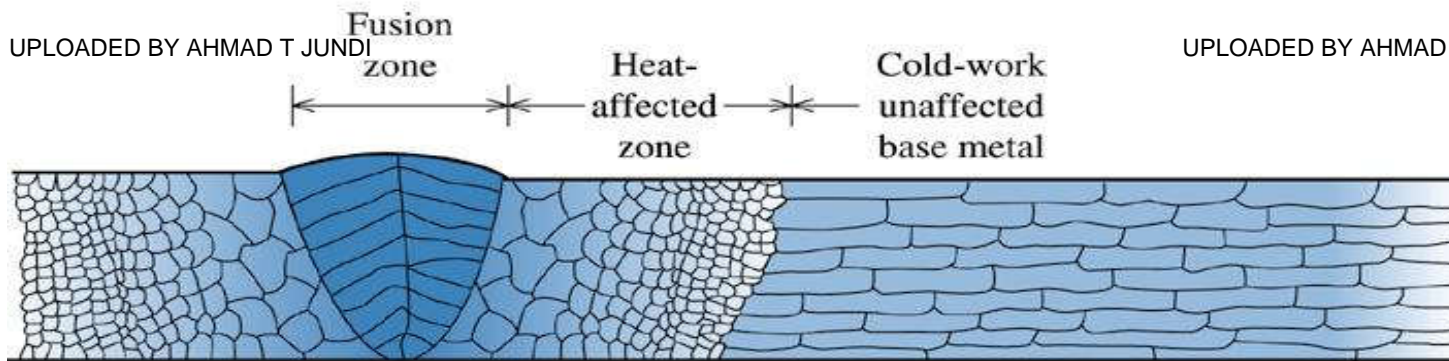
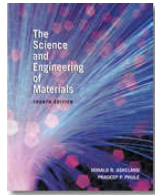
Example 7.6 SOLUTION

In Example 7-2, we found that the required properties can be obtained with a cold work of 40 to 45%. Therefore, the starting thickness must be between 0.167 cm and 0.182 cm, and this starting material must be as soft as possible— that is, in the annealed condition. Since we are able to purchase only 5-cm thick stock, we must reduce the thickness of the 5-cm strip to between 0.167 and 0.182 cm, then anneal the strip prior to final cold working. But can we successfully cold work from 5 cm to 0.182 cm?

$$\% \text{ CW} = \left[\frac{t_o - t_f}{t_o} \right] \times 100 = \left[\frac{5 \text{ cm} - 0.182 \text{ cm}}{5 \text{ cm}} \right] \times 100 = 96.4\%$$

Based on Figure 7.7, a maximum of about 90% cold work is permitted. Therefore, we must do a series of cold work and anneal cycles.





©2003 Brooks/Cole, a division of Thomson Learning, Inc. Thomson Learning[™] is a trademark used herein under license.

Figure 7.20 The structure and properties surrounding a fusion weld in a cold-worked metal. Note: only the right-hand side of the heat-affected zone is marked on the diagram. Note the loss in strength caused by recrystallization and grain growth in the heat-affected zone

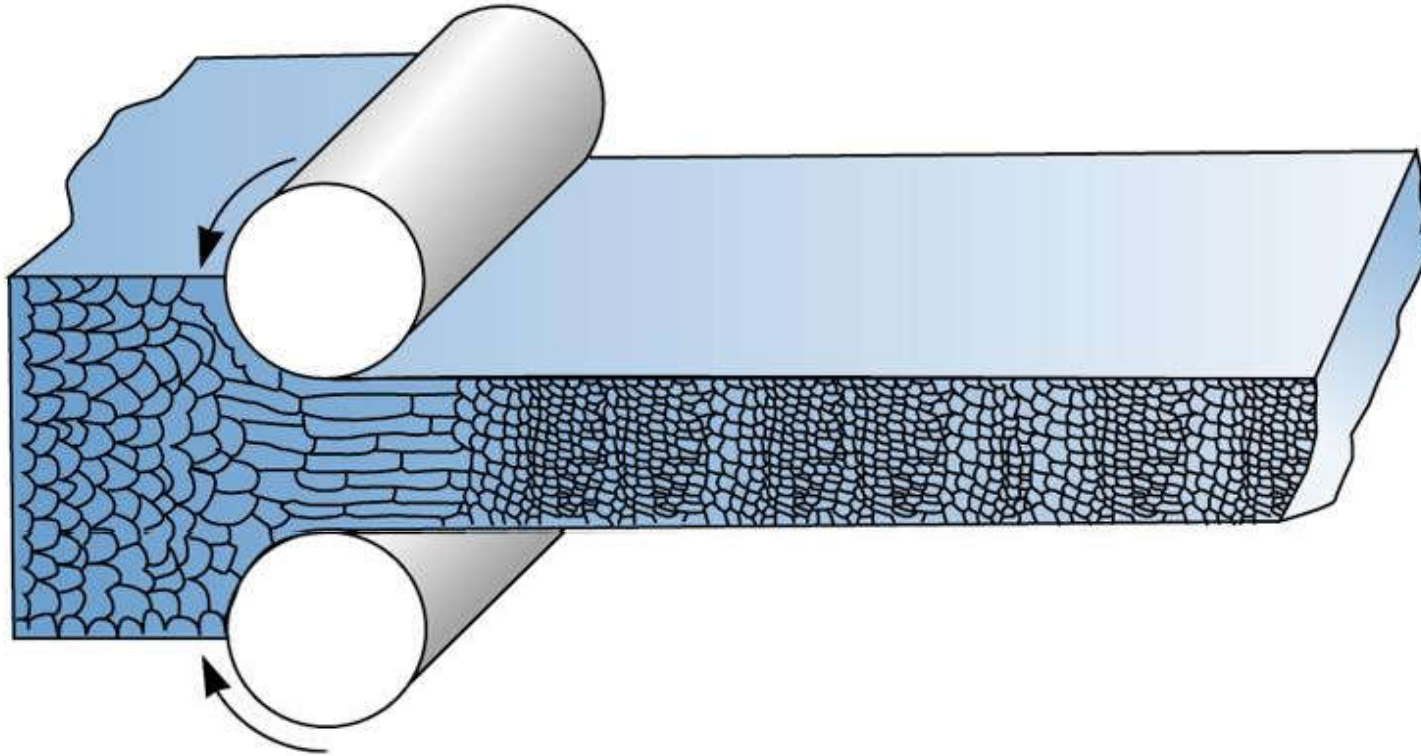


Section 7.9

Hot Working

- Lack of Strengthening
- Elimination of Imperfections
- Anisotropic Behavior
- Surface Finish and Dimensional Accuracy





©2003 Brooks/Cole, a division of Thomson Learning, Inc. Thomson Learning[™] is a trademark used herein under license.

Figure 7.21 During hot working, the elongated anisotropic grains immediately recrystallize. If the hot-working temperature is properly controlled, the final hot-worked grain size can be very fine





Example 7.7

Design of a Process to Produce a Copper Strip

We want to produce a 0.1-cm-thick, 6-cm-wide copper strip having at least 60,000 psi yield strength and at least 5% elongation. We are able to purchase 6-cm-wide strip only in thicknesses of 5 cm. Design a process to produce the product we need, but in fewer steps than were required in Example 7.6.



Example 7.7 SOLUTION

In Example 7.6, we relied on a series of cold work-anneal cycles to obtain the required thickness. We could reduce the steps by hot rolling to the required intermediate thickness:

$$\% \text{ HW} = \left[\frac{t_o - t_f}{t_o} \right] \times 100 = \left[\frac{5 \text{ cm} - 0.182 \text{ cm}}{5 \text{ cm}} \right] \times 100 = 96.4\%$$

$$\% \text{ HW} = \left[\frac{t_o - t_f}{t_o} \right] \times 100 = \left[\frac{5 \text{ cm} - 0.167 \text{ cm}}{5 \text{ cm}} \right] \times 100 = 96.7\%$$

Thus our design might be:

1. Hot work the 5-cm strip 96.4% to the intermediate thickness of 0.182 cm.
2. Cold work 45% from 0.182 cm to the final dimension of 0.1 cm. This design gives the correct dimensions and properties.



Section 7.10

Superplastic Forming (SPF)

- **Superplasticity** - The ability of a metallic or ceramic material to deform uniformly by an exceptionally large amount.
- **Strain rate** - The rate at which a material is deformed.



TABLE 7-5 ■ *Superplastic characteristics of several materials*[13,14]

Alloy	Superplastic Temperature	% Elongation (At Strain Rate Listed Here)	Strain Rate (s^{-1})	Strain Rate Sensitivity m	Flow Stress (MPa)
Ti-6% Al-4% V	927	1000–2000	2×10^{-4}	0.8	10
Al-4.5% Cu-0.5% Zn (Supral 100)	450	600–1000	10^{-3}	0.38	9
Al-4.5% Zn-4.5% Ca	565	500	10^{-3}	0.3	2.8
Fe-26% Cr-6.5% Ni	900	1000	5×10^{-5}	—	28
3mol.%Ytria-97%Zirconia	1450	>160	$\sim 10^{-4}$	0.53	—
Al ₂ O ₃ + 0.05%MgO + 0.05%Ytria	1550	65	$\sim 10^{-4}$	—	—
80wt.% of (3mol.%Ytria, 97%Zirconia) + 20wt.%Al ₂ O ₃	1650	~500	$\sim 10^{-3}$	0.5	—





©2003 Brooks/Cole, a division of Thomson Learning, Inc. Thomson Learning™ is a trademark used herein under license.

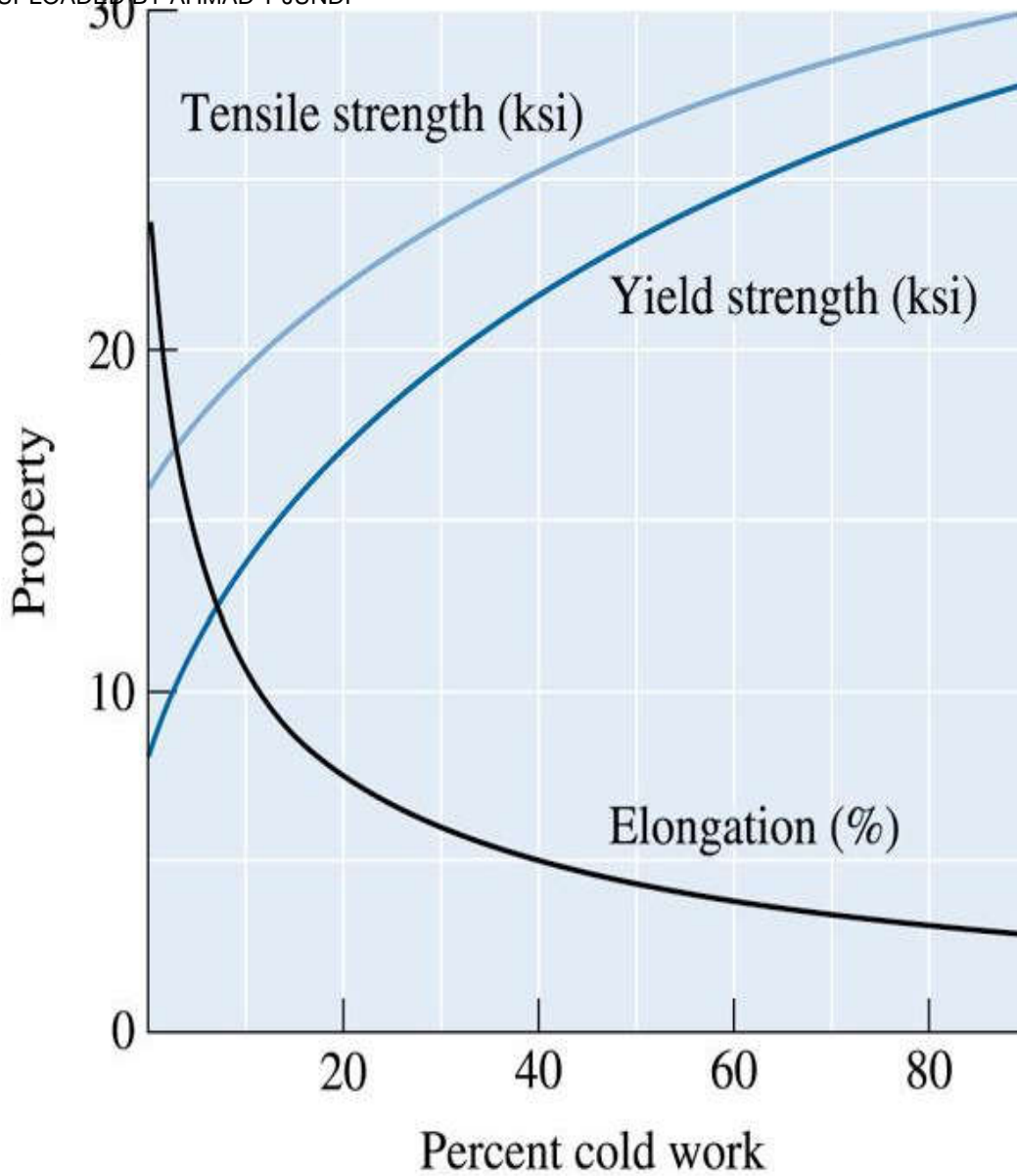


Figure 7.22 True stress-true strain curve (for Problem 7.9)





©2003 Brooks/Cole, a division of Thomson Learning, Inc. Thomson Learning, Inc. Thomson Learning, Inc. is a trademark used herein under license.

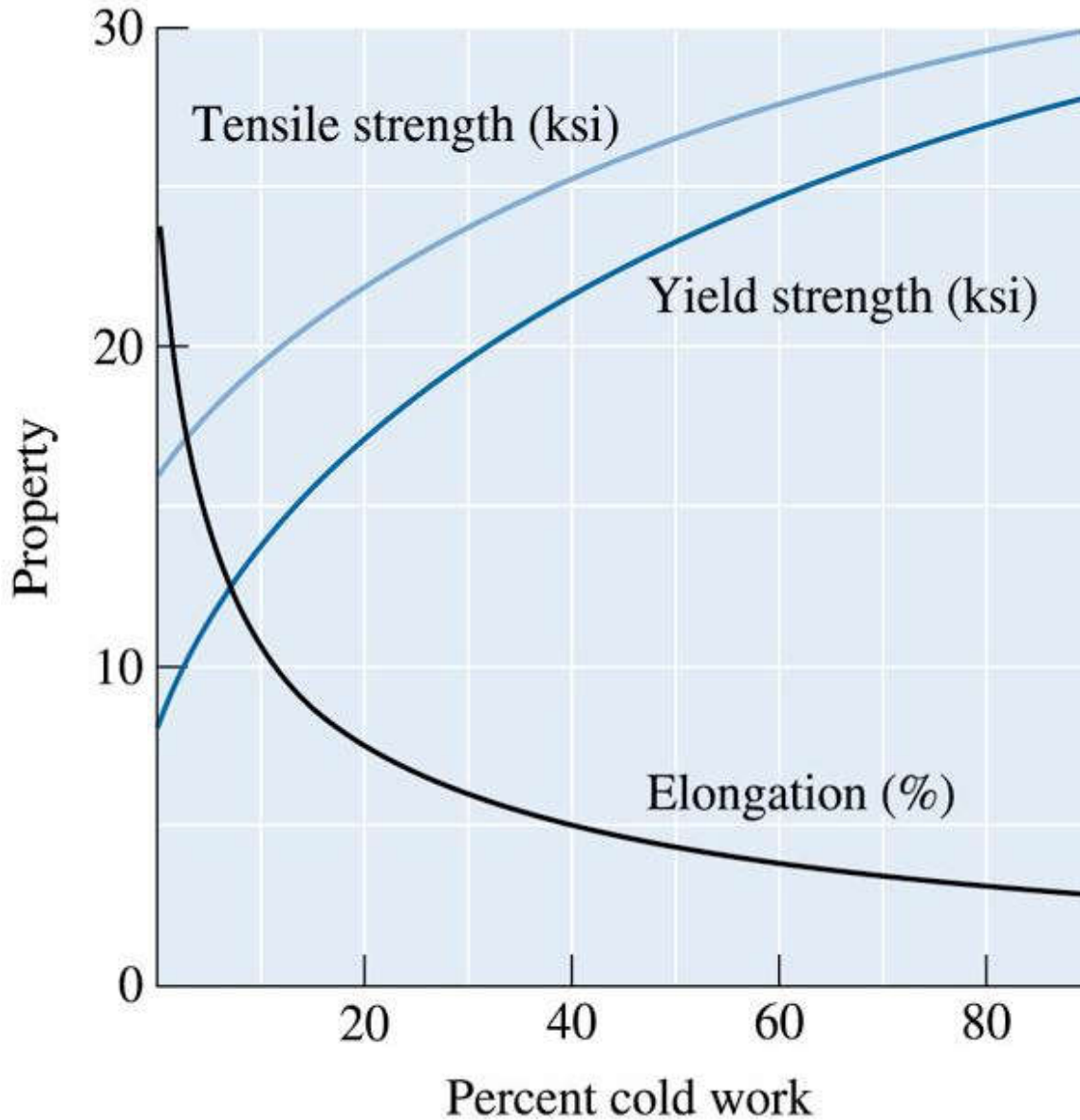


Figure 7.23 The effect of percent cold work on the properties of a 3105 aluminum alloy (for Problems 7.22 and 7.24)



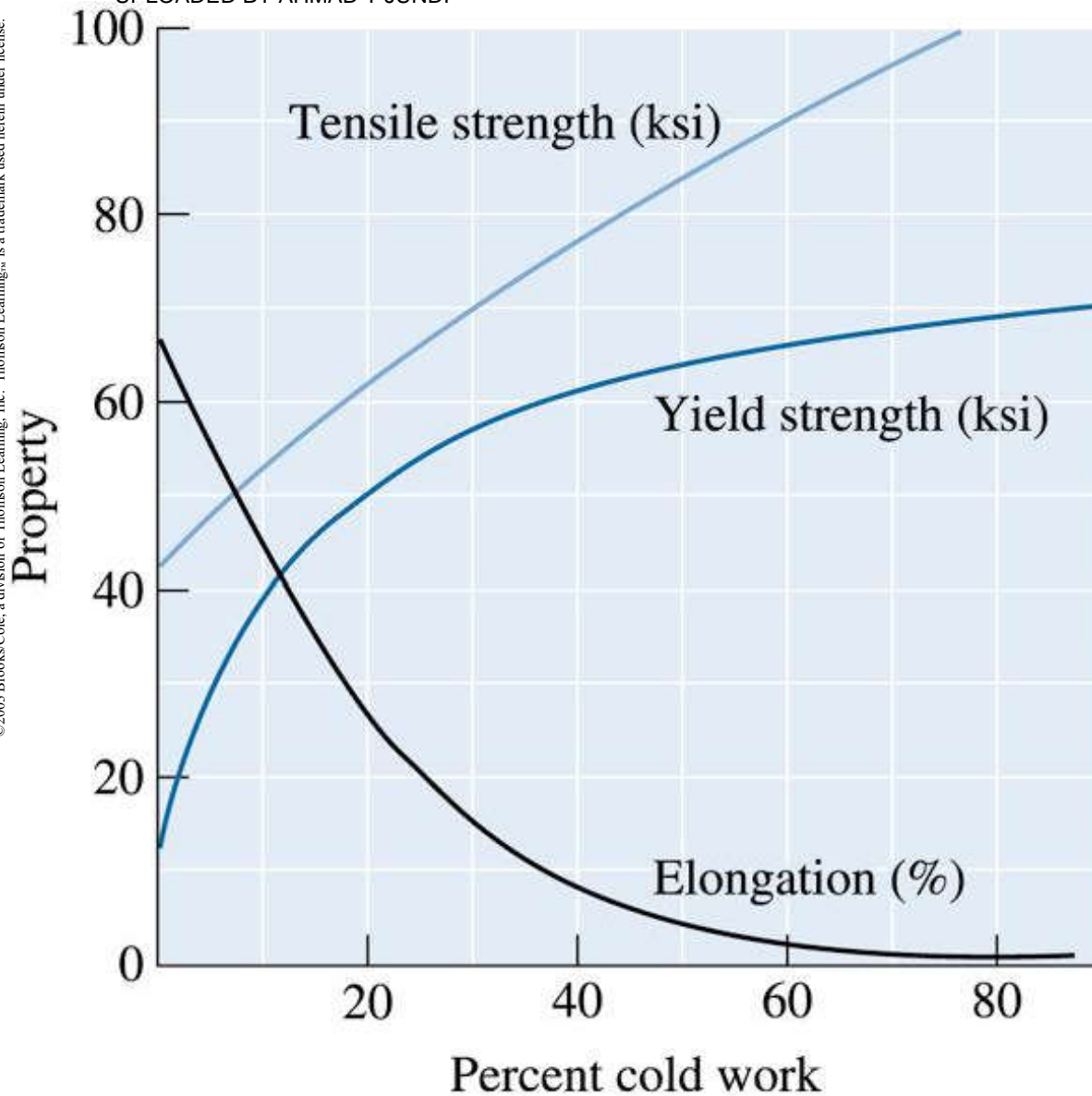
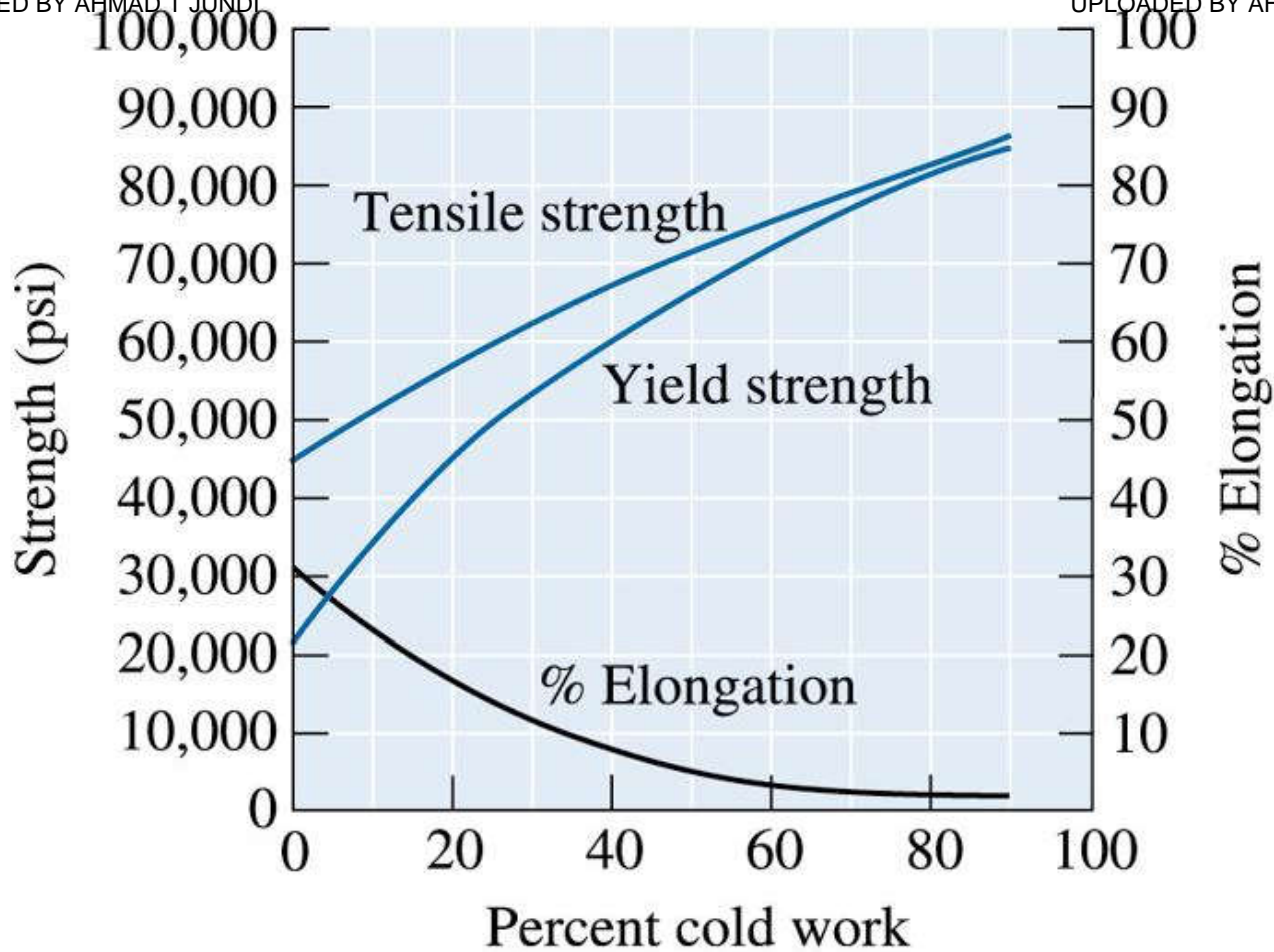
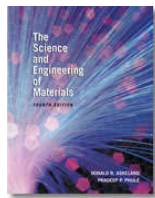


Figure 7.24 The effect of percent cold work on the properties of a Cu-30% Zn brass (for Problems 7.23 and 7.26)





©2003 Brooks/Cole, a division of Thomson Learning, Inc. Thomson Learning, is a trademark used herein under license.

**Figure 7.7 (Repeated for Problems 7.25 and 7.27 and 7.43)
The effect of cold work on the mechanical properties of copper**



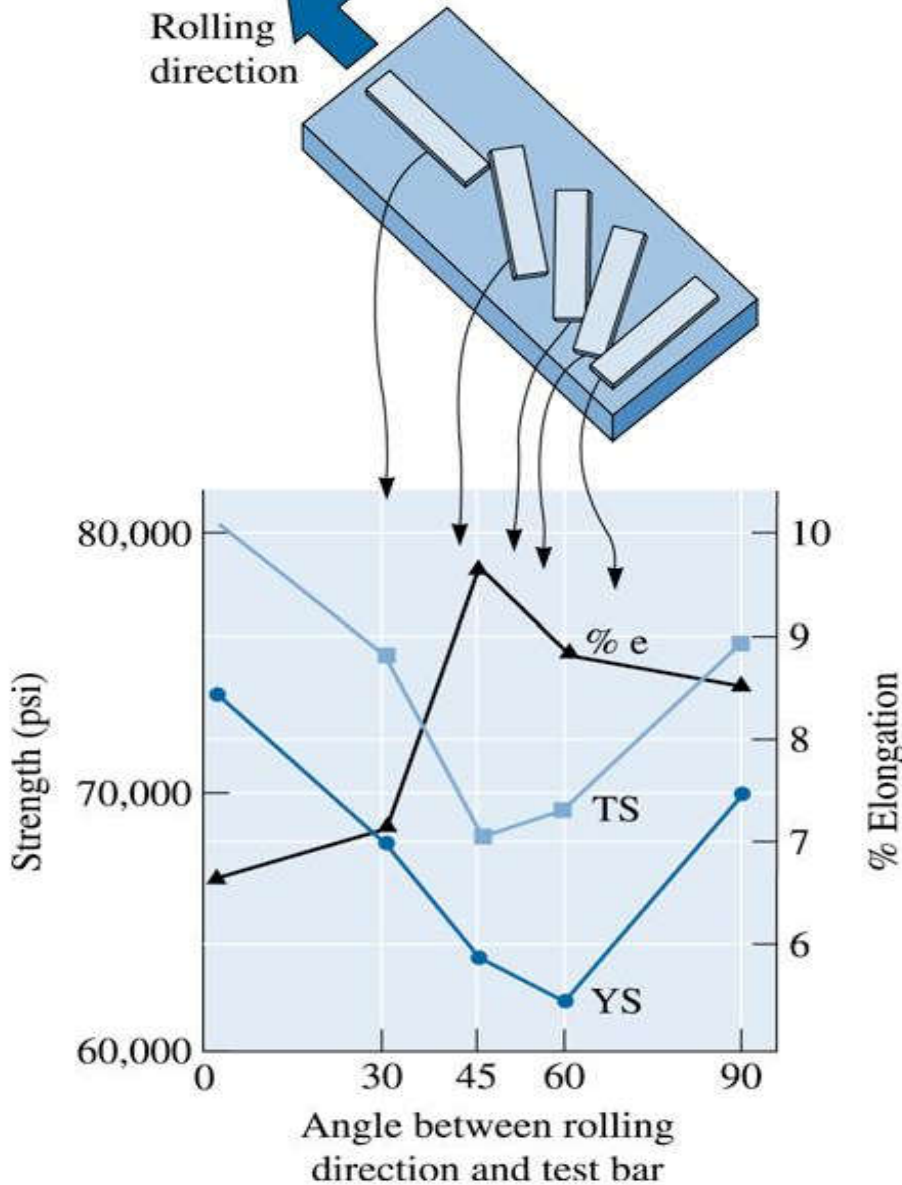


**Figure 7.10
(Repeated for Problem 7.29)
Anisotropic behavior
in a rolled
aluminum-lithium
sheet material used
in aerospace
applications. The
sketch relates the
position of tensile
bars to the
mechanical
properties that are
obtained**



The Science and Engineering of Materials, 4th ed

Donald R. Askeland – Pradeep P. Phulé

Chapter 8 – Principles of Solidification





Objectives of Chapter 8

- ❑ Study the principles of solidification as they apply to pure metals.
- ❑ Examine the mechanisms by which solidification occurs.
- ❑ Examine how techniques such as welding, brazing, and soldering are used for joining metals.





Chapter Outline

- 8.1 Technological Significance
- 8.2 Nucleation
- 8.3 Applications of Controlled Nucleation
- 8.4 Growth Mechanisms
- 8.5 Solidification Time and Dendrite Size
- 8.6 Cooling Curves
- 8.7 Cast Structure
- 8.8 Solidification Defects





Chapter Outline (Continued)

- 8.9 Casting Processes for Manufacturing Components
- 8.10 Continuous Casting and Ingot Casting
- 8.11 Directional Solidification (DS), Single Crystal Growth, and Epitaxial Growth
- 8.12 Solidification of Polymers and Inorganic Glasses
- 8.13 Joining of Metallic Materials





Section 8.1 Technological Significance

- **Primary processing** - Processes involving casting of molten metals into ingots or semi-finished useful shapes such as slabs.
- **Secondary processing** - Processes such as rolling, extrusion, etc. used to process ingots or slabs and other semi-finished shapes.

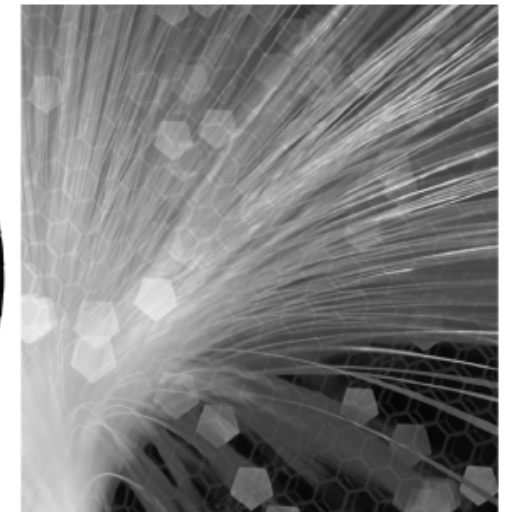




Figure 8.1 An image of a bronze object. This Canteen (bian hu) from China, Warring States period, circa 3rd century BCE (bronze inlaid with silver). (Courtesy of Freer Gallery of Art, Smithsonian Institution, Washington, D.C.)



(a)



(b)

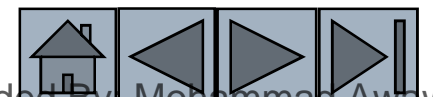
Figure 8.2 (a) Aluminum alloy wheels for automobiles, (b) optical fibers for communication. (Courtesy of PhotoDisc/Getty Images.)





Section 8.2 Nucleation

- **Nucleation** - The physical process by which a new phase is produced in a material.
- **Critical radius (r^*)** - The minimum size that must be formed by atoms clustering together in the liquid before the solid particle is stable and begins to grow.
- **Undercooling** - The temperature to which the liquid metal must cool below the equilibrium freezing temperature before nucleation occurs.
- **Homogeneous nucleation** - Formation of a critically sized solid from the liquid by the clustering together of a large number of atoms at a high undercooling (without an external interface).
- **Heterogeneous nucleation** - Formation of a critically sized solid from the liquid on an impurity surface.



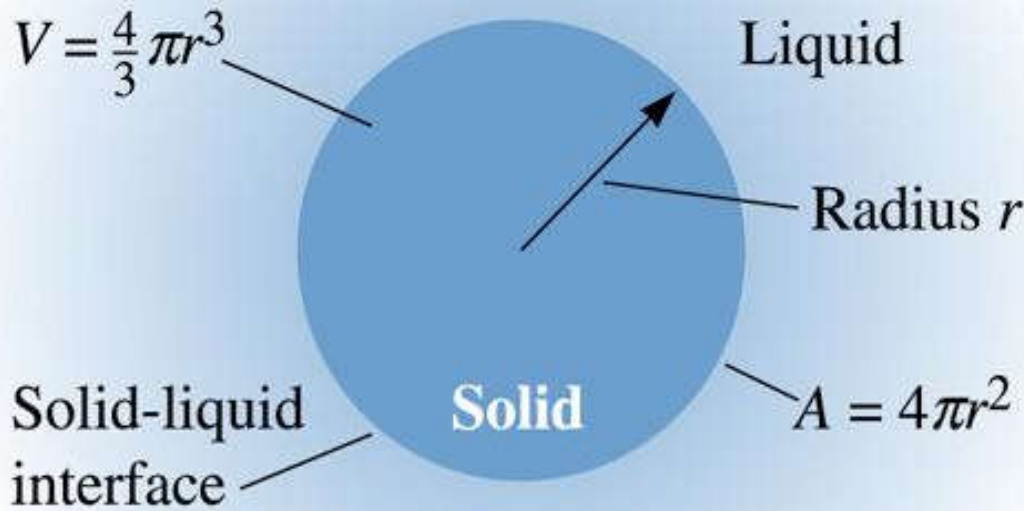
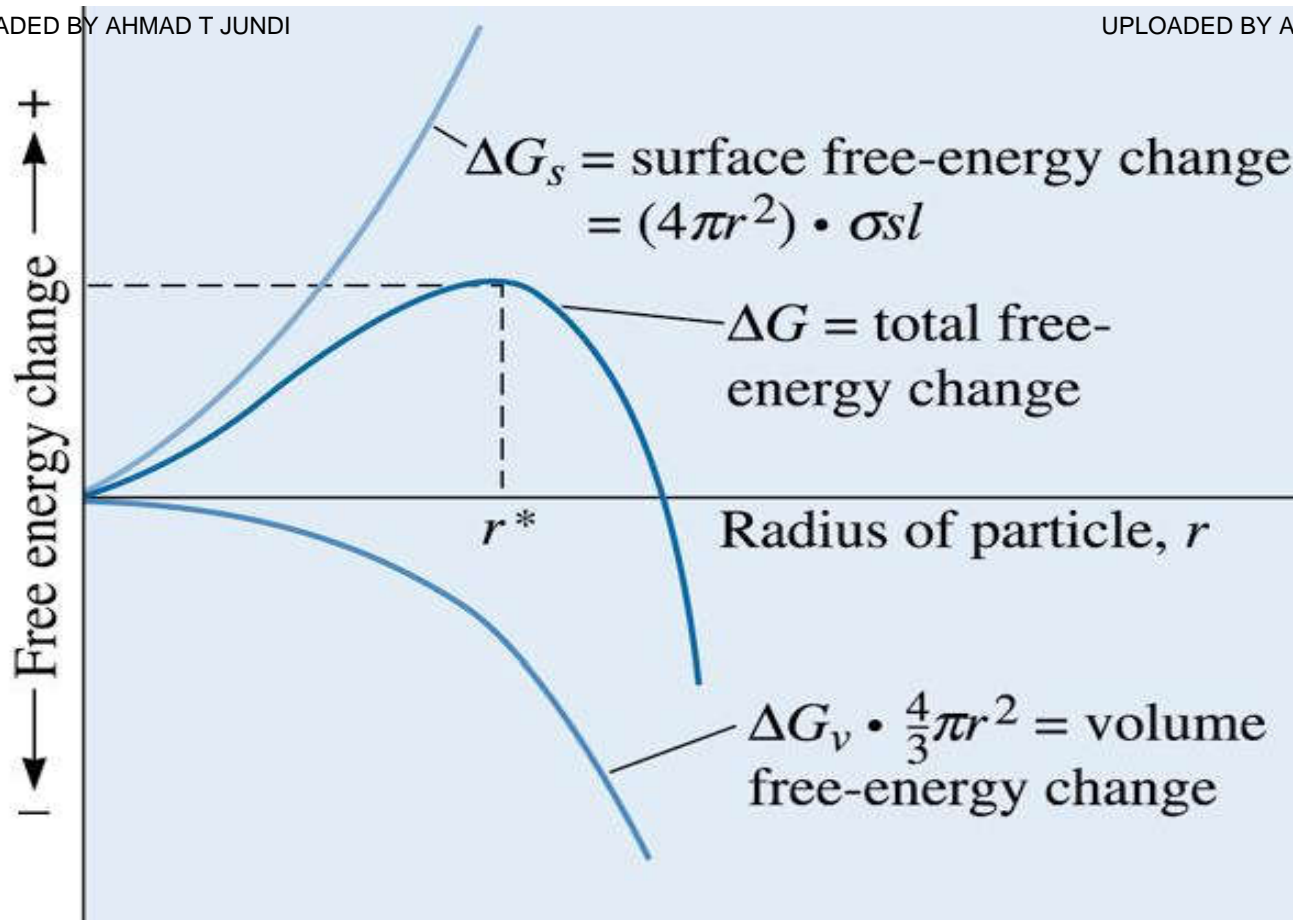


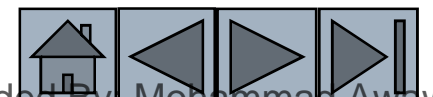
Figure 8.3 An interface is created when a solid forms from the liquid

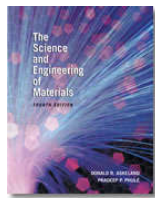




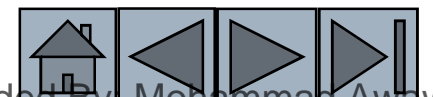
©2003 Brooks/Cole, a division of Thomson Learning, Inc. Thomson Learning,™ is a trademark used herein under license.

Figure 8.4 The total free energy of the solid-liquid system changes with the size of the solid. The solid is an embryo if its radius is less than the critical radius, and is a nucleus if its radius is greater than the critical radius



**TABLE 8-1** ■ Values for freezing temperature, latent heat of fusion, surface energy, and maximum undercooling for selected materials

	Freezing Temperature (T_m)	Heat of Fusion (ΔH_f)	Solid-Liquid Interfacial Energy (σ_{sl})	Typical Undercooling for Homogeneous Nucleation (ΔT)
Metal	(°C)	(J/cm ³)	(J/cm ²)	(°C)
Ga	30	488	56×10^{-7}	76
Bi	271	543	54×10^{-7}	90
Pb	327	237	33×10^{-7}	80
Ag	962	965	126×10^{-7}	250
Cu	1085	1628	177×10^{-7}	236
Ni	1453	2756	255×10^{-7}	480
Fe	1538	1737	204×10^{-7}	420
NaCl	801			169
CsCl	645			152
H ₂ O	0			40





Calculation of Critical Radius for the Solidification of Copper

Calculate the size of the critical radius and the number of atoms in the critical nucleus when solid copper forms by homogeneous nucleation. Comment on the size of the nucleus and assumptions we made while deriving the equation for radius of nucleus.

Example 8.1 SOLUTION

From Table 8-1:

$$\Delta T = 236^\circ\text{C} \quad T_m = 1085 + 273 = 1358 \text{ K}$$

$$\Delta H_f = 1628 \text{ J/cm}^3$$

$$\sigma_{sl} = 177 \times 10^{-7} \text{ J/cm}^2$$

$$r^* = \frac{2\sigma_{sl}T_m}{\Delta H_f\Delta T} = \frac{(2)(177 \times 10^{-7})(1358)}{(1628)(236)} = 12.51 \times 10^{-8} \text{ cm}$$





Example 8.1 SOLUTION (Continued)

The lattice parameter for FCC copper is $a_0 = 0.3615 \text{ nm} = 3.615 \times 10^{-8} \text{ cm}$

$$V_{\text{unit cell}} = (a_0)^3 = (3.615 \times 10^{-8})^3 = 47.24 \times 10^{-24} \text{ cm}^3$$

$$V_{r^*} = \frac{4}{3}\pi r^3 = \left(\frac{4}{3}\pi\right)(12.51 \times 10^{-8})^3 = 8200 \times 10^{-24} \text{ cm}^3$$

The number of unit cells in the critical nucleus is

$$\frac{8200 \times 10^{-24}}{47.24 \times 10^{-24}} = 174 \text{ unit cells}$$

Since there are four atoms in each unit cell of FCC metals, the number of atoms in the critical nucleus must be:

$$(4 \text{ atoms/cell})(174 \text{ cells/nucleus}) = 696 \text{ atoms/nucleus}$$



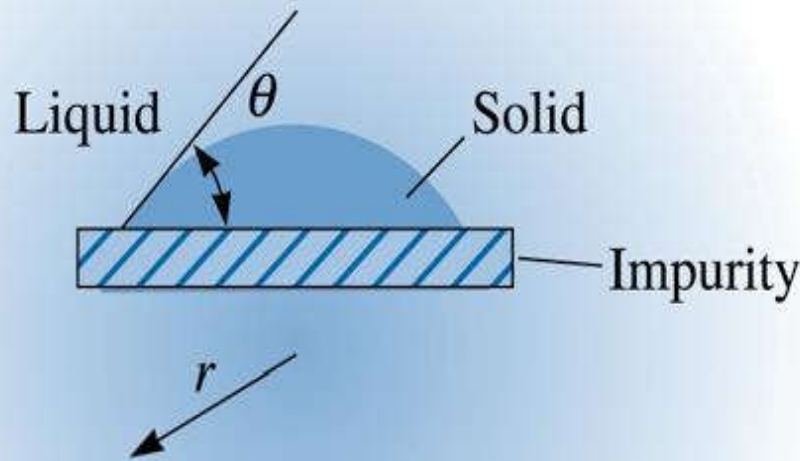
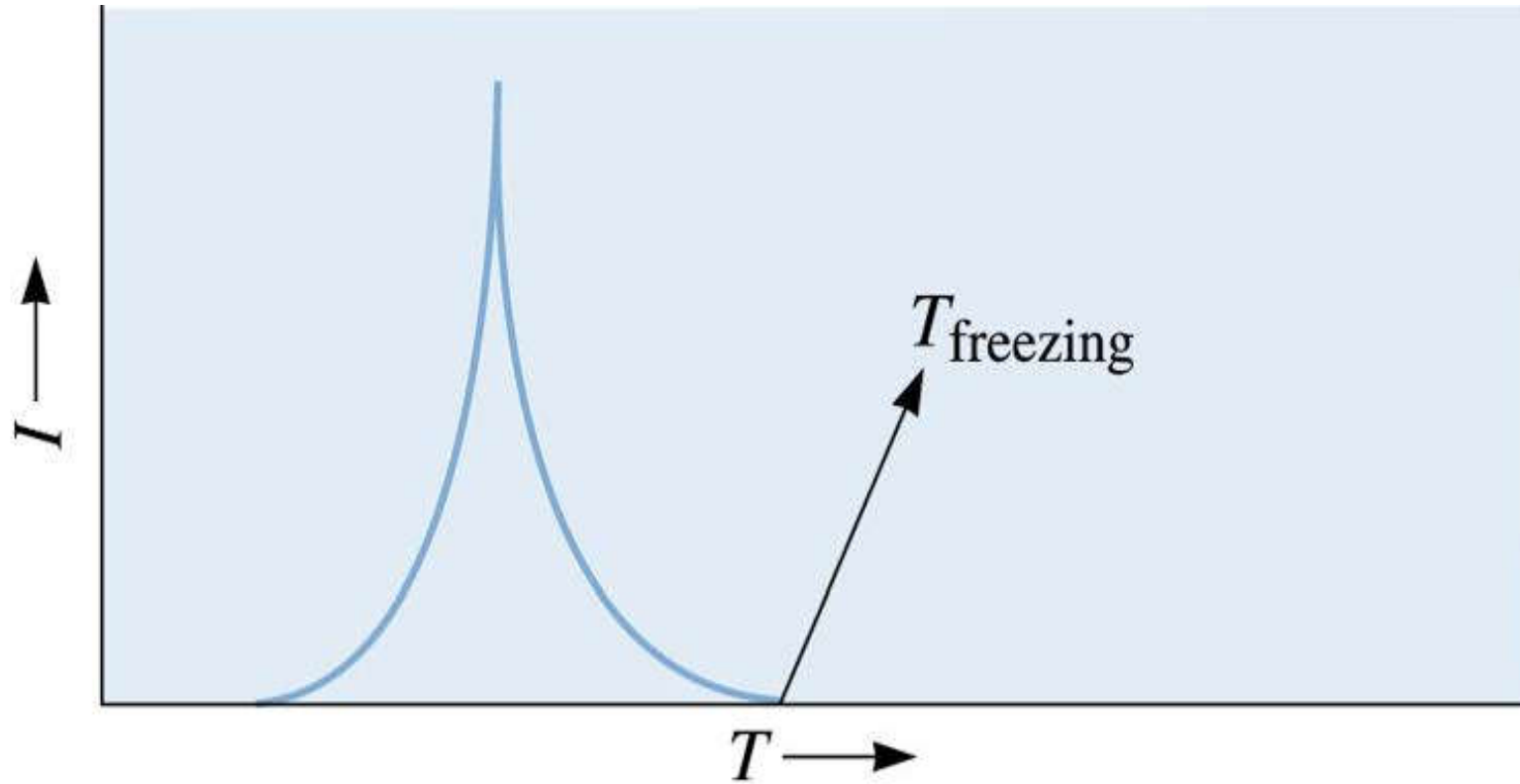


Figure 8.5 A solid forming on an impurity can assumed the critical radius with a smaller increase in the surface energy. Thus, heterogeneous nucleation can occur with relatively low undercoolings

©2003 Brooks/Cole, a division of Thomson Learning, Inc. Thomson Learning,™ is a trademark used herein under license.





©2003 Brooks/Cole, a division of Thomson Learning, Inc. Thomson Learning[®] is a trademark used herein under license.

Figure 8.6 Rate of nucleation (I) as a function of temperature of the liquid (T)





Section 8.3 Applications of Controlled Nucleation

- **Grain refinement** - The addition of heterogeneous nuclei in a controlled manner to increase the number of grains in a casting.
- **Dispersion strengthening** - Increase in strength of a metallic material by generating resistance to dislocation motion by the introduction of small clusters of a second material.
- **Solid-state phase transformation** - A change in phase that occurs in the solid state.
- **Rapid solidification processing** - Producing unique material structures by promoting unusually high cooling rates during solidification.

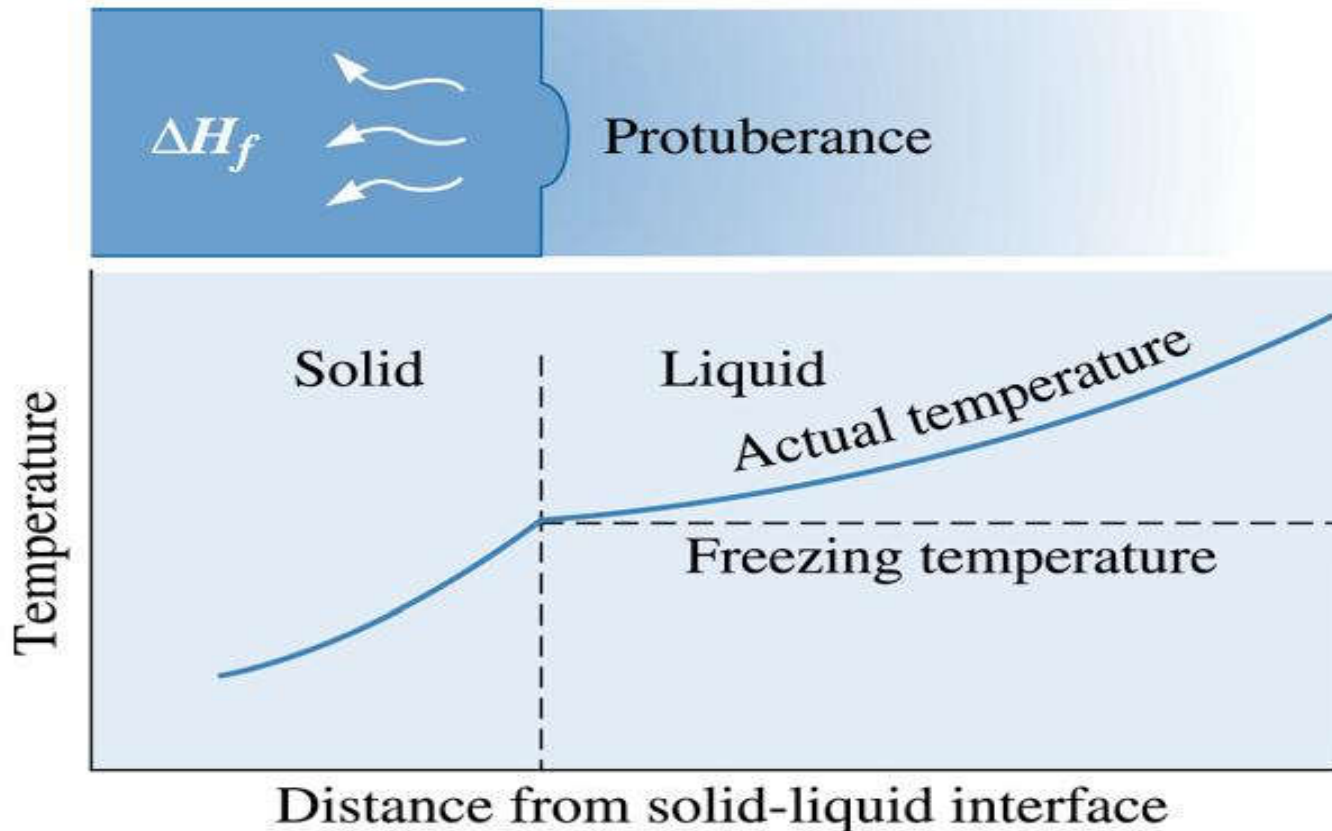




Section 8.4 Growth Mechanisms

- **Specific heat** - The heat required to change the temperature of a unit weight of the material one degree.
- **Solidification front** - Interface between a solid and liquid.
- **Planar growth** - The growth of a smooth solid-liquid interface during solidification, when no undercooling of the liquid is present.
- **Dendrite** - The treelike structure of the solid that grows when an undercooled liquid solidifies.

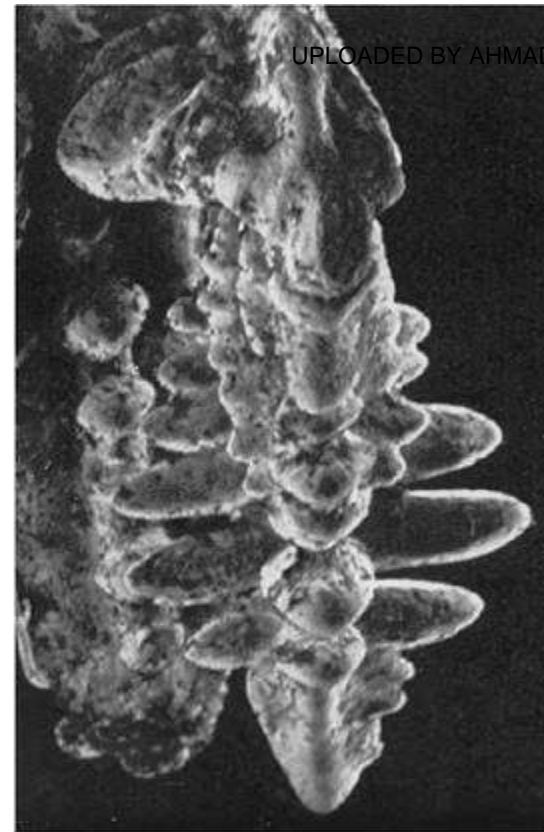
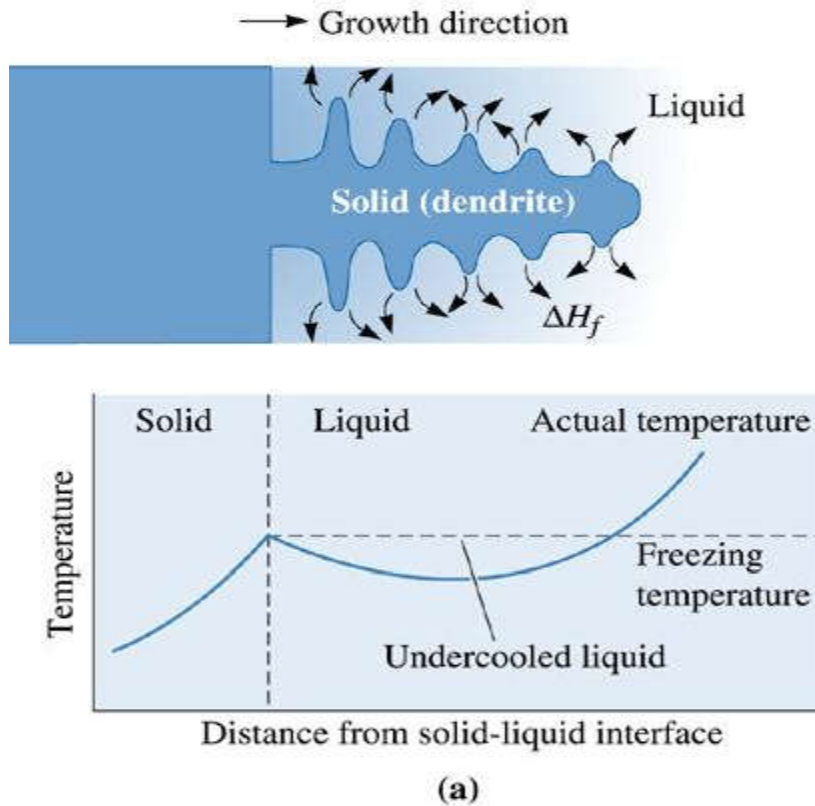




©2003 Brooks/Cole, a division of Thomson Learning, Inc. Thomson Learning[®] is a trademark used herein under license.

Figure 8.7 When the temperature of the liquid is above the freezing temperature a protuberance on the solid-liquid interface will not grow, leading to maintenance of a planer interface. Latent heat is removed from the interface through the solid





©2003 Brooks/Cole, a division of Thomson Learning, Inc. Thomson Learning[®] is a trademark used herein under license.

Figure 8.8 (a) If the liquid is undercooled, a protuberance on the solid-liquid interface can grow rapidly as a dendrite. The latent heat of fusion is removed by raising the temperature of the liquid back to the freezing temperature. (b) Scanning electron micrograph of dendrites in steel (x 15)





Section 8.5 Solidification Time and Dendrite Size

- **Chvorinov's rule** - The solidification time of a casting is directly proportional to the square of the volume-to-surface area ratio of the casting.
- **Mold constant (B)** - A characteristic constant in Chvorinov's rule.
- **Secondary dendrite arm spacing (SDAS)** - The distance between the centers of two adjacent secondary dendrite arms.





Redesign of a Casting for Improved Strength

Your company currently is producing a disk-shaped brass casting 2 in. thick and 18 in. in diameter. You believe that by making the casting solidify 25% faster, the improvement in the tensile properties of the casting will permit the casting to be made lighter in weight. Design the casting to permit this. Assume that the mold constant is 22 min/in.² for this process.





Example 8.2 SOLUTION

If d is the diameter and x is the thickness of the casting, then the volume, surface area, and solidification time of the 2-in.thick casting are:

$$V = (\pi/4)d^2x = (\pi/4)(18)^2(2) = 508.9 \text{ in.}^3$$

$$A = 2(\pi/4)d^2 + \pi dx = 2(\pi/4)(18)^2 + \pi(18)(2) = 622 \text{ in.}^2$$

$$t = B\left(\frac{V}{A}\right)^2 = (22)\left(\frac{508.9}{622}\right)^2 = 14.72 \text{ min}$$

The solidification time of the redesigned casting should be 25% shorter than the current time, or $t_r = 0.75t$, where:

$$t_r = 0.75t = (0.75)(14.72) = 11.04 \text{ min}$$





Example 8.2 SOLUTION (Continued)

Since the casting conditions have not changed, the mold constant B is unchanged. The V/A ratio of the new casting is:

$$t_r = B \left(\frac{V}{A} \right)^2 = (22) \left(\frac{V}{A} \right)^2 = 11.04 \text{ min}$$

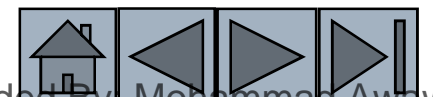
$$\left(\frac{V}{A} \right)^2 = 0.5018 \text{ in.}^2 \quad \text{or} \quad \frac{V}{A} = 0.708 \text{ in.}$$

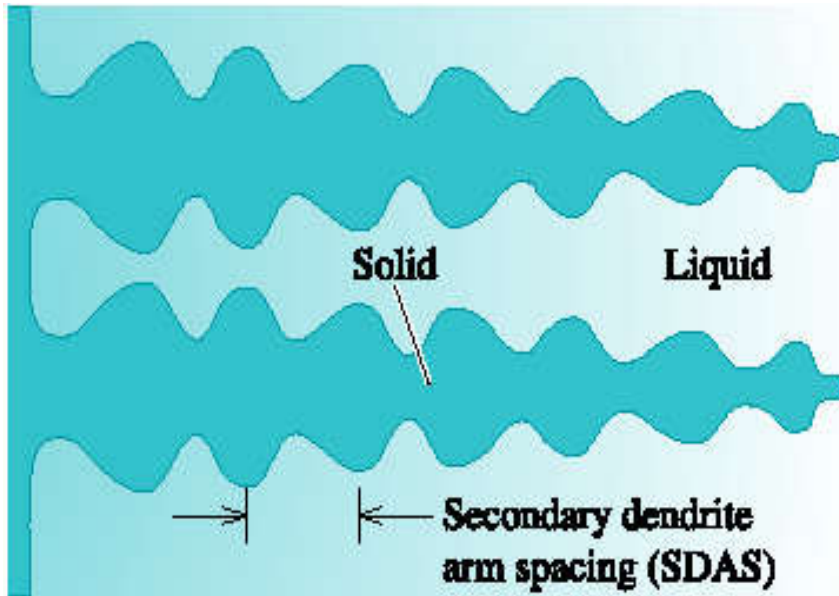
If x is the required thickness for our redesigned casting, then:

$$\frac{V_r}{A_r} = \frac{(\pi/4)d^2x}{2(\pi/4)d^2 + \pi dx} = \frac{(\pi/4)(18)^2(x)}{2(\pi/4)(18)^2 + \pi(18)(x)} = 0.708 \text{ in.}$$

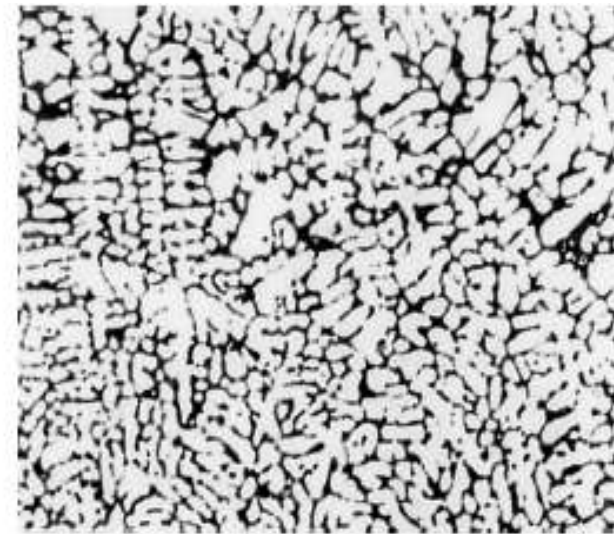
Therefore, $x = 1.68 \text{ in.}$

This thickness provides the required solidification time, while reducing the overall weight of the casting by nearly 15%.





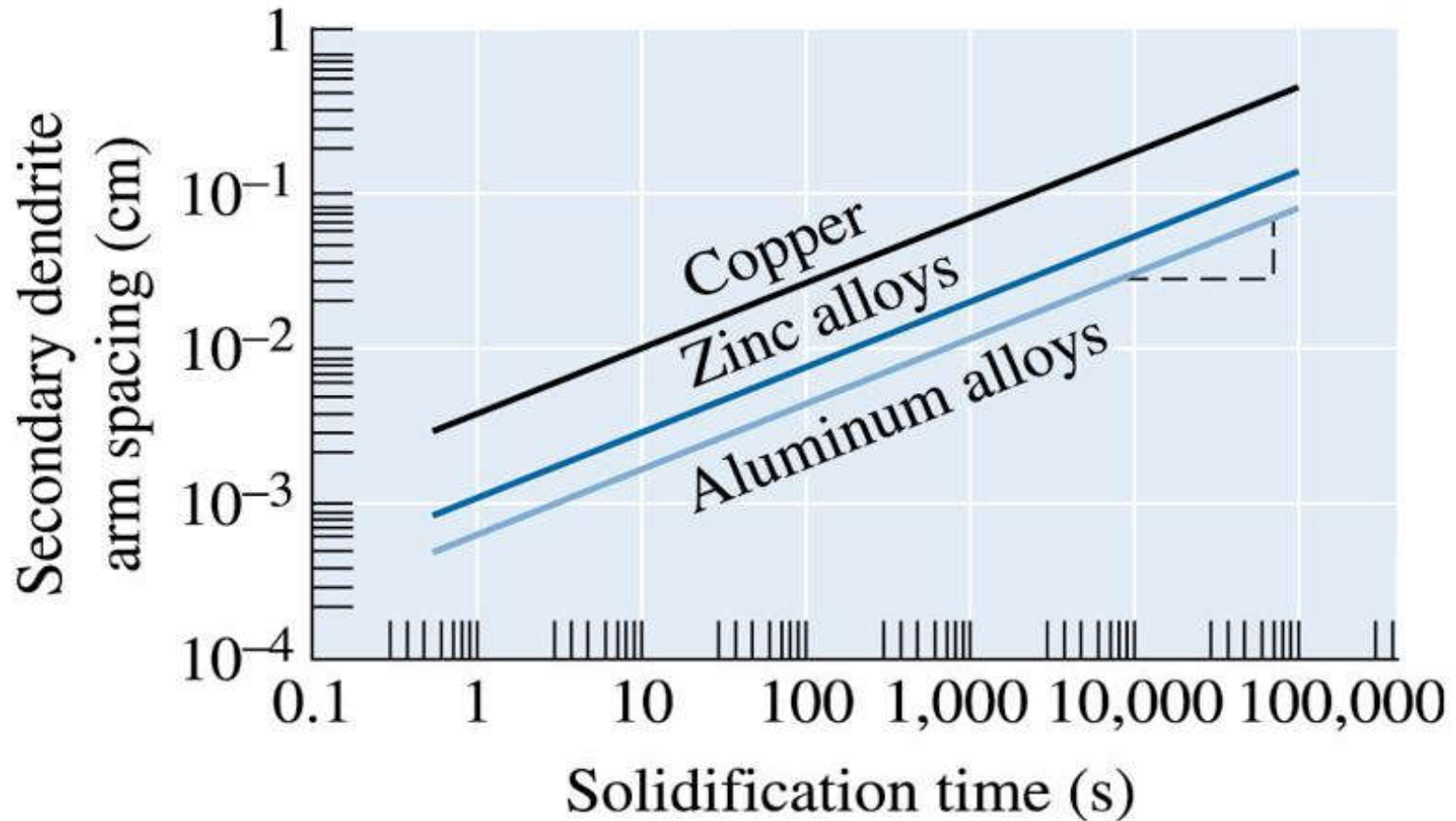
(a)



(b)

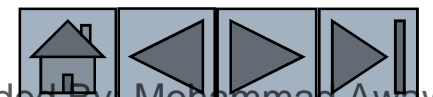
Figure 8.9 (a) The secondary dendrite arm spacing (SDAS). (b) Dendrites in an aluminum alloy (x 50). (From ASM Handbook, Vol. 9, Metallography and Microstructure (1985), ASM International, Materials Park, OH 44073-0002.)





©2003 Brooks/Cole, a division of Thomson Learning, Inc. Thomson Learning™ is a trademark used herein under license.

Figure 8.10 The effect of solidification time on the secondary dendrite arm spacings of copper, zinc and aluminum





©2003 Brooks/Cole, a division of Thomson Learning, Inc. Thomson Learning, Inc. is a trademark used herein under license.

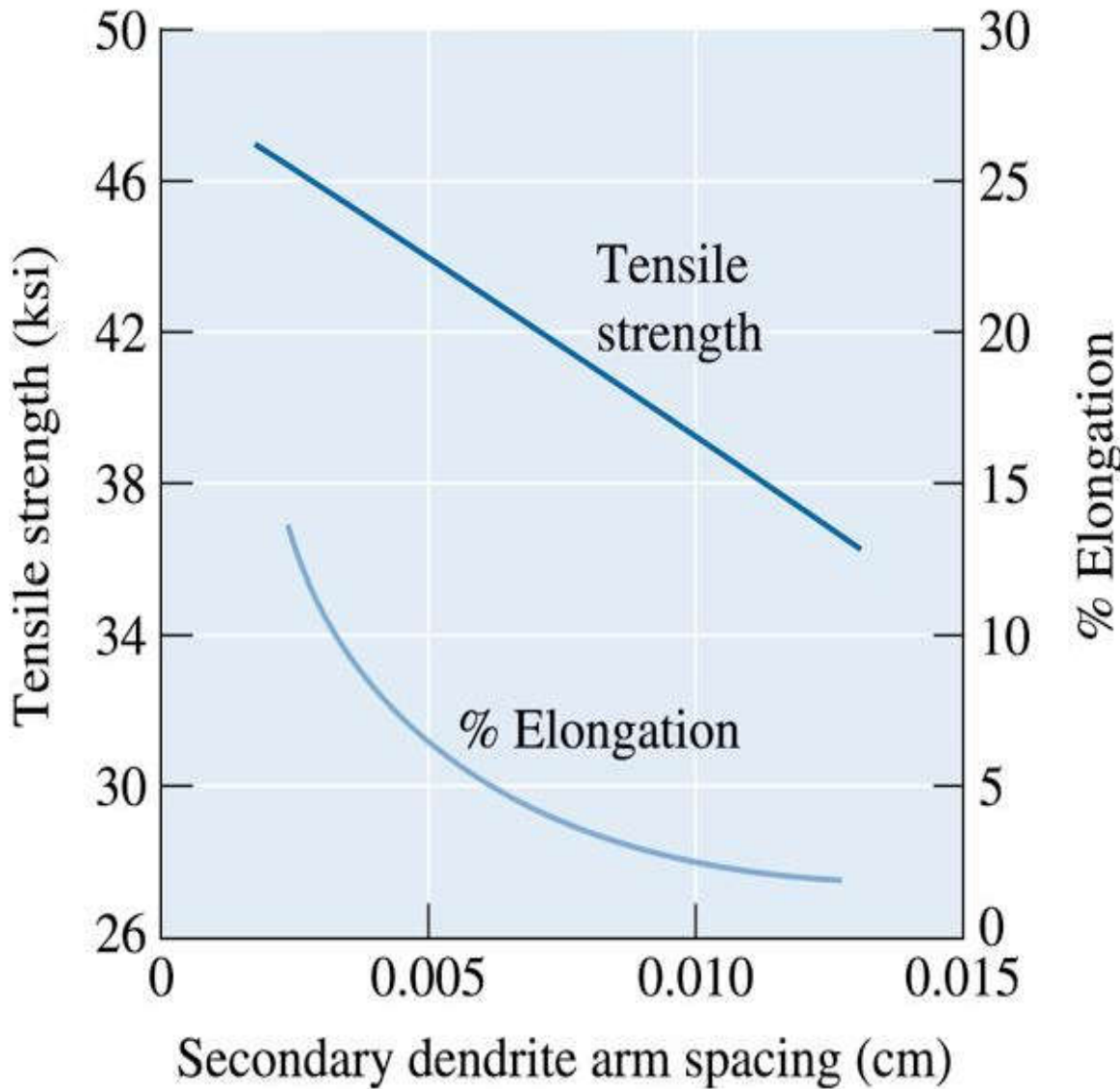
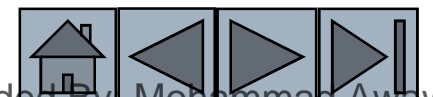


Figure 8.11 The effect of the secondary dendrite arm spacing on the properties of an aluminum casting alloy



Example 8.3



Secondary Dendrite Arm Spacing for Aluminum Alloys

Determine the constants in the equation that describe the relationship between secondary dendrite arm spacing and solidification time for aluminum alloys (Figure 8.10).

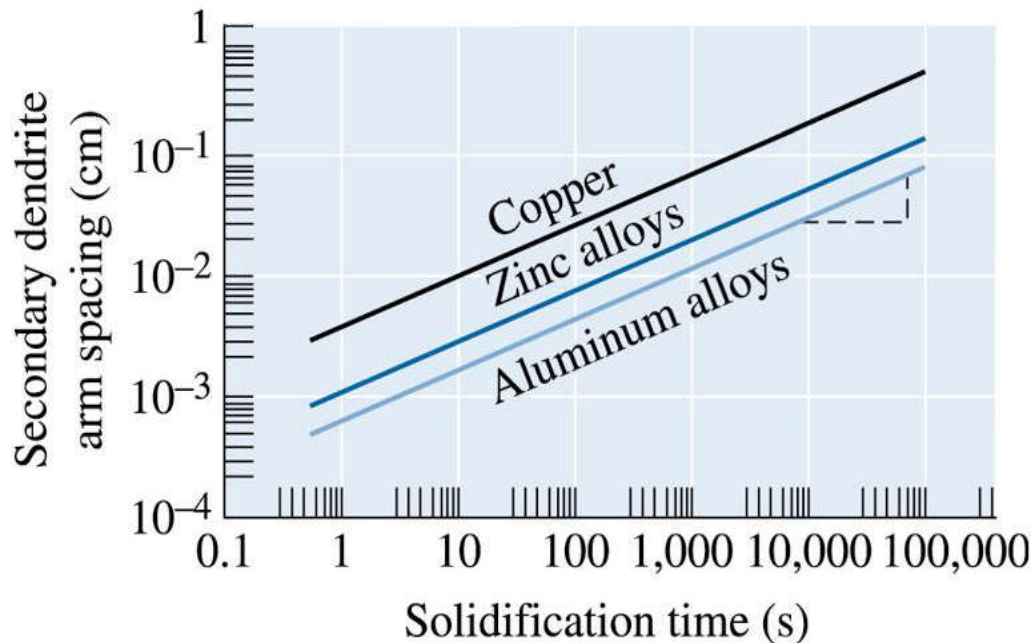


Figure 8.10 The effect of solidification time on the secondary dendrite arm spacings of copper, zinc and aluminum

©2003 Brooks/Cole, a division of Thomson Learning, Inc. Thomson Learning,™ is a trademark used herein under license.





Example 8.3 SOLUTION

Figure 8.10, we can mark five equal units on the vertical scale and 12 equal units on the horizontal scale. The slope is:

$$m = \frac{5}{12} = 0.42$$

The constant k is the value of SDAS when $t_s = 1$ s, since:

$$\log \text{SDAS} = \log k + m \log t_s$$

If $t_s = 1$ s, $m \log t_s = 0$, and $\text{SDAS} = k$, from Figure 8-10:

$$k = 8 \times 10^{-4} \frac{\text{cm}}{\text{s}^m}$$



Example 8.4

Time of Solidification



A 4-in.-diameter aluminum bar solidifies to a depth of 0.5 in. beneath the surface in 5 minutes. After 20 minutes, the bar has solidified to a depth of 1.5 in. How much time is required for the bar to solidify completely?

Example 8.4 SOLUTION

From our measurements, we can determine the constants $k_{\text{solidification}}$ and c_1 .

Solidification is complete when $d = 2$ in. (half the diameter, since freezing is occurring from all surfaces):

$$2 = 0.447\sqrt{t} - 0.4995$$

$$\sqrt{t} = \frac{2 + 0.4995}{0.447} = 5.59$$

$$t = 31.27 \text{ min}$$





Design of an Aluminum Alloy Casting

Design the thickness of an aluminum alloy casting whose length is 12 in. and width is 8 in., in order to produce a tensile strength of 40,000 psi. The mold constant in Chvorinov's rule for aluminum alloys cast in a sand mold is 45 min/in². Assume that data shown in Figures 8.10 and 8.11 can be used.

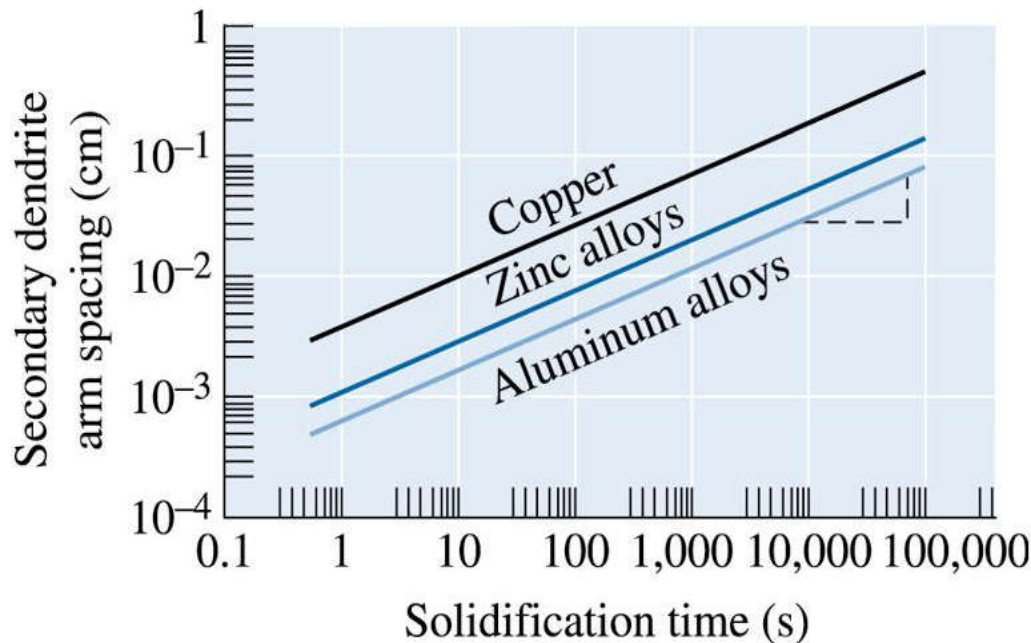
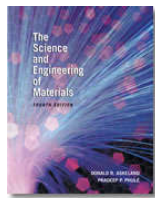


Figure 8.10 The effect of solidification time on the secondary dendrite arm spacings of copper, zinc and aluminum

©2003 Brooks/Cole, a division of Thomson Learning, Inc. Thomson Learning, is a trademark used herein under license.





Example 8.5 (Continued)

©2003 Brooks/Cole, a division of Thomson Learning, Inc. Thomson Learning, Inc. is a trademark used herein under license.

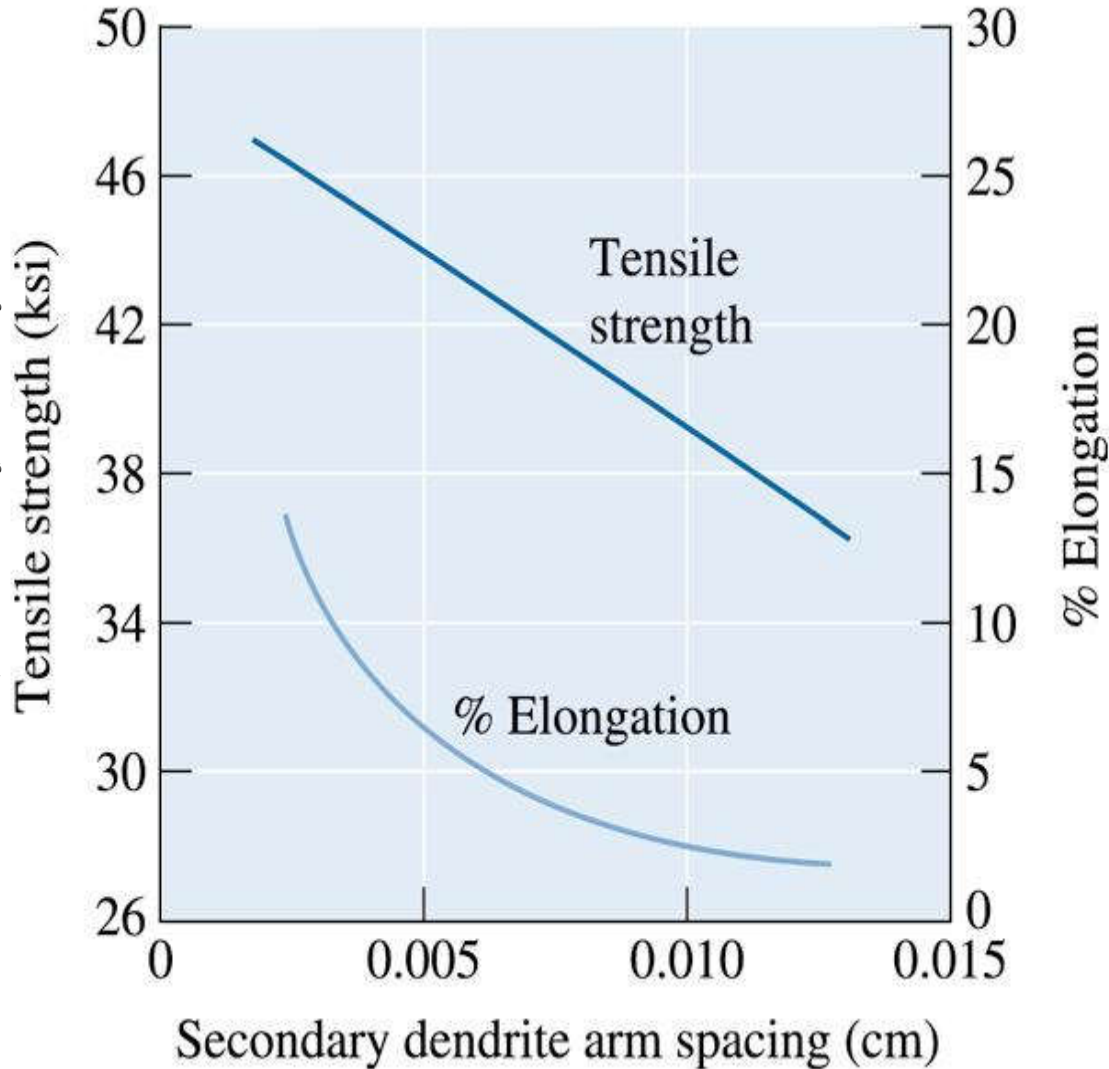


Figure 8.11 The effect of the secondary dendrite arm spacing on the properties of an aluminum casting alloy





Example 8.5 SOLUTION

Since the length is 12 in. and the width is 8 in.:

$$V = (8)(12)(x) = 96x$$

$$A = (2)(8)(12) + (2)(x)(8) + (2)(x)(12) = 40x + 192$$

$$5 \text{ min} = (45 \text{ min/in.}^2) \left(\frac{96x}{40x + 192} \right)^2$$

Thickness of an aluminum alloy casting

$$x = 0.77 \text{ in.}$$

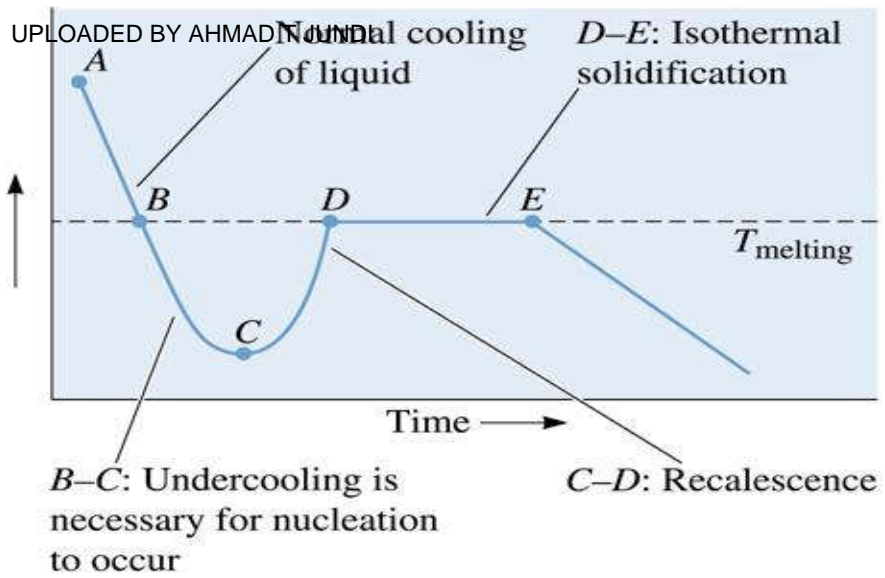
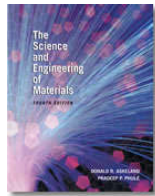




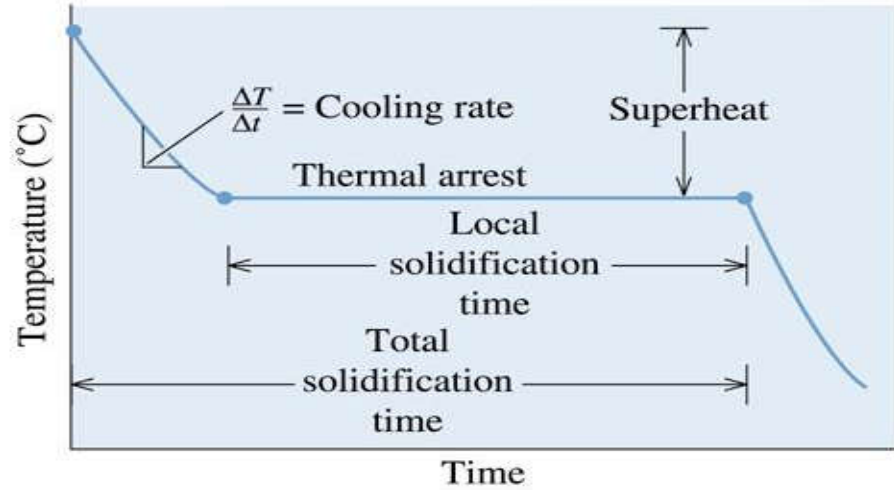
Section 8.6 Cooling Curves

- **Recalescence** - The increase in temperature of an undercooled liquid metal as a result of the liberation of heat during nucleation.
- **Thermal arrest** - A plateau on the cooling curve during the solidification of a material caused by the evolution of the latent heat of fusion during solidification.
- **Total solidification time** - The time required for the casting to solidify completely after the casting has been poured.
- **Local solidification time** - The time required for a particular location in a casting to solidify once nucleation has begun.





(a)



(b)

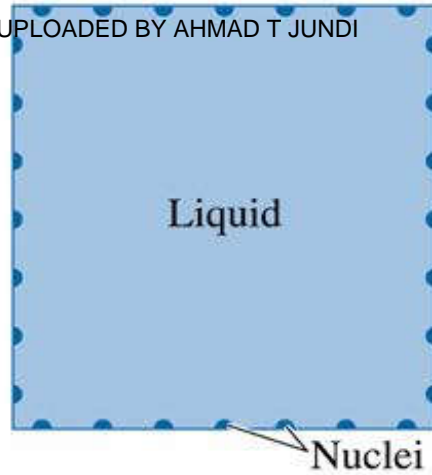
Figure 8.12 (a) Cooling curve for a pure metal that has not been well inoculated. Liquid cools as specific heat is removed (between points A and B). Undercooling is thus necessary (between points B and C). As the nucleation begins (point C), latent heat of fusion is released causing an increase in the temperature of the liquid. This process is known as recalescence (point C to point D). Metal continues to solidify at a constant temperature ($T_{melting}$). At point E, solidification is complete. Solid casting continues to cool from the point. (b) Cooling curve for a well inoculated, but otherwise pure metal. No undercooling is needed. Recalescence is not observed. Solidification begins at the melting temperature



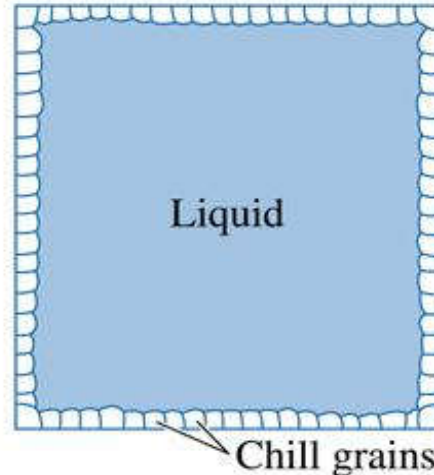
Section 8.7 Cast Structure

- **Chill zone** - A region of small, randomly oriented grains that forms at the surface of a casting as a result of heterogeneous nucleation.
- **Columnar zone** - A region of elongated grains having a preferred orientation that forms as a result of competitive growth during the solidification of a casting.
- **Equiaxed zone** - A region of randomly oriented grains in the center of a casting produced as a result of widespread nucleation.

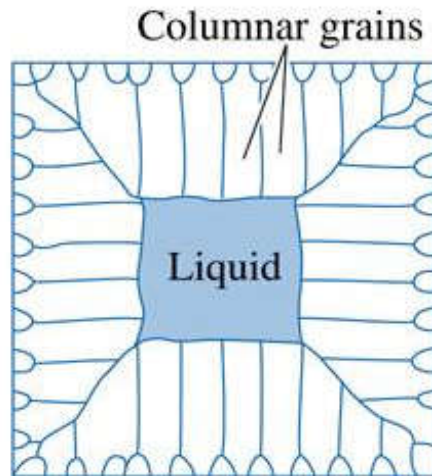




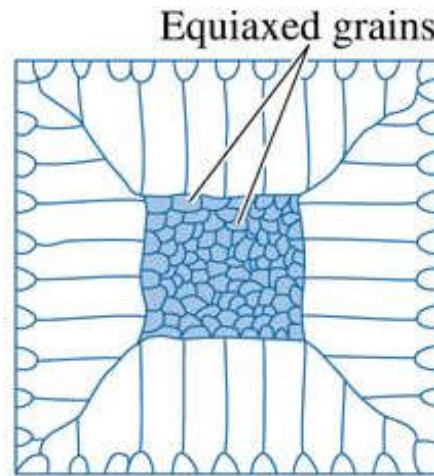
(a)



(b)

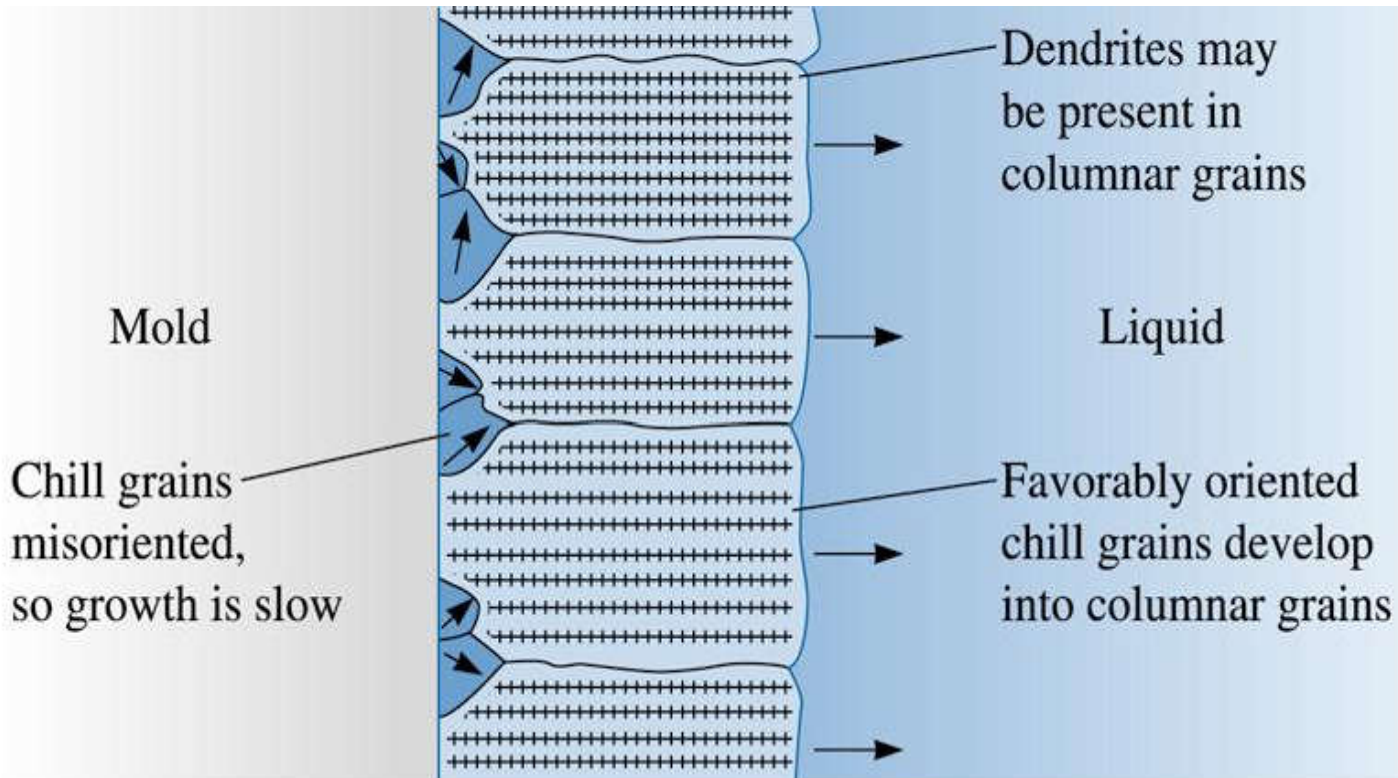


(c)



(d)

Figure 8.13
Development of the ingot structure of a casting during solidification: (a) Nucleation begins, (b) the chill zone forms, (c) preferred growth produces the columnar zone³, and (d) additional nucleation creates the equiaxed zone



©2003 Brooks/Cole, a division of Thomson Learning, Inc. Thomson Learning,™ is a trademark used herein under license.

Figure 8.14 Competitive growth of the grains in the chill zone results in only those grains with favorable orientations developing into columnar grains





Section 8.8 Solidification Defects

- **Shrinkage** - Contraction of a casting during solidification.
- **Microshrinkage** - Small, frequently isolated pores between the dendrite arms formed by the shrinkage that accompanies solidification.
- **Gas porosity** - Bubbles of gas trapped within a casting during solidification, caused by the lower solubility of the gas in the solid compared with that in the liquid.
- **Sievert's law** - The amount of a gas that dissolves in a metal is proportional to the partial pressure of the gas in the surroundings.



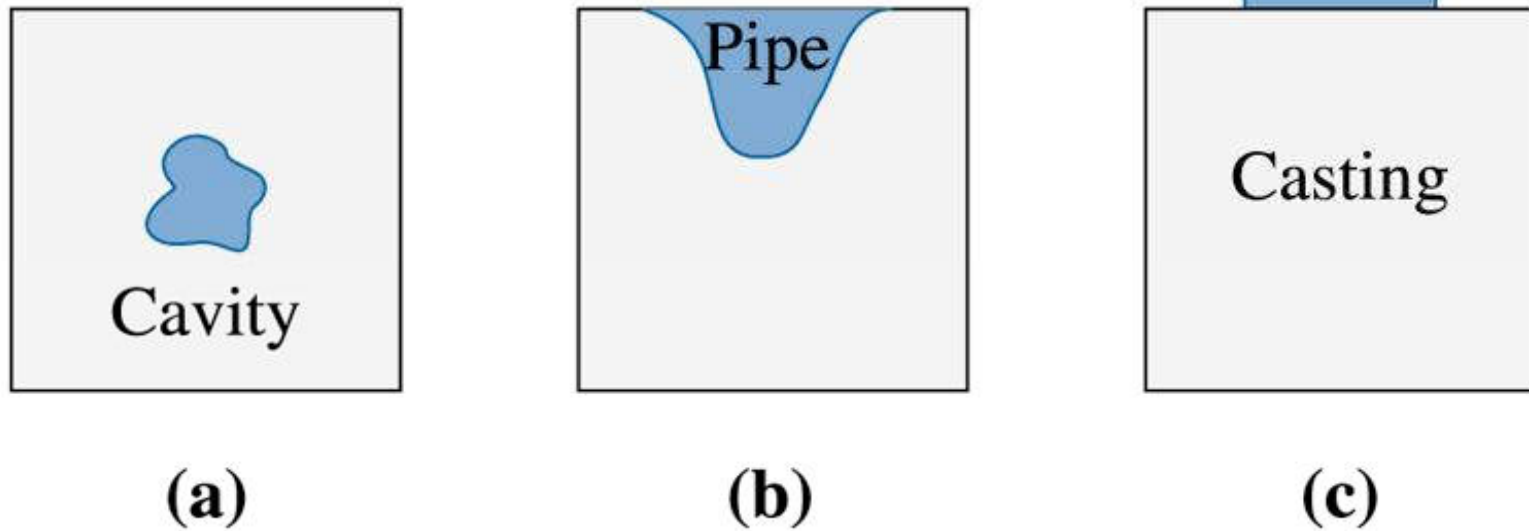


TABLE 8-2 ■ Shrinkage during solidification for selected materials

Material	Shrinkage (%)
Al	7.0
Cu	5.1
Mg	4.0
Zn	3.7
Fe	3.4
Pb	2.7
Ga	+3.2 (expansion)
H ₂ O	+8.3 (expansion)
Low-carbon steel	2.5–3.0
High-carbon steel	4.0
White Cast Iron	4.0–5.5
Gray Cast Iron	+1.9 (expansion)

Note: Some data from Ref. [9]





©2003 Brooks/Cole, a division of Thomson Learning, Inc. Thomson Learning[®] is a trademark used herein under license.

Figure 8.15 Several types of macroshrinkage can occur, including cavities and pipes. Risers can be used to help compensate for shrinkage





Example 8.6

Design of a Riser for a Casting

Design a cylindrical riser, with a height equal to twice its diameter, that will compensate for shrinkage in a 2 cm × 8 cm 16 cm casting (Figure 8.16).

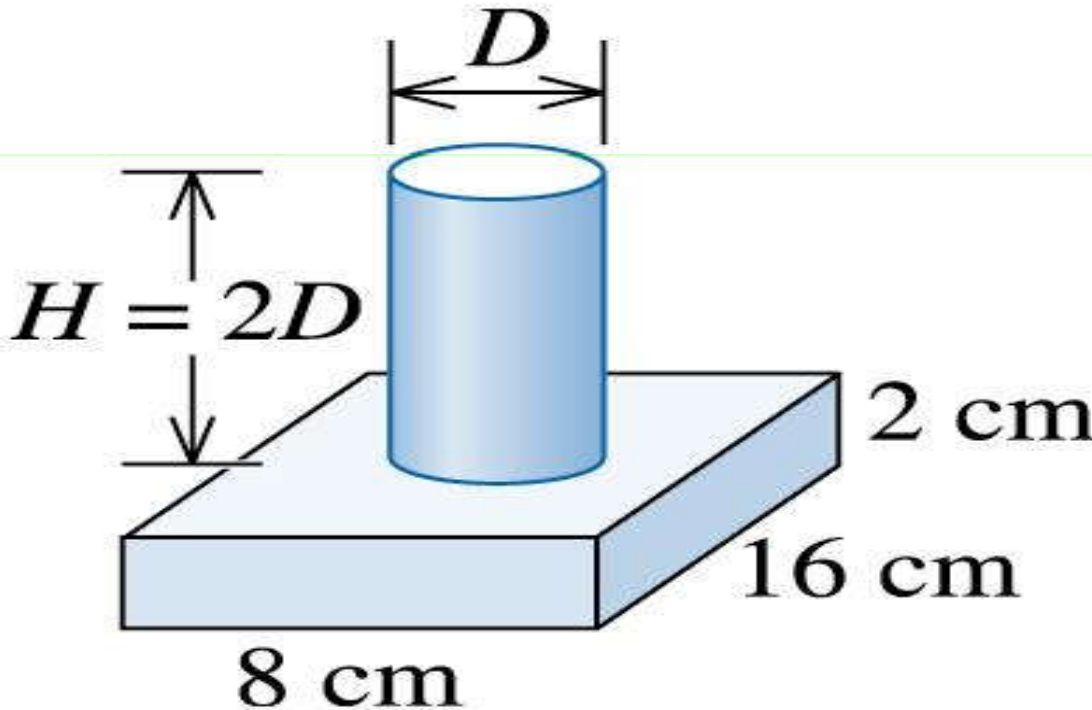
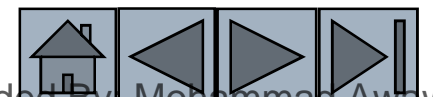


Figure 8.16 The geometry of the casting and riser (for Example 8.6)

©2003 Brooks/Cole, a division of Thomson Learning, Inc. Thomson Learning is a trademark used herein under license.





Example 8.6 SOLUTION

We know that the riser must freeze after the casting. To be conservative, however, we typically require that the riser take 25% longer to solidify than the casting.

Therefore:

$$t_{\text{riser}} = 1.25t_{\text{casting}} \quad \text{or} \quad B \left(\frac{V}{A} \right)_r^2 = 1.25B \left(\frac{V}{A} \right)_c^2$$

Subscripts r and c stand for riser and casting, respectively.

The mold constant B is the same for both casting and riser, so:

$$\left(\frac{V}{A} \right)_r = \sqrt{1.25 \left(\frac{V}{A} \right)_c}$$

$$V_c = (2)(8)(16) = 256 \text{ cm}^3$$

$$A_c = (2)(2)(8) + (2)(2)(16) + (2)(8)(16) = 352 \text{ cm}^2$$





Example 8.6 SOLUTION (Continued)

We can write equations for the volume and area of a cylindrical riser, noting that $H = 2D$:

$$V_r = (\pi/4)D^2H = (\pi/4)D^2(2D) = (\pi/2)D^3$$

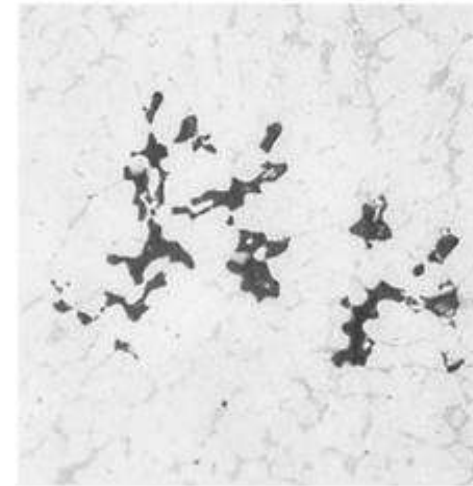
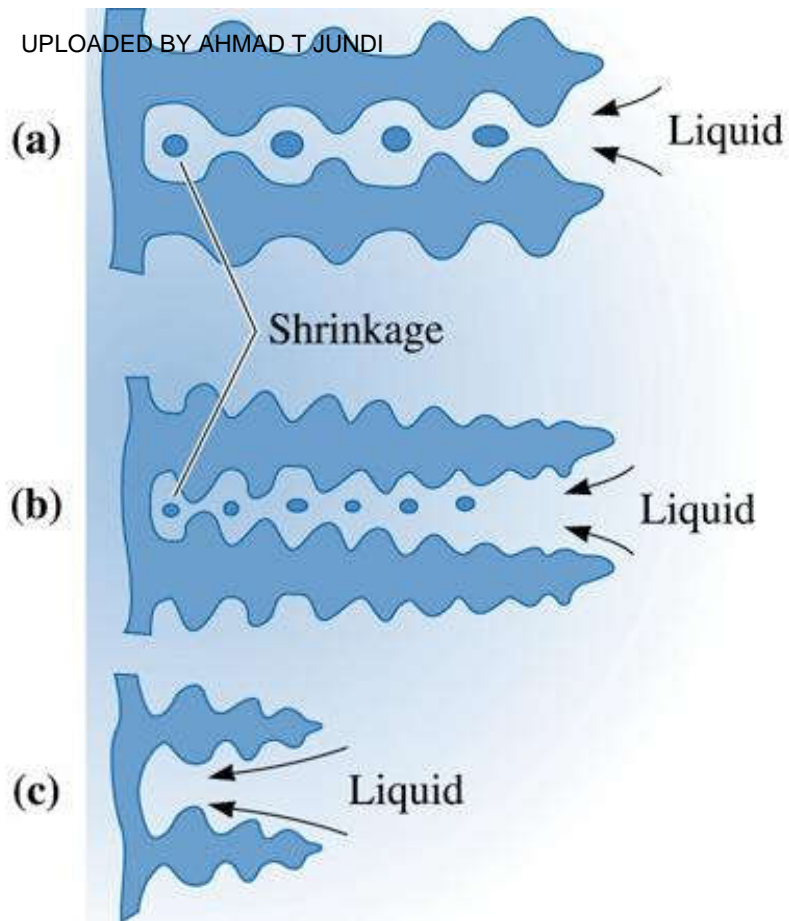
$$A_r = 2(\pi/4)D^2 + \pi DH = 2(\pi/4)D^2 + \pi D(2D) = (5\pi/2)D^2$$

$$\frac{V_r}{A_r} = \frac{(\pi/2)(D)^3}{(5\pi/2)(D)^2} = \frac{D}{5} > \sqrt{\frac{(1.25)(256)}{352}}$$

$$D = 4.77 \text{ cm} \quad H = 2D = 9.54 \text{ cm} \quad V_r = 170.5 \text{ cm}^3$$

Although the volume of the riser is less than that of the casting, the riser solidifies more slowly because of its compact shape.

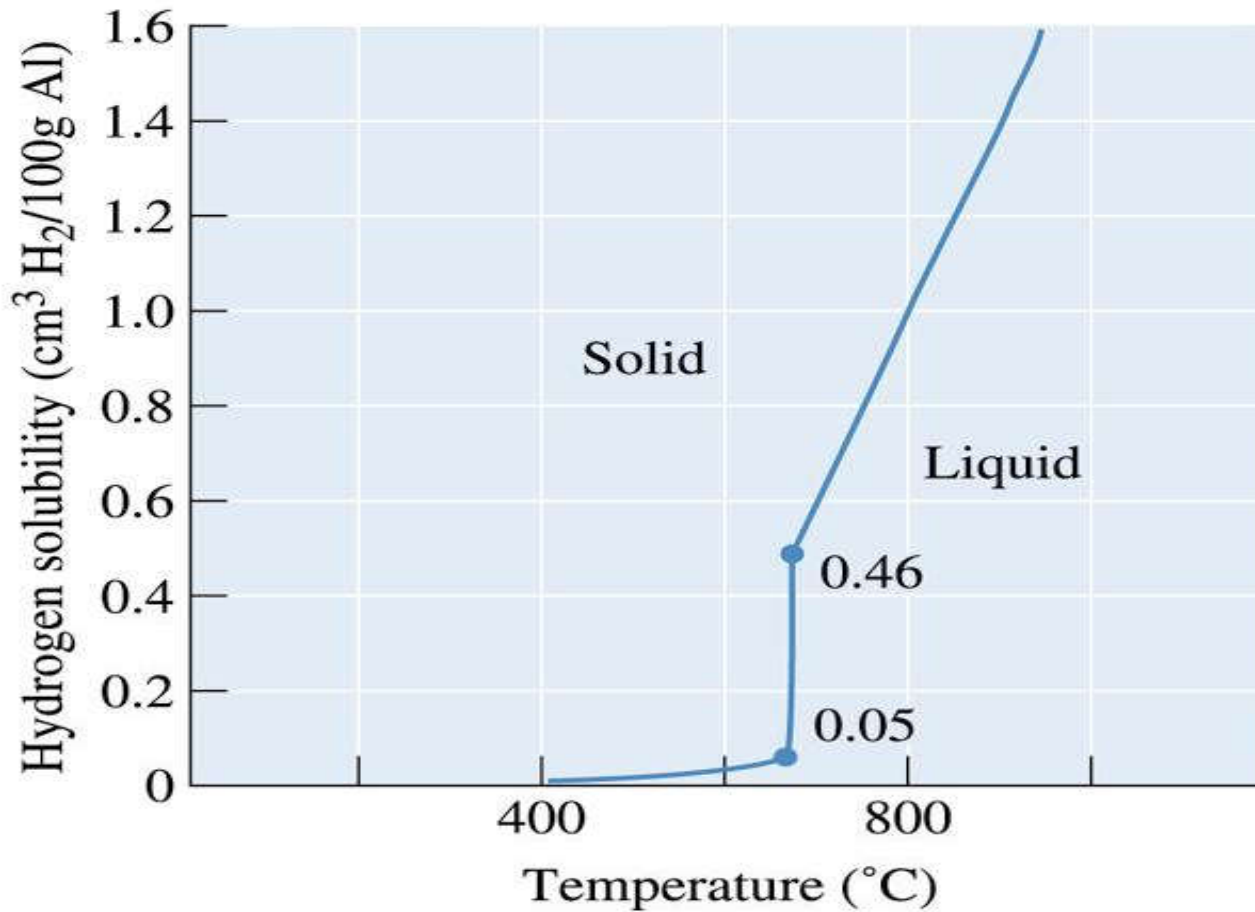




(d)

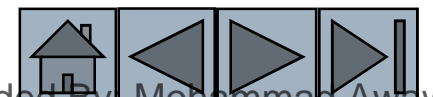
©2003 Brooks/Cole, a division of Thomson Learning, Inc. Thomson Learning[™] is a trademark used herein under license.

Figure 8.17 (a) Shrinkage can occur between the dendrite arms. (b) Small secondary dendrite arm spacings result in smaller, more evenly distributed shrinkage porosity. (c) Short primary arms can help avoid shrinkage. (d) Interdendritic shrinkage in an aluminum alloy is shown (x 80)



©2003 Brooks/Cole, a division of Thomson Learning, Inc. Thomson Learning,™ is a trademark used herein under license.

Figure 8.18 The solubility of hydrogen gas in aluminum when the partial pressure of H₂ = 1 atm.





Example 8.7

Design of a Degassing Process for Copper

After melting at atmospheric pressure, molten copper contains 0.01 weight percent oxygen. To assure that your castings will not be subject to gas porosity, you want to reduce the weight percent to less than 0.00001% prior to pouring. Design a degassing process for the copper.





Example 8.7 SOLUTION

In one approach, the liquid copper is placed in a vacuum chamber; the oxygen is then drawn from the liquid and carried away into the vacuum. The vacuum required can be estimated from Sievert's law:

$$\frac{\%O_{\text{initial}}}{\%O_{\text{vacuum}}} = \frac{K\sqrt{p_{\text{initial}}}}{K\sqrt{p_{\text{vacuum}}}} = \sqrt{\left(\frac{1 \text{ atm.}}{p_{\text{vacuum}}}\right)}$$

$$\frac{1 \text{ atm.}}{p_{\text{vacuum}}} = (1000)^2 \quad \text{or} \quad p_{\text{vacuum}} = 10^{-6} \text{ atm.}$$

Another approach would be to introduce a copper-15% phosphorous alloy. The phosphorous reacts with oxygen to produce P_2O_5 , which floats out of the liquid, by the reaction:





Section 8.9 Casting Processes for Manufacturing Components

- ❑ **Sand casting** - A casting process using sand molds.
- ❑ **Investment casting** - A casting process that is used for making complex shapes such as turbine blades, also known as the lost wax process.
- ❑ **Lost foam process** - A process in which a polymer foam is used as a pattern to produce a casting.
- ❑ **Permanent mold casting** - A casting process in which a mold can be used many times.
- ❑ **Pressure die casting** - A casting process in which molten metal/alloys is forced into a die under pressure.



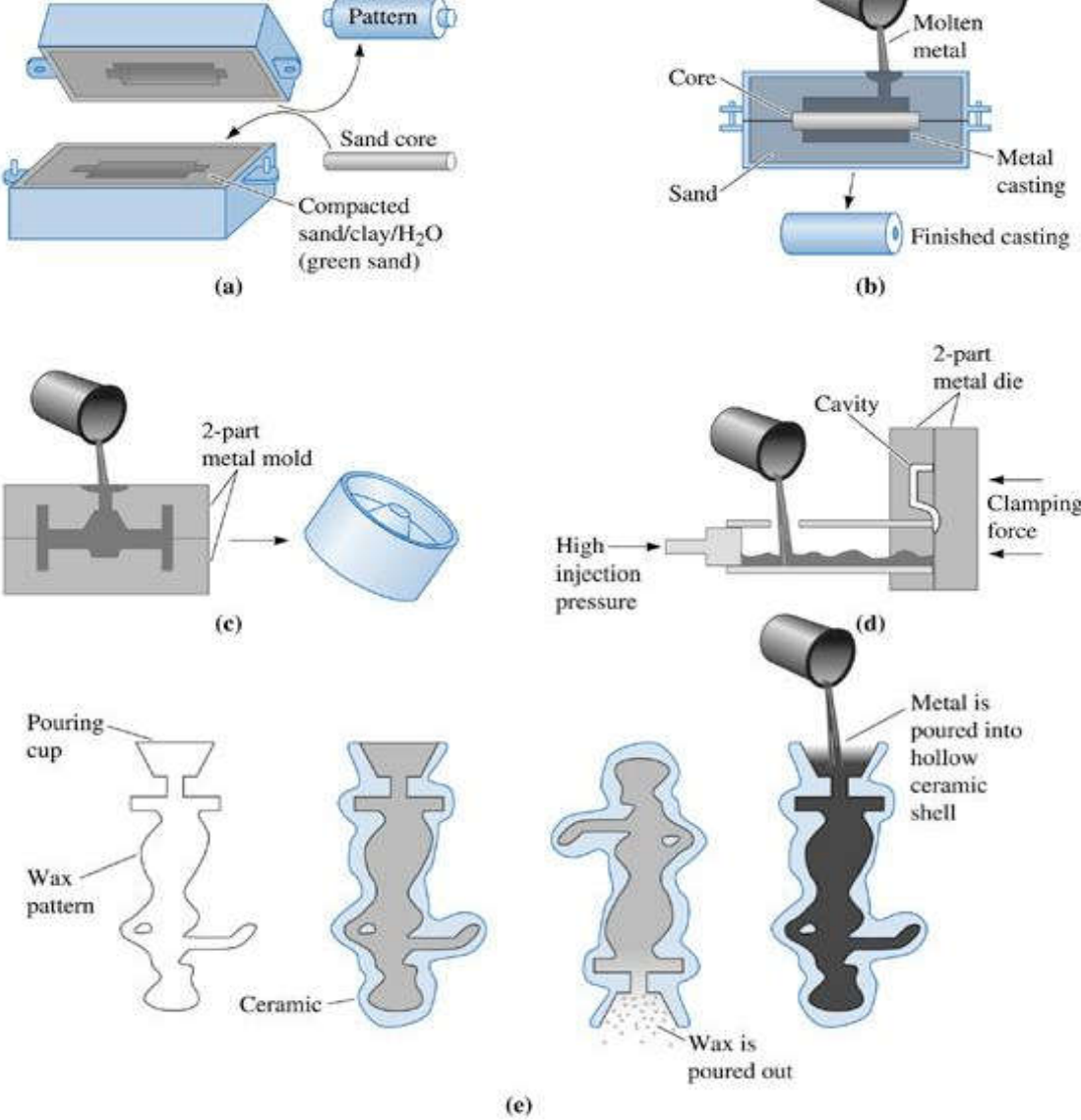


Figure 8.19 Four typical casting processes: (a) and (b) Green sand molding, in which clay-bonded sand is packed around a pattern. Sand cores can produce internal cavities in the casting. (c) The permanent mold process, in which metal is poured into an iron or steel mold. (d) Die casting, in which metal is injected at high pressure into a steel die. (e) Investment casting, in which a wax pattern is surrounded by a ceramic; after the wax is melted and drained, metal is poured into the mold

©2003 Brooks/Cole, a division of Thomson Learning, Inc. Thomson Learning is a trademark used herein under license.

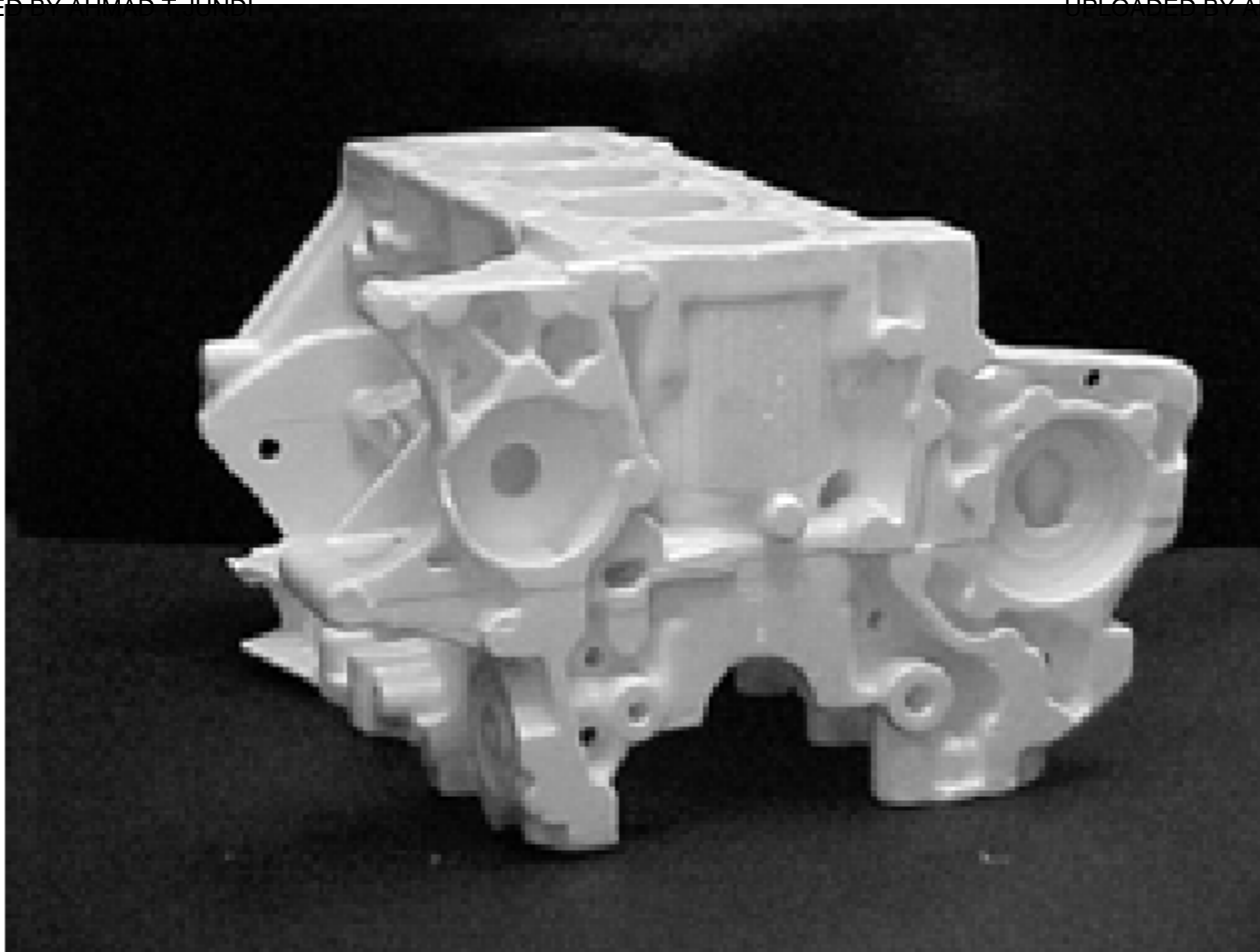


Figure 8-20 Engine block produced using the lost foam casting process. (Courtesy of Paul Arch, Nova Chemicals.)





Section 8.10 Continuous Casting and Ingot Casting

- **Ingot casting** - The process of casting ingots. This is different from the continuous casting route.
- **Continuous casting** - A process to convert molten metal or an alloy into a semi-finished product such as a slab.



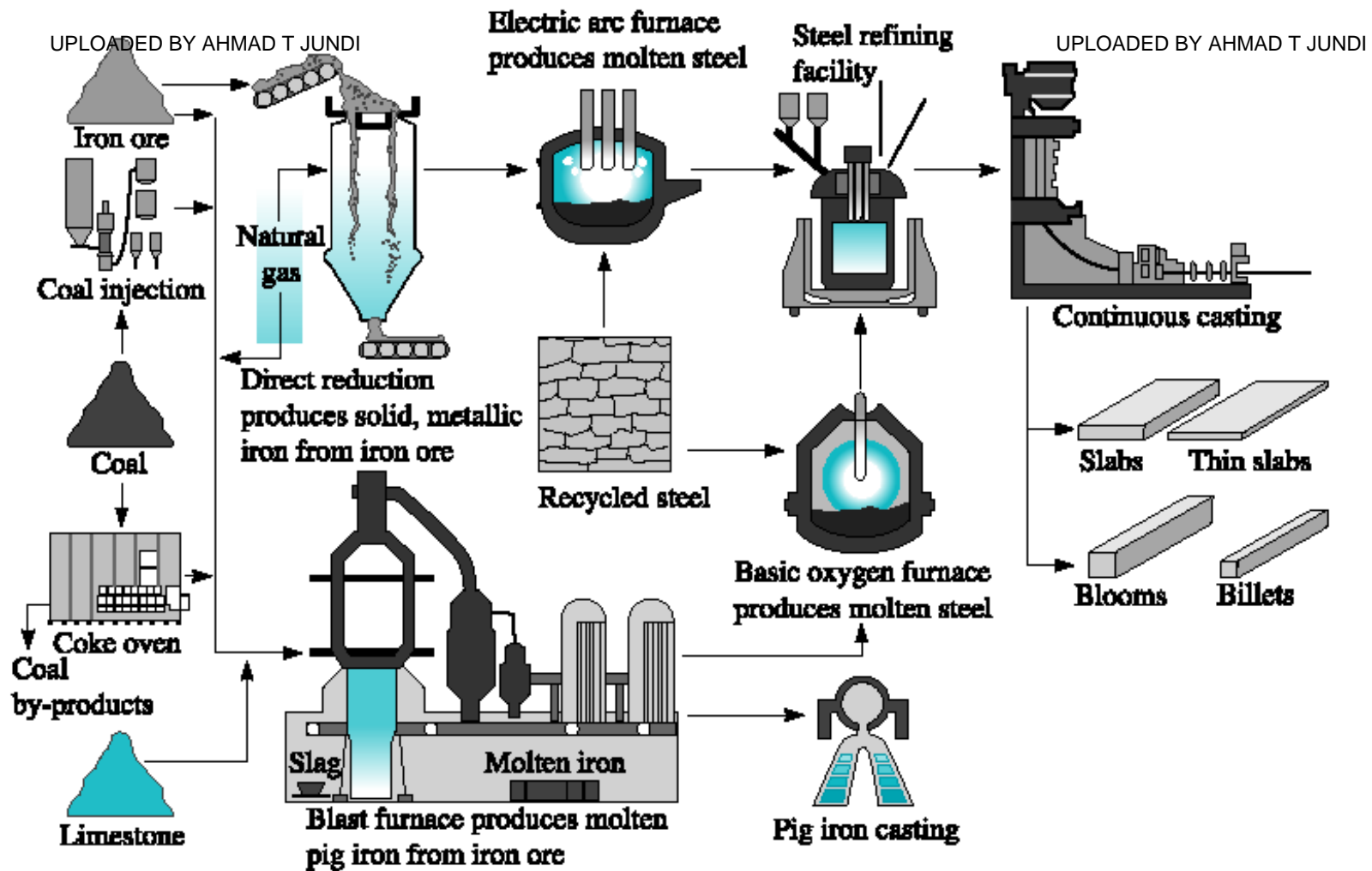


Figure 8.21 Summary of steps in the extraction of steels using iron ores, coke and limestone. (Source: www.steel.org. Used with permission of the American Iron and Steel Institute.)



©2003 Brooks/Cole, a division of Thomson Learning, Inc. Thomson Learning is a trademark used herein under license.

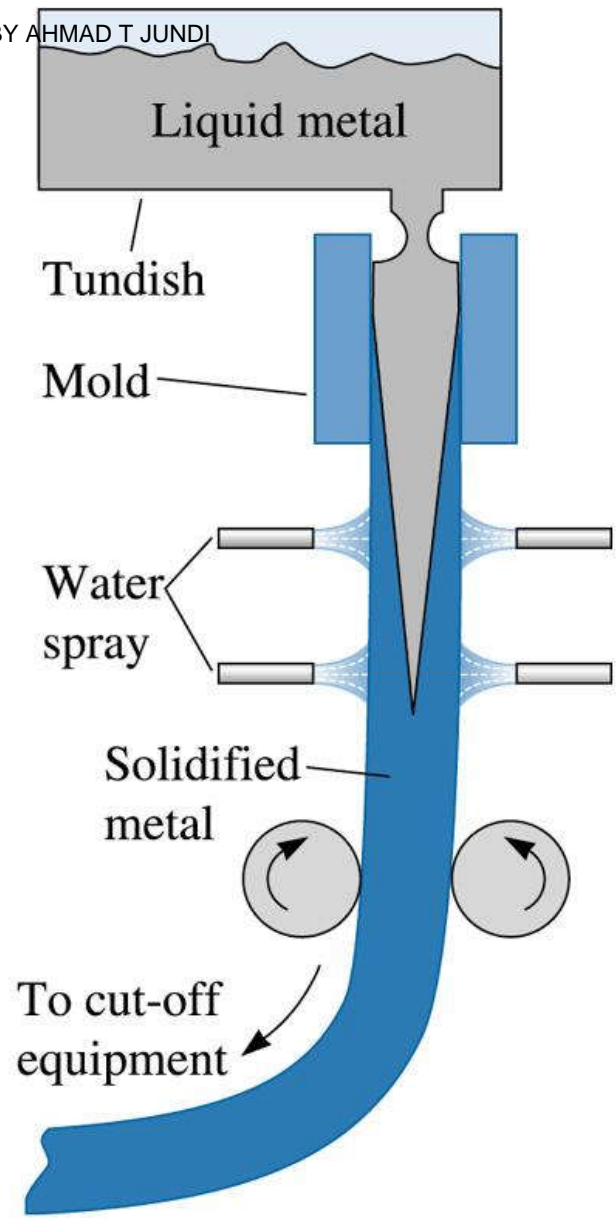


Figure 8.22 Vertical continuous casting, used in producing many steel products. Liquid metal contained in the tundish partially solidifies in a mold

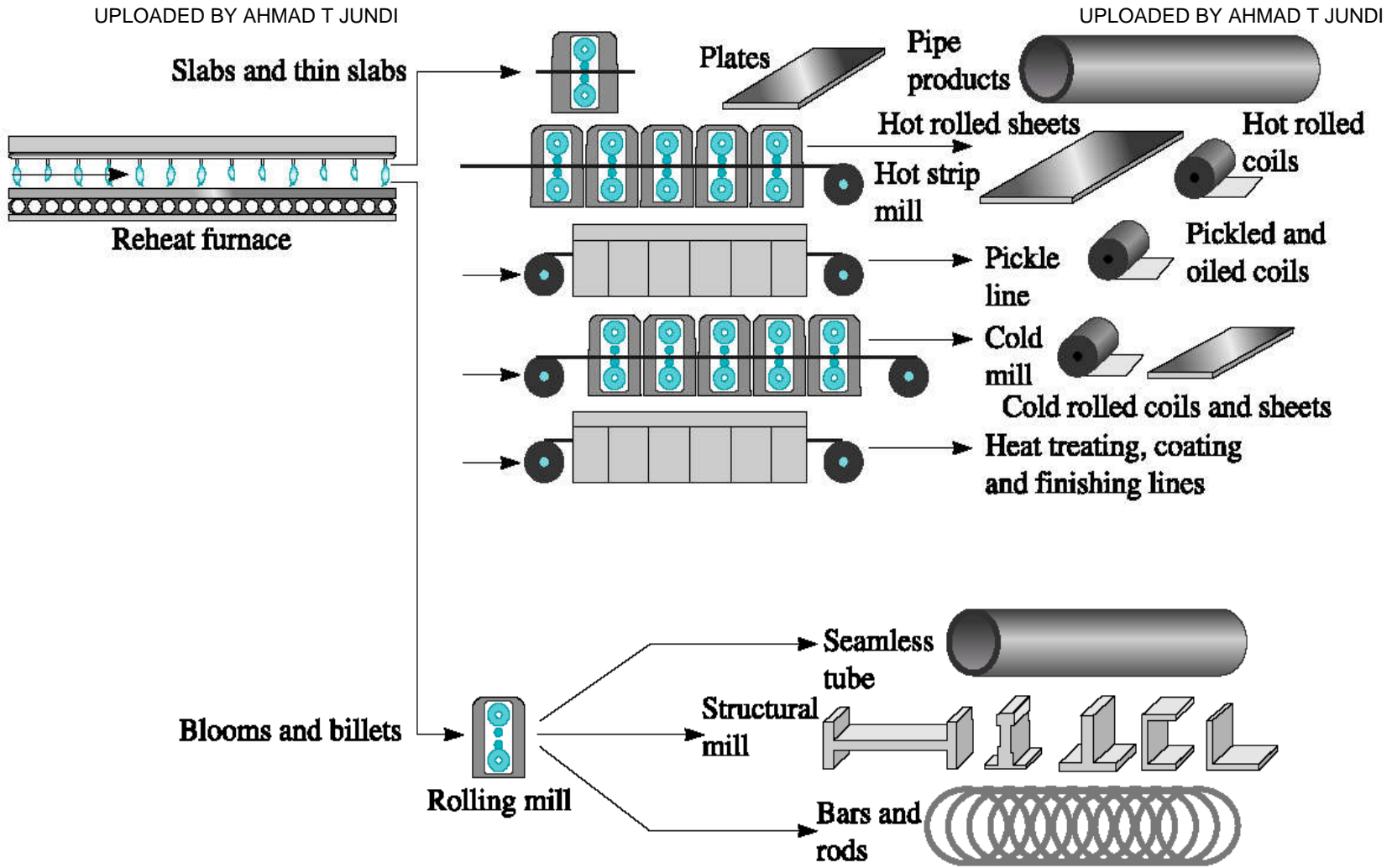


Figure 8.23 Secondary processing steps in processing of steel and alloys. (Source: www.steel.org. Used with permission of the American Iron and Steel Institute.)

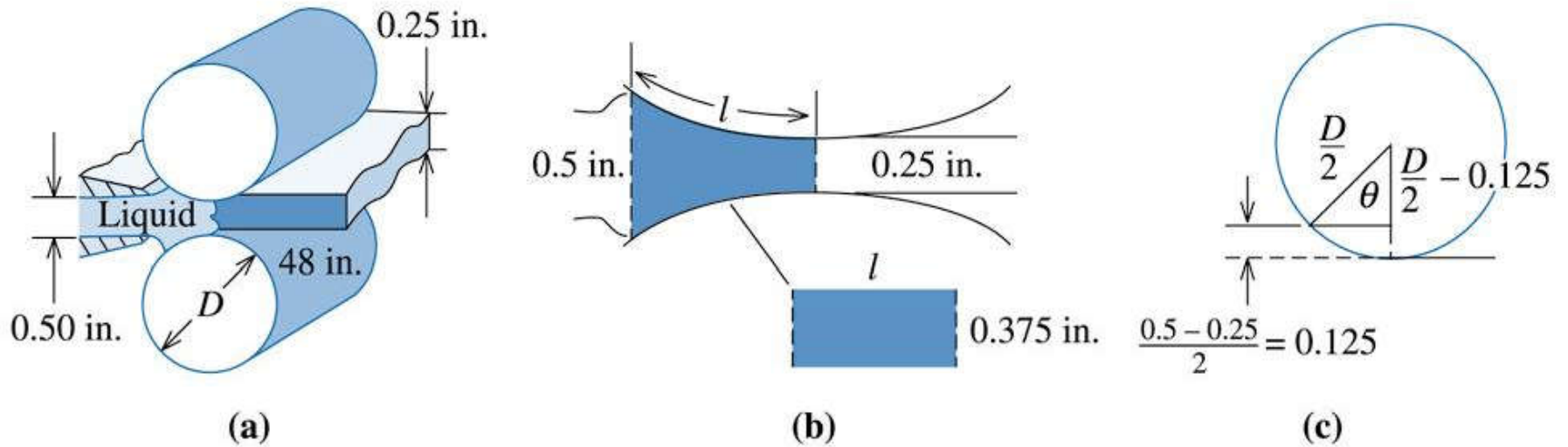


Example 8.8

Design of a Continuous Casting Machine

Figure 8.24 shows a method for continuous casting of 0.25-in.-thick, 48-in.-wide aluminum plate that is subsequently rolled into aluminum foil. The liquid aluminum is introduced between two large steel rolls that slowly turn. We want the aluminum to be completely solidified by the rolls just as the plate emerges from the machine. The rolls act as a permanent mold with a mold constant B of about 5 min/in.^2 when the aluminum is poured at the proper superheat. Design the rolls required for this process.





©2003 Brooks/Cole, a division of Thomson Learning, Inc. Thomson Learning_® is a trademark used herein under license.

Figure 8.24 Horizontal continuous casting of aluminum (for Example 8.8)



Example 8.8 SOLUTION



UPLOADED BY AHMAD T JUNDI

The average thickness is $(0.50 \text{ in.} + 0.25 \text{ in.})/2 = 0.375 \text{ in.}$ Then:

$$V = (\text{thickness})(\text{length})(\text{width}) = 0.375/w$$

$$A = 2(\text{length})(\text{width}) = 2/w$$

$$V/A = (0.375/w)/(2/w) = 0.1875 \text{ in.}$$

The length l is the fraction of the roll diameter that is in contact with the aluminum during freezing and can be given by

$$l = \frac{\pi D \theta}{360}$$

Then, by substituting for l and v in the equation for the time:

$$t = \frac{l}{v} = \frac{\pi D \theta}{360 \pi D R} = \frac{\theta}{360 R} = 0.175 \text{ min}$$

$$R = \frac{\theta}{(360)(0.175)} = 0.0159 \theta \text{ rev/min}$$





Example 8.8 SOLUTION (Continued)

A number of combinations of D and R provide the required solidification rate. Let's calculate θ for several diameters and then find the required R .

D	θ	l	$R = 0.0159\theta$	$v = \pi DR$
24 in.	8.2771	1.7334 in.	0.1316 rev/min	9.923 in./min
36 in.	6.7560	2.1230 in.	0.1074 rev/min	12.149 in./min
48 in.	5.8502	2.4505 in.	0.0930 rev/min	14.027 in./min
60 in.	5.2322	2.7396 in.	0.0832 rev/min	15.683 in./min

In selecting our final design, we prefer to use the **largest practical roll diameter** to assure high production rates. As the rolls become more massive, however, they and their supporting equipment become more expensive.

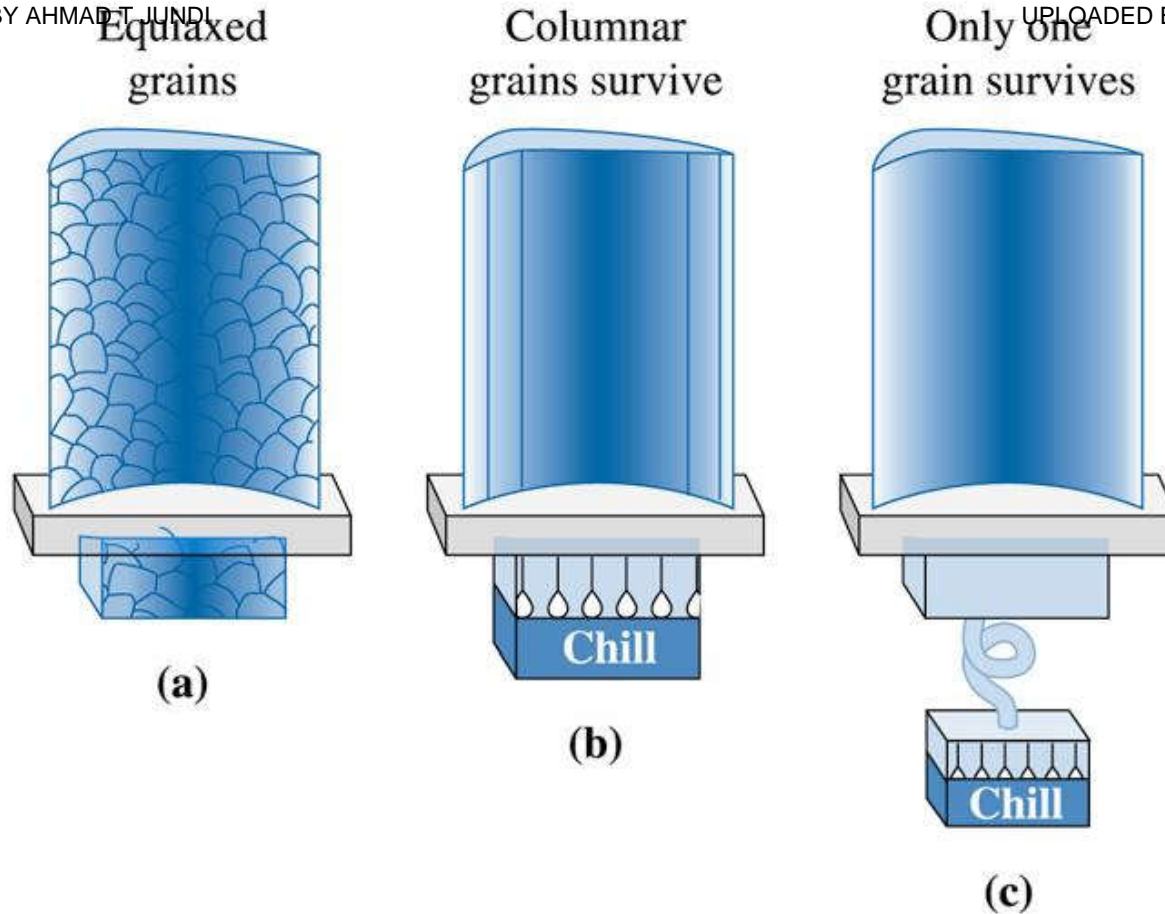




Section 8.11 Directional Solidification (DS), Single Crystal Growth, and Epitaxial Growth

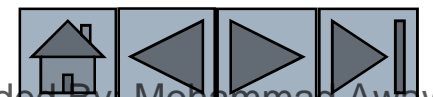
- **Directional solidification (DS)** - A solidification technique in which cooling in a given direction leads to preferential growth of grains in the opposite direction, leading to an anisotropic-oriented microstructure.
- **Bridgman processes** - A process to grow semiconductor and other single crystals.
- **Epitaxial growth** - Growth of a material via epitaxy.
- **Homoepitaxy** - Growth of a highly oriented material onto a crystal of the same material.
- **Heteroepitaxy** - Growth of a highly oriented material onto a different substrate material.

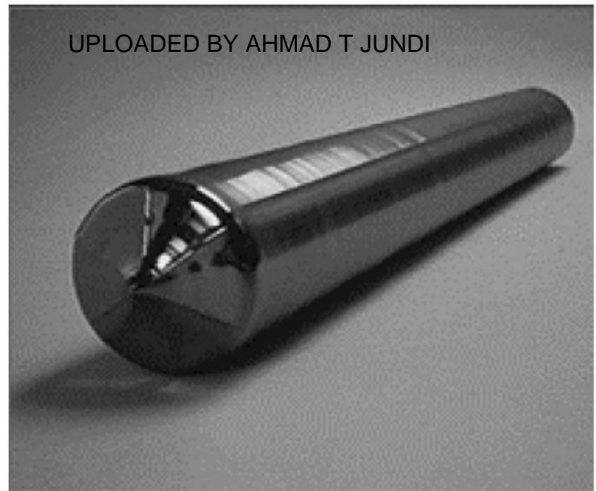




©2003 Brooks/Cole, a division of Thomson Learning, Inc. Thomson Learning, Inc. is a trademark used herein under license.

Figure 8.25 Controlling grain structure in turbine blades: (a) conventional equiaxed grains, (b) directionally solidified columnar grains, and (C) single crystal.





(a)



(b)



(c)

Figure 8.26 (a) Silicon single crystal, (b) silicon wafer, and (c) Bridgman technique. (Courtesy of PhotoDisc/Getty Images.)



Section 8.12 Solidification of Polymers and Inorganic Glasses

- **Lamellar** - A plate-like arrangement of crystals within a material.
- **Spherulite** - Spherical-shaped crystals produced when certain polymers solidify.
- **Preform** - A component from which a fiber is drawn or a bottle is made.



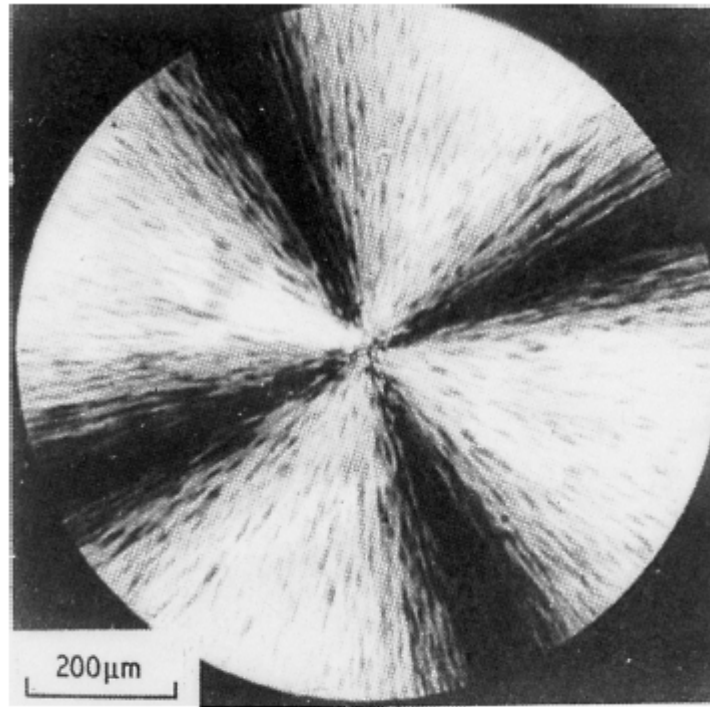


Figure 8.27 An amorphous boundary region separates the lamellae. A spherulite in polystyrene (8000). (From R. Young and P. Lovell, Introduction to Polymers, 2nd Ed., Chapman & Hall, 1991).

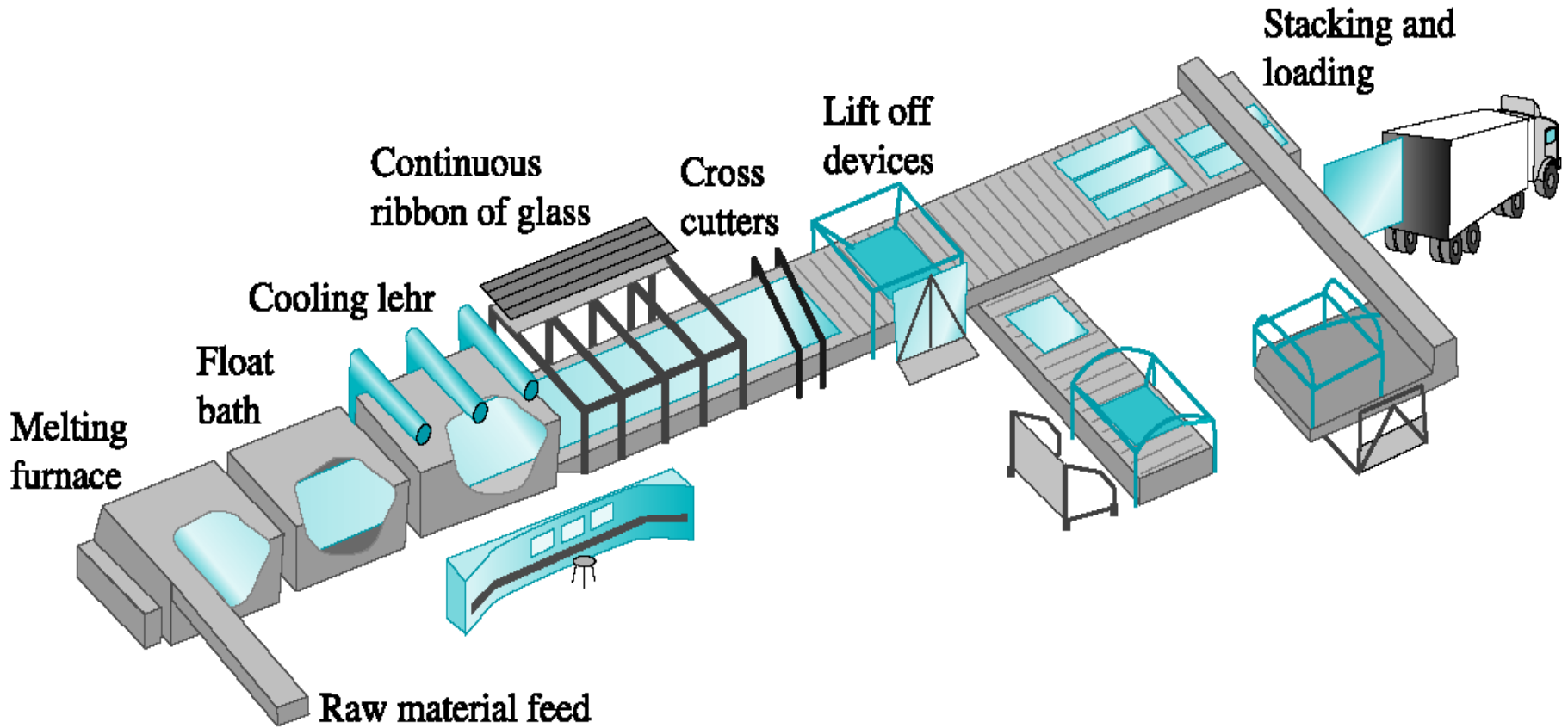
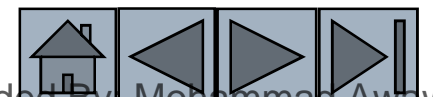


Figure 8.28 Processing scheme for float glasses. (Source: www.glassrecruiters.com.)





Section 8.13 Joining of Metallic Materials

- **Brazing** - An alloy, known as a filler, is used to join two materials to one another.
- **Soldering** - Soldering is a joining process in which the filler has a melting temperature below 450°C, no melting of the base materials occurs.
- **Fusion welding** - Joining processes in which a portion of the materials must melt in order to achieve good bonding.
- **Fusion zone** - The portion of a weld heated to produce all liquid during the welding process. Solidification of the fusion zone provides joining.



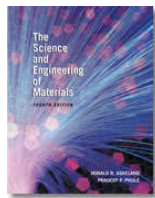
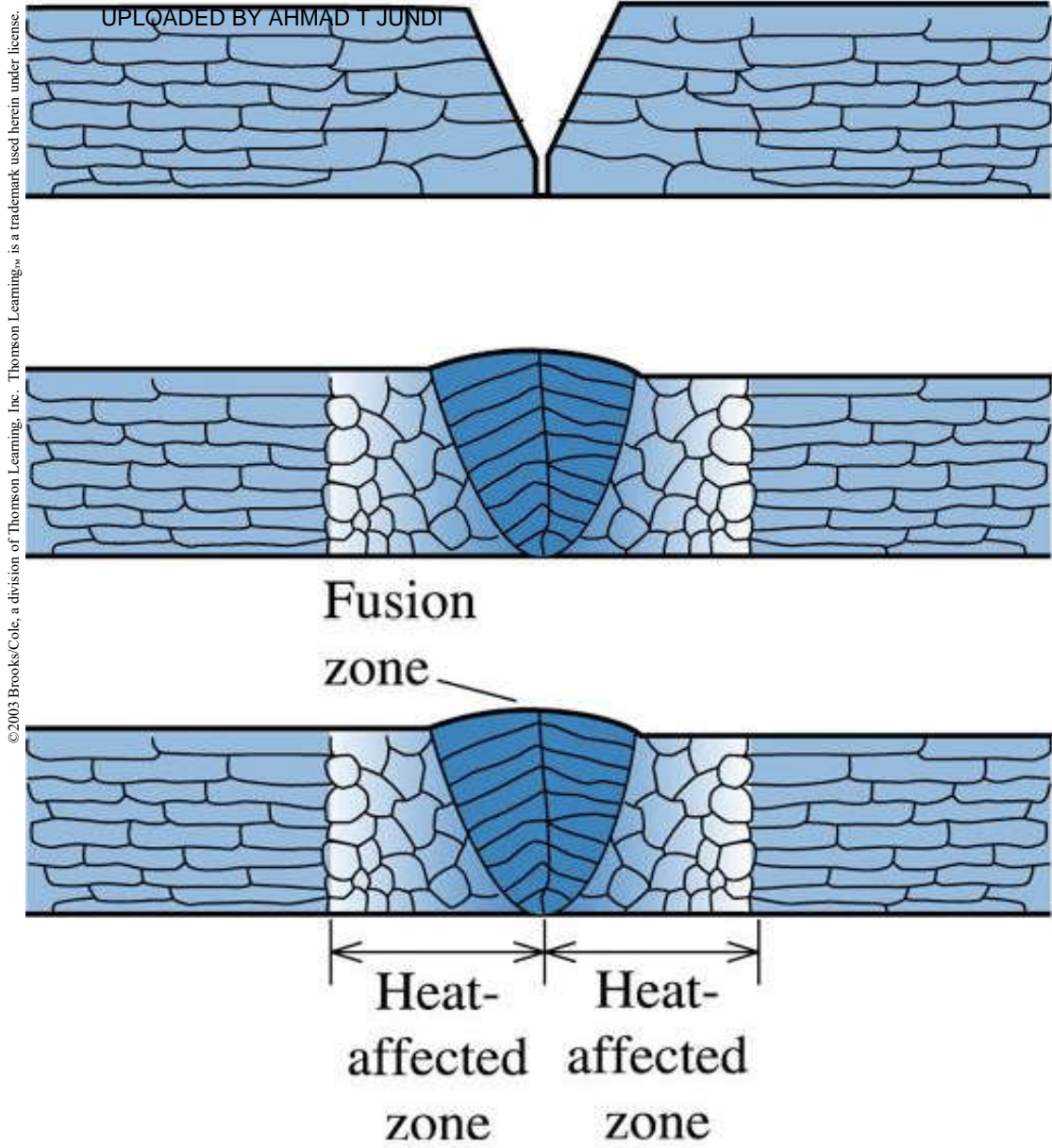


Figure 8.29 A schematic diagram of the fusion zone and solidification of the weld during fusion welding: (a) initial prepared joint, (b) weld at the maximum temperature, with joint filled with filler metal, and (c) weld after solidification.

©2003 Brooks/Cole, a division of Thomson Learning, Inc. Thomson LearningSM is a trademark used herein under license.

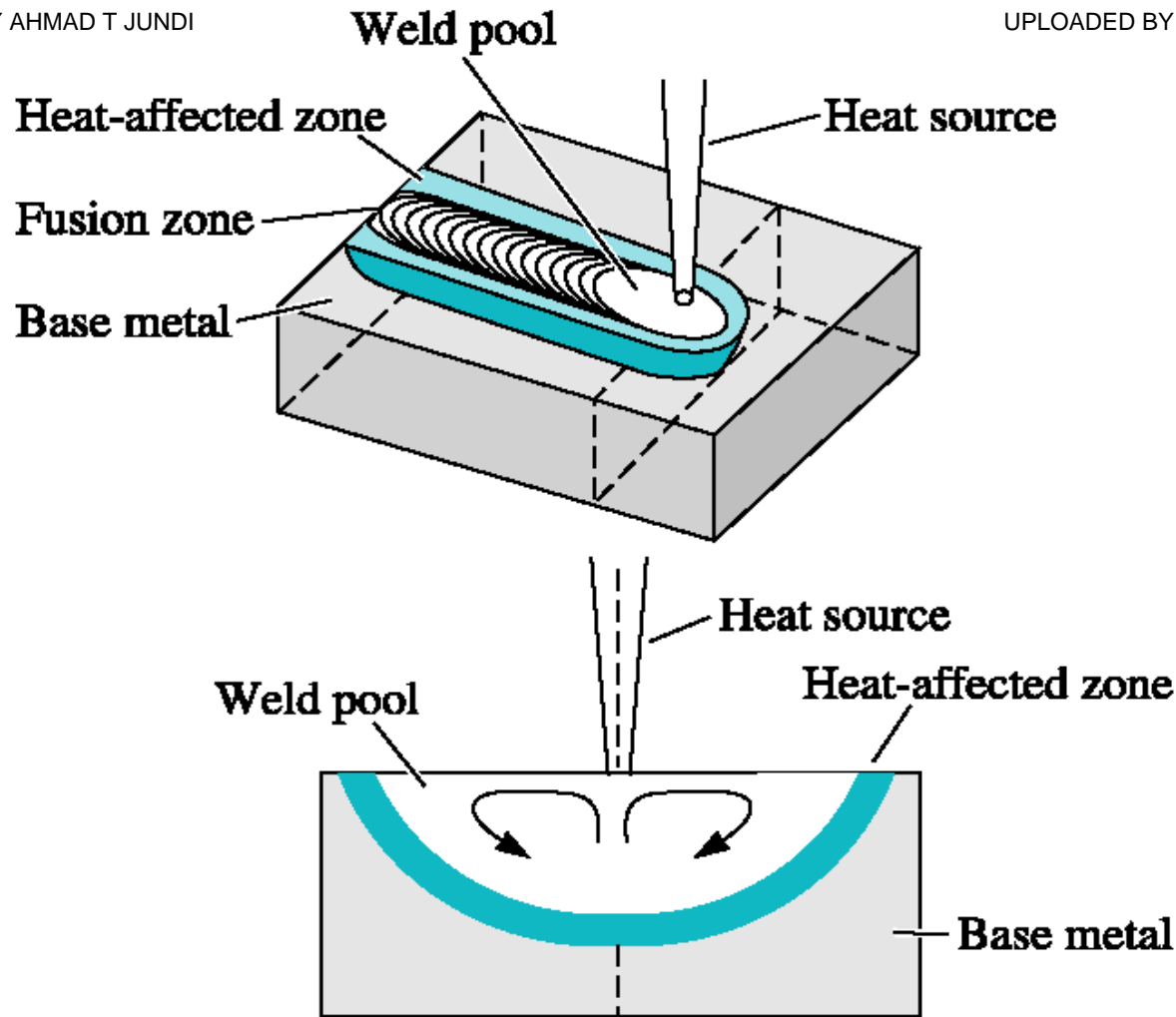
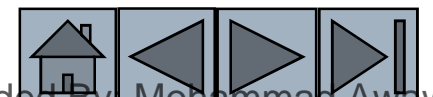


Figure 8.30 Schematic diagram showing interaction between the heat source and the base metal. Three distinct regions in the weldment are the fusion zone, the heat-affected zone, and the base metal. (Source: Reprinted with permission from "Current Issues and Problems in Welding Science," by S.A. David and T. DebRoy, 1992, Science, 257, pp. 497–502, Fig. 2. Copyright © 1992 American Association for the Advancement of Science.)



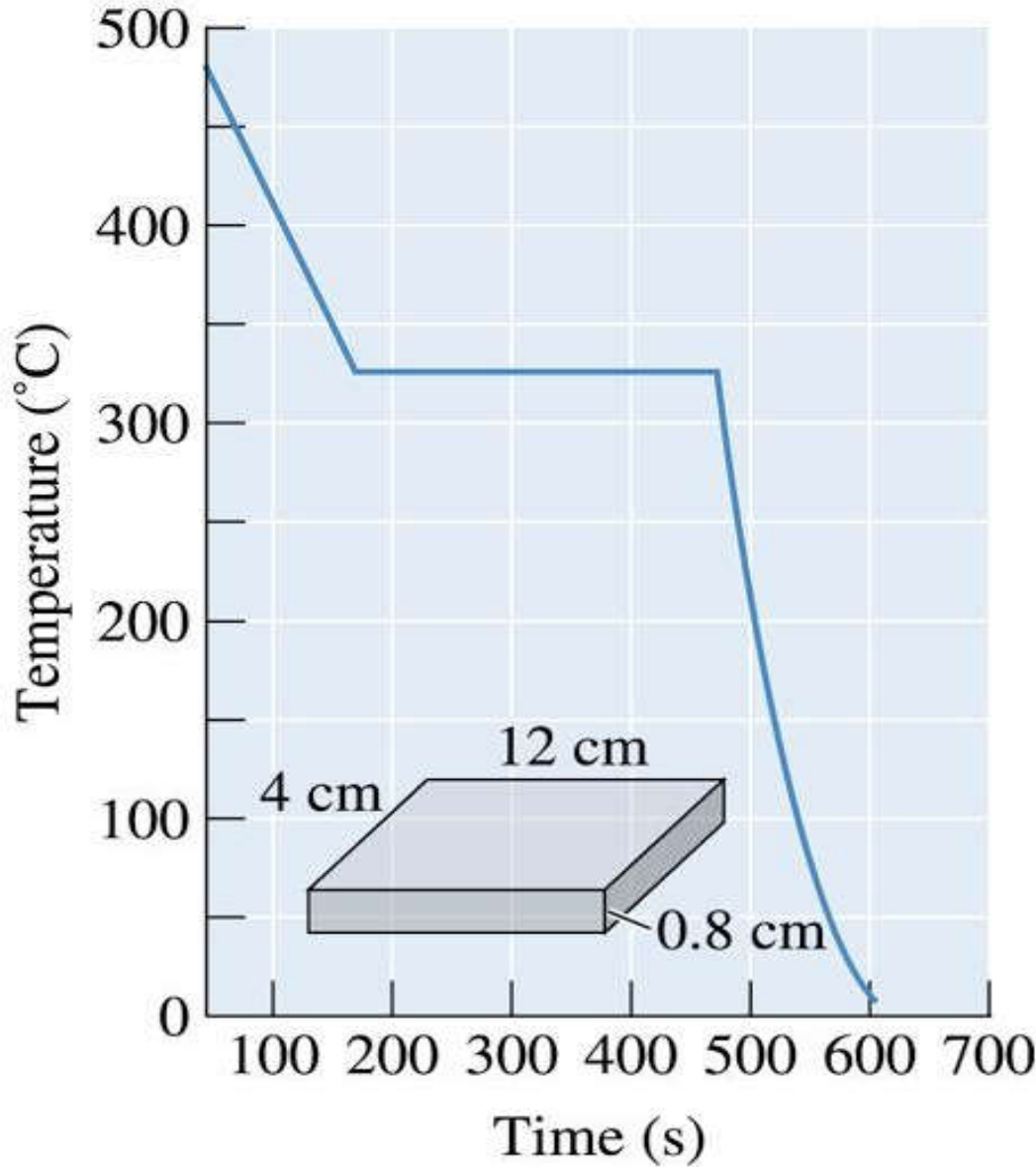


Figure 8.33 Cooling curve (for Problem 8.45)

©2003 Brooks/Cole, a division of Thomson Learning, Inc. Thomson Learning[™] is a trademark used herein under license.

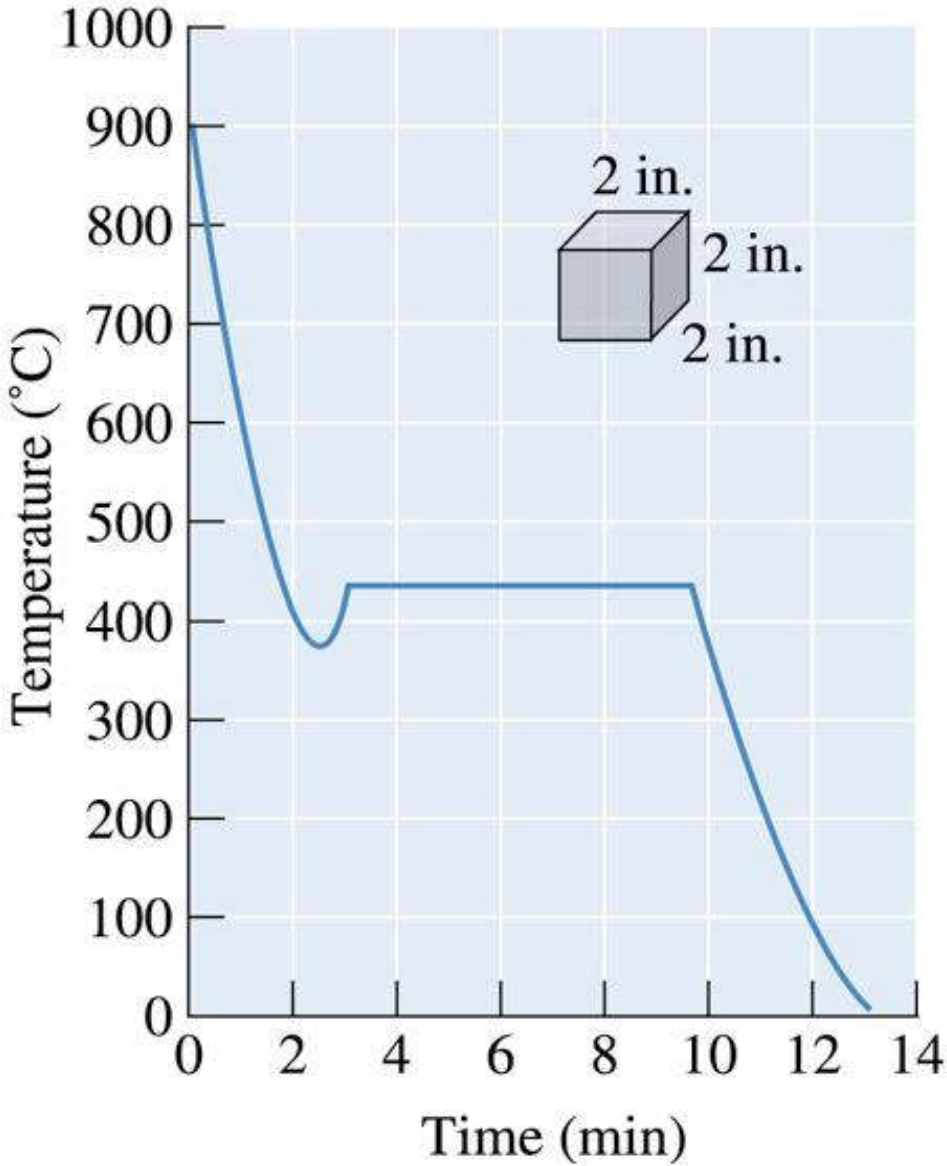
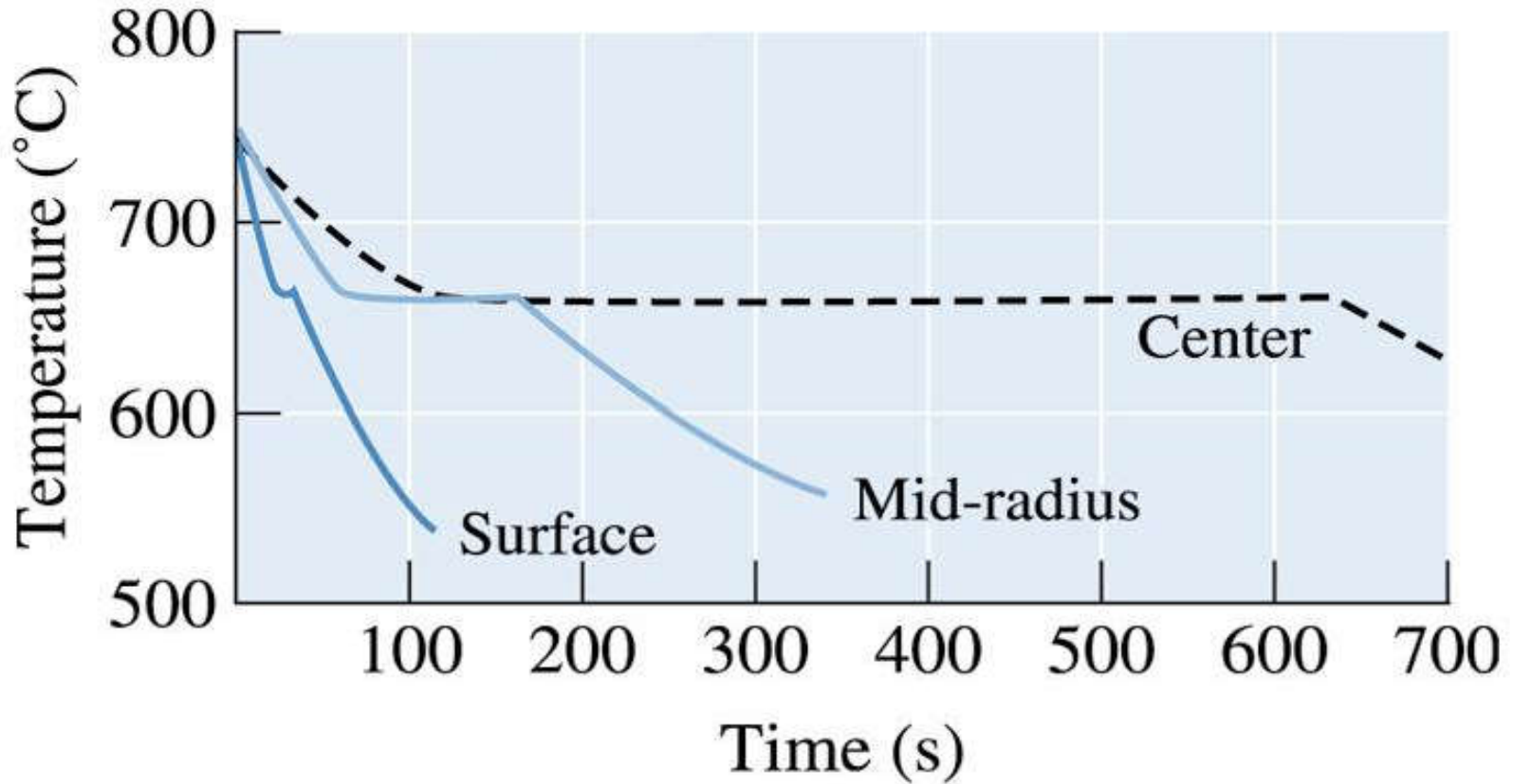


Figure 8.34 Cooling curve (for Problem 8.46)





©2003 Brooks/Cole, a division of Thomson Learning, Inc. Thomson Learning[®] is a trademark used herein under license.

Figure 8.35 Cooling curves (for Problem 8.47)



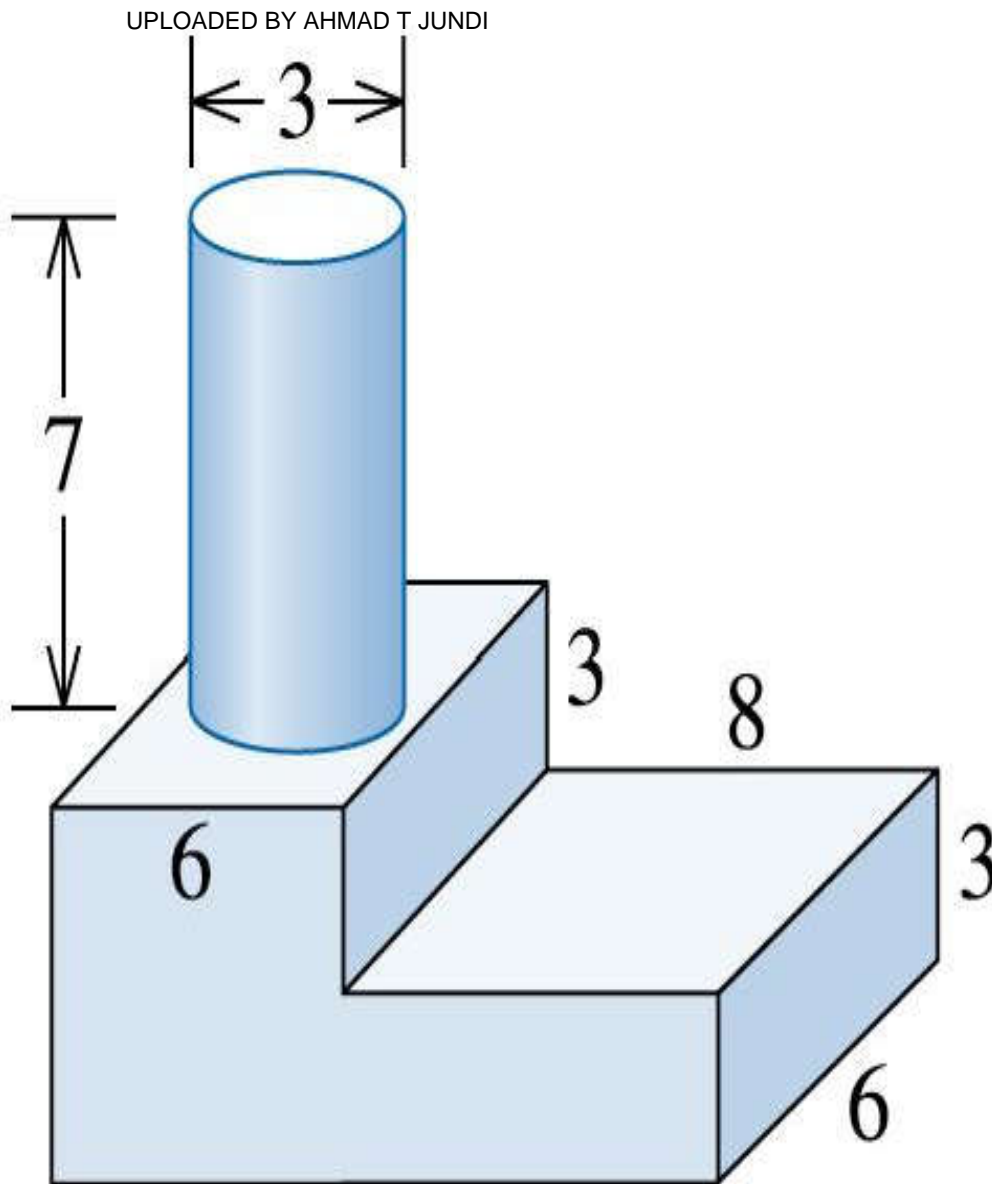
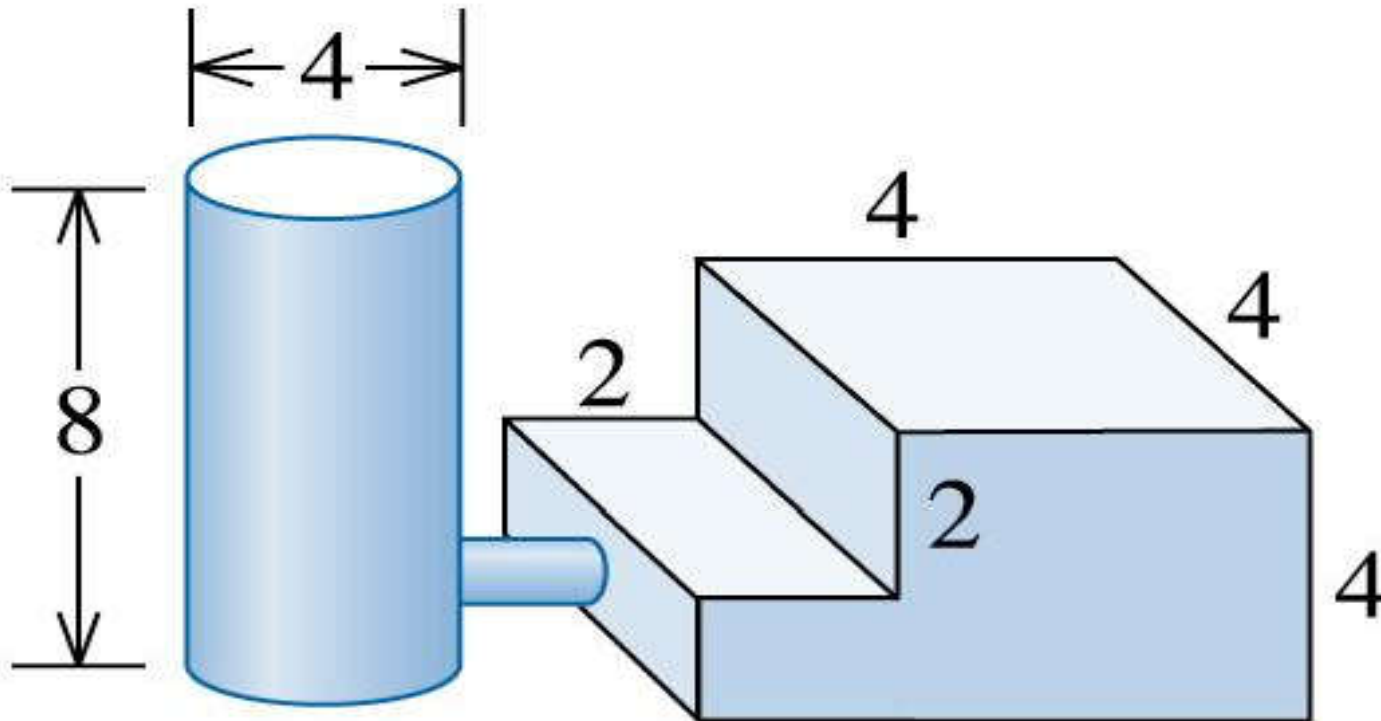


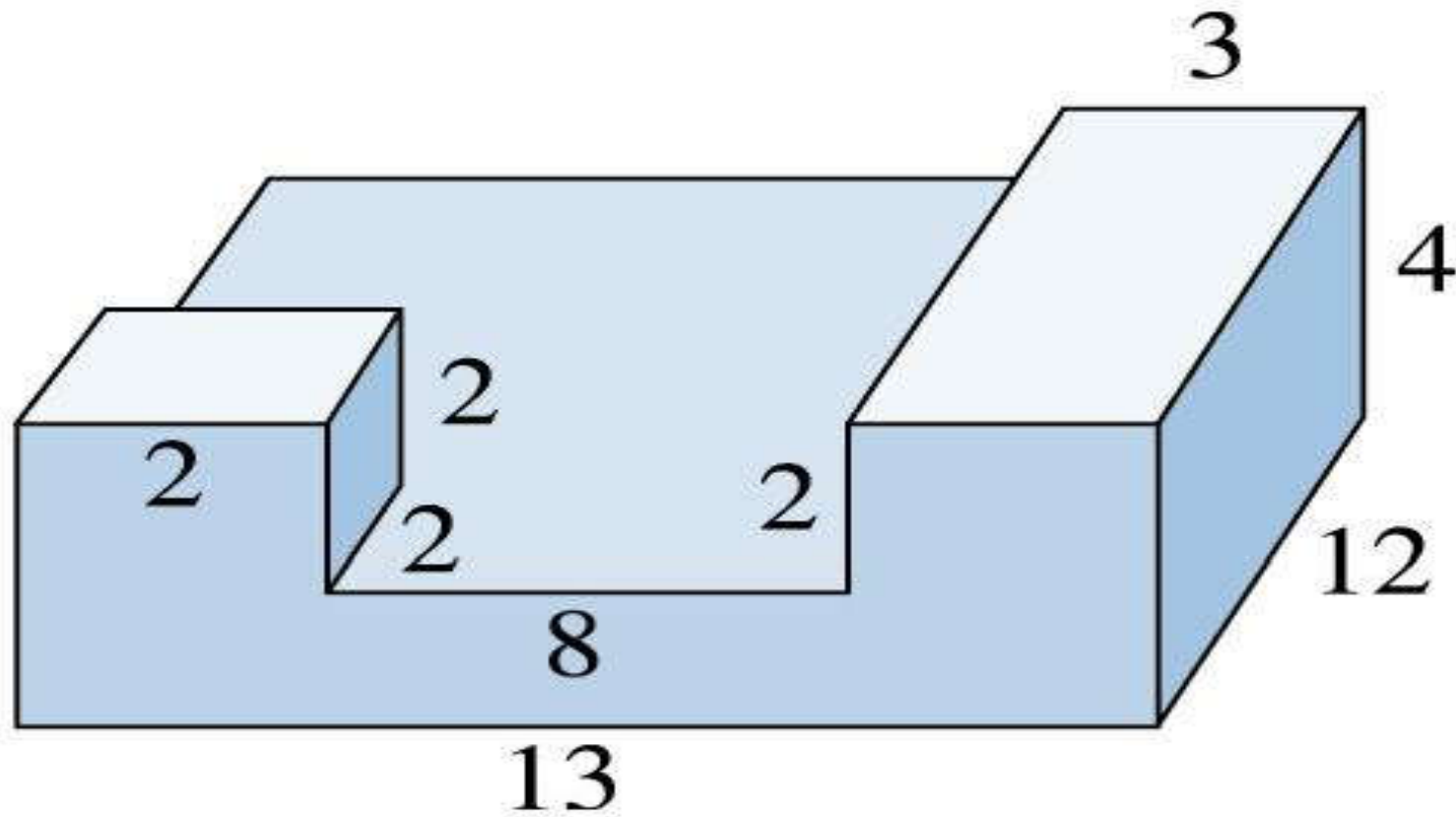
Figure 8.36 Step-block casting (for Problem 8.56).



©2003 Brooks/Cole, a division of Thomson Learning, Inc. Thomson Learning[™] is a trademark used herein under license.

Figure 8.37 Step-block casting (for Problem 8.57).





©2003 Brooks/Cole, a division of Thomson Learning, Inc. Thomson Learning, is a trademark used herein under license.

Figure 8.38 Casting to be risered (for Problem 8.97).





©2003 Brooks/Cole, a division of Thomson Learning, Inc. Thomson Learning™ is a trademark used herein under license.

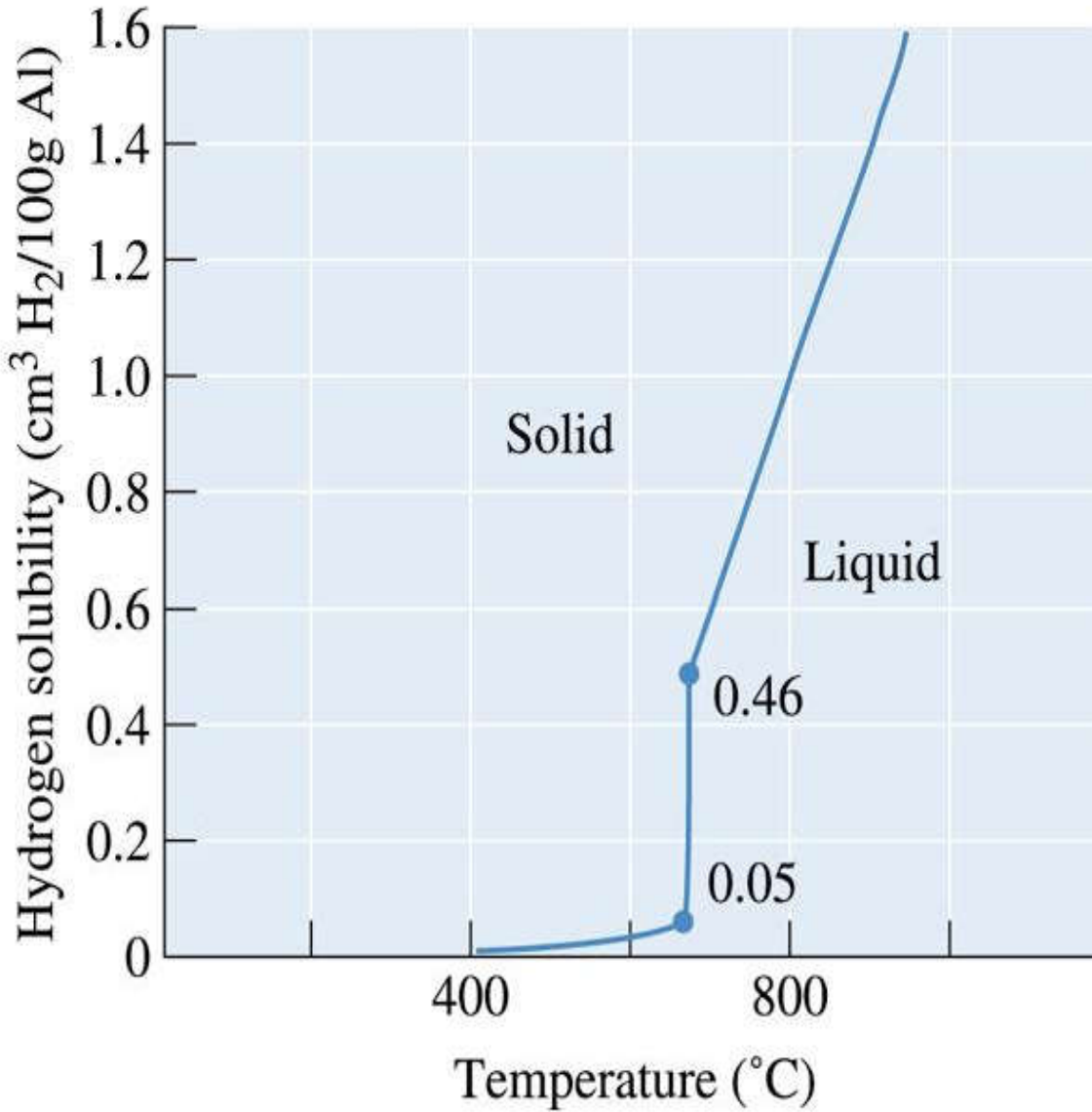


Figure 8.18
(repeated for
Problem 8.67) The
solubility of
hydrogen gas in
aluminum when the
partial pressure of
H₂ = 1 atm.



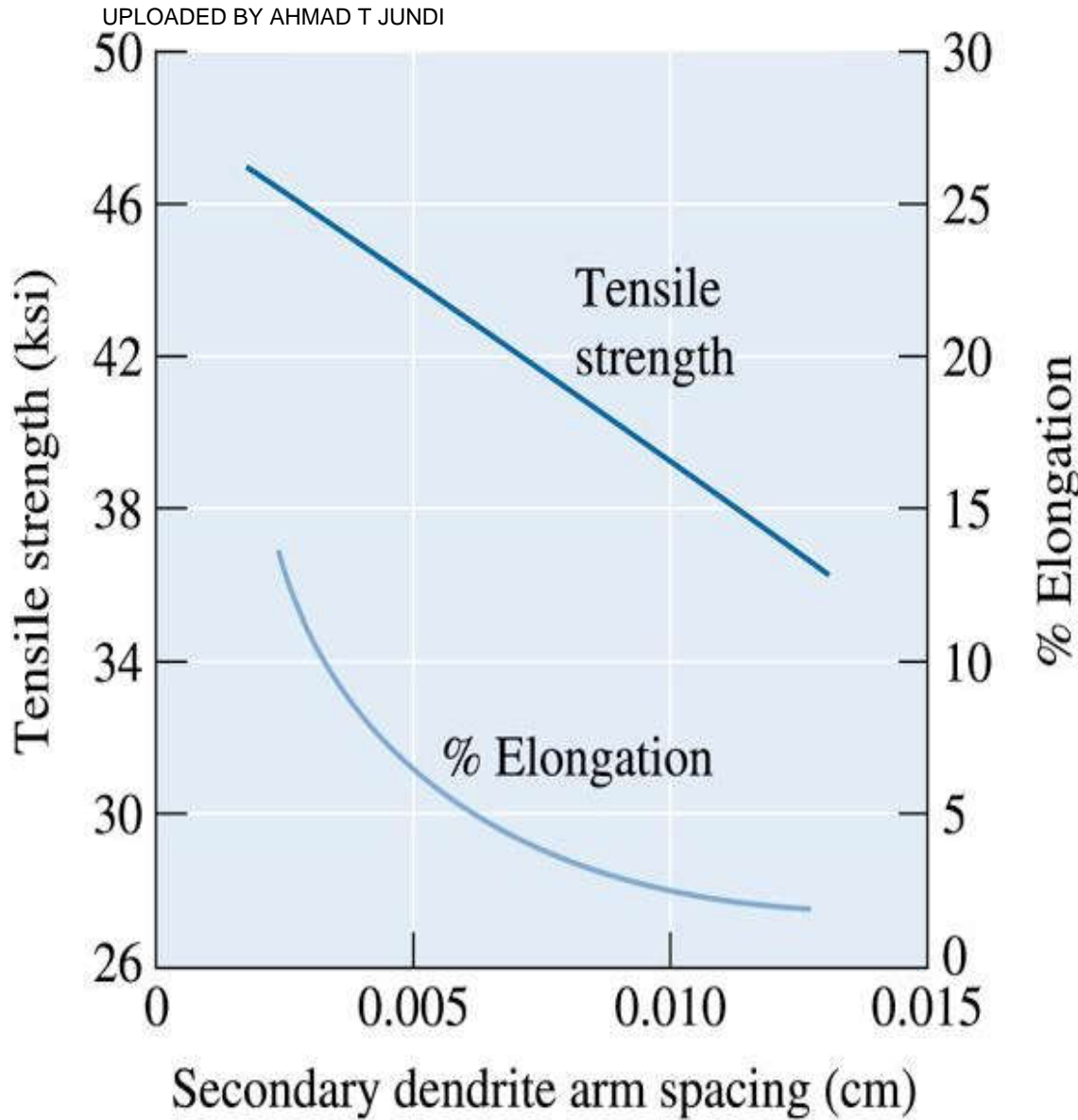
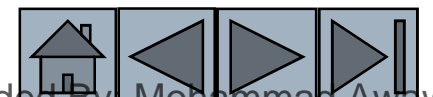


Figure 8.11
(Repeated for Problem 8.99) The effect of the secondary dendrite arm spacing on the properties of an aluminum casting alloy.





The Science and Engineering of Materials, 4th ed

Donald R. Askeland – Pradeep P. Phulé

Chapter 9 – Solid Solutions and Phase Equilibrium





Objectives of Chapter 9

- ❑ The goal of this chapter is to describe the underlying physical concepts related to the structure of matter.
- ❑ To examine the relationships between structure of atoms-bonds-properties of engineering materials.
- ❑ Learn about different levels of structure i.e. atomic structure, nanostructure, microstructure, and macrostructure.





Chapter Outline

- 9.1 Phases and the Phase Diagram
- 9.2 Solubility and Solid Solutions
- 9.3 Conditions for Unlimited Solid Solubility
- 9.4 Solid-Solution Strengthening
- 9.5 Isomorphous Phase Diagrams
- 9.6 Relationship Between Properties and the Phase Diagram
- 9.7 Solidification of a Solid-Solution Alloy
- 9.8 Nonequilibrium Solidification and Segregation

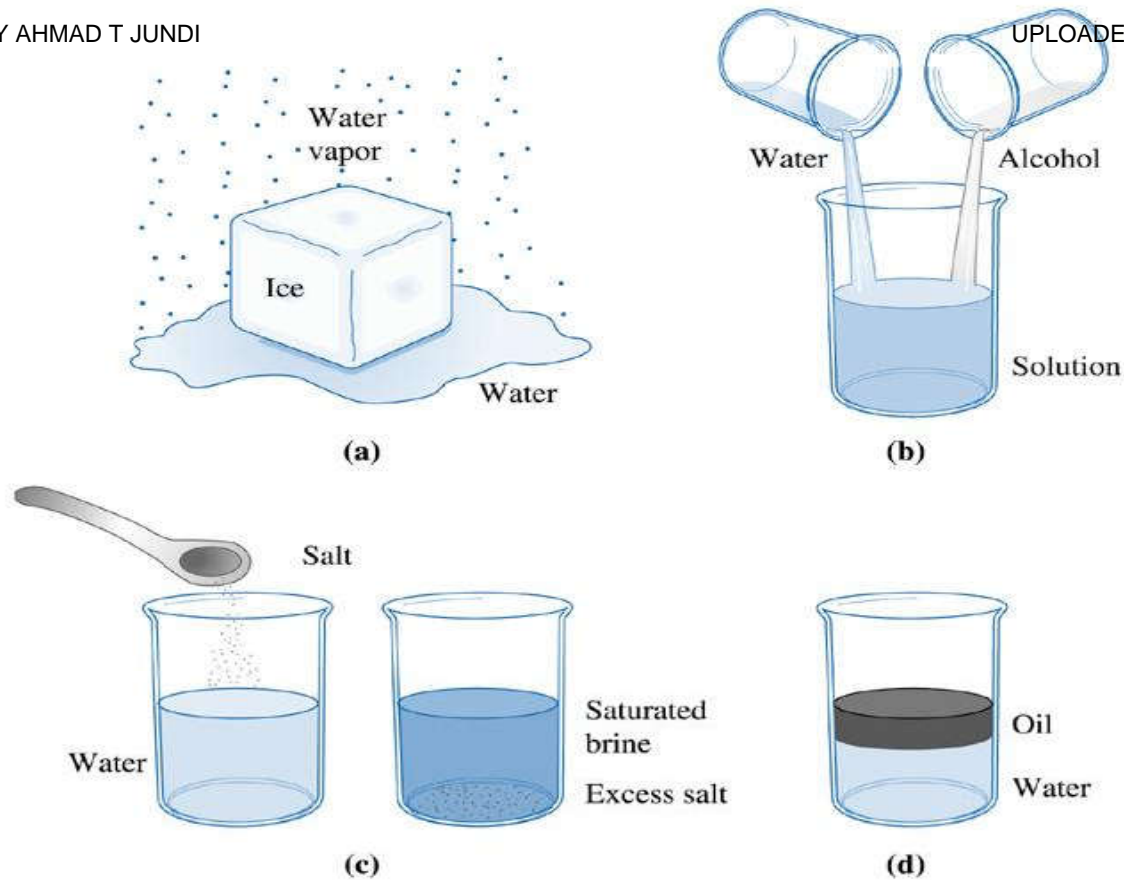




Section 9.1 Phases and the Phase Diagram

- **Phase** - Any portion including the whole of a system, which is physically homogeneous within it and bounded by a surface so that it is mechanically separable from any other portions.
- **Gibbs phase rule** - Describes the number of degrees of freedom, or the number of variables that must be fixed to specify the temperature and composition of a phase ($2 + C = F + P$, where pressure and temperature can change, $1 + C = F + P$, where pressure or temperature is constant).
- **P-T diagram** - A diagram describing thermodynamic stability of phases under different temperature and pressure conditions (same as a unary phase diagram).





©2003 Brooks/Cole, a division of Thomson Learning, Inc. Thomson Learning[®] is a trademark used herein under license.

Figure 9.1 Illustration of phases and solubility: (a) The three forms of water – gas, liquid, and solid – are each a phase. (b) Water and alcohol have unlimited solubility. (c) Salt and water have limited solubility. (d) Oil and water have virtually no solubility.



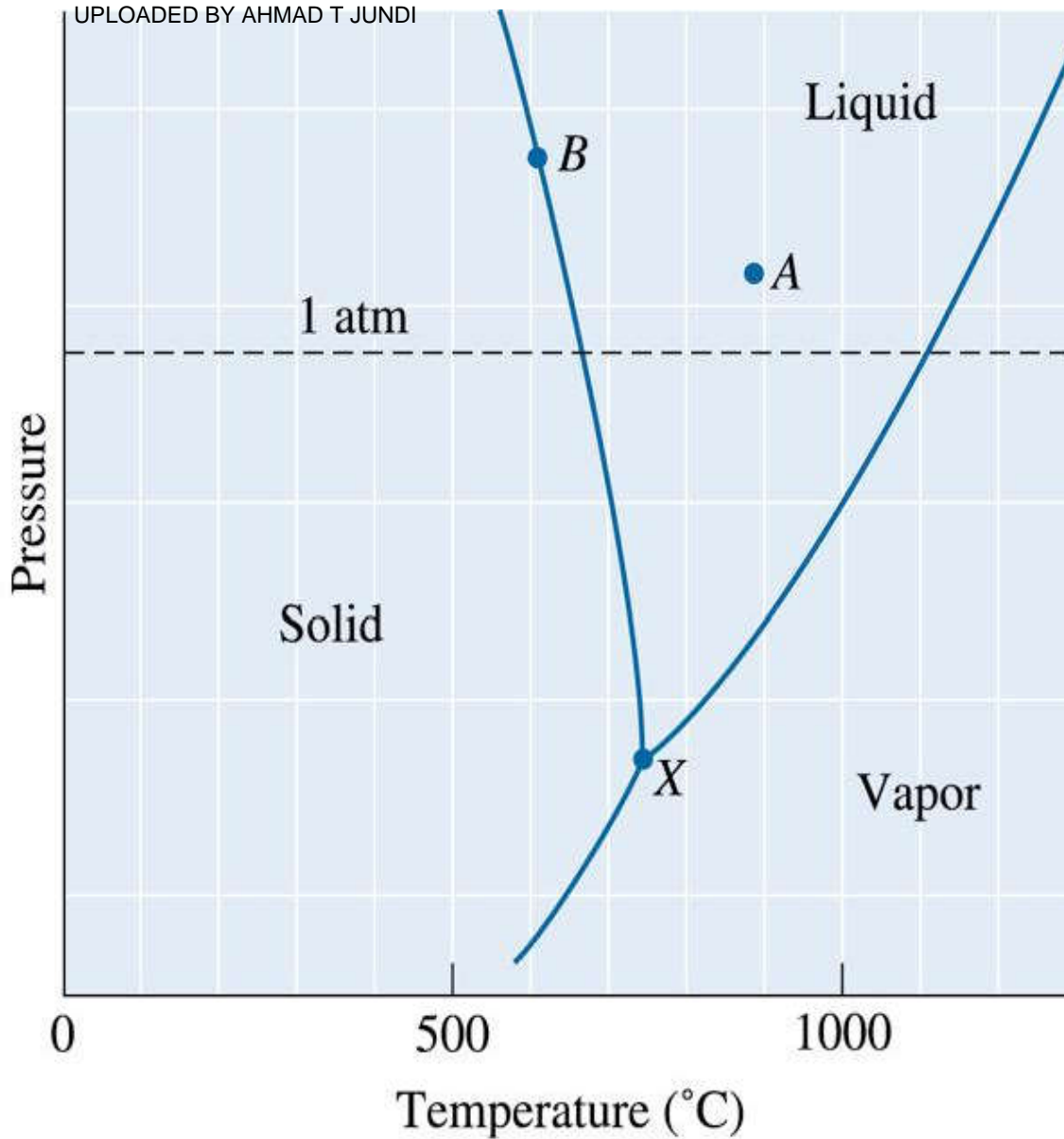
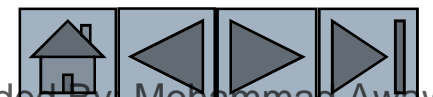


Figure 9.2 Schematic unary phase diagram for magnesium, showing the melting and boiling temperatures at one atmosphere pressure.





Design of an Aerospace Component

Because magnesium (Mg) is a low-density material ($\rho_{\text{Mg}} = 1.738 \text{ g/cm}^3$), it has been suggested for use in an aerospace vehicle intended to enter the outer space environment. Is this a good design?

Example 9.1 SOLUTION

- In space the pressure is very low. Even at relatively low temperatures, solid magnesium can begin to change to a vapor, causing metal loss that could damage a space vehicle.
- A low-density material with a higher boiling point (and, therefore, lower vapor pressure at any given temperature) might be a better choice.
- Other factors to consider: In load-bearing applications, we should not only look for density but also for relative strength. Therefore, the ratio of Young's modulus to density or yield strength to density could be a better parameter to compare different materials.





Example 9.2

Freeze Drying Synthesis of Ceramic Superconductors

Many ceramic materials are made into powders using different oxides and carbonates (Chapter 14). This is because ceramics melt at too high a temperature and tend to exhibit brittle behavior. For example, the synthesis process for $\text{YBa}_2\text{Cu}_3\text{O}_{7-x}$, a ceramic superconductor known as *YBCO*, involves mixing and reacting powders of yttrium oxide (Y_2O_3), copper oxide (CuO), and barium carbonate (BaCO_3). The barium carbonate decomposes to BaO during the high temperature reactions and reacts with yttria and copper oxide to form different phases. Often, this process, known as the “oxide mix” technique, produces ceramic powders that are relatively coarse. Some other undesired phases may also form, and deleterious impurities (from processing or raw materials) may become incorporated in the product.





Example 9.2 (Continued)

On the other hand, chemical techniques that make use of high-purity chemicals may offer a better product (most likely at a higher cost). One such chemical process, used in the food industry (e.g., coffee, spices, etc.) is **freeze drying**. [3] For example, freeze-dried coffee is made by extracting coffee from beans and then evaporating the water from the coffee using freeze drying.

An engineer decides to use water-based solutions to develop a freeze-drying synthesis of a YBCO superconductor. Using the unary phase diagram for water [Figure 9.3(a)], explain the different steps that could be followed to generate high-purity and chemically homogeneous powders of the *YBCO* superconductor.



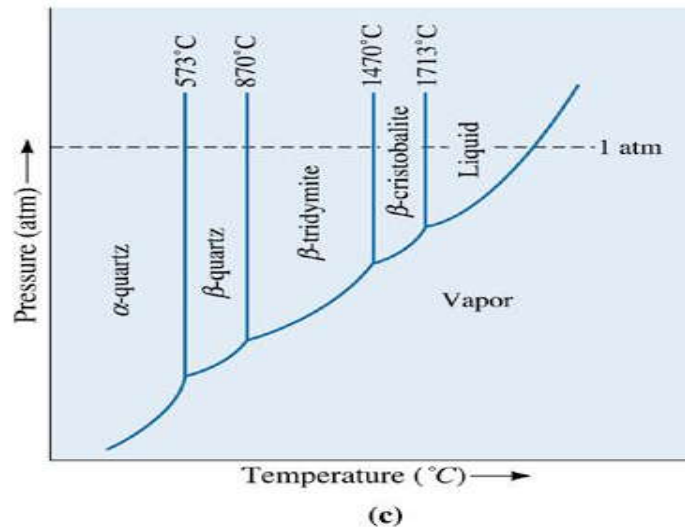
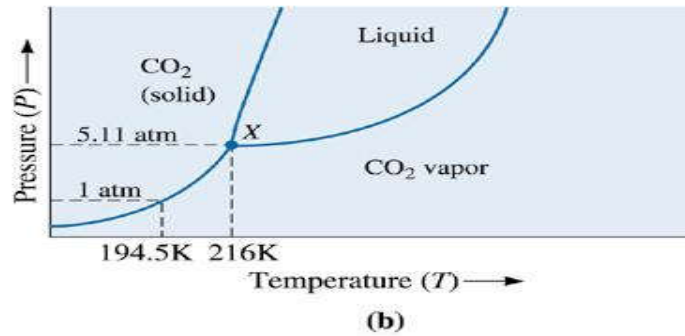
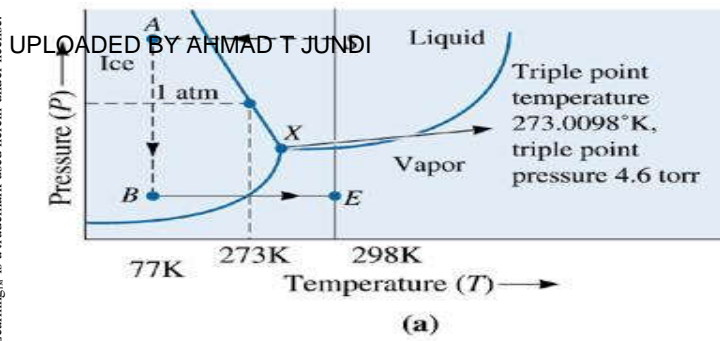
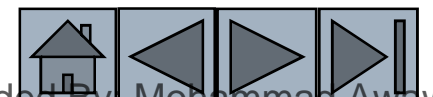


Figure 9.3 (a) Pressure-temperature diagram for H₂O. The triple point temperature is 273.0098 K and the triple point pressure is 4.6 torr. Notice the solid-liquid line sloping to the left. At normal pressure (1 atm or 760 torr), the melting temperature is 273 K. A possible scheme for freeze drying is shown as starting with point S and following the dashed line to the left. (b) Pressure-temperature diagram for CO₂. Many researchers are examining the applications of super-critical CO₂ for use as a solvent for applications related to the processing of plastics and pharmaceuticals. (c) Pressure-temperature diagram for SiO₂. The dotted line shows the 1 atm pressure.





Example 9.2 SOLUTION

- Prepare a solution of nitrates of yttrium, copper, and barium in proper cation stoichiometry.
- Remove the nitric acid (HNO_3) and H_2O without causing any melting by lowering the pressure to approximately 10^{-2} torr (point B).
- Increase the temperature while maintaining the low pressure causing the ice and nitric acid to sublime (solid \rightarrow vapor).
- The mixed metal nitrate powder will then be heated carefully and the nitrates can be decomposed to form a ceramic powder.

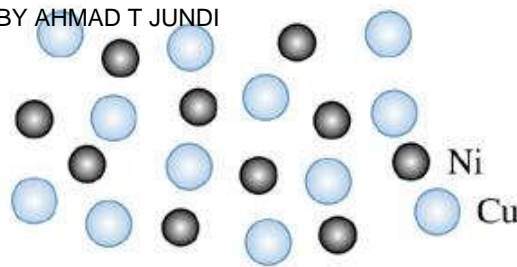




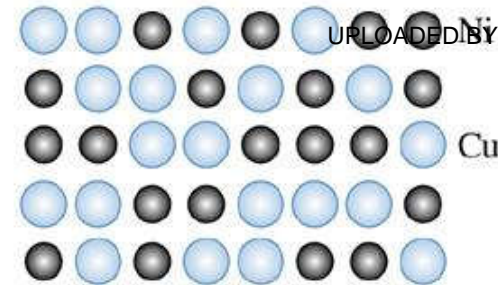
Section 9.2 Solubility and Solid Solutions

- **Solubility** - The amount of one material that will completely dissolve in a second material without creating a second phase.
- **Unlimited solubility** - When the amount of one material that will dissolve in a second material without creating a second phase is unlimited.
- **Limited solubility** - When only a maximum amount of a solute material can be dissolved in a solvent material.
- **Copolymer** - A polymer that is formed by combining two or more different types of monomers usually with the idea of blending the properties affiliated with individual polymers, example Dylark™ a copolymer of maleic anhydride and styrene.

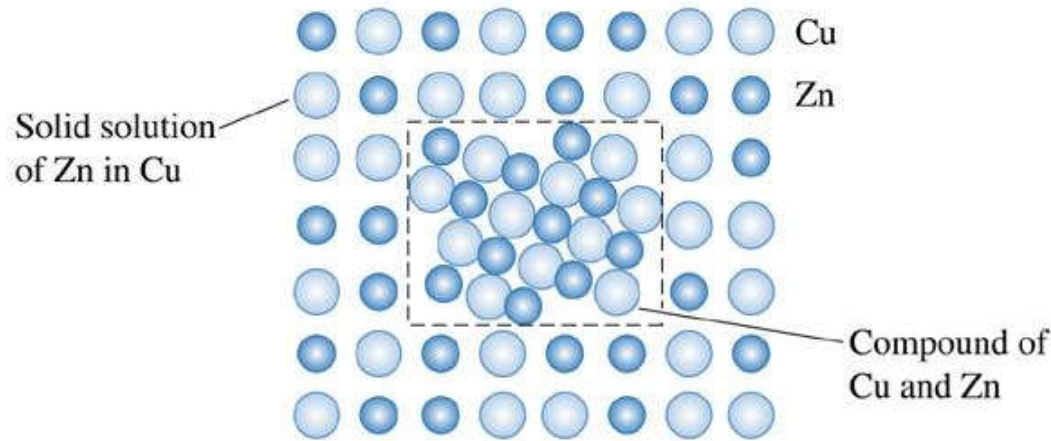




(a)



(b)



(c)

©2003 Brooks/Cole, a division of Thomson Learning, Inc. Thomson Learning, Inc. is a trademark used herein under license.

Figure 9.4 (a) Liquid copper and liquid nickel are completely soluble in each other. (b) Solid copper-nickel alloys display complete solid solubility, with copper and nickel atoms occupying random lattice sites. (c) In copper-zinc alloys containing more than 30% Zn, a second phase forms because of the limited solubility of zinc in copper.

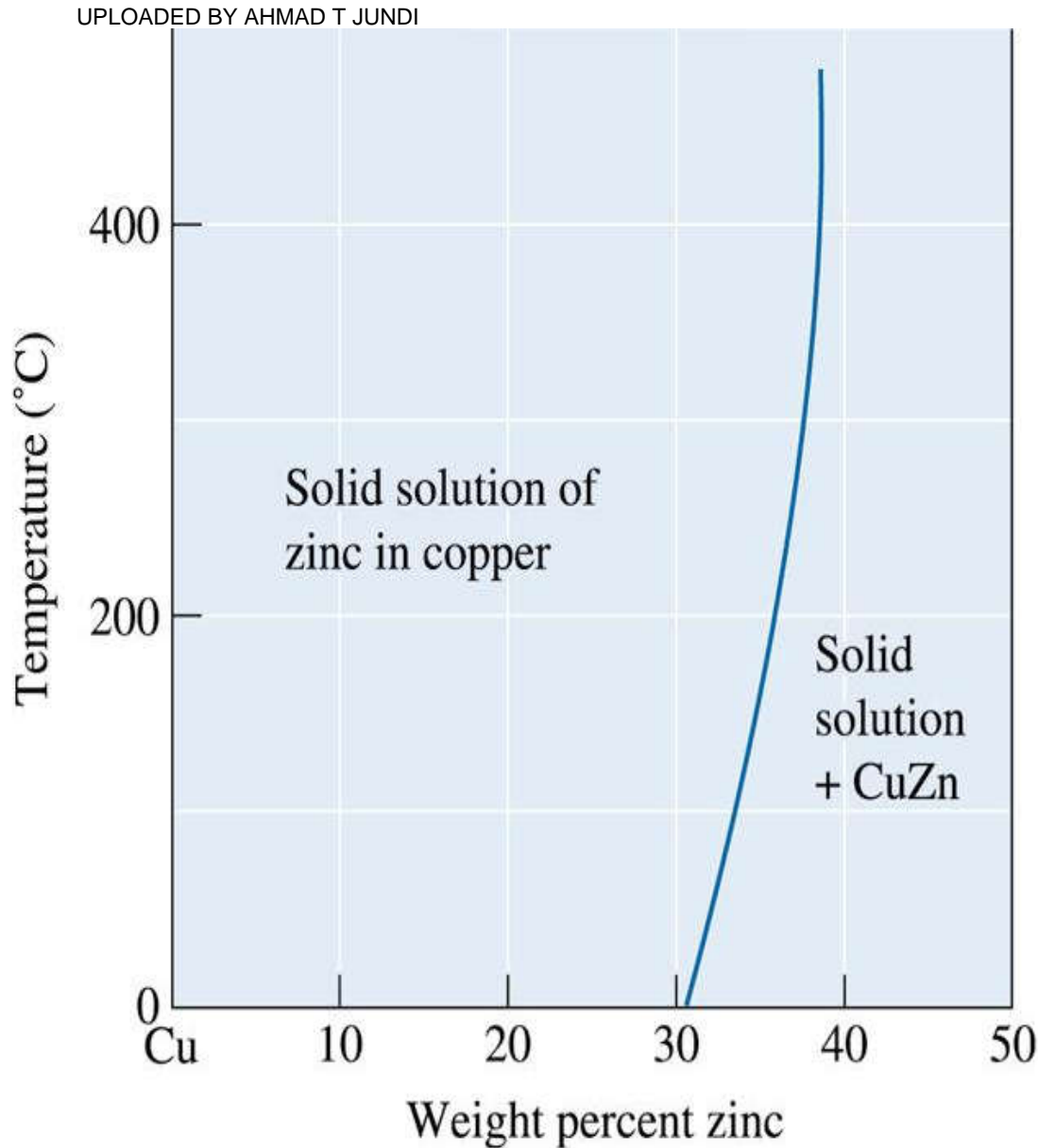


Figure 9.5 The solubility of zinc in copper. The solid line represents the solubility limit; when excess zinc is added, the solubility limit is exceeded and two phases coexist.

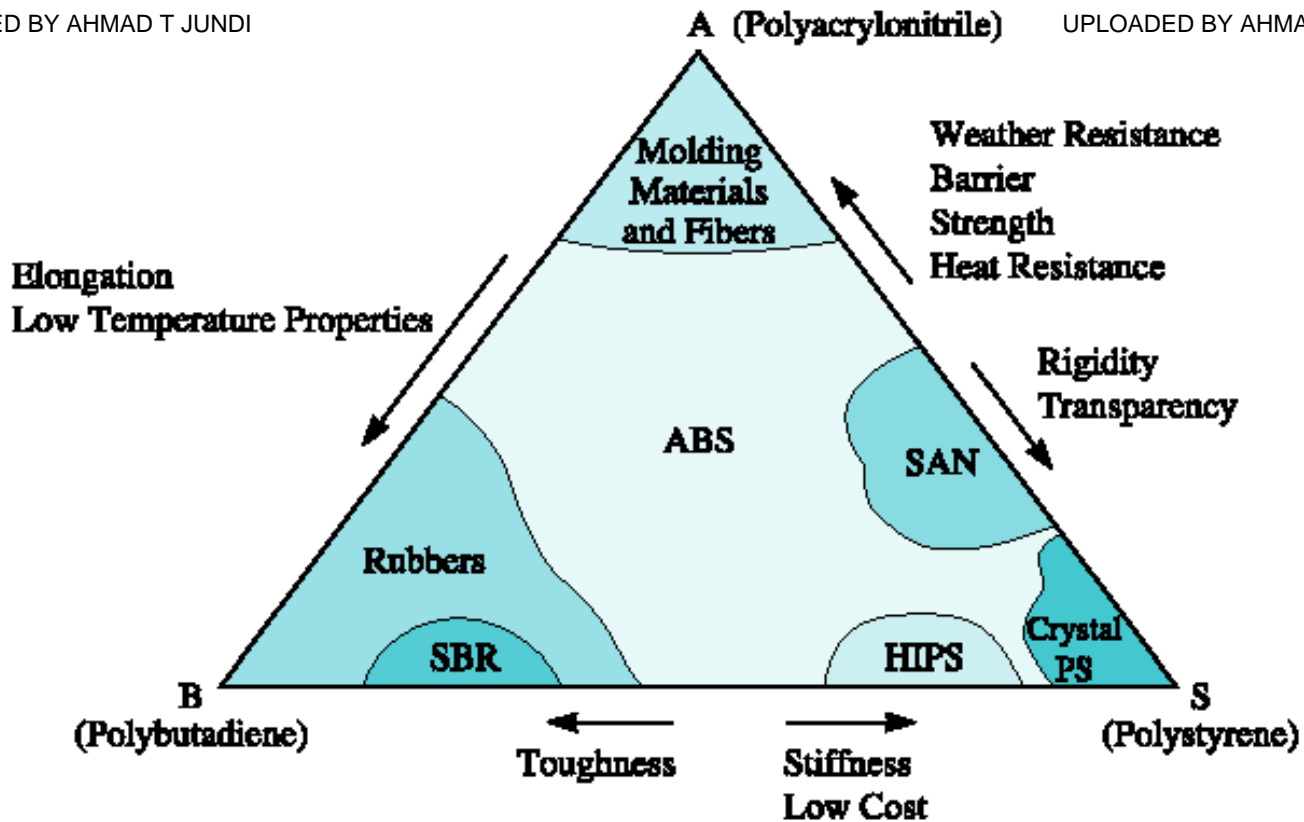
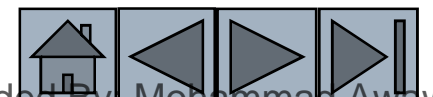


Figure 9.6 Diagram showing how the properties of copolymers formed in the ABS system vary. This is not a phase diagram. (Source: From *Plastics, Materials and Processing, Second Edition*, by B.A. Strong, p. 223, Fig. 6-14. Copyright © 2000 Prentice Hall. Reprinted by permission of Pearson Education.)

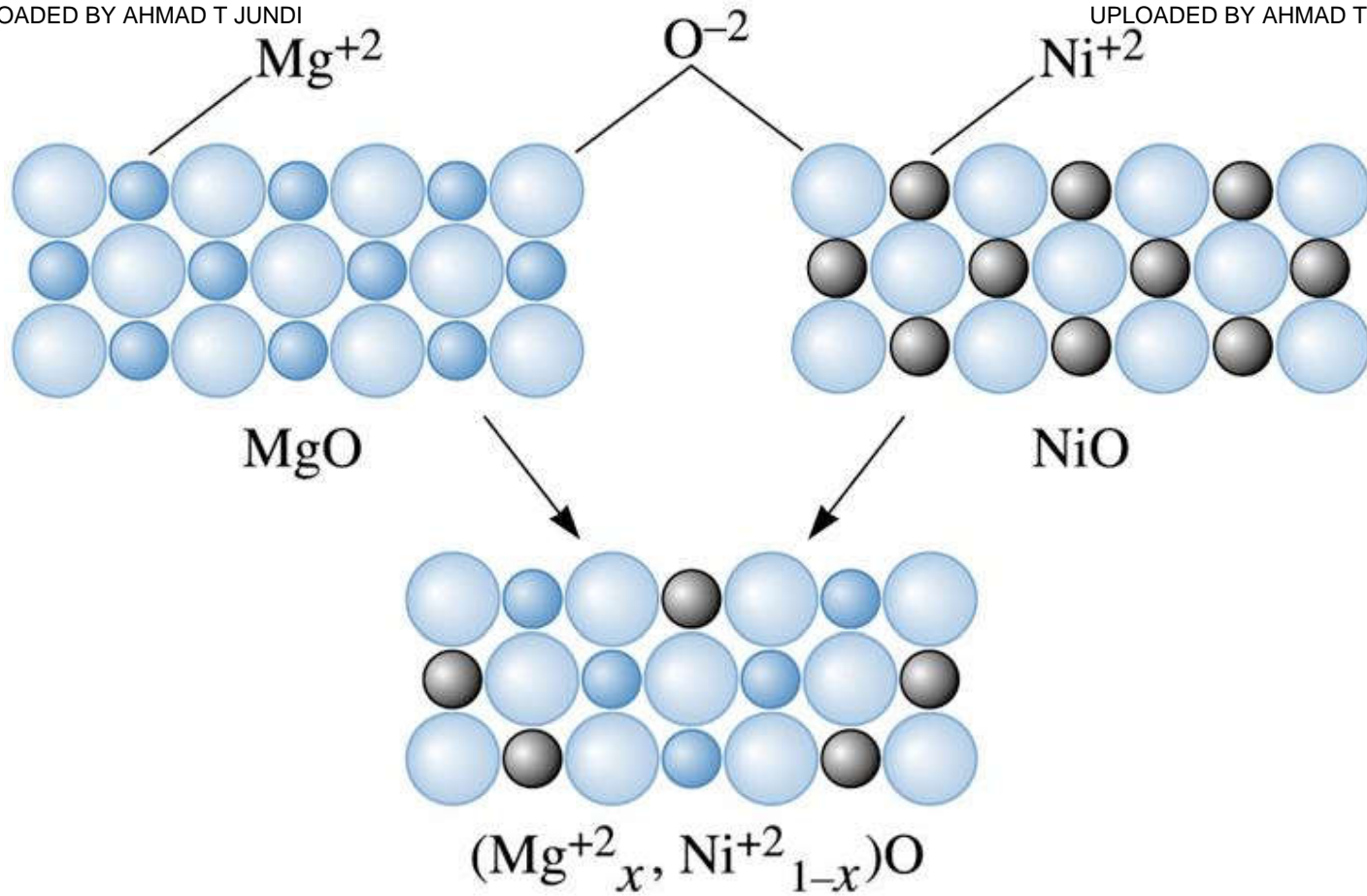




Section 9.3 Conditions for Unlimited Solid Solubility

- **Hume-Rothery rules** - The conditions that an alloy or ceramic system must meet if the system is to display unlimited solid solubility. Hume-Rothery's rules are necessary but are not sufficient for materials to show unlimited solid solubility.
- **Hume-Rothery rules:**
 - Size factor
 - Crystal structure
 - Valence
 - Electronegativity





©2003 Brooks/Cole, a division of Thomson Learning, Inc. Thomson Learning[™] is a trademark used herein under license.

Figure 9.7 MgO and NiO have similar crystal structures, ionic radii, and valences; thus the two ceramic materials can form solid solutions.



Ceramic Solid Solutions of MgO

NiO can be added to MgO to produce a solid solution. What other ceramic systems are likely to exhibit 100% solid solubility with MgO?

Example 9.3 SOLUTION

From Appendix B, some other possibilities in which the cation has a valence of +2 include the following:

	r (Å)	$\left[\frac{r_{\text{ion}} - r_{\text{Mg}^{+2}}}{r_{\text{Mg}^{+2}}} \right] \times 100\%$	Crystal Structure
Cd ⁺² in CdO	$r_{\text{Cd}^{+2}} = 0.97$	47	NaCl
Ca ⁺² in CaO	$r_{\text{Ca}^{+2}} = 0.99$	50	NaCl
Co ⁺² in CoO	$r_{\text{Co}^{+2}} = 0.72$	9	NaCl
Fe ⁺² in FeO	$r_{\text{Fe}^{+2}} = 0.74$	12	NaCl
Sr ⁺² in SrO	$r_{\text{Sr}^{+2}} = 1.12$	70	NaCl
Zn ⁺² in ZnO	$r_{\text{Zn}^{+2}} = 0.74$	12	NaCl





Example 9.3 SOLUTION (Continued)

The percent difference in ionic radii and the crystal structures are also shown and suggest that the FeO-MgO system will probably display unlimited solid solubility. The CoO and ZnO systems also have appropriate radius ratios and crystal structures.





Section 9.4 Solid-Solution Strengthening

- **Solid-solution strengthening** - Increasing the strength of a metallic material via the formation of a solid solution.
- **Dispersion strengthening** - Strengthening, typically used in metallic materials, by the formation of ultra-fine dispersions of a second phase.





©2003 Brooks/Cole, a division of Thomson Learning, Inc. Thomson Learning is a trademark used herein under license.

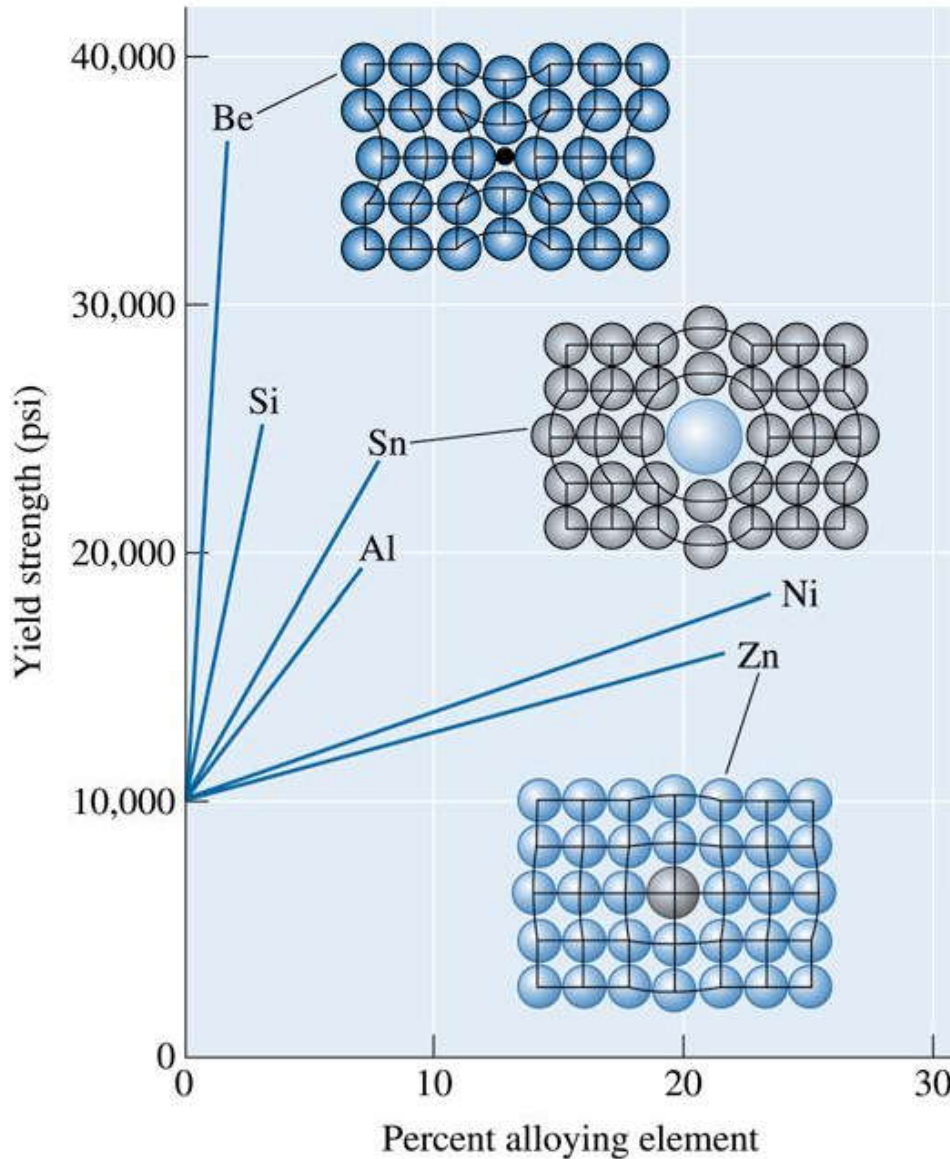
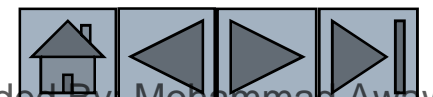
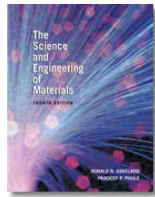


Figure 9.8 The effects of several alloying elements on the yield strength of copper. Nickel and zinc atoms are about the same size as copper atoms, but beryllium and tin atoms are much different from copper atoms. Increasing both atomic size difference and amount of alloying element increases solid-solution strengthening.





Example 9.4

Solid-Solution Strengthening

From the atomic radii, show whether the size difference between copper atoms and alloying atoms accurately predicts the amount of strengthening found in Figure 9.8.

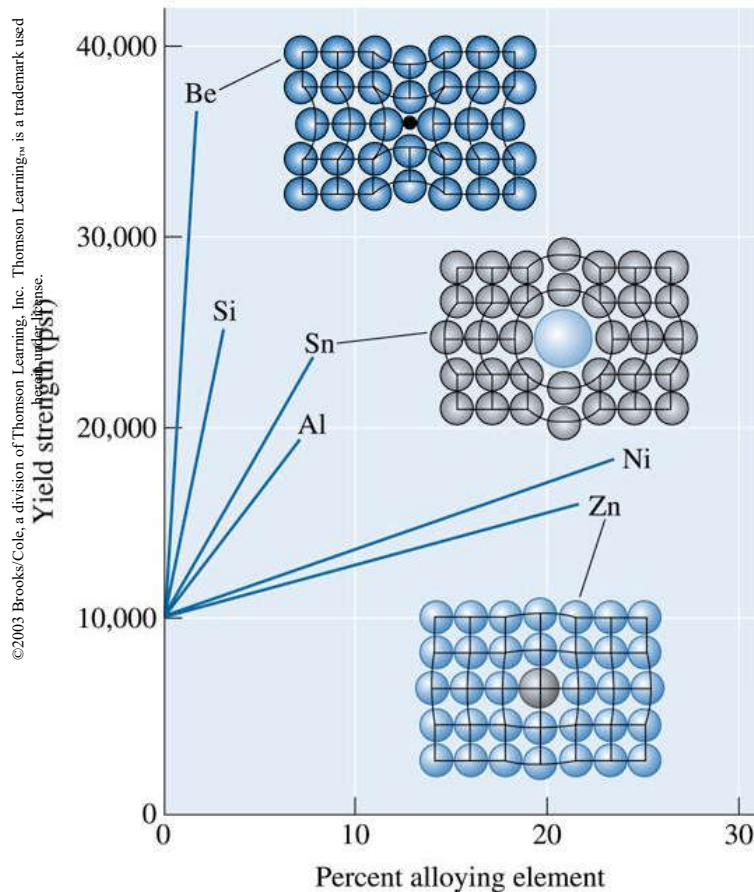
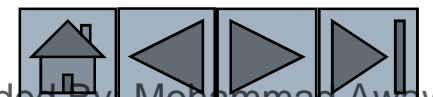
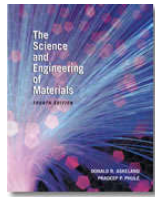


Figure 9.8 The effects of several alloying elements on the yield strength of copper. Nickel and zinc atoms are about the same size as copper atoms, but beryllium and tin atoms are much different from copper atoms. Increasing both atomic size difference and amount of alloying element increases solid-solution strengthening.





UPLOADED BY AHMAD T JUNDI

Example 9.4 SOLUTION

The atomic radii and percent size difference are shown below:

Metal	Atomic Radius (Å)	$\left[\frac{r - r_{\text{Cu}}}{r_{\text{Cu}}} \right] \times 100\%$
Cu	1.278	0
Zn	1.332	+4.2
Al	1.432	+12.1
Sn	1.509	+18.1
Ni	1.243	-2.7
Si	1.176	-8.0
Be	1.143	-10.6

For atoms larger than copper—namely, zinc, aluminum, and tin— increasing the size difference increases the strengthening effect. Likewise for smaller atoms, increasing the size difference increases strengthening.



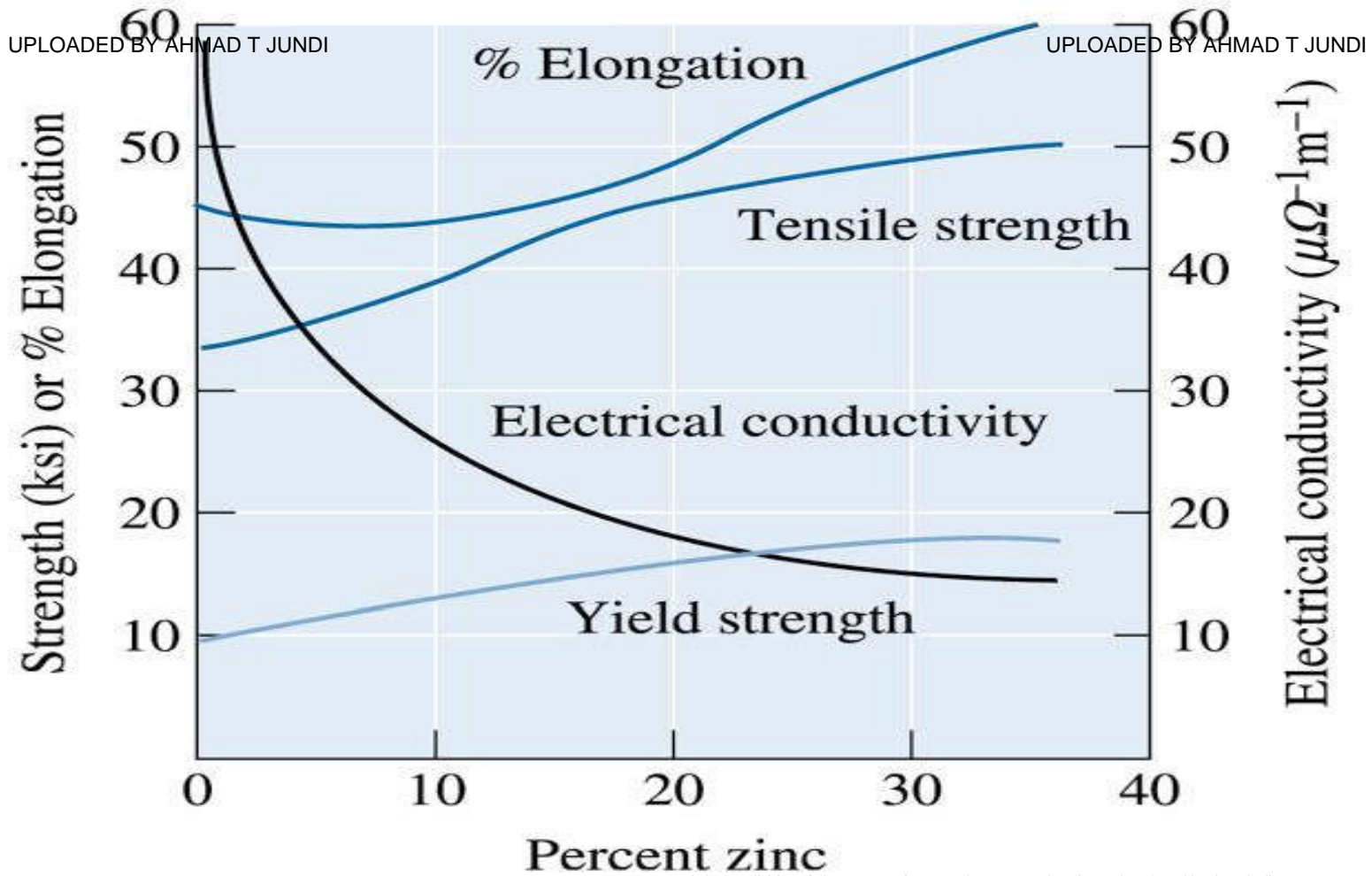
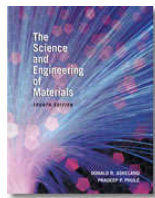


Figure 9.9 The effect of additions of zinc to copper on the properties of the solid-solution-strengthened alloy. The increase in % elongation with increasing zinc content is *not* typical of solid-solution strengthening.

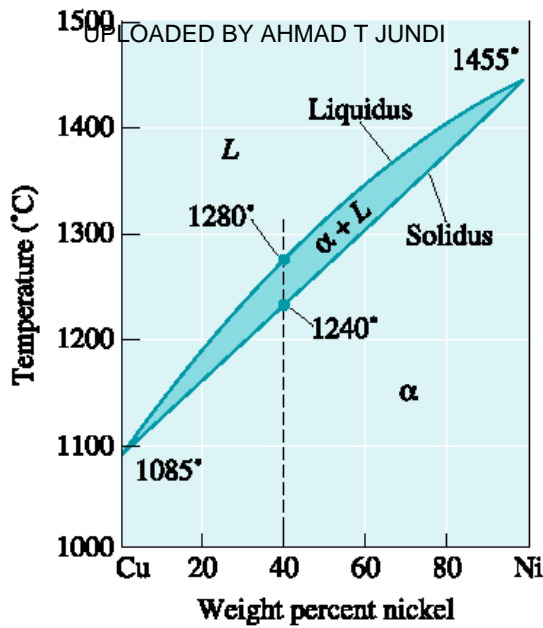




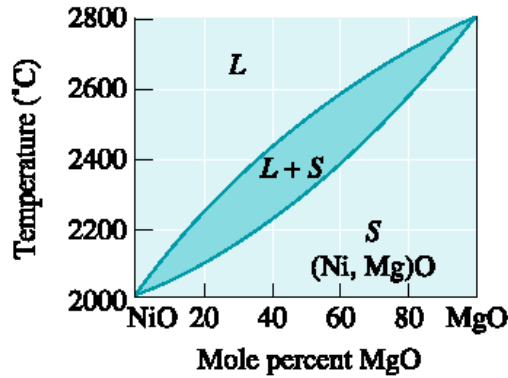
Section 9.5 Isomorphous Phase Diagrams

- ❑ **Binary phase diagram** - A phase diagram for a system with two components.
- ❑ **Ternary phase diagram** - A phase diagram for a system with three components.
- ❑ **Isomorphous phase diagram** - A phase diagram in which components display unlimited solid solubility.
- ❑ **Liquidus temperature** - The temperature at which the first solid begins to form during solidification.
- ❑ **Solidus temperature** - The temperature below which all liquid has completely solidified.

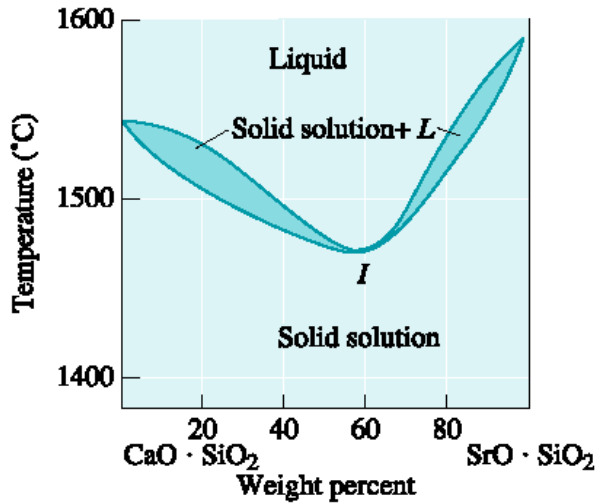




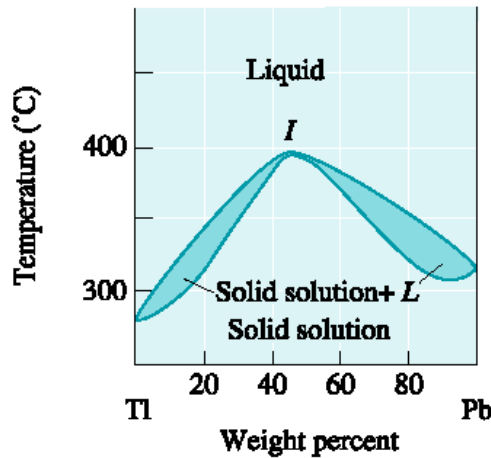
(a)



(b)



(c)



(d)

Figure 9.10 (a) The equilibrium phase diagrams for the Cu-Ni and NiO-MgO systems. (b) The liquidus and solidus temperatures are shown for a Cu-40% Ni alloy. (c) and (d) Systems with solid solution maxima and minima. (Source: Adapted from Introduction to Phase Equilibria, by C.G. Bergeron, and S.H. Risbud. Copyright © 1984 American Ceramic Society. Adapted by permission.)



Example 9.5

NiO-MgO Isomorphous System

From the phase diagram for the NiO-MgO binary system [Figure 9.10(b)], describe a composition that can melt at 2600°C but will not melt when placed into service at 2300°C.

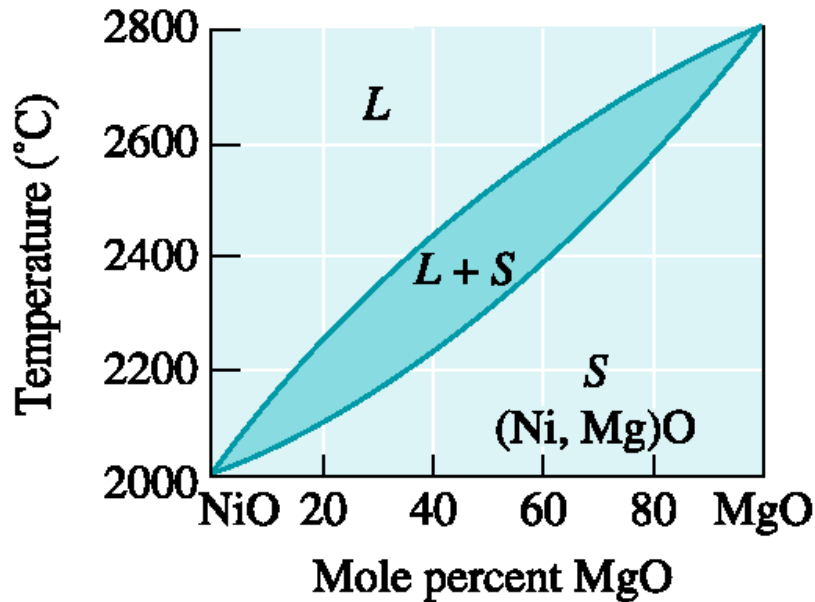
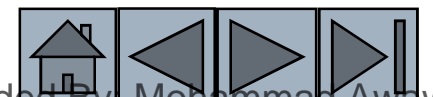


Figure 9.10 (b) The liquidus and solidus temperatures are shown for a Cu-40% Ni alloy.

(b)





Example 9.5 SOLUTION

To identify a composition with a liquidus temperature below 2600°C , there must be less than 65 mol% MgO in the refractory. To identify a composition with solidus temperature above 2300°C , there must be at least 50 mol% MgO present.

Consequently, we can use any composition between 50 mol% MgO and 65 mol% MgO.



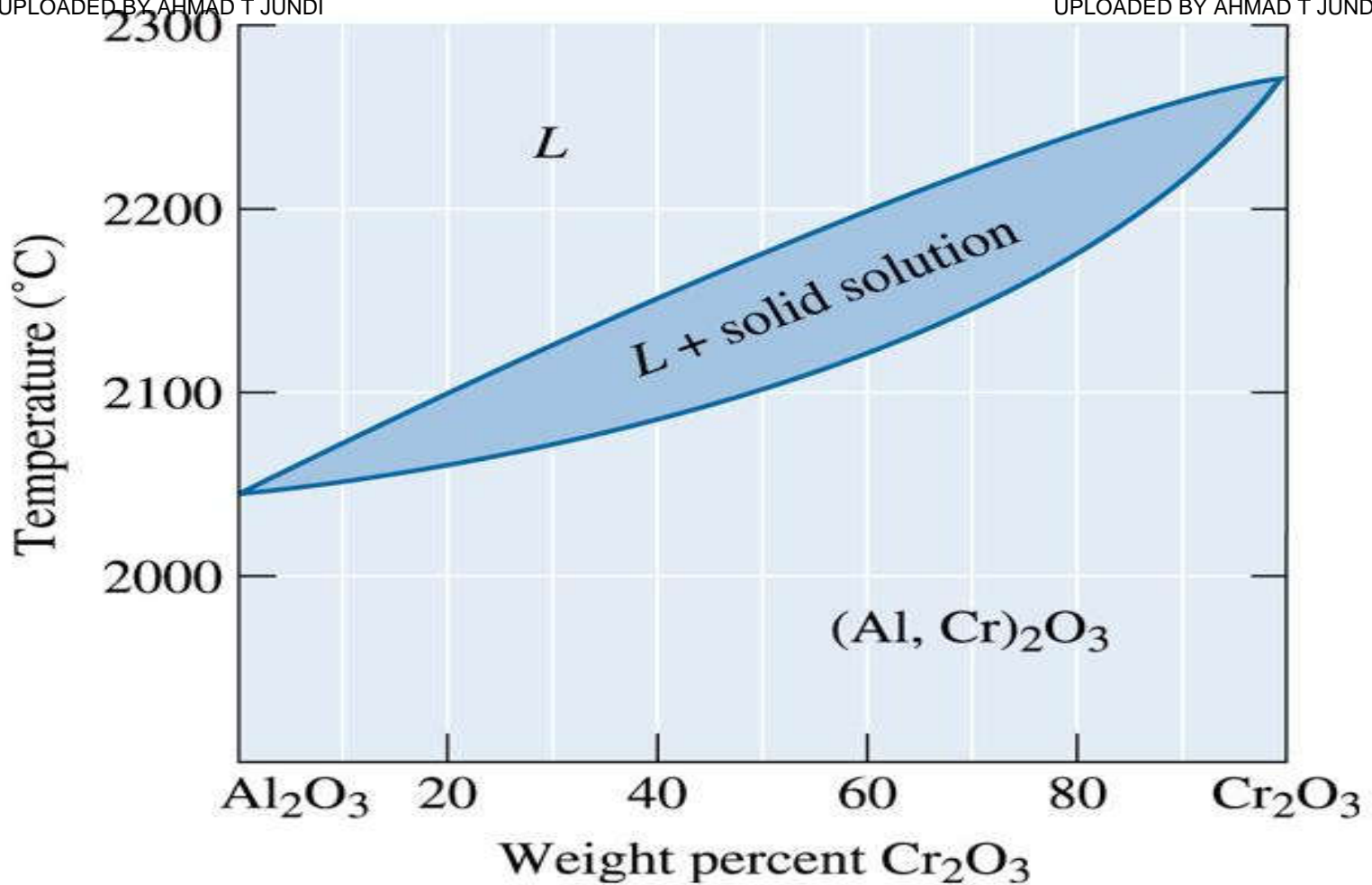


Example 9.6

Design of a Composite Material

One method to improve the fracture toughness of a ceramic material (Chapter 6) is to reinforce the ceramic matrix with ceramic fibers. A materials designer has suggested that Al_2O_3 could be reinforced with 25% Cr_2O_3 fibers, which would interfere with the propagation of any cracks in the alumina. The resulting composite is expected to operate under load at 2000°C for several months. Criticize the appropriateness of this design.

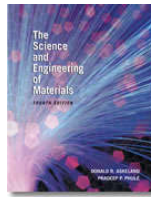




©2003 Brooks/Cole, a division of Thomson Learning, Inc. Thomson Learning™ is a trademark used herein under license.

Figure 9.11 The $\text{Al}_2\text{O}_3\text{-Cr}_2\text{O}_3$ phase diagram (for Example 9.6).





Example 9.6 SOLUTION

Since the composite will operate at high temperatures for a substantial period of time, the two phases—the Cr_2O_3 fibers and the Al_2O_3 matrix—must not react with one another. In addition, the composite must remain solid to at least 2000°C . The phase diagram in Figure 9.11 permits us to consider this choice for a composite.

Pure Cr_2O_3 , pure Al_2O_3 , and Al_2O_3 -25% Cr_2O_3 have solidus temperatures above 2000°C ; consequently, there is no danger of melting any of the constituents. However, Cr_2O_3 and Al_2O_3 display unlimited solid solubility. At the high service temperature, 2000°C , Al^{3+} ions will diffuse from the matrix into the fiber, replacing Cr^{3+} ions in the fibers. Simultaneously, Cr^{3+} ions will replace Al^{3+} ions in the matrix. Long before several months have elapsed, these diffusion processes cause the fibers to completely dissolve into the matrix. With no fibers remaining, the fracture toughness will again be poor.





Example 9.7

Gibbs Rule for Isomorphous Phase Diagram

Determine the degrees of freedom in a Cu-40% Ni alloy at (a) 1300°C, (b) 1250°C, and (c) 1200°C.

Example 9.7 SOLUTION

This is a binary system ($C = 2$). Two components are Cu and Ni. We will assume constant pressure. Therefore, Equation 9-2 ($1 + C = F + P$) can be used as follows:

(a) At 1300°C, $P = 1$, since only one phase (liquid) is present; $C = 2$, since both copper and nickel atoms are present. Thus:

$$1 + C = F + P \quad \text{So, } 1 + 2 = F + 1 \quad \text{or } F = 2$$





Example 9.7 SOLUTION (Continued)

(b) At 1250°C , $P = 2$, since both liquid and solid are present; $C = 2$, since copper and nickel atoms are present. Now:

$$1 + C = F + P \quad \text{So, } 1 + 2 = F + 2 \text{ or } F = 1$$

(c) At 1200°C , $P = 1$, since only one phase, solid, is present; $C = 2$, since both copper and nickel atoms are present. Again,

$$1 + C = F + P \quad \text{So, } 1 + 2 = F + 1 \text{ or } F = 2$$



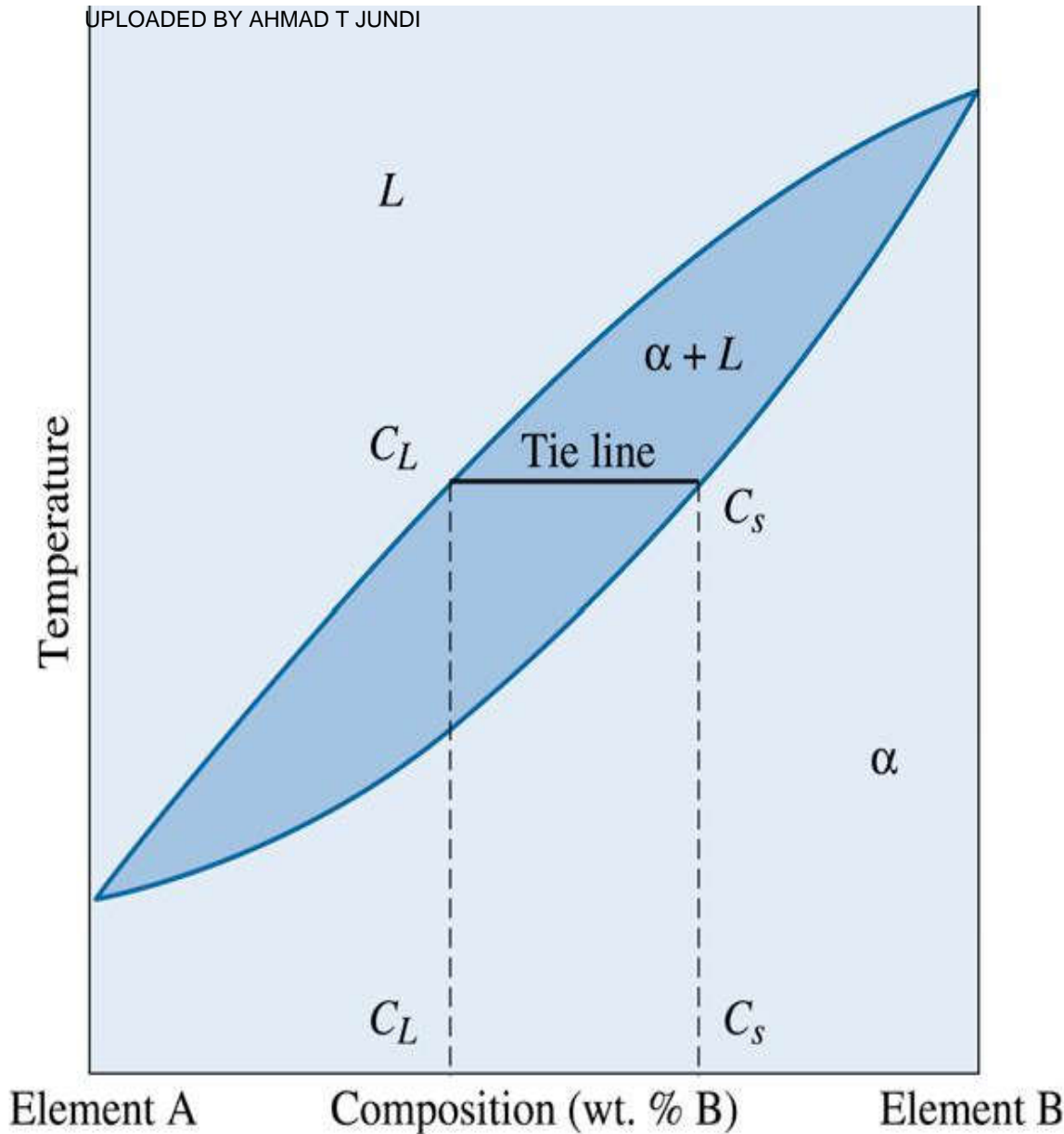


Figure 9.12 A hypothetical binary phase diagram between elements A and B. When an alloy is present in a two-phase region, a tie line at the temperature of interest fixes the composition of the two phases. This is a consequence of the Gibbs phase rule, which provides only one degree of freedom.

Example 9.8



Compositions of Phases in Cu-Ni Phase Diagram

Determine the composition of each phase in a Cu-40% Ni alloy at 1300°C, 1270°C, 1250°C, and 1200°C. (See Figure 9.13.)

©2003 Brooks/Cole, a division of Thomson Learning, Inc. Thomson Learning is a trademark used herein under license.

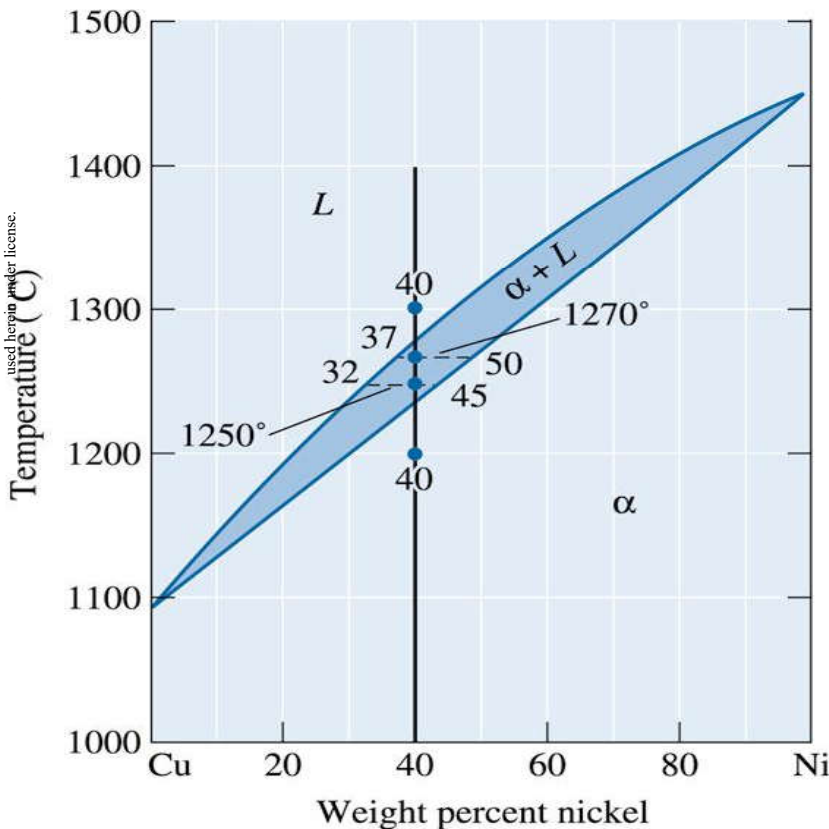
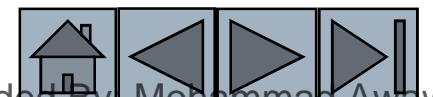


Figure 9.13 Tie lines and phase compositions for a Cu-40% Ni alloy at several temperatures (for Example 9.8).





Example 9.8 SOLUTION

The vertical line at 40% Ni represents the overall composition of the alloy:

- 1300°C: Only liquid is present. The liquid must contain 40% Ni, the overall composition of the alloy.
- 1270°C: Two phases are present. The liquid contains 37% Ni and the solid contains 50% Ni.
- 1250°C: Again two phases are present. The tie line drawn at this temperature shows that the liquid contains 32% Ni and the solid contains 45% Ni.
- 1200°C: Only solid α is present, so the solid must contain 40% Ni.



Example 9.9

Application of Lever Rule



Calculate the amounts of α and L at 1250°C in the Cu-40% Ni alloy shown in Figure 9.14.

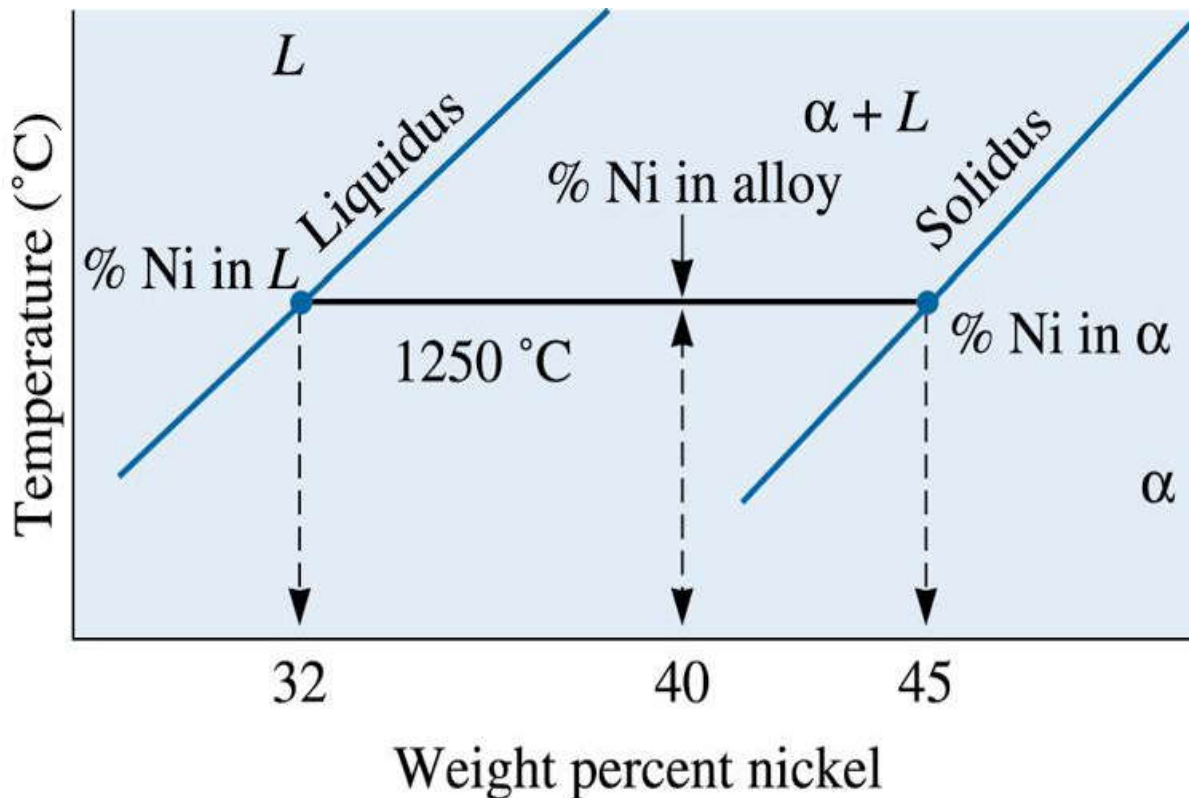


Figure 9.14 A tie line 1250°C in the copper-nickel system that is used in Example 9.9 to find the amount of each phase.

©2003 Brooks/Cole, a division of Thomson Learning, Inc. Thomson Learning[®] is a trademark used herein under license.





Example 9.9 SOLUTION

Let's say that x = mass fraction of the alloy that is solid α . Since we have only two phases, the balance of nickel must be in the liquid phase (L). Thus, the mass fraction of nickel in liquid will be $1 - x$.

Total mass of nickel in 100 grams of the alloy = mass of nickel in liquid + mass of nickel in α

So, $100 \times (\% \text{ Ni in alloy}) = [(100)(1 - x)](\% \text{ Ni in L}) + (100)[x](\% \text{ Ni in } \alpha)$

$$x = (40-32)/(45-32) = 8/13 = 0.62$$

If we convert from mass fraction to mass percent, the alloy at 1250°C contains 62% α and 38% L . Note that the concentration of Ni in alpha phase (at 1250°C) is 45% and concentration of nickel in liquid phase (at 1250°C) is 32%.



Example 9.10



Solidification of a Cu-40% Ni Alloy

Determine the amount of each phase in the Cu-40% Ni alloy shown in Figure 9.13 at 1300°C, 1270°C, 1250°C, and 1200°C.

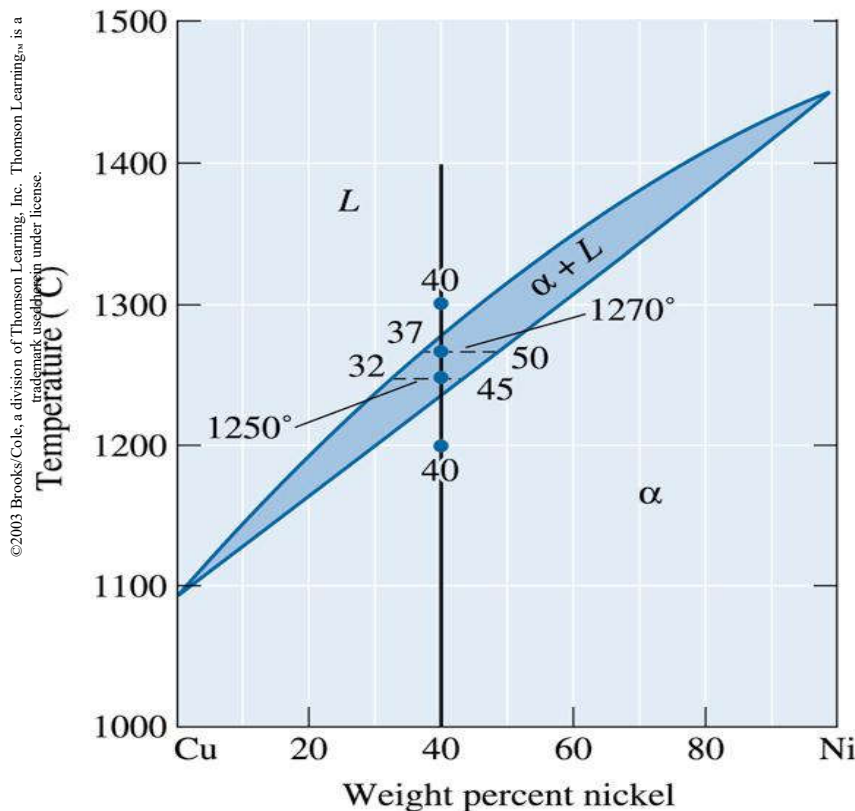


Figure 9.13 Tie lines and phase compositions for a Cu-40% Ni alloy at several temperatures





Example 9.10 SOLUTION

$$- 1300^{\circ}C : 100\%L$$

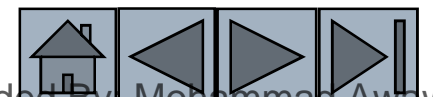
$$- 1270^{\circ}C : \%L = \frac{50 - 40}{50 - 37} \times 100 = 77\%$$

$$\% \alpha = \frac{40 - 37}{50 - 37} \times 100 = 23\%$$

$$- 1250^{\circ}C : \%L = \frac{45 - 40}{45 - 32} \times 100 = 38\%$$

$$\% \alpha = \frac{40 - 32}{45 - 32} \times 100 = 62\%$$

$$- 1200^{\circ}C : 100\% \alpha$$





Section 9.6 Relationship Between Properties and the Phase Diagram



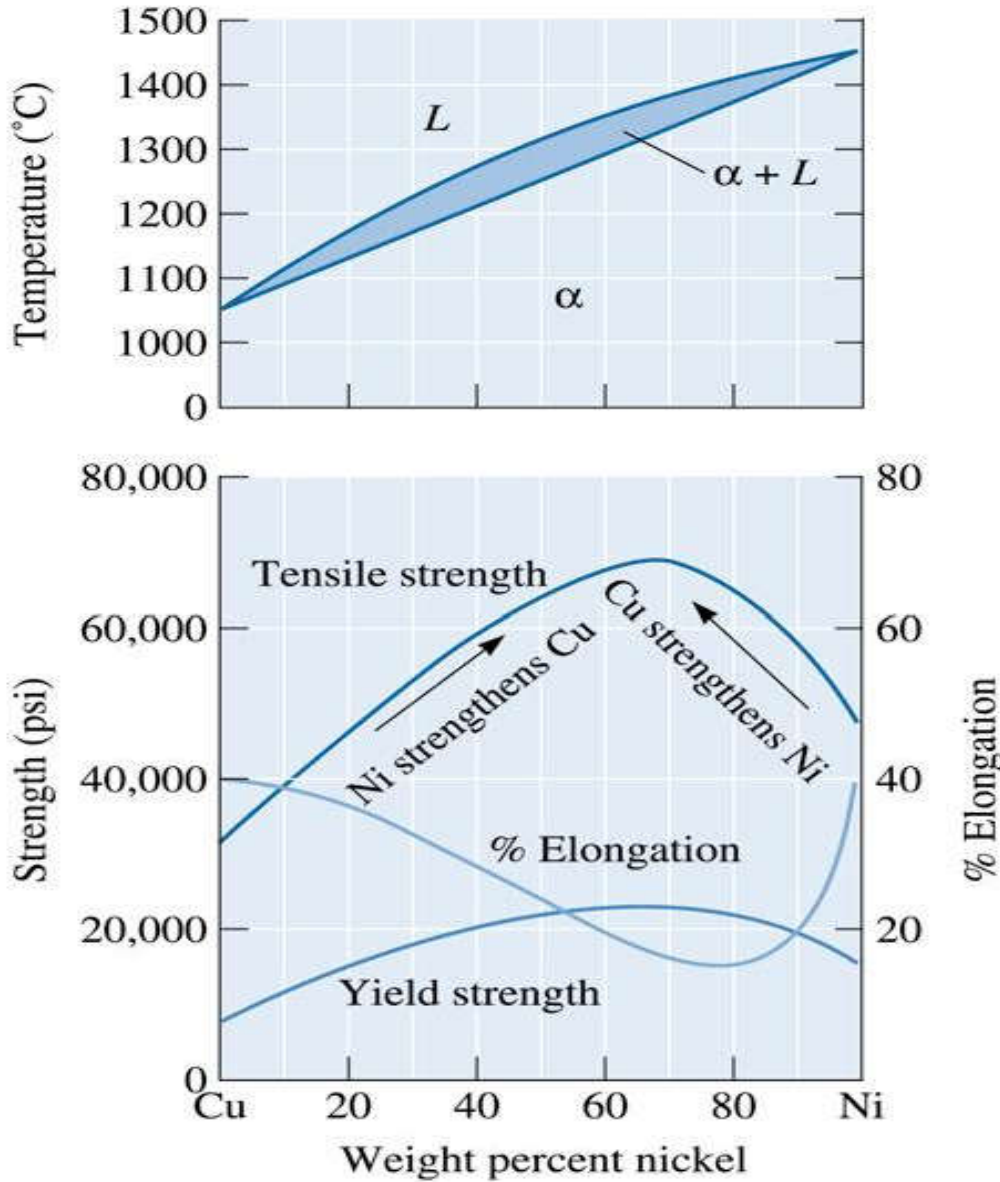


Figure 9.15 The mechanical properties of copper-nickel alloys. Copper is strengthened by up to 60% Ni and nickel is strengthened by up to 40% Cu.

Example 9.11



Design of a Melting Procedure for a Casting

You need to produce a Cu-Ni alloy having minimum yield strength of 20,000 psi, a minimum tensile strength of 60,000 psi, and a minimum % elongation of 20%. You have in your inventory a Cu-20% Ni alloy and pure nickel. Design a method for producing castings having the required properties.

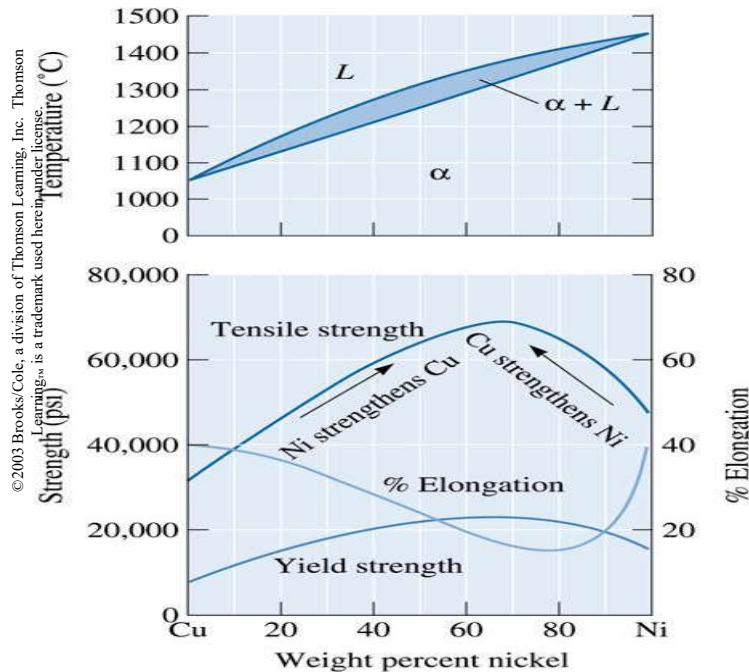


Figure 9.15 The mechanical properties of copper-nickel alloys. Copper is strengthened by up to 60% Ni and nickel is strengthened by up to 40% Cu.





Example 9.11 SOLUTION

From Figure 9.15, we determine the required composition of the alloy. To satisfy all of these conditions, we could use:

Cu-90% Ni or Cu-33% to 60% Ni

We prefer to select a low nickel content, since nickel is more expensive than copper. In addition, the lower nickel alloys have a lower liquidus, permitting castings to be made with less energy being expended. Therefore, a reasonable alloy might be Cu-35% Ni.





Example 9.11 SOLUTION (Continued)

To produce this composition from the available melting stock, we must blend some of the pure nickel with the Cu-20% Ni ingot. Assume we wish to produce 10 kg of the alloy. Let x be the mass of Cu-20% Ni alloy we will need. The mass of pure Ni needed will be $10 - x$.

Since the final alloy consists of 35% Ni, the total mass of Ni needed will be:

$$(10 \text{ Kg})(35\% \text{ Ni} / 100\%) = 3.5 \text{ Kg Ni}$$

Now let's write a mass balance for nickel. Nickel from the Cu-20% alloy + pure nickel added = total nickel in the 35% alloy being produced.

$$0.2x + 10 - x = 3.5$$

$$6.5 = 0.8x$$

$$x = 8.125 \text{ kg}$$



Section 9.7 Solidification of a Solid-Solution Alloy

- **Segregation** - The presence of composition differences in a material, often caused by insufficient time for diffusion during solidification.



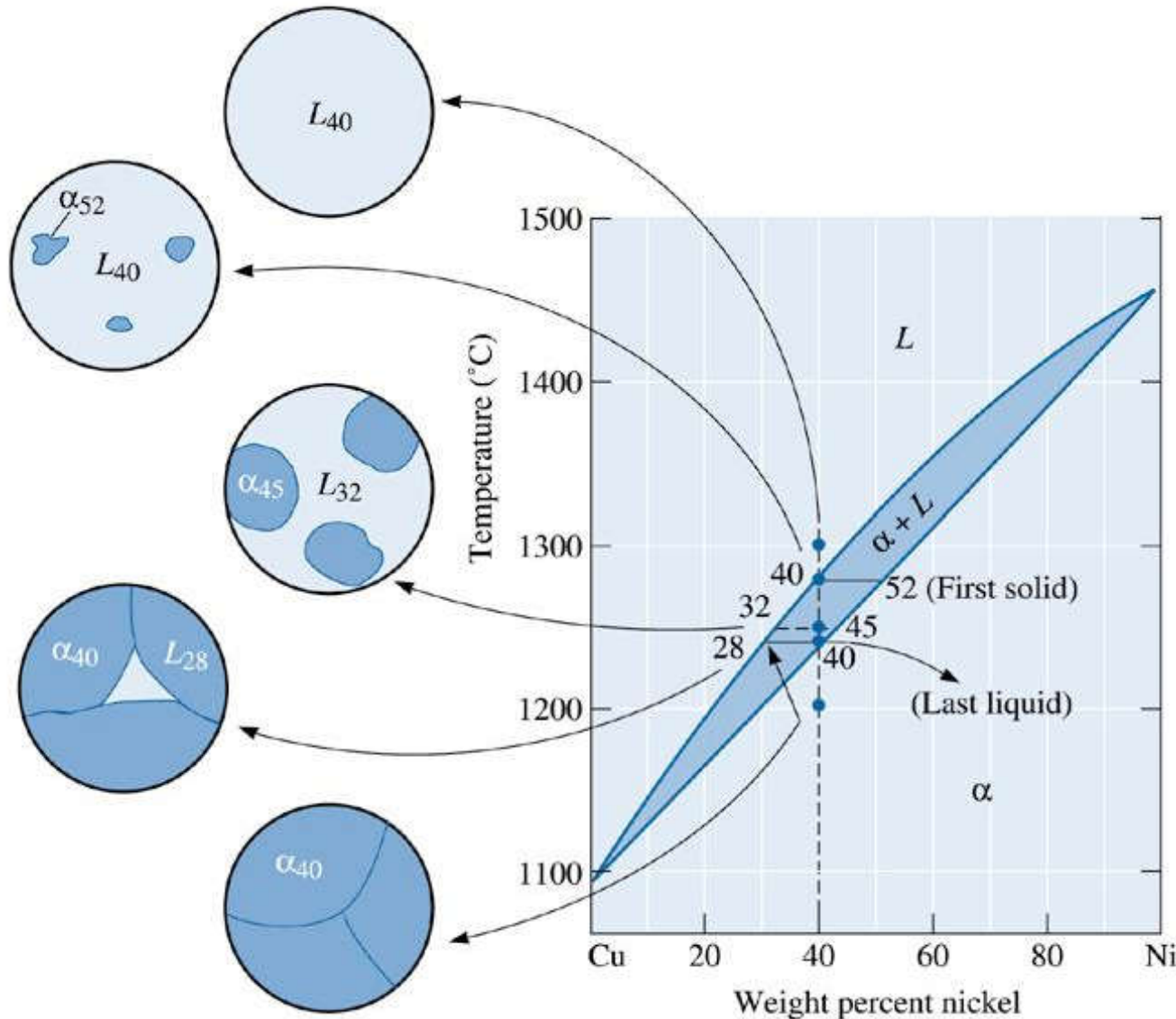
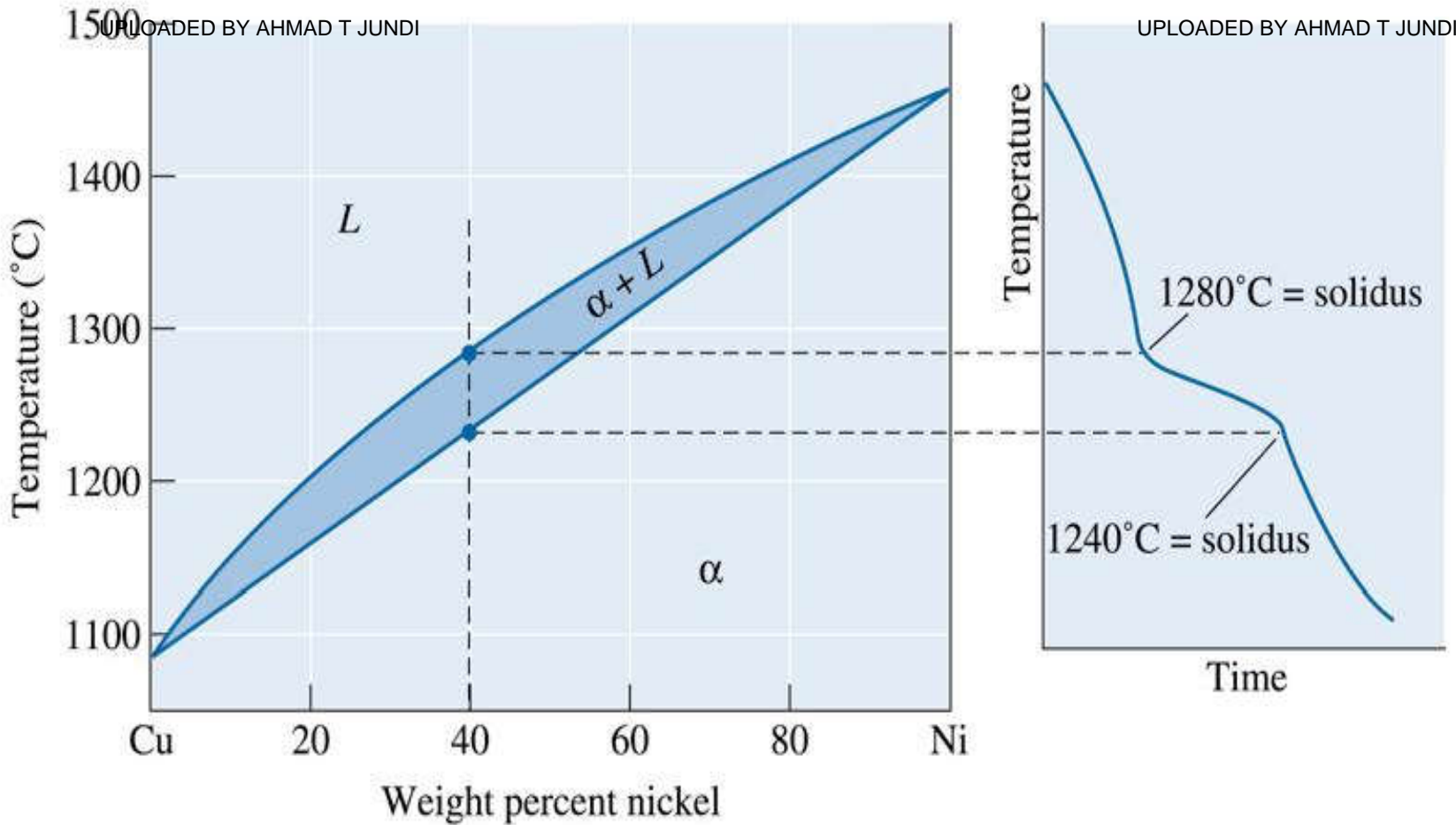


Figure 9.16 The change in structure of a Cu-40% Ni alloy during equilibrium solidification. The nickel and copper atoms must diffuse during cooling in order to satisfy the phase program and produce a uniform equilibrium structure.





©2003 Brooks/Cole, a division of Thomson Learning, Inc. Thomson Learning, is a trademark used herein under license.

Figure 9.17 The cooling curve for an isomorphous alloy during solidification. We assume that cooling rates are small so as to allow thermal equilibrium to take place. The changes in slope of the cooling curve indicate the liquidus and solidus temperatures, in this case for a Cu-40% Ni alloy.



Section 9.8 Nonequilibrium Solidification and Segregation

- ❑ **Coring** - Chemical segregation in cast products, also known as microsegregation or interdendritic segregation.
- ❑ **Homogenization heat treatment** - The heat treatment used to reduce the microsegregation caused during nonequilibrium solidification.
- ❑ **Macrosegregation** - The presence of composition differences in a material over large distances caused by nonequilibrium solidification.
- ❑ **Spray atomization** - A process in which molten alloys or metals are sprayed using a ceramic nozzle.



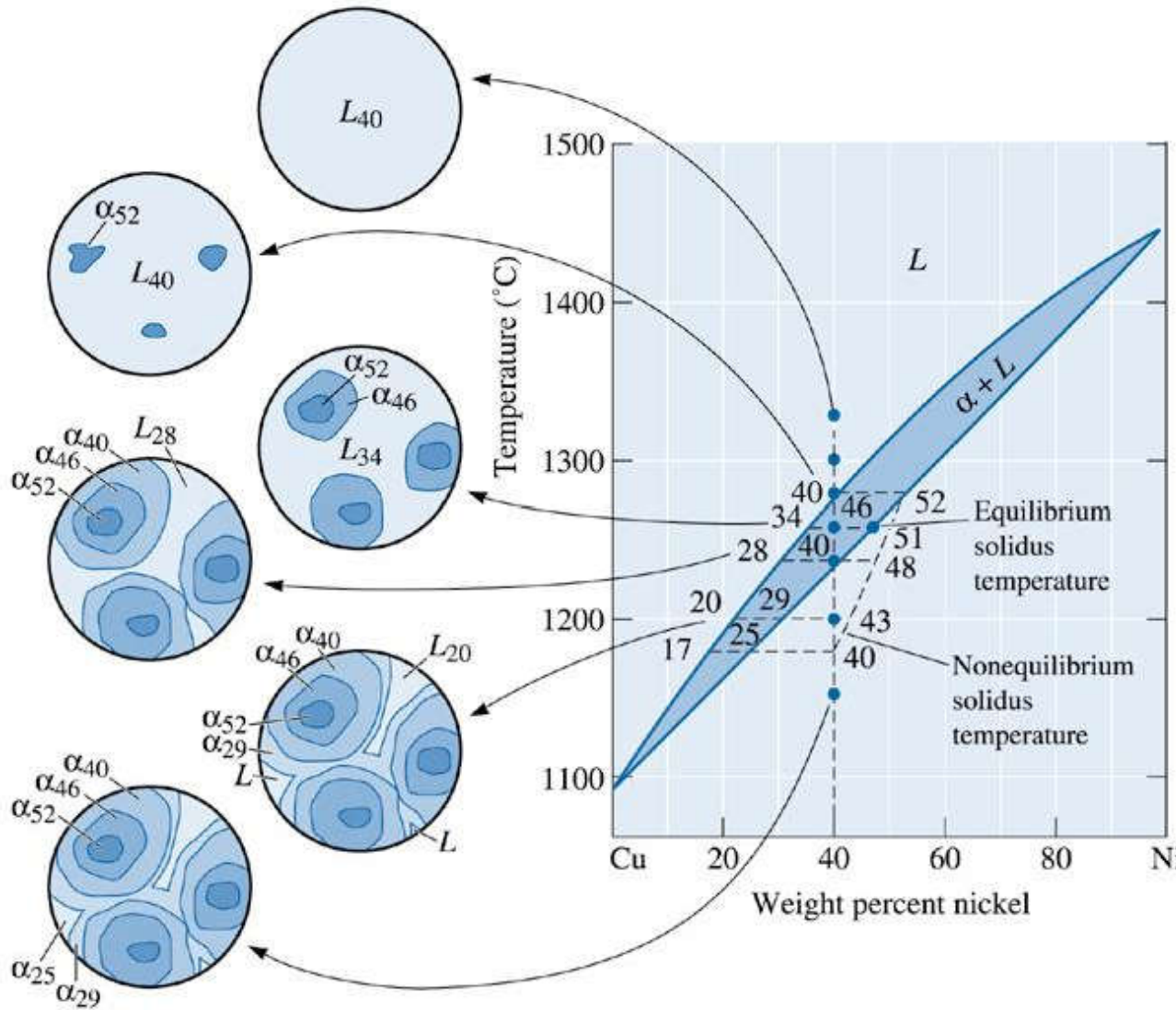
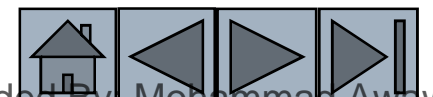


Figure 9.18 The change in structure of a Cu-40% Ni alloy during nonequilibrium solidification. Insufficient time for diffusion in the solid produces a segregated structure.

©2003 Brooks/Cole, a division of Thomson Learning, Inc. Thomson Learning, Inc. is a trademark used herein under license.





Example 9.12

Nonequilibrium Solidification of Cu-Ni Alloys

Calculate the composition and amount of each phase in a Cu-40% Ni alloy that is present under the nonequilibrium conditions shown in Figure 9.18 at 1300°C, 1280°C, 1260°C, 1240°C, 1200°C, and 1150°C. Compare with the equilibrium compositions and amounts of each phase.



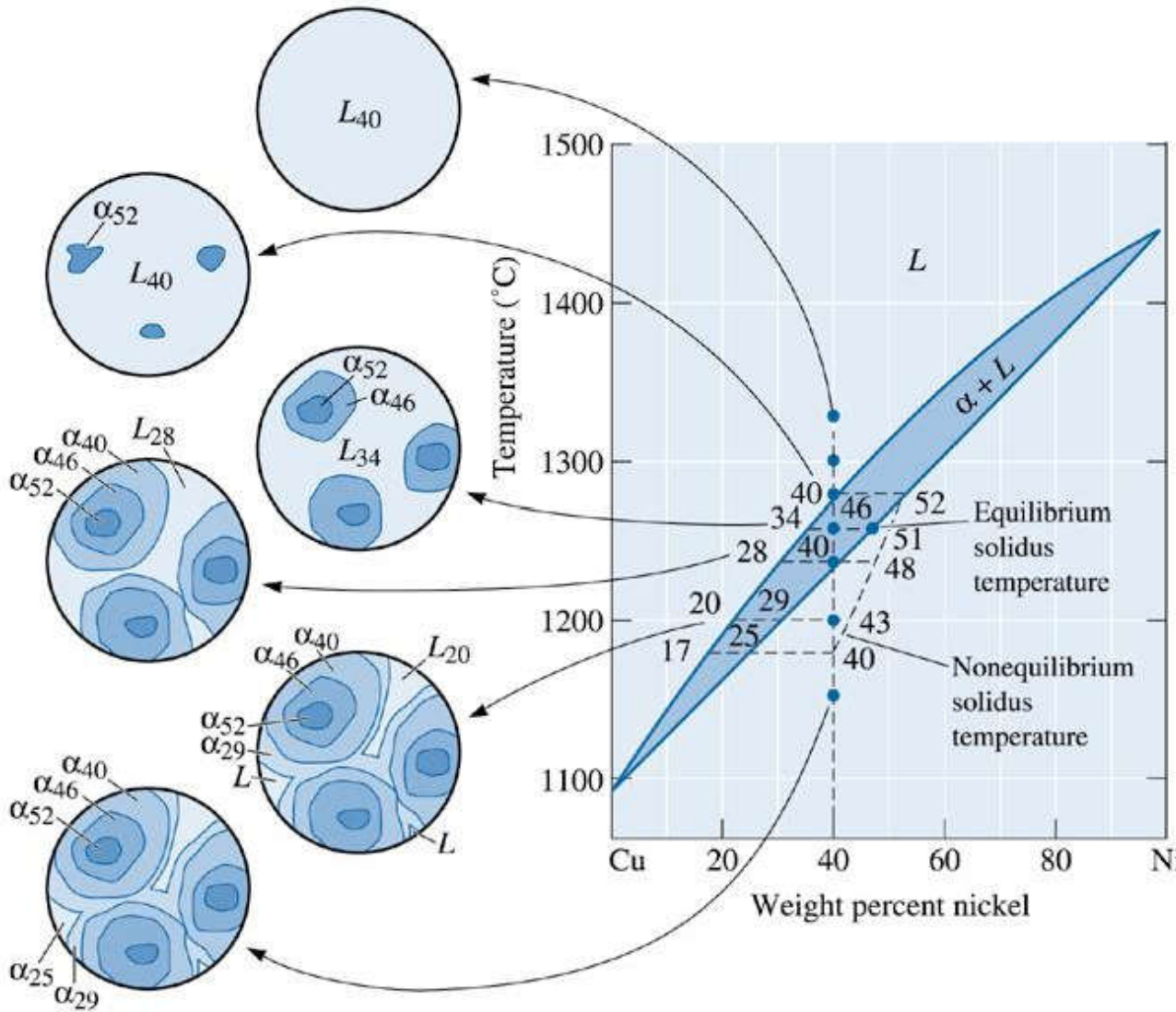


Figure 9.18 The change in structure of a Cu-40% Ni alloy during nonequilibrium solidification. Insufficient time for diffusion in the solid produces a segregated structure.

©2003 Brooks/Cole, a division of Thomson Learning, Inc. Thomson Learning, is a trademark used herein under license.





Example 9.12 SOLUTION

We use the tie line upto the equilibrium solidus temperature to calculate composition and percentages of phases as per the lever rule. Similarly, the nonequilibrium solidus temperature curve is used to calculate percentages and concentrations of different phases formed under nonequilibrium conditions.





Example 9.12 SOLUTION (Continued)

Temperature	Equilibrium	Nonequilibrium
1300°C	$L: 40\% \text{ Ni } 100\% L$	$L: 40\% \text{ Ni } 100\% L$
1280°C	$L: 40\% \text{ Ni } 100\% L$ $\alpha: 52\%, \text{ Ni } \sim 0\%$	$L: 40\% \text{ Ni } 100\% L$
1260°C	$L: 34\% \text{ Ni } \frac{46 - 40}{46 - 34} = 50\% L$ $\alpha: 46\% \text{ Ni } \frac{40 - 34}{46 - 34} = 50\% \alpha$	$L: 34\% \text{ Ni } \frac{51 - 40}{51 - 34} = 65\% L$ $\alpha: 51\% \text{ Ni } \frac{40 - 34}{51 - 34} = 35\% \alpha$
1240°C	$L: 28\% \text{ Ni } \sim 0\% L$ $\alpha: 40\% \text{ Ni } 100\% \alpha$	$L: 28\% \text{ Ni } \frac{48 - 40}{48 - 28} = 40\% L$ $\alpha: 48\% \text{ Ni } \frac{40 - 28}{48 - 28} = 60\% \alpha$
1200°C	$\alpha: 40\% \text{ Ni } 100\% \alpha$	$L: 20\% \text{ Ni } \frac{43 - 40}{43 - 20} = 13\% L$ $\alpha: 43\% \text{ Ni } \frac{40 - 20}{43 - 20} = 87\% \alpha$
1150°C	$\alpha: 40\% \text{ Ni } 100\% \alpha$	$\alpha: 40\% \text{ Ni } 100\% \alpha$



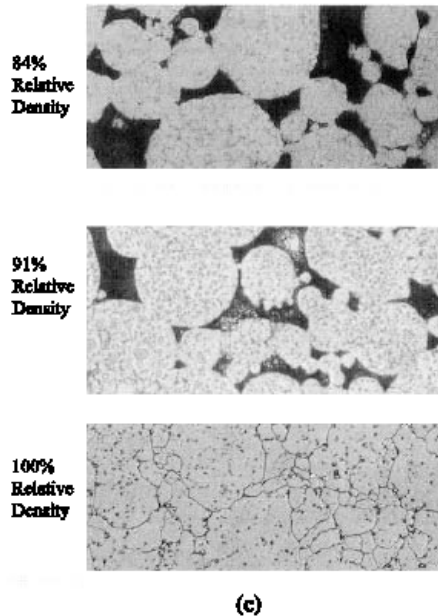
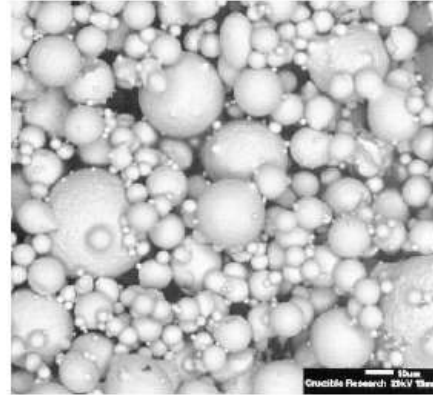
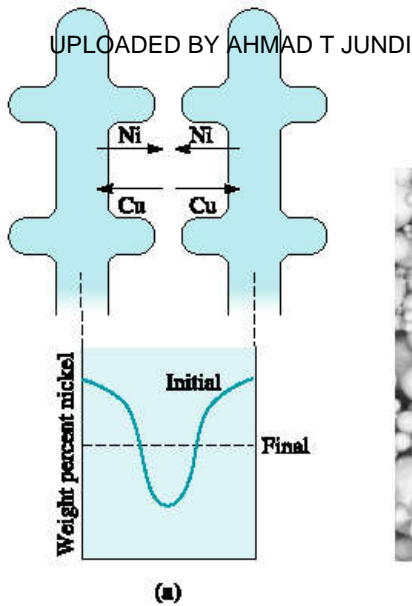


Figure 9.19 (a) Microsegregation between dendrites can be reduced by a homogenization heat treatment. Counterdiffusion of nickel and copper atoms may eventually eliminate the composition gradients and produce a homogeneous composition. (b) Spray atomized powders of superalloys. (c) Progression of densification in low carbon Astroalloy sample processed using HIP. (Courtesy of J. Staite, Hann, B. and Rizzo, F., Crucible Compaction Metals.)

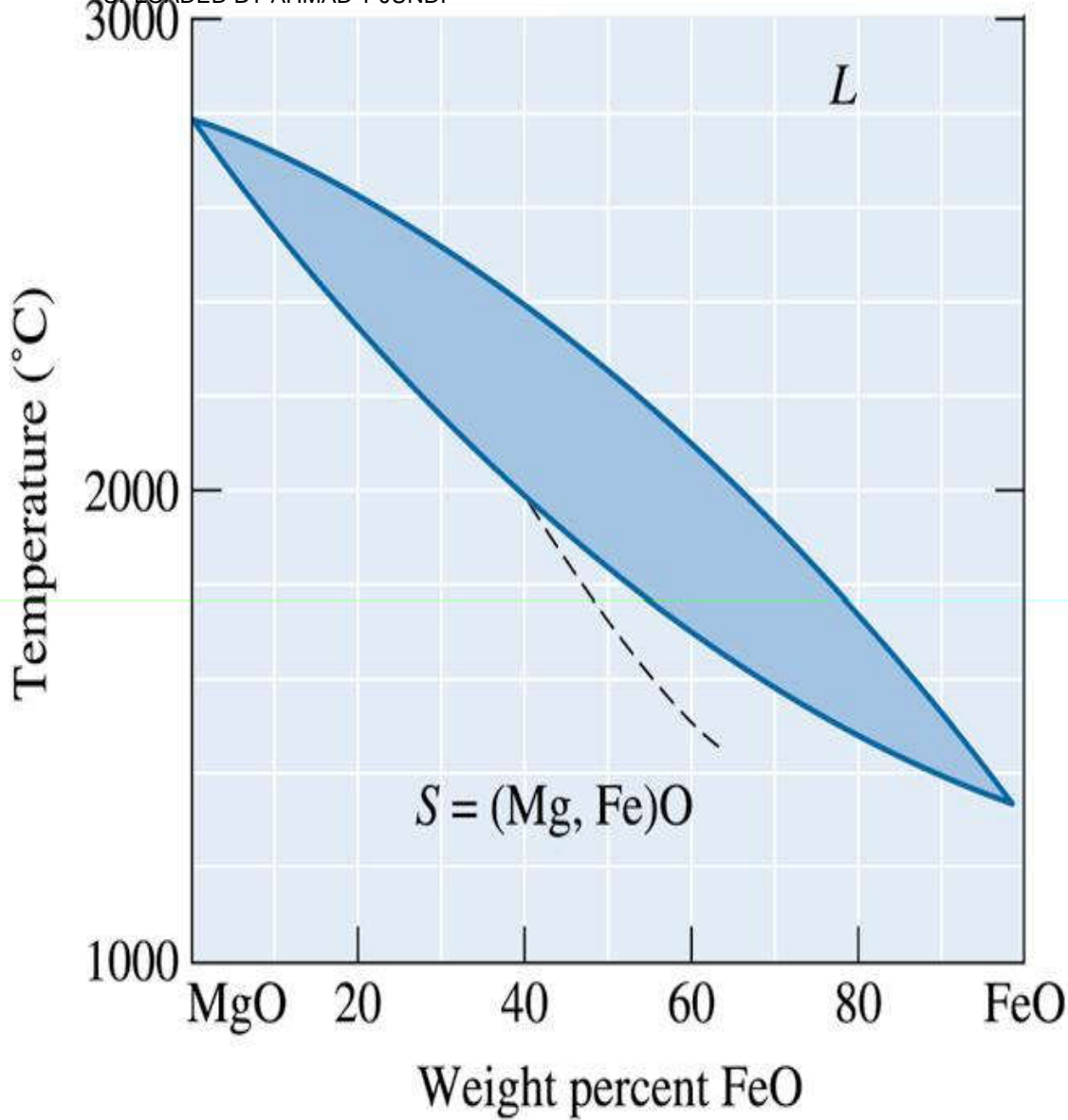
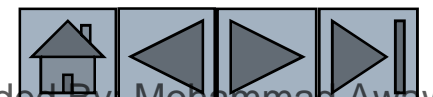


Figure 9.21 The equilibrium phase diagram for the MgO-FeO system.





©2003 Brooks/Cole, a division of Thomson Learning, Inc. Thomson Learning, Inc. is a trademark used herein under license.

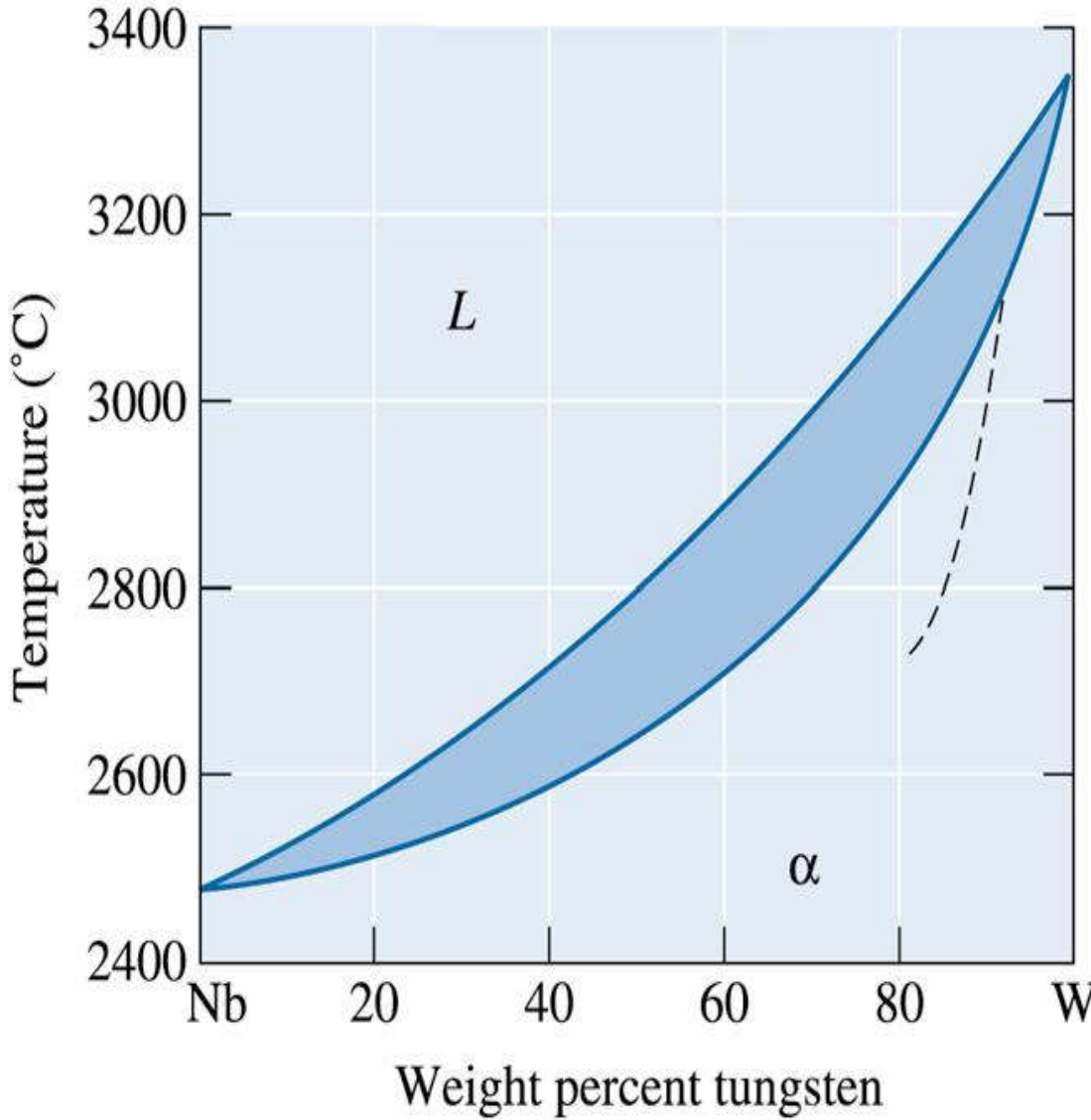
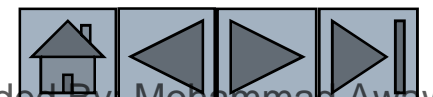


Figure 9.22 The equilibrium phase diagram for the Nb-W system.





©2003 Brooks/Cole, a division of Thomson Learning, Inc. Thomson LearningSM is a trademark used herein under license.

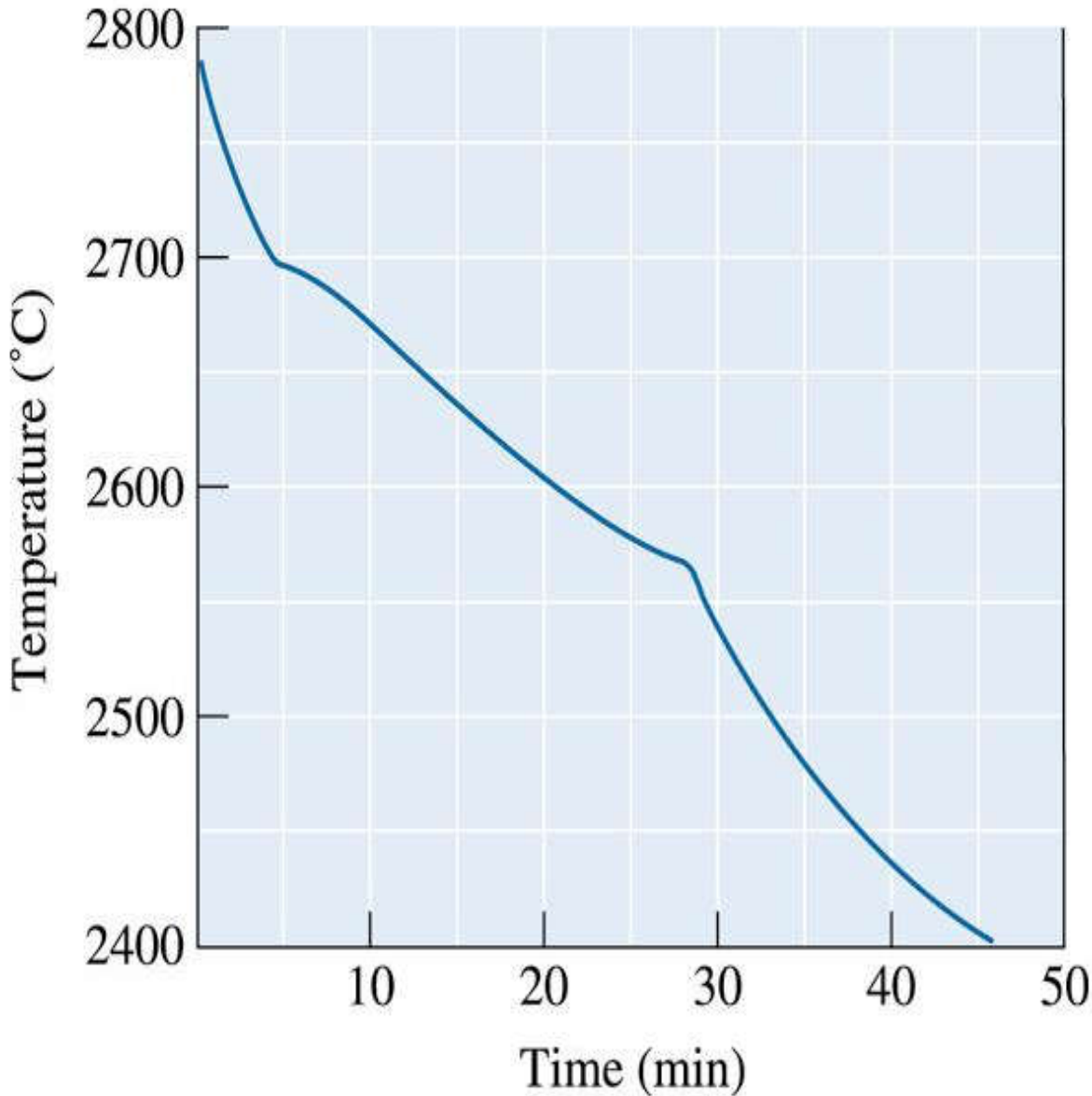


Figure 9.23
Cooling curve
for a NiO-MgO
ceramic (for
Problem 9.66).



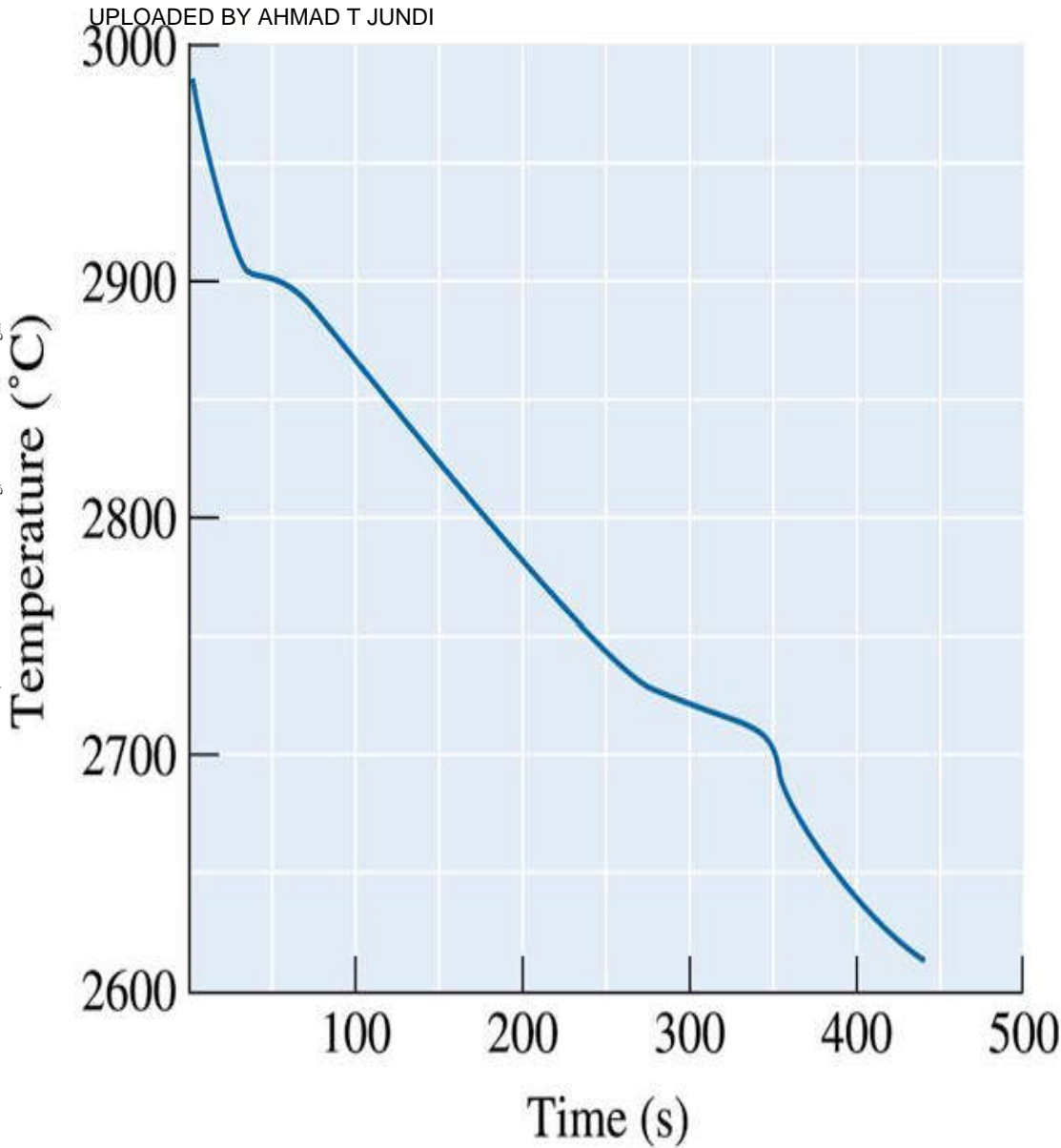
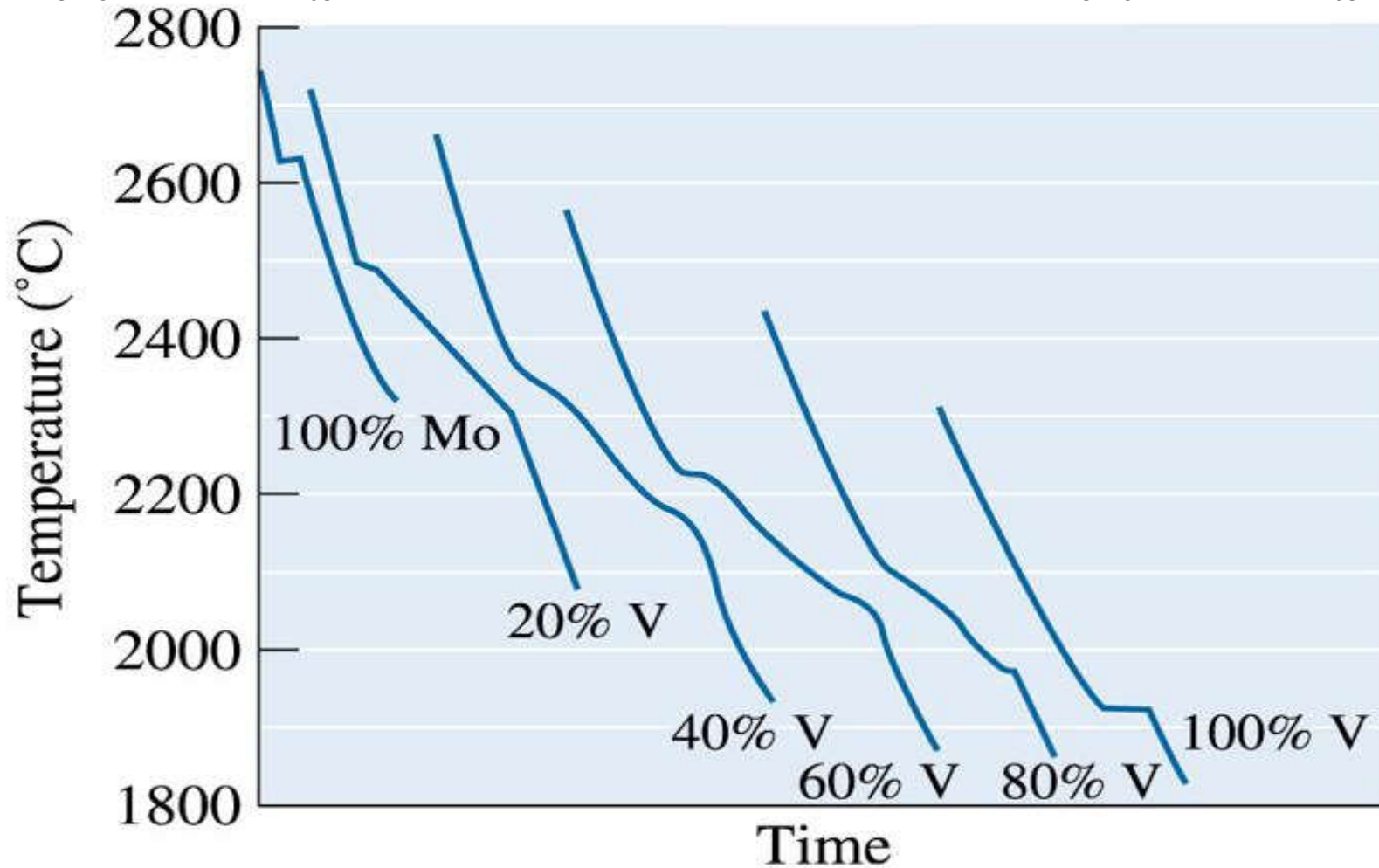


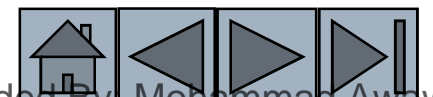
Figure 9.24
Cooling curve for a
Nb-W alloy (for
Problem 9.68).





©2003 Brooks/Cole, a division of Thomson Learning, Inc. Thomson Learning[®] is a trademark used herein under license.

Figure 9.25 Cooling curves for a series of Mo-V alloys (for Problem 9.69).





The Science and Engineering of Materials, 4th ed

Donald R. Askeland – Pradeep P. Phulé

Chapter 10 – Dispersion Strengthening and Eutectic Phase Diagrams





Objectives of Chapter 10

- ❑ Discuss the fundamentals of dispersion strengthening to determine the microstructure.
- ❑ Examine the types of reactions that produce multiple-phase alloys.
- ❑ Examine in some detail the methods to achieve dispersion strengthening by controlling the solidification process.





Chapter Outline

- 10.1 Principles and Examples of Dispersion Strengthening
- 10.2 Intermetallic Compounds
- 10.3 Phase Diagrams Containing Three-Phase Reactions
- 10.4 The Eutectic Phase Diagram
- 10.5 Strength of Eutectic Alloys
- 10.6 Eutectics and Materials Processing
- 10.7 Nonequilibrium Freezing in the Eutectic System
- 10.8 Ternary Phase Diagrams

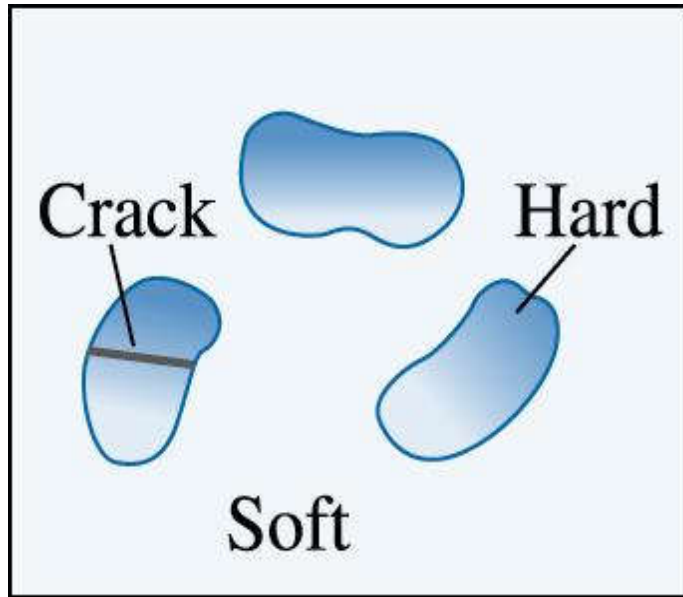




Section 10.1 Principles and Examples of Dispersion Strengthening

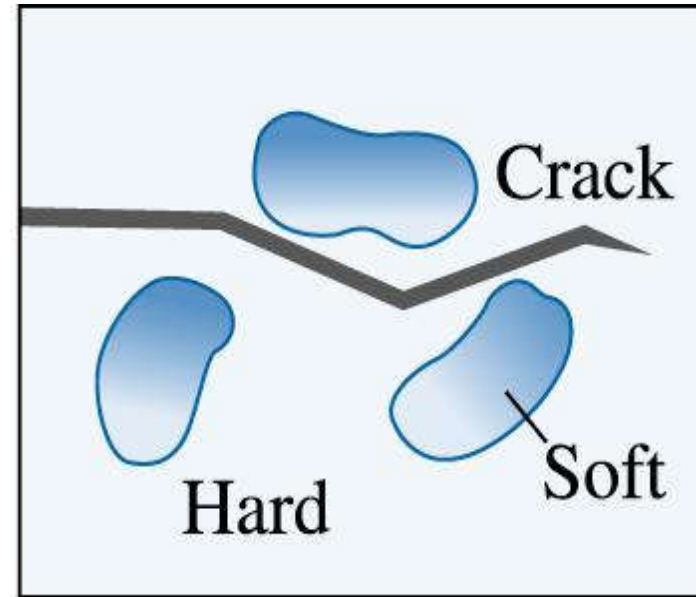
- **Dispersion strengthening** - Increasing the strength of a material by forming more than one phase.
- **Matrix** - The continuous solid phase in a complex microstructure.
- **Precipitate** - A solid phase that forms from the original matrix phase when the solubility limit is exceeded.
- **Eutectic** - A three-phase invariant reaction in which one liquid phase solidifies to produce two solid phases.





Good

vs.

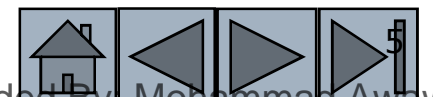


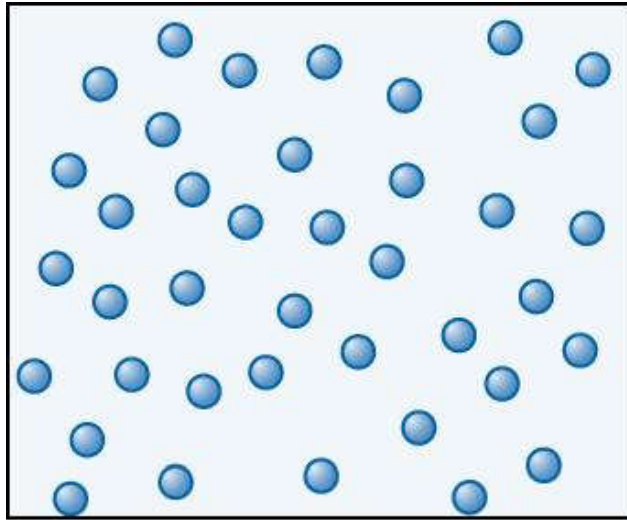
Poor

(a)

(c)2003 Brooks/Cole, a division of Thomson Learning, Inc. Thomson Learning, is a trademark used herein under license.

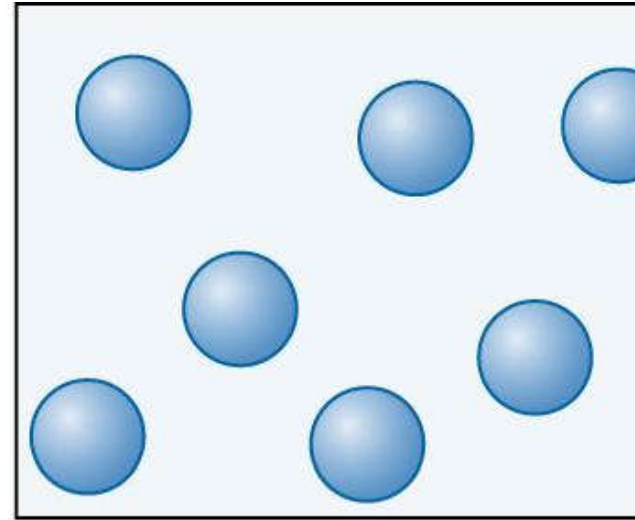
Figure 10.1 Considerations for effective dispersion strengthening: (a) The precipitate phase should be hard and discontinuous.





Good

VS.



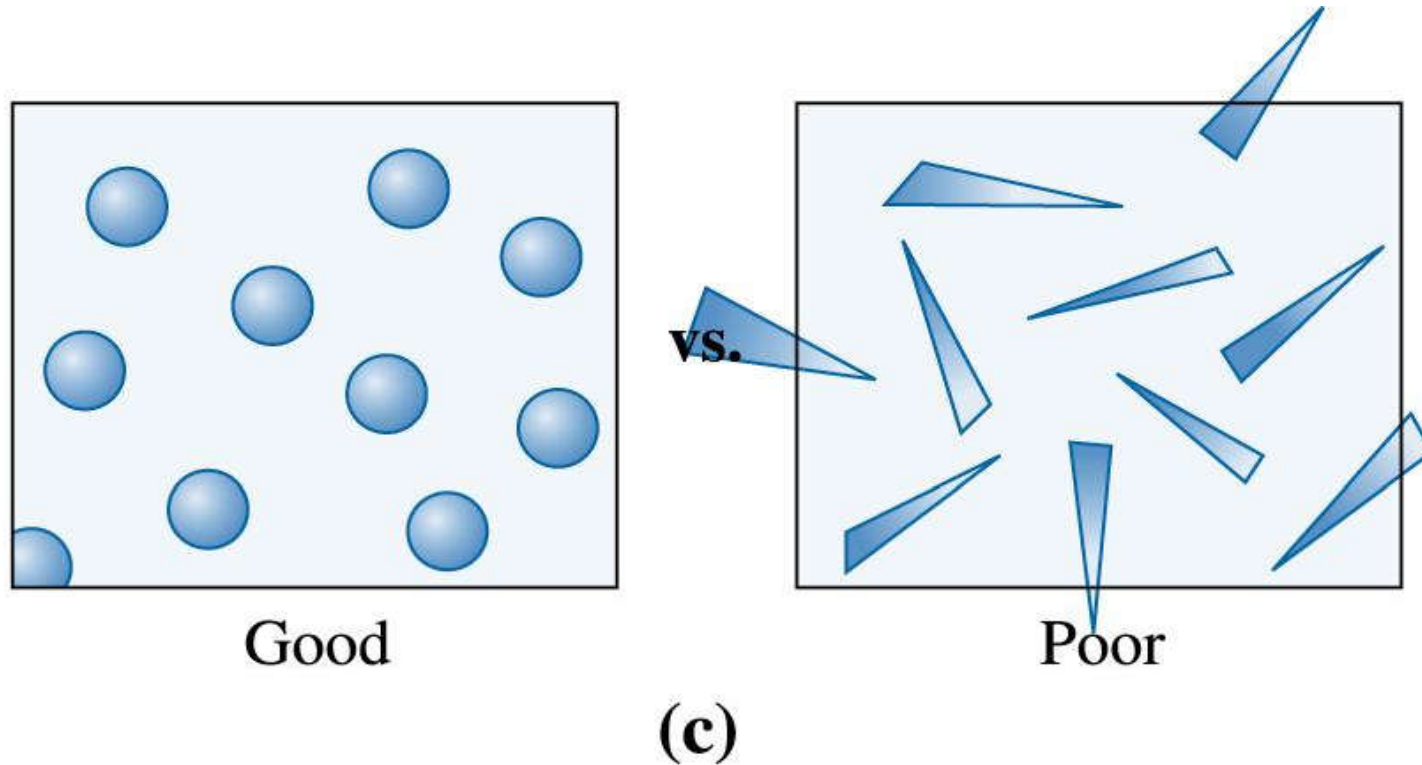
Poor

(b)

(c)2003 Brooks/Cole, a division of Thomson Learning, Inc. Thomson Learning[®] is a trademark used herein under license.

Figure 10.1 Considerations for effective dispersion strengthening: (b) The dispersed phase particles should be small and numerous.

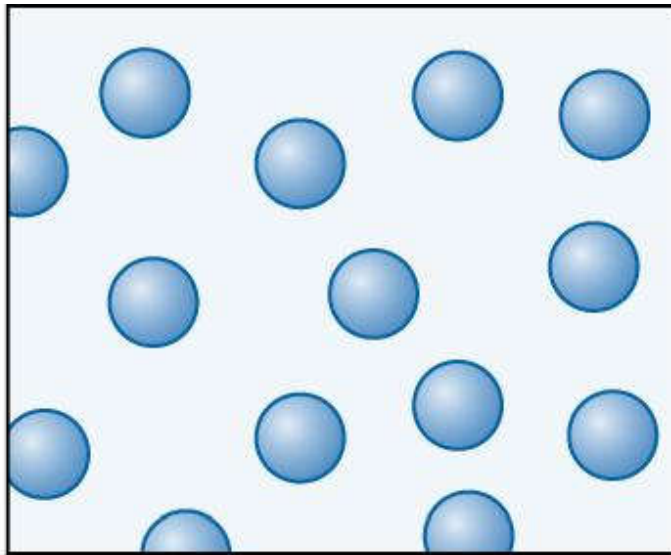




(c)2003 Brooks/Cole, a division of Thomson Learning, Inc. Thomson Learning™ is a trademark used herein under license.

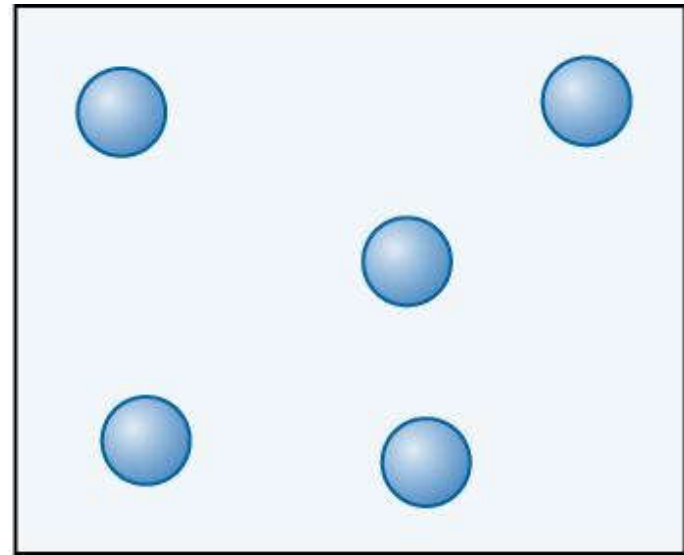
Figure 10.1 Considerations for effective dispersion strengthening: (c) The dispersed phase particles should be round rather than needlelike.





Good

vs.



Poor

(d)

(c)2003 Brooks/Cole, a division of Thomson Learning, Inc. Thomson Learning, is a trademark used herein under license.

Figure 10.1 Considerations for effective dispersion strengthening: (d) Larger amounts of dispersed phase increase strengthening.





Section 10.2 Intermetallic Compounds

- ❑ **Intermetallic compound** - A compound formed of two or more metals that has its own unique composition, structure, and properties.
- ❑ **Stoichiometric intermetallic compound** - A phase formed by the combination of two components into a compound having a structure and properties different from either component.
- ❑ **Nonstoichiometric intermetallic compound** - A phase formed by the combination of two components into a compound having a structure and properties different from either component.
- ❑ **Ordered crystal structure** - Solid solutions in which the different atoms occupy specific, rather than random, sites in the crystal structure.



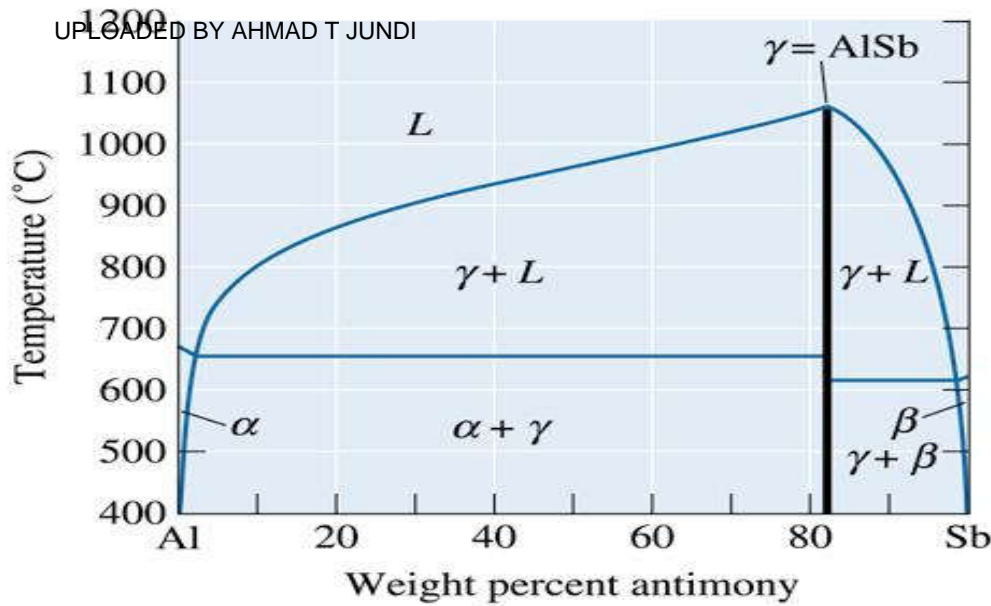


TABLE 10-1 ■ *Properties of some intermetallic compounds*

Intermetallic Compound	Crystal Structure	Melting Temperature (°C)	Density ($\frac{\text{g}}{\text{cm}^3}$)	Young's Modulus (GPa)
FeAl	Ordered BCC	1250–1400	5.6	263
NiAl	Ordered FCC (B2)*	1640	5.9	206
Ni ₃ Al	Ordered FCC (L1 ₂)*	1390	7.5	337
TiAl	Ordered tetragonal (L1 ₀)*	1460	3.8	94
Ti ₃ Al	Ordered HCP	1600	4.2	210
MoSi ₂	Tetragonal	2020	6.31	430

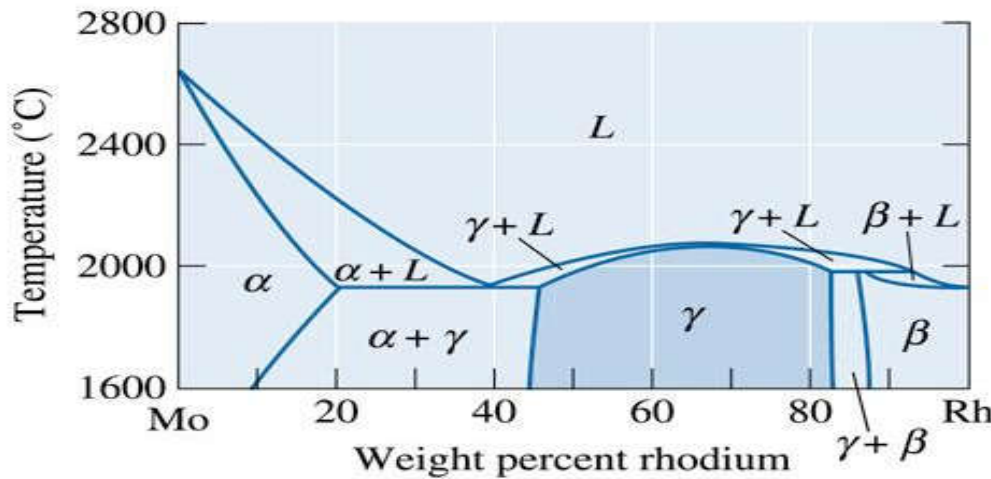
**Also known as. (Source: Adapted from Mechanical Behavior of Materials, by M.A. Meyers and K.K. Chawla. Copyright © 1998 Prentice Hall. Adapted by permission of Pearson Education.)*





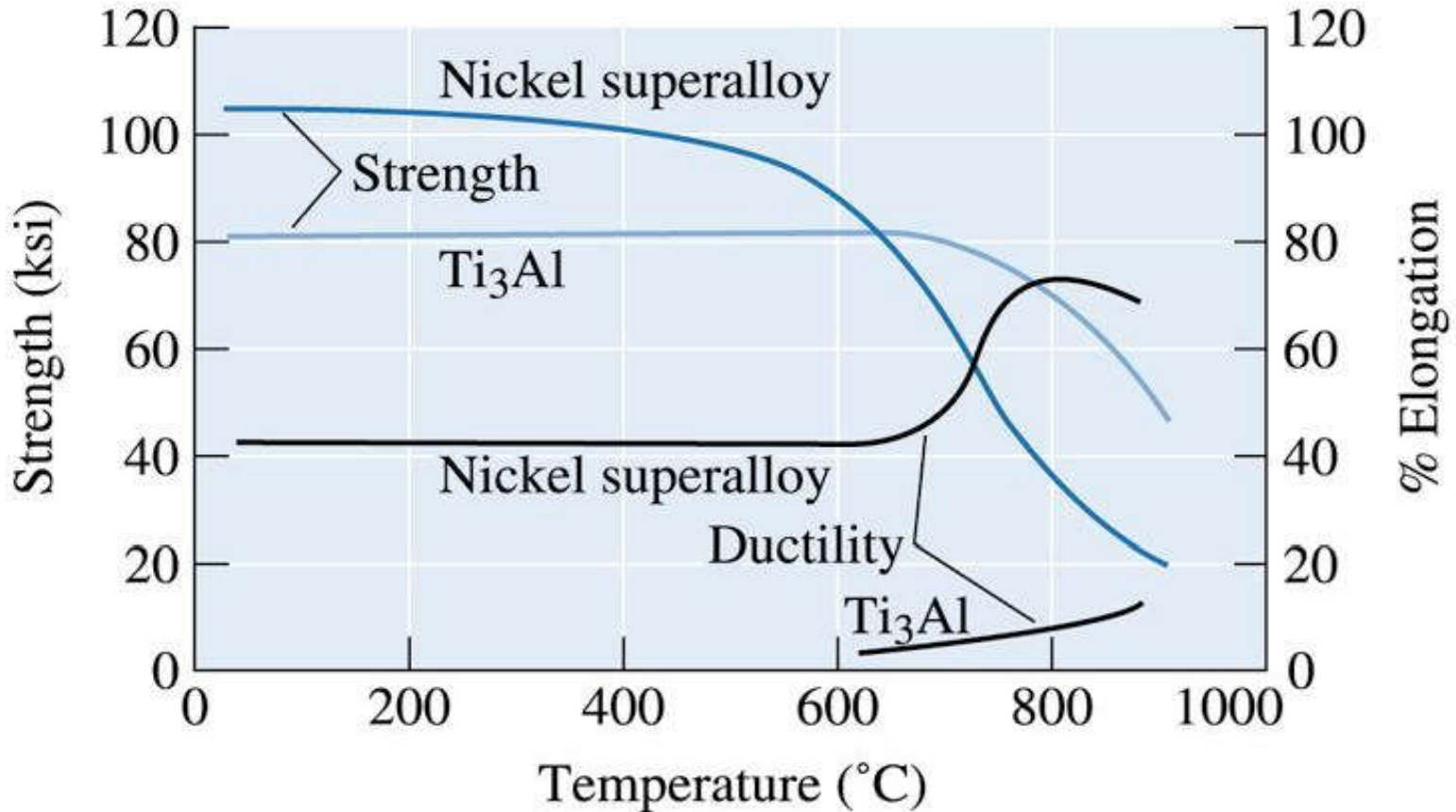
(a)

Figure 10.2 (a) The aluminum-antimony phase diagram includes a stoichiometric intermetallic compound γ .



(b)

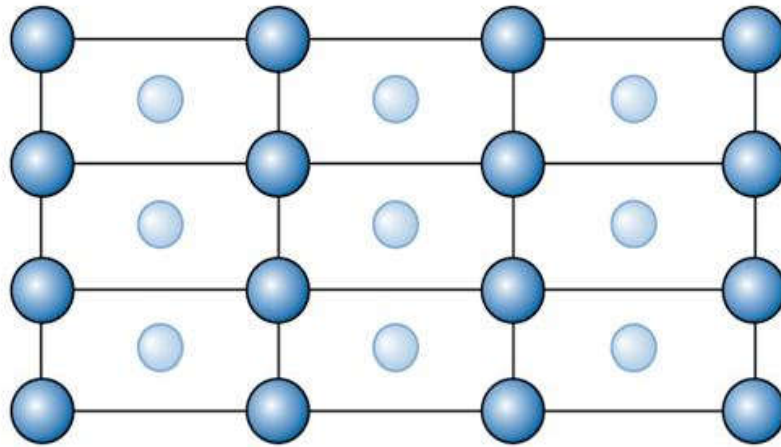




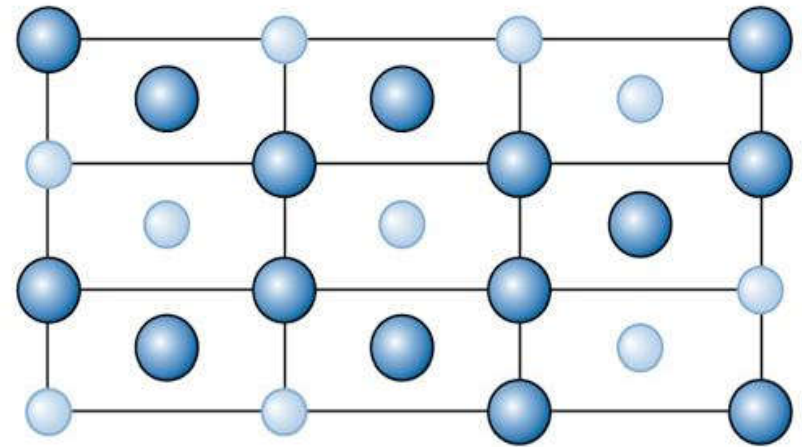
(c)2003 Brooks/Cole, a division of Thomson Learning, Inc. Thomson Learning[®] is a trademark used herein under license.

Figure 10.3 The strength and ductility of the intermetallic compound Ti₃Al compared with that of a conventional nickel superalloy. The Ti₃Al maintains its strength to higher temperatures longer than does the nickel superalloy.





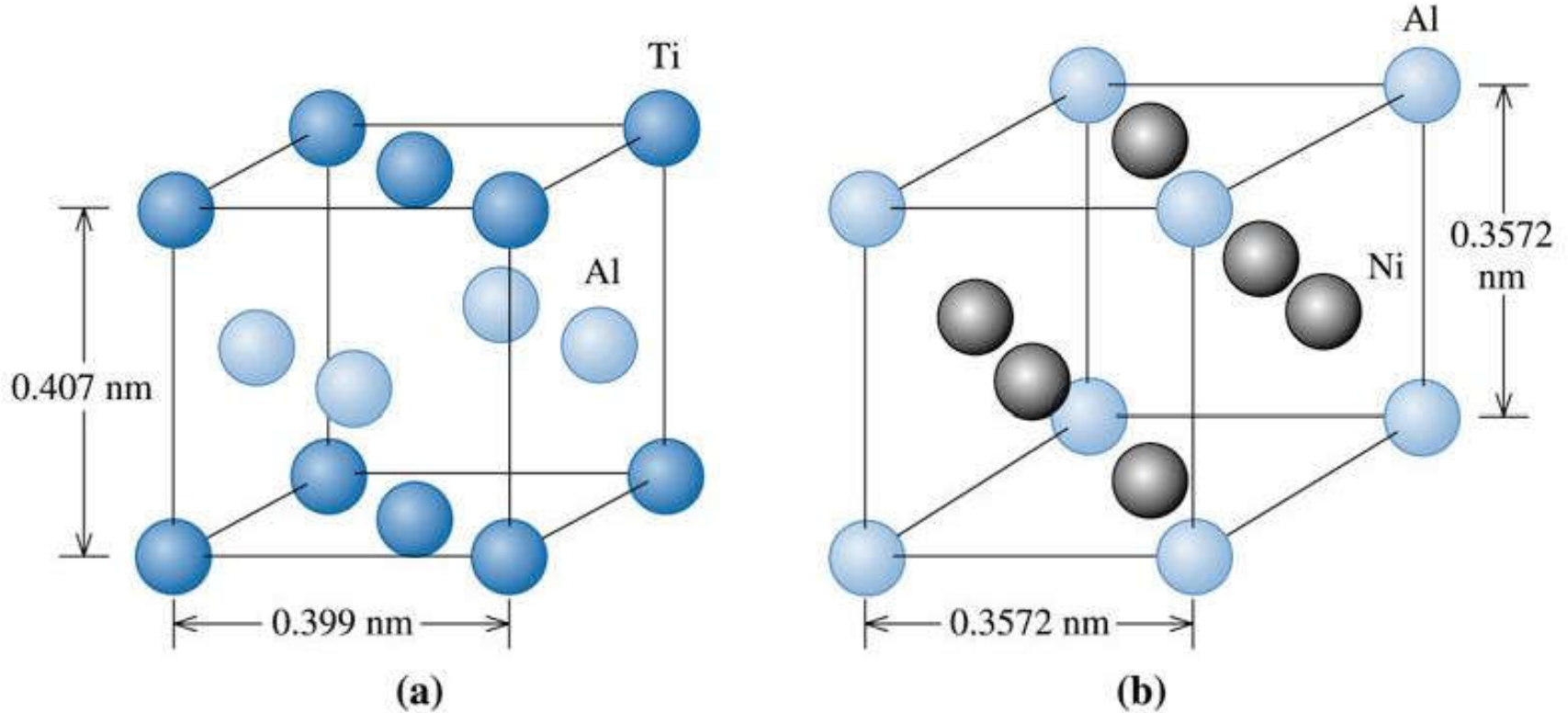
(a)



(b)

(c)2003 Brooks/Cole, a division of Thomson Learning, Inc. Thomson Learning, is a trademark used herein under license.

Figure 10.4 (a) In an ordered structure, the substituting atoms occupy specific lattice points,(b) while in normal structure, the constituent atoms are randomly located at different lattice points.



(c)2003 Brooks/Cole, a division of Thomson Learning, Inc. Thomson Learning[®] is a trademark used herein under license.

Figure 10.5 The unit cells of two intermetallic compounds: (a) TiAl has an ordered tetragonal structure, and (b) Ni₃Al has an ordered cubic structure.



Materials Selection for an Aerospace Vehicle

Design a material suitable for the parts of an aerospace vehicle that reach high temperatures during re-entry from Earth orbit.

Example 10.1 SOLUTION

- ❑ The material must **withstand the high temperatures** (1600°C - 1700°C) generated as the vehicle enters Earth's atmosphere.
- ❑ Some **ductility** is needed to provide damage tolerance to the vehicle. Finally, the material should have a **low density**.
- ❑ **TiAl and Ni₃Al** have good high-temperature properties and oxidation resistance and, at high temperatures, have at least some ductility.
- ❑ Thus, **carbon or aramid fiber-matrix composites** (based on Kevlar™), coated properly to protect oxidation, also will be very good choices for outer space applications.



Section 10.3 Phase Diagrams Containing Three-Phase Reactions

- ❑ **Peritectic** - A three-phase reaction in which a solid and a liquid combine to produce a second solid on cooling.
- ❑ **Monotectic** - A three-phase reaction in which one liquid transforms to a solid and a second liquid on cooling.
- ❑ **Miscibility gap** - A region in a phase diagram in which two phases, with essentially the same structure, do not mix, or have no solubility in one another.
- ❑ **Metastable miscibility gap** - A miscibility gap that extends below the liquidus or exists completely below the liquidus.



Eutectic	$L \rightarrow \alpha + \beta$	
Peritectic	$\alpha + L \rightarrow \beta$	
Monotectic	$L_1 \rightarrow L_2 + \alpha$	
Eutectoid	$\gamma \rightarrow \alpha + \beta$	
Peritectoid	$\alpha + \beta \rightarrow \gamma$	

(c)2003 Brooks/Cole, a division of Thomson Learning, Inc. Thomson Learning,™ is a trademark used herein under license.

Figure 10.6 The five most important three-phase reactions in binary phase diagrams.





Example 10.2

Identifying Three-Phase Reactions

Consider the binary phase diagram in Figure 10.7. Identify the three-phase reactions that occur.



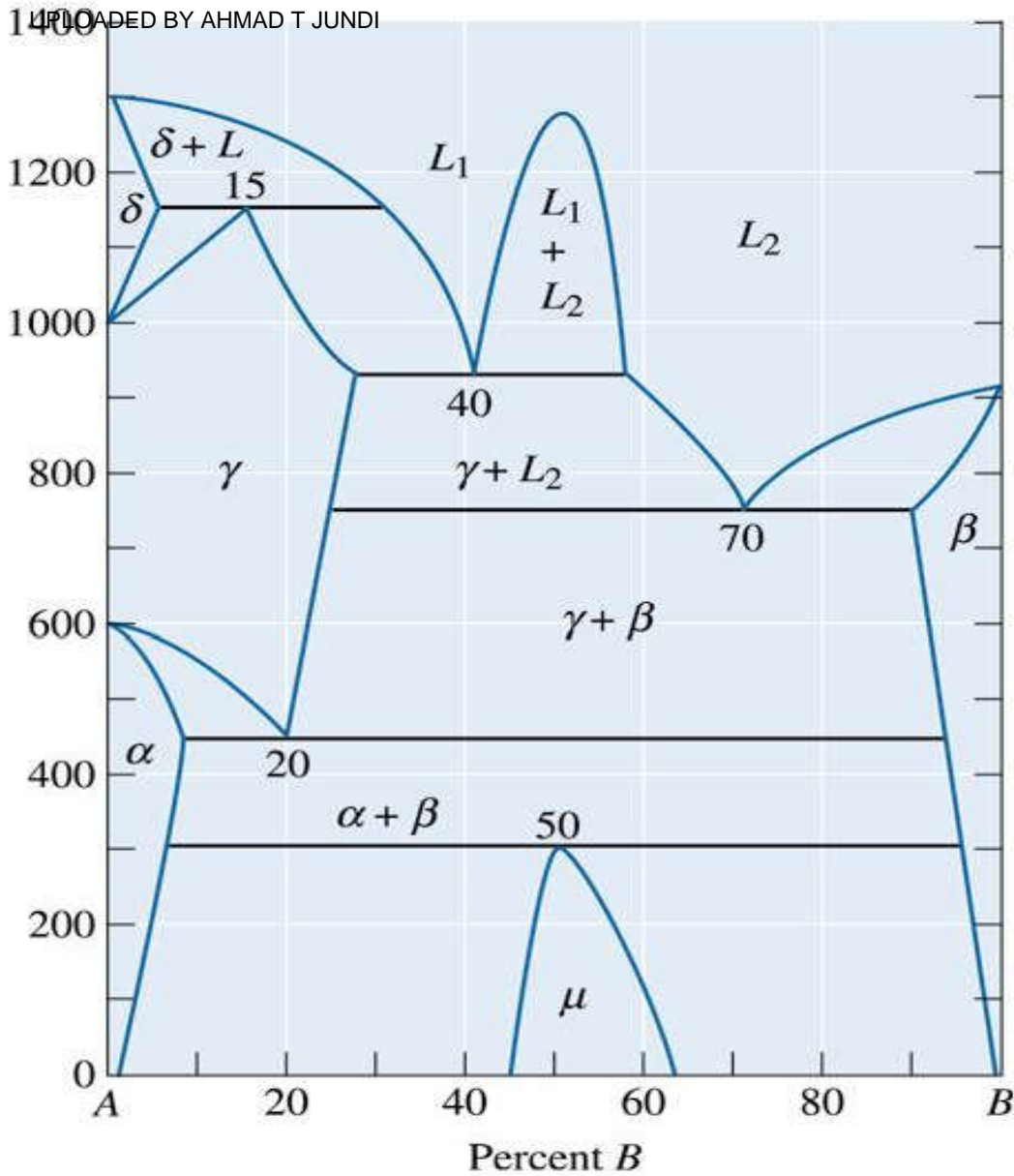


Figure 10.7 A hypothetical phase diagram (for Example 10.2)



UPLOADED BY AHMAD T JUNDI

Example 10.2 SOLUTION

We find horizontal lines at 1150°C, 920°C, 750°C, 450°C, and 300°C: 1150°C: The in-between point is at 15% B. $\delta + L$ are present above the point, γ is present below. The reaction is:



920°C: This reaction occurs at 40% B:



750°C: This reaction occurs at 70% B:



450°C: This reaction occurs at 20% B:



300°C: This reaction occurs at 50% B:

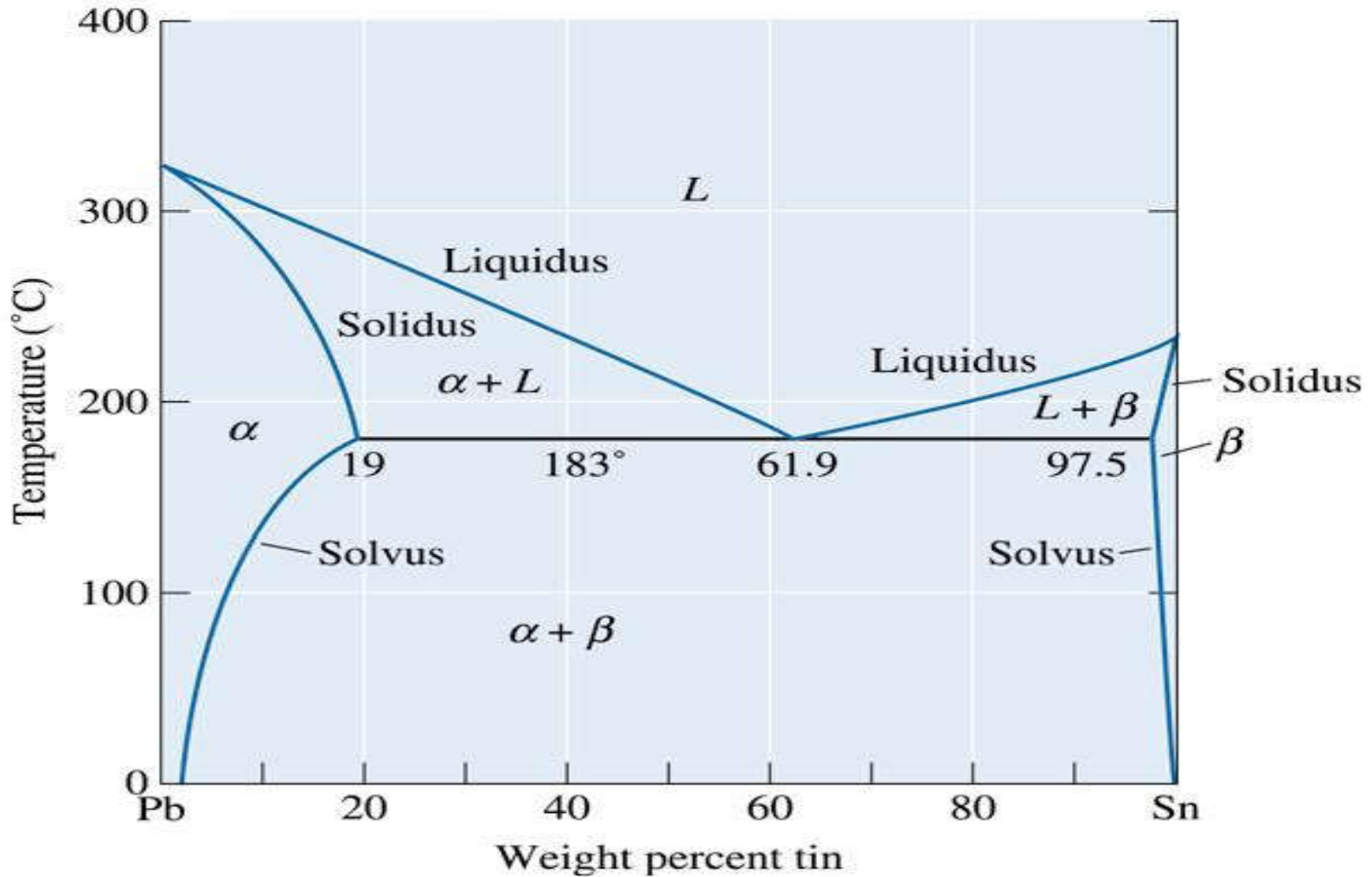




Section 10.4 The Eutectic Phase Diagram

- **Solvus** - A solubility curve that separates a single-solid phase region from a two-solid phase region in the phase diagram.
- **Isopleth** - A line on a phase diagram that shows constant chemical composition.
- **Hypoeutectic alloy** - An alloy composition between that of the left-hand-side end of the tie line defining the eutectic reaction and the eutectic composition.
- **Hypereutectic alloys** - An alloy composition between that of the right-hand-side end of the tie line defining the eutectic reaction and the eutectic composition.





(c)2003 Brooks/Cole, a division of Thomson Learning, Inc. Thomson Learningsm is a trademark used herein under license.

Figure 10.8 the lead-tin equilibrium phase diagram.





(c)2003 Brooks/Cole, a division of Thomson Learning, Inc. Thomson Learning is a trademark used herein under license.

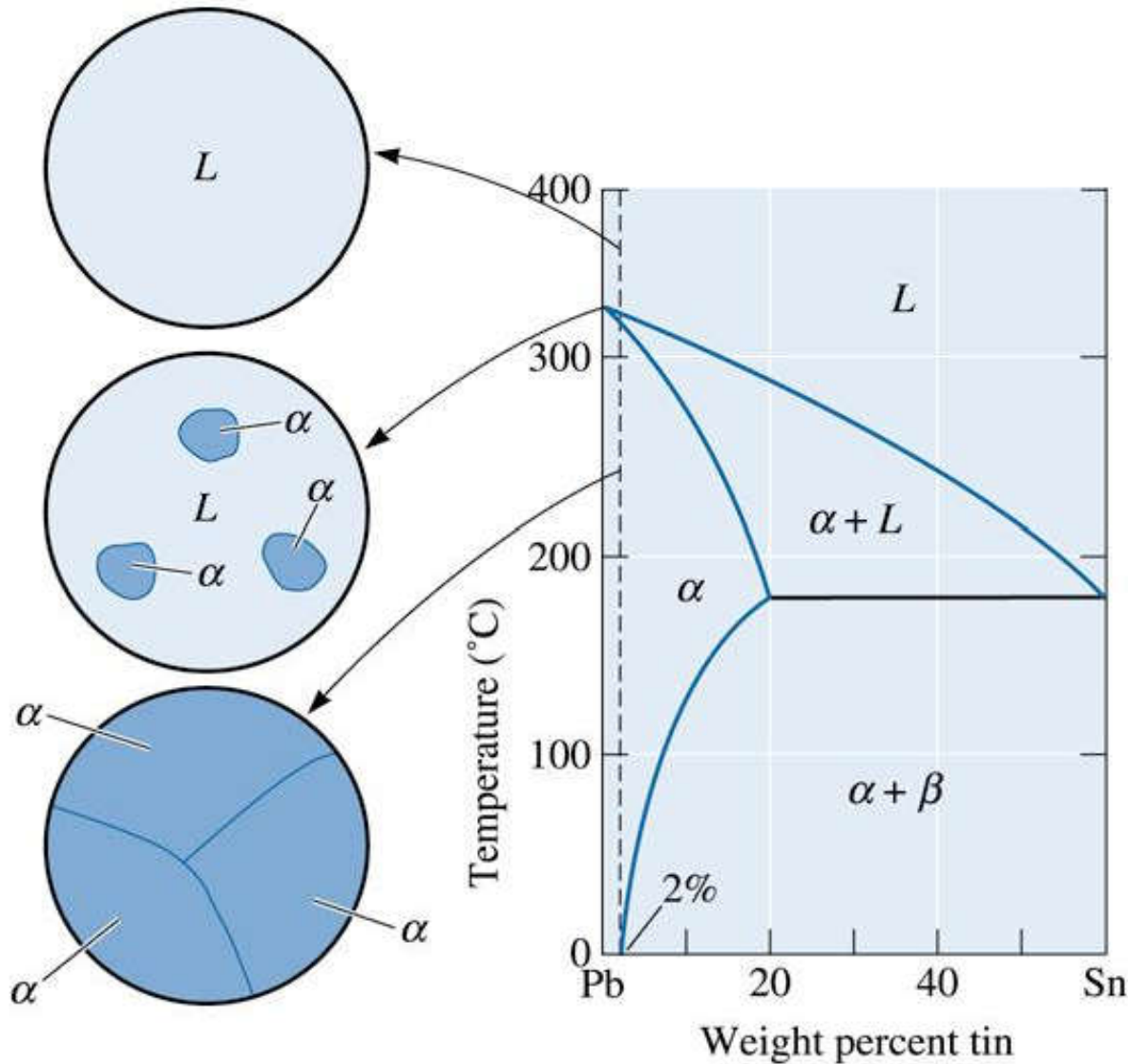
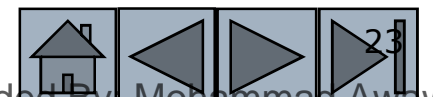
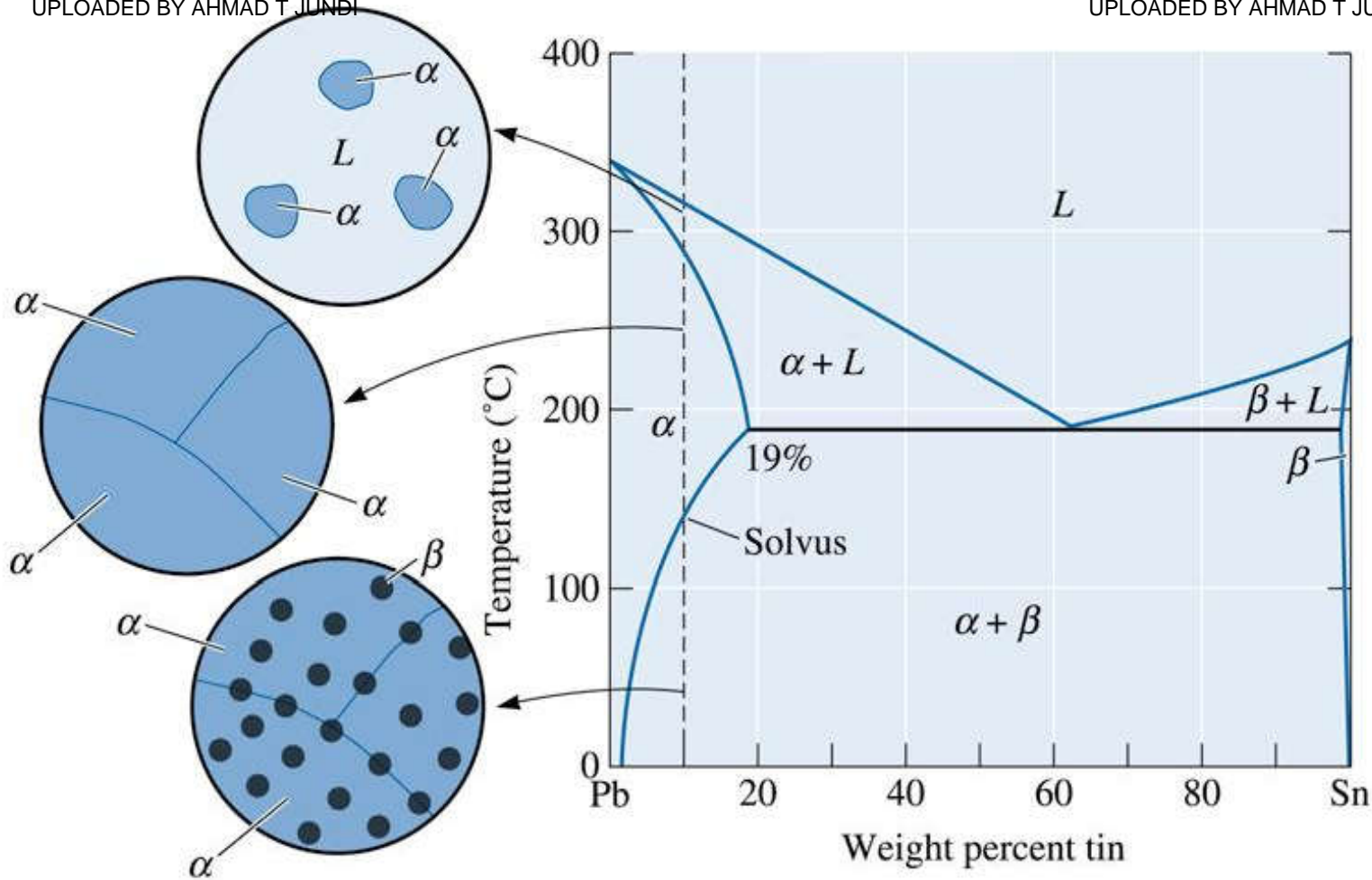


Figure 10.9
Solidification and
microstructure of a
Pb-2% Sn alloy.
The alloy is a
single-phase solid
solution.





(c)2003 Brooks/Cole, a division of Thomson Learning, Inc. Thomson Learning,™ is a trademark used herein under license.

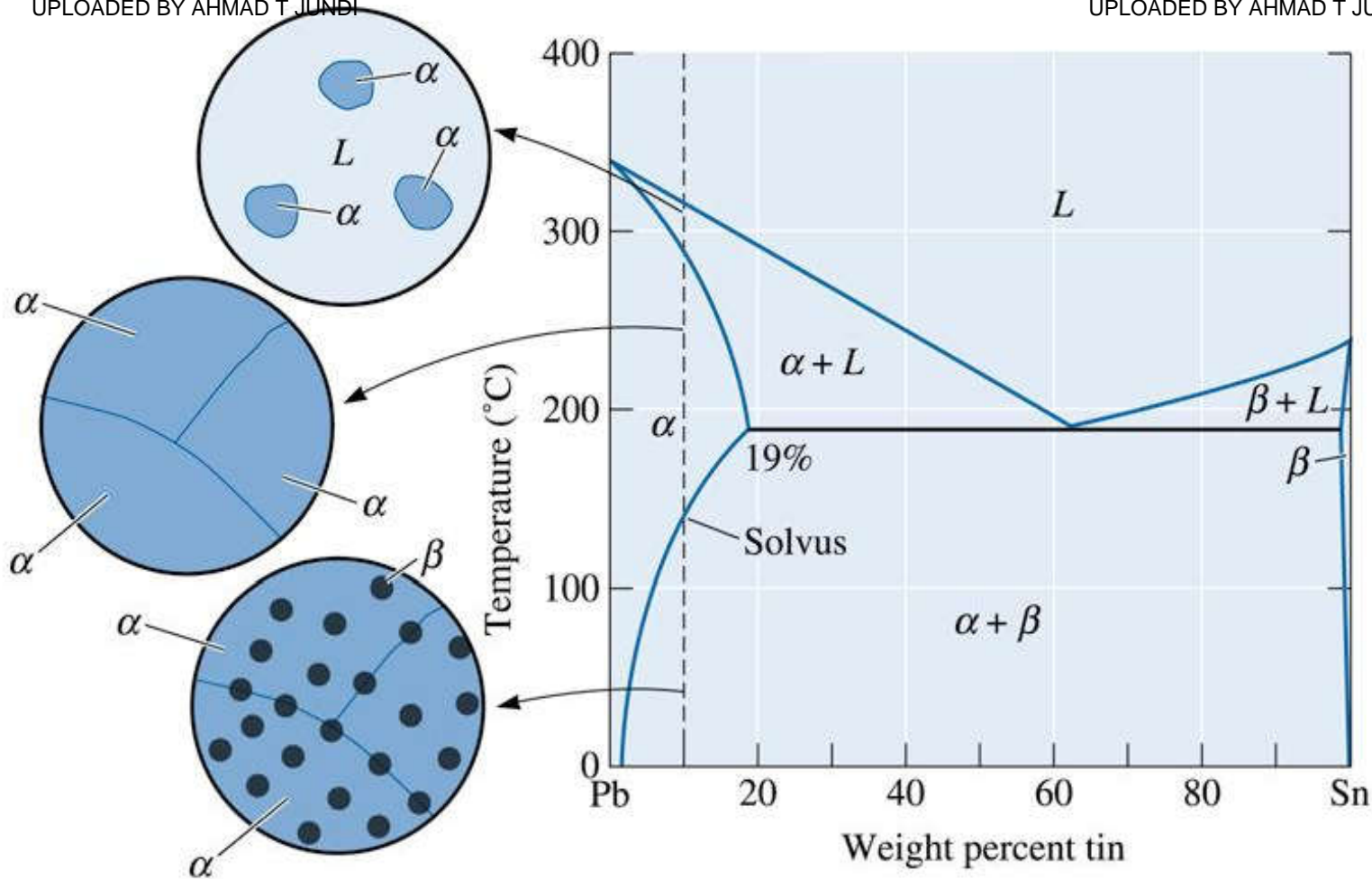
Figure 10.10 Solidification, precipitation, and microstructure of a Pb-10% Sn alloy. Some dispersion strengthening occurs as the β solid precipitates.



Example 10.3

Phases in the Lead–Tin (Pb–Sn) Phase Diagram

Determine (a) the solubility of tin in solid lead at 100°C, (b) the maximum solubility of lead in solid tin, (c) the amount of β that forms if a Pb-10% Sn alloy is cooled to 0°C, (d) the masses of tin contained in the α and β phases, and (e) mass of lead contained in the α and β phases. Assume that the total mass of the Pb-10% Sn alloy is 100 grams.



(c)2003 Brooks/Cole, a division of Thomson Learning, Inc. Thomson Learning,™ is a trademark used herein under license.

Figure 10.10 Solidification, precipitation, and microstructure of a Pb-10% Sn alloy. Some dispersion strengthening occurs as the β solid precipitates.



Example 10.3 SOLUTION

(a) The 100°C temperature intersects the solvus curve at 5% Sn. The solubility of tin (Sn) in lead (Pb) at 100°C therefore is 5%.

(b) The maximum solubility of lead (Pb) in tin (Sn), which is found from the tin-rich side of the phase diagram, occurs at the eutectic temperature of 183°C and is 97.5% Sn.

(c) At 0°C, the 10% Sn alloy is in a $\alpha + \beta$ region of the phase diagram. By drawing a tie line at 0°C and applying the lever rule, we find that:

$$\% \beta = \frac{10 - 2}{100 - 2} \times 100 = 8.2\%$$



Example 10.3 SOLUTION (Continued)

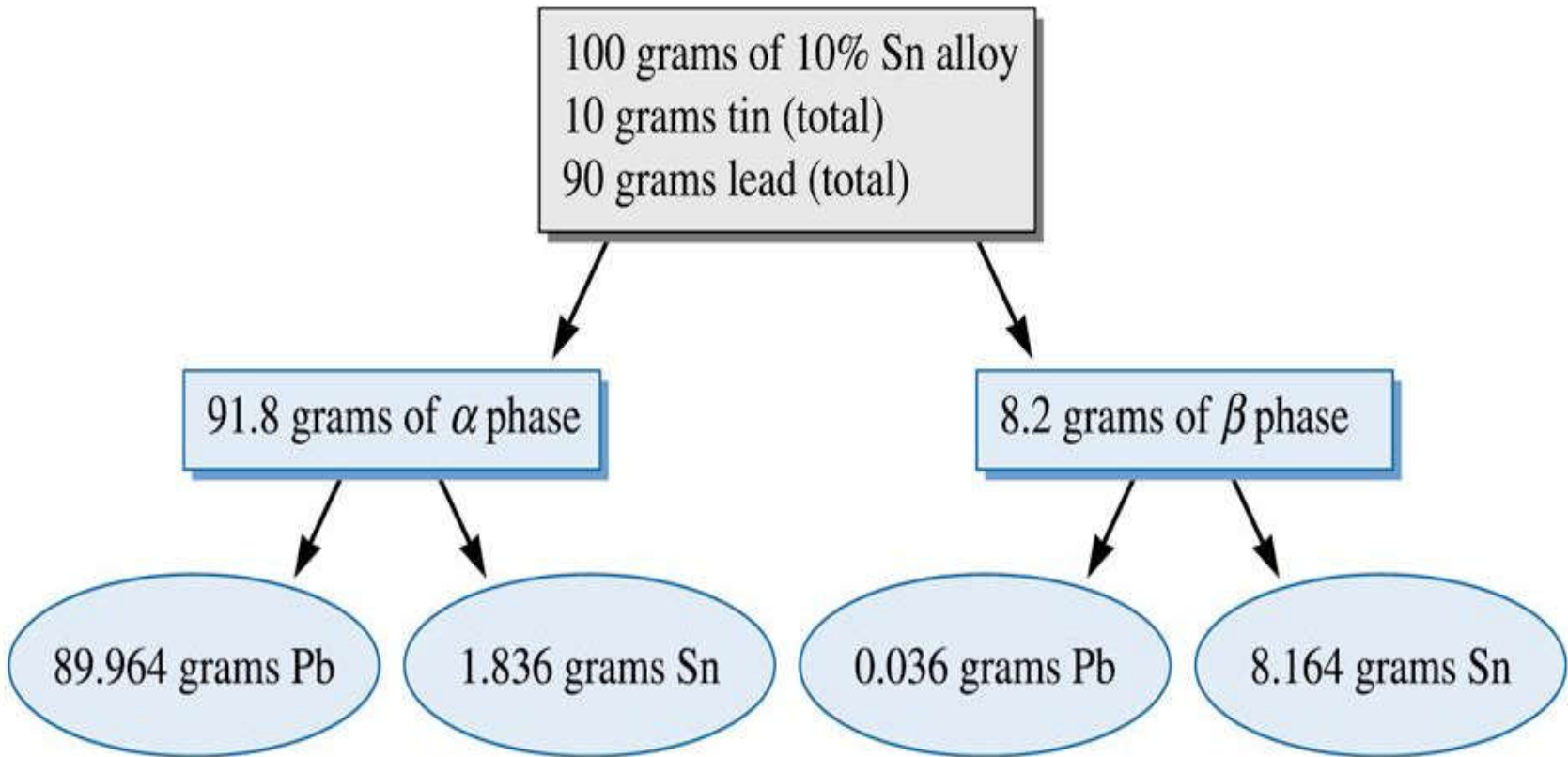
(d) The mass of Sn in the α phase = $2\% \text{ Sn} \times 91.8 \text{ g}$
of α phase = $0.02 \times 91.8 \text{ g} = 1.836 \text{ g}$. Since tin (Sn)
appears in both the α and β phases, the mass of Sn
in the β phase will be = $(10 - 1.836) \text{ g} = 8.164 \text{ g}$.

(e) Mass of Pb in the α phase

= $98\% \text{ Sn} \times 91.8 \text{ g}$ of α phase = $0.98 \times 91.8 \text{ g} =$
 89.964 g

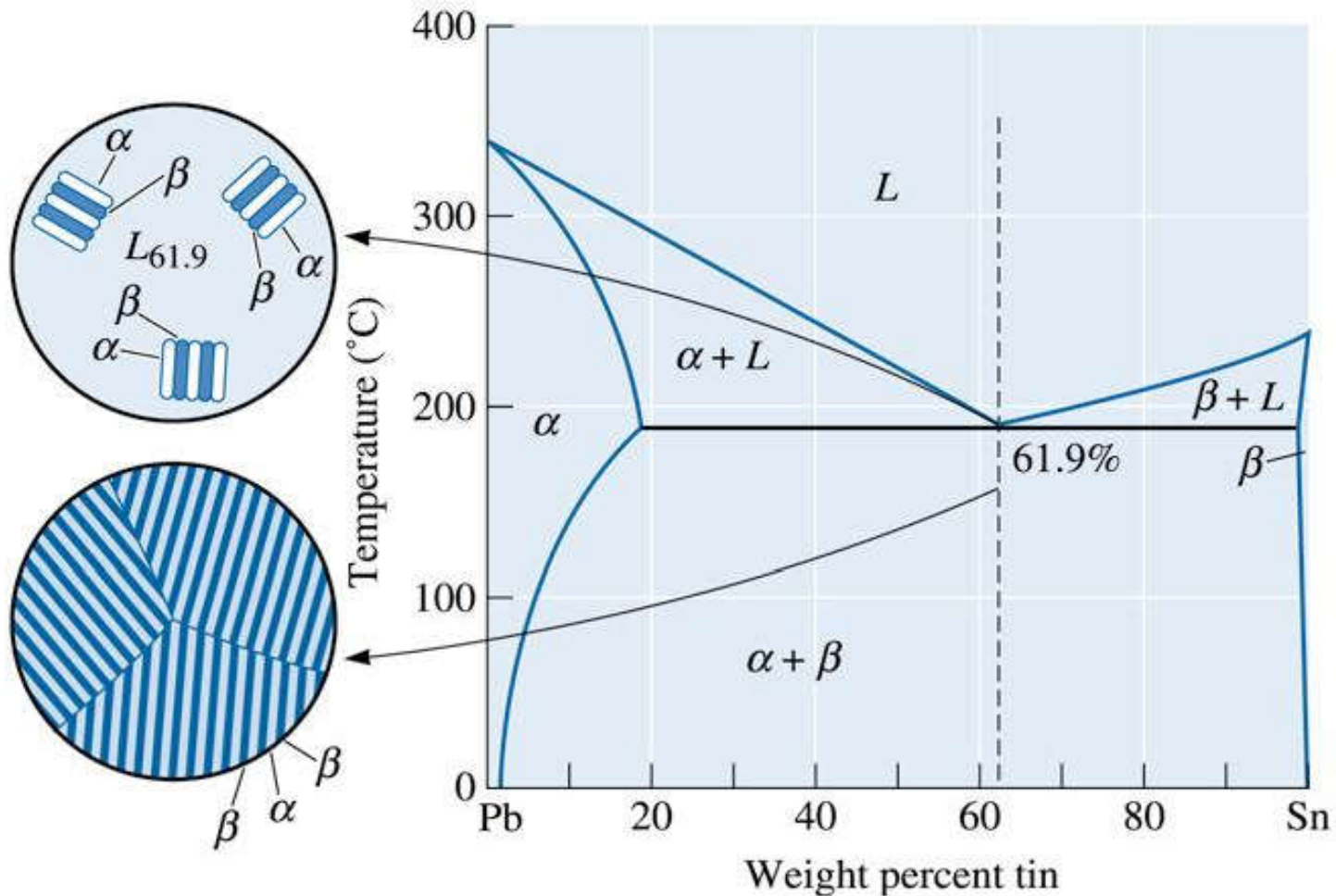
Mass of Pb in the β phase

= $90 - 89.964 = 0.036 \text{ g}$.



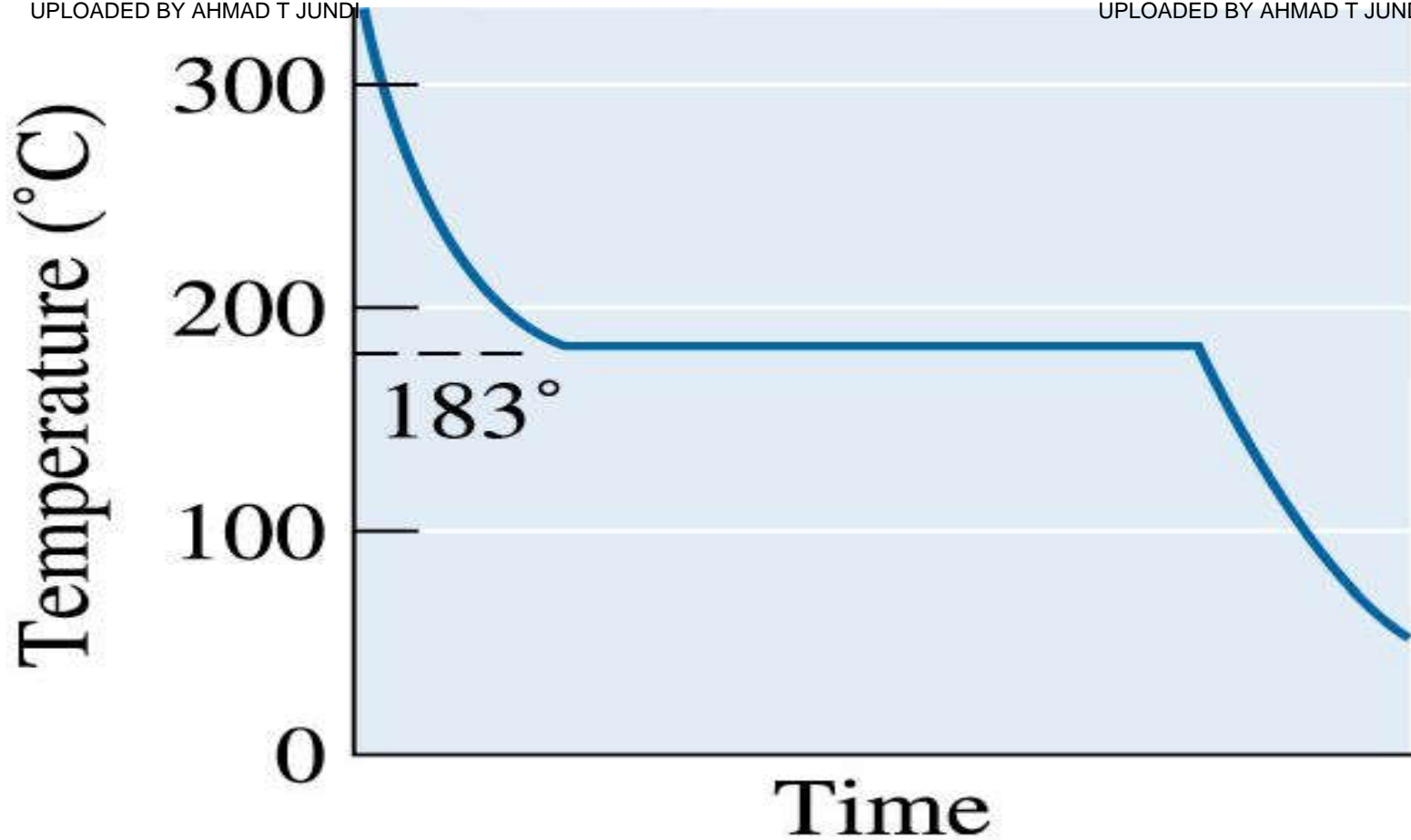
(c)2003 Brooks/Cole, a division of Thomson Learning, Inc. Thomson Learning, Inc. is a trademark used herein under license.

Figure 10.11 Summary of calculations (for example 10.3).



(c)2003 Brooks/Cole, a division of Thomson Learning, Inc. Thomson Learningsm is a trademark used herein under license.

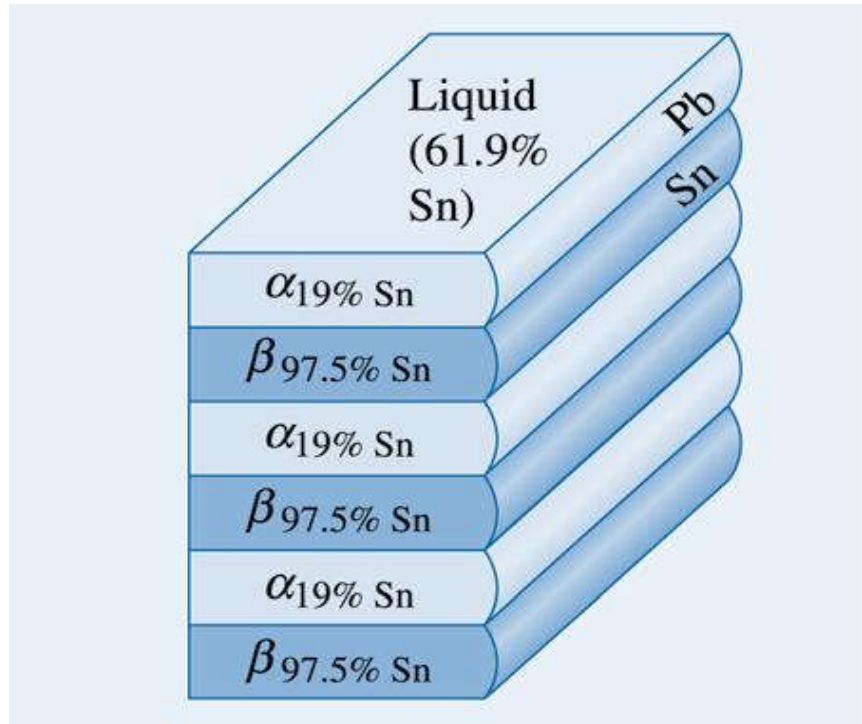
Figure 10.12 Solidification and microstructure of the eutectic alloy Pb-61.9% Sn.



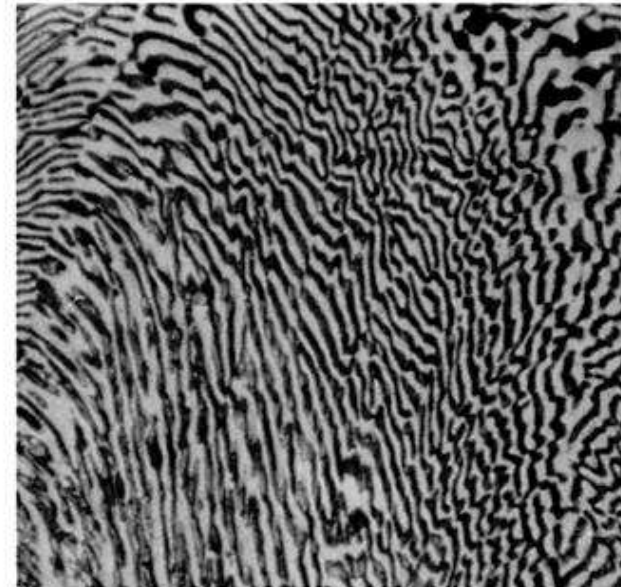
(c)2003 Brooks/Cole, a division of Thomson Learning, Inc. Thomson Learning, is a trademark used herein under license.

Figure 10.13 The cooling curve for a eutectic alloy is a simple thermal arrest, since eutectics freeze or melt at a single temperature.





(a)



(b)

(c)2003 Brooks/Cole, a division of Thomson Learning, Inc. Thomson Learning[™] is a trademark used herein under license.

Figure 10.14 (a) Atom redistribution during lamellar growth of a lead-tin eutectic. Tin atoms preferentially diffuse to the β plates, and lead atoms diffuse to the α plates. (b) Photomicrograph of the lead-tin eutectic microconstituent (x400).



Example 10.4

Amount of Phases in the Eutectic Alloy

(a) Determine the amount and composition of each phase in a lead-tin alloy of eutectic composition. (b) Calculate the mass of phases present. (c) Calculate the amount of lead and tin in each phase, assuming you have 200 g of the alloy.

Example 10.4 SOLUTION

(a) The eutectic alloy contains 61.9% Sn.

$$\alpha : (Pb - 19\% Sn) \quad \% \alpha = \frac{97.5 - 61.9}{97.5 - 19.0} \times 100 = 45.35\%$$

$$\beta : (Pb - 97.5\% Sn) \quad \% \beta = \frac{61.9 - 19.0}{97.5 - 19.0} \times 100 = 54.65\%$$





Example 10.4 SOLUTION (Continued)

(b) At a temperature just below the eutectic:

The mass of the α phase in 200 g of the alloy =

mass of the alloy \times fraction of the α phase

$$= 200 \text{ g} \times 0.4535 = 90.7 \text{ g}$$

The amount of the β phase in 200 g of the alloy =

(mass of the alloy \times mass of the α phase)

$$= 200.0 \text{ g} \times 90.7 \text{ g} = 109.3 \text{ g}$$

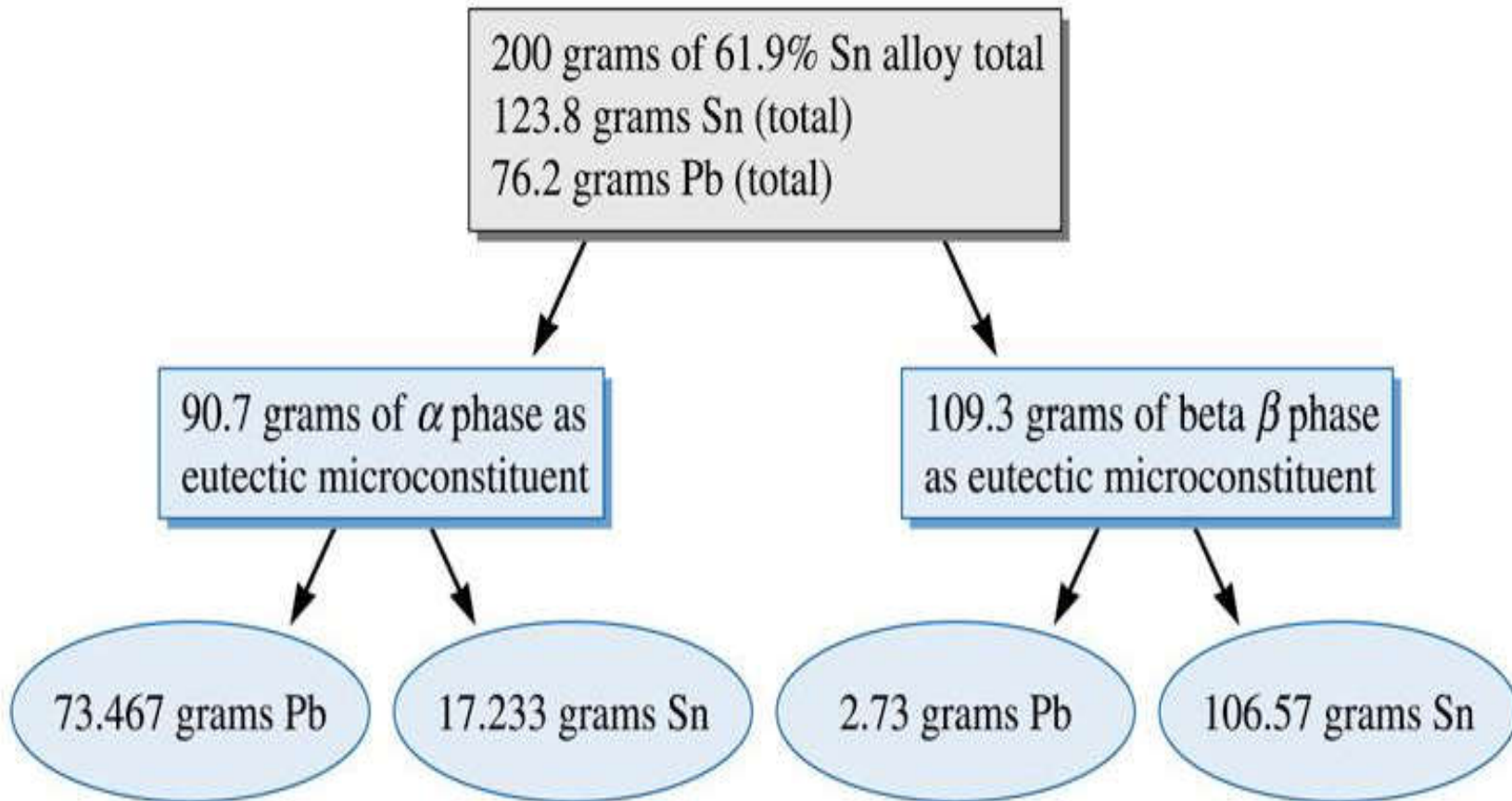




Example 10.4 SOLUTION (Continued)

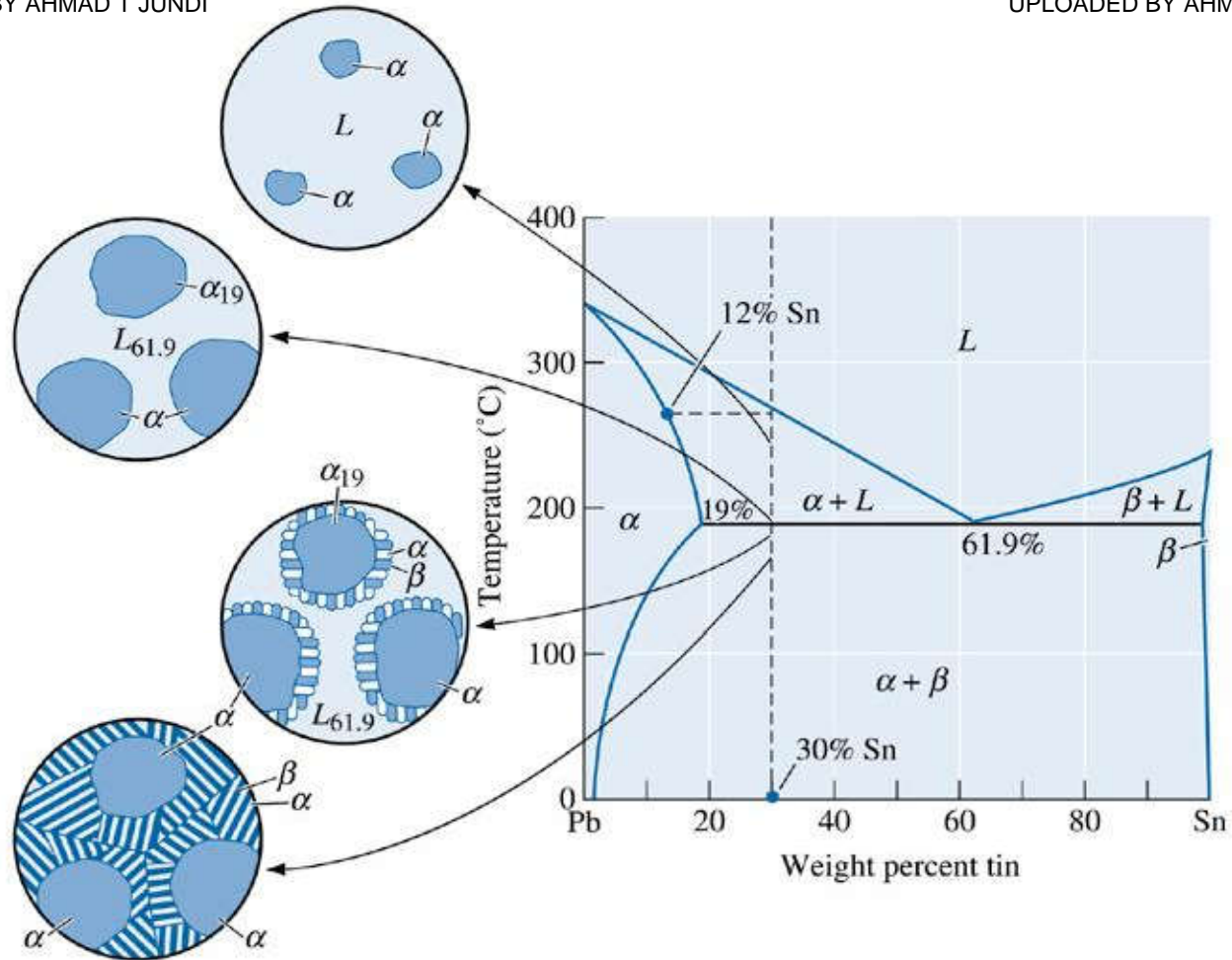
- Mass of Pb in the α phase = mass of the a phase in 200 g \times (concentration of Pb in α) = $(90.7 \text{ g}) \times (1 - 0.190) = 73.467 \text{ g}$
- Mass of Sn in the α phase = mass of the a phase - mass of Pb in the a phase = $(90.7 - 73.467 \text{ g}) = 17.233 \text{ g}$
- Mass of Pb in β phase = mass of the b phase in 200 g \times (wt. fraction Pb in β) = $(109.3 \text{ g}) \times (1 - 0.975) = 2.73 \text{ g}$
- Mass of Sn in the β phase = total mass of Sn - mass of Sn in the α phase = $123.8 \text{ g} - 17.233 \text{ g} = 106.57 \text{ g}$





(c)2003 Brooks/Cole, a division of Thomson Learning, Inc. Thomson Learning[™] is a trademark used herein under license.

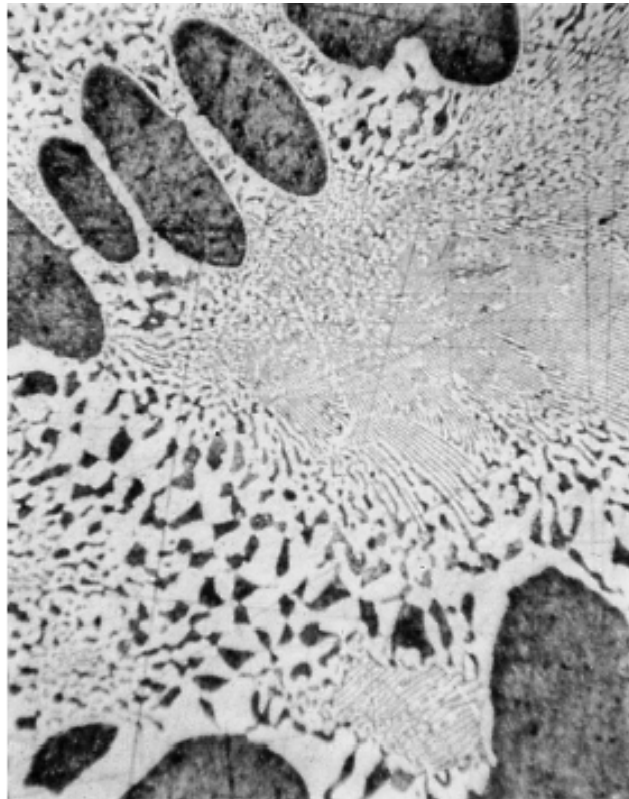
Figure 10.15 Summary of calculations (for Example 10.4).



(c)2003 Brooks/Cole, a division of Thomson Learning, Inc. Thomson Learningsm is a trademark used herein under license.

Figure 10.16 The solidification and microstructure of a hypoeutectic alloy (Pb-30% Sn).





(a)



(b)

Figure 10.17 (a) A hypoeutectic lead-tin alloy. (b) A hypereutectic lead-tin alloy. The dark constituent is the lead-rich solid α , the light constituent is the tin-rich solid β , and the fine plate structure is the eutectic (x400).



Example 10.5

Determination of Phases and Amounts in a Pb-30% Sn Hypoeutectic Alloy

For a Pb-30% Sn alloy, determine the phases present, their amounts, and their compositions at 300°C, 200°C, 184°C, 182°C, and 0°C.



Example 10.5 SOLUTION

Temperature (°C)	Phases	Compositions	Amounts
300	L	L : 30% Sn	$L = 100\%$
200	$\alpha + L$	L : 55% Sn	$L = \frac{30 - 18}{55 - 18} \times 100 = 32\%$
		α : 18% Sn	$\alpha = \frac{55 - 30}{55 - 18} \times 100 = 68\%$
184	$\alpha + L$	L : 61.9% Sn	$L = \frac{30 - 19}{61.9 - 19} \times 100 = 26\%$
		α : 19% Sn	$\alpha = \frac{61.9 - 30}{61.9 - 19} \times 100 = 74\%$
182	$\alpha + \beta$	α : 19% Sn	$\alpha = \frac{97.5 - 30}{97.5 - 19} \times 100 = 86\%$
		β : 97.5% Sn	$\beta = \frac{30 - 19}{97.5 - 19} \times 100 = 14\%$
0	$\alpha + \beta$	α : 2% Sn	$\alpha = \frac{100 - 30}{100 - 2} \times 100 = 71\%$
		β : 100% Sn	$\beta = \frac{30 - 2}{100 - 2} \times 100 = 29\%$





Example 10.6

Microconstituent Amount and Composition for a Hypoeutectic Alloy

Determine the amounts and compositions of each microconstituent in a Pb-30% Sn alloy immediately after the eutectic reaction has been completed.

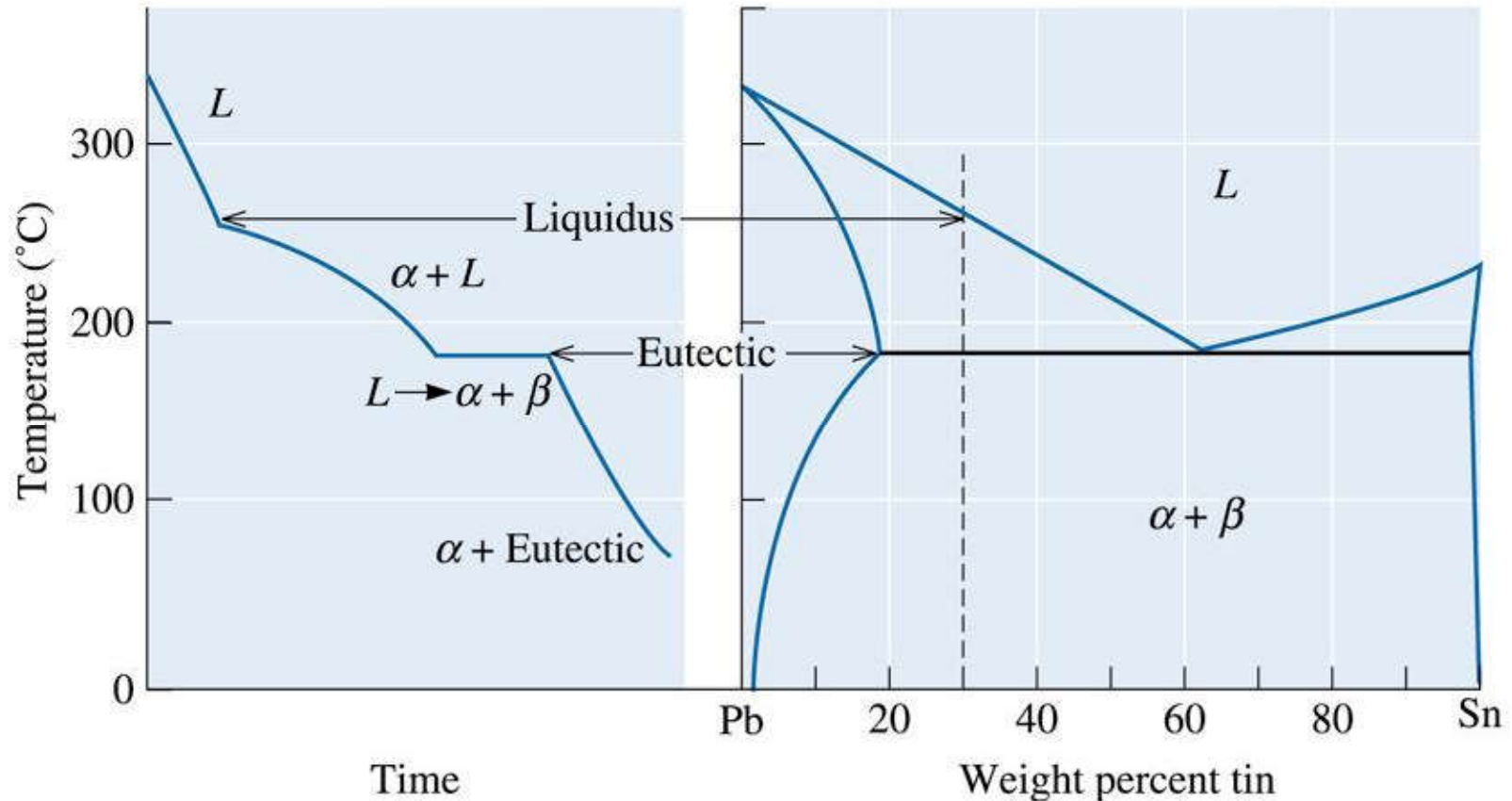
Example 10.6 SOLUTION

At a temperature just above the eutectic—say, 184°C—the amounts and compositions of the two phases are:

$$\alpha : 19\% \text{ Sn} \quad \% \alpha = \frac{61.9 - 30}{61.9 - 19} \times 100 = 74\% = \% \text{ Primary } \alpha$$

$$L : 61.9\% \text{ Sn} \quad \% L = \frac{30 - 19}{61.9 - 19} \times 100 = 26\% = \% \text{ eutectic at } 182^\circ\text{C}$$





(c)2003 Brooks/Cole, a division of Thomson Learning, Inc. Thomson Learning™ is a trademark used herein under license.

Figure 10.18 The cooling curve for a hypo-eutectic Pb-30% Sn alloy.

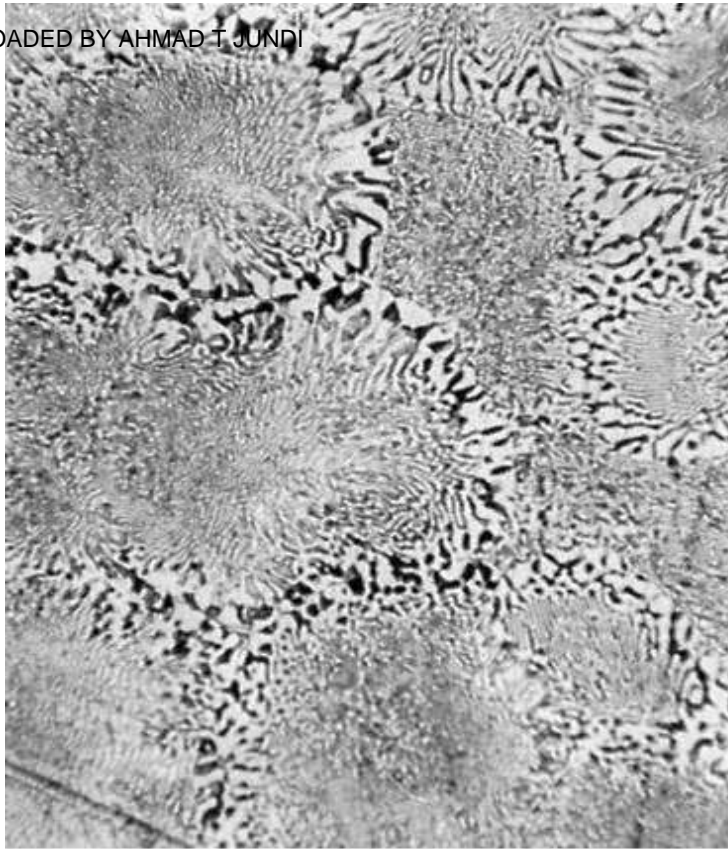




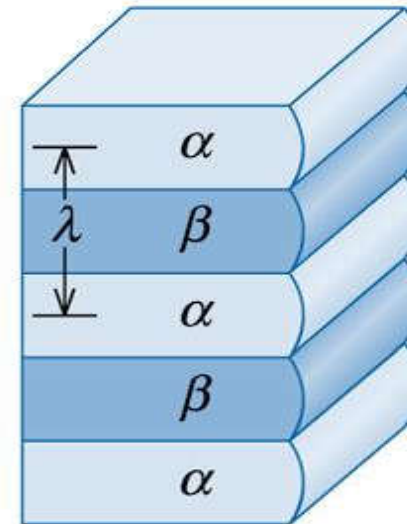
Section 10.5

Strength of Eutectic Alloys

- Eutectic Colony Size
- Interlamellar Spacing
- Amount of Eutectic
- Microstructure of the Eutectic



(a)

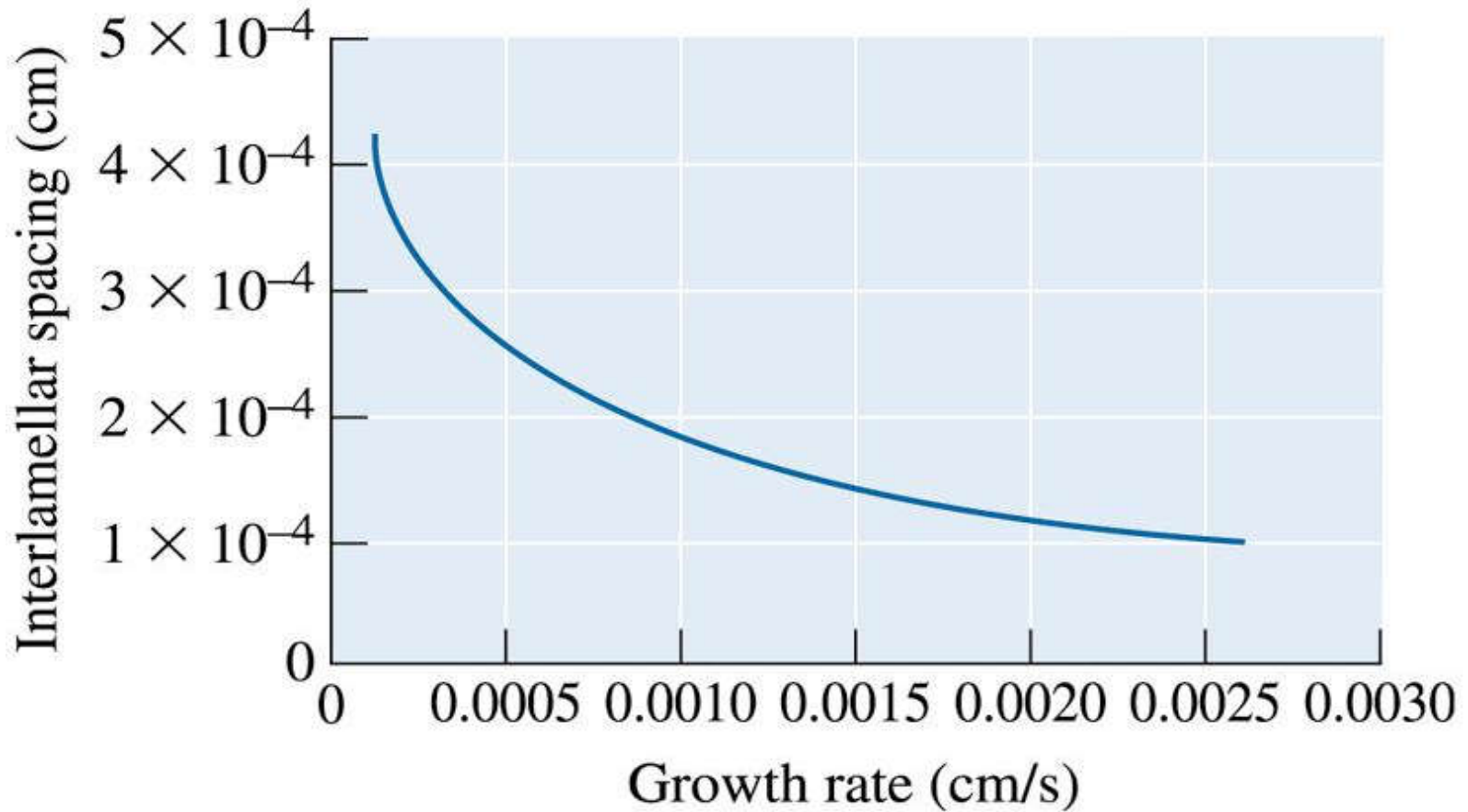


(b)

(c)2003 Brooks/Cole, a division of Thomson Learning, Inc. Thomson Learningsm is a trademark used herein under license.

Figure 10.19 (a) Colonies in the lead-tin eutectic (x300). (b) The interlamellar spacing in a eutectic microstructure.





(c)2003 Brooks/Cole, a division of Thomson Learning, Inc. Thomson Learning[®] is a trademark used herein under license.

Figure 10.20 The effect of growth rate on the interlamellar spacing in the lead-tin eutectic.



Design of a Directional Solidification Process

Design a process to produce a single “grain” of Pb-Sn eutectic microconstituent in which the interlamellar spacing is 0.00034 cm.

Example 10.7 SOLUTION

We could use a directional solidification (DS) process to produce the single grain, while controlling the growth rate to assure that the correct interlamellar spacing is achieved.

Figure 10.21 shows how we might achieve this growth rate. The Pb- 61.9% Sn alloy would be melted in a mold within a furnace. The mold would be withdrawn from the furnace at the rate of 0.00025 cm/s, with the mold quenched with a water spray as it emerges from the furnace.

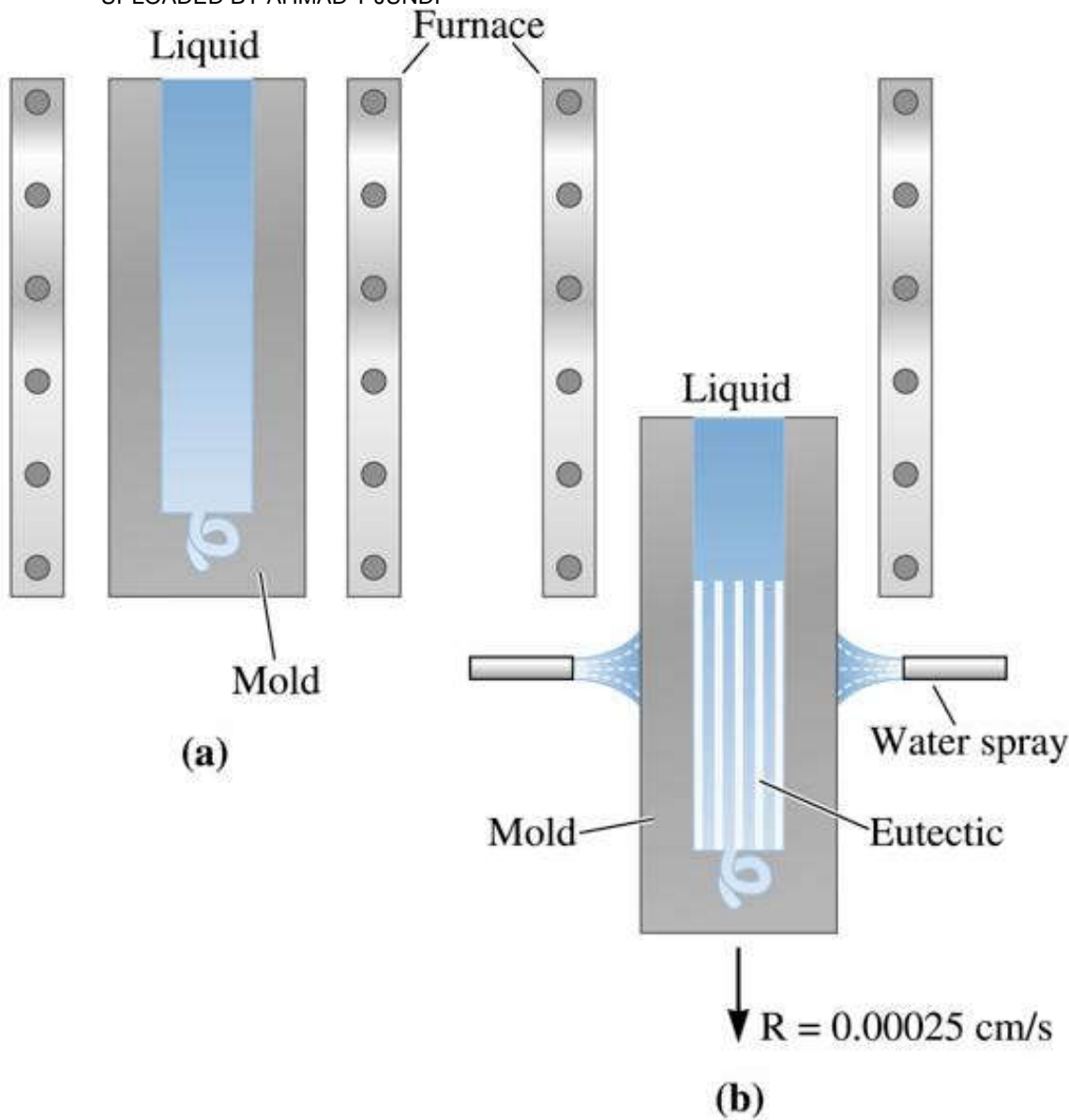


Figure 10.21
Directional solidification of a Pb-Sn eutectic alloy: (a) The metal is melted in the furnace, and (b) the mold is slowly withdrawn from the furnace and the casting is cooled (for Example 10.7).

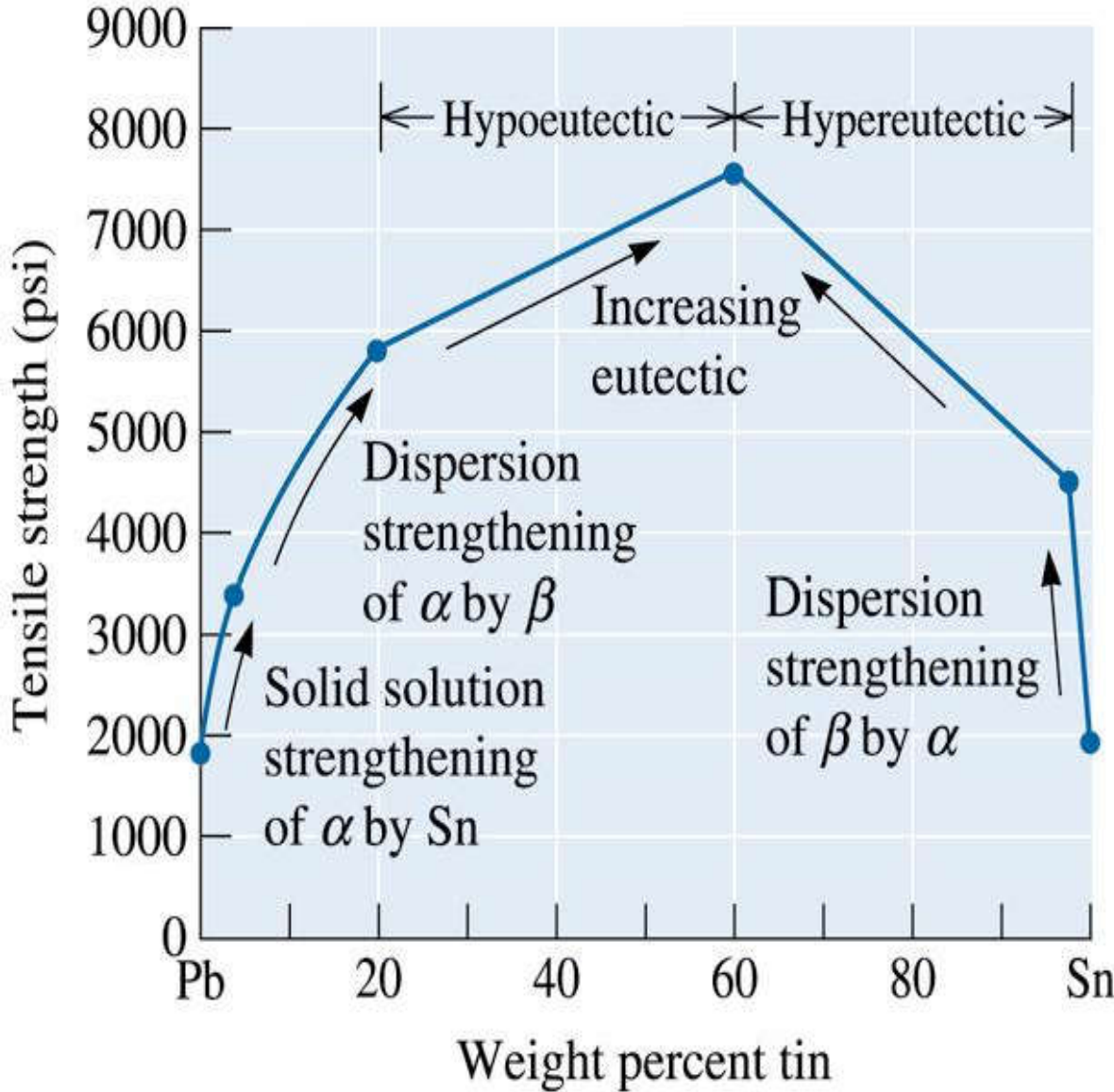


Figure 10.22 The effect of the composition and strengthening mechanism on the tensile strength of lead-tin alloys.

(c)2003 Brooks/Cole, a division of Thomson Learning, Inc. Thomson Learning is a trademark used herein under license.

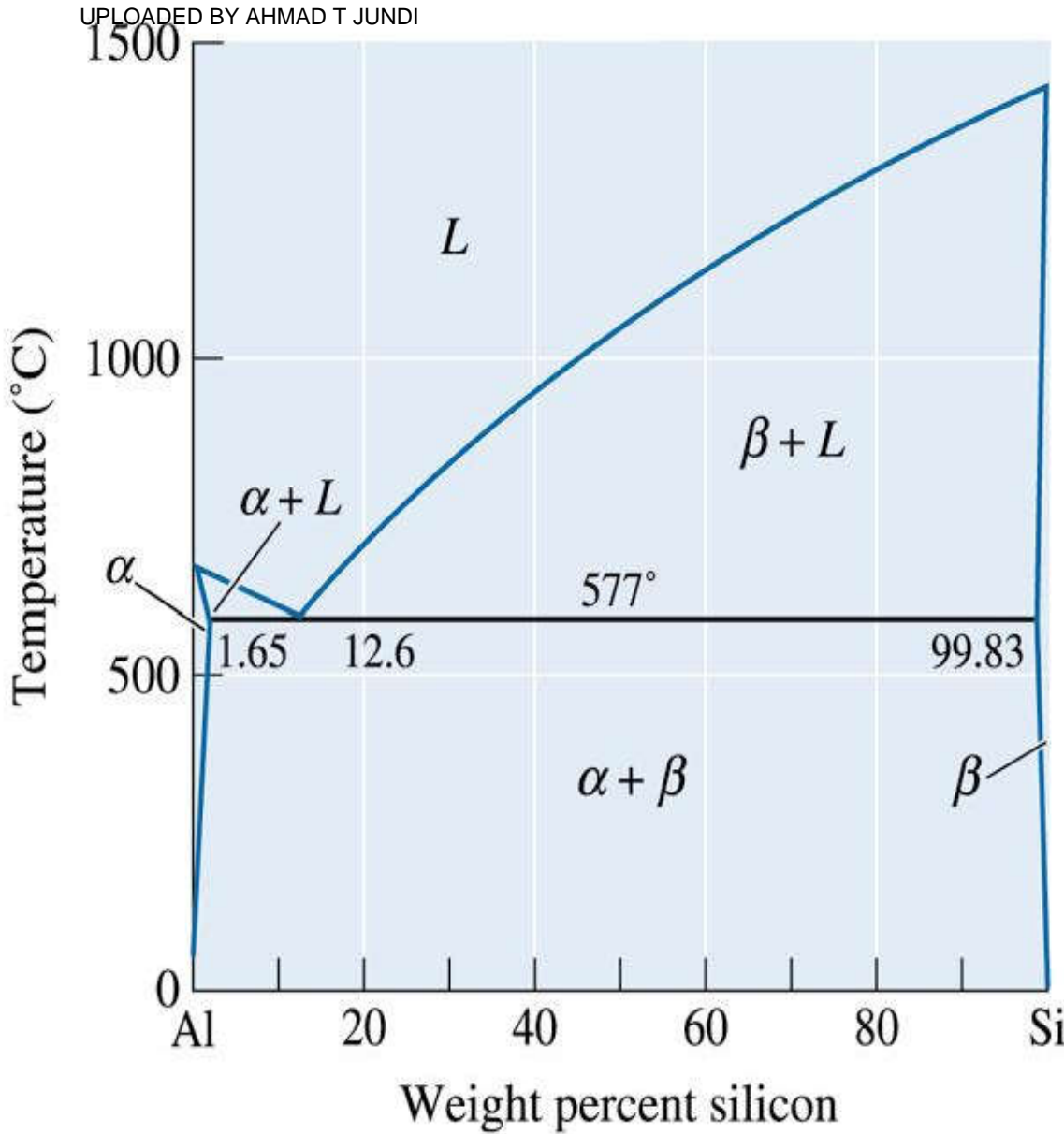


Figure 10.23
the aluminum-
silicon phase
diagram.



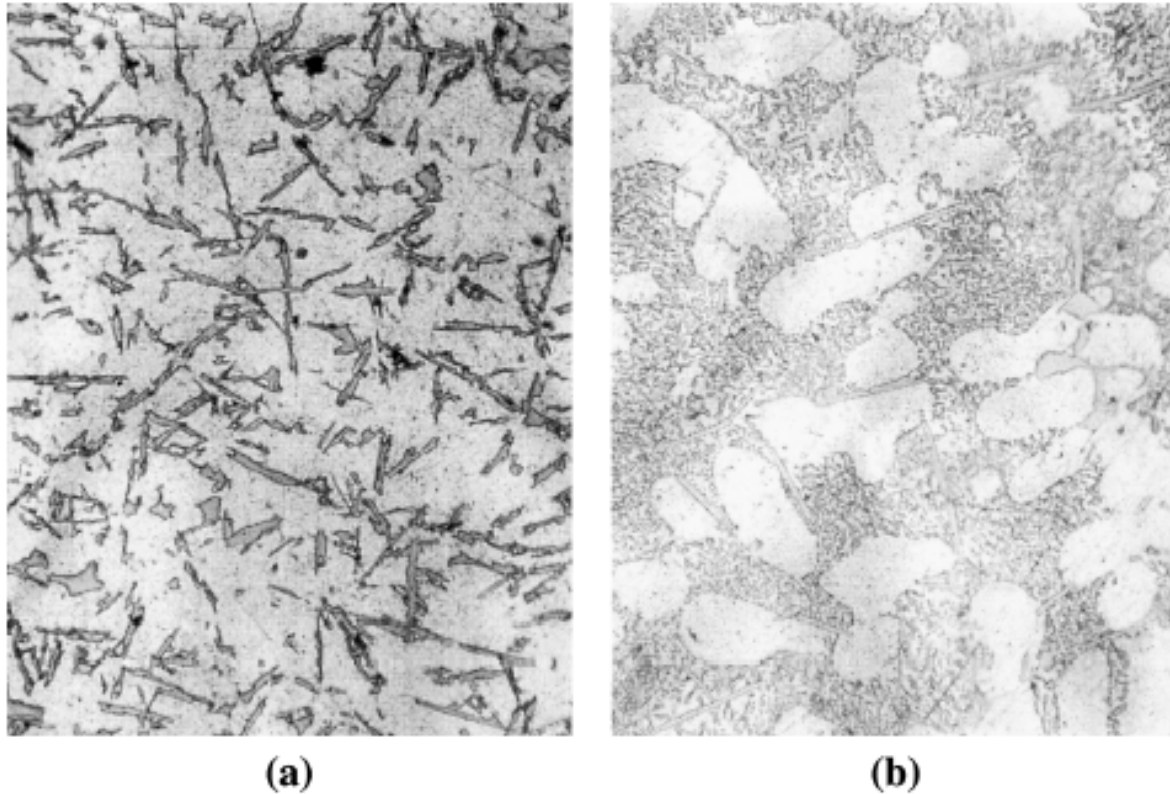
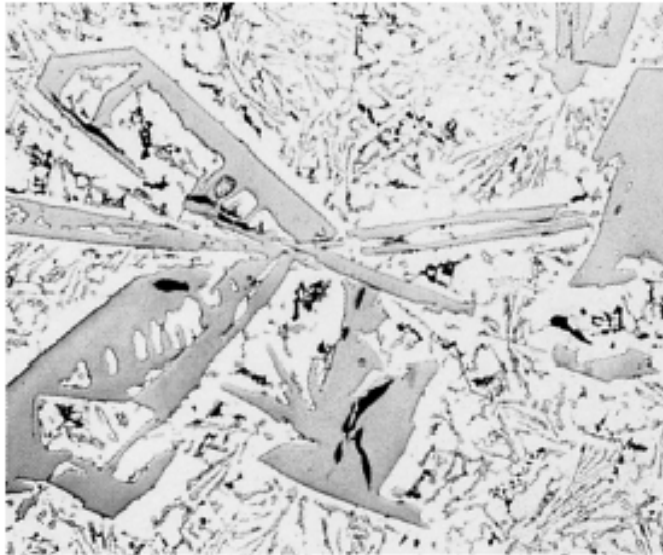
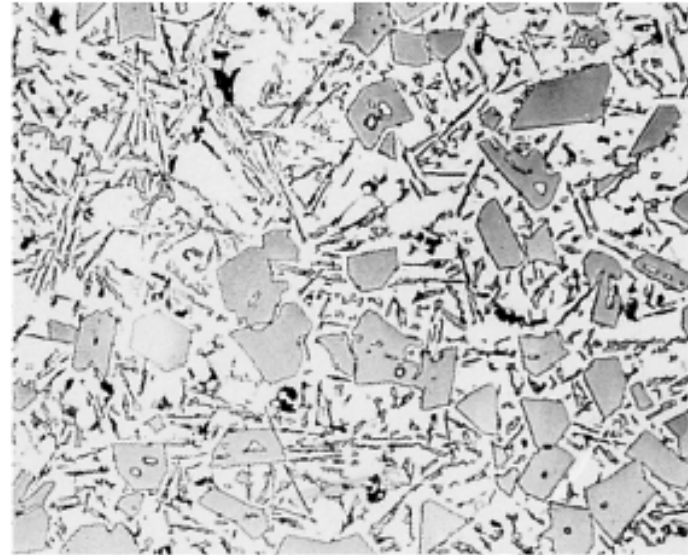


Figure 10.24 Typical eutectic microstructures: (a) needle-like silicon plates in the aluminum silicon eutectic (x100), and (b) rounded silicon rods in the modified aluminum-silicon eutectic (x100).



(a)



(b)

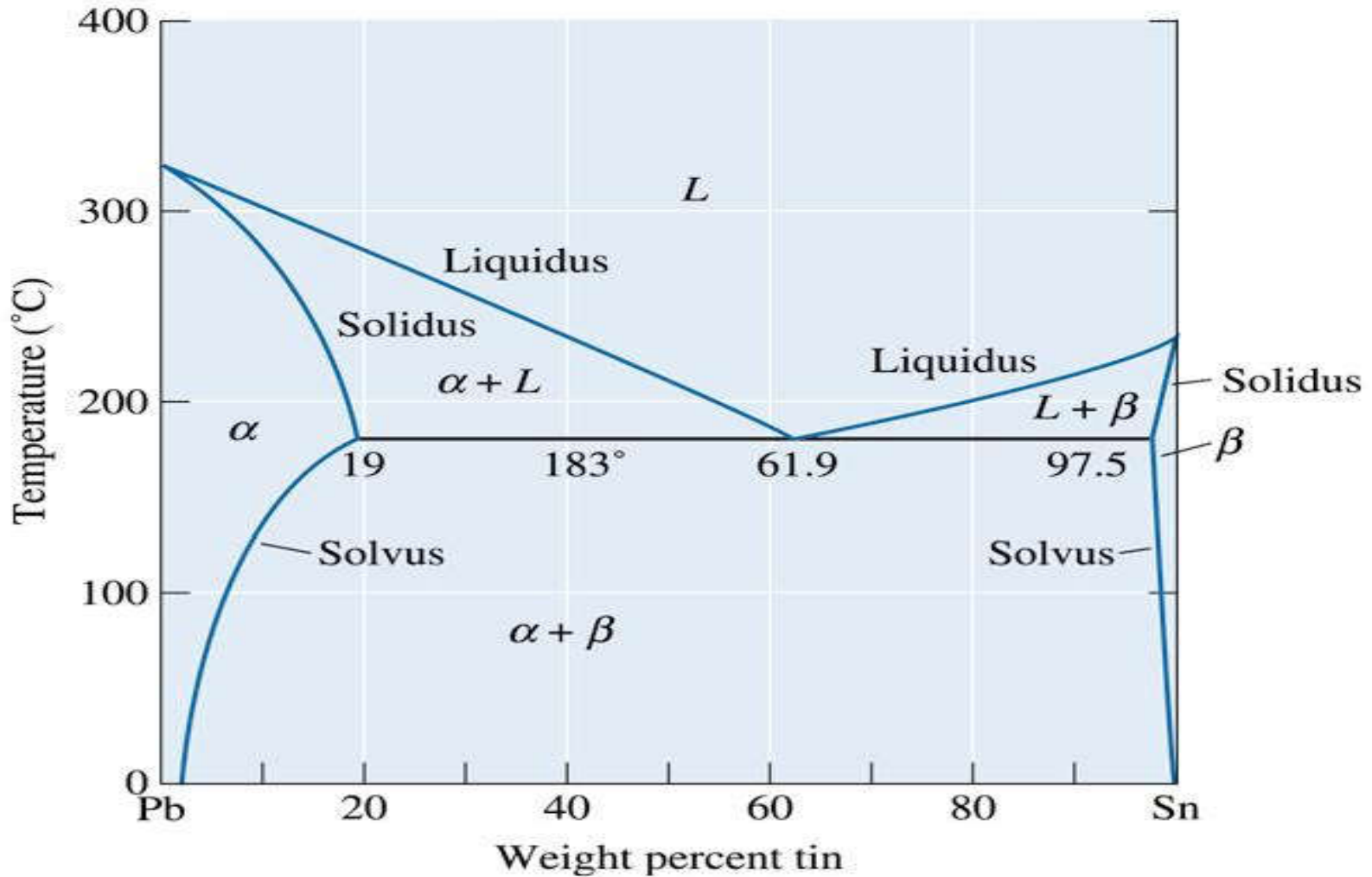
Figure 10.25 The effect of hardening with phosphorus on the microstructure of hypereutectic aluminum-silicon alloys: (a) coarse primary silicon, and (b) fine primary silicon, as refined by phosphorus addition (x75). (From ASM Handbook, Vol. 7, (1972), ASM International, Materials Park, OH 44073.)



Example 10.8

Design of Materials for a Wiping Solder

One way to repair dents in a metal is to wipe a partly liquid-partly solid material into the dent, then allow this filler material to solidify. For our application, the wiping material should have the following specifications: (1) a melting temperature below 230°C , (2) a tensile strength in excess of 6000 psi, (3) be 60% to 70% liquid during application, and (4) the lowest possible cost. Design an alloy and repair procedure that will meet these specifications.



(c)2003 Brooks/Cole, a division of Thomson Learning, Inc. Thomson Learningsm is a trademark used herein under license.

Figure 10.8 the lead-tin equilibrium phase diagram.



Example 10.8 SOLUTION

Our recommendation, therefore, is to use a Pb-40% Sn alloy applied at 205°C, a temperature at which there will be 65% liquid and 35% primary α . As mentioned before, we should also pay attention to the toxicity of lead and any legal liabilities the use of such materials may cause. A number of new lead free solders have been developed.





Example 10.9

Design of a Wear-Resistant Part

Design a lightweight, cylindrical component that will provide excellent wear-resistance at the inner wall, yet still have reasonable ductility and toughness overall. Such a product might be used as a cylinder liner in an automotive engine.

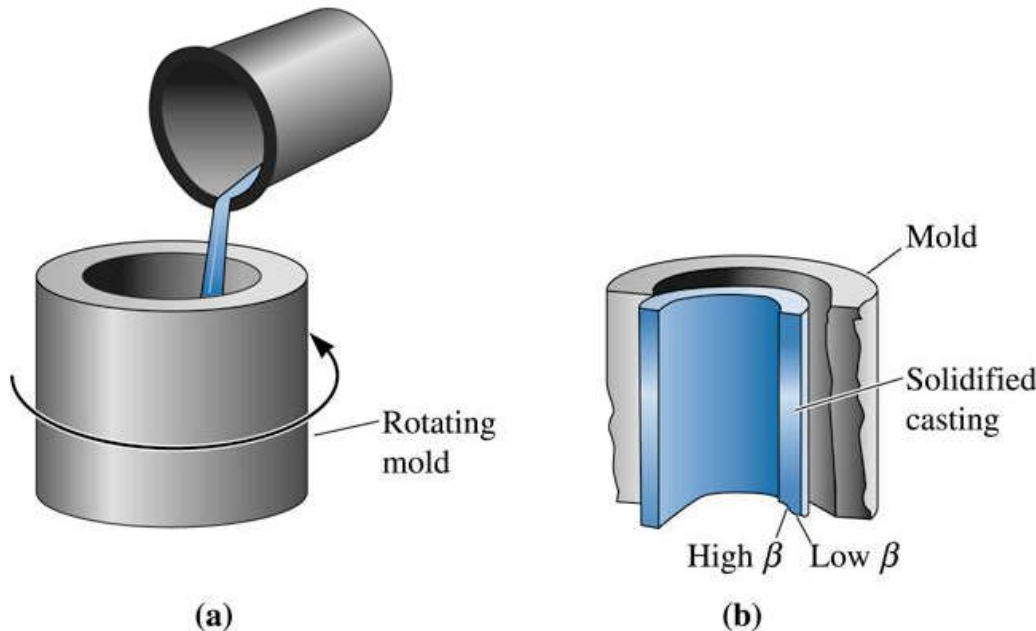


Figure 10.26
Centrifugal casting of a hypereutectic Al-Si alloy: (a) Liquid alloy is poured into a rotating mold, and (b) the solidified casting is hypereutectic at the inner diameter and eutectic at the outer diameter (for Example 10.9).

(c)2003 Brooks/Cole, a division of Thomson Learning, Inc. Thomson Learning,™ is a trademark used herein under license.



Example 10.9 SOLUTION

The hypereutectic Al-Si alloys containing primary β may provide the wear-resistance that we wish at one-third the weight of the steel.

Since the part to be produced is cylindrical in shape, centrifugal casting (Figure 10.26) might be a unique method for producing it.

A typical alloy used to produce aluminum engine components is Al-17% Si. From Figure 10.23, the total amount of primary β that can form is calculated at 578°C, just above the eutectic temperature:

$$\% \text{ Primary } \beta = \frac{17 - 12.6}{99.83 - 12.6} \times 100 = 5.0\%$$

Section 10.6 Eutectics and Materials Processing

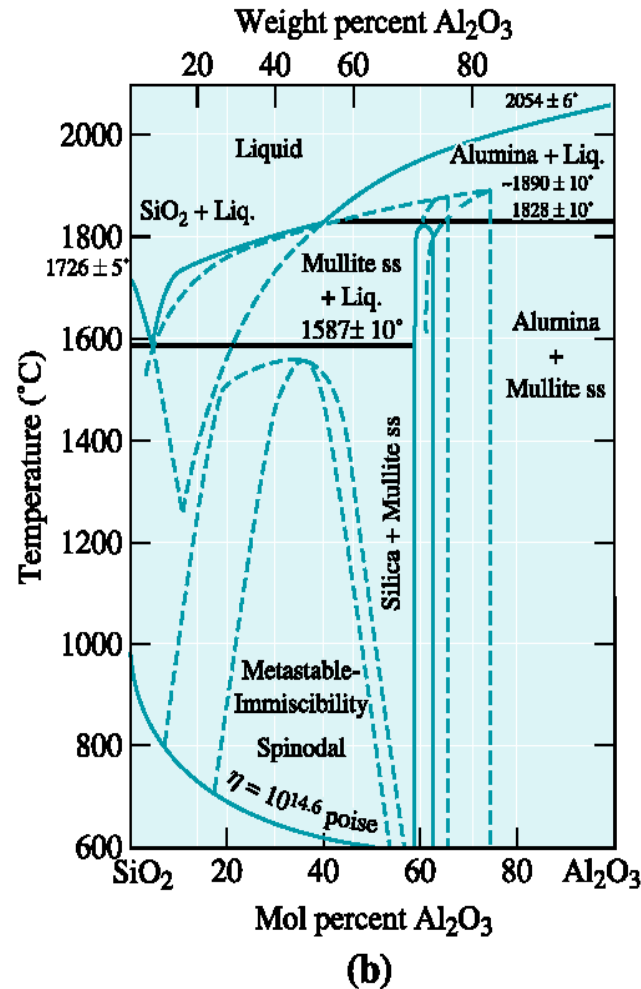
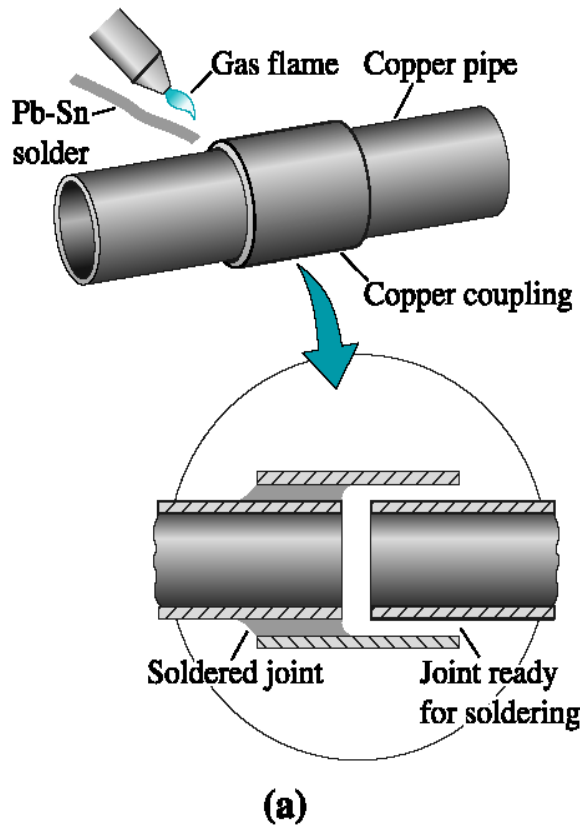
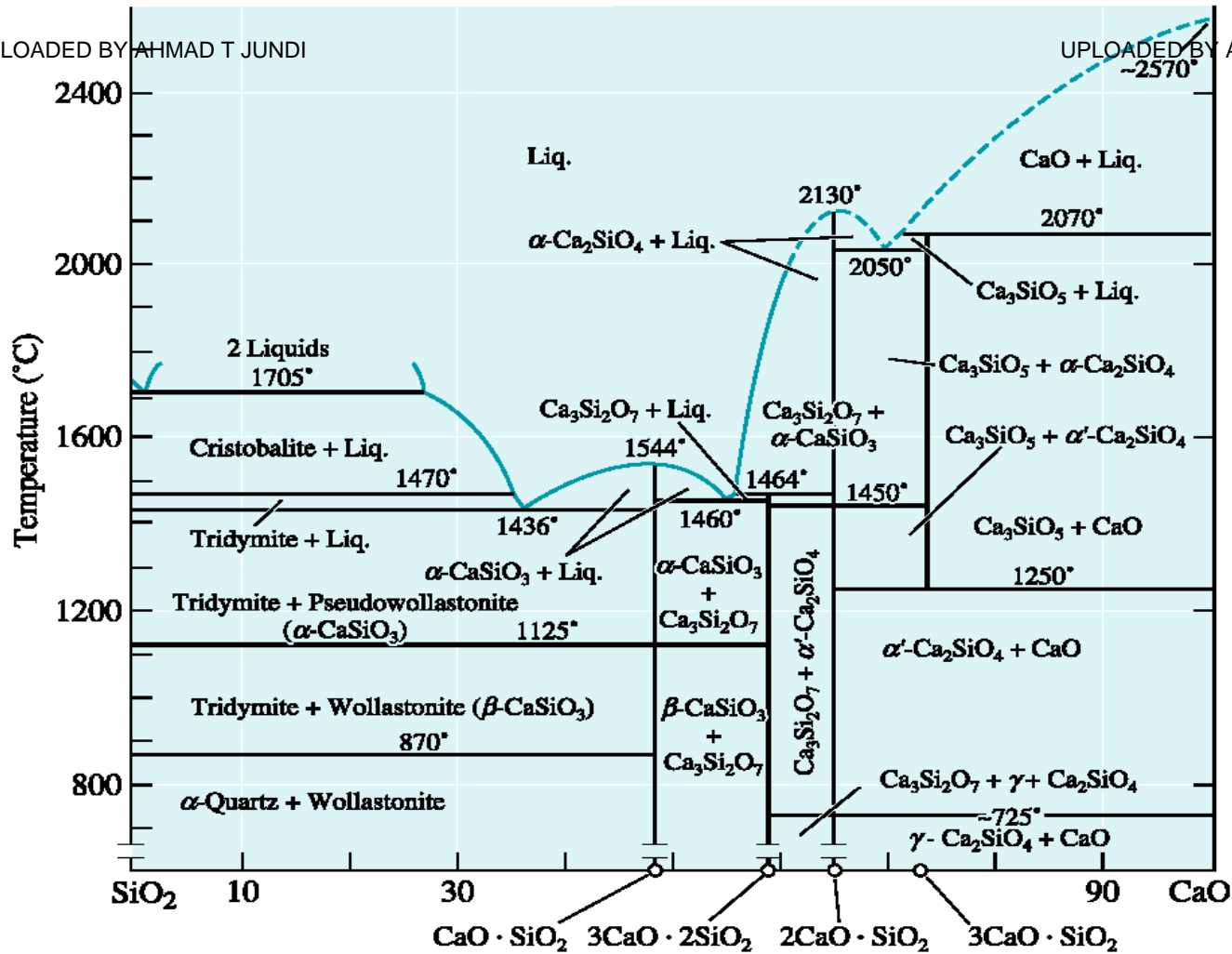


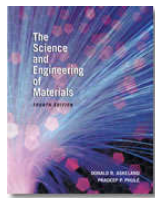
Figure 10.27 (a) A Pb-Sn eutectic alloy is often used during soldering to assemble parts. A heat source, such as a gas flame, heats both the parts and the filler material. The filler is drawn into the joint and solidifies. (b) A phase diagram for $\text{Al}_2\text{O}_3\text{-SiO}_2$. [9] (*Adapted from Introduction to Phase Equilibria in Ceramics, by Bergeron, C.G. and Risbud, S.H., The American Ceramic Society, Inc., 1984, page 44.*)



(c)

Figure 10.27 (c) A phase diagram for the CaO-SiO₂ system. (Source: Adapted from Introduction to Phase Equilibria, by C.G. Bergeron and S.H. Risbud, pp. 44 and 45, Figs. 3-36 and 3-37. Copyright © 1984 American Ceramic Society.)





Section 10.7 Nonequilibrium Freezing in the Eutectic System

©2003 Brooks/Cole, a division of Thomson Learning, Inc. Thomson Learning is a trademark used herein under license.

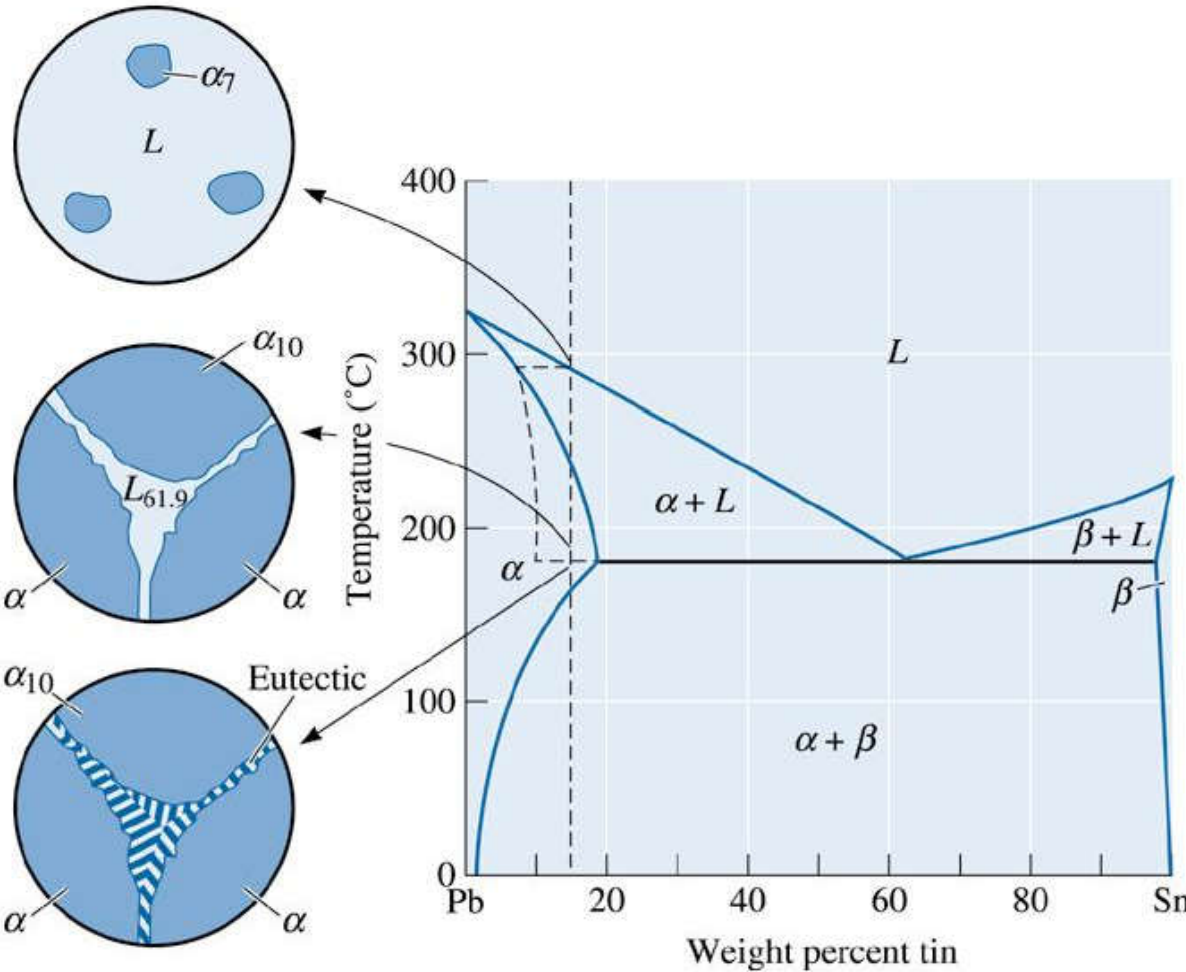


Figure 10.28
Nonequilibrium solidification and microstructure of a Pb-15% Sn alloy. A nonequilibrium eutectic microconstituent can form if the solidification is too rapid.





Section 10.8

Ternary Phase Diagrams

- **Ternary alloy** - An alloy formed by combining three elements or components.
- **Ternary phase diagram** - A phase diagram between three components showing the phases present and their compositions at various temperatures. This diagram requires a three-dimensional plot or is presented as two-dimensional isothermal sections of a three-dimensional diagram.

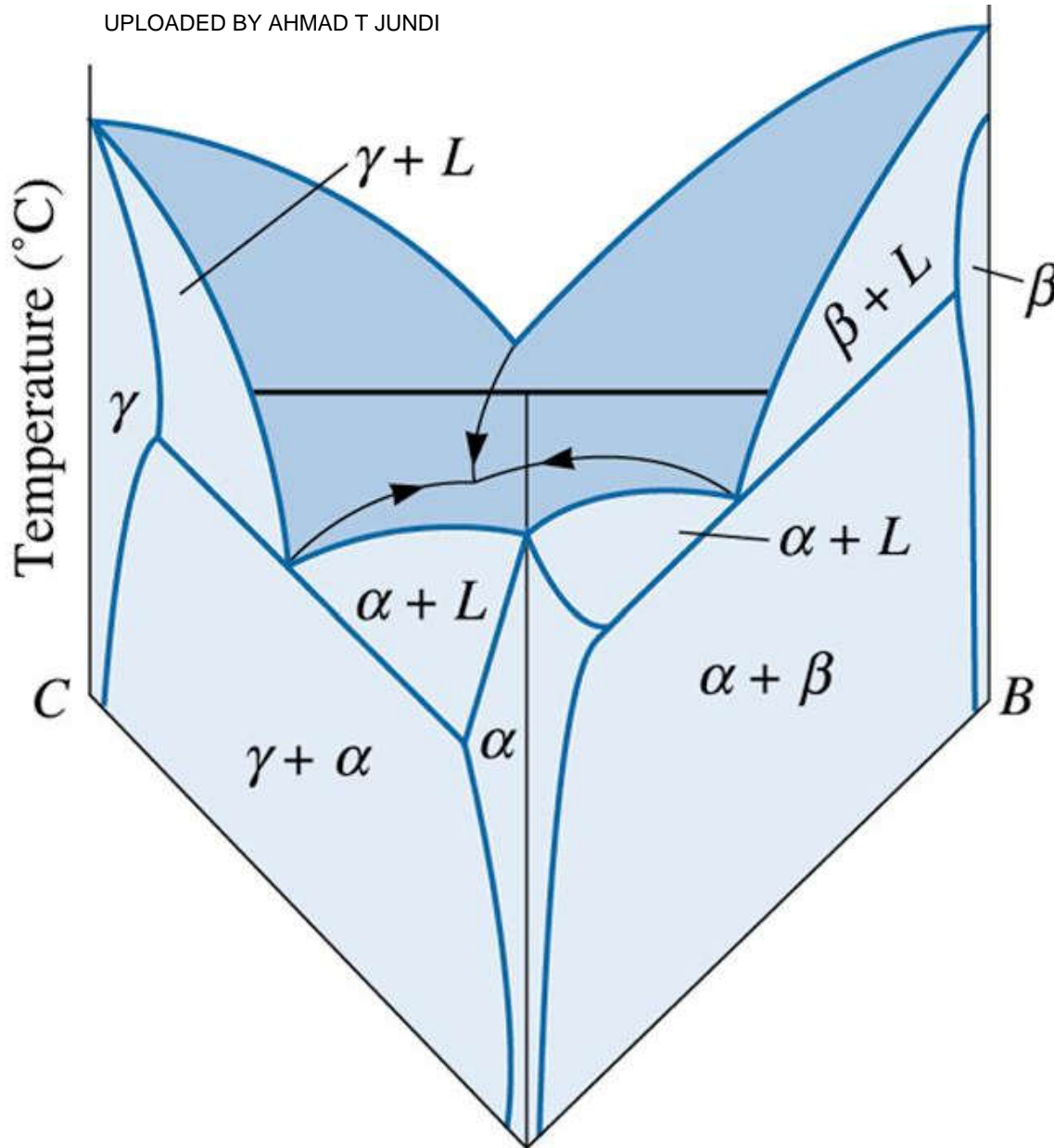


Figure 10.29
Hypothetical
ternary phase
diagram. Binary
phase diagrams
are present at the
three faces.

(c)2003 Brooks/Cole, a division of Thomson Learning, Inc. Thomson Learning is a trademark used herein under license.



Example 10.10

Determination of Liquidus on a Ternary Phase Diagram

Using the ternary plots in Figures 10.30 and 10.31, determine the liquidus temperature, the primary phase that forms during solidification, and the phases at room temperature for the following materials:

Point x : 10% B , 10% C , balance A

Point y : 10% B , 60% C , balance A

Point z : 40% B , 40% C , balance A

Melting temperatures
 A — 450°
 B — 600°
 C — 500°
 Eutectic — 150°

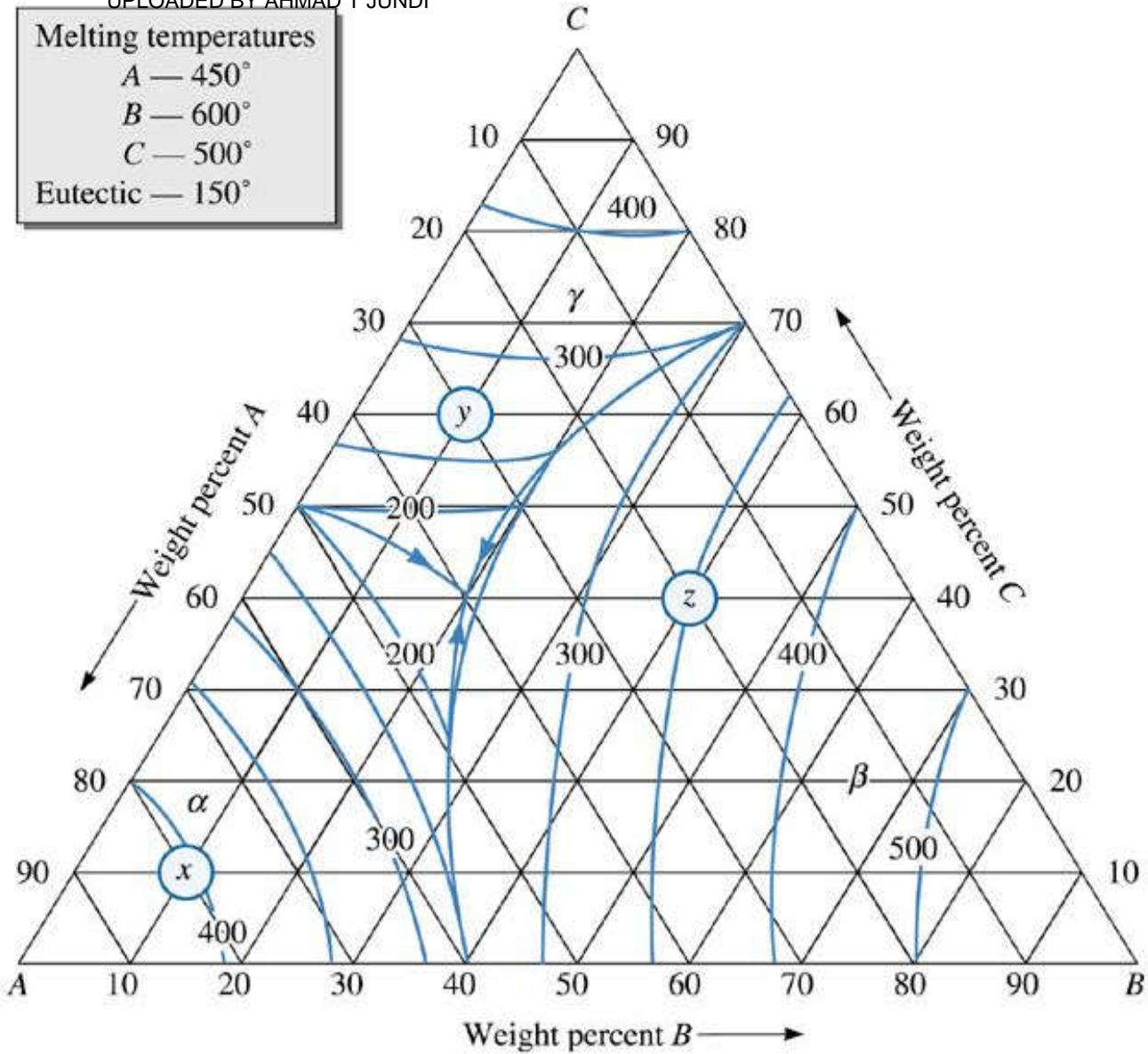


Figure 10.30 A liquidus plot for the hypothetical ternary phase diagram. The circles labeled x, y, and z refer to the different compositions discussed in Example 10.10.



©2003 Brooks/Cole, a division of Thomson Learning, Inc. Thomson LearningSM is a trademark used herein under license.

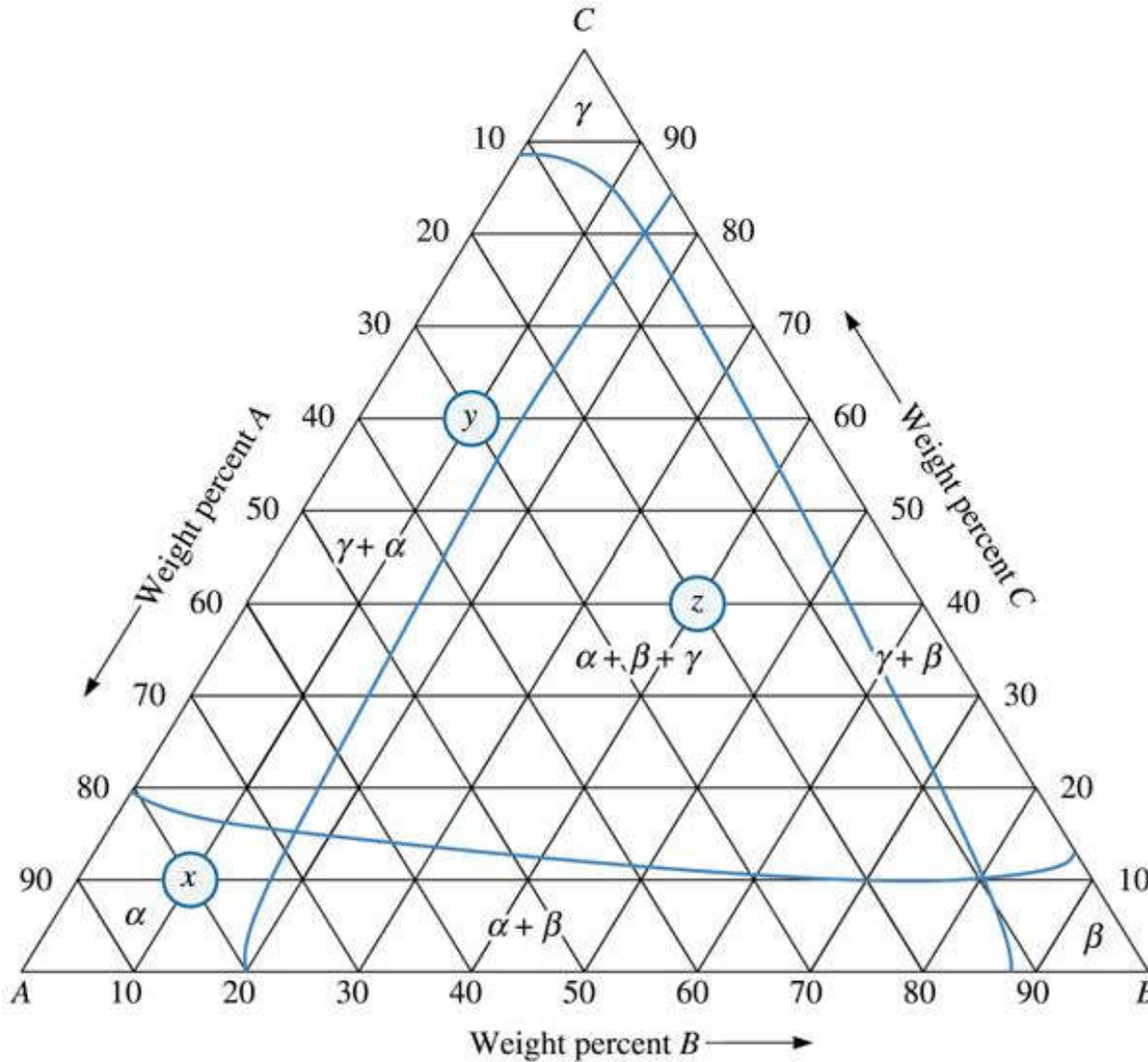


Figure 10.31 An isothermal plot at room temperature for the hypothetical ternary phase diagram. The circles labeled x, y, and z correspond to the different compositions discussed in Example 10.10.





Example 10.10 SOLUTION

The composition 10% B-10% C balance A is located at point x in the figures; from the isotherm in this region, the liquidus temperature is 400°C . The primary phase, as indicated in the diagram, is α . The final structure (Figure 10.31) is all α .

The composition 10% B-60% C balance A is located at point y ; by interpolating the isotherms in this region, the liquidus temperature is about 270°C . The primary phase that forms in this section of the diagram is γ , and the room temperature phases are α and γ .

The composition 40% B-40% C balance A is located at point z ; the liquidus temperature at this point is 350°C , and the point is in the primary β region. The room temperature phases are α , β , and γ .

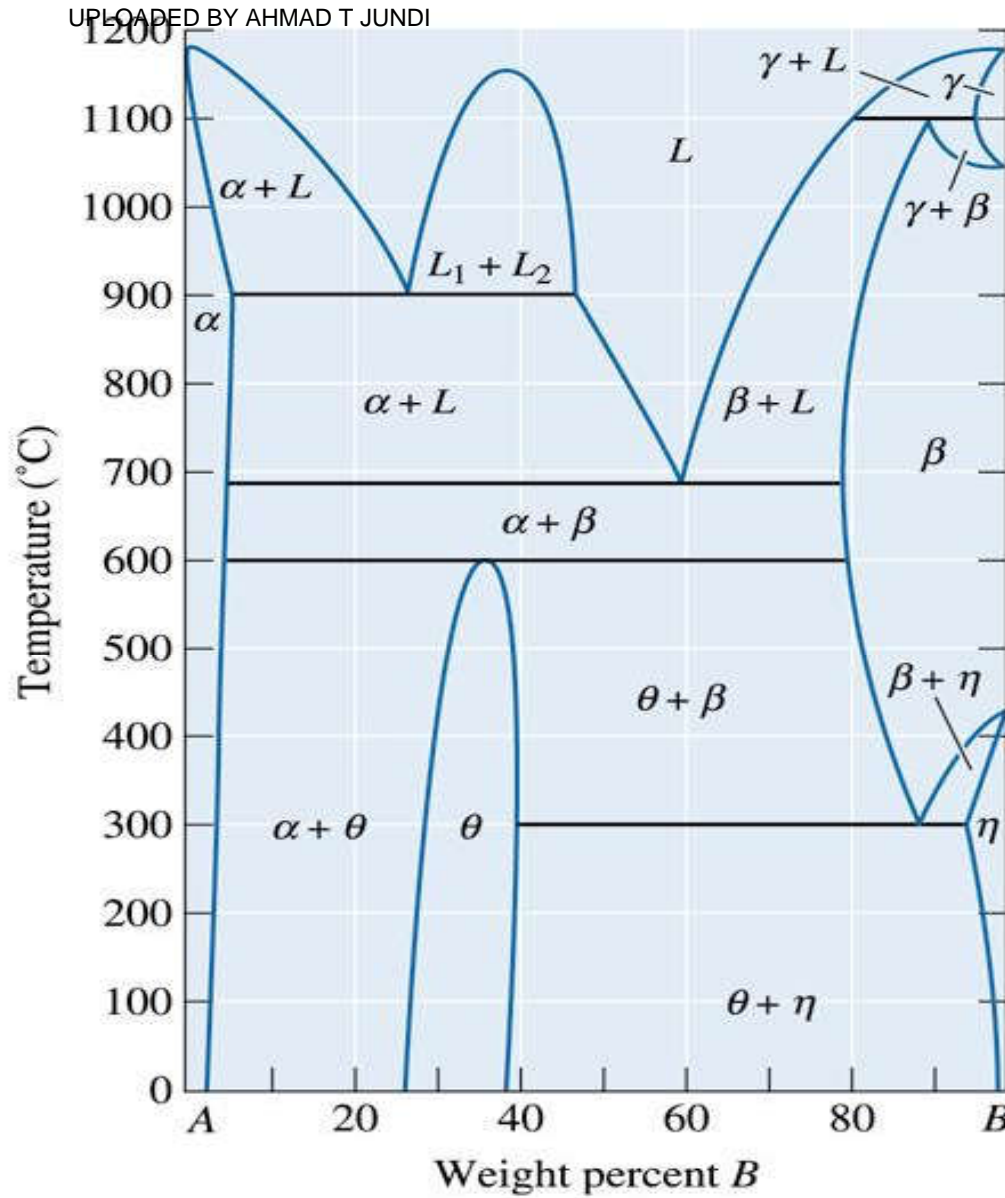
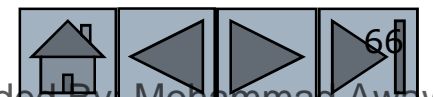


Figure 10.32
Hypothetical phase
diagram (for Problem
10.22).



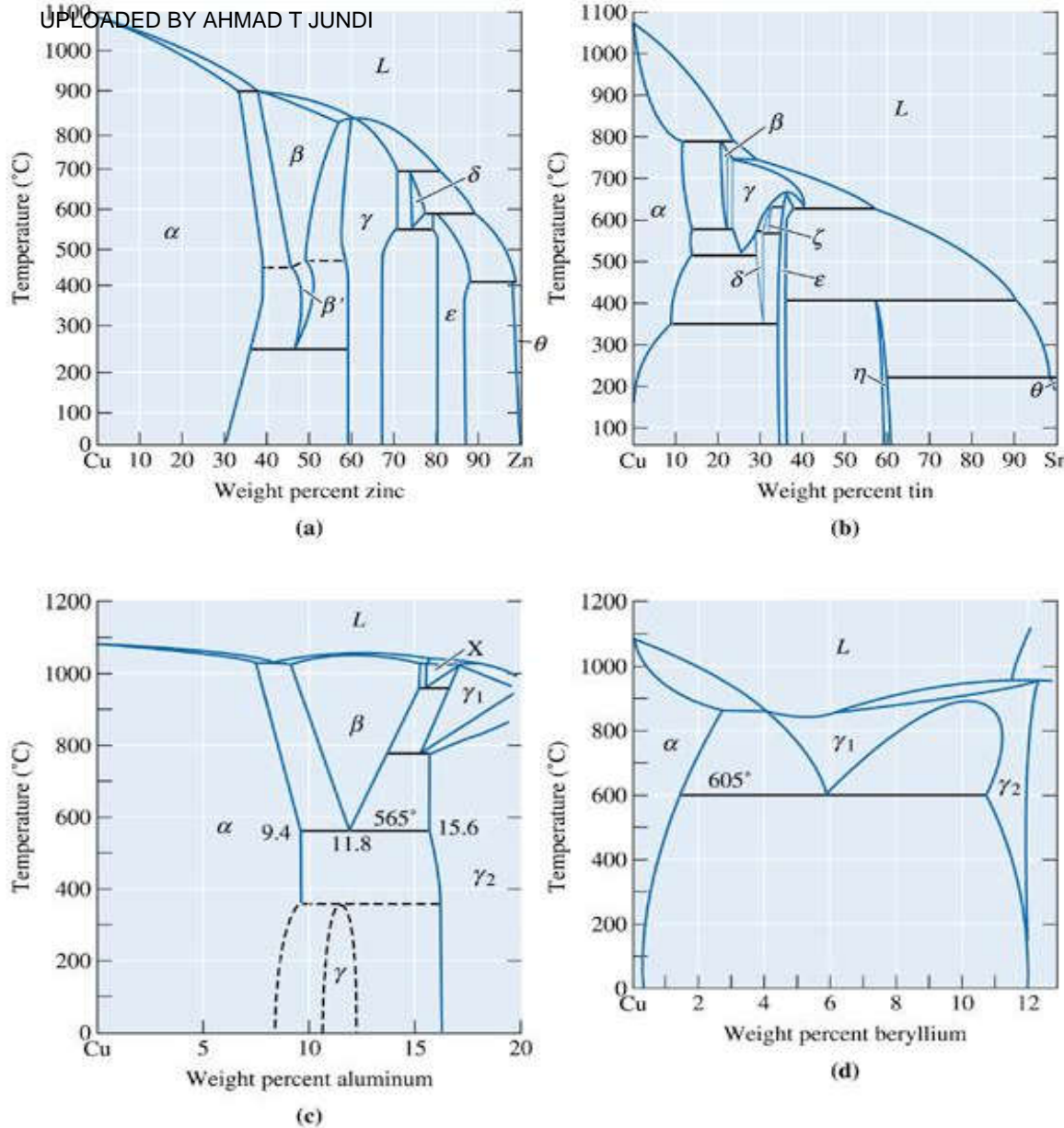
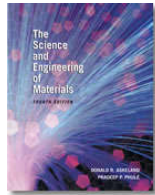
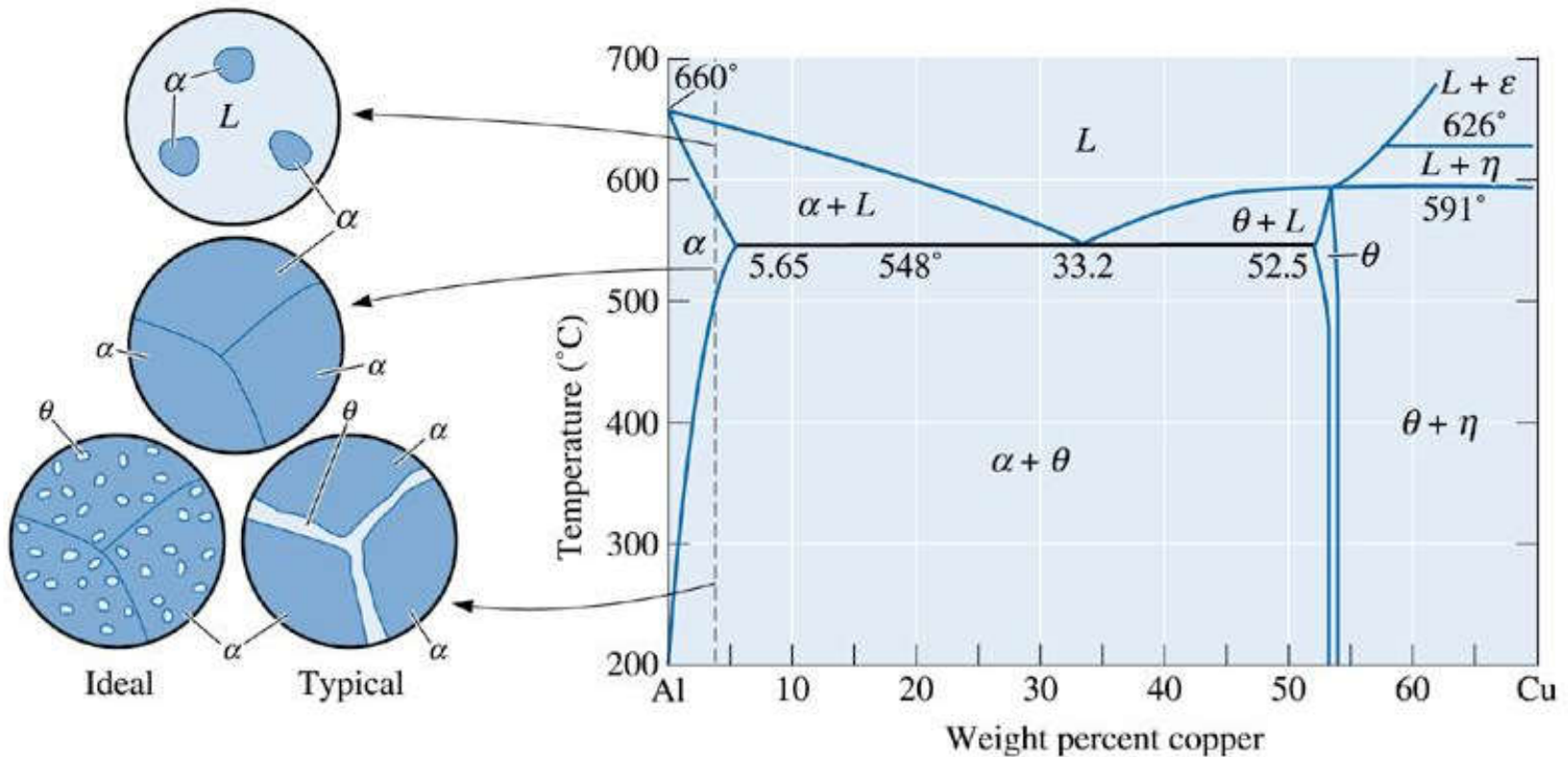


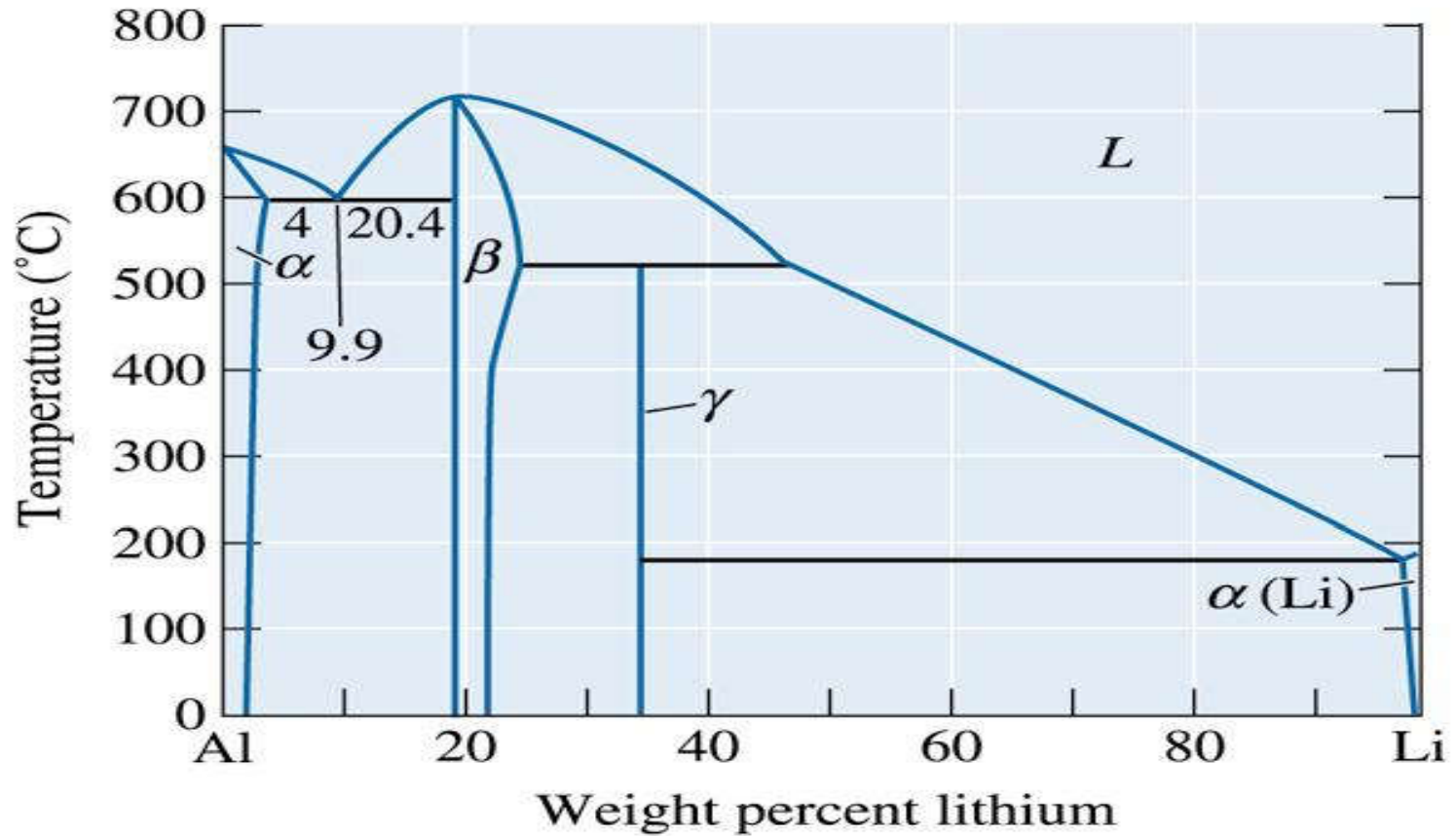
Figure 10.33
Binary phase
diagrams for the
(a) copper-zinc,
(b) copper-tin,
(c) copper-
aluminum, and
(d) copper-
beryllium
systems (for
Problem 10.23).





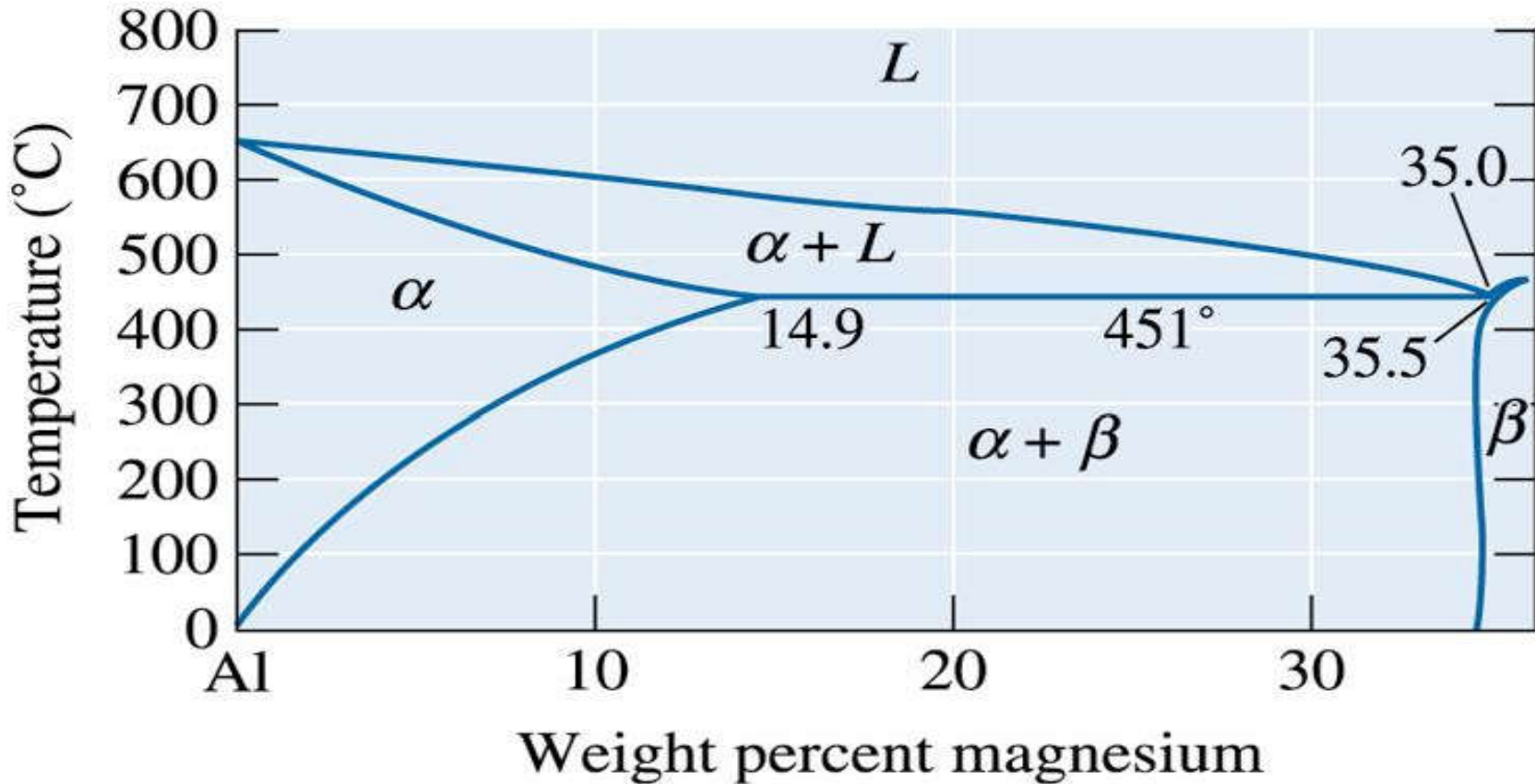
(c)2003 Brooks/Cole, a division of Thomson Learning, Inc. Thomson Learning™ is a trademark used herein under license.

Figure 10.34 The aluminum-copper phase diagram and the microstructures that may develop during cooling of an Al-4%-Cu alloy (for Problem 10.24).



(c)2003 Brooks/Cole, a division of Thomson Learning, Inc. Thomson Learning, is a trademark used herein under license.

Figure 10.35 The aluminum-lithium phase diagram (for Problem 10.25).



(c)2003 Brooks/Cole, a division of Thomson Learning, Inc. Thomson Learning, Inc. is a trademark used herein under license.

Figure 10.36 Portion of the aluminum-magnesium phase diagram (for Problem 10.31).





©2003 Brooks/Cole, a division of Thomson Learning, Inc. Thomson Learning is a trademark used herein under license.

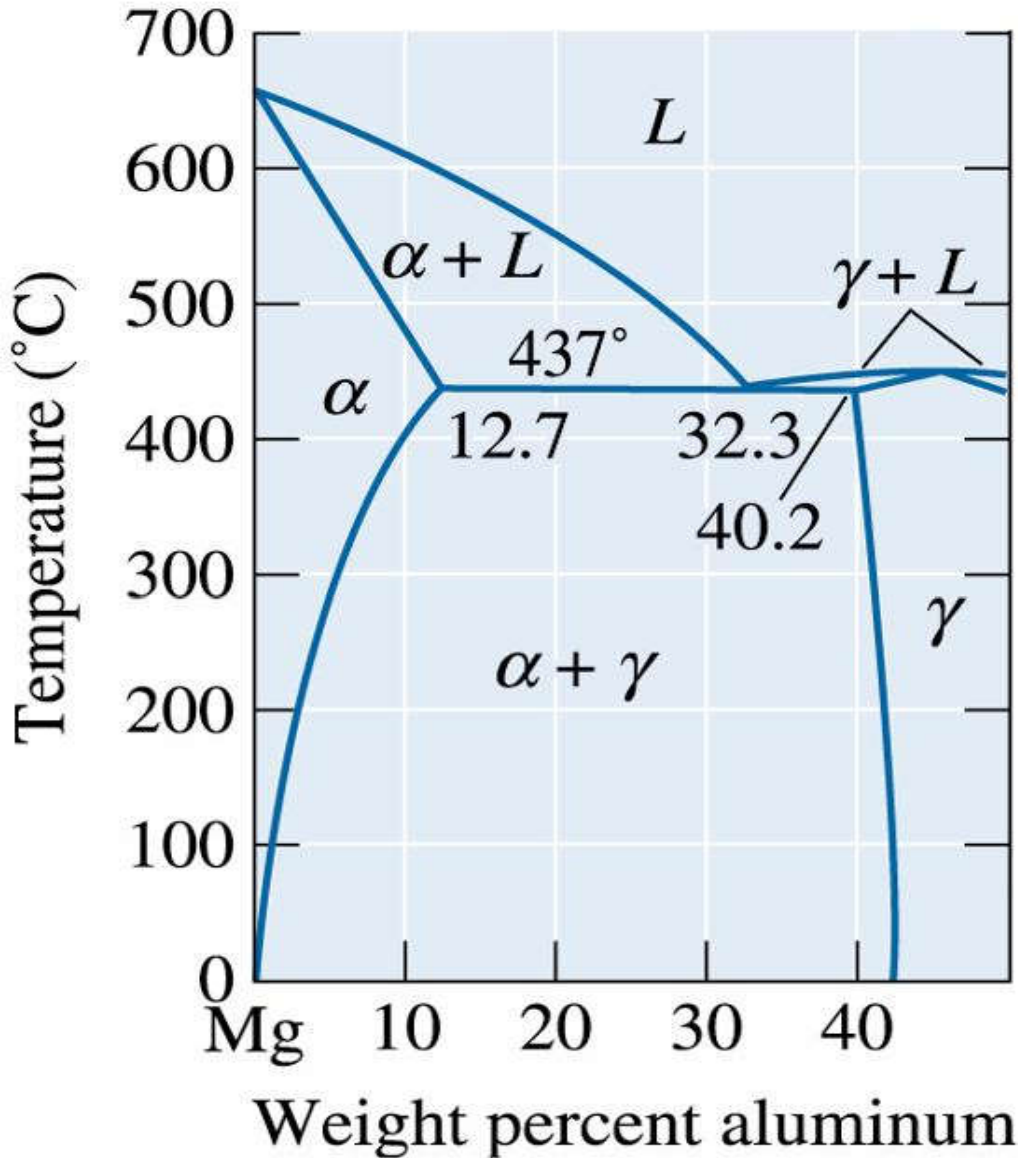
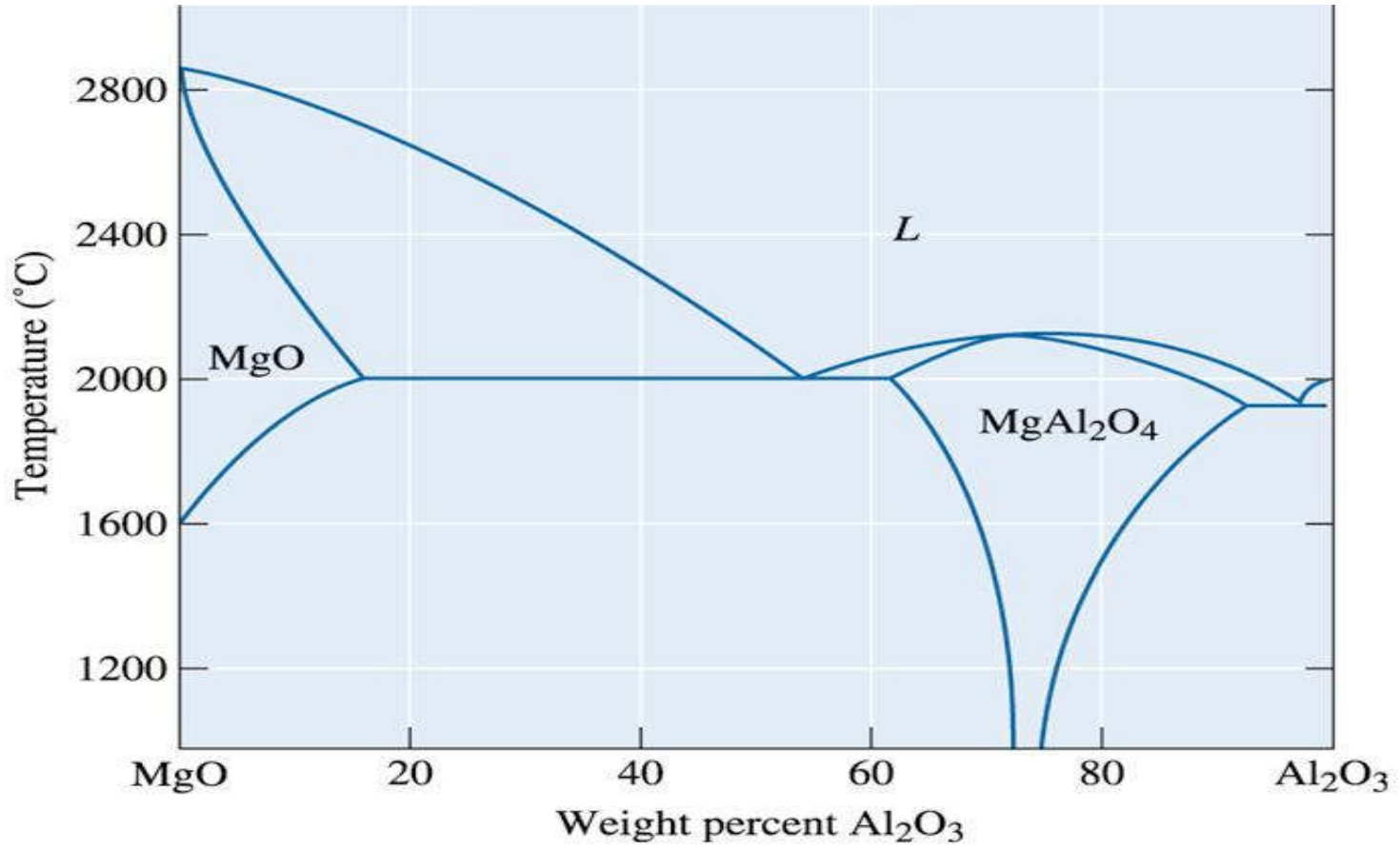


Figure 10.37 A portion of the magnesium-aluminum phase diagram (for Problem 10.41).





(c)2003 Brooks/Cole, a division of Thomson Learning, Inc. Thomson Learningsm is a trademark used herein under license.

Figure 10.39 The MgO-Al₂O₃ phase diagram, showing limited solid solubility and the presence of MgAl₂O₄ or spinel (for Problem 10.42).



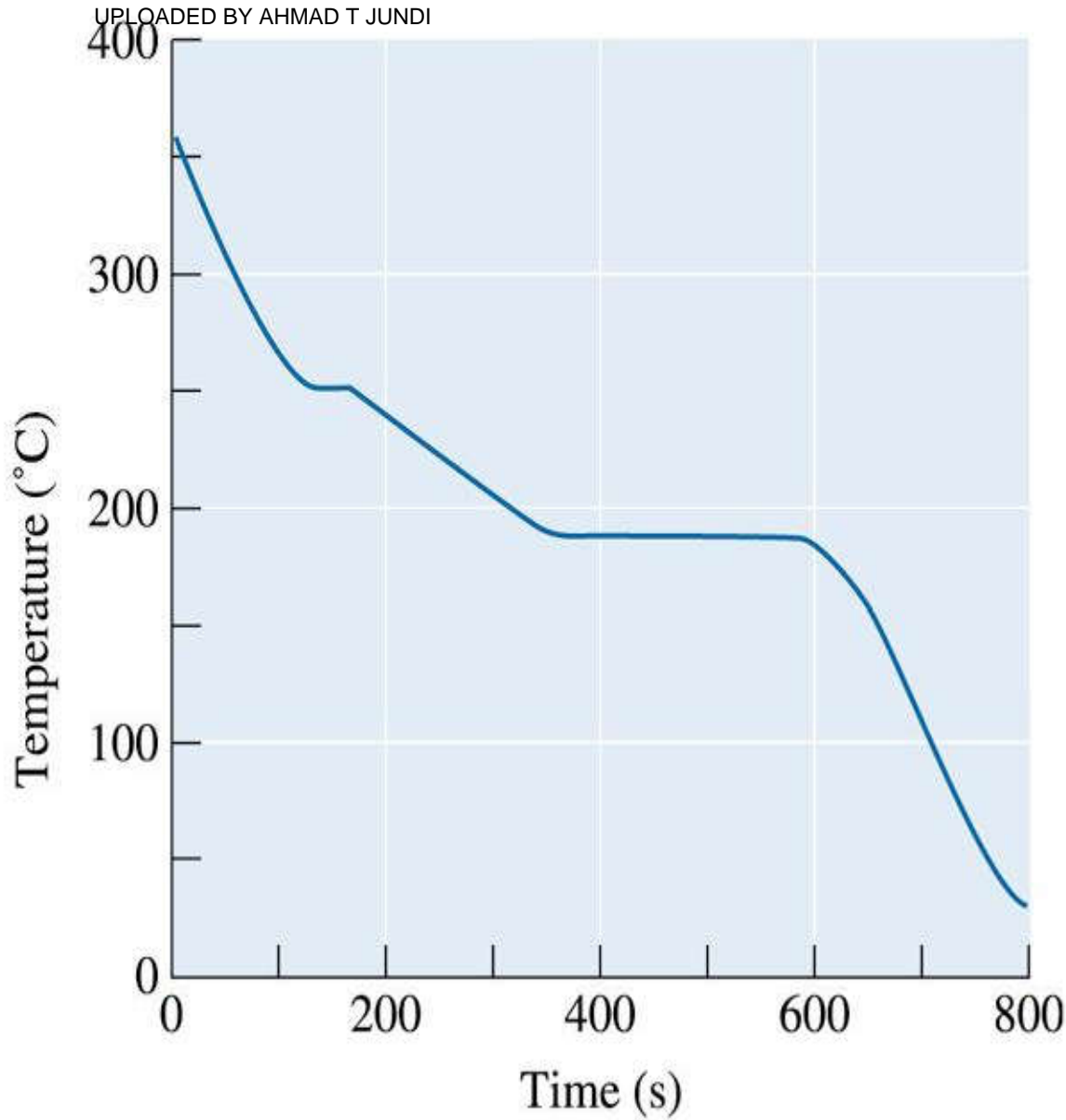
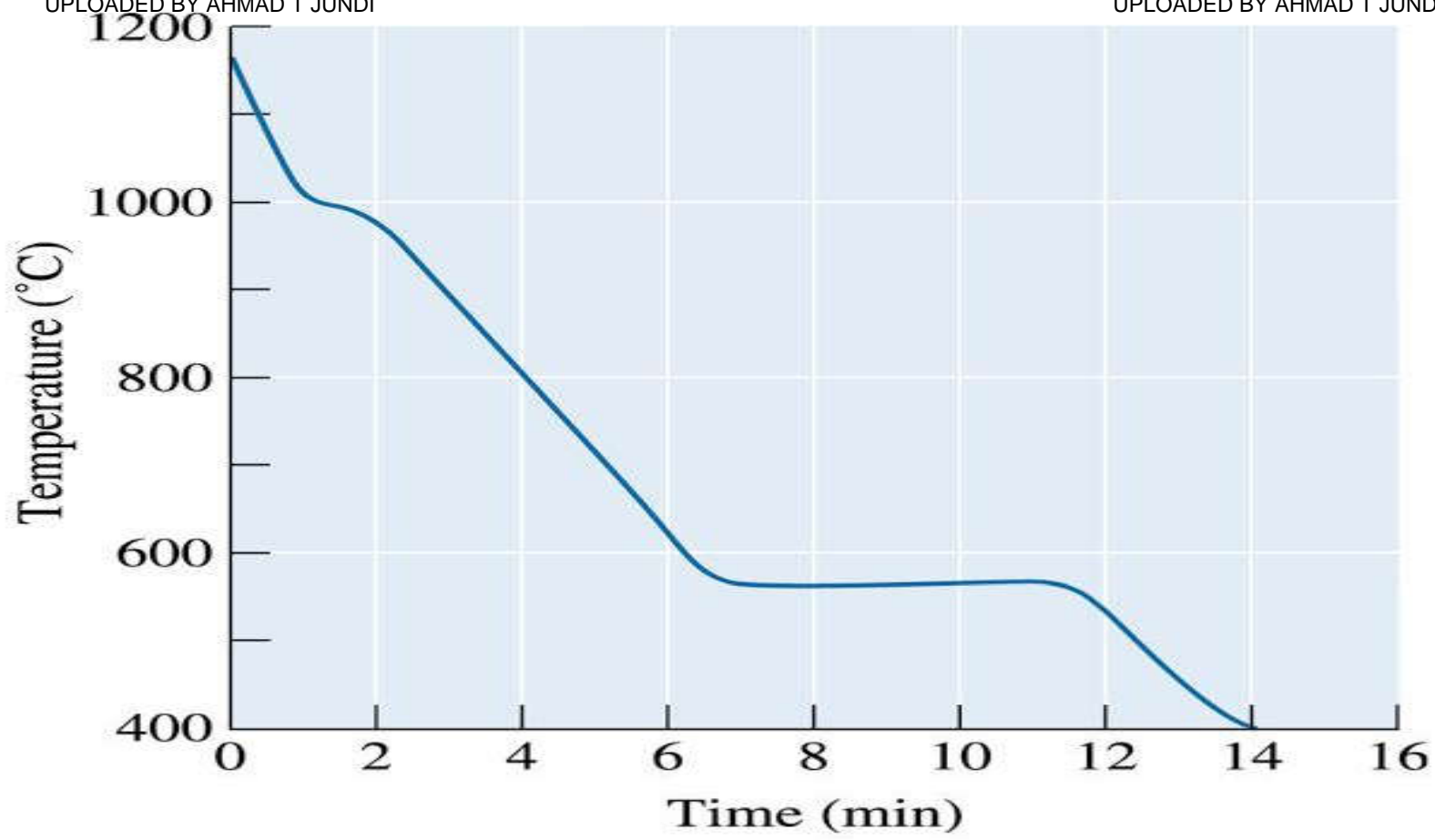
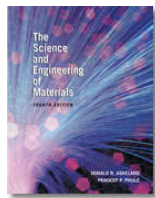


Figure 10.40
Cooling curve for a
Pb-Sn alloy (for
Problem 10.46).

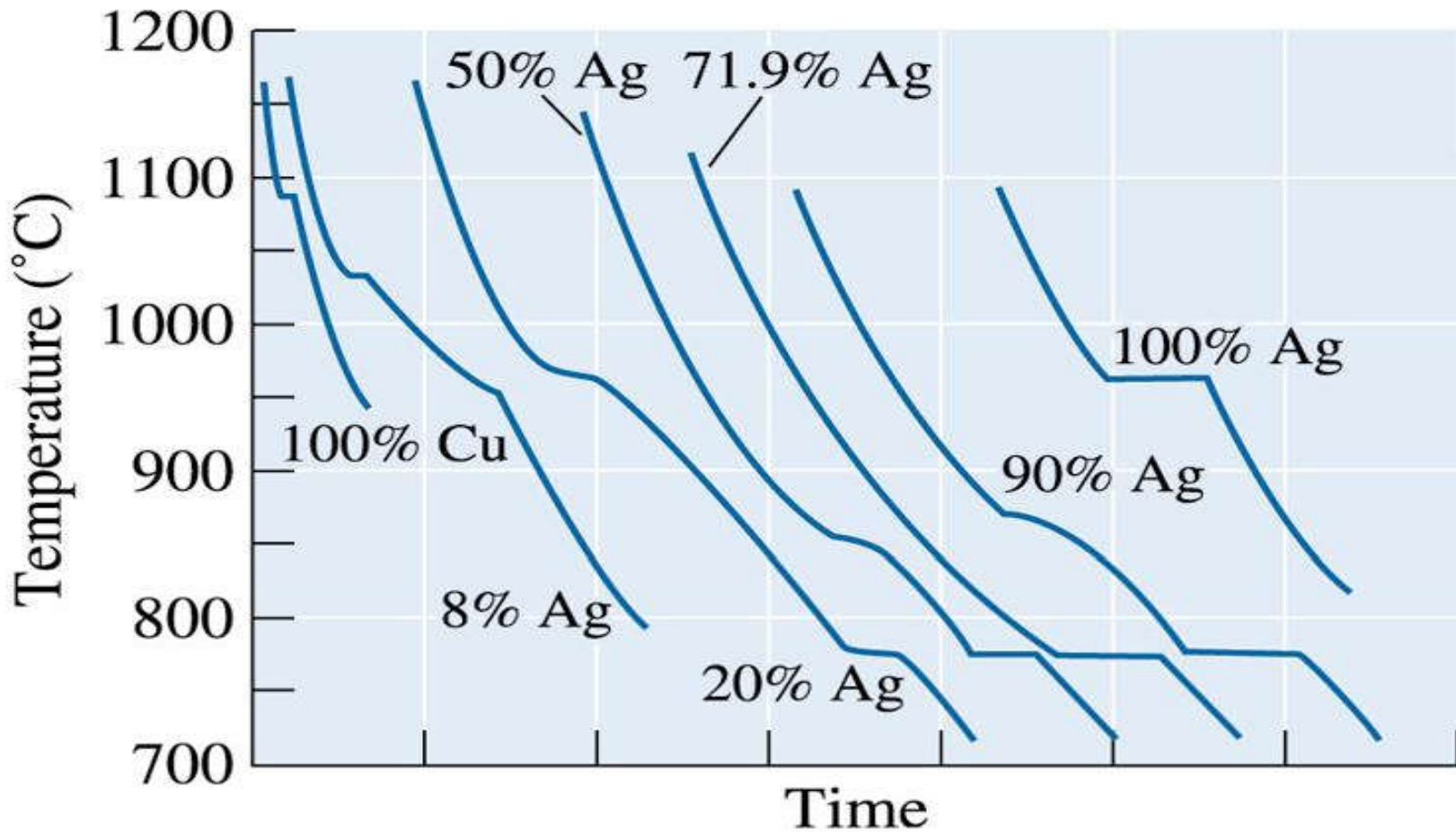




(c)2003 Brooks/Cole, a division of Thomson Learning, Inc. Thomson Learning, is a trademark used herein under license.

Figure 10.41 Cooling curve for an Al-Si alloy (for Problem 10.47).





(c)2003 Brooks/Cole, a division of Thomson Learning, Inc. Thomson Learningsm is a trademark used herein under license.

Figure 10.42 Cooling curves for a series of Cu-Ag alloys (for Problem 10.50).